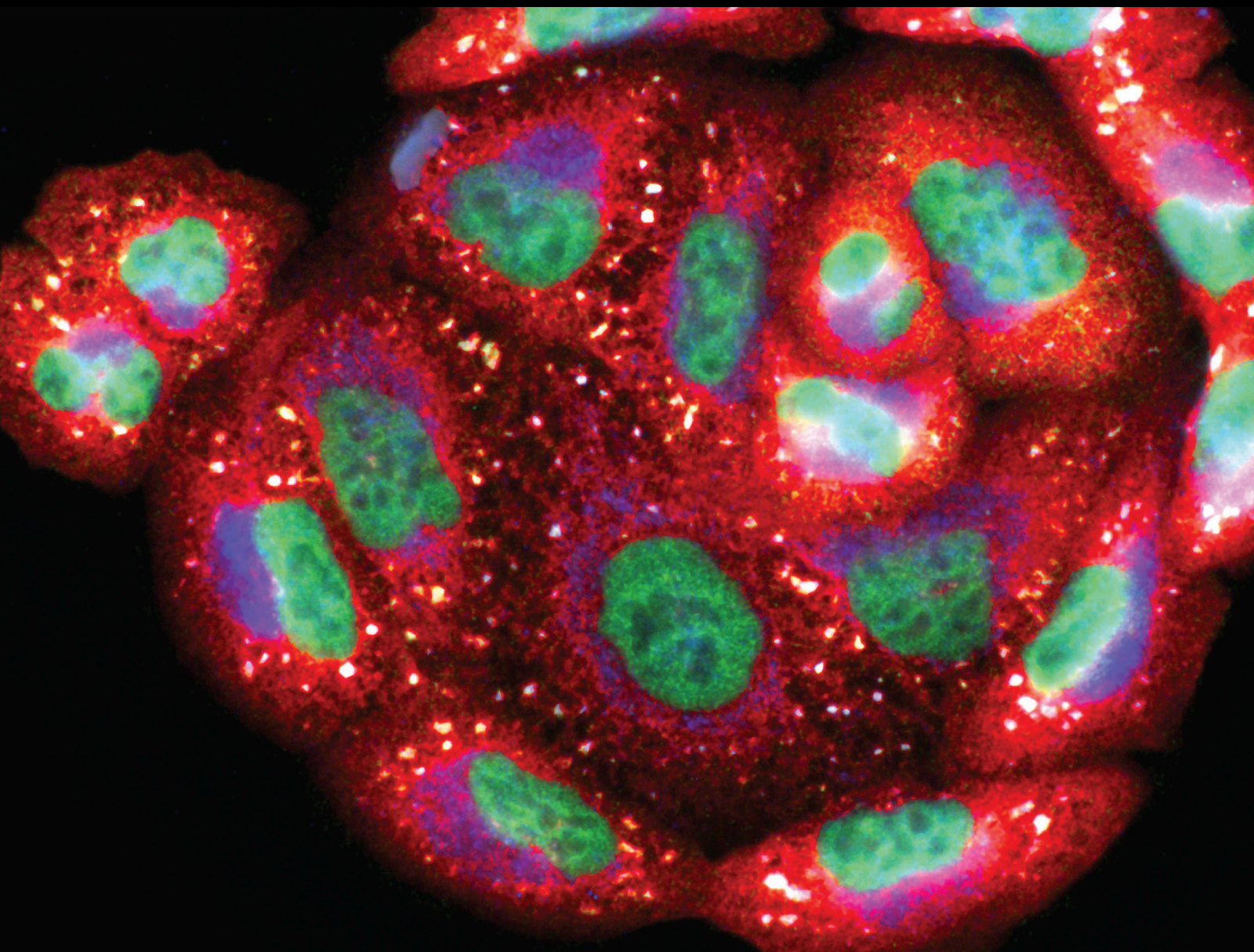


Natural Bioactive Products with Antioxidant Properties Useful in Neurodegenerative Disease 2020

Lead Guest Editor: Francisco Jaime B. Mendonça Junior

Guest Editors: Luciana Scotti, Marcus Tullius Scotti, Anuraj Nayarisseri, and Eugene N. Muratov





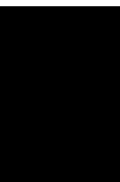
**Natural Bioactive Products with Antioxidant
Properties Useful in Neurodegenerative
Disease 2020**

Oxidative Medicine and Cellular Longevity

**Natural Bioactive Products with
Antioxidant Properties Useful in
Neurodegenerative Disease 2020**

Lead Guest Editor: Francisco Jaime B. Mendonça
Junior

Guest Editors: Luciana Scotti, Marcus Tullius Scotti,
Anuraj Nayarisseri, and Eugene N. Muratov



Copyright © 2021 Hindawi Limited. All rights reserved.

This is a special issue published in "Oxidative Medicine and Cellular Longevity" All articles are open access articles distributed under the Creative Commons Attribution License, which permits unrestricted use, distribution, and reproduction in any medium, provided the original work is properly cited.

Chief Editor

Jeannette Vasquez-Vivar, USA

Editorial Board

Ivanov Alexander, Russia
Fabio Altieri, Italy
Fernanda Amicarelli, Italy
José P. Andrade, Portugal
Cristina Angeloni, Italy
Antonio Ayala, Spain
Elena Azzini, Italy
Peter Backx, Canada
Damian Bailey, United Kingdom
Sander Bekeschus, Germany
Ji C. Bihl, USA
Consuelo Borrás, Spain
Nady Braidy, Australia
Ralf Braun, Austria
Laura Bravo, Spain
Amadou Camara, USA
Gianluca Carnevale, Italy
Roberto Carnevale, Italy
Angel Catalá, Argentina
Peter Celec, Slovakia
Giulio Ceolotto, Italy
Shao-Yu Chen, USA
Ferdinando Chiaradonna, Italy
Zhao Zhong Chong, USA
Xinxin Ci, China
Alin Ciobica, Romania
Ana Cipak Gasparovic, Croatia
Giuseppe Cirillo, Italy
Maria R. Ciriolo, Italy
Massimo Collino, Italy
Graziamaria Corbi, Italy
Manuela Corte-Real, Portugal
Mark Crabtree, United Kingdom
Manuela Curcio, Italy
Andreas Daiber, Germany
Felipe Dal Pizzol, Brazil
Francesca Danesi, Italy
Domenico D'Arca, Italy
Sergio Davinelli, Italy
Claudio De Lucia, USA
Yolanda de Pablo, Sweden
Cinzia Domenicotti, Italy
Joël R. Drevet, France
Grégory Durand, France
Anne Eckert, Switzerland
Javier Egea, Spain
Pablo A. Evelson, Argentina
Stefano Falone, Italy
Ioannis G. Fatouros, Greece
Qingping Feng, Canada
Gianna Ferretti, Italy
Giuseppe Filomeni, Italy
Swaran J. S. Flora, India
Teresa I. Fortoul, Mexico
Rodrigo Franco, USA
Joaquin Gadea, Spain
Juan Gambini, Spain
José Luís García-Giménez, Spain
Gerardo García-Rivas, Mexico
Janusz Gebicki, Australia
Alexandros Georgakilas, Greece
Husam Ghanim, USA
Jayeeta Ghose, USA
Rajeshwary Ghosh, USA
Eloisa Gitto, Italy
Daniela Giustarini, Italy
Saeid Golbidi, Canada
Aldrin V. Gomes, USA
Arantxa González, Spain
Tilman Grune, Germany
Chi Gu, China, China
Nicoletta Guaragnella, Italy
Solomon Habtemariam, United Kingdom
Ying Han, China
Eva-Maria Hanschmann, Germany
Tim Hofer, Norway
John D. Horowitz, Australia
Silvana Hrelia, Italy
Juan Huang, China
Stephan Immenschuh, Germany
Maria Isagulians, Latvia
Luigi Iuliano, Italy
FRANCO J. L, Brazil
Vladimir Jakovljevic, Serbia
Peeter Karihtala, Finland
Kum Kum Khanna, Australia
Neelam Khaper, Canada
Thomas Kietzmann, Finland

Demetrios Kouretas, Greece
Andrey V. Kozlov, Austria
Jean-Claude Lavoie, Canada
Simon Lees, Canada
Xin-Feng Li, China
Qiangqiang Li, China
Jialiang Liang, China
Christopher Horst Lillig, Germany
Paloma B. Liton, USA
Ana Lloret, Spain
Lorenzo Loffredo, Italy
Daniel Lopez-Malo, Spain
Antonello Lorenzini, Italy
Hai-Chun Ma, China
Nageswara Madamanchi, USA
Kenneth Maiese, USA
Marco Malaguti, Italy
Tullia Maraldi, Italy
Reiko Matsui, USA
Juan C. Mayo, Spain
Steven McAnulty, USA
Antonio Desmond McCarthy, Argentina
Bruno Meloni, Australia
Pedro Mena, Italy
Victor M. Mendoza-Núñez, Mexico
Alexandra Miller, USA
Sanjay Misra, USA
Raffaella Molteni, Italy
Sandra Moreno, Italy
Maria U. Moreno, Spain
Trevor A. Mori, Australia
Ryuichi Morishita, Japan
Fabiana Morroni, Italy
Luciana Mosca, Italy
Ange Mouithys-Mickalad, Belgium
Iordanis Mourouzis, Greece
Danina Muntean, Romania
Colin Murdoch, United Kingdom
Pablo Muriel, Mexico
Ryoji Nagai, Japan
Amit Kumar Nayak, India
David Nieman, USA
Hassan Obied, Australia
Julio J. Ochoa, Spain
Pál Pacher, USA
Pasquale Pagliaro, Italy
Valentina Pallottini, Italy






Rosalba Parenti, Italy
Vassilis Paschalis, Greece
Visweswara Rao Pasupuleti, Malaysia
Daniela Pellegrino, Italy
Ilaria Peluso, Italy
Claudia Penna, Italy
Serafina Perrone, Italy
Tiziana Persichini, Italy
Shazib Pervaiz, Singapore
Vincent Pialoux, France
Alessandro Poggi, Italy
Ada Popolo, Italy
Aijuan Qu, China
José L. Quiles, Spain
Zsolt Radak, Hungary
Namakkal Soorappan Rajasekaran, USA
Sid D. Ray, USA
Hamid Reza Rezvani, France
Alessandra Ricelli, Italy
Paola Rizzo, Italy
Francisco J. Romero, Spain
Joan Roselló-Catafau, Spain
H. P. Vasantha Rupasinghe, Canada
Kunihiro Sakuma, Japan
Gabriele Saretzki, United Kingdom
Luciano Saso, Italy
Nadja Schroder, Brazil
Sebastiano Sciarretta, Italy
Ratanesh K. Seth, USA
Xiaolei Shi, China
Cinzia Signorini, Italy
Mithun Sinha, USA
Yi-Rui Sun, China
Carla Tatone, Italy
Frank Thévenod, Germany
Shane Thomas, Australia
Carlo Gabriele Tocchetti, Italy
Angela Trovato Salinaro, Italy
Paolo Tucci, Italy
Rosa Tundis, Italy
Giuseppe Valacchi, Italy
Daniele Vergara, Italy
Victor M. Victor, Spain
László Virág, Hungary
Kai Wang, China
Min-qi Wang, China
Natalie Ward, Australia



Philip Wenzel, Germany
Georg T. Wondrak, USA
Qiongming Xu, China
Sho-ichi Yamagishi, Japan
Liang-Jun Yan, USA
Guillermo Zalba, Spain
Jia Zhang, First Affiliated Hospital of Xi'an
Jiaotong University, Xi'an, Shaanxi Province,
China, China
Ziwei Zhang, China
Yong Zhou, China
Mario Zoratti, Italy


Contents

Natural Bioactive Products with Antioxidant Properties Useful in Neurodegenerative Diseases 2020

Francisco Jaime Bezerra Mendonça-Junior , Marcus Tullius Scotti , Eugene N. Muratov , Luciana Scotti , and Anuraj Nayarisseri 



Editorial (2 pages), Article ID 6262316, Volume 2021 (2021)

Secondary Metabolites with Antioxidant Activities for the Putative Treatment of Amyotrophic Lateral Sclerosis (ALS): “Experimental Evidences”

Jamire M. Silva, Michelangela S. C. Nobre, Sonaly L. Albino, Lucas L. Lócio, Agnis P. S. Nascimento, Luciana Scotti, Marcus T. Scotti, João A. Oshiro-Junior, Maria C. A. Lima, Francisco J. B. Mendonça-Junior , and Ricardo O. Moura



Review Article (22 pages), Article ID 5642029, Volume 2020 (2020)

Curcumin Attenuates Chronic Unpredictable Mild Stress-Induced Depressive-Like Behaviors via Restoring Changes in Oxidative Stress and the Activation of Nrf2 Signaling Pathway in Rats

Dehua Liao, Chuanfeng Lv, Lizhi Cao, Dunwu Yao, Yi Wu, Minghui Long, Ni Liu , and Pei Jiang 




Research Article (11 pages), Article ID 9268083, Volume 2020 (2020)

Identifying Plant-Based Natural Medicine against Oxidative Stress and Neurodegenerative Disorders

Rahul Chandran  and Heidi Abrahamse 

Review Article (9 pages), Article ID 8648742, Volume 2020 (2020)

Identification of New Targets and the Virtual Screening of Lignans against Alzheimer’s Disease

Mayara dos Santos Maia, Gabriela Cristina Soares Rodrigues, Natália Ferreira de Sousa, Marcus Tullius Scotti , Luciana Scotti , and Francisco Jaime B. Mendonça-Junior 

Research Article (19 pages), Article ID 3098673, Volume 2020 (2020)

The Effects of Alpha-Linolenic Acid on the Secretory Activity of Astrocytes and β Amyloid-Associated Neurodegeneration in Differentiated SH-SY5Y Cells: Alpha-Linolenic Acid Protects the SH-SY5Y cells against β Amyloid Toxicity

Anna Litwiniuk , Anita Domańska, Magdalena Chmielowska, Lidia Martyńska, Wojciech Bik, and Małgorzata Kalisz




Research Article (20 pages), Article ID 8908901, Volume 2020 (2020)

Honeybush Extracts (*Cyclopia* spp.) Rescue Mitochondrial Functions and Bioenergetics against Oxidative Injury

Anastasia Agapouda , Veronika Butterweck , Matthias Hamburger , Dalene de Beer , Elizabeth Joubert , and Anne Eckert 



Research Article (14 pages), Article ID 1948602, Volume 2020 (2020)

Foods with Potential Prooxidant and Antioxidant Effects Involved in Parkinson’s Disease

Alejandra Guillermina Miranda-Díaz , Andrés García-Sánchez , and Ernesto Germán Cardona-Muñoz 

Review Article (17 pages), Article ID 6281454, Volume 2020 (2020)

A Dihydroflavonoid Naringin Extends the Lifespan of *C. elegans* and Delays the Progression of Aging-Related Diseases in PD/AD Models via DAF-16

Qing Zhu, Yuan Qu, Xiao-Gang Zhou, Jian-Ning Chen, Huai-Rong Luo , and Gui-Sheng Wu 



Research Article (14 pages), Article ID 6069354, Volume 2020 (2020)

Amarogentin from *Gentiana rigescens* Franch Exhibits Antiaging and Neuroprotective Effects through Antioxidative Stress

Dejene Disasa , Lihong Cheng , Majid Manzoor , Qian Liu , Ying Wang , Lan Xiang , and Jianhua Qi 

Research Article (15 pages), Article ID 3184019, Volume 2020 (2020)

Olive Leaf Polyphenols Attenuate the Clinical Course of Experimental Autoimmune Encephalomyelitis and Provide Neuroprotection by Reducing Oxidative Stress, Regulating Microglia and SIRT1, and Preserving Myelin Integrity

Jasminka Giacometti  and Tanja Grubić-Kezele 





Research Article (20 pages), Article ID 6125638, Volume 2020 (2020)

Hydroxy- α -sanshool Possesses Protective Potentials on H₂O₂-Stimulated PC12 Cells by Suppression of Oxidative Stress-Induced Apoptosis through Regulation of PI3K/Akt Signal Pathway

Ruo-Lan Li , Qing Zhang , Jia Liu , Jia-yi Sun , Li-Ying He , Hu-Xinyue Duan , Wei Peng , and Chun-Jie Wu 



Research Article (12 pages), Article ID 3481758, Volume 2020 (2020)

Integrated Metabolomic and Lipidomic Analysis Reveals the Neuroprotective Mechanisms of Bushen Tiansui Formula in an A β 1-42-Induced Rat Model of Alzheimer's Disease

Min Yi , Chunhu Zhang , Zheyu Zhang , Pengji Yi, Panpan Xu, Jianhua Huang, and Weijun Peng 


Research Article (18 pages), Article ID 5243453, Volume 2020 (2020)

Antia, a Natural Antioxidant Product, Attenuates Cognitive Dysfunction in Streptozotocin-Induced Mouse Model of Sporadic Alzheimer's Disease by Targeting the Amyloidogenic, Inflammatory, Autophagy, and Oxidative Stress Pathways

Nesrine S. El Sayed  and Mamdooh H. Ghoneum 

Research Article (14 pages), Article ID 4386562, Volume 2020 (2020)

Characterization of Polysaccharides Extracted from Pulps and Seeds of *Crataegus azarolus* L. var. *aronia*: Preliminary Structure, Antioxidant, Antibacterial, α -Amylase, and Acetylcholinesterase Inhibition Properties

Ilhem Rjeibi , Rihab Zaabi, and Warda Jouida

Research Article (11 pages), Article ID 1903056, Volume 2020 (2020)


Neuroprotective Effect of Chlorogenic Acid on Mitochondrial Dysfunction-Mediated Apoptotic Death of DA Neurons in a Parkinsonian Mouse Model

Saumitra Sen Singh , Sachchida Nand Rai , Hareram Birla , Walia Zahra , Aaina Singh Rathore, Hagera Dilynashin , Richa Singh, and Surya Pratap Singh 

Research Article (14 pages), Article ID 6571484, Volume 2020 (2020)


Contents

Baicalin Represses C/EBP β via Its Antioxidative Effect in Parkinson's Disease

Kecheng Lei , Yijue Shen, Yijing He, Liwen Zhang, Jingxing Zhang, Weifang Tong, Yichun Xu, and Lingjing Jin 

Research Article (14 pages), Article ID 8951907, Volume 2020 (2020)

Apigenin Protects Mouse Retina against Oxidative Damage by Regulating the Nrf2 Pathway and Autophagy

Yuanzhong Zhang, Yan Yang, Haitao Yu, Min Li, Li Hang, and Xinrong Xu 

Research Article (14 pages), Article ID 9420704, Volume 2020 (2020)

Tetragonia hemsleyanum Vine Flavone Ameliorates Glutamic Acid-Induced Neurotoxicity via MAPK Pathways

Qiang Chu, Yonglu Li, Zheng Hua, Yaxuan Wang, Xin Yu, Ruoyi Jia, Wen Chen, and Xiaodong Zheng 

Research Article (12 pages), Article ID 7509612, Volume 2020 (2020)

Editorial

Natural Bioactive Products with Antioxidant Properties Useful in Neurodegenerative Diseases 2020

Francisco Jaime Bezerra Mendonça-Junior ^{1,2} **Marcus Tullius Scotti** ¹
Eugene N. Muratov ³ **Luciana Scotti** ^{1,4} and **Anuraj Nayariseri** ^{5,6}

¹Postgraduate Program in Natural and Synthetic Bioactive Products, Federal University of Paraiba, João Pessoa, PB, Brazil

²Laboratory of Synthesis and Drug Delivery, Department of Biological Science, State University of Paraiba, João Pessoa, PB, Brazil

³Laboratory for Molecular Modeling, UNC Eshelman School of Pharmacy, University of North Carolina, Chapel Hill, North Carolina 27599, USA

⁴Teaching and Research Management-University Hospital, Federal University of Paraiba, João Pessoa, PB, Brazil

⁵In Silico Research Laboratory, Eminent Biosciences, Indore, 452010 Madhya Pradesh, India

⁶Bioinformatics Research Laboratory, LeGene Biosciences Pvt. Ltd., Indore, 452010 Madhya Pradesh, India

Correspondence should be addressed to Francisco Jaime Bezerra Mendonça-Junior; franciscojbmendonca@yahoo.com.br

Received 14 September 2020; Accepted 14 September 2020; Published 10 February 2021

Copyright © 2021 Francisco Jaime Bezerra Mendonça-Junior et al. This is an open access article distributed under the Creative Commons Attribution License, which permits unrestricted use, distribution, and reproduction in any medium, provided the original work is properly cited.

Neurodegenerative diseases (NDs) are a group of diseases that affect millions of people worldwide and which are characterized by the progressive degeneration of the nervous system, compromising cognitive and/or motor functions. The most common NDs are Parkinson's disease (PD), Alzheimer's disease (AD), Huntington's disease, Prion disease, amyotrophic lateral sclerosis (ALS), and multiple sclerosis (MS). These pathologies have multifactorial causes, many of which are not yet fully understood; however, recent studies show that ageing and oxidative stress play important roles in the appearance and evolution of these pathologies; to which, the therapeutic options available are not curative and only slow their progression. Despite this, it is very well established that antioxidant therapy that can control free radicals and reactive oxygen species (ROS) levels is a promising strategy to delay, prevent, and/or treat NDs.

In this context, natural bioactive compounds isolated from plants, animals, bacteria, fungi, and algae are widely known and employed since the beginning of human life on Earth, to treat many pathologies. In recent years, in silico, in vitro, and in vivo studies, performed with natural products and its isolated bioactive compounds, have proven its biological activities and large therapeutic benefits, including its

antioxidant properties, reducing ROS levels, and modulating the cellular redox balance, thus stating its great potential to delay, prevent, and/or treat NDs.

In this special issue, articles were selected that address new therapeutic alternatives on the antioxidant role with related neuroprotective effects of natural bioactive compounds in the prevention/treatment or improvement of neurodegenerative diseases. This special issue compiles eighteen (18) manuscripts including three (3) reviews and fifteen (15) research papers, which show recent research about the discovery of plant-derived antioxidants with application in NDs.

In their minireview, R. Chandran and H. Abrahamse describe several plants, plant parts, and isolated phytochemicals (especially phenolic compounds) with the potential to prevent the progression of neurodegenerative diseases due to its antioxidant properties. In the second review, A. G. Miranda-Díaz, E. G. García-Sánchez, and A. Cardona-Muñoz report the pro-oxidant effect of consumption of processed meat and the neuroprotective effects of some foods constituents with antioxidant properties, like melatonin, N-acetylcysteine, vitamin B3, ascorbic acid, and vitamin D, on brain health in PD. In the review by J. M. Silva et al., the

authors summarize the natural bioactive compounds with antioxidant properties useful against ALS.

Fourteen of the fifteen research articles addressed to deal with the proof of the neuroprotective activity associated with the antioxidant properties of plants, mushrooms, plant extracts, isolated phytoconstituents, herbal medicines, and compositions containing phytochemicals. The only article that is out of this theme is the work of M. S. Maia et al. which performed a virtual screening based on studies of QSAR (quantitative structure-activity relationship), molecular docking, and ADMET (absorption, distribution, metabolism, excretion, and toxicity) properties, allowing to identify lignans with potential multitarget action against enzymes related to the oxidative pathway which represent a potential alternative for AD treatment.

K. Lei et al. demonstrated that the flavonoid baicalin improved PD model's behavioral performance, reducing dopaminergic neuron loss in the substantia nigra. Additionally, baicalin has the ability to protect dopaminergic neurons against ROS, decreasing the expression of the transcription factors such as α -synuclein and CCAAT/enhancer-binding protein β (C/EBP β). Y. Zhang et al., using a model of age-related macular degeneration (AMD), demonstrated that solid dispersion of the flavonoid apigenin is able to reduce retinal oxidative injury by upregulation of autophagy and of the expression of antioxidant enzymes through the Nrf2 pathway. Q. Chu et al. demonstrated that purified flavones (3-caffeoylquinic acid, 5-caffeoylquinic acid, quercetin-3-O-rutinoside, and kaempferol-3-O-rutinoside) from the vine part of *Tetragium hemsleyanum* present in vitro and in vivo neuroprotective effects through mitogen-activated protein kinase (MAPK) pathways in models induced by glutamic acid. Q. Zhu et al. found that the dihydro flavonoid naringin is capable of increasing tolerance to oxidative stress and delaying the evolution of ageing-related diseases like AD and PK, via the transcription factor DAF-16.

I. Rjeibia, et al. demonstrated that polysaccharides from the pulps of *Crataegus azarolus* L. var. *Aronia* exhibit the neuroprotective activity mediated by its antioxidant, α -amylase, and acetylcholinesterase inhibitory activities. S. S. Singh et al.'s group observed that chlorogenic acid has a neuroprotective effect and decreased the loss of dopaminergic neurons in the PD mouse model. The effect was associated with the attenuation of mitochondrial dysfunction, inhibition of proapoptotic proteins caspase-3 and Bax, and with phosphorylation of GSK3 β via activating Akt/ERK signaling in the mitochondrial intrinsic apoptotic pathway. R.-L. Li et al. demonstrated that hydroxy- α -sanshool (isolated from *Zanthoxylum bungeanum* pericarps) promotes neuroprotection by reduction of intracellular ROS and suppression of oxidative stress caused by H₂O₂.

D. Liao et al. observed that the polyphenol curcumin reduces the depressive state by decreasing the expression of oxidative stress markers and activating the Nrf2-ARE pathway. D. Disana et al. demonstrated that the secoiridoid glycoside amarogentin (isolated from *Gentiana rigescens* Franch) promotes anti-ageing and neuroprotective effects by reduction of oxidative stress, promoted by the increase of catalase, superoxide dismutase, and glutathione peroxi-

dase activities. A. Litwiniuk et al. demonstrated that alpha-linolenic acid stimulates the release of insulin from astrocytes, and these astrocytes were capable to protect cells against A β 1-42-induced mitochondrial dysfunction promoting neuroprotection.

J. Giacometti and T. Grubić-Kezele demonstrated that olive leaf polyphenols promote neuroprotection through the reduction of oxidative stress, regulation of microglia and SIRT1, and maintaining the myelin sheath integrity, which can be effective for the treatment of multiple sclerosis and other neurodegenerative diseases. A. Agapouda et al. evidenced the anti-ageing and neuroprotective effects of Honeybush extracts (*Cyclopia* spp.). The authors associated these properties to the extract's ability to recover the mitochondrial function under oxidative stress conditions.

N. S. El Sayed and M. H. Ghoneum proved that Antia, a natural product extracted from yamabushitake mushroom, can exert protective effects attenuating cognitive dysfunction against sporadic AD. The action is associated to its interference in amyloidogenic, inflammatory, and oxidative stress pathways, including the JAK2/STAT3 pathway. M. Yi et al. investigated the effects on the cognitive performance and the interference of Bushen Tiansui formula on the metabolomic and lipidomic profiles in the cerebral cortices of the rat AD model. The authors found that the Bushen Tiansui formula can restore the metabolic balance acting on the metabolism of sphingolipids, glycerol phospholipids, alanine, aspartate, glutamine, and glutamate, thus exerting its neuroprotective effect.

Taken together, these studies provide readers with an updated view of the evidence and mechanisms of action of herbal medicines, compositions containing natural products, and several classes of secondary metabolites including polysaccharides, flavonoids, lignans, polyphenols, iridoids, fatty acids, phenolic acids, and alkyl amides in reducing oxidative stress in the context of NDs. We are sure that these findings will be useful and will contribute to the success of new therapies for NDs.

Conflicts of Interest

The authors declare that there is no conflict of interest regarding the publication of this article.


Acknowledgments

We would like to thank all authors, reviewers, and editorial staff who contributed to the organization of this special issue: Francisco J. B. Mendonça-Junior, Marcus T. Scotti, Anuraj Nayariseri, Eugene N. Muratov, and Luciana Scotti.

Francisco Jaime Bezerra Mendonça-Junior
 Marcus Tullius Scotti
 Eugene N. Muratov
 Luciana Scotti
 Anuraj Nayariseri

Review Article

Secondary Metabolites with Antioxidant Activities for the Putative Treatment of Amyotrophic Lateral Sclerosis (ALS): “Experimental Evidences”

Jamire M. Silva,^{1,2} Michelangela S. C. Nobre,^{1,2} Sonaly L. Albino,^{2,3} Lucas L. Lócio,^{2,3} Agnis P. S. Nascimento,^{2,4} Luciana Scotti,⁵ Marcus T. Scotti,⁵ João A. Oshiro-Junior,³ Maria C. A. Lima,¹ Francisco J. B. Mendonça-Junior ,⁶ and Ricardo O. Moura^{2,3,4}

¹Postgraduate Program in Pharmaceutical Sciences-PPGCF, Department of Pharmacy, Federal University of Pernambuco, 50670-901 Recife PB, Brazil

²Drug Development and Synthesis Laboratory, Department of Pharmacy, State University of Paraiba, 58429-500 Campina Grande PB, Brazil

³Postgraduate Program in Pharmaceutical Sciences-PPGCF, Department of Pharmacy, State University of Paraiba, 58429-500 Campina Grande PB, Brazil

⁴Graduate Program in Chemistry-PPGQ, Department of Chemistry, State University of Paraiba, 58429-500 Campina Grande PB, Brazil

⁵Laboratory of Cheminformatics, Program of Natural and Synthetic Bioactive Products, Federal University of Paraiba, João Pessoa PB, Brazil

⁶Laboratory of Synthesis and Drug Delivery, Department of Biological Sciences, State University of Paraiba, 58071-160 João Pessoa PB, Brazil

Correspondence should be addressed to Francisco J. B. Mendonça-Junior; xicolouco@gmail.com

Received 24 April 2020; Revised 2 October 2020; Accepted 4 October 2020; Published 24 November 2020

Academic Editor: Bruno Meloni

Copyright © 2020 Jamire M. Silva et al. This is an open access article distributed under the Creative Commons Attribution License, which permits unrestricted use, distribution, and reproduction in any medium, provided the original work is properly cited.

Amyotrophic lateral sclerosis (ALS) is a fatal motor neuron disorder that is characterized by progressive loss of the upper and lower motor neurons at the spinal or bulbar level. Oxidative stress (OS) associated with mitochondrial dysfunction and the deterioration of the electron transport chain are factors that contribute to neurodegeneration and perform a potential role in the pathogenesis of ALS. Natural antioxidant molecules have been proposed as an alternative form of treatment for the prevention of age-related neurological diseases, in which ALS is included. Researches support that regulations in cellular reduction/oxidation (redox) processes are being increasingly implicated in this disease, and antioxidant drugs are aimed at a promising pathway to treatment. Among the strategies used for obtaining new drugs, we can highlight the isolation of secondary metabolite compounds from natural sources that, along with semisynthetic derivatives, correspond to approximately 40% of the drugs found on the market. Among these compounds, we emphasize oxygenated and nitrogenous compounds, such as flavonoids, coumarins, and alkaloids, in addition to the fatty acids, that already stand out in the literature for their antioxidant properties, consisting in a part of the diets of millions of people worldwide. Therefore, this review is aimed at presenting and summarizing the main articles published within the last years, which represent the therapeutic potential of antioxidant compounds of natural origin for the treatment of ALS.

1. Introduction

Amyotrophic lateral sclerosis (ALS), also known as Charcot's or Lou Gehrig's disease, is a progressive and ultimately fatal

neurodegenerative disorder characterized by affecting cortical and spinal motor neurons that control the voluntary motions of muscles [1, 2]. It is currently classified according to the mode of the emergence of the pathology in familial

(10% of cases), also referred as fALS, inherited in an autosomal dominant, autosomal recessive, or X-linked manner, and sporadic (90% of cases), also known as sALS, which is not genetically inherited [3]. Both types of ALS share the most common symptoms, which manifests as muscle weakness, twitching, and cramping, subsequently leading to the impairment of muscles. In the most advanced stages, the symptoms extend to dyspnea, dysphagia, paralysis, and eventual death from respiratory failure within 3 to 5 years after symptom onset [4, 5].

ALS is the most common motor neuron disease, even though the mechanism evolved in the neurodegenerative dysfunction that leads to motor neurons' loss is not entirely known [6, 7]. Histopathological data shows reduction in neuron size, loss and atrophy of nerve fibers, vacuolization, large empty spaces near neurons, and sponge-like appearance caused by spongiosis [8].

Its incidence is associated with increased age, as it onsets mostly in adults between 50-65 years, and is slightly more prevalent in males than females, with a ratio of approximately 1.6:1 [4, 9]. The majority of the epidemiological studies have been conducted in Europe, in which the incidence of ALS is 2-3 people per year per 100,000 general population. Furthermore, an increase in the prevalence of ALS to 8.58 cases per 100,000 inhabitants in the United Kingdom population is expected by the year of 2020 [5, 10].

Multiple pathophysiological mechanisms and cellular dysfunctions are involved as possible causative factors in the disease. Among these, the following stand out: accumulation of reactive oxygen species, mitochondrial dysfunction, neuroinflammation, alterations on RNA processing, glutamate excitotoxicity, apoptosis, protein misfolding and aggregation, autophagy, impaired axonal transport and neurofilament aggregation, and endoplasmic reticulum stress. Moreover, environmental factors have shown to contribute to the pathogeny, such as alcohol, tobacco, physical activity, chemical exposure and metals, and exposure to radiation [1, 10-12].

The oxidative stress is highly correlated with the development and progression of the neurodegeneration in ALS. Changes in the homeostatic balance of ROS production are particularly associated with mutant forms of the antioxidant enzyme SOD1 (encodes for copper/zinc ion-binding superoxide dismutase), which is reported to be the most common causative factor for ALS. Over 150 different mutations have been described in different parts of the enzyme, which include G93A (glycine 93 changed to alanine), H46R (histidine at codon 46 changed to arginine), and A4V (alanine at codon 4 changed to valine). This particular enzyme is responsible for catalyzing the conversion of superoxide (O_2^-) into hydrogen peroxide and oxygen. Its mutation provokes a structural instability that promotes enzyme misfolding, and consequent formation of cytotoxic protein aggregates alone or with other proteins. Consequently, there is a loss of enzyme activity and an increase in the production of ROS that results in deterioration in the regulation of vital cell processes and mitochondrial dysfunction [4, 13-16].

There is no cure for ALS, and current drug treatment is limited since only two drugs are approved by the Food and

Drug Administration for the treatment of the disease: Riluzole, a neuroprotective drug that blocks glutamatergic neurotransmission and, more recently, the antioxidant drug Edaravone. These assist in delaying the progression of the disease, extending life expectancy by 2-3 months [2, 17].

Therefore, the obtainment of new drugs, capable of effectively fulfilling the gap in the therapeutic arsenal in order to assist in the treatment and in the decrease of the disease's progression, presents itself as a priority. Among the strategies used for obtaining new drugs, we can highlight the isolation of secondary metabolite compounds from natural products that, along with semisynthetic derivatives, correspond to approximately 40% of the drugs found on the market [18].

Focusing on the influence of ROS for the onset and progression of the disease, the interest in natural compounds with antioxidant potential has become increasing. According to epidemiological studies focused on neurodegenerative diseases, it was observed that there is a significant difference in the incidence of such diseases among ethnic groups with different eating habits, recording that the diet rich in antioxidants is related to a decrease in the incidence rate. Thus, different types of compounds with antioxidant properties can be highlighted, such as the following: polyphenols, which provide protection against ROS and modulate metabolic cascades [19, 20]; carotenoids, which perform antioxidant and neutralizing activities against ROS [19-22]; antioxidant vitamins such as vitamins C and E, among others [13, 14, 23]. Hence, this review is aimed at presenting and summarizing the main articles published within the last years, which represent the therapeutic potential of antioxidant compounds of natural origin for the treatment of ALS. In this sense, the keywords "antioxidant activity," "amyotrophic lateral sclerosis," "natural products," and "secondary metabolites," among others, were included in the search into the databases "ScienceDirect," "Pubmed," "Periódicos Capes," "Clinical Trials," "Web of Science," and "Google Acadêmico," during the period of March 14 to April 10 2020.

2. Secondary Metabolites with Potential Antioxidant Action and Their Possible Applications for ALS

2.1. Alkaloids. Alkaloids comprise the largest group of nitrogen compounds, characterized by containing one or more nitrogen atoms within a heterocyclic ring. Over 12,000 compounds are known to be provided by a variety of sources such as animals, bacteria, plants, and fungi [24, 25]. Figure 1 presents the chemical structure of some well-known alkaloids, such as nicotine (1), morphine (2), and caffeine (3). Nitrogen, oxygen, carbon, and hydrogen are the chemical elements that constitute its basic formula, so that its molecular weight varies between 100 and 900 $g\ mol^{-1}$. This class of compounds has revealed to be one of the most promising secondary metabolites for ALS treatment due to their diverse mechanism of action, which can collaborate to prevent the disease evolution [26-28].

It has been suggested that the increase of extracellular glutamate occurs mainly due to an anomaly in glutamate

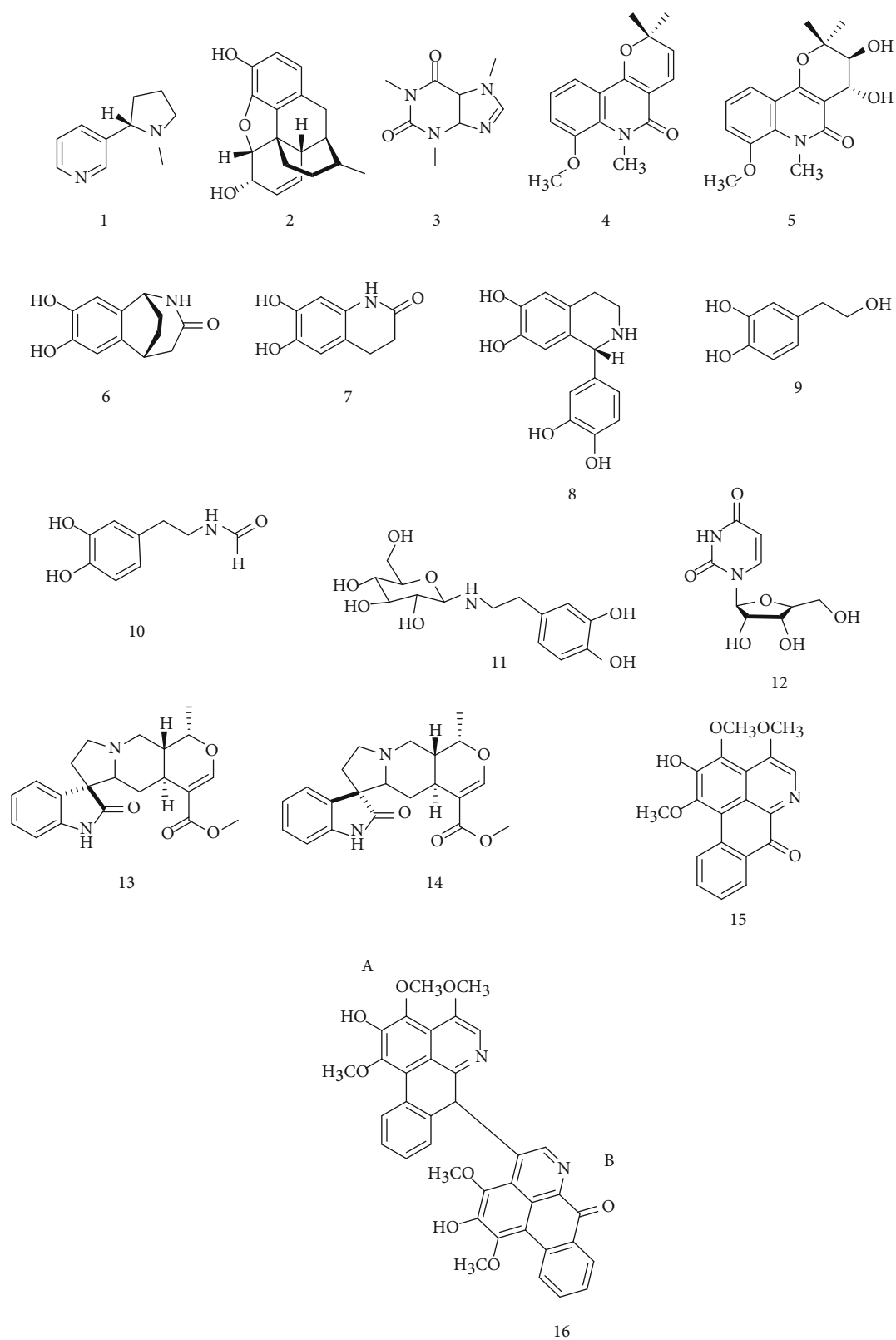


FIGURE 1: Chemical structure of the well-known alkaloids (nicotine (1), morphin (2), and caffeine (3)), such as those used in preclinical antioxidant studies (8-methoxy-*N*-methylflindersine (4), zanthodioline (5), alternamide A (6), alternamide B (7), alternamine A (8), hydroxytyrosol (9), formamide (10), alternamine B (11), uridine (12), mitraphylline (13), isomitraphylline (14), iraqiine (15), and kareemine (16)).

transporter EAAT2/GLT-1 and leads to ALS. Harmine, a beta-carboline alkaloid, may act by activating EAAT2/GLT-1 gene expression increasing the cellular uptake of glutamate [29]. The indirect mechanism was suggested by the use of alkaloids with commercial drug Riluzole, aiming to block the increased levels of P-glycoprotein in the blood-brain barrier (BBB) [30]. In this sense, Lopez and Martinez-Luis showed that polyaromatic alkaloids from *prosobranch* mollusk (*Lamellaria* sp.) restrain P-gp, demonstrating an increased cellular uptake to different drugs in resistant cell line [31]. However, in this review, we will highlight the benefits of its mechanism of action as antioxidants, since alkaloids have the ability to convert free radical species in inactive substances [32, 33]. Thus, researches have explored the advantages of employing alkaloids with this purpose, alone or included in a pharmaceutical form and from several sources [34–37].

For example, in order to evaluate the antioxidant activity of two quinoline isolated alkaloids from *Zanthoxylum rhetsa* root bark, Zohora and collaborators showed through DPPH assay that the compounds 8-methoxy-*N*-methylflindersine (4) and zanthodioline (5) (Figure 1) presented free radical scavenging activity (IC_{50} in $\mu\text{g/mL}$) of 71.18 ± 1.74 and 101.90 ± 5.24 , respectively, revealing potent antioxidant activity [38].

Alternanthera littoralis P. Beauv. is a tree common in tropical, subtropical, and temperate regions. Koolen et al. isolated seven chemical alkaloids from the aerial parts of this plant, which include two known alkaloids, hydroxytyrosol (9) and uridine (12), and five new alkaloids, namely, alternamide A (6), alternamide B (7), alternamine A (8), *N*-(3,4-dihydroxyphenethyl) formamide (10), and alternamine B (11) (Figure 1). The biological evaluations showed the high antioxidant free radical scavenging effect of the ethanolic extract containing alkaloids alternamide B (1.10 relative Trolox equivalent—RTE), alternamide A (0.85 RTE), and alternamine B (0.65 RTE) in relation to positive control quercetin (5.62 RTE) [39].

Azevedo et al. studied the alkaloids mitraphylline (13) and isomitraphylline (14) (Figure 1) obtained from extracts of the aqueous leaf extract (ALE) from *Uncaria tomentosa* which present high phenolic content ($153.51 \mu\text{g}$ gallic acid equivalents per milligram extract). The ALE *in vitro* antioxidant activity investigation, performed using DPPH, ABTS, and ferric reducing antioxidant power (FRAP) assays, obtained values of $IC_{50} = 10.68 \pm 0.64 \mu\text{g mL}^{-1}$, $2.15 \pm 0.29 \text{ mmol Trolox/mg AA}$ and extract, and $2.9 \pm 0.15 \text{ mM Fe-SO}_4/\text{mg AA}$ and extract, respectively, presenting a moderate activity [40].

Aiming to obtain new alkaloids, Aldulaimi and collaborators isolated from *Alphonsea cylindrical* King two novel isoquinoline alkaloids, namely, iraqiine (15) and kareemine (16) (Figure 1). *In vitro* antioxidant activity was performed, and the results showed IC_{50} values of 48.77 and $101.66 \mu\text{g mL}^{-1}$, respectively. In this same test, five additional known alkaloids were tested and among them, *O*-methylmoschatoline ($144.15 \mu\text{g/mL}$) was better than kareemine [41].

Nevertheless, despite of examples above, researching for papers about this matter, using “antioxidant activity” and “alkaloids” as keywords on the Scholar, with range of last 5 years, it is possible to found 822 papers that cite these terms in the abstract and/or title [42]. When the term “ALS” is added, no articles are found and similar results are observed in other databases (Web of Science, Pubmed, and ScienceDirect). These works always present alkaloids obtained from different sources and evaluate their biocompatibility and antioxidant activity *in vitro* using different methods [43, 44]. The association with ALS always happens in a generalized way because one treatment option to neurodegenerative diseases is using this approach [45].

The lack of studies in the literature performing specific preclinical or clinical tests for ALS and no therapy consolidate to alkaloids despite advantages can be by two main problems, not to easy standardization in batch-to-batch reproducibility and scale-up [46]. For these reasons, the use of isolated alkaloid molecules can circumvent these drawbacks. Another possibility is alkaloids-loaded in nanoscale systems to develop new formulation in terms of tissue/organ targeting and BBB penetration as shown in literature [47, 48].

Finally, alkaloids can slow down ALS by three hypothetical mechanisms of action, as mentioned above. Several studies evidenced satisfactory results in terms of antioxidant activity; thus, clinical trials (phase I) are necessary in order to better understand the previously mentioned mechanisms and advance this treatment proposal to improve patients' life quality.

2.2. Flavonoids. Flavonoids are phenolic compounds derived from the aromatic amino acids phenylalanine and tyrosine, which are widely found in plants. Its structure consists of a flavin nucleus (17) containing 15 carbon atoms arranged in three rings (C6-C3-C6), labeled as A, B, and C, as illustrated in Figure 2. These compounds have a broad pharmacological spectrum, in which their antioxidant and anti-inflammatory stand out, which mainly associated with the fight against neurodegenerative diseases such as ALS [49].

It is known that processes such as oxidative stress, neuroinflammation, and neural apoptosis collaborate with ALS progression; in this sense, Winter et al. evaluated the effects of strawberry extract enriched with anthocyanin (18) (Figure 2) in mice with ALS model (G93ASOD1 mutation), as this class of flavonoids has antioxidant, anti-inflammatory, and antiapoptotic activity established in previous studies [50–52]. The trials showed that at a dose of 2 mg/kg/day , guinea pigs suffered a marked delay of approximately 17 days at the onset of the disease, in addition to an increase in life expectancy of approximately 11 days. Histological analysis exhibited a significant reduction in spinal cord injury when compared to mutant guinea pigs not treated with the extract. For that reason, this study emphasizes that anthocyanins have therapeutic potential for this disease and can evolve to more complex pharmacological tests [53].

There are reports in the literature suggesting that the mutation in superoxide dismutase (SOD1) at position 85 of glycine and arginine is a fundamental cause for the onset of ALS. Taking advantage of the antioxidant activity of the

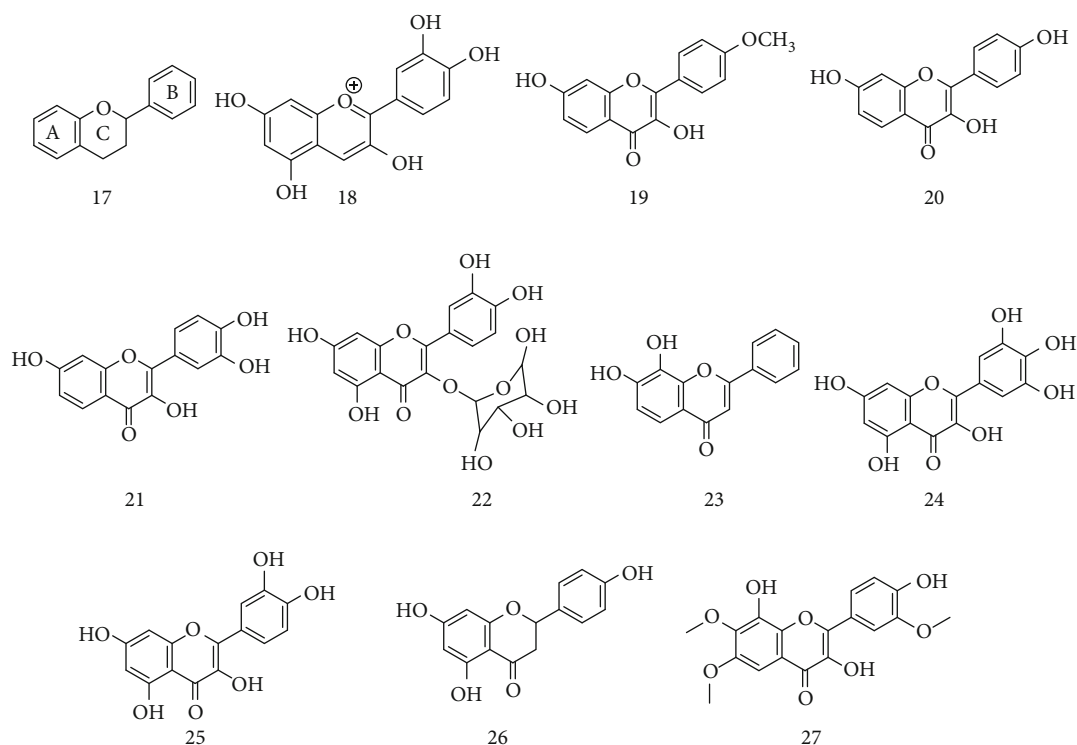


FIGURE 2: Structure of flavin (17) and anthocyanin (18), kaempferida (19), kaempferol (20), fisetin (21), compound 22, 7,8 dihydroxy flavone (23), myricetin (24), quercetin (25), naringin (26), and 3,5,4'-trihydroxy-6,7,3'-trimethoxy flavone (27).

flavonoids kaempferida (19) and kaempferol (20) (Figure 2), the study performed by Srinivasan and Rajasekarab evaluated through molecular docking their aggregation affinity towards SOD1. Kaempferol portrayed stronger hydrophobic interactions with the target in comparison to kaempferida, thus qualifying it as a possible prototype for the design of new drugs for the treatment of ALS [54].

Ueda and collaborators also proved the action of kaempferida and kaempferol, extracted from Brazilian green propolis, as a possible alternative for the treatment and prevention of ALS. In this study, kaempferida ($15 \mu\text{M}$) and kaempferol ($3.0 \mu\text{M}$) were tested against Na^{2+} cells (superoxide induced) with mutant SOD1. The results showed significant inhibition of mutant SOD1, as well as in Western blot analysis, which showed that kaempferol induced autophagy through the protein kinase activated by AMP, suggesting this as a probable mechanism for neuroprotection and emphasizing this compound as a good therapeutic alternative on the treatment of ALS [55].

A flavonoid known as fisetin (21) (Figure 2), a natural antioxidant, already presented several benefits in some degenerative diseases such as Alzheimer's and Parkinson's. Therefore, Wang et al. performed *in vitro* assays on mutant cells (hSOD1G85R and hSOD1G93A) and *in vivo* assays with hSOD1 transgenic mice in order to evaluate the efficiency of the compound to SOD1 associated with ALS. Treatment with fisetin improved motor impairment, prolonged life span, and confirmed the neuroprotective antioxidant effects, proposing this flavonoid as a strong drug candidate with therapeutic value for the treatment of ALS [56].

Studies in mice revealed that the first steps in the development of ALS may comprehend the increased presence of SOD1 monomers and their aggregation to motor neurons. In this perspective, Ip and collaborators carried out tests *in silico* with a library of 4,400 drugs and natural compounds that were coupled in the SOD1 dimer. Between these compounds, seven with best results were tested for aggregation and splitting of SOD1 induced by hydrogen peroxide *in vitro* at concentrations ranging from $20 \mu\text{M}$ to $100 \mu\text{M}$. Compound 22 (Figure 2) revealed that quercetin-3- β -D-glucoside presented one of the best results, and for that, it may be a potential therapeutic inhibitor of misfolding and aggregation of SOD1 and, therefore, can delay clinical symptoms of ALS [57].

The use of *Panax ginseng* for the alternative treatment of ALS is recurrent, but without scientific proof, these effects may be related to the increase in the expression of the growth factor for cells of the nervous system and high antioxidant activity. For these reasons, Jiang et al. studied the effects of ginseng extract, rich in flavonoids, at doses of 40 and 80 mg/kg in B6SJL-TgN (SOD1G93A) transgenic mice. Results showed a delay in the appearance of diseases' signs and increase in survival [58], pointing out the potential of this root and possible mechanism action.

Korkmaza et al. observed that the chronic administration of 5 mg/kg of flavonoid 7,8-dihydroxyflavone (23) (Figure 2), generally found in the plants *Godmania aesculifolia* and *Tri-dax procumbens*, in mice with ALS (SOD1G93A) by up to 105 days caused a significant improvement in motor deficits. This result is believed to be associated with the compound's

ability to cross the blood-brain barrier and exercise neuroprotective activity therefore can decrease the clinical manifestations of the disease [59].

As previously mentioned, the formation of poorly folded protein aggregates inside or outside neural cells is one of the causes of neurodegenerative diseases, such as ALS. In this sense, Joshi and collaborators presented, through *in vitro* studies with Cos-7 cells in immunofluorescence staining assay with primary antibodies of E6-AP and Hsp70, that at a concentration of 15 $\mu\text{g}/\text{mL}$, mycetin flavonoid (24) (Figure 2) is capable to eliminate or suppress the aggregation of different proteins and reduce the inclusion of folded proteins and leading to a decrease in the symptoms of muscle paralysis [60].

Excessive neuronal stimulation of glutamate leads to a large influx of Ca^{2+} which, when accumulated in mitochondria, triggers an increase in the production of reactive oxygen species for the formation of oxygen free radicals, just as this excitation leads to the activation of caspase3, which seem to be involved in the etiology of many neurodegenerative disorders, such as ALS. In this context, Shimmyo et al., through *in vivo* studies with mice induced by glutamate and *in vitro* tests with neuronal cells, showed that myricetin 24 (Figure 2) inhibited the glutamate-induced excitotoxicity by three routes: reduction of intracellular calcium through the phosphorylation of NMDAR (*N*-methyl *D*-aspartate receptor), inhibition of free oxygen radicals, and inhibition of caspase-3 [61].

Aluminum has been associated with several neurological diseases, including Alzheimer's disease, Parkinson's disease, and ALS; it is suggested that this neurotoxicity may be associated with the fact that aluminum is capable of generating reactive oxygen species (ROS) [60]. In this perspective, Sharma et al. [62] evaluated the antioxidant activity of quercetin (25) (Figure 2), at a dose of 10 mg/kg body weight/day in mice whose oxidative stress was induced by aluminum (10 mg/kg of body weight/day). The results revealed that quercetin decreased neuronal apoptosis and decreased the production of free radicals, in addition to obstructing neurodegenerative histological changes induced by aluminum.

Zhuang et al. analyzed through mass spectrometry and molecular docking the noncovalent interactions between SOD1 and selected flavonoid compounds, such as quercetin, rutin, naringin, and hesperidin, among others. The study is aimed at identifying which compound has a more prominent capacity to inhibit the aggregation of the apo-SOD1 complex. Through these techniques, the results showed that naringin (26) (Figure 2) presented better aggregation inhibition profile, being considered as an interesting compound for the treatment of ALS [63].

As mentioned in the literature, glutamate toxicity is a major contributor to the appearance of neurodegenerative diseases such as ALS and Alzheimer's disease. Hence, Elmann and collaborators [64] isolated the sesquiterpene lactone achillolide A and the flavonoid 3,5,4'-trihydroxy-6,7,3'-trimethoxyflavone (27) (Figure 2) from the *Achillea fragrantissima* plant and tested in Na^{2+} cells of neuroblastoma of mice intoxicated with glutamate. The results show that the

compounds protected astrocytes from cell death induced by oxidative stress and inhibited microglia activation, demonstrating its significant protective effect. In this sense, we highlight the importance of flavonoids as a therapeutic potential tool against the decrease in the time of onset of symptoms and the increased survival of patients with ALS, whether by antioxidant, neuroanti-inflammatory, and antiprotein aggregation mechanisms.

In silico and *in vivo* tests of the cited studies demonstrated that extracts enriched with flavonoids, as well as their isolated, may act in the treatment of ALS by different mechanisms of action, such as decreased spinal cord injury, SOD1 inhibition, inhibition of motor neuron aggregation, inhibition caspase3, and decrease reactive oxygen species. These compounds may cause a delay in the appearance of the disease's signs and decrease the clinical manifestations. Therefore, by evaluating the toxicity of these compounds and establishing a therapeutic dose, they could potentially be qualified to undergo more advanced pharmacological tests, such as clinical trials.

2.3. Coumarins. Coumarins are another class of secondary metabolites implemented in the literature as promising molecules due to their results against neurodegenerative diseases such as ALS. Based on these facts, Mogana et al. tested the antioxidant capacity *in vitro* of scopoletin (28) isolated from *Canarium patentinervium* (Figure 3), starting from chloroform extract and purification by silica gel chromatography using the hydrogen atom transfer (HAT) and simple electronic transfer (SET) method. This coumarin presented strong antioxidant potential (EC_{50} 191.51 \pm 0.01 μM), demonstrating its ability to act in diseases caused by oxidative stress [65].

In vitro studies for DPPH, hydroxyl, and ABTS radical scavenging activity carried out by Kumar et al. to determine the antioxidant capacity of substances present in fenugreek seed extract (*Trigonella foenum-graecum*), such as trigocoumarin (29) (Figure 3), were performed. The antioxidant activity of the extract was expressed in IC_{50} and showed its efficiency in reducing DPPH free radicals, being able to reduce them by 50% at a concentration of 395 $\mu\text{g}/\text{mL}$ ($R^2 = 0.9712$) [66].

Oxidative stress was induced in NSC34 motor neurons of rats by Barber and collaborators in the presence and absence of several compounds. Among them, the coumarin esculetin (30) (Figure 3) was the only one of the studied compounds capable of directly buffering the radicals, promoting protective effects for cells. This article does not present the form of obtainment of these compounds [67].

Hasnat and collaborators presented results for inhibition of acetylcholinesterase, as well as *in vitro* and *in vivo* antioxidant activity of *Ganoderma lucidum* that grows in germinated brown rice (GLBR), in which coumarin (31) (Figure 3) is presented as the fourth most predominant compound between the thirteen identified by HPLC analysis of the GLBR extract. *In vitro* results revealed the occurrence of inhibition of peroxidation induced in brain cells of rats by Fe^{2+} . However, in *in vivo* results, no significant variations

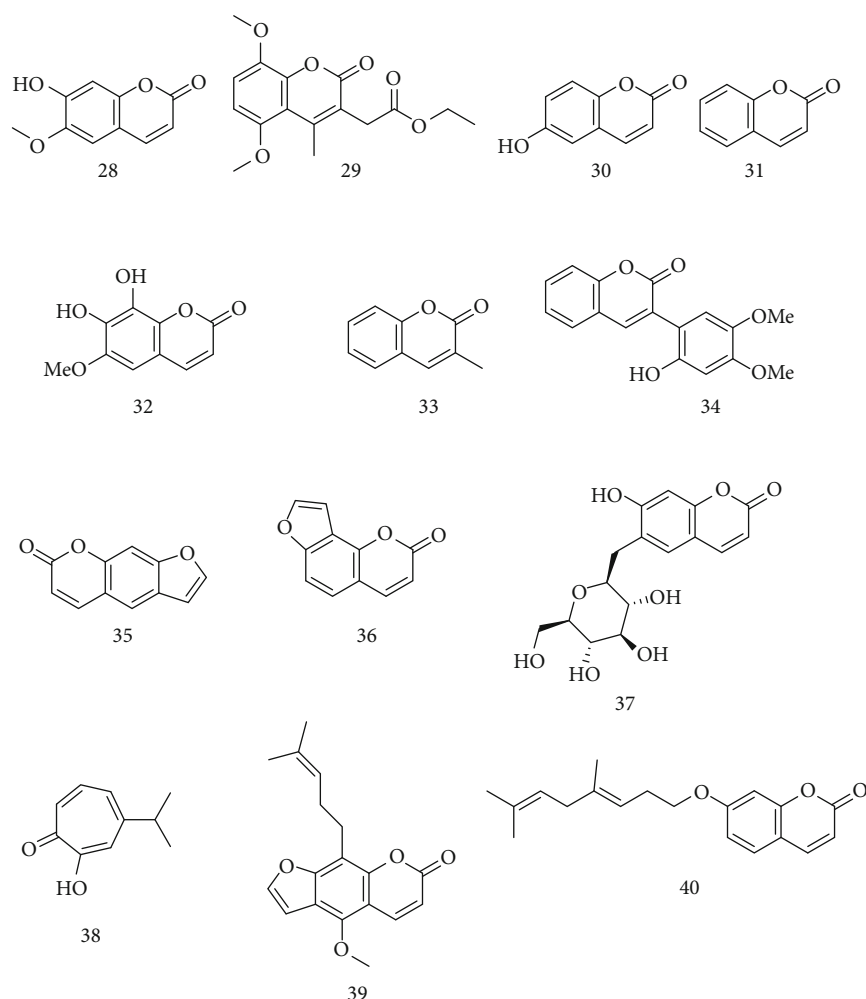


FIGURE 3: Structure of coumarins scopoletin (28), trigocoumarin (29), esculetin (30), coumarin (31), fraxetin (32), methyl-3-coumarin (33), caraganolide A (34), psoralen (35), isopsoralen (36), esculin (37), hinokitol (38), fellopterin (39), and auraptene (40).

could be observed when doses of 100 mg/kg were administered in the treatment group [68].

Li and Seeram identified the presence of seven lignans, as well as two coumarins isolated from the butanol extract of the maple syrup (MS-BuOH), being identified as scopoletin and fraxetin (32) (Figure 3). These coumarins were evaluated for their antioxidant activity and obtained IC_{50} values of 68.2 ± 31.2 and $46.5 \pm 3.6 \mu\text{g/mL}$, respectively. Therefore, these compounds better result in comparison to the seven isolated lignans (values ranging between 101.5 ± 5.9 and $1335.9 \pm 47.6 \mu\text{g/mL}$) and stilbenes contained in sugar fraction of maple syrup ($>2600 \mu\text{g/mL}$). Moreover, fraxetin also showed a better result when compared to vitamin C ($IC_{50} = 58.6 \pm 10.7 \mu\text{g/mL}$) [69].

Glutamatergic excessive transmission is associated with several neurodegenerative diseases such as ALS. In order to analyze the antioxidant and neurodegenerative capacity of the seed extract of *Amburana cearenses*, Pereira and collaborators promoted studies in PC12 cell cultures which were induced by glutamate excitotoxicity. Among the isolated compounds, methyl-3-coumarin (33) was identified (Figure 3). In the isolate containing mainly coumarins,

including compound 33, promoted, after 24 h, a reduction of 17% in death induced by glutamate, in addition to inducing neuroprotection in $1000 \mu\text{g/mL}$ [70].

To test the ability to inhibit oxidative stress from the extract of *Angelicae dahuricae radix*, which presents furanocoumarin as a secondary metabolite, Moon and colleagues examined its effect on reducing the level of ROS in BV2 cells activated by lipopolysaccharides (LPS). It was observed a significant decrease in ROS levels at the concentrations of 10 and $50 \mu\text{g/mL}$. *In vivo* tests were performed using a dose of 100 mg/kg administered orally to rats during 14 days. The results indicated the extract's neuroprotective effect after spinal cord injury. In this way, the extract has a possible neuroprotective capacity for diseases such as ALS, mainly due to the decrease in cytokine levels when damage to BV2 cells is inferred [71].

A plant of the same genus, *Angelicae gigas*, was evaluated for its antioxidative effect directed to neurodegenerative diseases by Park and collaborators, where the presence of coumarins in this plant has been identified in previous works published by Ryu et al. [72]. *In vitro* tests on DPPH and determination of the reducing capacity demonstrated that

the ethanol extract showed an EE_{50} of 31.47 ± 0.68 mg/mL in the elimination of DPPH. The ethanol extract also showed strong antioxidant activity with an IC_{50} of 43.22 ± 1.67 μ g/mL, demonstrating to be more effective in comparison to the aqueous and methanolic extracts, and to the positive control α -tocopherol (68.64 ± 5.47 μ g/mL). The initiation and propagation of free radicals in the body can be related to transition metals in which elements such as iron and copper act as powerful catalysts in oxidation reactions. Complementing the tests, metal chelating activity was carried out, which consists of adding different concentrations of the extract, methanol, and $FeCl_2$. For the ethanolic extract, an accentuated binding capacity with Fe^{2+} was verified [73].

The effects of *Caragana turfanensis* on neuroinflammation inhibition were evaluated by Song et al. Among the 36 compounds present in the extract, a new coumarin, caraganolide A (34), was observed (Figure 3). The evaluation of each compound was performed on LPS-induced BV2 cells, and caraganolide A demonstrated an IC_{50} of 1.01 ± 1.57 μ g/mL, portraying the best activity among all isolated compounds, including in comparison to the positive control (minocycline) of 9.07 ± 0.86 μ g/mL [74].

From the extract of aerial parts from *Ducrosia ismaelis asch*, Morgan and collaborators were able to isolate psoralen (35) and isopsoralen (36), among other compounds (Figure 3). *In vitro* antioxidant activity of these coumarins demonstrated that the elimination of peroxy radicals and the reducing capacity were inferior to the other components of this extract; however, the inhibition of soluble epoxide hydrolase (sEH) by psoralen was favorable, indicating that this compound can act improving the antioxidant defense mechanism, thus being considered a promising compound for diseases such as ALS [75].

Varier et al. performed molecular docking, using Auto Dock tools 1.5.6 program and the MGL tools 1.5.6 package, to predict the inhibitory capacity of esculin and hinokitol. In the target monooxidase b, esculin (37) (Figure 3) obtained a more favorable binding affinity, with free energy result of -9.6 Kcal/mol, while the cocrystallized ligand levodopa and hinokitol (38) presented binding energies of -7.7 Kcal/mol and -7.2 Kcal/mol, respectively. For all six evaluated different targets, esculin exhibited the best results in comparison to the aforementioned ligands. Monooxidase B is found in the external mitochondrial membrane, whose dysfunction of this organelle may be associated with common neurodegenerative diseases such as ALS and Alzheimer's disease [76].

In neurodegenerative diseases such as ALS, compounds that activate signal-regulated kinase phosphorylation (ERK) and element response-binding protein (CREB) are considered as possible neuroprotective agents. Based on this information, Nakamura et al. tested phosphorylation capacity in human A172 cells of felopterin (39) and auraptene (40) isolated from citrus fruits (Figure 3). Both coumarins promoted an activation of ERK and CREB, indicating that the coumarin ring is a possible pharmacophore responsible for activating the neuroprotective effect on the central nervous system [77].

In general, there is an improvement in coping with neurodegenerative diseases such as ALS through the use of iso-

lated coumarins or plant extracts containing them. The results were promising when performed *in silico*, *in vitro*, and experimentally *in vivo*, revealing its antioxidant effect, prolongation of the programmed death of neural cells, and neuroprotection, beyond the reduction of free radicals.

Most coumarins from natural products could potentially be tested for antioxidant activity, reduction of DPPH, inhibition of induced peroxidation, reduction of glutathione-induced death, and induction of neuroprotection. In general, there is an improvement in dealing with neurodegenerative diseases, such as ALS, through the use of isolated coumarins or plant extracts containing them. The results were promising when performed *in silico*, *in vitro*, and experimentally *in vivo*, revealing its antioxidant effect, prolongation of the programmed death of neural cells, and neuroprotection, beyond the reduction of free radicals.

2.4. Other Metabolites. In addition to the secondary metabolites present in natural products with antioxidant action already mentioned for the treatment of ALS, it is also common the presence of other metabolites in extracts or fractions of extracts present in leaves, fruits, and roots, as well as in other natural products such as fungi and algae [78–80]. From here, we will present the presence and antioxidant mechanisms of tannins, terpenoids, lignans, quinones, saponins, methylxanthines, glucosinolates, and fatty acids directed to the treatment of ALS.

2.5. Tannins. Tannins are secondary polyphenolic plant metabolites commonly found in extracts from a wide variety of plants [81, 82]. Studies of extracts of several plants containing tannins have already reported their biological activity for the treatment of various diseases, such as neurodegenerative diseases, diabetes, lung infections, rheumatism, and kidney diseases, among others [83, 84].

In this perspective, Auddy and collaborators evaluated through *in vitro* and *in vivo* tests, in an unprecedented way, the toxicity and the effect of eliminating radicals with ethanolic and aqueous extracts of three plants commonly used in Indian medicine: *Sida cordifolia*, *Evolvulus alsinoides*, and *Cynodon dactylon*. The results demonstrated that the water infusion of the three plants (up to 1 mg/mL) did not show toxic effects on the PC12 cell line in the MTT tests. As for the verification of antioxidant effects, it was shown that in the ABTS test, the ethanolic extract of *S. cordifolia* presented a better result, with an IC_{50} of 16.07 μ g/mL, followed by *E. alsinoides* and *C. dactylon*, with IC_{50} values of 33.39 μ g/mL and 78.62 μ g/mL, respectively. As for water infusions, the IC_{50} values were, respectively: 172.25 μ g/mL for *E. alsinoides*, 273.64 μ g/mL for *C. dactylon*, and 342.82 μ g/mL for *S. cordifolia*. In the results of lipid peroxidation (TBARS), the water infusion of *E. alsinoides* demonstrated the best result out of the three infusions with an IC_{50} of 89.23 μ g/mL. *In vivo* studies have not shown significant results, and the author attributes the experimental model as being ineffective due to the high, rapid, and extensive degradation of the antioxidant inside the body. The results were promising for the continuity of tests and verification of activity in neurodegenerative diseases [85].

Banerjee et al. reported an *in vitro* study that evaluated the antioxidant activity of black plum peel and juice extract scientifically known as *Syzygium cumini* of the *myrtaceae* family. The antioxidant activities of the aqueous extracts were verified for hydroxyl radicals, superoxide radicals, and stable free radicals 1,1-diphenyl-2-picryl-hydrazil (DPPH). The IC_{50} values for the fruit peel were 468 $\mu\text{g}/\text{mL}$, 260 $\mu\text{g}/\text{mL}$, and 168 $\mu\text{g}/\text{mL}$, respectively. Thus, it can be said that the antioxidant activity of *S. cumini* has significant antioxidant activity. The author attributes this activity to the presence of tannins in the extracts and the peel of the fruit may be important for further studies in the fight against diseases, including ALS [86].

The antioxidant activity of polyphenols is mainly linked to its redox properties and hydrogen donation [87, 88]. Aware of these properties, Mahesh and collaborators carried out studies to evaluate the antioxidant effect and of a plant native to India, *Terminalia chebula* (*combretaceae*), traditionally used to treat various diseases in Asia. The elimination of superoxide radicals, hydroxyl radicals, and nitric oxide radicals with the aqueous extract of the fruit peel of *T. chebula* was evaluated showing significant results with IC_{50} values of 0.031 mg/mL, 0.097 mg/mL and 0.744 mg/mL, respectively. Thus, although the tannin fraction has not been isolated, the author attributes a greater contribution to the antioxidant properties. It also highlights the importance of studying *T. chebula* for possible applications in the treatment of neurodegenerative diseases [89].

A plant-based multicomponent, called Padma® 28, contains, in addition to other compounds, flavonoids and tannins. It has had its antioxidant activity reported by Ginsburg and collaborators, who also evaluated the neuroprotective activity of the extract in a PC12 neuronal cell strain against the toxins $A\beta_{25-35}$ (10 mM), glutamate (40 mM), MPTB (5 mM), and 3-NP (10 mM). Faced with these neurotoxins, PC12 cells demonstrated reduced mitochondrial dysfunction following Padma 28 treatment, thus decreasing cellular oxidative capacity. The decrease induced by Padma® 28 can be attributed to the direct elimination of reactive oxygen species generated in PC12 cells or by the interference with the generation of hydroxyl radicals [90].

Chang and colleagues evaluated *in vitro* the antioxidant activity and neuroprotective effects of five methanolic extracts from dry parts of the plants *Spatholobus suberectus* (SSE), *Uncaria rhynchophylla* (URE), *Alpinia officinarum* (AOE), *Drynaria fortune* (DFE), and *Crataegus pinnatifida* (CPE). Analyzing the extracted fractions, it was verified that the SSE extract contained a higher content of flavonoids, while the URE and AOE extracts contained a higher percentage of tannins and triterpenoids, respectively. Their antioxidant effects were evaluated by 4 means: HRP-luminol- H_2O_2 , pyrogallol-luminol, CuSO_4 -Phen-Vc- H_2O_2 , and Luminol- H_2O_2 . The URE extract demonstrated good antioxidant activities in the HRP-luminol- H_2O_2 and CuSO_4 -Phen-Vc- H_2O_2 assays, with respective IC_{50} values of $3.6 \pm 0.4 \mu\text{g}/\text{mL}$ and $5.9 \pm 0.5 \mu\text{g}/\text{mL}$. These values approximated and, in some cases, better than, the positive controls: vitamin C ($14.8 \pm 6.2 \mu\text{g}/\text{mL}$ and $688.3 \pm 29.7 \mu\text{g}/\text{mL}$) and Trolox ($3.2 \pm 0.1 \mu\text{g}/\text{mL}$ and $5.8 \pm 1.0 \mu\text{g}/\text{mL}$) [91].

Regarding the neuroprotective evaluation, the neuro-growth effects in H_2O_2 of the five extracts in PC12 were evaluated. The extracts that had the best neuroprotective effects were CPE, URE, and SSE in the concentrations ranging from 0.5 to 5.0 $\mu\text{g}/\text{mL}$, with a percentage of neuroprotection from 78.1 to 107.2% for CPE, 54.1 to 85.7% for URE, and 46.3 to 65.7% for SSE, compared to the positive control AC-DEVCHO (N-acetyl-Asp-Glu-Val-Asp-al) with values from 23.9 to 37.5%. Therefore, the extracts have the potential to be deepened into *in vivo* studies for the treatment of neurodegenerative diseases, in which ALS is included [91].

In the study conducted by Adewale and colleagues with the leaves of *Solanum macrocarpon*, a plant typical of India, had its antioxidant activity verified in the protection of the tissues of rats, especially the liver and brain, against iron-induced lipids (Fe^{2+}). Aqueous extracts showed levels of flavonoids and phenolic compounds (with the presence of tannins). The results demonstrated that the aqueous extract of the leaves of *S. macrocarpon* showed high inhibition of lipid peroxidation induced by iron sulfate II with an inhibition value of $92.91 \pm 1.56\%$ at a concentration of 3.33 $\mu\text{g}/\text{mL}$, showing to be more effective than the quercetin control (concentration of $90.15 \pm 1.35 \mu\text{g}/\text{mL}$). Thus, the aqueous extract of the leaves of *S. macrocarpon* presented with a strong antioxidant agent, offering protection against oxidative damage of liver and brain tissues, which places it as a potential for future analyses in the treatment of ALS and neurodegenerative diseases [92].

Another *in vitro* study was carried out by Hamamcioglu and collaborators, in which the evaluation of the potential of the neuroprotective effect in PC12 (dPC12) cells, as well as the antimutagenic and antigenotoxic effects of the species of the plant *Glaucium acutidentatum* of the *papaveraceae* family was carried out. The methanolic extract, at a concentration of 500 $\mu\text{g}/\text{mL}$, showed better results for cell damage, caused by H_2O_2 , with values between 80 and 90% of neuroprotection, in comparison to the aqueous extract that presented a rate between 65 and 75%. It was also observed that the aqueous extract presented no cytotoxicity (90 to 96%), while the methanolic extract presented moderate cytotoxicity (67 to 75%) at any concentration. Another important data demonstrated in the same study is concerning the neuritis index, which is strongly linked to the neuroprotective effect. The higher the value, the better the neuroprotective result [93], as it indicates neural regeneration. It was found that in the presence of only H_2O_2 , neuritis concentration dropped to $50.7 \pm 0.4 \mu\text{M}$, while the control untreated cells presented a value of $80.3 \pm 0.3 \mu\text{M}$ and the extracts (methanolic and aqueous), in a concentration of 500 $\mu\text{g}/\text{mL}$, exhibited values of $78.8 \pm 0.5 \mu\text{M}$ and $78.2 \pm 0.3 \mu\text{M}$, respectively. Furthermore, the extracts showed antimutagenic activity (75.0 and 74.8% inhibition) and antigenotoxic activity. This is a pioneering study for antigenotoxic activity. The results demonstrate strong candidates for the treatment of multiple degenerative diseases, including ALS [94].

The studies presented above with extracts containing tannins in the treatment of ALS demonstrate the lack of in-depth studies, considering that they do not perform *in vivo* experiments, therefore limited to *in vitro* studies, and,

consequently, there are no subsequent preclinical tests and specific clinical trials for ALS. Possibly this continuity of the experiments is linked to the isolation and quantification of the compounds, considering that the majority of the studies did not present gas chromatography techniques.

2.6. Terpenoids. Terpenoids are terpenic compounds that have undergone oxidation. Many studies have been reported with the use of terpenoids in the treatment of diseases [95–97]. One of these studies was carried out by Kiaei and collaborators through the evaluation of the neurodegenerative activities of celastrol (41) (Figure 4), a triterpenoid, isolated from a Chinese plant *Tripterygium wilfordii* of the family *Celastraceae*. In this study, the neuroprotective effects were examined in the G93A SOD1 transgenic mice model for ALS. Studies have shown that the treatment with celastrol significantly improved motor function, delaying ALS symptoms, and also causing a decrease in mice's weight. Another relevant result was the increase in survival of the G93A mice treated with celastrol, registering 9.4% and 13% at the dosages of 2 mg/kg/day and 8 mg/kg/day, respectively. Moreover, an increase of 30% of the neuronal concentration in the lumbar spine suggests a protective effect. Histological analysis revealed a reduction in TNF- α , iNOS, CD40, and GFAP immunoreactivity. Thus, celastrol can be a promising therapeutic agent for the treatment of ALS [98].

In silico and *in vivo* evaluations of phytochemicals present in the root extract of the *Asparagus adscendens* (AAE) plant of the *Liliaceae* family were carried out by Pahwa and Goel, aiming to evaluate the nootropic, anti-amnesic, and antioxidative activities. Prediction of Activity Spectra for Substances (PASS) and Pharmaexpert were used for *in silico* studies. *In vivo* studies of anti-amnesic activity were assessed by scopolamine induction. Finally, nootropic activity was assessed by evaluating the effect of the extract of AAE against antioxidant enzymes on the cortex and hippocampus of mice and acetylcholinesterase. The extracts showed, in addition to other secondary metabolites, the presence of terpenoids. The results *in silico* pointed to a significant decrease in memory loss that was proven by *in vivo* studies. Besides, the AAE extract considerably reduced the levels of oxidative stress in the cortex and hippocampus of mice [99].

Lee et al. investigated the neuroprotective effects of a sesquiterpenoid, ECN (7β -(3-ethylcis-crotonoyloxy)- 1α -(2-methylbutyryloxy)-3,14-dehydro-Z-notonipetranone) (42) (Figure 4) obtained from *Tussilago farfara* sprout, from the *Asteraceae* family, mediated by Nrf2 (nuclear factor erythroid 2) against oxidative stress in the PC12 cell line, as well as the potential of ECN to activate Nrf2 inducing OH⁻¹, also observing the protective effects of ECN (10 μ M) in an experimental model of animals with neurodegeneration. The results demonstrated a protective effect against H₂O₂ and 6-hydroxydopamine (6-OHDA) with 91.8 \pm 6.6% and 87.9 \pm 1.7% inhibition in the concentration of 500 μ M of H₂O₂ and 250 μ M of 6-OHDA, respectively. The ECN also showed good results in the positive regulation of ARE-luciferase activity (cell line designed to monitor the induction of antioxidant response elements), as well as in the induction of

Nrf2 and OH⁻¹ mRNA expression. The results also suggested an interaction between ECN and Keap1 modifying the cysteine thiols of Nrf2, causing a positive regulation of OH⁻¹. Furthermore, the administration of ECN improved dopaminergic and motor neuronal damage [100].

2.7. Lignans. Lignans are a group of phytochemicals, which are produced by oxidative dimerization of two phenylpropanoid units [101]. Studies related to the use of plant extracts containing lignans have also been reported in the literature for the treatment of neurodegenerative diseases [102, 103] mainly by the mechanism of peroxidation dismutase-SOD1. In one of these reports, Lahaie-Collins et al. evaluated sesamine (43) (Figure 5), a lignan isolated from sesame seed (*Sesamum indicum* L) and bark of *fagara* plants, for neuroprotective, antioxidant, and anti-inflammatory effects on neuronal cells PC12. The compound 1-methylphenylpyridine (MPP+) was used as an oxidative damage inducer. The results showed that in picomolar doses (10⁻¹² M), sesamine protected the PC12 neuronal cells from oxidative stress, attenuating by up to 60% the cell death caused by MPP+, in addition to reducing the production of reactive oxygen species. Further results revealed an increase in the production of SOD proteins, as well as a reduction in catalase. Sesamine showed potential in preventing neurodegenerative diseases [104].

Mei et al. isolated 12 lignans from the fruit of the *Broussonetia papyrifera* plant, among which 9 were unpublished. The ethanolic extracts of each lignan were evaluated for its antioxidant activities via MTT and DPPH in PC12 neuronal cells induced by H₂O₂ and also for the capability of eliminating DPPH radicals. The results showed that all ethanolic extracts were efficient in antioxidant activities, reducing the action of H₂O₂ in the CP12 cell line. Compounds 44, 45, 46, 47, and 48 (Figure 5) demonstrated DPPH radical scavenging activity with IC₅₀ values of 236.8 μ M, 156.3 μ M, 273.9 μ M, 281.1 μ M, and 60.9 μ M, respectively, with H₂O₂ concentrations ranging from 0.16 to 100 μ M. Lignan 48 showed the best antioxidant activity. Subsequent studies may apply these lignans for pharmacotherapeutic treatments of ALS and additional neurodegenerative diseases [105].

Sesamine (Figure 5), as reported previously, was also the object of the study of Shimoyoshi et al. They examined the possibility of sesamine affecting the cognitive decline in mice accelerated by senescence (SAMP10). Analytical methods showed changes in oxidative stress related to age in reactive brain carbonyl species (CRs) in mice treated with sesamine. The results showed that mice treated with sesamine obtained better results in tasks of avoidance and forced swimming with aging. Oxidative stress in the cerebral cortex and liver showed a reduction in mice treated with lignan. These results suggest that sesamine prevents brain dysfunction by antioxidative activity [106].

2.8. Quinones. Similar to the other secondary metabolites, quinones present in extracts have been reported in studies looking for ALS treatments and different neurodegenerative diseases [107–109].

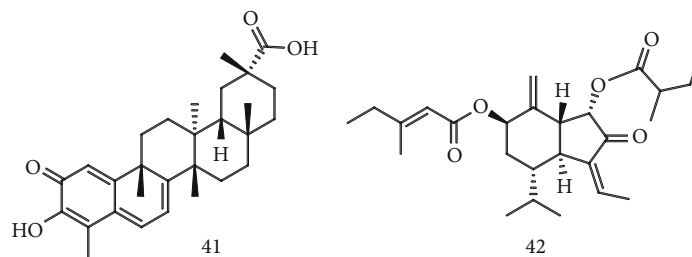


FIGURE 4: Structure of celastrol (41), a natural triterpenoid isolated from a Chinese plant *Tripterygium wilfordii*, and ECN (42), isolated from the plant *Tussilago farfara*.

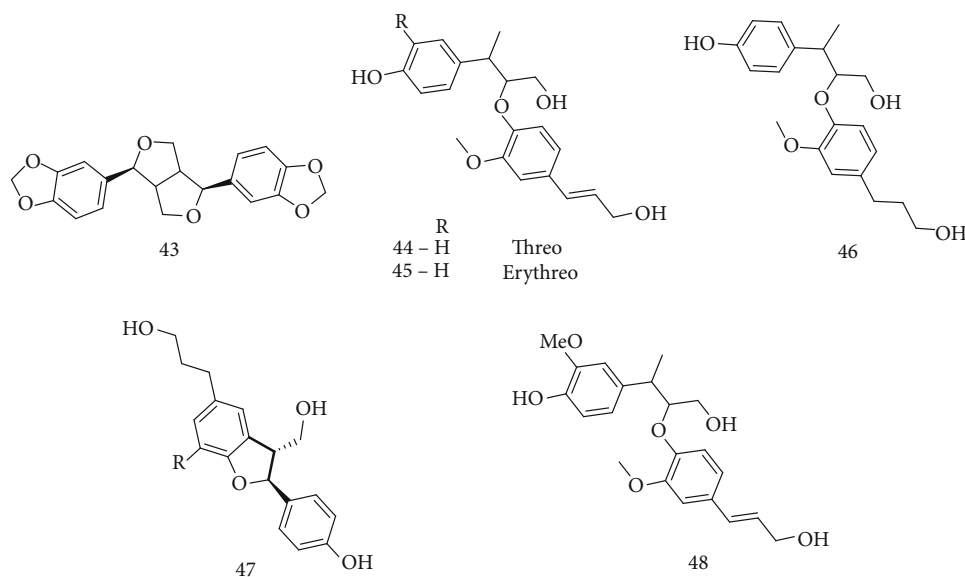


FIGURE 5: Structures of sesamine (43), a lignan isolated from sesame seed (*Sesamum indicum* L) and other lignans (44, 45, 46, 47, and 48) isolated 12 lignans from the fruit of the plant *Broussonetia papyrifera*.

One of these reports, presented by Lu et al., demonstrated the antioxidant effects of ethanolic extracts from the roots of the *Rheum officinale baill* plant of the *Polygonaceae* family, popularly known as rhubarb. Phytochemical analysis of the extracts demonstrated the presence of anthraquinones (emodine 49) and dianthraquinones (aloe-emodine 50) (Figure 6), in addition to other constituents. Rhubarb extract considerably decreased the number of neurons with condensed and fragmented DNA, especially at a concentration of 10 $\mu\text{g}/\text{mL}$ (at concentrations 2 and 5 $\mu\text{g}/\text{mL}$ the results were inferior). The study showed a protective role for rhubarb extract against cell oxidation, which may bring significant results in further studies in the treatment of ALS and other neurodegenerative diseases [109].

Vegás-Hernández and collaborators evaluated the antioxidant effects of rapanone (51) (Figure 6), a natural benzoquinone isolated from the *Myrsine* plant, against the chelation, iron removal activity, and protective potential against damage induced by *tert*-butyl hydroperoxide in mitochondria. The results showed the formation of complexes with irons II and III, oxidation of iron II, and peroxide radicals, inhibiting Fenton-Haber-Weiss reactions, effectively demonstrating the protective effect against oxidative stress

at concentrations of 50 and 300 μM . The results demonstrate the protective potential of rapanone against mitochondrial lipid peroxidation with IC_{50} 10.33 \pm 1.29 at 50 μM values better than the positive glycol-bis(2-aminoethylether)-*N,N,N',N'*-tetraacetic acid (EGTA) IC_{50} 15.47 \pm 2.01 μM at 200 μM . Thus, rapanona appears with pharmacological potential in the treatment of diseases that occur oxidative stress such as neurodegenerative diseases [110].

Studies with terpenoids, lignans, and quinones are more limited in the literature; however they exhibit greater depth of studies aimed at treating ALS. Unlike studies with tannins, these three metabolites, despite the few studies found, have advanced to *in vivo* studies, presenting significant results in different pathways. Few studies have reported the isolation of the main compound and do not report the extraction methodology transparently. Finally, despite having been carried out *in vivo*, the studies have not yet been reported or evaluated in clinical tests. It may be related to difficulties in isolation, since the extractive methods were not well understood in the study.

2.9. Saponins. The classic definition of saponins is based on its surface activity and its detergent properties, forming stable

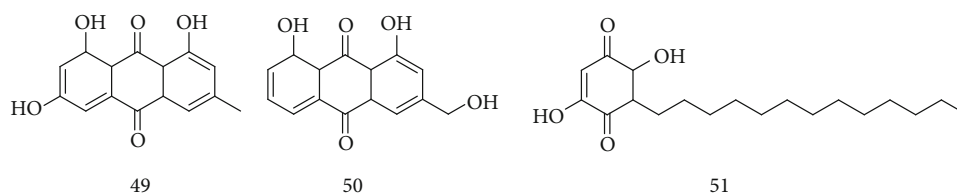


FIGURE 6: Structure of emodin (49), aloe-emodin (50) quinones found in the roots of the *Rheum officinale baill* plant, and rapanone (51), a benzoquinone isolated from the *Myrsine* plant.

foams in water. Saponin is a class of glycosidic compounds that can be classified as steroidal saponins and triterpene saponins, which can form colloidal solutions that foam in water, like soap, if the mixture is stirred. Saponins can be found in the roots and leaves of plants and present antimicrobial, antibacterial, antiviral, anticancer, and antioxidants activities, in addition to its ability to stimulate the formation of collagen, a protein that plays a role in the healing process of wounds [111–113].

Many saponins have been reported for neuroprotection purposes, including madecassoside (52) [114–117], ginsenoside (53) [118–120], and astragaloside IV (54) [121] (Figure 7). Saponin's neuroprotection property is not correlated to a single process, but to a spectrum of independent and related processes, which promotes its ability to regenerate the neural network directly promoting cell survival, improving neurite growth, and recovering the activities of axons and synapses. These metabolites can also prevent neuron malfunctions by changing levels of neurotransmitters, receptors, and messengers [114, 121]. In this sense, madecassoside (52) is one of the bioactive compounds of the triterpenoid saponins isolated from *Centella asiatica* (L) Urban, reported with the potential to protect the degeneration of motor neurons and also increase the longevity of transgenic mice SOD1G93A with ALS [114].

In a model of ALS using a type of lipopolysaccharide-induced rats (LPS), two different doses of madecassoside were tested, 61.1 ± 11.0 and 185.6 ± 18.7 mg/kg/day, respectively. Compared to the control group (mice without madecassoside treatment), madecassoside failed to delay the onset of the disease, but can significantly prolong the mice's survival time by 11.4 and 9.4 days, respectively ($P < 0.05$) [113, 114]. Also, madecassoside inhibits the production of nitric oxide (NO) (a harmless component when present in small quantities, but undesirable when secreted in large quantities), prostaglandin E2 (PGE2), and additional inflammatory factors in RAW264.7 macrophage cells lipopolysaccharide-induced (LPS) and collagen-induced arthritis in a rat model, which could explain its neuroprotective and anti-inflammatory effect [113].

According to a study by Sasmita et al., madecassoside (52) is introduced as a potent antineuroinflammatory agent, which is able to influence genetic and protein components that are implicated in neuroinflammation and to reduce the intracellular levels of reactive oxygen species (ROS) by 56.84% in BV2 microglia cell line, in comparison to the group stimulated only with LPS. The results of the present study suggest that madecassoside successfully and significantly reg-

ulated the gene and protein expression of inducible nitric oxide synthase (iNOS), cyclooxygenase 2 (COX-2), signal transducer and transcription activator 1 (STAT1), and nuclear factor kappa B (NF- κ B), which are all proneuroinflammatory components. In addition, madecassoside significantly increased the gene expression of the anti-inflammatory component heme oxygenase 1 (HO⁻¹) by 175.22% compared to the LPS group, suggesting that this compound is an important ally in the treatment of neurodegenerative diseases [115].

In another study by Liu et al., in which researchers evaluated the protective effect of madecassoside (52) on the cognitive process induced by LPS and neuroinflammation in rats, it was observed that the treatment with madecassoside (120 mg/kg, i.g.) for 14 days reduced LPS-induced neurotoxicity, decreasing cognitive deficiencies and suppressing the production of inflammatory cytokines, such as interleukin 1-beta (IL-1 β), tumor necrosis factor alpha (TNF- α), and interleukin 6 (IL-6), through the activation of nuclear factor 2 signaling related to erythroid nuclear factor 2 (Nrf2). In addition, the treatment improved heme oxygenase (HO⁻¹) protein levels, through the positive regulation of Nrf2 in LPS-stimulated neurotoxicity. Collectively, these results suggest that madecassoside is effective in preventing neurodegenerative diseases by improving memory functions due to its anti-inflammatory activities and activation of Keap1-Nrf2/HO⁻¹ signaling [113].

Additional studies with madecassoside (52) extracted from *Centella asiatica* (CA) were also carried out evolving the evaluation of its potential to inhibit the enzyme Serine Racemase (SR), an enzyme responsible for converting L-serine into D-serine, an amino acid coagonist at glutamate N-methyl-D-aspartate (NMDA) receptors, whose hyperexcitation is involved in several neurodegenerative diseases, including ALS. The authors observed that the activity of the SR enzyme was significantly inhibited in the presence of CA extract. The CA extract at a concentration of 20 μ g/mL and 40 μ g/mL inhibited 85% and 99% of SR activity ($P = 0.0001$), respectively. The enzyme inhibition assay indicates that madecassoside is an inhibitor of human SR. The I C₅₀ value for madecassoside is 26 μ M, which is the lowest I C₅₀ among SR inhibitors reported up to date, giving this compound anti-inflammatory, neuroprotective, antiapoptotic, and antioxidative activity in animal models of ALS [116].

Ginsenosides are saponins found in the medicinal herb *Panax ginseng* that can be classified into three groups (Figure 8) based on structural differences: the protopanaxadiol group (55) (including Rb1, Rb2, Rb3, Rc, and Rd), the

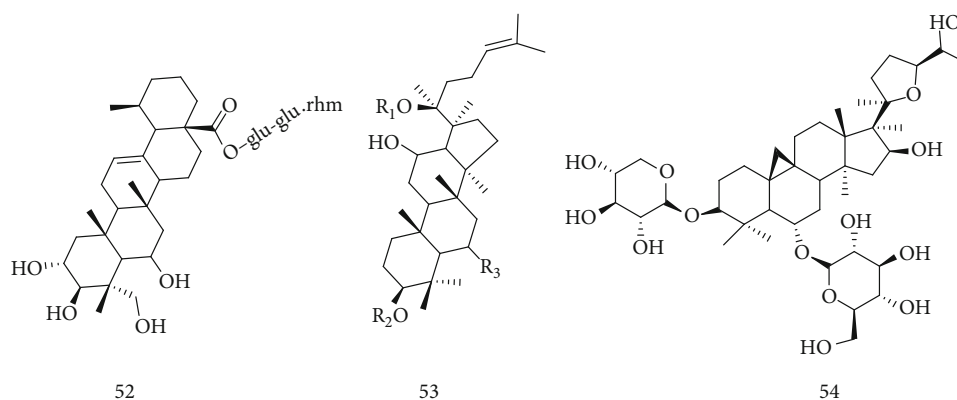


FIGURE 7: Chemical structure of madecassoside (52), ginsenoside (53), and astragaloside IV (54),

protopanaxatriol group (56) (as the Re, Rf, Rg1, and Rg2 derivatives), and the Oleanano group (as the Ro variant) (57) [117–119]. Different studies have shown that the components of *Panax L.*, especially the ginsenosides Rb1, Rb2, Rb3, Rc, Rd, Re, Rg1, Rg2, and Rg3, have significant therapeutic effects in various neurological disorders such as memory, anxiety, depression, epilepsy, accident stroke, ALS, Alzheimer's disease (AD), Parkinson's disease (PD), and Huntington's disease [119]. Each ginsenoside molecule is potentially effective in the treatment of various diseases of the central nervous system (CNS). For example, the biologically active ginsenoside component Rg1 reduces reactive oxygen species (ROS) and cytotoxicity by negatively regulating proapoptotic proteins, neutralizing oxidative stress, resulting in neuroprotection of cells treated with lipopolysaccharides (LPS) [117, 118]. The ginsenosides present in ginseng have shown the potential to be an excellent compound for the treatment of neurodegenerative diseases, possibly its neuroprotective effect occurs due to the modulation of neuronal calcium channels. Some studies suggest that ginsenoside Rg1 (58) (Figure 8), panaxatriol saponin, reduces the production of reactive oxygen species (ROS), releases cytochrome c in the cytosol, inhibits caspase3 activity, and lowers nitric oxide production (NO), reducing the level of inducible protein of nitric oxide synthase (iNOS), in addition to being reported rescue of cellular damage caused by hydrogen peroxide through the negative regulation of the NF- κ B signaling pathway, as well as activation of the AKT and ERK1/2 [118, 122, 123].

A preliminary study by Jiang et al. [58] with ginseng root showed beneficial effects in an ALS model using SOD1G93A transgenic mice, portraying a delay in disease onset and a prolonged survival rate. This study, combined with the anti-inflammatory, antioxidant, antiapoptotic, and immunological effects on the CNS reported in the literature, encouraged Ratan et al. [119] to evaluate the effects of the ginsenoside Re (G-Re) (59) (Figure 8) on neuroinflammation and its action on human superoxide dismutase 1 (SOD1) through the administration of 2.5 μ g/g of the compound in symptomatic ALS hSOD1G93A mice. The authors observed that treatment with G-Re reduced the loss of motor neurons and the expression of Iba-1 (ionized calcium binding adapter molecule 1), a microglia-specific calcium-binding protein, in

the spinal cord of transgenic mice hSOD1G93A, indicating a possible neuroprotective effect. Besides, compared to hSOD1G93A mice of the same age, those treated with G-Re showed a significant reduction in the expression of proinflammatory proteins, like the CD14 protein and TNF- α related to the TLR4 signaling pathway. G-Re administration also led to a decrease in phospho-p38 protein levels related to cell death and had an antioxidant effect by reducing the expression of HO⁻¹. These results suggest that ginsenoside-Re has a potent antineuroinflammatory effect on ALS, inhibiting the TLR4 pathway.

Astragaloside IV (AST-IV) (54) is a small saponin and the main active component in *Astragalus membranaceus*, holding anti-inflammatory, antiviral, antiaging, immunomodulatory, and neuroprotective effects. The neuroprotective effect of this compound was observed in neural microglia cells, in which the presence of AST-IV in the concentration of 1 to 5 μ mol/L protected the microglia from death caused by LPS and negatively regulated the release of proinflammatory mediators, including interleukin IL-1 β , IL-6, tumor necrosis factor α (TNF- α), and nitric oxide, as well as the expression of Toll-like 4 receptors (TLR4), MyD88, and nuclear factor κ B (NF- κ B) of these cells. These results indicate that AST-IV exerts an anti-inflammatory effect on microglia, possibly by inhibiting the TLR4/NF- κ B signaling pathways and protects neurons from microglia-mediated cell death by converting the inflammatory M1 microglia into a M2 anti-inflammatory phenotype, indicating the potential of this compound for the treatment of neurodegenerative diseases [120].

The evidence of possible beneficial effects during *in vitro* and *in vivo* studies, shown in the studies above, is a starting point for the achievement of new therapeutic alternatives in the treatment of ALS. However, it is important to note that such studies demonstrate a lack of methodological standardization of the samples used, ranging from commercially obtained saponins [113, 117, 120, 124] to plant extracts [116]. The lack of standardization of the samples can influence the reproducibility of the results obtained in these initial tests.

2.10. Methylxanthines. Methylated xanthines (methylxanthines) are heterocyclic organic compounds that are

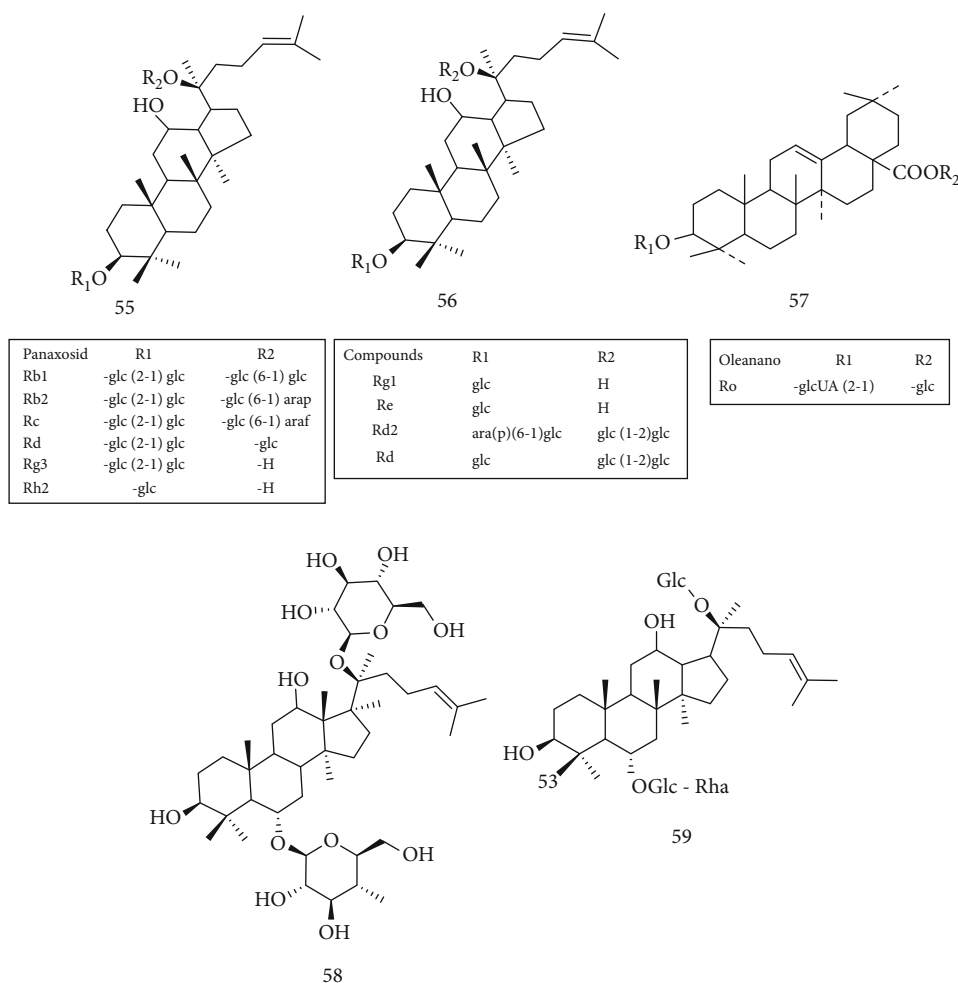


FIGURE 8: Chemical structure of (55), protopanaxatriol (56), Oleanano (57), ginsenoside Rg1 (58), and ginsenosideo Re (59).

methylated derivatives of xanthine, therefore comprising coupled rings of pyrimidinedione and imidazole. They are present in almost 100 species of 13 orders from the plant kingdom, including tea (*Camellia sinensis L.*), coffee (*Coffea sp.*), and cocoa (*Theobroma cacao L.*), being normally included in the daily human diet in many drinks and foods extremely common, such as coffee, tea, cocoa, yerba mate, and cola. Caffeine (60), theophylline (61), and theobromine (62) (Figure 9) are the main methylxanthines available from natural sources [125, 126].

Methylxanthines have been widely used as therapeutic agents, in a range of medicinal fields, such as CNS stimulants, bronchodilators, coronary dilators, diuretics, anticancer adjuvant treatments, and, more recently, they have been suggested with a potential beneficial health effect in the treatment of neurodegenerative diseases, cardioprotection, diabetes, and fertility [126].

Caffeine is a methylxanthine that nonselectively antagonizes adenosine receptors and is the most widely used psychoactive substance in the world. Its chronic consumption has proven to be protective against neurodegenerative diseases, such as Parkinson [127], Alzheimer [128], and ALS [129]. For many years, it was believed that caffeine consumption could be associated with an increased risk of neurode-

generative diseases. However, Fondell and colleagues [129] performed a longitudinal analysis based on more than 1,010,000 men and women in five large cohort studies, in which they evaluated the association between caffeine, coffee, and tea consumption and ALS risk. The results showed that a total of 1,279 cases of ALS were documented during an average of 18 years of follow-up. Caffeine intake was not associated with the risk of ALS; the combined multivariate adjusted risk (RR) ratio was 0.96 (95% CI 0.81-1.16). Similarly, neither coffee nor tea has been associated with ALS risk. Therefore, the results of this large study did not demonstrate any associations of caffeine or caffeine drinks with the risk of ALS [130, 131].

The data found by Fondell and collaborators [129] reaffirm the results obtained by Herden and Weissert [132] when investigating in 377 patients with newly diagnosed ALS the relationship between coffee consumption and ALS risk in which they evidenced an inverse correlation between the consumption of coffee and the risk of disease.

Onatibia-Astibia et al. and Sonsalla et al. [125, 127] report that caffeine consumption improves cognitive function, prevents neurodegeneration, and restores neuronal plasticity and mitochondrial production in middle-aged rats and in the APPswe mouse model of Alzheimer's disease.

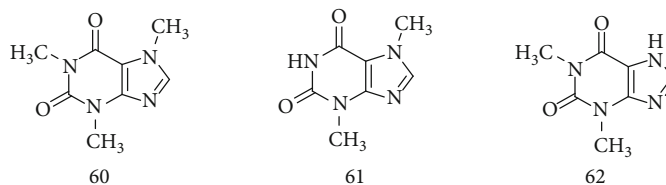


FIGURE 9: Chemical structure of methyl xanthine: caffeine (60), theophylline (61), and theobromine (62).

Regarding ALS, caffeine is believed to be neuroprotective, antagonizing A_{2A} adenosine receptors in the brain and thus protecting motor neurons from excitotoxicity [128, 129]. In this sense, Monteiro et al. [126], Kolahdouzan and Hamadeh [130], and Herden and Weissert [132] also reinforce the beneficial effects of caffeine consumption in improving motor activity in the context of neurodegenerative diseases through mechanisms of neuroprotection and neurorestoration by trophic proteins, suggesting that caffeine is a promising compound for the treatment of neurodegenerative diseases.

Caffeine is the most studied methylxanthine concerning its effect on neurodegenerative diseases. According to the studies with patients reported above, the consumption of caffeine has shown a protective effect in patients with ALS. On the other hand, there is a lack of evidence on the neuroprotective mechanism of action of this compound, and it is necessary to expand research in this area, using *in silico*, *in vitro*, and *in vivo* experiments, not only to elucidate the effect of caffeine on neurodegenerative diseases, but also to investigate new methylxanthines that may show a potential effect on these diseases. So these structures can be explored for the design of new compounds that may be more promising, facilitating the understanding of their possible mechanisms of action.

2.11. Glucosinolates. Glucosinolates are abundant compounds in the *Moringa* species, mainly in the *Moringa oleifera*, having been reported to have anti-inflammatory, antioxidant, anticancer, and antidiabetic activities. The most abundant glucosinolate present in the species is 4-O-(α -L-rhamnopyranosyloxy)-benzyl glucosinolate, also known as glucomoringin (GMG) (63). Glucosinolates and related hydrolytic products, isothiocyanates (ITCs) (64), have attracted researchers due to their neuroprotective effect [133–136]. ITCs are phytochemicals containing sulfur and nitrogen obtained from glucosinolates after myrosinase action. Myrosinase-catalyzed hydrolysis at neutral pH of GMG releases the biologically active compound 4-(α -L-ranosiloxy)-benzylisothiocyanate (GMG-ITC) (65) (Figure 10) [135, 136].

Many studies have revealed the benefits of consuming vegetables from *Brassicaceae* and *moringaceae*, which are the main sources of ITCs. These compounds are considered to contribute to the massive reduction of risk for the development of neurodegenerative diseases, due to their anti-amyloidogenic, antioxidant, and anti-inflammatory properties. The preventive and treatment capacity of ITCs for NDDs is being extensively explored over the last years [135].

In this sense, Jaafaru and collaborators [137] evaluated the neuroprotective activity of GMG-ITC (65) by eliminating ROS in SH-SY5Y neuroblastoma cells (ATCC® CRL-2266

TM), observing that the presence of GMG-ITC (1.25 μ g/mL) before the development of the oxidative stress condition decreased the expression of cyt-c (cytochrome C), p53 (also called TP53 gene and tumor protein p53 gene), Apaf-1 (apoptosis-activating factor 1), Bax (BCL-2-associated protein X), CASP3, CASP8, and CASP9 (proteins involved in the caspase pathway) with simultaneous positive regulation of the Bcl-2 gene (B cell lymphoma protein 2) in the mitochondrial apoptotic signaling pathway. In view of these results, the authors suggest that pretreatment with GMG-ITC can relieve the condition of oxidative stress in neuronal cells, reducing the level of ROS production and protecting cells against apoptosis through possible neurodegenerative pathways of disease [137].

In another study, Galuppo et al. [136] evaluated the therapeutic efficacy of GMG-ITC against ALS *in vivo* using SOD1tg mice, which physiologically develop SOD1G93A at around 16 weeks of age and can be considered a genetic model of the disease. The rats were treated once a day with GMG (10 mg/kg) bioactivated with myrosinase (20 μ L/rat) by intraperitoneal injection for two weeks before the onset of the disease, and the treatment was prolonged for another two weeks before sacrifice. The results showed statistically significant differences between mice treated and untreated with GMG-IT ($P = 0.003$), demonstrating that the administration of GMG-IT was able to delay the onset of the disease for approximately two weeks, probably due to its immunomodulatory, anti-inflammatory, antioxidant, and antiapoptotic effects, suggesting that this compound could be a potential drug for the treatment of this disease.

Glucosinolates have been extensively studied in recent years due to their anti-inflammatory and antioxidant potential. However, few studies in the literature report their action on neurodegenerative diseases, such as ALS. Preliminary studies in both cells and animals show neuroprotective effects of these compounds, but the mechanism of action and the extent of the effects have yet to be further investigated in more robust preclinical and clinical studies.

2.12. Fatty Acids. The growing amount of researches involving neurodegenerative diseases shows that neurons are particularly vulnerable to oxidative damage due to their high content of polyunsaturated fatty acids in the membranes, high oxygen consumption, and weak antioxidant defense [138]. Fatty acids are essential lipid molecules to support the structural integrity of cell membranes, providing energy and assisting in signaling pathways. Studies show that a higher intake of polyunsaturated fatty acids ω 3, considered neuroprotectives, was associated with a reduced risk of ALS [139].

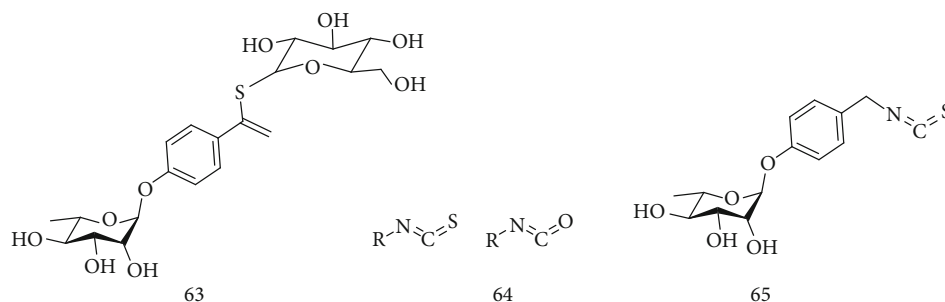


FIGURE 10: Chemical structure of 4-O-(α -L-ramnopyranosyloxy)-benzyl (GMG) (63), isothiocyanates (ITCs) (64), and 4-(α -L-rhamnosyloxy)-benzylisothiocyanate (GMC-ITC) (65).

On the other hand, Boumil et al. estimated the impact of omega-3 (Ω -3) (66) and omega-6 (Ω -6) (67) (Figure 11) in the function of the motor neuron in mice expressing the mutant human superoxide dismutase-1 (SOD1). The authors noted that supplementation with Ω -3 and Ω -6 equivalents hastened the pathology and death of motor neurons; however, 10x Ω -6 with no change in Ω -3 (1 mg/kg) significantly delayed pathology in motor neurons, including preservation of minor motor neuron function during the terminal stage, suggesting that a critical balance of Ω -6 and Ω -3 may temporarily preserve motor neuron function during the terminal stages of ALS, which could provide a substantial improvement in the quality of life of the affected individuals [140].

Assessing the therapeutic potential of fatty acids for the treatment of ALS, Tefera and collaborators [141] observed the effects of triheptanoin fatty acid (68) (Figure 11), a heptanoate triglyceride, in the treatment of mice that overexpress the SOD1G93A human gene mutant. They observed that rats fed the SF11-028 diet (composed of ingredients typical of other rat diets), modified with 35% oral triheptanoin, starting at P35 (35th day), showed attenuation in the loss of motor neurons at 70-day old by 33%. This result, combined with the pressure strength of the hind limbs, which demonstrated a delay in the loss of strength in hSOD1G93A mice treated with triheptanoin, suggests that this compound delays the loss of motor neurons and the appearance of motor symptoms in mice.

According to Días-Amarilla et al., nitro-fatty acids (NO_2 -FA) are electrophilic signaling mediators formed in tissues during inflammation, capable of inducing cytoprotective pathways and pleiotropic antioxidants, including the regulation of genes responsive to factor 2 (Nrf2) related to the erythroid nuclear factor. These researchers demonstrated that nitro-arachidonic acid (NO_2 -AA) or nitro-oleic acid (NO_2 -OA) administered in astrocytes that express hSOD1G93A bound to ALS at a concentration of 5 μM induces an antioxidant effect through the activation of Nrf2 concomitantly with the increased levels of glutathione. In addition, the treatment of astrocytes expressing hSOD1G93A with NO_2 -FA prevented its toxicity to motor neurons, proving its antioxidant effect on astrocytes capable of preventing the death of motor neurons in an ALS culture model [142].

Trostchansky and collaborators also evaluated the response of transgenic SOD1G93A mice with ALS after the treatment with 16 mg/kg/day of nitro-oleic electrophilic acid

(NO_2 -OA) subcutaneously. It was observed that NO_2 -OA significantly improved the grip strength and performance on rotarod (also called rotating bar that assesses motor coordination and balance) compared to animals treated with vehicle or oleic acid (AO), suggesting NO_2 -OA as a promising therapeutic compound [143].

Another fatty acid of importance in ALS is docosahexaenoic acid (DHA) (69) (Figure 11), an essential fatty acid that modulates the main functions of the nervous system, including neuroinflammation, and regulation of pre- and postsynaptic membrane formation, being reduced in patients with amyotrophic lateral sclerosis and preclinical murine models [144]. Based on this information, Torres et al. [144] performed dietary supplementation of DHA in a murine model fASL B6SJL-Tg (SOD1 * G93A), in which they observed that a diet rich in DHA significantly increases the survival of male rats by 7% (average of 10 days over 130 days of life expectancy) and delays motor dysfunction (based on stride length) and loss of weight associated with ALS transgene ($P < 0.01$). Also, DHA supplementation led to an increase in the profile of anti-inflammatory fatty acids ($P < 0.01$), a lower concentration of circulating proinflammatory such as the cytokine $\text{TNF-}\alpha$ ($P < 0.001$ in males), reduced immunoreactivity to markers of oxidative DNA damage (8-oxodG) in the lumbar spinal cord (LSC), and preserved the number of motor neurons compared to untreated. The literature also suggests the antioxidant action of fatty acids as the main mechanism of action.

Due to the importance of fatty acids for the structure and integrity of cell membranes, these compounds have been investigated with a potential neuroprotective effect. Studies in murine models have shown a beneficial effect obtained by the supplementation with fatty acids, such as DHA, omega-3 (Ω -3), and omega-6 (Ω -6). Nonetheless, it is important to emphasize that the amount to be supplemented is not yet well established. Some studies have suggested that the neuroprotective effect is derived from a balance between fatty acids [140]. Therefore, further research is required to establish the neuroprotective potential, the neuroprotective mechanism, and the amount of fatty acids to be used to ensure this effect.

3. Conclusions

Unfortunately, there is still no effective and/or curative treatment for the disease, and the few drugs on the market are

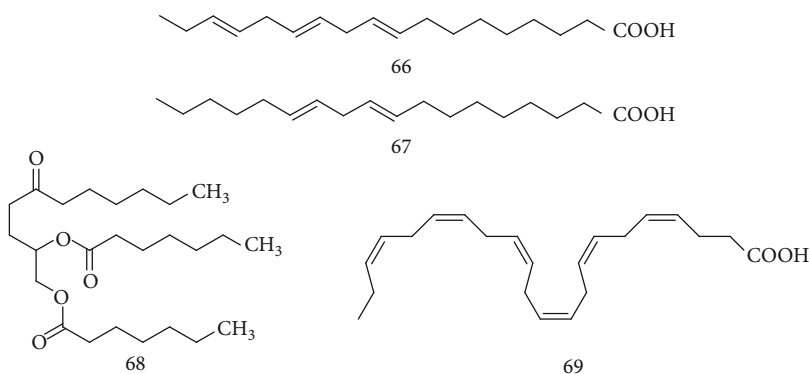


FIGURE 11: Chemical structure of omega-3 (66), omega-6 (67), triheptanoin (68), and docosahexaenoic acid (DHA) (69).

intended to only slow the progress of the disease. Among the most promising treatment alternatives, the effectiveness of antioxidants can be highlighted, since the disease is directly related to oxidative stress and cell death. In this context, the relevance of natural products with potential antioxidant action was reported in this review, emphasizing on oxygenated and nitrogenous compounds that are capable of acting in redox balance, attenuating or decreasing the impact of these effects on neuronal and motor cells. Among them, we highlight polyphenols, flavonoids, coumarins, and alkaloids as main metabolites, as well as unsaturated hydrocarbons, such as fatty acids and their esters, which are part of the diet worldwide and are considered promising alternatives. The mechanisms of action associated with the activity of these metabolites are not yet entirely elucidated, but researches point out that natural products capable of regulating redox effects are fundamental for cellular processes, maintaining an appropriate environment for metabolic activities and healthy functioning, as they present, in some cases, low collateral effects and multiple targets. Nevertheless, there are still few studies related to toxic effects, mechanisms of action, and strategies of molecular modifications using these prototypes through total synthesis or semisynthesis, which could lead to further preclinical and clinical trials, and eventual obtainment of safe and effective compounds that can improve the ALS patient's outcome.

Conflicts of Interest

The authors declare no conflict of interests regarding the publication of this paper.

Acknowledgments

The authors acknowledge the financial support from Fundação de Amparo a Ciência e Tecnologia do Estado de Pernambuco (FACEPE), Federal University of Pernambuco (UFPE), State University of Paraíba (UEPB), Conselho Nacional de Desenvolvimento Científico e Tecnológico (CNPq), Coordenação de Aperfeiçoamento de Pessoal de Nível Superior (CAPES), Fundação de Apoio à Pesquisa do Estado da Paraíba (FAPESQ), and Pro-rectory of Post-graduate Studies (PROPESQ/PB).

References

- [1] S. Parakh, D. M. Spencer, M. A. Halloran, K. Y. Soo, and J. D. Atkin, "Redox regulation in amyotrophic lateral sclerosis," *Oxidative medicine and cellular longevity*, vol. 2013, 12 pages, 2013.
- [2] K. Valko and L. Ciesla, *Amyotrophic Lateral Sclerosis*, Elsevier B.V, 2019.
- [3] S. Chen, P. Sayana, X. Zhang, and W. Le, "Genetics of amyotrophic lateral sclerosis: an update," *Molecular Neurodegeneration*, vol. 8, no. 1, p. 28, 2013.
- [4] S. Zarei, K. Carr, L. Reiley et al., "A comprehensive review of amyotrophic lateral sclerosis," *Surgical neurology international*, vol. 6, no. 1, p. 171, 2015.
- [5] A. Gowland, S. Opie-Martin, K. M. Scott et al., "Predicting the future of ALS: the impact of demographic change and potential new treatments on the prevalence of ALS in the United Kingdom, 2020–2116," *Amyotrophic Lateral Sclerosis and Frontotemporal Degeneration*, vol. 20, no. 3–4, pp. 264–274, 2019.
- [6] L. Rechtman, L. Wagner, W. Kaye, and J. Villanacci, "Updated prevalence and demographic characteristics for ALS cases in Texas, 2009–2011," *Southern Medical Journal*, vol. 108, no. 8, pp. 483–486, 2015.
- [7] A. M. G. Ragagnin, S. Shadfar, M. Vidal, M. S. Jamali, and J. D. Atkin, "Motor neuron susceptibility in ALS/FTD," *Frontiers in Neuroscience*, vol. 13, 2019.
- [8] S. Saberi, J. E. Stauffer, D. J. Schulte, and J. Ravits, "Neuropathology of amyotrophic lateral sclerosis and its variants," *Neurologic Clinics*, vol. 33, no. 4, pp. 855–876, 2015.
- [9] J. W. Nieves, C. Gennings, P. Factor-Litvak et al., "Association between dietary intake and function in amyotrophic lateral sclerosis," *JAMA Neurology*, vol. 73, no. 12, pp. 1425–1432, 2016.
- [10] P. Couratier, P. Corcia, G. Lautrette, M. Nicol, P.-M. Preux, and B. Marin, "Epidemiology of amyotrophic lateral sclerosis: a review of literature," *Revue Neurologique*, vol. 172, no. 1, pp. 37–45, 2016.
- [11] V. S. de Souza, W. B. V. de Rezende Pinto, M. A. T. Chieia, and A. S. B. Oliveira, "Clinical and genetic basis of familial amyotrophic lateral sclerosis," *Arquivos de Neuro-Psiquiatria*, vol. 73, no. 12, pp. 1026–1037, 2015.
- [12] M. Yusuf, M. Khan, M. A. Robaian, and R. A. Khan, "Biomechanistic insights into the roles of oxidative stress in generating complex neurological disorders," *Biological Chemistry*, vol. 399, no. 4, pp. 305–319, 2018.

- [13] S. Carrera-Juliá, M. L. Moreno, C. Barrios, J. E. de la Rubia Ortí, and E. Drehmer, "Antioxidant alternatives in the treatment of amyotrophic lateral sclerosis: a comprehensive review," *Frontiers in Physiology*, vol. 11, p. 63, 2020.
- [14] S. L. Albarracín, B. Stab, Z. Casas et al., "Effects of natural antioxidants in neurodegenerative disease," *Nutritional Neuroscience*, vol. 15, no. 1, pp. 1–9, 2013.
- [15] E. Niedzielska, I. Smaga, M. Gawlik et al., "Oxidative stress in neurodegenerative diseases," *Molecular Neurobiology*, vol. 53, no. 6, pp. 4094–4125, 2016.
- [16] M. C. Kiernan, S. Vucic, B. C. Cheah et al., "Amyotrophic lateral sclerosis," *Lancet*, vol. 377, no. 9769, pp. 942–955, 2011.
- [17] R. Bhattacharya, R. A. Harvey, K. Abraham, J. Rosen, and P. Mehta, "Amyotrophic lateral sclerosis among patients with a Medicare Advantage prescription drug plan; prevalence, survival and patient characteristics," *Amyotrophic Lateral Sclerosis and Frontotemporal Degeneration*, vol. 20, no. 3–4, pp. 251–259, 2019.
- [18] M. Lahlou, "The Success of Natural Products in Drug Discovery," *Pharmacology & Pharmacy*, vol. 4, no. 3, pp. 17–31, 2013.
- [19] K. C. Fitzgerald, É. J. O'Reilly, E. Fondell et al., "Intakes of vitamin C and carotenoids and risk of amyotrophic lateral sclerosis: pooled results from 5 cohort studies," *Annals of Neurology*, vol. 73, no. 2, pp. 236–245, 2013.
- [20] R. N. Krishnaraj, S. S. S. Kumari, and S. S. Mukhopadhyay, "Antagonistic molecular interactions of photosynthetic pigments with molecular disease targets: a new approach to treat AD and ALS," *Journal of Receptors and Signal Transduction*, vol. 36, no. 1, pp. 67–71, 2016.
- [21] D. Ribeiro, M. Freitas, A. M. S. Silva, F. Carvalho, and E. Fernandes, "Antioxidant and pro-oxidant activities of carotenoids and their oxidation products," *Food and Chemical Toxicology*, vol. 120, pp. 681–699, 2017.
- [22] Z. Yan, Y. Zhong, Y. Duan, Q. Chen, and F. Li, "Antioxidant mechanism of tea polyphenols and its impact on health benefits," *Animal Nutrition*, vol. 6, no. 2, pp. 115–123, 2020.
- [23] S. Nabavi, M. Daglia, G. D'Antona, E. Sobarzo-Sanchez, Z. Talas, and S. Nabavi, "Natural compounds used as therapies targeting to amyotrophic lateral sclerosis," *Current Pharmaceutical Biotechnology*, vol. 16, no. 3, pp. 211–218, 2015.
- [24] M. Ur Rashid, M. Alamzeb, S. Ali et al., "The chemistry and pharmacology of alkaloids and allied nitrogen compounds from Artemisia species: a review," *Phytotherapy Research*, vol. 33, no. 10, pp. 2661–2684, 2019.
- [25] A. L. Souto, J. F. Tavares, M. S. da Silva, M. F. F. M. Diniz, P. F. de Athayde-Filho, and J. M. Barbosa Filho, "Anti-inflammatory activity of alkaloids: an update from 2000 to 2010," *Molecules*, vol. 16, no. 10, pp. 8515–8534, 2011.
- [26] B. Debnath, W. S. Singh, M. Das et al., "Role of plant alkaloids on human health: a review of biological activities," *Materials Today Chemistry*, vol. 9, pp. 56–72, 2018.
- [27] S. Bunsupa, M. Yamazaki, and K. Saito, "Lysine-derived alkaloids: overview and update on biosynthesis and medicinal applications with emphasis on quinolizidine alkaloids," *Mini-Reviews in Medicinal Chemistry*, vol. 17, no. 12, pp. 1002–1012, 2017.
- [28] A. Roy, "A review on the alkaloids an important therapeutic compound from plants," *International Journal of Plant Biotechnology*, vol. 3, no. 2, pp. 1–9, 2017.
- [29] Y. Li, R. Sattler, E. J. Yang et al., "Harmine, a natural beta-carboline alkaloid, upregulates astroglial glutamate transporter expression," *Neuropharmacology*, vol. 60, no. 7–8, pp. 1168–1175, 2011.
- [30] L. A. Mohamed, S. Markandaiah, S. Bonanno, P. Pasinelli, and D. Trotti, "Blood–brain barrier driven pharmacoresistance in amyotrophic lateral sclerosis and challenges for effective drug therapies," *AAPS Journal*, vol. 19, no. 6, pp. 1600–1614, 2017.
- [31] D. Lopez and S. Martinez-Luis, "Marine natural products with P-glycoprotein inhibitor properties," *Marine Drugs*, vol. 12, no. 1, pp. 525–546, 2014.
- [32] A. A. Skhalyakhov, H. R. Siyukhov, and Z. T. Tazova, "Phenolic compounds and antioxidant potential of wild-growing plant materials of the North Caucasus region," *International Journal of Engineering and Advanced Technology*, vol. 9, no. 2, pp. 5062–5071, 2019.
- [33] P. Roy, S. Amdekar, A. Kumar, and V. Singh, "Preliminary study of the antioxidant properties of flowers and roots of *Pyrostegia venusta* (Ker Gawl) Miers," *BMC Complementary and Alternative Medicine*, vol. 11, no. 1, pp. 1–8, 2011.
- [34] V. Palomo, I. D. Perez, C. Gil, and A. Martínez, "The potential role of glycogen synthase kinase 3 inhibitors as amyotrophic lateral sclerosis pharmacological therapy," *Current Medicinal Chemistry*, vol. 18, no. 20, pp. 3028–3034, 2011.
- [35] S. Hossain, M. El-Sayed, and H. Aoshima, "Antioxidative and anti- α -amylase activities of four wild plants consumed by pastoral nomads in Egypt," *Oriental Pharmacy and Experimental Medicine*, vol. 9, no. 3, pp. 217–224, 2009.
- [36] B. L. Nanda, "Determination of phytochemicals and antioxidant activity of *Acorus Calamus Rhizome*," *Journal of Drug Delivery and Therapeutics*, vol. 4, no. 6, pp. 117–121, 2014.
- [37] N. Cortes, C. Castañeda, E. H. Osorio, G. P. Cardona-Gomez, and E. Osorio, "Amaryllidaceae alkaloids as agents with protective effects against oxidative neural cell injury," *Life Sciences*, vol. 203, pp. 54–65, 2018.
- [38] F. T. Zohora, S. N. Islam, S. A. Khan, C. M. Hasan, and M. Ahsan, "Antioxidant, cytotoxic, thrombolytic and antimicrobial activity of *Zanthoxylum rhetsa* root bark with two isolated quinolone alkaloids," *Pharmacology & Pharmacy*, vol. 10, no. 3, pp. 137–145, 2019.
- [39] H. H. F. Koolen, E. M. F. Pral, S. C. Alfieri et al., "Antiprotozoal and antioxidant alkaloids from *Alternanthera littoralis*," *Phytochemistry*, vol. 134, pp. 106–113, 2017.
- [40] C. B. Azevedo, M. Roxo, C. M. Borges et al., "Antioxidant activity of an aqueous leaf extract from *Uncaria tomentosa* and its major alkaloids mitraphylline and isomitraphylline in *Caenorhabditis elegans*," *Molecules*, vol. 24, no. 18, p. 3299, 2019.
- [41] A. K. O. Aldulaimi, S. S. Azziz, Y. M. Bakri et al., "Two New isoquinoline alkaloids from the bark of *Alphonsea cylindrica* King and their antioxidant activity," *Phytochemistry Letters*, vol. 29, pp. 110–114, 2019.
- [42] A. Mundaragi, D. Thangadurai, K. A. A. Appaiah, C. J. Dandin, and J. Sangeetha, "Physicochemical characterization, antioxidant potential and sensory quality of wine from wild edible fruits of *Flacourtia montana* J. Graham," *Brazilian Archives of Biology and Technology*, vol. 62, pp. 1–12, 2019.
- [43] C. O. Akoto, A. A. Acheampong, P. D. Tagbor, and K. Bortey, "Determination of the antimicrobial and antioxidant activities of the leaf extracts of *Griffonia simplicifolia*," *Journal of*

- Pharmacognosy and Phytochemistry*, vol. 9, no. 2, pp. 537–545, 2020.
- [44] A. Sikandar, M. Zhang, Y. Wang et al., “Mycochemical screening and analysis, antioxidant activity, and biochemical composition of fermentation strain Snef1216 (*Penicillium chrysogenum*),” *Journal of Analytical Methods in Chemistry*, vol. 2020, Article ID 3073906, 8 pages, 2020.
- [45] M. A. Rahman, M. R. Rahman, T. Zaman et al., “Emerging potential of naturally occurring autophagy modulator against neurodegeneration,” *Current Pharmaceutical Design*, vol. 26, no. 7, pp. 4–6, 2020.
- [46] D. J. McNally, K. Wurms, C. Labbé, and R. R. Bélanger, “A standardized methodology for the study of induced glycosylated plant phenolics,” *Canadian Journal of Plant Pathology*, vol. 24, no. 4, pp. 429–436, 2002.
- [47] T. B. Soares, L. Loureiro, A. Carvalho et al., “Lipid nanocarriers loaded with natural compounds: potential new therapies for age related neurodegenerative diseases?,” *Progress in Neurobiology*, vol. 168, pp. 21–41, 2018.
- [48] L. Wen, Y. Tan, S. Dai et al., “VEGF-mediated tight junctions pathological fenestration enhances doxorubicin-loaded glycolipid-like nanoparticles traversing bbb for glioblastoma-targeting therapy,” *Drug Delivery*, vol. 24, no. 1, pp. 1843–1855, 2017.
- [49] P. G. Pietta, “Flavonoids as antioxidants,” *Journal of Natural Products*, vol. 63, no. 7, pp. 1035–1042, 2000.
- [50] A. N. Winter, E. K. Ross, H. M. Wilkins et al., “An anthocyanin-enriched extract from strawberries delays disease onset and extends survival in the hSOD1G93A mouse model of amyotrophic lateral sclerosis,” *Nutritional Neuroscience*, vol. 21, no. 6, pp. 414–426, 2017.
- [51] C. L. Bordignon Junior, V. Francescato, A. A. Nienow, E. Calvete, and F. H. Reginatto, “Influence of the extraction solution pH on the content of anthocyanins in strawberry fruits,” *Food Science and Technology*, vol. 29, no. 1, pp. 183–188, 2009.
- [52] M. L. Cardoso, J. P. V. Leite, and M. C. G. Peluzio, “Biological effects of anthocyanins on the atherosclerotic process,” *Colombian Journal of Chemical and Pharmaceutical Sciences*, vol. 40, no. 1, 2011.
- [53] D. R. Sari, A. Safitri, J. R. Cairns, and F. Fatchiyah, “Anti-apoptotic activity of anthocyanins has potential to inhibit caspase-3 signaling,” *Journal of Tropical Life Science*, vol. 10, no. 1, pp. 15–25, 2020.
- [54] E. Srinivasan and R. Rajasekaran, “Comparative binding of kaempferol and kaempferide on inhibiting the aggregate formation of mutant (G85R) SOD1 protein in familial amyotrophic lateral sclerosis: a quantum chemical and molecular mechanics study,” *BioFactors*, vol. 44, no. 5, pp. 431–442, 2018.
- [55] T. Ueda, M. Inden, K. Shirai et al., “The effects of Brazilian green propolis that contains flavonols against mutant copper-zinc superoxide dismutase-mediated toxicity,” *Scientific Reports*, vol. 7, no. 1, pp. 1–11, 2017.
- [56] T. H. Wang, S. Y. Wang, X. D. Wang et al., “Fisetin exerts antioxidant and neuroprotective effects in multiple mutant hSOD1 models of amyotrophic lateral sclerosis by activating ERK,” *Neuroscience*, vol. 379, pp. 152–166, 2018.
- [57] P. Ip, P. R. Sharda, A. Cunningham, S. Chakrabarty, V. Pande, and A. Chakrabarty, “Quercitrin and quercetin 3- β -d-glucoside as chemical chaperones for the A4V SOD1 ALS-causing mutant,” *Protein Engineering, Design and Selection*, vol. 30, no. 6, pp. 431–440, 2017.
- [58] F. Jiang, S. De Silva, and J. Turnbull, “Beneficial effect of ginseng root in SOD-1 (G93A) transgenic mice,” *Journal of the Neurological Sciences*, vol. 180, no. 1-2, pp. 52–54, 2000.
- [59] O. T. Korkmaz, N. Ayta, I. Carreras et al., “7,8-Dihydroxyflavone improves motor performance and enhances lower motor neuronal survival in a mouse model of amyotrophic lateral sclerosis,” *Neuroscience Letters*, vol. 566, pp. 286–291, 2014.
- [60] V. Joshi, R. Mishra, A. Upadhyay et al., “Polyphenolic flavonoid (myricetin) upregulated proteasomal degradation mechanisms: eliminates neurodegenerative proteins aggregation,” *Journal of Cellular Physiology*, vol. 234, no. 11, pp. 20900–20914, 2019.
- [61] Y. Shimmyo, T. Kihara, A. Akaike, T. Niidome, and H. Sugimoto, “Three distinct neuroprotective functions of myricetin against glutamate-induced neuronal cell death: involvement of direct inhibition of caspase-3,” *Journal of Neuroscience Research*, vol. 86, no. 8, pp. 1836–1845, 2008.
- [62] D. R. Sharma, W. Y. Wani, A. Sunkaria et al., “Quercetin attenuates neuronal death against aluminum-induced neurodegeneration in the rat hippocampus,” *Neuroscience*, vol. 324, pp. 163–176, 2016.
- [63] X. Zhuang, B. Zhao, S. Liu et al., “Noncovalent interactions between superoxide dismutase and flavonoids studied by native mass spectrometry combined with molecular simulations,” *Analytical Chemistry*, vol. 88, no. 23, pp. 11720–11726, 2016.
- [64] A. Elmann, A. Telerman, R. Ofir, and Y. Kashman, “Glutamate toxicity to differentiated neuroblastoma N2a cells is prevented by the sesquiterpene lactone achillolide A and the flavonoid 3, 5, 4'-trihydroxy-6, 7, 3'-trimethoxyflavone from *Achillea fragrantissima*,” *Journal of Molecular Neuroscience*, vol. 62, no. 1, pp. 99–105, 2017.
- [65] R. Mogana, K. T. Jin, and C. Wiart, “Anti-inflammatory, anticholinesterase, and antioxidant potential of scopoletin isolated from *Canarium patentinervium* Miq. (*Burseraceae* Kunth),” *Evidence-based complementary and alternative medicine*, vol. 2013, Article ID 734824, 7 pages, 2013.
- [66] G. P. Kumar, T. Anand, D. Singsit, F. Khanum, and K. R. Anilakumar, “Evaluation of antioxidant and anti-fatigue properties of *Trigonella foenum-graecum* L. in rats subjected to weight loaded forced swim test,” *Pharmacognosy Journal*, vol. 5, no. 2, pp. 66–71, 2013.
- [67] S. C. Barber, A. Higginbottom, R. J. Mead, S. Barber, and P. J. Shaw, “An in vitro screening cascade to identify neuroprotective antioxidants in ALS,” *Free Radical Biology and Medicine*, vol. 46, no. 8, pp. 1127–1138, 2009.
- [68] M. A. Hasnat, M. Pervin, and B. O. Lim, “Acetylcholinesterase inhibition and in vitro and in vivo antioxidant activities of *Ganoderma lucidum* grown on germinated brown rice,” *Molecules*, vol. 18, no. 6, pp. 6663–6678, 2013.
- [69] L. Li and N. P. Seeram, “Maple syrup phytochemicals include lignans, coumarins, a stilbene, and other previously unreported antioxidant phenolic compounds,” *Journal of Agricultural and Food Chemistry*, vol. 58, no. 22, pp. 11673–11679, 2010.
- [70] E. P. Pereira, S. Braga-de-Souza, C. C. Santos et al., “Amburana cearensis seed extracts protect PC-12 cells against toxicity induced by glutamate,” *Brazilian Journal of Pharmacognosy*, vol. 27, no. 2, pp. 199–205, 2017.

- [71] Y. J. Moon, J. Y. Lee, M. S. Oh et al., "Inhibition of inflammation and oxidative stress by *Angelica dahuricae* radix extract decreases apoptotic cell death and improves functional recovery after spinal cord injury," *Journal of Neuroscience Research*, vol. 90, no. 1, pp. 243–256, 2012.
- [72] S. J. Park, J. H. Yoon, Y. E. Kim, W. B. Yoon, and J. D. Kim, "In vitro antioxidant activity of the aqueous of *Angelicae gigas Nakai* leaves," *Korean Journal of Food Preservation*, vol. 18, no. 6, pp. 817–823, 2011.
- [73] K. S. Ryu, N. D. Hong, N. J. Kim, and Y. Y. Kong, "Studies on the coumarin constituents of the root of *Angelica gigas Nakai* isolation of decursinol angelate and assay of decursinol angelate and decursin," *Korean Journal of Pharmacognosy*, vol. 21, no. 1, pp. 64–68, 1990.
- [74] Y. Song, L. Pan, W. Li et al., "Natural neuro-inflammatory inhibitors from *Caragana turfanensis*," *Bioorganic & Medicinal Chemistry Letters*, vol. 27, no. 20, pp. 4765–4769, 2017.
- [75] A. M. Morgan, J. H. Kim, H. W. Lee et al., "Phytochemical constituents from the aerial part of *Ducrosia ismaelis Asch.*" *Natural Product Sciences*, vol. 21, pp. 6–13, 2015.
- [76] M. V. Krishnapriya, T. Sumathi, A. Chinnasamy, G. Balakrishnan, and P. Renjith, "Comparative analysis of potentiality of esculin and hinokitol (B-thujaplicin) as anti-parkinsonism drugs: a pilot *in silico* study," *International Journal of Pharmacy and Pharmaceutical Sciences*, vol. 9, no. 1, pp. 108–115, 2017.
- [77] M. Nakamura, T. Suzuki, M. Takagi, H. Tamura, and T. Masuda, "Stimulation of phosphorylation of ERK and CREB by phellopterin and auraptene isolated from *Citrus junos*," *Natural product communications*, vol. 9, no. 10, 2014.
- [78] M. S. Butler, "Natural products to drugs: natural product derived compounds in clinical trials," *Natural Product Reports*, vol. 22, no. 2, pp. 162–195, 2005.
- [79] B. Morrison, K. Hensley, E. P. Pioro, S. Petri, and M. Kiaei, "Amyotrophic lateral sclerosis and novel therapeutic strategies," *Neurology Research International*, vol. 2012, Article ID 798028, 3 pages, 2012.
- [80] F. J. B. Mendonça-Junior, M. T. Scotti, A. Nayariseri, E. N. T. Zondegoumba, and L. Scotti, "Natural bioactive products with antioxidant properties useful in neurodegenerative diseases," *Oxidative Medicine and Cellular Longevity*, vol. 2019, Article ID 7151780, 2 pages, 2019.
- [81] C. Casalini, M. Lodovici, C. Briani et al., "Effect of complex polyphenols and tannins from red wine (WCPT) on chemically induced oxidative DNA damage in the rat," *European Journal of Nutrition*, vol. 38, no. 4, pp. 190–195, 1999.
- [82] L. Giovannelli, G. Testa, C. de Filippo, V. Cheyner, M. N. Clifford, and P. Dolara, "Effect of complex polyphenols and tannins from red wine on DNA oxidative damage of rat colon mucosa *in vivo*," *European Journal of Nutrition*, vol. 39, no. 5, pp. 207–212, 2000.
- [83] O. I. Aruoma, T. Bahorun, and L. S. Jen, "Neuroprotection by bioactive components in medicinal and food plant extracts," *Mutation Research*, vol. 544, no. 2-3, pp. 203–215, 2003.
- [84] J. Serrano, R. Puupponen-Pimiä, A. Dauer, A. M. Aura, and F. Saura-Calixto, "Tannins: current knowledge of food sources, intake, bioavailability and biological effects," *Molecular Nutrition Food Research*, vol. 53, pp. 310–329, 2009.
- [85] B. Auddy, M. Ferreira, F. Blasina et al., "Screening of antioxidant activity of three Indian medicinal plants, traditionally used for the management of neurodegenerative diseases," *Journal of Ethnopharmacology*, vol. 84, no. 2-3, pp. 131–138, 2003.
- [86] A. Banerjee et al., "In vitro study of antioxidant activity of fruit," *Food Chemistry*, vol. 90, no. 4, pp. 727–733, 2005.
- [87] C. A. Rice-evans, N. J. Miller, P. G. Bolwell, P. M. Bramley, and J. B. Pridham, "The relative antioxidant activities of plant derived polyphenolic flavonoids," *Free Radical Research*, vol. 22, pp. 375–383, 1995.
- [88] Y. Qingming, P. Xianhui, K. Weibao et al., "Antioxidant activities of malt extract from barley (*Hordeum vulgare L.*) toward various oxidative stress *in vitro* and *in vivo*," *Food Chemistry*, vol. 118, no. 1, pp. 84–89, 2010.
- [89] R. Mahesh, K. Nagulendran, S. Velavan, T. Ramesh, and V. Hazeena Begum, "Studies on the antioxidative and free radical scavenging activities of *myrobalan (terminaliachebularetz)* through various *in vitro* models," *Pharmacology*, vol. 2, pp. 1–11, 2007.
- [90] I. Ginsburg, L. Rozenstein-Tsalkovich, E. Koren, and H. Rosenmann, "The herbal preparation Padma® 28 protects against neurotoxicity in PC12 cells," *Phytotherapy Research*, vol. 25, no. 5, pp. 740–743, 2011.
- [91] C. L. Chang, C. S. Lin, and G. H. Lai, "Phytochemical characteristics, free radical scavenging activities, and neuroprotection of five medicinal plant extracts," *Evidence-Based Complementary and Alternative Medicine*, vol. 2012, Article ID 984295, 8 pages, 2012.
- [92] O. Adewale, A. Onasanya, A. Fadaka et al., "In vitro antioxidant effect of aqueous extract of *Solanum macrocarpon* leaves in rat liver and brain," *Oxidants and Antioxidants in Medical Science*, vol. 3, no. 3, pp. 225–229, 2014.
- [93] B. Hamamcioglu, F. G. Kocanci, and B. Aslim, "Phytochemical screening and evaluation of neuroprotective, anti-mutagenic and anti-genotoxic effects of Turkish endemic *Glaucium acutidentatum*," *South African Journal of Botany*, vol. 117, pp. 232–239, 2018.
- [94] P. J. Mitchell, J. C. Hanson, A. T. Quets-Nguyen, M. Bergeron, and R. C. Smith, "A quantitative method for analysis of *in vitro* neurite outgrowth," *Journal of Neuroscience Methods*, vol. 164, no. 2, pp. 350–362, 2007.
- [95] G. P. Kumar and F. Khanum, "Neuroprotective potential of phytochemicals," *Pharmacognosy Reviews*, vol. 6, no. 12, pp. 81–90, 2012.
- [96] X. Jin, M. Y. Liu, D. F. Zhang et al., "Natural products as a potential modulator of microglial polarization in neurodegenerative diseases," *Pharmacological Research*, vol. 145, p. 104253, 2019.
- [97] D. Li, D. Liu, M. Lv, P. Gao, and X. Liu, "Isolation of triterpenoid saponins from *Medicago sativa L.* with neuroprotective activities," *Bioorganic & Medicinal Chemistry Letters*, vol. 30, no. 4, p. 126956, 2020.
- [98] M. Kiaei, K. Kipiani, S. Petri, J. Chen, N. Y. Calingasan, and M. F. Beal, "Celastrol blocks neuronal cell death and extends life in transgenic mouse model of amyotrophic lateral sclerosis," *Neurodegenerative Diseases*, vol. 2, no. 5, pp. 246–254, 2005.
- [99] P. Pahwa and R. K. Goel, "*Asparagus adscendens* root extract enhances cognition and protects against scopolamine induced amnesia: an *in-silico* and *in-vivo* studies," *Chemico-Biological Interactions*, vol. 260, no. 25, pp. 208–218, 2016.
- [100] J. Lee, K. Song, E. Huh, M. S. Oh, and Y. S. Kim, "Neuroprotection against 6-OHDA toxicity in PC12 cells and mice

- through the Nrf2 pathway by a sesquiterpenoid from *Tussilago farfara*,” *Redox Biology*, vol. 18, pp. 6–15, 2018.
- [101] D. E. Sok, H. Cui, and M. Kim, “Isolation and Bioactivities of furfuran type lignan compounds from edible plants,” *Recent Patents on Food, Nutrition & Agriculture*, vol. 1, no. 1, pp. 87–95, 2009.
- [102] L. Tavares, G. J. McDougall, S. Fortalezas, D. Stewart, R. B. Ferreira, and C. N. Santos, “The neuroprotective potential of phenolic-enriched fractions from four *Juniperus* species found in Portugal,” *Food Chemistry*, vol. 135, no. 2, pp. 562–570, 2012.
- [103] C. Wiart, *Chapter 3 – Phenolics, Lead Compounds from Medicinal Plants for the Treatment of Neurodegenerative Diseases*, 2014.
- [104] V. Lahaie-Collins, J. Bournival, M. Plouffe, J. Carange, and M. G. Martinoli, “Sesamin modulates tyrosine hydroxylase, superoxide dismutase, catalase, inducible NO synthase and interleukin-6 expression in dopaminergic cells under MPP+ induced oxidative stress,” *Oxidative Medicine and Cellular Longevity*, vol. 1, Article ID 875974, 9 pages, 2008.
- [105] R. Q. Mei, Y. H. Wang, G. H. du, G. M. Liu, L. Zhang, and Y. X. Cheng, “Antioxidant lignans from the fruits of *Broussonetia papyrifera*,” *Journal Natural Products*, vol. 72, no. 4, pp. 621–625, 2009.
- [106] S. Shimoyoshi, D. Takemoto, Y. Ono et al., “Sesame lignans suppress age-related cognitive decline in senescence-accelerated mice,” *Nutrients*, vol. 11, no. 7, p. 1582, 2019.
- [107] H. Erlank, A. Elmann, R. Kohen, and J. Kanner, “Polyphenols activate Nrf2 in astrocytes via H₂O₂, semiquinones, and quinones,” *Free Radical Biology and Medicine*, vol. 51, no. 12, pp. 2319–2327, 2011.
- [108] M. Iranshahy, M. Iranshahi, S. R. Abtahi, and G. Karimi, “The role of nuclear factor erythroid 2-related factor 2 in hepatoprotective activity of natural products: a review,” *Food and Chemical Toxicology*, vol. 120, pp. 261–276, 2018.
- [109] K. Lu, C. Zhang, W. Wu, M. Zhou, Y. Tang, and Y. Peng, “Rhubarb extract has a protective role against radiation-induced brain injury and neuronal cell apoptosis,” *Molecular Medicine Reports*, vol. 12, no. 2, pp. 2689–2694, 2015.
- [110] K. de la Vega-Hernández, M. Antuch, O. Cuesta-Rubio, Y. Núñez-Figueroa, and G. L. Pardo-Andreu, “Discerning the antioxidant mechanism of rapanone: a naturally occurring benzoquinone with iron complexing and radical scavenging activities,” *Journal of Inorganic Biochemistry*, vol. 170, pp. 134–147, 2017.
- [111] S. M. Astuti, A. M. Mimi Sakinah, B. M. Retno Andayani, and A. Risch, “Determination of saponin compound from *Anredera cordifolia* (Ten) Steenis plant (*binahong*) to potential treatment for several diseases,” *Journal of Agricultural Science*, vol. 3, no. 4, 2011.
- [112] L. Ravi, V. Manasvi, and L. B. Praveena, “Antibacterial and antioxidant activity of saponin from *Abutilon indicum* leaves,” *Asian Journal of Pharmaceutical and Clinical Research*, vol. 9, no. 9, pp. 344–347, 2016.
- [113] S. Liu, G. Li, H. Tang et al., “Madecassoside ameliorates lipopolysaccharide-induced neurotoxicity in rats by activating the Nrf2-HO⁻¹ pathway,” *Neuroscience Letters*, vol. 709, p. 134386, 2019.
- [114] X. Zhang, Y. L. Hong, D. S. Xu et al., “A review of experimental research on herbal compounds in amyotrophic lateral sclerosis,” *Phytotherapy Research*, vol. 28, no. 1, pp. 9–21, 2014.
- [115] A. O. Sasmita, A. P. K. Ling, K. G. L. Voon, R. Y. Koh, and Y. P. Wong, “Madecassoside activates anti-neuroinflammatory mechanisms by inhibiting lipopolysaccharide-induced microglial inflammation,” *International Journal of Molecular Medicine*, vol. 41, no. 5, pp. 3033–3040, 2018.
- [116] K. Rani, M. Tyagi, M. Mazumder et al., “Accelerated identification of serine racemase inhibitor from *Centella asiatica*,” *Scientific Reports*, vol. 10, no. 4640, pp. 1–12, 2020.
- [117] M. Cai and E. J. Yang, “Ginsenoside Re attenuates neuroinflammation in a symptomatic ALS animal model,” *The American Journal of Chinese Medicine*, vol. 44, no. 2, pp. 401–413, 2016.
- [118] G. Ratheesh, L. Tian, J. R. Venugopal et al., “Role of medicinal plants in neurodegenerative diseases,” *Bio-manuf Reviews*, vol. 2, no. 1, pp. 1–16, 2017.
- [119] Z. A. Ratan, M. F. Haidere, Y. H. Hong et al., “Pharmacological potential of ginseng and its major component ginsenosides,” *Journal of Ginseng Research*, pp. 1–36, 2020.
- [120] J. Yu, M. Guo, Y. Li et al., “Astragaloside IV protects neurons from microglia-mediated cell damage through promoting microglia polarization,” *Folia Neuropathologica*, vol. 57, no. 2, pp. 170–181, 2019.
- [121] A. Sun, X. Xu, J. Lin, X. Cui, and R. Xu, “Neuroprotection by saponins,” *Phytotherapy Research*, vol. 29, no. 2, pp. 187–200, 2014.
- [122] X. C. Chen, Y. G. Zhu, L. A. Zhu et al., “Ginsenoside Rg1 attenuates dopamine-induced apoptosis in PC12 cells by suppressing oxidative stress,” *European Journal of Pharmacology*, vol. 473, no. 1, pp. 1–7, 2003.
- [123] Q. Liu, J. P. Kou, and B. Y. Yu, “Ginsenoside Rg1 protects against hydrogen peroxide-induced cell death in PC12 cells via inhibiting NF- κ B activation,” *Neurochemistry International*, vol. 58, no. 1, pp. 119–125, 2011.
- [124] S. Zoccolella, A. Santamato, and P. Lamberti, “Current and emerging treatments for amyotrophic lateral sclerosis,” *Neuropsychiatric Disease and Treatment*, vol. 5, pp. 577–595, 2009.
- [125] A. Onatibia-Astibia, R. Franco, and E. Martínez-Pinilla, “Health benefits of methyl xanthines in neurodegenerative diseases,” *Molecular Nutrition & Food Research*, vol. 61, no. 6, pp. 1–47, 2017.
- [126] J. Monteiro, M. G. Alves, P. F. Oliveira, and B. M. Silva, “Pharmacological potential of methylxanthines: retrospective analysis and future expectations,” *Critical Reviews in Food Science and Nutrition*, vol. 59, no. 16, pp. 2597–2625, 2019.
- [127] P. K. Sonsalla, L. Y. Wong, S. L. Harris et al., “Delayed caffeine treatment prevents nigral dopamine neuron loss in a progressive rat model of Parkinson’s disease,” *Experimental Neurology*, vol. 234, no. 2, pp. 482–487, 2012.
- [128] N. Dragicevic, V. Delic, C. Cao et al., “Caffeine increases mitochondrial function and blocks melatonin signaling to mitochondria in Alzheimer’s mice and cells,” *Neuropharmacology*, vol. 63, no. 8, pp. 1368–1379, 2012.
- [129] E. Fondell, É. I. J. O’Reilly, K. C. Fitzgerald et al., “Intakes of caffeine, coffee and tea and risk of amyotrophic lateral sclerosis: results from five cohort studies,” *Amyotrophic Lateral Sclerosis and Frontotemporal Degeneration*, vol. 16, no. 5-6, pp. 366–371, 2015.
- [130] M. K. Olahdouzan and M. J. Hamadeh, “The neuroprotective effects of caffeine in neurodegenerative diseases,” *CNS Neuroscience and Therapeutic*, vol. 23, no. 4, pp. 272–290, 2017.

- [131] L. Herden and R. Weissert, "The impact of coffee and caffeine on multiple sclerosis compared to other neurodegenerative diseases," *Frontiers in Nutrition*, vol. 5, no. 133, pp. 1–12, 2018.
- [132] E. Beghi, E. Pupillo, P. Messina et al., "Coffee and amyotrophic lateral sclerosis: a possible preventive role," *American Journal of Epidemiology*, vol. 174, no. 9, pp. 1002–1008, 2011.
- [133] N. Z. B. Rani, K. Husain, and E. Kumolosasi, "Moringa genus: a review of phytochemistry and pharmacology," *Frontiers in Pharmacology*, vol. 9, no. 108, pp. 1–26, 2018.
- [134] O. O. Igado and J. O. Olopade, "A review on the possible neuroprotective effects of *Moringa oleifera*," *Nigerian Journal of Physiological Sciences*, vol. 31, no. 2, pp. 183–187, 2016.
- [135] M. S. Jaafaru, N. A. Abd Karim, M. E. Enas, P. Rollin, E. Mazzon, and A. F. Abdull Razis, "Protective effect of glucosinolates hydrolytic products in neurodegenerative diseases (NDDs)," *Nutrients*, vol. 10, no. 580, pp. 1–15, 2018.
- [136] M. Galuppo, S. Giacoppo, R. Iori, G. R. de Nicola, P. Bramanti, and E. Mazzon, "Administration of 4-(α -L-Rhamnosyloxy)-benzyl isothiocyanate delays disease phenotype in SOD1G93ARats: a transgenic model of amyotrophic lateral sclerosis," *BioMed Research International*, vol. 2015, Article ID 259417, 12 pages, 2015.
- [137] M. S. Jaafaru, N. Nordin, R. Rosli et al., "Prospective role of mitochondrial apoptotic pathway in mediating GMG-ITC to reduce cytotoxicity in H₂O₂-induced oxidative stress in differentiated SH-SY5Y cells," *Biomedicine and Pharmacotherapy*, vol. 119, p. 109445, 2019.
- [138] Z. Liu, T. Zhou, A. C. Ziegler, P. Dimitrion, and L. Zuo, "Oxidative stress in neurodegenerative diseases: from molecular mechanisms to clinical applications," *Oxidative Medicine and Cellular Longevity*, vol. 2017, Article ID 2525967, 11 pages, 2017.
- [139] J. L. G. Aguiar, "Lipid biomarkers for amyotrophic lateral sclerosis," *Frontiers in Neurology*, vol. 10, no. 284, pp. 1–6, 2019.
- [140] E. F. Boumil, R. B. Vohnoutka, Y. Liu, S. Lee, and T. B. Shea, "Omega-3 hastens and omega-6 delays the progression of neuropathology in a murine model of familial ALS," *The Open Neurology Journal*, vol. 11, no. 1, pp. 84–91, 2017.
- [141] T. W. Tefera, Y. Wong, M. E. Barkl-Luke et al., "Triheptanoin protects motor neurons and delays the onset of motor symptoms in a mouse model of amyotrophic lateral sclerosis," *PLoS One*, vol. 11, no. 8, pp. 1–24, 2016.
- [142] P. Diaz-Amarilla, E. Miquel, A. Trostchansky et al., "Electrophilic nitro-fatty acids prevent astrocyte-mediated toxicity to motor neurons in a cell model of familial amyotrophic lateral sclerosis via nuclear factor erythroid 2-related factor activation," *Free Radical Biology and Medicine*, vol. 95, pp. 112–120, 2016.
- [143] A. Trostchansky, M. Mastrogiovanni, E. Miquel et al., "Profile of arachidonic acid-derived inflammatory markers and its modulation by nitro-oleic acid in an inherited model of amyotrophic lateral sclerosis," *Frontiers in Molecular Neuroscience*, vol. 11, no. 131, 2018.
- [144] P. Torres, D. Cacabelos, J. Pairada et al., "Gender-specific beneficial effects of docosahexaenoic acid dietary supplementation in G93A-SOD1 amyotrophic lateral sclerosis mice," *Neurotherapeutics*, vol. 17, no. 1, pp. 269–281, 2020.

Research Article

Curcumin Attenuates Chronic Unpredictable Mild Stress-Induced Depressive-Like Behaviors via Restoring Changes in Oxidative Stress and the Activation of Nrf2 Signaling Pathway in Rats

Dehua Liao,¹ Chuanfeng Lv,² Lizhi Cao,¹ Dunwu Yao,¹ Yi Wu,¹ Minghui Long,¹ Ni Liu ¹ and Pei Jiang ²

¹Department of Pharmacy, Hunan Cancer Hospital, Changsha, 410013 Hunan, China

²Institute of Clinical Pharmacy & Pharmacology, Jining First People's Hospital, Jining, 272000 Shandong, China

Correspondence should be addressed to Ni Liu; liuni@hnca.org.cn and Pei Jiang; jiangpeicsu@sina.com

Received 14 April 2020; Revised 21 August 2020; Accepted 27 August 2020; Published 18 September 2020

Academic Editor: Francisco Jaime B. Mendonça Junior

Copyright © 2020 Dehua Liao et al. This is an open access article distributed under the Creative Commons Attribution License, which permits unrestricted use, distribution, and reproduction in any medium, provided the original work is properly cited.

Accumulating evidence has demonstrated that oxidative stress is associated with depression. Our present study aimed at investigating the antidepressant effect and the possible mechanisms of curcumin (CUR) in chronic unpredictable mild stress-(CUMS-) induced depression model in rats. After exposure to CUMS for four weeks, the rats showed depressive-like behavior, and the depressive-like behaviors in CUMS-treated rats were successfully corrected after administration of CUR. In addition, CUR could effectively decrease protein expression of oxidative stress markers (Nox2, 4-HNE, and MDA) and increase the activity of CAT. CUR treatment also reversed CUMS-induced inhibition of Nrf2-ARE signaling pathway, along with increasing the mRNA expression of NQO-1 and HO-1. Furthermore, the supplementation of CUR also increased the ratio of pCREB/CREB and synaptic-related protein (BDNF, PSD-95, and synaptophysin). In addition, CUR could effectively reverse CUMS-induced reduction of spine density and total dendritic length. In conclusion, the study revealed that CUR relieves depressive-like state through the mitigation of oxidative stress and the activation of Nrf2-ARE signaling pathway.

1. Introduction

As one of the most common neuropsychiatric illness, depression has affected 300 million people of all ages in the modern world [1]. According to the WHO's prediction, depression is expected to become the world's second leading cause of disability by 2020 [2], leading to a huge social and economic burden on the modern society [3]. In currently clinical practice, many chemical treatments are used for depression, such as tricyclic antidepressants, monoamine oxidase inhibitors, and selective serotonin reuptake inhibitors [4, 5]. However, the existing treatments were not effective to all patients [6] and also accompanied with unwanted side effects [7, 8]. Thus, it is necessary to develop a more effective and safer pharmacological intervention.

Increasing evidence suggested that oxidative stress is responsible for the development of depression [9]. Oxidative stress mainly focused on brain which has a limited

amount of antioxidant capacity [10]. It was reported that antidepressants could effectively reduced oxidative damage in depressed patients [11, 12]. The antioxidant subjects like polyphenolic compounds exhibit antidepressant activity in experimentally induced depression models by modulating the brain oxidative stress status [13].

Oxidative stress is an etiologic factor in depressive/neurodegenerative disorders that it is often accompanied by deregulation of nuclear factor erythroid-2-related factor 2 (Nrf2) pathway, a key antioxidant mechanism indicated as a promising target for treatment of depression [14]. As a pivotal transcription factor, Nrf2 was involved in the regulation of the antioxidant response in the brain. Under oxidative stress circumstances, Nrf2 isolate from Kelch-like ECH-associated protein 1 (Keap1) and translocate from cytoplasm into the nucleus [15, 16]. Furthermore, antioxidant response element (ARE) could be upregulated after the activation of the Nrf2 and finally regulates the expressions of a variety

of antioxidant enzymes like heme oxygenase-1 (HO-1) and NADPH: quinone oxidoreductase-1 (NQO-1) [17, 18]. Buendia et al. [19] has reported that Nrf2-ARE pathway is proved to reduce oxidative stress and neuroinflammation and play a protective role in neurodegenerative diseases.

Numerous evidence has indicated that depression was associated with a range of changes in synaptic form [20, 21]. Cyclic AMP response element-binding protein (CREB) was a major transcription factor involved in the regulation of genes associated with synaptic and neural plasticity. As an important neurotrophic factor, brain-derived neurotrophic factor (BDNF) supports growth and survival of neurons. Recent study has showed that CREB-BDNF signaling pathway in hippocampus was closely related to depression and the pathogenesis of cognitive function impairments [22]. PSD-95 and synaptophysin were postsynaptic marker and presynaptic marker, respectively, which play an important role in the maintenance of synaptic plasticity.

Curcumin (CUR) is the major active component extracted from *Curcuma longa*, which exhibited anti-inflammatory, antioxidant, immunomodulatory, and neuroprotective activities [23, 24]. It has been increasingly recognized that CUR has the potential to cross blood brain barrier and exert antidepressant-like action. Xu et al. have reported that chronic administration of CUR produced a significant antidepressant property in the treatment of depression in mice model [25]. Notably, CUR's antioxidative properties hold a great deal of potential for the treatment of depression. More and more evidences also showed that the activation of Nrf2 was the main mechanism of CUR in the treatment of oxidant stress-related diseases [26, 27]. Shen et al. have reported that CUR exerts its chemopreventive effects via the induction of antioxidant enzymes by activating Nrf2-ARE signaling [28]. Oxidative stress in the diabetic rat-induced by STZ could be attenuated by CUR through activation of the Keap1-Nrf2-ARE signaling pathway [29]. In addition, CUR augments the cardioprotective effect of metformin in an experimental model of type I diabetes mellitus via the Nrf2/HO-1 pathway which is also reported in previous study [30]. However, the detailed mechanism underlying the antidepressant effects of CUR as related to Nrf2 in the brain remains seldom studied.

Therefore, in our present study, we aimed to investigate the antidepressant-like effect of CUR in CUMS-induced rats. In addition, to further investigate the possible molecular mechanisms underlying the therapeutic effects of CUR, we also assessed whether the possible antidepressant-like effects of CUR are associated with oxidative stress status and the changes on the activation of Nrf2 in the brain.

2. Materials and Methods

2.1. Animals. Male Sprague-Dawley rats (180-220 g) were provided by the Hunan Cancer Hospital Animal Centre. The rats were housed in standard conditions ($23 \pm 2^\circ\text{C}$, 12 h light/dark cycle). Except prior to sucrose preference test (SPT), food and water were freely available in the whole experiment. This study was approved by the Animal Care and Use Committee of Hunan Cancer Hospital (protocol number 016/2018). All experiments were performed in

TABLE 1: Specific modeling methods of CUMS.

Number	CUMS procedure
1	24 h food deprivation
2	24 h water deprivation
3	45° cage tilting for 24 h
4	Restraint for 4 h in an empty water bottle
5	20 min of noise
6	1 min tail clamping
7	Damp bedding

accordance with the Guide for Care and Use of Laboratory Animals (Chinese Council).

2.2. CUMS Procedure. The rats were adapted for one week and the CUMS procedure was performed for four weeks as previously described [31]. 24 h food deprivation followed by 24 h water deprivation, 45° cage tilting for 24 h, restraint for 4 h in an empty water bottle, 20 min of noise, 1 min tail clamping, and damp bedding were selected as stressors in our study. All stressors were applied individually, continuously, and randomly, so that the stress procedure is unpredictable. The detailed information for specific modeling methods of CUMS are shown in Table 1.

2.3. Experimental Design. Rats were randomly divided into three groups ($n = 8$): control, CUMS, and CUMS+CUR. CUR (suspended in 0.5% Tween 80, purchased from Sigma Chemical Co., USA) was administrated by oral gavage (100 mg/kg/day) in the CUMS+CUR group, and the rats in control group were treated with the same volume of saline.

At the end of four weeks, behavioral tests were carried out, and the rats were sacrificed under anesthesia with an intraperitoneal injection of 1% sodium pentobarbital (50 mg/kg). Blood samples and the hippocampus were collected in our study. The whole experimental protocols are shown in Figure 1.

2.4. Behavioral Test

2.4.1. SPT. The SPT was performed as our previous study [32]. Prior to testing conditions, all the rats were separated in 1 cage each and habituated to 48 h of forced 1% sucrose solution consumption in two bottles on each side. After deprivation of water for 14 h, two preweighted bottles containing 1% sucrose solution and tap water were given to each rat. After 1 h, the bottles were weighed again, and the consumed weights of 1% sucrose solution and tap water were recorded. The percentage preference for sucrose was calculated as follows: sucrose preference (%) = sucrose consumption / (sucrose consumption + water consumption).

2.4.2. Forced Swimming Test (FST). The FST was performed as described previously [33] with minor modifications. In brief, rats were separated and were forced to swim in an open cylindrical container (45 cm height, 25 cm diameter) containing 35 cm of water ($24 \pm 1^\circ\text{C}$) for a 15 min pretest. The rats were then dried and removed from their cages. 24 hours later, the rats were exposed to the same experimental conditions

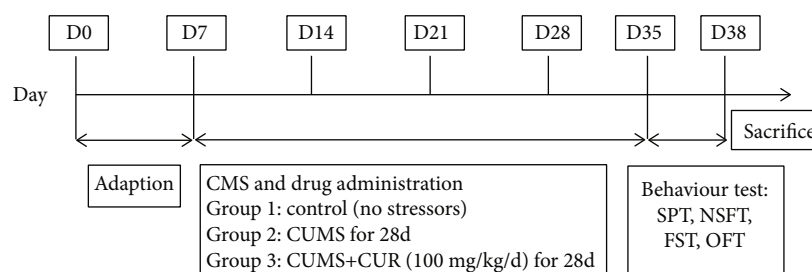


FIGURE 1: Schematic representation of experimental protocol.

TABLE 2: Primers used in real-time PCR analyses of mRNA expression.

Gene	Sense primer (5'-3')	Antisense primer (5'-3')
HO-1	TGCTCGCATGAACACTCTGGAGAT	ATGGCATAAATTCCCCTGCCACG
NQO-1	GTGAGAAGAGCCCTGATTGT	CCTGTGATGTCGTTTCTGGA
Nrf2	CCCAGCACATCCAGACAG	TATCCAGGGCAAGCGACT
β -Actin	CATCCTGCGTCTGGACCTGG	TAATGTCACGCACGATTTCC

outlined above for a 5 min FST. Immobility time was scored by an experienced observer blind to the experiment design, defined as floating with only small movement necessary to keep the head above water.

2.4.3. Novelty-Suppressed Feeding Test (NSFT). All the rats were food deprived for 24 h in their home cages before NSFT. A piece of white paper (10 × 10 cm) was placed in an open field (75 × 75 × 40 cm), and a small amount of food was placed on this paper. The rats were allowed to explore the open field for 8 min. The time it took for the rat to approach and take the first bite of the food was defined as the latency time and was recorded in our study. Immediately afterwards, the animals were transferred to their home cage, and the total food intake for the next 5 min was also weighed to avoid the influence of the animals' appetite.

2.4.4. Open Field Test (OFT). The open field apparatus consisted of a 76 × 76 cm gray wooden box with 42 cm high boundary walls. The floor was divided into 25 equal squares by black lines. Each rat was placed in the center of the square and left to explore it freely for 5 min. The number of crossing and rearing was recorded by the observer blind to the treatment condition of the animal. The apparatus was cleaned with ethanol and water to remove olfactory cues.

2.5. Determination of Serum Corticosterone. For the determination of serum corticosterone, the blood samples were collected at 13:00-15:00 on day 38 before sacrifice. The collected plasma was centrifuged (3500×g, 15 min) at 4°C and stored at -80°C until analysis. The serum corticosterone levels were measured using a commercial ELISA kit (Cayman Chemical, USA) according to the manufacturer's instructions. The standards and samples were all run in duplicates, and the averaged data were used for statistical analysis.

2.6. Real-Time PCR Analysis. According to the instruction of manufactory, total RNA was extracted from the hippocampus using TRIzol reagent (Invitrogen Corp., Carlsbad, CA,

USA). The mRNA expression of Nrf2, NQO-1, and HO-1 was determined in our present study. Quantitative PCR was performed on Bio-Rad Cx96 Detection System (Bio-Rad, Hercules, CA, USA) using the SYBR green PCR kit (Applied Biosystems Inc., Woburn, MA, USA) and gene-specific primers. The sequences of gene-specific primers are listed in Table 2. A 5 ng cDNA sample was used with 40 cycles of amplification. Each cDNA was determined in triplicate. The signals were normalized to β -actin as an internal standard.

2.7. Determination of Antioxidant Enzyme Activities and Lipid Peroxidation. Malondialdehyde (MDA) content was determined according to the previous report [34]. Briefly, 1 ml of 15% trichloroacetic acid was added to 500 μ l of brain homogenate supernatant and mixed well, and then, the solutions were centrifuged at 1006×g for 10 min. One milliliter of the supernatant was added to 0.5 ml of 0.7% TBA, and then, the mixture was heated for 60 min at 90°C. The absorbance was recorded at 532 nm using UV spectrophotometer. CAT activity was assayed by H₂O₂ consumption, following Aebi's [35].

2.8. Western Blot Analysis. For western blot analysis, total protein was prepared from the hippocampus, and the Bradford method was used to determine its concentration. The hippocampus sample was loaded on a precast 12% SDS-PAGE gel with 10 μ g proteins in each lane. Proteins in the gels were transferred to a polyvinylidene fluoride membrane and blocked for 1 h in 5% nonfat dry milk in TBS-T (25 mM Tris, pH 7.5, 150 mM NaCl, 0.05% Tween-20). The antibodies and concentrations listed below were used overnight at a temperature of 4°C: Nox2 (Santa Cruz; sc-130549; 1:800); 4-HNE (Abcam ab48506; 1:1000); Nrf2 (Abcam; ab137550; 1:200); pCREB (Cell Signaling; 9198; 1:1000); CREB (Cell Signaling; 9197; 1:1000); BDNF (Abcam; ab108319; 1:2000); PSD-95 (ProteinTech; 20665-1-AP; 1:2000); synaptophysin (ProteinTech; 17785-1-AP; 1:1000); PCNA (ProteinTech; 10205-2-AP; 1:3000); and

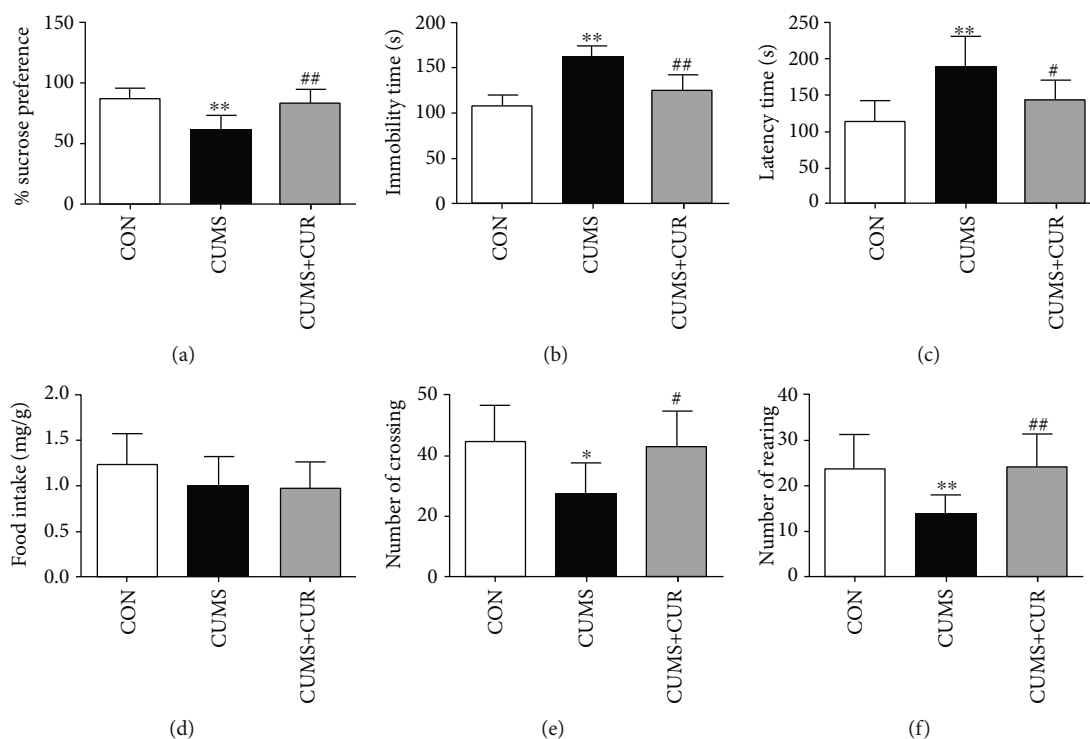


FIGURE 2: Effect of CUR on CUMS-induced behavior changes. (a) Sucrose preference in SPT, (b) immobility time in FST, (c) latency time in NSFT, (d) food intake in NSFT, (e) number of crossing in OPT, and (f) number of rearing in OPT. Data are expressed as means \pm SD ($n = 8$). * $p < 0.05$ and ** $p < 0.01$ compared to the control group. # $p < 0.05$ and ## $p < 0.01$ compared to the CUMS group.

β -actin (ProteinTech; 60008-1-Ig; 1:4000). Membranes were then probed with horseradish peroxidase-conjugated secondary antibody for 40 min. After washing, the membranes were dipped in electrochemiluminescence, and immunoblots were analyzed by using the Bioprofil Biolight PC software (Vulber Lourmat, France). β -Actin was used as an internal standard to normalize the signals.

2.9. TUNEL Staining. According to the manufacturer's instructions, the terminal deoxynucleotidyl transferase-mediated deoxyuridine triphosphate nick-end labeling (TUNEL) detection kit (KeyGen Biotech, Nanjing, China) was used to assess apoptosis. Apoptotic index was defined as the average percentage of TUNEL-positive cells in 20 nonoverlapping cortical fields under $\times 200$ magnification.

2.10. Immunohistochemical Staining. Paraffin-embedded tissue sections were rehydrated first in xylene and then in graded ethanol solutions. The slides were then blocked with 5% bovine serum albumin (BSA) in Tris-buffered saline (TBS) for 2 h. After incubation with anti-8-OHdG and anti-Nox2 overnight at 4°C , the sections were then washed with PBS and incubated with secondary antibodies. Counter staining was performed using hematoxylin, and the slides were visualized under a light microscope.

2.11. Golgi Staining. Golgi staining was performed as previous report [36]. In brief, the brain tissues of the rat were kept in the Golgi-Cox solution for 14 days in the darkness, and the solution was replaced every 48 h. After dehydration with 30%

sucrose solution, the tissues were cut into $100\ \mu\text{m}$ section. The following steps included treatment with ammonia water and acid hardening fixing bath and dehydration with increasing concentrations of alcohol. A digital camera attached with microscopy was used to take images of the tissues for dendritic structure analyzing. Dendritic spine density and total dendritic length analysis were done manually using the Fiji software under $\times 400$ magnification.

2.12. DHE Staining. Reactive oxygen species (ROS) was measured by dihydroethidium (DHE) microfluorography as previous study [37]. In brief, freshly prepared frozen brain sections ($15\ \mu\text{m}$ thick) were incubated with $5\ \mu\text{M}$ DHE in PBS at 37°C for 30 min in a dark humidified chamber. The sections were then imaged by using the Leica fluorescence microscope (Leica Microsystems, Germany).

2.13. Statistical Analysis. Statistical Package for Social Science (SPSS) version 18 (SPSS Inc., Chicago, IL, USA) was used for data analysis in our study. All data were analyzed by one-way analysis of variance (ANOVA) with least significant difference (LSD) post hoc multiple comparisons. All data were presented as means \pm SD, and $p < 0.05$ was considered statistically significant.

3. Results

3.1. Effects of CUR on Behavioral Tests. The CUMS group showed reduced sucrose preference in SPT (Figure 2(a), $p < 0.01$), prolonged immobility time in FST (Figure 2(b),

$p < 0.01$), and latency time in NSFT (Figure 2(c), $p < 0.01$) in comparison with the rats in control group. Our study also observed that the number of crossing (Figure 2(e), $p < 0.05$) and rearing (Figure 2(f), $p < 0.01$) in OPT was all significantly decreased in the CUMS group. In comparison with the CUMS group, the administration of CUR successfully increased the sucrose preference (Figure 2(a), $p < 0.01$), decreased immobility time (Figure 2(b), $p < 0.01$) and latency time (Figure 2(c), $p < 0.01$), and increased the number of crossing (Figure 2(e), $p < 0.05$) and rearing (Figure 2(f), $p < 0.01$) in the CUMS+CUR group. In addition, no significant difference of food intake was observed in NSFT.

3.2. Effects of CUR on Corticosterone Level. As displayed in Figure 3, the serum corticosterone level significantly increased ($p < 0.01$) in the CUMS group compared with the control group. However, the administration of CUR markedly decreased ($p < 0.01$) the corticosterone level when compared with the rats in the CUMS group.

3.3. Effect of CUMS and CUR on Oxidative Stress. The immunohistochemical staining results of 8-OHdG and Nox2 are shown in Figure 4(a); the results showed that the expressions of 8-OHdG and Nox2 were all increased in CUMS-treated rats when compared to control group, and the supplementation of CUR markedly moderated CUMS-induced increasing of 8-OHdG and Nox2. The results of DHE immunostaining showed that ROS production was significantly increased in the CUMS group, and this increase in ROS generation was markedly alleviated by the pretreatment with CUR (Figure 4(a)). The protein expressions of Nox2 (Figure 4(b), $p < 0.01$) and 4-HNE (Figure 4(c), $p < 0.01$) were significantly increased in the CUMS group as compared to the rats in the control group, and the administration of CUR effectively mitigated CUMS-induced increasing of Nox2 (Figure 4(b), $p < 0.05$) and 4-HNE (Figure 4(c), $p < 0.01$); the western blot result of Nox2 was in accordance with immunohistochemical staining results. The content of MDA (Figure 4(d), $p < 0.01$) was significantly increased in the CUMS group when compared to the control group. The CUR treatment successfully decreased the content of MDA in the CUMS+CUR group when compared to the CUMS group (Figure 4(d), $p < 0.01$). In comparison with the rats in the control group, the activity of CAT (Figure 4(e), $p > 0.05$) was decreased in CUMS-treated rats but without significance difference. Furthermore, the administration of CUR significantly increased CAT activity in the CUMS+CUR group when compared to the CUMS group (Figure 4(e), $p < 0.05$).

3.4. Effects of CUR on the Activation of Nrf2 in CUMS-Treated Rats. The Nrf2 levels in cytoplasmic (Figure 5(a), $p < 0.05$) and nuclear (Figure 5(b), $p < 0.01$) all significantly decreased in the CUMS group when compared with the rats in the normal-treated group, and the Nrf2 in nuclear obviously (Figure 5(b), $p < 0.01$) increased in the CUMS+CUR group compared to the CUMS group. Interestingly, as shown in Figure 5(c), the gene expression of Nrf2 was similar with the protein expression of Nrf2 in the

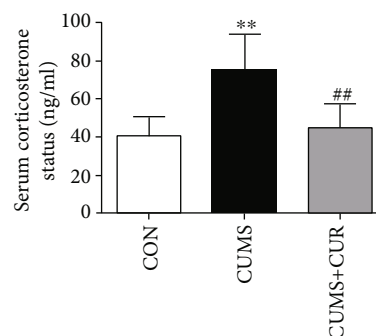


FIGURE 3: Effect of CUR on CUMS-induced serum corticosterone level. Data are expressed as means \pm SD ($n = 8$). * $p < 0.05$ and ** $p < 0.01$ compared to the control group. # $p < 0.05$ and ## $p < 0.01$ compared to the CUMS group.

nuclear. The mRNA expressions of NQO-1 (Figure 5(d), $p < 0.01$) and HO-1 (Figure 5(e), $p < 0.05$) all significantly decreased in the CUMS model rats, and CUR treatment significantly prevented the decrease of NQO-1 (Figure 5(d), $p < 0.01$) and HO-1 (Figure 5(e), $p < 0.05$) in the CUMS+CUR group when compared with the rats in the CUMS group.

3.5. Effect of CUMS and CUR on Synaptic Plasticity. As shown in Figure 6(b), the pCREB/CREB ratio was significantly decreased in the CUMS group compared to vehicle control group (Figure 6(b), $p < 0.05$). Administration of CUR significantly increased pCREB/CREB ratio in the hippocampus compared to the CUS-treated rats (Figure 6(b), $p < 0.01$). The protein expression of BDNF (Figure 6(c), $p < 0.01$), PSD-95 (Figure 6(d), $p < 0.05$), and synaptophysin (Figure 6(e), $p < 0.01$) all significantly decreased in the CUMS-treated rats, and CUR successfully reversed the CUMS-induced decrease of these three proteins ($p < 0.01$). Previous studies have reported that dynamic alterations in synaptic and dendritic structure and function play a pivotal role in the development of depression [38, 39]. In our present study, Golgi staining showed that spine density (Figure 6(g), $p < 0.01$) and total dendritic length (Figure 6(i), $p < 0.01$) significantly decreased in the dentate gyrus (DG) granule neurons of CUMS-induced rats, and the administration of CUR markedly reversed this effect (Figure 6(g), $p < 0.01$, Figure 6(i), $p < 0.05$).

4. Discussion

Our present study demonstrated that the administration of CUR exhibited antidepressant-like activities in CUMS-induced depression model. We investigated the depressive-like behaviors (SFT, FST, NSFT, and OFT) in rats under CUMS, and chronic administration of CUR normalized behavioral changes in rats exposed to stress. CUR could effectively decrease protein expression of oxidative stress marker (MDA, Nox2, and 4-HNE). CUR could also activate stress-induced Nrf2-ARE axis inhibition. In addition, long-term treatment with CUR markedly prevented CUMS-induced reduction of BDNF, PSD-95, and synaptophysin expressions.

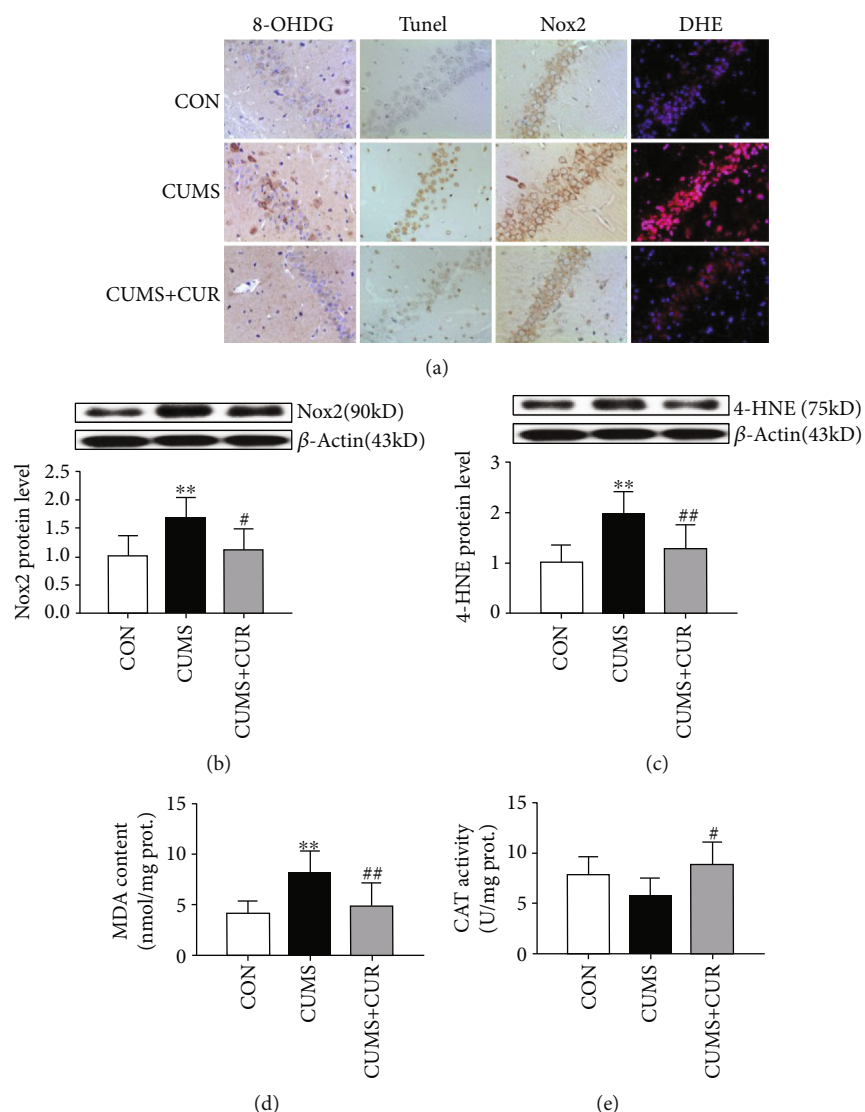


FIGURE 4: Effects of CUR on CUMS-induced oxidative stress change. (a) Immunohistochemical staining, TUNEL staining, and DHE staining, (b) protein expression of Nox2, (c) protein expression of 4-HNE, (d) content of MDA, and (e) activity of CAT. Data are expressed as means \pm SD ($n = 8$). * $p < 0.05$ and ** $p < 0.01$ compared to the control group. # $p < 0.05$ and ## $p < 0.01$ compared to the CUMS group.

These findings indicate the potential benefits of administration of CUR to reverse the development of depression. Furthermore, the antidepressant mechanism of CUR may be mediated by restoring changes in oxidative stress and the activation of the Nrf2-ARE signaling pathway.

The CUMS model has long been used as an animal model of depression, and previous study showed that most effects of CUMS could be effectively reversed by antidepressant agents [40]. In our present study, reduced sucrose preference in SPT and prolonged immobility time in FST were observed in the CUMS group, which indicated the depressive-like state. In comparison with the rats in the CUMS group, chronic administration of CUR successfully increased sucrose preference and decreased immobility time, which was consistent with the former studies [41, 42]. Anxiety status was assessed by NSFT and OFT. Our study observed that CUR treatment could successfully reverse CUMS-induced increase in latency time in NSFT and decrease in crossing number and rearing

number in OFT. Motaghinejad et al. have also reported that chronic administration of CUR could effectively improve ambulation number and ambulation distance in nicotine-treated rats, indicating neuroprotective effect of CUR against nicotine-induced neurotoxicity [43]. Therefore, CUR exhibited antidepressant-like properties basing on the above-mentioned results.

As a stress marker, corticosterone level is widely used for accessing the stress state. More and more evidences showed that the elevated corticosterone level was associated with depressive-like behaviors, and antidepressant-like activity could always induce a reduction of corticosterone level [44–46]. In the present study, the corticosterone serum level was significantly increased in rats exposed to CUMS model compared to the nonstressed group, and chronic administration of CUR successfully reversed CUMS-induced the elevation of the corticosterone serum level. The results that serum corticosterone in the rats of the CUMS

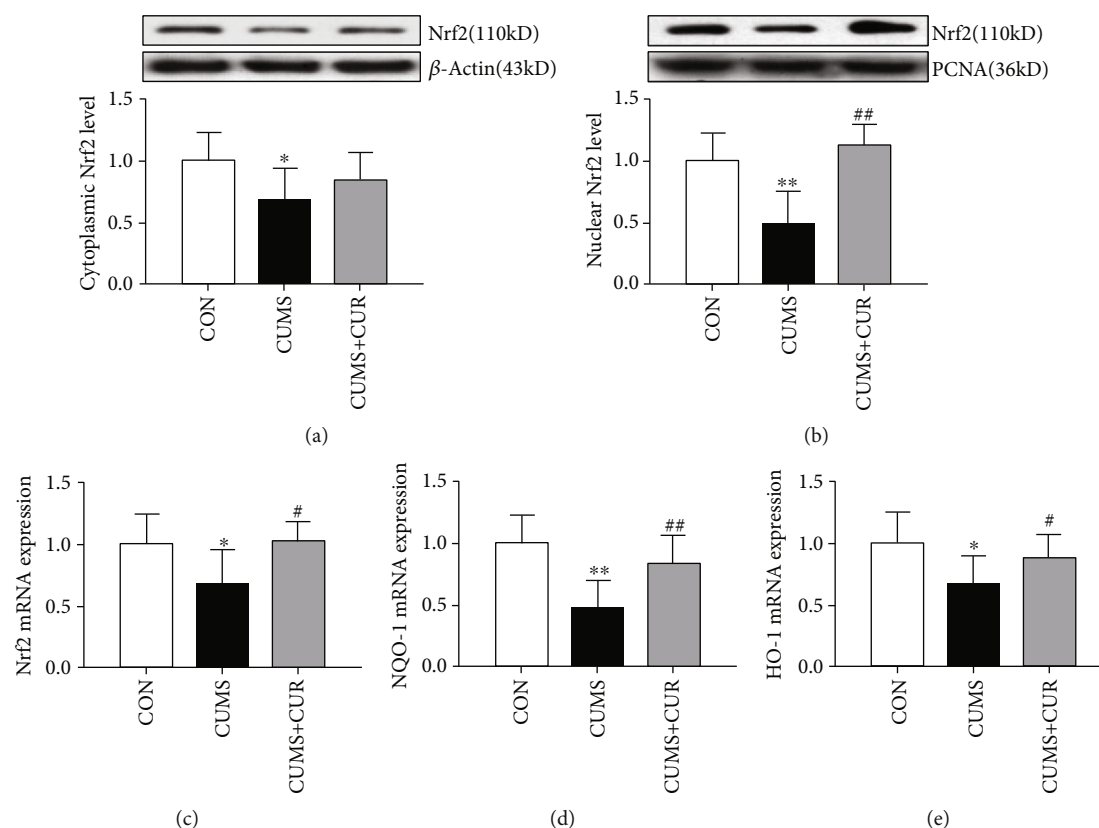


FIGURE 5: Effects of CUR on the activation of Nrf2 in CUMS-treated rats. (a) Protein expression of Nrf2 in cytoplasmic, (b) protein expression of Nrf2 in nuclear, (c) mRNA expression of Nrf2 in the hippocampus, (d) mRNA expression of NOQ-1 in the hippocampus, and (e) mRNA expression of HO-1 in the hippocampus. Data are expressed as means \pm SD ($n = 8$). * $p < 0.05$ and ** $p < 0.01$ compared to the control group. # $p < 0.05$ and ## $p < 0.01$ compared to the CUMS group.

group increased significantly were in accordance with previous studies [2, 47]. As a typical antidepressant agent, fluoxetine could effectively prevent the elevation of serum corticosterone level in CUMS-treated rats [1, 48]. Disrupting the HPA axis and elevating the levels of serum corticosterone by CUMS were increasingly recognized [49, 50]. In addition, CUMS-induced increase of serum corticosterone level may be due to an impaired negative feedback in the HPA [51, 52] and lack of the inhibitory role of the hippocampus in glucocorticoid synthesis [53].

The elevated free radical generation and decreased activity of antioxidants break the balance between oxidant-antioxidant systems, which will always induce oxidative stress [54]. More and more evidence showed that the brain is highly susceptible to oxidative damage [55], and oxidative stress plays a pivotal role in CUMS-induced depression [54]. The release of excitatory amino acid and the expression of specific gene may be enhanced by ROS, which will always induce lipid peroxidation and DNA oxidation, subsequently resulting in neuronal apoptosis [56]. Our present study observed that the intensity of DHE staining and TUNEL-positive cells significantly increased in CUMS-treated rats, which indicated oxidative stress induced a severe neuronal apoptosis. Fortunately, as a natural antioxidant agent, the administration of CUR significantly alleviated CUMS-induced oxidative stress and neuronal apoptosis in the

CUMS+CUR group. In our present study, signs of oxidative stress were observed as exemplified by the decrease of antioxidant enzyme activity, such as CAT. In addition, as lipid peroxidation markers, MDA and 4-HNE levels all significantly increased in the CUMS group when compared to the control group. Previous study has reported that CUR has shown to counteract oxidative stress by reducing lipid peroxidation and improving the activity of antioxidant enzymes [54]. Our study results were consistent with this report, which expressed a significantly decrease in MDA and 4-HNE levels and a markedly increase in CAT activity in the CUMS+CUR group. Furthermore, DNA is an important and recognized target of free radicals attack. 8-OHdG is one of the most widely studied biomarkers of oxidative DNA damage. The immunohistochemical staining results coincide with a previous study, which indicated that CUR effectively reversed the increase of 8-OHdG expression under CUMS. ROS and oxidative stress are mainly generated from Nox which is a multiunit enzyme [57]. In particular, the primary mechanism underlying the development of oxidative stress in various neurodegenerative conditions is the activation of Nox2 [58]. In our present study, the protein expression of Nox2 significantly increased in CUMS-treated rats, and the administration of CUR successfully alleviated this phenomenon in the CUMS+CUR group. These results supported that oxidative stress plays a pivotal role in CUMS-induced depression.

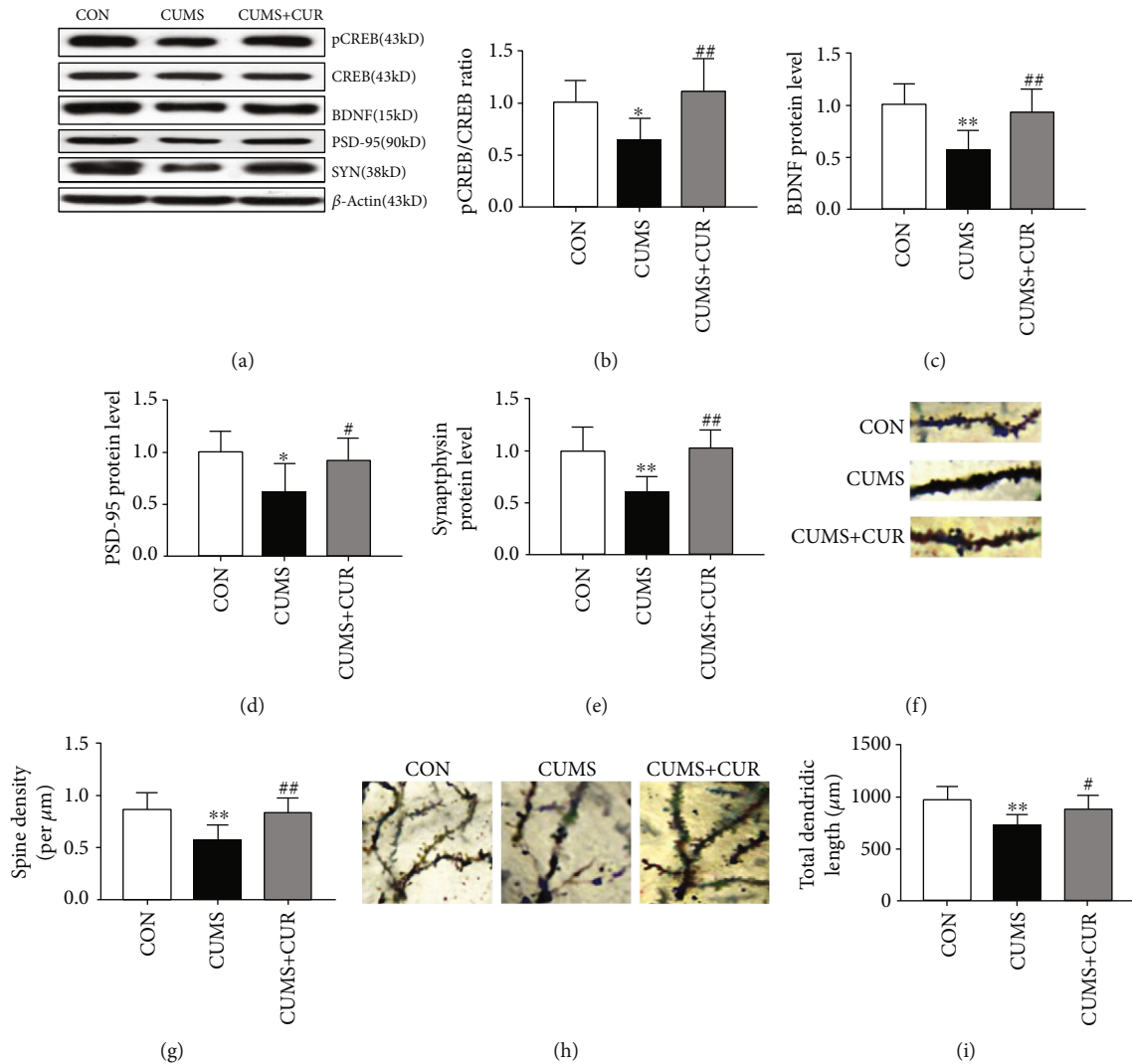


FIGURE 6: Effect of CUR on synaptic plasticity. (b) pCREB/CREB ratio in the hippocampus, (c) protein expression of BDNF in the hippocampus, (d) protein expression of PSD-95 in the hippocampus, (e) protein expression of synaptophysin in the hippocampus, (f) representative images of dendritic spines from DG granule neurons in the rat, (g) spine density in different groups, (h) representative images of DG granule neurons in the rats, and (i) total dendritic length in different groups. Data are expressed as means \pm SD ($n = 8$). * $p < 0.05$ and ** $p < 0.01$ compared to the control group. # $p < 0.05$ and ## $p < 0.01$ compared to the CUMS group.

In addition, our results also demonstrated that the neuroprotective effect of CUR was mediated via its antioxidative ability.

As a transcription factor, Nrf2 is known to play a pivotal role in modulating oxidative stress and exhibiting an important protective role in brain injury and neurodegenerative diseases. As it is known to us, Nrf2 is mainly located in the cytoplasm under physical conditions. However, Nrf2 translocates into the nucleus in response to oxidative stress [15]. In our present study, the results of western blot showed that CUR administration promoted Nrf2 nuclear translocation. This indicates that the Nrf2 level markedly increased in CUMS+CUR-treated rats when compared with the rats in the CUMS group. And the protein expression of Nrf2 was without significant difference in both the CUMS+CUR group and the CUMS group. The above observations revealed that Nrf2 was inhibited when rats exposed to CUMS and CUR

had the ability to activate Nrf2. Previous studies have also reported that CUR had the ability to activate Nrf2 and provide neuroprotection from a traumatic brain injury [16, 56]. In order to investigate the regulation effects of CUR on the Nrf2 downstream pathway, the mRNA levels of Nrf2, NQO-1, and HO-1 were evaluated in our study. NQO-1 and HO-1 are important antioxidant enzymes in the Nrf2-ARE pathway [59]. The results showed that chronic administration of CUR could significantly reverse CUMS-induced decrease in the mRNA level of Nrf2, NQO-1, and HO-1. The above results indicated that the Nrf2 downstream pathway was inhibited under CUMS, and chronic administration of CUR could effectively activate this signal pathway. Our results indicated that the Nrf2 signal pathway was inhibited under CUMS, and chronic administration of CUR enhanced Nrf2 translocation from cytoplasm to nucleus and increased expression of antioxidant enzymes through

Nrf2 signal pathway, thereby protecting the brain against CUMS-induced depression.

CREB is involved in the regulation of genes associated with synaptic and neural plasticity [43]. CREB has been reported to be phosphorylated by many signaling events on serine 133 [60]. The results in our study showed that the ratio of pCREB/CREB significantly decreased in the CUMS group, and chronic administration of CUR successfully reversed this reduction. These results were in conformity with previous studies which have shown that CUR can increase the pCREB/CREB ratio in rats exposed to CUMS [61]. In addition, a previous study also showed that CUR could function as a potential agent that suppresses depressive-like behavior via the prevention of protein changes associated with synaptic plasticity [62]. As the most abundant neurotrophin in the brain, BDNF plays a crucial role in the regulation of survival as well as synaptic plasticity. Our study investigated whether BDNF was involved in the antidepressant effects induced by CUR. The results indicated that the expression of BDNF in rats exposed to CUMS was significantly increased after chronic administration of CUR. Furthermore, other synapse-associated proteins were also accessed in our study. PSD-95 and synaptophysin were postsynaptic marker and presynaptic marker respectively. In accordance with BDNF, CUR successfully alleviated CUMS-induced reduction in the protein level of PSD-95 and synaptophysin. Zhang et al. have reported that CUR can reverse the decreased expression of BDNF, PSD-95, and synaptophysin in CMS-induced rats [62]. Previous studies have shown that spine densities and synaptic plasticity were closely correlated with the function of neuron and cognitive performance [63, 64]. Our present study shows that CUR could effectively reverse CUMS-induced decrease of spine density and total dendritic length. Hence, the alteration of the above-mentioned synaptic plasticity-associated proteins may underlie changes in functional plasticity associated with CUMS-induced depression.

5. Conclusion

In conclusion, our present study suggests that the administration of CUR is effective in preventing CUMS-induced depression. Furthermore, the current results suggested that the antidepressant action of CUR may be mediated by restoring changes in oxidative stress, the Nrf2-ARE signaling pathway, and the synaptic and neural plasticity, which might ultimately contribute to its antidepressant-like effect.

Data Availability

The data used to support the findings of this study are available from the corresponding author upon request.

Conflicts of Interest

The authors declare no conflict of interest.

Authors' Contributions

Pei Jiang and Ni Liu designed the study and wrote the protocol. Dehua Liao, Chuanfeng Lv, Lizhi Cao, Yi Wu, and Minghui Long performed the experiments and analyzed the data. Dunwu Yao contributed to the reagents and materials. Dehua Liao and Chuanfeng Lv drafted the manuscript. Pei Jiang and Dehua Liao revised the manuscript content. All authors read and approved the final manuscript. Dehua Liao and Chuanfeng Lv contributed equally to this manuscript.

Acknowledgments

This study was supported by the National Natural Science Foundation of China (NSFC: 81603206), Health and Family Planning Commission Foundation of Hunan Province (grant numbers B20180402 and C2019064), the Project of Hunan Provincial Science & Technology Department (grant numbers 2019JJ80093 and 2020JJ8093), the Key Research and Development Program of Jining Science and Technology (2019SMNS012), the Traditional Chinese Medicine Science and Technology Development Plan of Shandong Province (2019-0747), and the Shandong Science and Technology Development Plan on Medicine and Hygiene in China (No. 2017WS348).

References

- [1] Y. H. Kim, A. R. Im, B.-K. Park et al., "Antidepressant-like and neuroprotective effects of ethanol extract from the root bark of *Hibiscus syriacus* L.," *BioMed Research International*, vol. 2018, Article ID 7383869, 13 pages, 2018.
- [2] G.-F. Wu, S. Ren, R.-Y. Tang et al., "Antidepressant effect of taurine in chronic unpredictable mild stress-induced depressive rats," *Scientific Reports*, vol. 7, 2017.
- [3] J. B. Potash, A. J. Ferrari, F. J. Charlson et al., "The epidemiological modelling of major depressive disorder: application for the Global Burden Of Disease Study 2010," *PLoS One*, vol. 8, article e69637, 2013.
- [4] E. Holtzheimer Paul and NCB, "Advances in the treatment of depression," *NeuroRx*, vol. 3, p. 14, 2006.
- [5] D. Badyal, R. Deswal, A. Sharma, and P. Matreja, "Efficacy and safety of add on low-dose mirtazapine in depression," *Indian Journal of Pharmacology*, vol. 44, no. 2, pp. 173–177, 2012.
- [6] R. Mojtabai, M. Olfson, N. A. Sampson et al., "Barriers to mental health treatment: results from the National Comorbidity Survey Replication," *Psychological Medicine*, vol. 41, no. 8, pp. 1751–1761, 2011.
- [7] W. M.-L. Licinio Julio, "Depression, antidepressants and suicidality a critical appraisal," *Nature Reviews. Drug Discovery*, vol. 4, p. 6, 2005.
- [8] C. Taylor, A. D. Fricker, L. A. Devi, and I. Gomes, "Mechanisms of action of antidepressants: from neurotransmitter systems to signaling pathways," *Cellular Signalling*, vol. 17, no. 5, pp. 549–557, 2005.
- [9] V. N. Thakare, V. D. Dhakane, and B. M. Patel, "Potential antidepressant-like activity of silymarin in the acute restraint stress in mice: modulation of corticosterone and oxidative stress response in cerebral cortex and hippocampus," *Pharmacological Reports*, vol. 68, no. 5, pp. 1020–1027, 2016.

- [10] M. Gazal, M. R. Valente, B. A. Acosta et al., "Neuroprotective and antioxidant effects of curcumin in a ketamine-induced model of mania in rats," *European Journal of Pharmacology*, vol. 724, pp. 132–139, 2014.
- [11] F. Ng, M. Berk, O. Dean, and A. I. Bush, "Oxidative stress in psychiatric disorders: evidence base and therapeutic implications," *The International Journal of Neuropsychopharmacology*, vol. 11, no. 6, 2008.
- [12] M. Maes, P. Galecki, Y. S. Chang, and M. Berk, "A review on the oxidative and nitrosative stress (O&NS) pathways in major depression and their possible contribution to the (neuro)degenerative processes in that illness," *Progress in Neuro-Psychopharmacology and Biological Psychiatry*, vol. 35, no. 3, pp. 676–692, 2011.
- [13] R. Chhillar and D. Dhingra, "Antidepressant-like activity of gallic acid in mice subjected to unpredictable chronic mild stress," *Fundamental & Clinical Pharmacology*, vol. 27, no. 4, pp. 409–418, 2013.
- [14] L. Cigliano, M. S. Spagnuolo, F. Boscaino et al., "Dietary supplementation with fish oil or conjugated linoleic acid relieves depression markers in mice by modulation of the Nrf2 pathway," *Molecular Nutrition & Food Research*, vol. 63, article e1900243, 2019.
- [15] A. Kobayashi, M. I. Kang, H. Okawa et al., "Oxidative stress sensor Keap1 functions as an adaptor for Cul3-based E3 ligase to regulate proteasomal degradation of Nrf2," *Molecular and Cellular Biology*, vol. 24, no. 16, pp. 7130–7139, 2004.
- [16] W. Dong, B. Yang, L. Wang et al., "Curcumin plays neuroprotective roles against traumatic brain injury partly via Nrf2 signaling," *Toxicology and Applied Pharmacology*, vol. 346, pp. 28–36, 2018.
- [17] H. E. de Vries, M. Witte, D. Hondius et al., "Nrf2-induced antioxidant protection: a promising target to counteract ROS-mediated damage in neurodegenerative disease?," *Free Radical Biology and Medicine*, vol. 45, no. 10, pp. 1375–1383, 2008.
- [18] W. Li and A.-N. Kong, "Molecular mechanisms of Nrf2-mediated antioxidant response," *Molecular Carcinogenesis*, vol. 48, no. 2, pp. 91–104, 2009.
- [19] I. Buendia, P. Michalska, E. Navarro, I. Gameiro, J. Egea, and R. Leon, "Nrf2-ARE pathway: an emerging target against oxidative stress and neuroinflammation in neurodegenerative diseases," *Pharmacology & Therapeutics*, vol. 157, pp. 84–104, 2016.
- [20] S. H. Christiansen, M. V. Olesen, G. Wortwein, and D. P. Woldbye, "Fluoxetine reverts chronic restraint stress-induced depression-like behaviour and increases neuropeptide Y and galanin expression in mice," *Behavioural Brain Research*, vol. 216, no. 2, pp. 585–591, 2011.
- [21] M. Popoli, Z. Yan, B. S. McEwen, and G. Sanacora, "The stressed synapse: the impact of stress and glucocorticoids on glutamate transmission," *Nature Reviews. Neuroscience*, vol. 13, no. 1, pp. 22–37, 2011.
- [22] A. C. Conti, J. F. Cryan, A. Dalvi, I. Lucki, and J. A. Blendy, "cAMP response element-binding protein is essential for the upregulation of brain-derived neurotrophic factor transcription, but not the behavioral or endocrine responses to antidepressant drugs," *The Journal of Neuroscience*, vol. 22, no. 8, pp. 3262–3268, 2002.
- [23] B. B. Aggarwal and K. B. Harikumar, "Potential therapeutic effects of curcumin, the anti-inflammatory agent, against neurodegenerative, cardiovascular, pulmonary, metabolic, autoimmune and neoplastic diseases," *The International Journal of Biochemistry & Cell Biology*, vol. 41, no. 1, pp. 40–59, 2009.
- [24] R. K. Maheshwari, A. K. Singh, J. Gaddipati, and R. C. Simal, "Multiple biological activities of curcumin: a short review," *Life Sciences*, vol. 78, no. 18, pp. 2081–2087, 2006.
- [25] Y. Xu, B.-S. Ku, H.-Y. Yao et al., "The effects of curcumin on depressive-like behaviors in mice," *European Journal of Pharmacology*, vol. 518, no. 1, pp. 40–46, 2005.
- [26] C. Yang, X. Zhang, H. Fan, and Y. Liu, "Curcumin upregulates transcription factor Nrf2, HO-1 expression and protects rat brains against focal ischemia," *Brain Research*, vol. 1282, pp. 133–141, 2009.
- [27] I. S. Carmona-Ramírez, A. Tobón-Velasco, J. C. Orozco-Ibarra et al., "Curcumin restores Nrf2 levels and prevents quinolinic acid-induced neurotoxicity," *The Journal of Nutritional Biochemistry*, vol. 24, pp. 14–24, 2013.
- [28] X. C. Shen Guoxiang, H. Rong, R. Jain Mohit et al., "Modulation of nuclear factor E2-related factor 2-mediated gene expression in mice liver and small intestine by cancer chemopreventive agent curcumin," *Molecular Cancer Therapeutics*, vol. 5, pp. 39–51, 2006.
- [29] Z. Xie, B. Wu, G. Shen, X. Li, and Q. Wu, "Curcumin alleviates liver oxidative stress in type 1 diabetic rats," *Molecular Medicine Reports*, vol. 17, pp. 103–108, 2017.
- [30] E. M. Abdelsamia, S. A. Khaleel, A. Balah, and N. A. Abdel Baky, "Curcumin augments the cardioprotective effect of metformin in an experimental model of type I diabetes mellitus; impact of Nrf2/HO-1 and JAK/STAT pathways," *Biomedicine & Pharmacotherapy*, vol. 109, pp. 2136–2144, 2019.
- [31] G. G. Ducottet Cecile and B. Catherine, "Effects of the selective nonpeptide corticotropin-releasing factor receptor 1 antagonist antalarmin in the chronic mild stress model of depression in mice," *Progress in Neuro-Psychopharmacology & Biological Psychiatry*, vol. 27, p. 6, 2003.
- [32] D. Liao, D. Xiang, R. Dang et al., "Neuroprotective effects of dl-3-n-butylphthalide against doxorubicin-induced neuroinflammation, oxidative stress, endoplasmic reticulum stress, and behavioral changes," *Oxidative Medicine and Cellular Longevity*, vol. 2018, Article ID 9125601, 13 pages, 2018.
- [33] S. Kumar and A. C. Mondal, "Neuroprotective, neurotrophic and anti-oxidative role of Bacopa monnieri on CUS induced model of depression in rat," *Neurochemical Research*, vol. 41, no. 11, pp. 3083–3094, 2016.
- [34] H. O. N. Ohkawa and K. Yagi, "Assay for lipid peroxides in animal tissues by thiobarbituric acid reaction," *Analytical Biochemistry*, vol. 95, p. 7, 1979.
- [35] H. Aebi, "Catalase in vitro," *Methods in Enzymology*, vol. 105, p. 5, 1984.
- [36] N. Abe-Higuchi, S. Uchida, H. Yamagata et al., "Hippocampal sirtuin 1 signaling mediates depression-like behavior," *Biological Psychiatry*, vol. 80, no. 11, pp. 815–826, 2016.
- [37] J. Mo, B. Enkhjargal, Z. D. Travis et al., "AVE 0991 attenuates oxidative stress and neuronal apoptosis via Mas/PKA/CREB/UCP-2 pathway after subarachnoid hemorrhage in rats," *Redox Biology*, vol. 20, pp. 75–86, 2019.
- [38] R. S. Duman and G. K. Aghajanian, "Synaptic dysfunction in depression: potential therapeutic targets," *Science*, vol. 338, no. 6103, pp. 68–72, 2012.
- [39] V. Krishnan and E. J. Nestler, "The molecular neurobiology of depression," *Nature*, vol. 455, no. 7215, pp. 894–902, 2008.

- [40] P. Willner, "Validity, reliability and utility of the chronic mild stress model of depression a 10-year review and evaluation," *Psychopharmacology*, vol. 134, no. 4, pp. 319–329, 1997.
- [41] Y.-C. Li, F.-M. Wang, Y. Pan et al., "Antidepressant-like effects of curcumin on serotonergic receptor-coupled AC-cAMP pathway in chronic unpredictable mild stress of rats," *Progress in Neuro-Psychopharmacology and Biological Psychiatry*, vol. 33, no. 3, pp. 435–449, 2009.
- [42] M. K. Bhutani, M. Bishnoi, and S. K. Kulkarni, "Anti-depressant like effect of curcumin and its combination with piperine in unpredictable chronic stress-induced behavioral, biochemical and neurochemical changes," *Pharmacology Biochemistry and Behavior*, vol. 92, no. 1, pp. 39–43, 2009.
- [43] M. Motaghinejad, M. Motevalian, S. Fatima, F. Faraji, and S. Mozaffari, "The neuroprotective effect of curcumin against nicotine-induced neurotoxicity is mediated by CREB–BDNF signaling pathway," *Neurochemical Research*, vol. 42, no. 10, pp. 2921–2932, 2017.
- [44] M. E. Crupi Rosalia, M. Angela, L. S. Giuseppina, B. Placido, C. Salvatore, and S. Edoardo, "Melatonin treatment mimics the antidepressant action in chronic corticosterone-treated mice," *Journal of Pineal Research*, vol. 49, p. 6, 2010.
- [45] B. Lee, I. Shim, H. J. Lee, Y. Yang, and D. H. Hahm, "Effects of acupuncture on chronic corticosterone-induced depression-like behavior and expression of neuropeptide Y in the rats," *Neuroscience Letters*, vol. 453, no. 3, pp. 151–156, 2009.
- [46] Y. Zhao, W. Xie, J. Dai, Z. Wang, and Y. Huang, "The varying effects of short-term and long-term corticosterone injections on depression-like behavior in mice," *Brain Research*, vol. 1261, pp. 82–90, 2009.
- [47] N. Jiang, B.-Y. Zhang, L.-M. Dong et al., "Antidepressant effects of dammarane sapogenins in chronic unpredictable mild stress-induced depressive mice," *Phytotherapy Research*, vol. 32, no. 6, pp. 1023–1029, 2018.
- [48] V. N. Thakare, R. R. Patil, R. J. Oswal, V. D. Dhakane, M. K. Aswar, and B. M. Patel, "Therapeutic potential of silymarin in chronic unpredictable mild stress induced depressive-like behavior in mice," *Journal of Psychopharmacology*, vol. 32, pp. 223–235, 2017.
- [49] Z. Ma, G. Wang, L. Cui, and Q. Wang, "Myricetin attenuates depressant-like behavior in mice subjected to repeated restraint stress," *International Journal of Molecular Sciences*, vol. 16, no. 12, pp. 28377–28385, 2015.
- [50] W. Quan, F. Liu, Y. Zhang et al., "Antidepressant-like effects of magnesium lithospermate B in a rat model of chronic unpredictable stress," *Pharmaceutical Biology*, vol. 53, no. 8, pp. 1168–1175, 2015.
- [51] J. G. Tasker and J. P. Herman, "Mechanisms of rapid glucocorticoid feedback inhibition of the hypothalamic–pituitary–adrenal axis," *Stress*, vol. 14, no. 4, pp. 398–406, 2011.
- [52] M. Keller-Wood, "Hypothalamic-pituitary-adrenal axis-feedback control," *Comprehensive Physiology*, vol. 5, pp. 1161–1182, 2015.
- [53] H. F. Sakr, A. M. Abbas, A. Z. Elsamanoudy, and F. M. Ghoneim, "Effect of fluoxetine and resveratrol on testicular functions and oxidative stress in a rat model of chronic mild stress-induced depression," *Journal of Physiology and Pharmacology*, vol. 66, p. 12, 2015.
- [54] S. Samarghandian, M. Azimi-Nezhad, T. Farkhondeh, and F. Samini, "Anti-oxidative effects of curcumin on immobilization-induced oxidative stress in rat brain, liver and kidney," *Biomedicine & Pharmacotherapy*, vol. 87, pp. 223–229, 2017.
- [55] M. Motaghinejad, M. Motevalian, and B. Shabab, "Effects of chronic treatment with methylphenidate on oxidative stress and inflammation in hippocampus of adult rats," *Neuroscience Letters*, vol. 619, pp. 106–113, 2016.
- [56] W. Dai, H. Wang, J. Fang et al., "Curcumin provides neuroprotection in model of traumatic brain injury via the Nrf2-ARE signaling pathway," *Brain Research Bulletin*, vol. 140, pp. 65–71, 2018.
- [57] L. M. Fan, S. Cahill-Smith, L. Geng, J. Du, G. Brooks, and J.-M. Li, "Aging-associated metabolic disorder induces Nox2 activation and oxidative damage of endothelial function," *Free Radical Biology and Medicine*, vol. 108, pp. 940–951, 2017.
- [58] S. J. Cooney, S. L. Bermudez-Sabogal, and K. R. Byrnes, "Cellular and temporal expression of NADPH oxidase (NOX) isoforms after brain injury," *Journal of Neuroinflammation*, vol. 10, p. 13, 2013.
- [59] Y. Xie, Q. Y. Zhao, H. Y. Li, X. Zhou, Y. Liu, and H. Zhang, "Curcumin ameliorates cognitive deficits heavy ion irradiation-induced learning and memory deficits through enhancing of Nrf2 antioxidant signaling pathways," *Pharmacology Biochemistry and Behavior*, vol. 126, pp. 181–186, 2014.
- [60] R. Wang, Y.-H. Li, Y. Xu et al., "Curcumin produces neuroprotective effects via activating brain-derived neurotrophic factor/TrkB-dependent MAPK and PI-3K cascades in rodent cortical neurons," *Progress in Neuro-Psychopharmacology and Biological Psychiatry*, vol. 34, no. 1, pp. 147–153, 2010.
- [61] Y. Xu, B. Ku, L. Tie et al., "Curcumin reverses the effects of chronic stress on behavior, the HPA axis, BDNF expression and phosphorylation of CREB," *Brain Research*, vol. 1122, no. 1, pp. 56–64, 2006.
- [62] L. Zhang, J. Luo, M. Zhang, W. Yao, X. Ma, and S. Y. Yu, "Effects of curcumin on chronic, unpredictable, mild, stress-induced depressive-like behaviour and structural plasticity in the lateral amygdala of rats," *The International Journal of Neuropsychopharmacology*, vol. 17, no. 5, pp. 793–806, 2014.
- [63] J. I. Luebke, C. M. Weaver, A. B. Rocher et al., "Dendritic vulnerability in neurodegenerative disease: insights from analyses of cortical pyramidal neurons in transgenic mouse models," *Brain Structure & Function*, vol. 214, no. 2-3, pp. 181–199, 2010.
- [64] S. T. Tsai, S. Y. Chen, S. Z. Lin, and G. F. Tseng, "Rostral intralaminar thalamic deep brain stimulation ameliorates memory deficits and dendritic regression in beta-amyloid-infused rats," *Brain Structure & Function*, vol. 225, no. 2, pp. 751–761, 2020.

Review Article

Identifying Plant-Based Natural Medicine against Oxidative Stress and Neurodegenerative Disorders

Rahul Chandran  and **Heidi Abrahamse** 

Laser Research Centre, Faculty of Health Sciences, University of Johannesburg, P.O. Box 17011, Doornfontein, 2028 Johannesburg, South Africa

Correspondence should be addressed to Heidi Abrahamse; h Abrahamse@uj.ac.za

Received 6 May 2020; Revised 9 June 2020; Accepted 27 August 2020; Published 16 September 2020

Academic Editor: Ayman M. Mahmoud

Copyright © 2020 Rahul Chandran and Heidi Abrahamse. This is an open access article distributed under the Creative Commons Attribution License, which permits unrestricted use, distribution, and reproduction in any medium, provided the original work is properly cited.

Free radicals and oxidative stress are among the most studied factors leading to the imbalance in mental health. With no exception, free radicals also damage neuronal cells, leading to various degenerative diseases. With existing modern medications, around 80% of the world population relies on herbal medicine for various ailments. Phytochemicals in plants have a wide range of pharmacological properties, the major being their ability to scavenge free radicals. Plant polyphenols are among the major class of antioxidants identified in plants. This antioxidative property of plant compounds and their ability to downgrade the process of oxidative stress can be used to treat neurodegenerative diseases. However, selecting plants and their active compounds is a crucial step in framing the mechanism of action underlying their therapeutic potential.

1. Introduction

Herbal medicine and their active ingredients are trusted source of medicine since ancient times. Herbal products with plant parts in crude form or their bioactive compounds are gaining interest in the treatment of diseases [1]. Plant are rich in medicinal compounds and almost all the parts of a plant can be considered as a medicine in one way or another. However, the most commonly used parts are flowers, fruits, seeds, roots, leaves, bark, etc. Due to increasing disease forms, resistance to existing drugs and demand for drugs with lesser side effects, concern has raised to explore the best source of medicine with modern science/technology and ideas. Global pharmaceutical companies are in the run to find novel medicinal sources and plants being their best choice [2–4]. The popularity of herbal products has increased worldwide in the past few decades [5]. These days, herbal products with well-defined constituents are more preferred over crude forms due to their reliability in preclinical and clinical studies.

Depression and anxiety are among the most common neurodegenerative disorders and also highly associated with substantial comorbidity and mortality. Free radicals and oxidative stress might induce conditions pertaining to nervous

disorders and behavioral changes [6]. Further, a better understanding of oxidative stress-induced mitochondrial dysfunction, neuroinflammatory response, and intracellular signaling pathways may help to draw up a relation among free radicals, oxidative stress, and neurodegenerative disorders [7, 8].

Plant based-therapy targeting the relative link between oxidative stress and neurodegeneration through cellular and molecular levels may improve strategies of treatment and drug development.

2. Oxidative Stress and Neurodegeneration

Oxygen is an essential molecule, which during metabolic conditions may generate free radicals. Free radicals are also an essential and fundamental molecule in any biochemical process and are essential in redox reactions [9]. However, these radicals are highly unstable and target easily accessible biomolecules like lipids, nucleic acids, and proteins. This establishes a chain reaction and plays an important role in the pathogenesis of many disease conditions [10]. In recent years, the research community has witnessed new developments in free radical biology and their role in health and disease incidence (Figure 1). Compared to other organs, the

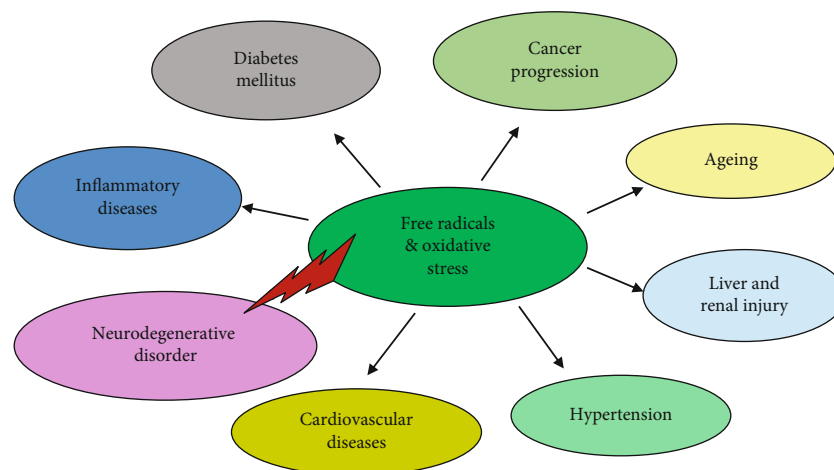


FIGURE 1: Pathogenesis of free radicals. Free radicals and oxidative stress are responsible for the development of various diseases through various cellular and molecular processes. Among them, neurodegeneration is the most commonly noted disorder induced by free radicals.

brain uses a major portion of oxygen and has relatively less antioxidant enzymes, making them more prone to free radical attack [11]. Free radicals like reactive oxygen species (ROS) and reactive nitrogen species (RNS) are prime generators of stress.

Due to high reactivity, superoxide radicals generated in the brain mitochondria limit their movement and cause damage to its DNA and lead to impaired function [12] and neurodegenerative diseases. Hydrogen peroxide (H_2O_2) is the major precursor of superoxide radical in mitochondria. Reduced nicotinamide adenine dinucleotide phosphate (NADPH) oxidase (NOX1 and NOX4) being another sources, are expressed in neurons [13]. Increased NOX activity in the microglia induces neuroinflammation [14] and neurodegenerative diseases [15]. The level of free radical damage increases when nitric oxide interacts with superoxide to become more toxic to neurons [16]. Brain-derived neurotrophic factor (BDNF) is one of the major factors determining the bipolar disorder and depression. Increased free radical concentration and oxidative stress are directly proportional to low concentrations of BDNF and promote depression and anxiety. The use of an antidepressant will increase BDNF, regenerate brain cells, and reduce oxidative stress, depression, and anxiety [17, 18]. Depression is characterized by mood fluctuation and short-term emotional changes leading to serious health. A similar mental disorder is observed in patients with anxiety showing symptoms such as insensitiveness, unpleasant feeling, and loss of interest [19]. The irregular production of neurotransmitters like serotonin, dopamine, and glutamate in the brain is also associated with neurodegeneration [20, 21]. Oxidative stress, increased levels of nuclear factor κ B (NF κ B) and insulin-like growth factor (IGF) is also linked with the progression of these disease conditions [22]. Oxidative stress and mechanisms leading to neurodegenerative and neuropsychiatric disorders have been well studied [23–26]. Antioxidants can remove these free radicals and suppress the conditions leading to depression and anxiety (Figure 2) [27–29].

3. Phytochemicals and Their Pharmacological Significance

According to the World Health Organization [30], around 5% of the population has anxiety and depression disorders. Plant medicine has shown wonders in the treatment of diseases, and traditional plant formulations have been well documented by many researchers [31–33]. Pharmacological reports using these traditional medicines are promising; the research on medicinal plants and neurological disorders are progressing worldwide [34]. With an extensive research on the biological and clinical aspects of depression and anxiety and existing side effects of synthetic drugs, it has become possible to offer new treatment strategies using herbal medicine. The clinical importance of a plant can be related to its biologically active compounds present in them. These compounds are produced in plants as primary and secondary metabolites for the defense mechanism against pathogens, abiotic stress, and other similar adverse conditions [35]. However, these phytochemicals are known to have therapeutic properties, provide nutrition for normal cell health and repairs, enhance the immune system, fight disease-causing agents, inhibit carcinogens, and act as antioxidants [36]. Some of them such as polyphenols, flavonoids, terpenoids, catechins, ascorbic acid, alpha-tocopherol, and beta-carotene may act as an effective nutraceutical supplement. Though their mechanism of actions is yet to be studied completely, their role in preventing the progression of neurodegenerative disorders including Parkinson's disease [37] and Alzheimer's disease are well evaluated [38]. These phytochemicals may exert their therapeutic effects as a single active compound or synergistically. Furthermore, additive action of crude extracts eliminates side effects associated with the predominance of a single xenobiotic compound, giving them a broad spectrum activity and reducing chances of developing resistance by pathogens [39].

Plants produce three major classes of phytochemicals, *viz.* phenolic metabolites and alkaloids, terpenoids, and other nitrogen-containing compounds [40]. Figure 3 represents

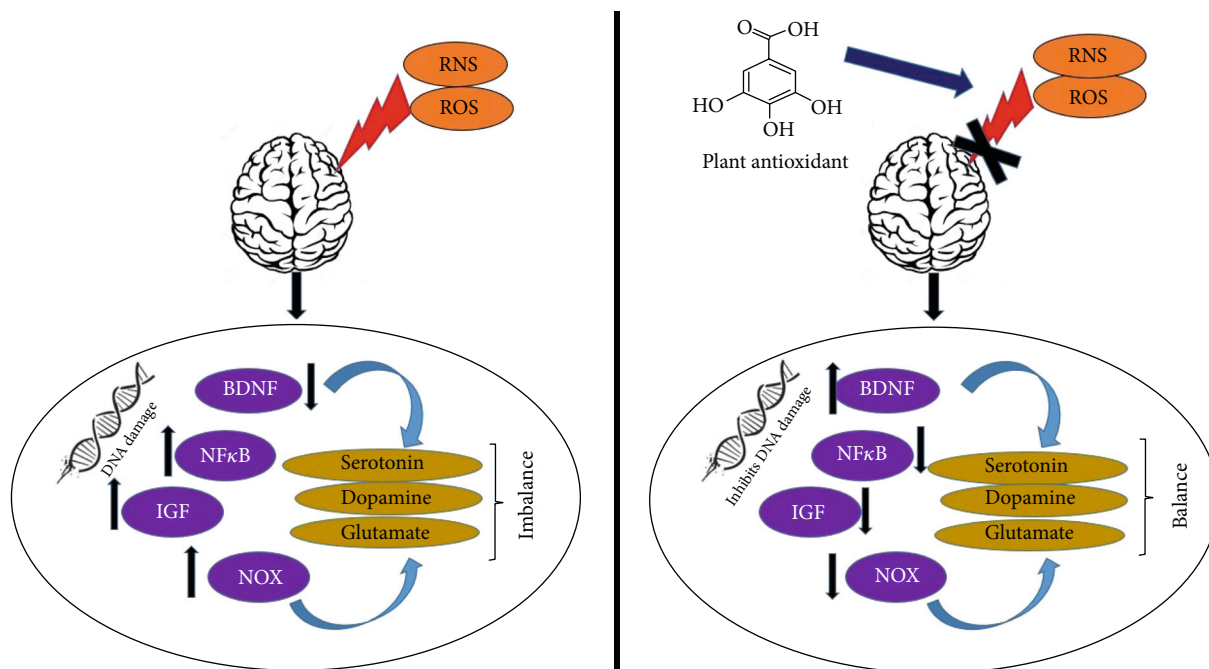


FIGURE 2: Antioxidant defense in neurodegenerative disorder. The radicals generated in the brain mitochondria cause damage to its DNA. Increased NADPH oxidase (NOX), nuclear factor κ B (NF κ B), and insulin-like growth factor (IGF) and low levels of brain-derived neurotrophic factor (BDNF) may cause imbalance in the neurotransmitter production. Antioxidant, on the other hand, reverses this action.

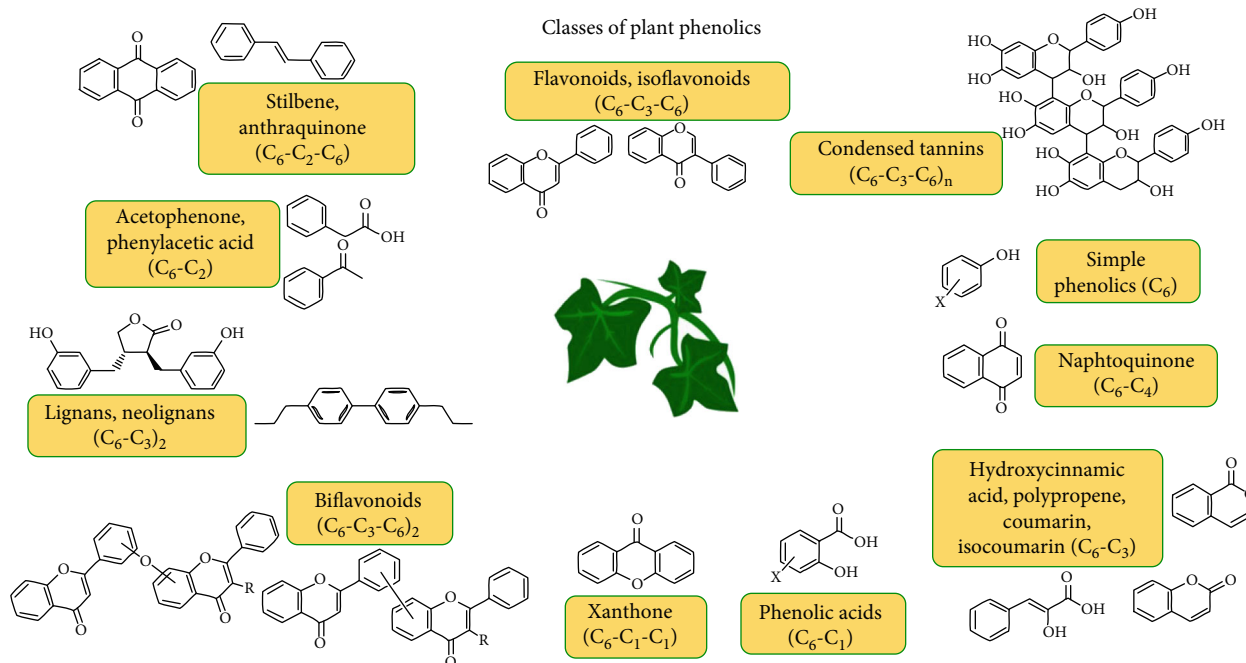


FIGURE 3: Classes of plant phenolics. The figure illustrates plant-derived compounds belonging to different classes of polyphenolics. These phenolic compounds have shown various forms of action to protect the brain from neurodegeneration.

major classes of plant-derived phenolic compounds. Among these, polyphenolics are well known for their high antioxidant capacity [41, 42]. Phenolics are compounds possessing one or more aromatic rings with one or more hydroxyl groups. Plant polyphenols, such as epicatechin, β -catechin,

epicatechin gallate, epigallocatechin, tannic acid, isoflavones, glycyrrhizin, saponins, and chlorogenic acid, have an antidiabetic property [43]. Flavanoids have been reported to show therapeutic activity in cardiovascular diseases and atherosclerosis [44]. Basirnejad et al. [45] reviewed the protective role

of carotenoids including lycopene, γ -carotene, lutein, and xanthophyll against cancer progression. In animals, phytosterols exhibit anti-inflammatory, antineoplastic, antipyretic, and immune-modulating activities [46]. Flavonoids perform a wide range of actions against free radical-mediated inflammation, tumors, and cellular signaling, [47]. These impaired signaling may cause neurodegenerative disorders.

Researchers have also reported neurotrophin induction properties of plant-derived natural compounds. Phytocompounds like 3,5-dicaffeoyl-muquinic acid (*Aster scaber*), furostanol saponins, diosgenin, diosnipsoside A-B, diosniponol C-D, (*Dioscorea* spp.), 6-shogaol (*Zingiber officinale*), and lignans (*Abies holophylla*) were found to possess nerve growth factor (NGF) mimicking property. Other compounds like 3,7-dihydroxy-2,4,6-trimethoxy-phenanthrene, ginkgolide B, lignan derivatives, 4,6-dimethoxyphenanthrene-2,3,7-triol, spicatoside A, ginsenoside Rg3, quercetin, apigenin derivatives, cyanidin-3-*O*- β -glucopyranoside, quinic acid derivatives, and clerodane diterpenoids have been well reported in inducing neuronal cell differentiation and upregulating BDNF [48, 49]. Plant parts as a raw material in traditional medicine or their defined active compounds in modern natural medicine are an interesting source of treatment against neurodegenerative disorders (Table 1).

4. Selection of Plant

There are certain strategies used for the selection of plant species: random screening and ethnobotany. With over 500,000 plant species on earth, and each of these with flowers, fruits, leaves, stem, bark, and roots with different chemical compositions, geographical and seasonal, the likelihood of finding an appropriate plant sample for a desired disease through random search is fairly difficult [60, 61]. In some cases, the compounds isolated from such plants may not be novel and show good activity compared to those available in the market. However, a plant with its ethnobotanical background could be selected with the belief that it is being used traditionally with some medicinal purpose. Traditional knowledge also includes detail of the season during which a particular plant species is medicinally active, part of the plant used, geographical region in which a species abundant [62–64]. Long-term use of a medicinal plant in traditional medicines, including folklore remedies, is generally considered safe and active against prevention of many diseases, and has been proven to be a trustworthy source of active compounds. Such a correlation between traditional medicine and their use in research and the isolation of compounds are well studied by many researchers [65–67].

5. Extraction and Isolation of Bioactive Compounds

As discussed, plant polyphenolics are the major class of antioxidants, which are widely studied for their disease prevention, free radical scavenging property, and reducing oxidative stress. Extraction of these and other compounds is the crucial step in the analysis of plants for its medicinal property. It is necessary to extract the desired chemical compo-

nents from the plant materials for further separation and characterization. Extraction and isolation of active compounds from plants are tedious processes. Hence, definitive measures must be taken to restore the bioactive compounds while extraction and to assure that they are not destroyed, lost, or distorted. It is important to follow traditional uses of a medicinal plant and prepare an extract to mimic as closely as possible the traditional 'herbal' drug [68]. The selection of a solvent system largely depends on the specific nature of the bioactive compound being targeted. Different solvent systems are available to extract the bioactive compound from natural products. As the target compounds may vary from polar to nonpolar, the suitability of the methods of extraction must be considered. Various methods, such as sonication, Soxhlet extraction, heating under reflux, and others are commonly used [69–71] for the extraction of compounds from plant samples. In addition, maceration or percolation of fresh green plants or dried powdered plant material in water and/or organic solvent systems is also being used. In order to reduce the consumption of solvents and time, several modern techniques have been introduced. These include solid-phase microextraction, supercritical-fluid extraction, pressurized-liquid extraction, microwave-assisted extraction, solid-phase extraction, and surfactant-mediated techniques, which possess certain advantages [72]. These steps improve extraction efficiency, kinetics of extraction, and selectivity [73]. But the conventional methods like Soxhlet and maceration are still under use due to their high efficiency in extracting the phytochemicals with higher extract yield. However, the wide range of compounds in plants makes separation and isolation of unknown active compounds a difficult task. Activity-guided fractionation is the most frequently used technique for isolating plant compounds [74]. The optimum recovery of antioxidant compounds like polyphenolics is different from one sample to the other and relies on the type of plant used. The choice of extraction solvents such as ethyl acetate, acetone, alcohols (methanol, ethanol, and propanol), water and their mixtures [75] will influence the yields of phenolics extracted.

According to research findings, increasing time and temperature will increase the solubility and extractability of compounds; however, plant phenolics may undergo enzymatic oxidation and reactions forming undesirable compounds under such conditions [76, 77]. Sample matrix and particle size also strongly influence phenolic extraction from plant materials [78]. Flavonoids are often extracted with methanol, ethanol, acetone, water, or mixtures of these solvents using heated reflux extraction methods [79–81]. Similarly, maximum extractability of flavonoids can be achieved using polar organic solvents alone or in combination [82, 83].

Maceration, Soxhlet, and heated reflux extraction are simple, require relatively cheap apparatus, and result in adequately high phenolic extraction rates [84, 85]. However, the need for large volumes of hazardous organic solvents, long extraction times, and degradation of targeted components due to air, light, high temperatures, and enzymatic reactions are few noted disadvantages [86, 87] which needs standardization. Other modern techniques include pressurized liquid extraction (PLE), super critical fluid extraction (SFC), and microwave-assisted extraction (MAE) [74].

TABLE 1: Commonly used plants against neurodegenerative disorders.

Plant name	Parts used	Active compound	Action	References
<i>Ginkgo biloba</i> L	Leaves	Quercetin, kaempferol, and isorhamnetin	Improves cerebral blood flow	[50]
<i>Panax ginseng</i> C.A. Meyer	Arial parts and root	Aglycones, protopanaxadiol, and propanaxatriol	Promotes neuron survival, increasing the levels of neurotrophic factors	[51]
<i>Scutellaria baicalensis</i> Georgi	Arial parts and root	Baicalin, baicalin, and wogonin	Protect neurons from oxidative damage	[52]
<i>Curcuma longa</i> L	Rhizome	Curcumin	Inhibition of cytokine production and microglia activation	[53]
<i>Vitis vinifera</i> L.	Fruits and seeds	Resveratrol, quercetin, and catechin	Neuroprotective effects	[54]
<i>Salvia officinalis</i> L.	Leaves and flowers	1,8-Cineole, camphor, borneol, caryophyllene, and linalool	Anticholinesterase activity	[55]
<i>Coffea</i> spp.	Seeds	Caffeine	Acts on adenosine receptors	[56]
<i>Camellia sinensis</i> Kuntze	Leaves	Epigallocatechin, epigallocatechin-3-gallate, myricetin, quercetin, kaempferol, epicatechin	Antioxidants, protects from oxidative stress, reduces amyloid proteins	[57]
<i>Bacopa monniera</i> (L.) Pennel	Whole plant	Herpestine, d-mannitol, hersaponin, and monnierin	Enhancing neuronal synthesis, kinase activity, restoration of synaptic activity, and nerve impulse transmission	[58]
<i>Centella asiatica</i> (L.) urban	Leaves	Asiaticoside, brahmoside, brahminoside, asiatic acid, madecassic acid, brahmic acid, isobrahmic acid, and betulic acid	Antioxidant action, acetylcholine esterase inhibitor activity	[59]
<i>Picrothiza scrophulariiflora</i> Pennell	Roots	Glycosides, terpenoids, phenylethanoid, glycosides, and phenolic glycosides	Neuritogenic activity	[58]

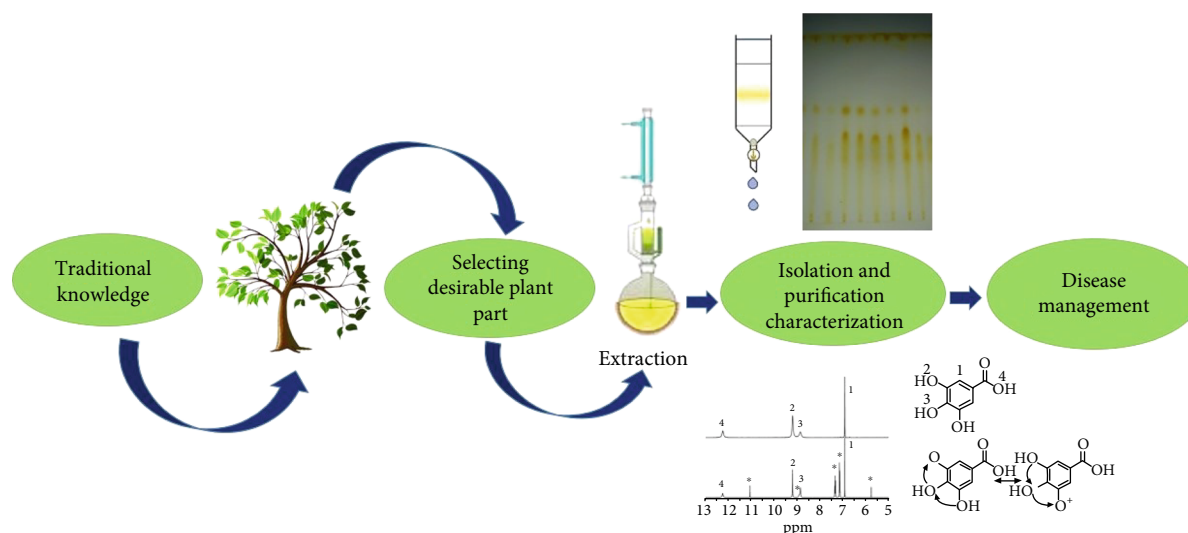


FIGURE 4: Process of activity-guided isolation of compounds. Based on the traditional knowledge, plants were collected and processed for extraction. Extraction and solvent systems are influenced by the plant part, desired activity, targeted class of compounds, etc. Finally, the purified compound alone or in combination as crude extract is used in disease management.

6. Purification and Structural Determination

Purification of the phytochemicals from the crude extract is a difficult and crucial part. Advances in modern techniques of isolation and purification have opened up possibilities for large-scale production of active compounds from plants [78]. Based on the solvent system and techniques used, the crude extract displays combination of bioactive compounds or phytochemicals with different polarities. Chromatographic separations are the best used techniques implemented for efficient isolation and purification of targeted phytochemicals. Paper, thin layer, and column chromatography are the best used conventional isolation and purification method to achieve maximum yield [88, 89]. Finally, the structural determination of compounds after isolation can be done by accumulating data from a wide range of spectroscopic techniques, such as UV-visible, infrared (IR), and nuclear magnetic resonance (NMR) spectroscopy (Figure 4). Although almost all parts of the electromagnetic spectrum are used for studying matter in organic chemistry, but natural products are concerned with energy absorption from three or four regions—ultraviolet (UV), visible, infrared (IR), radio frequency, and electron beam [90].

In clinical trials, isolating active principle and their use are frequently investigated compared to crude extract in order to determine the exact mechanism of action. However, the combination of various active principles of crude extracts promotes synergistic effects, leading to an antioxidant-based defense mechanism in patients with neurodegeneration [91]. Moreover, natural antioxidants with multitarget drug profiles can suppress oxidative stress and the combination of single active principle or crude extracts needs further investigation.

7. Conclusion and Future Perspective

In conclusion, free radicals and oxidative stress could act as one of the prime precursors in building up neurodegenerative

disorders. Phytochemicals with a broad range of activities has increased interest among researchers to explore plant species with significant traditional use. Moreover, it is important to note that natural products, especially from plants with antioxidant property can present a reliable source of medicine. The process of identifying plants and using them for desired medication is a tedious process. But, once identified, herbal medicine could noticeably have maximum impact with lesser side effects due to the synergistic action of compounds present in them. However, more research is needed in this direction to justify their use in the disease management.

Data Availability

All the data used in this study are available with the corresponding author upon request.

Disclosure

The funders had no role in the design of the study; in the collection, analyses, or interpretation of data; in the writing of the manuscript, or in the decision to publish the results.

Conflicts of Interest

The authors declare no conflict of interest.

Acknowledgments

This work is based on the research supported by the South African Research Chairs Initiative of the Department of Science and Technology and National Research Foundation of South Africa (Grant No. 98337), as well as grants received from the University of Johannesburg (URC), the National Research Foundation (NRF), and the CSIR (Council for Scientific and Industrial Research)–NLC (National Laser Centre) Laser Rental Pool Programme.

References




- [1] M. Ekor, "The growing use of herbal medicines: issues relating to adverse reactions and challenges in monitoring safety," *Frontiers in Pharmacology*, vol. 4, p. 177, 2014.
- [2] B. M. Schmidt, D. M. Ribnicky, P. E. Lipsky, and I. Raskin, "Revisiting the ancient concept of botanical therapeutics," *Nature Chemical Biology*, vol. 3, no. 7, pp. 360–366, 2007.
- [3] L. Li, L. S. Adams, S. Chen, C. Killian, A. Ahmed, and N. P. Seeram, "Eugenia jambolana Lam. berry extract inhibits growth and induces apoptosis of human breast cancer but not non-tumorigenic breast cells," *Journal of Agriculture and Food Chemistry*, vol. 57, no. 3, pp. 826–831, 2009.
- [4] S. Y. Pan, S. Pan, Z. L. Yu et al., "New perspectives on innovative drug discovery: an overview," *International Journal of Pharmacy and Pharmaceutical Sciences*, vol. 13, no. 3, pp. 450–471, 2010.
- [5] J. M. Humber, "The role of complementary and alternative medicine: accommodating pluralism," *Journal of American Medical Association*, vol. 288, no. 13, pp. 1655–1656, 2001.
- [6] W. Kessler, W. Numtip, W. Völkel et al., "Kinetics of di(2-ethylhexyl) phthalate (DEHP) and mono(2-ethylhexyl) phthalate in blood and of DEHP metabolites in urine of male volunteers after single ingestion of ring-deuterated DEHP," *Toxicology and Applied Pharmacology*, vol. 264, no. 2, pp. 284–291, 2012.
- [7] S. Moylan, H. A. Eyre, M. Maes, B. T. Baune, F. N. Jacka, and M. Berk, "Exercising the worry away: how inflammation, oxidative and nitrogen stress mediates the beneficial effect of physical activity on anxiety disorder symptoms and behaviours," *Neuroscience and Biobehavioral Reviews*, vol. 37, no. 4, pp. 573–584, 2013.
- [8] A. Jindal, R. Mahesh, and S. Bhatt, "Etazolate, a phosphodiesterase 4 inhibitor reverses chronic unpredictable mild stress-induced depression-like behavior and brain oxidative damage," *Pharmacology Biochemistry and Behaviour*, vol. 105, pp. 63–70, 2013.
- [9] A. Phaniendra, D. B. Jestadi, and L. Periyasamy, "Free radicals: properties, sources, targets, and their implication in various diseases," *Indian Journal of Clinical Biochemistry*, vol. 30, no. 1, pp. 11–26, 2015.
- [10] F. Khan, V. K. Garg, A. K. Singh, and T. Kumar, "Role of free radicals and certain antioxidants in the management of Huntington's disease: a review," *Journal of Analytical and Pharmaceutical Research*, vol. 7, no. 4, pp. 386–392, 2018.
- [11] B. Halliwell, "Reactive oxygen species and the central nervous system," *Journal of Neurochemistry*, vol. 59, no. 5, pp. 1609–1623, 1992.
- [12] C. Gemma, J. Vila, A. Bachstetter, and P. C. Bickford, "Oxidative stress and the aging brain: from theory to prevention," in *Brain Aging: Models, Methods, and Mechanisms*, D. R. Riddle, Ed., pp. 353–374, CRS Press, Taylor & Francis Group, Boca Raton, FL, 2007.
- [13] K. T. Kishida and E. Klann, "Sources and targets of reactive oxygen species in synaptic plasticity and memory," *Antioxidant and Redox Signaling*, vol. 9, no. 2, pp. 233–244, 2007.
- [14] D. J. Hall, S. H. Han, A. M. Chepetan, E. G. Inui, M. Rogers, and L. L. Dugan, "Dynamic optical imaging of metabolic and NADPH oxidase-derived superoxide in live mouse brain using fluorescence lifetime unmixing," *Journal of Cerebral Blood Flow and Metabolism*, vol. 32, no. 2, pp. 23–32, 2011.
- [15] S. H. Chen, E. A. Oyarzabal, and J. S. Hong, "Critical role of the Mac1/NOX2 pathway in mediating reactive microgliosis-generated chronic neuroinflammation and progressive neurodegeneration," *Current Opinion in Pharmacology*, vol. 26, pp. 54–60, 2016.
- [16] P. Pacher, J. S. Beckman, and L. Liaudet, "Nitric oxide and peroxynitrite in health and disease," *Physiological Reviews*, vol. 87, no. 1, pp. 315–424, 2007.
- [17] A. R. Brunoni, M. Lopes, and F. Fregni, "A systematic review and meta-analysis of clinical studies on major depression and BDNF levels: implications for the role of neuroplasticity in depression," *International Journal of Neuropsychopharmacology*, vol. 11, no. 8, pp. 1169–1180, 2008.
- [18] A. Vander Meij, H. C. Comijs, A. Dols, J. G. E. Janzing, and R. C. O. Voshaar, "BDNF in late-life depression: effect of SSRI usage and interaction with childhood abuse," *Psychoneuroendocrinology*, vol. 43, pp. 81–89, 2014.
- [19] W. Y. A. Wahed and S. K. Hassan, "Prevalence and associated factors of stress, anxiety and depression among medical Fayoum University students," *Alexandria Journal of Medicine*, vol. 53, no. 1, pp. 77–84, 2017.
- [20] A. L. Lopresti, S. D. Hood, and P. D. Drummond, "A review of lifestyle factors that contribute to important pathways associated with major depression: diet, sleep and exercise," *Journal of Affective Disorders*, vol. 148, no. 1, pp. 12–27, 2013.
- [21] N. Ye, Z. Song, and A. Zhang, "Dual ligands targeting dopamine D2 and serotonin 5-HT1A receptors as new antipsychotic or anti-parkinsonian agents," *Current Medicinal Chemistry*, vol. 21, no. 4, pp. 437–457, 2014.
- [22] I. Lukic, M. Mitic, J. Djordjevic et al., "Lymphocyte levels of redox-sensitive transcription factors and antioxidative enzymes as indicators of pro-oxidative state in depressive patients," *Neuropsychobiology*, vol. 70, no. 1, pp. 1–9, 2014.
- [23] T. Ma and E. Klann, "Amyloid β : linking synaptic plasticity failure to memory disruption in Alzheimer's disease," *Journal of Neurochemistry*, vol. 120, no. 1, pp. 140–148, 2012.
- [24] B. Parajuli, Y. Sonobe, H. Horiuchi, H. Takeuchi, T. Mizuno, and A. Suzumura, "Oligomeric amyloid β induces IL-1 β processing via production of ROS: implication in Alzheimer's disease," *Cell Death and Disease*, vol. 4, no. 12, p. e975, 2013.
- [25] M. Maes, P. Galecki, Y. S. Chang, and M. Berk, "A review on the oxidative and nitrosative stress (O&NS) pathways in major depression and their possible contribution to the (neuro)degenerative processes in that illness," *Progressive Neuropsychopharmacology Biological Psychiatry*, vol. 35, no. 3, pp. 676–692, 2011.
- [26] J. Q. Wu, T. R. Kosten, and X. Y. Zhang, "Free radicals, antioxidant defense systems, and schizophrenia," *Progressive Neuropsychopharmacology Biological Psychiatry*, vol. 46, pp. 200–206, 2013.
- [27] M. Berk, O. Dean, S. M. Cotton et al., "The efficacy of N-acetylcysteine as an adjunctive treatment in bipolar depression: an open label trial," *Journal of Affective Disorder*, vol. 135, no. 1-3, pp. 389–394, 2011.
- [28] P. V. Magalhães, O. M. Dean, A. I. Bush et al., "N-Acetylcysteine for major depressive episodes in bipolar disorder," *Revista Brasileira de Psiquiatria*, vol. 33, no. 4, pp. 374–378, 2011.
- [29] Y. Xu, C. Wang, J. J. Klabnik, and J. M. O'Donnell, "Novel therapeutic targets in depression and anxiety: antioxidants as a candidate treatment," *Current Neuropharmacology*, vol. 12, no. 2, pp. 108–119, 2014.

- [30] WHO, "Depression and other related disorders-Global health estimates," April 2020, <https://apps.who.int/iris/bitstream/handle/10665/254610/WHO-MSD-MER-2017.2-eng.pdf>.
- [31] W. H. Farah, M. Alsawas, M. Mainou et al., "Non-pharmacological treatment of depression: a systematic review and evidence map," *Evidence Based Medicine*, vol. 21, no. 6, pp. 214–221, 2016.
- [32] L. F. Zeng, Y. Cao, L. Wang et al., "Role of medicinal plants for liver-qi regulation adjuvant therapy in post-stroke depression: a systematic review of literature," *Phytotherapy Research*, vol. 31, no. 1, pp. 40–52, 2017.
- [33] B. Muszynska, M. Lojewski, J. Rojowski, W. Opoka, and K. Sulkowska-Ziaja, "Natural products of relevance in the prevention and supportive treatment of depression," *Psychiatria Polska*, vol. 49, no. 3, pp. 435–453, 2015.
- [34] X. Zhang, J. M. Beaulieu, T. D. Sotnikova, R. R. Gainetdinov, and M. G. Caron, "Tryptophan hydroxylase-2 controls brain serotonin synthesis," *Science*, vol. 305, no. 5681, p. 217, 2004.
- [35] T. Isah, "Stress and defense responses in plant secondary metabolites production," *Biological Research*, vol. 52, no. 39, pp. 1–25, 2013.
- [36] S. N. Ngoci, C. M. Mwendia, and C. G. Mwaniki, "Phytochemical and cytotoxicity testing of *Indigofera lupatana* Baker F," *Journal of Animal and Plant Science*, vol. 11, no. 1, pp. 1364–1373, 2011.
- [37] Z. Shahpiri, R. Bahramsoltani, M. H. Farzaei, F. Farzaei, and R. Rahimi, "Phytochemicals as future drugs for Parkinson's disease: a comprehensive review," *Reviews in the Neurosciences*, vol. 27, no. 6, pp. 651–668, 2016.
- [38] G. P. Kumar and F. Khanum, "Neuroprotective potential of phytochemicals," *Pharmacognosy Reviews*, vol. 6, no. 12, pp. 81–90, 2012.
- [39] D. Olila, J. Opuda-Asibo, and D. Olwa, "Antibacterial and antifungal activities of extracts of *Zanthoxylum chalybeum* and *Warburgia ugandensis*, Ugandan medicinal plants," *African Health Sciences*, vol. 1, no. 2, pp. 66–72, 2001.
- [40] J. B. Harborne, *Classes and functions of secondary products from plants. Chemicals from Plants*, John Wiley and Sons, Norwich, UK, 1999.
- [41] R. Murugan and T. Parimelazhagan, "Study of anti-nociceptive, anti-inflammatory properties and phytochemical profiles of *Osbeckia parvifolia* Arn. (Melastomataceae)," *Industrial Crops and Products*, vol. 51, pp. 360–369, 2013.
- [42] R. Chandran, T. Sajeesh, and T. Parimelazhagan, "Total phenolic content, anti-radical property and HPLC profiles of *Caralluma diffusa* (Wight) N.E. Br.," *Journal of Biologically Active Products from Nature*, vol. 4, no. 3, pp. 188–195, 2014.
- [43] S. K. Jung, "Myricetin suppresses UVB-induced wrinkle formation and MMP-9 expression by inhibiting Raf," *Biochemical Pharmacology*, vol. 79, no. 10, pp. 1455–1461, 2010.
- [44] A. M. Mahmood, J. Rene, H. Bautista, M. A. Sandhu, and O. E. Hussein, "Beneficial effects of citrus flavonoids on cardiovascular and metabolic health," *Oxidative medicine and cellular longevity*, vol. 2019, Article ID 5484138, 19 pages, 2019.
- [45] M. Basirnejad, A. Milani, and A. Bolhassani, "Carotenoids and cancer: biological functions," *Acta Scientific Pharmaceutical Sciences*, vol. 1, no. 6, pp. 11–20, 2017.
- [46] C. J. Dillard and J. B. German, "Phytochemicals: nutraceuticals and human health," *Journal of Science of Food and Agriculture*, vol. 80, no. 12, pp. 1744–1756, 2000.
- [47] S. Kumar and A. K. Pandey, "Chemistry and activities of Flavonoids: Overview," *The Scientific world journal*, vol. 2013, Article ID 162750, 16 pages, 2013.
- [48] K. W. Woo, O. W. Kwon, S. Y. Kim et al., "Phenolic derivatives from the rhizomes of *Dioscorea nipponica* and their anti-neuroinflammatory and neuroprotective activities," *Journal of Ethnopharmacology*, vol. 155, no. 2, pp. 1164–1170, 2014.
- [49] R. Venkatesan, E. Ji, and S. Y. Kim, "Phytochemicals that regulate neurodegenerative disease by targeting neurotrophins: a comprehensive review," *BioMed research international*, vol. 2015, Article ID 814068, 22 pages, 2015.
- [50] J. Birks and E. J. Grimley, "Ginkgo biloba for cognitive impairment and dementia," *Cochrane Database Systematic reviews*, vol. 4, article CD003120, 2002.
- [51] K. Radad, G. Gille, L. Liu, and W. D. Rausch, "Use of ginseng in medicine with emphasis on neurodegenerative disorders," *Journal of Pharmacological Sciences*, vol. 100, no. 3, pp. 175–186, 2006.
- [52] D. E. Shieh, L. T. Liu, and C. C. Lin, "Antioxidant and free radical scavenging effects of baicalein, baicalin and wogonin," *Anticancer Research*, vol. 20, no. 5, pp. 2861–2865, 2000.
- [53] L. Baum and A. Ng, "Curcumin interaction with copper and iron suggests one possible mechanism of action in Alzheimer's disease animal models," *Journal of Alzheimers Disease*, vol. 6, no. 4, pp. 367–377, 2004.
- [54] M. Iriti, S. Vitalini, G. Fico, and F. Faoro, "Neuroprotective herbs and foods from different traditional medicines and diets," *Molecules*, vol. 15, no. 5, pp. 3517–3555, 2010.
- [55] N. S. L. Perry, P. J. Houghton, A. Theobald, P. Jenner, and E. K. Perry, "In-vitro inhibition of human erythrocyte acetylcholinesterase by *Salvia lavandulaefolia* essential oil and constituent terpenes," *Journal of Pharmacy and Pharmacology*, vol. 52, no. 7, pp. 895–902, 2000.
- [56] O. Cauli and M. Morelli, "Caffeine and the dopaminergic system," *Behavioral Pharmacology*, vol. 16, no. 2, pp. 63–77, 2005.
- [57] S. Bastianetto, C. Ramassamy, S. Dore, Y. Christen, J. Poirier, and R. Quirion, "The ginkgo biloba extract (EGb 761) protects hippocampal neurons against cell death induced by β -amyloid," *European Journal of Neuroscience*, vol. 12, no. 6, pp. 1882–1890, 2000.
- [58] G. P. Kumar, K. R. Anilakumar, and S. Naveen, "Phytochemicals having neuroprotective properties from dietary sources and medicinal herbs," *Pharmacognosy Journal*, vol. 7, no. 1, pp. 01–17, 2015.
- [59] M. H. Veerendra Kumar and Y. K. Gupta, "Effect of different extracts of *Centella asiatica* on cognition and markers of oxidative stress in rats," *Journal of Ethnopharmacology*, vol. 79, no. 2, pp. 253–260, 2002.
- [60] M. Setzer, W. Setzer, B. Jackes, G. Gentry, and D. Moriarity, "The medicinal value of tropical rainforest plants from Paluma, North Queensland, Australia," *Pharmaceutical Biology*, vol. 39, no. 1, pp. 67–78, 2008.
- [61] M. S. Lesney, "Nature's pharmaceuticals-natural products from plants remain at the core of modern medicinal chemistry," *Today's chemist at work*, vol. 13, pp. 26–33, 2004.
- [62] A. L. Okundae, "Ageratum conyzoides L. (Asteraceae)," *Fitoterapia*, vol. 73, no. 1, pp. 1–16, 2002.
- [63] S. Chandra, "Effect of altitude on energy exchange characteristics of some alpine medicinal crops from Central Himalayas," *Journal of Agronomy and Crop Science*, vol. 190, no. 1, pp. 13–20, 2004.

- [64] G. C. Jagetia and M. Baliga, "The effect of seasonal variation on the antineoplastic activity of *Alstonia scholaris* R. Br. in HeLa cells," *Journal of Ethnopharmacology*, vol. 96, no. 1-2, pp. 37-42, 2005.
- [65] J. Murillo-Alvarez, D. Encarnacion, and S. Franzblau, "Antimicrobial and cytotoxic activity of some medicinal plants from Baja California Sur (Mexico)," *Pharmaceutical Biology*, vol. 36, no. 6, pp. 445-449, 2001.
- [66] E. Palombo and S. Semple, "Antibacterial activity of traditional Australian medicinal plants," *Journal of Ethnopharmacology*, vol. 77, no. 2-3, pp. 151-157, 2001.
- [67] J. McRae, E. Palombo, I. Harding, and R. Crawford, "Antimicrobial activity of traditional medicinal plants," in *Proceedings of 7th Annual EERE Conference, December 2003, Environmental Engineering Research Event*, pp. 225-233, Victoria, Australia, December 2003.
- [68] D. S. Fabricant and N. R. Farnsworth, "The value of plants used in traditional medicine for drug discovery," *Environmental Health Perspectives*, vol. 109, no. S1, pp. 69-75, 2001.
- [69] Pharmacopoeia of the People's Republic of China, *English ed*, The Pharmacopoeia Commission of PRC, Beijing, 2005.
- [70] The Japanese Pharmacopoeia, *Fourteenth ed.*, JP XVI, The Society of Japanese Pharmacopoeia, Japan, 2016.
- [71] United States Pharmacopoeia and National Formulary, *USP 25, NF 19*, United States Pharmacopoeial Convention Inc., Rockville, 2002.
- [72] S. C. Mahugo, S. Z. Ferrera, E. T. M. Padrón, and J. S. J. Rodríguez, "Methodologies for the extraction of phenolic compounds from environmental samples: new approaches," *Molecules*, vol. 14, no. 1, pp. 298-320, 2009.
- [73] C. W. Huie, "A review of modern sample-preparation techniques for the extraction and analysis of medicinal plants," *Analytical and Bioanalytical Chemistry*, vol. 373, no. 1-2, pp. 23-30, 2002.
- [74] Q. Zhang, L. Lin, and W. Ye, "Techniques for extraction and isolation of natural products: a comprehensive review," *Chinese Medicine*, vol. 13, no. 1, p. 20, 2018.
- [75] P. Garcia-Salas, A. Morales-Soto, A. Segura-Carretero, and A. Fernández-Gutiérrez, "Phenolic-compound-extraction systems for fruit and vegetable samples," *Molecules*, vol. 15, no. 12, pp. 8813-8826, 2010.
- [76] M. Biesaga and K. Pyrzyńska, "Stability of bioactive polyphenols from honey during different extraction methods," *Food Chemistry*, vol. 136, no. 1, pp. 46-54, 2013.
- [77] G. Davidov-Pardo, M. R. I. Arozarena, and M. R. Marin-Arroyo, "Stability of polyphenolic extracts from grape seeds after thermal treatments," *European Food Research and Technology*, vol. 232, no. 2, pp. 211-220, 2011.
- [78] M. Pinelo, B. Zornoza, and A. S. Meyer, "Selective release of phenols from apple skin: mass transfer kinetics during solvent and enzyme-assisted extraction," *Separation and Purification Technology*, vol. 63, no. 3, pp. 620-627, 2008.
- [79] H. B. Zhu, Y. Z. Wang, Y. X. Liu, Y. L. Xia, and T. Tang, "Analysis of flavonoids in *Portulaca oleracea* L. by UV-Vis spectrophotometry with comparative study on different extraction technologies," *Food Analytical Methods*, vol. 3, no. 2, pp. 90-97, 2010.
- [80] M. Biesaga, "Influence of extraction methods on stability of flavonoids," *Journal of Chromatography A*, vol. 1218, no. 18, pp. 2505-2512, 2011.
- [81] W. Routray and V. Orsat, "Microwave-assisted extraction of flavonoids: a review," *Food Bioprocess Technology*, vol. 5, no. 2, pp. 409-424, 2012.
- [82] G. Patil, M. C. Madhusudhan, B. Ravindra Babu, and K. S. M. S. Raghavarao, "Extraction, dealcoholization and concentration of anthocyanin from red radish," *Chemical Engineering and Processing*, vol. 48, no. 1, pp. 364-369, 2009.
- [83] A. Amr and E. Al-Tamimi, "Stability of the crude extracts of *Ranunculus asiaticus* anthocyanins and their use as food colourants," *International Journal of Food Science and Technology*, vol. 42, no. 8, pp. 985-991, 2007.
- [84] K. Kalpana, S. Kapil, P. S. Harsh, and S. Bikram, "Effects of extraction methods on phenolic contents and antioxidant activity in aerial parts of *Potentilla atrosanguinea* Lodd. and quantification of its phenolic constituents by RP-HPLC," *Journal of Agriculture and Food Chemistry*, vol. 56, no. 21, pp. 10129-10134, 2008.
- [85] H. I. Castro-Vargas, L. I. Rodríguez-Varela, S. R. S. Ferreira, and F. Parada-Alfonso, "Extraction of phenolic fraction from guava seeds (*Psidium guajava* L.) using supercritical carbon dioxide and co-solvents," *Journal of Supercritical Fluids*, vol. 51, no. 3, pp. 319-324, 2010.
- [86] E. Aspé and K. Fernández, "The effect of different extraction techniques on extraction yield, total phenolic, and anti-radical capacity of extracts from *Pinus radiata* Bark," *Industrial Crops and Products*, vol. 34, no. 1, pp. 838-844, 2011.
- [87] E. M. Altuner, C. İşlek, T. Çeter, and H. Alpas, "High hydrostatic pressure extraction of phenolic compounds from *Maclura pomifera* fruits," *African Journal of Biotechnology*, vol. 11, no. 4, pp. 930-937, 2012.
- [88] S. Sasidharan, Y. Chen, D. Saravanan, K. M. Sundram, and L. Y. Latha, "Extraction, isolation and characterization of bioactive compounds from plant's extracts," *African Journal of Traditional, Complementary and Alternative Medicine*, vol. 8, no. 1, pp. 1-10, 2011.
- [89] M. Zeeshan, S. M. D. Rizvi, M. S. Khan, and A. Kumar, "Isolation, partial purification and evaluation of bioactive compounds from leaves of *Ageratum houstonianum*," *EXCLI Journal*, vol. 11, pp. 78-88, 2012.
- [90] A. Altemimi, N. Lakhssassi, A. Baharlouei, D. G. Watson, and D. A. Lightfoot, "Phytochemicals: extraction, isolation, and identification of bioactive compounds from plant extracts," *Plants*, vol. 22, no. 6, p. 42, 2017.
- [91] K. J. Kemper, S. Vohra, and R. Walls, "Task force on complementary and alternative medicine; provisional section on complementary, holistic, and integrative medicine. American Academy of Pediatrics. The use of complementary and alternative medicine in pediatrics," *Pediatrics*, vol. 122, no. 6, pp. 1374-1386, 2008.

Research Article

Identification of New Targets and the Virtual Screening of Lignans against Alzheimer's Disease

Mayara dos Santos Maia,¹ Gabriela Cristina Soares Rodrigues,¹ Natália Ferreira de Sousa,¹ Marcus Tullius Scotti ,¹ Luciana Scotti ,¹ and Francisco Jaime B. Mendonça-Junior ²

¹Laboratory of Cheminformatics, Program of Natural and Synthetic Bioactive Products (PgPNSB), Health Sciences Center, Federal University of Paraíba, João Pessoa, PB, Brazil

²Laboratory of Synthesis and Drug Delivery, State University of Paraíba, João Pessoa, PB, Brazil

Correspondence should be addressed to Luciana Scotti; luciana.scotti@gmail.com

Received 22 April 2020; Revised 22 June 2020; Accepted 17 July 2020; Published 17 August 2020

Academic Editor: Pedro Mena

Copyright © 2020 Mayara dos Santos Maia et al. This is an open access article distributed under the Creative Commons Attribution License, which permits unrestricted use, distribution, and reproduction in any medium, provided the original work is properly cited.

Alzheimer's disease (AD) is characterized by the progressive disturbance in cognition and affects approximately 36 million people worldwide. However, the drugs used to treat this disease are only moderately effective and do not alter the course of the neurodegenerative process. This is because the pathogenesis of AD is mainly associated with oxidative stress, and current drugs only target two enzymes involved in neurotransmission. Therefore, the present study sought to identify potential multitarget compounds for enzymes that are directly or indirectly involved in the oxidative pathway, with minimal side effects, for AD treatment. A set of 159 lignans were submitted to studies of QSAR and molecular docking. A combined analysis was performed, based on ligand and structure, followed by the prediction of absorption, distribution, metabolism, excretion, and toxicity (ADMET) properties. The results showed that the combined analysis was able to select 139 potentially active and multitarget lignans targeting two or more enzymes, among them are c-Jun N-terminal kinase 3 (JNK-3), protein tyrosine phosphatase 1B (PTP1B), nicotinamide adenine dinucleotide phosphate oxidase 1 (NOX1), NADPH quinone oxidoreductase 1 (NQO1), phosphodiesterase 5 (PDE5), nuclear factor erythroid 2-related factor 2 (Nrf2), cyclooxygenase 2 (COX-2), and inducible nitric oxide synthase (iNOS). The authors conclude that compounds (06) austrobailignan 6, (11) anolignan c, (19) 7-epi-virolin, (64) 6-[(2R,3R,4R,5R)-3,4-dimethyl-5-(3,4,5-trimethoxyphenyl)oxolan-2-yl]-4-methoxy-1,3-benzodioxole, (116) ococymosin, and (135) mappidoinin b have probabilities that confer neuroprotection and antioxidant activity and represent potential alternative AD treatment drugs or prototypes for the development of new drugs with anti-AD properties.

1. Introduction

Although Alzheimer's disease is a multifactorial disease [1, 2], it is characterized by the increased generation and/or accumulation of amyloidogenic peptides (particularly A β), which are derived from the proteolysis of APP [3]. The presence of senile plaques in the cerebral cortex is thought to result in the activation of inflammatory and neurotoxic processes, culminating in the production of NO, cytokines, and ROS [3–9]. This process contributes to neurodegeneration and the loss of neuronal cells in AD [10, 11].

ROS can have beneficial and negative effects on cellular functions, depending on their concentrations. Low concen-

trations of ROS can regulate cellular functions, through redox-dependent signaling and redox-dependent transcription factors [8, 9]. However, high concentrations of ROS can impair vital cell processes, causing damage to proteins, lipids, and DNA [10]. Therefore, a balance between the production and removal of ROS is essential for normal cellular functions. Homeostasis imbalances can result in oxidative stress and the subsequent development of pathological conditions [11]. Stress precedes A β deposition, tau hyperphosphorylation, and impaired cognitive function. Endogenous antioxidant systems decrease with aging, favoring the appearance of AD. Therefore, oxidative stress is at the heart of AD pathogenesis [12, 13].

Currently, drugs for the treatment of AD include donepezil, galantamine, and rivastigmine, which are inhibitors of the enzyme acetylcholinesterase, while memantine is a noncompetitive inhibitor drug against N-methyl-D-aspartate (NMDA) [14–16]. These inhibitors act on cholinergic receptors and glutamate, respectively. This is because the oxidative glutamate toxicity [13] which is an excitatory neurotransmitter in the central nervous system (CNS) is associated with AD [16]. The excess of glutamate causes the suppression of cysteine uptake by the x_c^- system, which subsequently causes the inhibition of glutathione synthesis (GSH), triggering the accumulation of ROS [17, 18]. In addition to this mechanism, the neurochemical impairment of cholinergic neurons in the central nervous system (CNS) can contribute to the pathology of AD [17]. Although these drugs represent the best pharmacological treatments available at the time of AD, they have a relatively small average overall effect and do not alter the course of the underlying neurodegenerative process [19] probably because AD is multifactorial and is related to several deregulated mechanisms, due to the activation or inactivation of several enzymes important for homeostasis.

Knowing that oxidative stress is the center of the pathogenesis of AD, oxidative defense mechanisms appear to be important targets for the development of new and promising AD drugs. The Kelch-like ECH-associated protein 1 (Keap1)/Nrf2/ARE pathway is one of the most potent defensive systems against oxidative stress [20]. In addition, cyclooxygenase-2 (COX-2), inducible nitric oxide synthase (iNOS), NADPH oxidase (NOX), lipoxygenase (LOX), c-Jun N-terminal kinase 3 (JNK-3), protein tyrosine phosphatase 1B (PTP1B), phosphodiesterase type 5 (PDE5), NADPH oxidase, sodium-glucose cotransporter (SGLT)1, SGLT2, and DJ-1 have been associated with the expression of anti-inflammatory mediators, neuroprotection, and ROS regulation and therefore represent promising AD targets [21–29].

Natural products are important alternatives for AD treatment because they contain widely known and reported classes of molecules associated with antioxidant activities, especially polyphenol compounds [23]. Lignans are a class of polyphenol compounds, which, according to Barbosa Filho in Simões (1999) [24], are chemically characterized as dimers formed by the oxidative homocoupling of cinnamic alcohols or the coupling with cinnamic acids.

Drug design is an important strategy in the field of medicinal chemistry, which increasingly requires the use of modern tools to ensure the increased practicality and speed of obtaining results. For example, we often utilize *in silico* studies that seek to understand the properties between a ligand and its respective receptor [25].

1.1. c-Jun N-Terminal Kinases (JNKs). JNKs represent a family of serine-threonine protein kinases that are encoded by 3 genes (JNK1, JNK2, and JNK3) [26]. JNK1 and JNK2 are ubiquitously expressed, whereas JNK3 is primarily expressed in the brain. JNKs are activated by phosphorylation (pJNK), through the activation of mitogen-activated protein (MAP) kinase kinase (MAPK2), by extracellular stimuli, such as ultraviolet light, cytokines, and A β peptides [27]. In addition, studies have indicated that JNK can be activated by stress and

triggered by harmful external stimuli, via the kinase cascade and oxidative stress, in patients with AD [21]. JNKs are associated with several important functions in the cell, such as inflammation, the regulation of gene expression, cell proliferation, and apoptosis. JNK3 has been implicated in the pathogenesis of AD because JNK3 phosphorylates amyloid precursor protein (APP), which increases the production of A β [27]. Due to its fundamental role in neurodegeneration, JNK pathway signaling has been a target for the design of pharmacological and potential therapeutic agents [28].

The activation of the JNK pathway depends on the coordinated interaction among the scaffold proteins that belong to the JNK activation complex, which is capable of mediating signal amplification, ensuring substrate specificity, and coordinating a signaling cascade [29]. Different stimuli can trigger JNK activation, including JNK interaction protein 1a (JIP1a) and JIP1b (also called IB1), JIP2, JIP3 (initially called JSAP1) JNK-associated leucine zipper protein (JLP), and various SRC homology 3 (SH3) domain-containing proteins. Substrates are activated by JNK phosphorylation, mediated by c-Jun, which in turn interact with JunB, JunD, c-Fos, and activating transcription factor (ATF), which constitute the transcription factor activator protein 1 (AP-1), which regulates the maturation of the cellular response to stress and modulates the signals that ultimately lead to the activation of caspases and proteins associated with apoptosis [30, 31].

Studies have found elevated levels of JNK-3 in the brains of living patients with AD compared to levels in controls and that inhibitors kinases, including JNK-3, are able to reduce the effects of neuronal injury induced by A β [28, 32–34].

1.2. Phosphodiesterases (PDEs). PDEs represent a group of enzymes, consisting of 11 subtypes (PDE1–PDE11), that control the cAMP and cGMP hydrolysis rates [31]. Variant PDEs play specific roles in different physiological characteristics and pathological processes. Although most PDE isoforms are expressed in the brain (PDE1, PDE2, PDE3, PDE4, PDE5A, PDE7A, PDE7B, PDE8B, PDE9A, PD10A, and PDE11A), their levels of expression vary among regions [33]. For example, PDE5 and PDE1 are located in the cerebellum, but only in Purkinje neurons; PDE1B is located in subsets of Purkinje cells; PDE6 is restricted to the retina and pineal gland; PDE3B is expressed in proopiomelanocortin and neuropeptide neurons; PDE1 exhibits distribution patterns in the hippocampus, cerebral cortex, thalamus, and striatum [34]; PDE2A is widely expressed in the brain, with the strongest expression in the cortex, striatum, and hippocampus; and PDE4 is widely expressed in the CNS [22].

PDEs can affect neuronal cell survival, and when PDEs malfunction, they can play roles in neurodegenerative diseases, such as AD [23]. PDE5 produces anti-inflammatory and neuroprotective effects, increasing NOS expression and cGMP accumulation and activating the protein kinase G (PKG) signaling pathway, which plays an important role in the development of several neurodegenerative diseases, including AD, Parkinson's disease (PD), and multiple sclerosis (MS) [24].

During AD pathogenesis, PDE5 hydrolyzes cGMP, an important intracellular messenger that activates PKG, triggering a wide range of intracellular signals [25]. The cyclic regulation of AMP/cGMP plays a determining role in several memory-related processes because these molecules are critical secondary messengers in the brain that are specifically associated with the memory recovery processes [34]. The levels of these messengers are maintained by the balance between production, catalysis, by adenylyl cyclase and guanylyl cyclase, and degradation, which is mediated by PDEs [35]. PDE5 specifically hydrolyzes cGMP [31]. Therefore, PDE5 inhibitors act to increase the levels of cGMP in neurons. Age-associated decreases in cGMP levels have been related to increased PDE5 expression and activity and the accumulation of A β peptide, which inhibits the activation of the NO/cGMP pathway [23]. Many studies have shown that PDE5 inhibitors exhibit therapeutic effects on AD by stimulating NO/cGMP signaling. PDE5 inhibitors can trigger vasodilation in the brain, resulting in the increased or sustained activation of signaling pathways that impact neuroprotective processes [36]. Therefore, elevating cGMP levels through PDE5 inhibition represents an alternative strategy for improving the learning and memory functions of AD patients.

1.3. Protein Tyrosine Phosphatase 1B (PTP1B). PTP1B is a member of the nontransmembrane phosphotyrosine phosphatase family [37] and is a regulator of several processes in the CNS, many of which are therapeutically relevant to AD. Increased PTP1B activity is associated with insulin deficiency and signaling pathways that are impaired in AD [38]. In addition, increased PTP1B activity can be activated with endoplasmic reticulum neuroinflammation and stress, which are both associated with amyloidosis [36]. The neuroinflammatory response includes the activation of innate immune cells in the brain (microglia), the infiltration of macrophages, and the release of inflammatory mediators, such as NO, cytokines, and chemokines, which are associated with the progression of neurodegenerative diseases [37]. Inflammatory processes and amyloid aggregates have been implicated in neuronal loss and cognitive decline. When activated, PTP1B suppresses many signaling pathways that activate GSK3 and are involved in neurodegeneration.

Trodusquemina is a highly selective PTP1B inhibitor that has been used for the intervention of diabetes and obesity in clinical trials and has been investigated for the selective inhibition of PTP1B in neurons. The results showed that trodusquemina was sufficient to improve spatial learning and memory deficits in hAPP-J20 mice and to prevent the loss of neurons in the hippocampus [39]. In another study, PTP1B expression was found to be regulated by inflammatory stimuli, and PTP1B promotes microglial activation and functions as a critical positive regulator of neuroinflammation [37]. Thus, the inhibition of PTP1B provides a new therapeutic strategy for neuroinflammatory and neurodegenerative diseases.

1.4. Nicotinamide Adenine Dinucleotide Phosphate (NADPH) Oxidase (NOX). NOX is the most studied ROS-generating

system [6]. NOX family members are transmembrane proteins that utilize electrons from cytosolic NADPH to reduce oxygen, generating a superoxide anion [16]. Seven known isoforms, NOX1, NOX2, NOX3, NOX4, NOX5, DUOX1, and DUOX2, combined with several subunits to form active enzyme complexes [40, 41]. The only known function of these membrane proteins is the catalysis superoxide anion formation from hydrogen peroxide. Hydrogen peroxide easily permeates cell membranes and can directly damage cells by oxidizing deoxyribonucleic acid (DNA), proteins, and lipids [41].

NOX primarily functions to generate free radicals, and some isoforms can be overregulated by a variety of neurodegenerative factors [41]. Studies have suggested that the genetic and pharmacological inhibition of NOX enzymes may reduce harmful aspects associated with brain injuries and neurodegenerative disorders, resulting in a neuroprotective effect [41]. In particular, the observed lack of benefits associated with various antioxidant strategies may be due to the ineffectiveness of antioxidant molecules *in vivo* or the concomitant attenuation of oxidant regulatory roles [40]. Shimohama et al. [42] reported the translocation of p47phox and p67phox, which strongly suggested that NOX is activated in the AD brain.

Studies with NOX inhibitors exert neuroprotective effects against AD, due to anti-inflammatory properties, through the oligomeric A β - (oA β -) induced microglial proliferation and the production of proinflammatory factors, including ROS, NO, tumor necrosis factor (TNF)- α , and interleukin (IL)-1 β [42–45].

1.5. NADPH Quinone Oxidoreductase 1 (NQO1). NADPH quinone oxidoreductase 1 (NQO1) is a flavin adenine dinucleotide- (FAD-) dependent cytoplasmic flavoprotein that catalyzes the reduction of two electrons from quinones, quinonimines, and nitroaromatic naphthoquinones and substituted by glutathione, dichlorophenolindophenol (DCPIP) dyes, and an NADPH as an electron donor [12]. Therefore, NQO1, plays a central role in monitoring cellular redox status, protecting against oxidative stress induced by a variety of metabolic situations [44], including the metabolism of quinones and other xenobiotics, through the following mechanisms: (i) functioning as a two-electron donor, to provide a derivation that competes with the formation of ROS; (ii) maintaining reduced coenzyme Q; and (iii) regulating the stress-activated kinase pathway [45].

According to Chhetri et al. [12], the inactivation of the detoxifying enzyme NQO1 has been linked to the progression of AD. Factors that alter NQO1 activity can include genetic predispositions, such as the C690T NQO1 polymorphism, advanced age, cigarette smoking, and various medications [12]. The early expression of NQO1 in astrocytes may reflect a partially protective neuronal cell antioxidant protection system that activates at the beginning of the disease process, whereas the late expression of NQO1 may indicate the delayed activation of this system, as a final attempt to prevent neuronal cell death [46].

The antioxidant activity of NQO1 is essential; however, further studies are necessary to determine whether it should be targeted in the treatment of AD.

1.6. Nuclear Factor Erythroid 2-Related Factor 2 (Nrf2). Nrf2 is a transcription factor that facilitates adaptation and survival under stress by regulating the gene expression of different networks of cytoprotective proteins, including anti-inflammatory and antioxidant proteins and proteins that repair or remove damaged macromolecules [47]. Nrf2 plays a crucial role in maintaining cellular redox homeostasis and regulating the production of ROS by mitochondria. Nrf2 affects changes in the mitochondrial membrane potential ($\Delta\psi_m$), ATP synthesis, and lipid peroxidation, and Nrf2 activation under stress conditions or by growth factors can neutralize increases in ROS production by the mitochondria, contributing to neuroprotection [48, 49].

Nrf2 is a key regulator of the body's antioxidant response and is responsible for inducing the expression of genes that encode antioxidant proteins and enzymes, in addition to metabolism detoxification phase II enzymes, which is a critical mechanism associated with cell protection and survival. Nrf2 targets include HO-1, superoxide dismutase (SOD), catalase (CAT), NADPH, NQO1, GSH S transferase (GST), GSH reductase (GR), GSH peroxidase (GPx), thioredoxin (Trx), and glutamate-cysteine ligase (GCL) [50, 51].

In addition to mediating antioxidant and detoxification mechanisms, Nrf2 is responsible for modulating the expression of 200 genes associated with other cellular processes, including the inflammatory response, metabolic regulation, cell proliferation, senescence, and mitochondrial function [52, 53].

Recent studies have investigated the participation of Nrf2, in the mechanisms of apoptosis and neuroprotection associated with Alzheimer's disease and traumatic brain injury, as well as the reduction of the expression of EROs [54].

1.7. Sodium-Glucose Transport Protein (SGLT). Glucose transporters can be divided into two primary families: facilitative glucose transporters (GLUTs) and sodium-dependent glucose cotransporters (SGLTs) [54]. Five primary SGLT isoforms have been identified, SGLT1, SGLT2, SGLT3, SGLT4, and SGLT5; however, SGLT1 and SGLT2, in particular, are associated with the pathways involved in the cellular mechanisms of AD [55].

The SGLT1 isoform is encoded by the SLC5A1 gene and performs glucose transport through a secondary active transport mechanism that uses the Na⁺ gradient established by the Na⁺/K⁺ ATPase pump. This receptor is primarily expressed in the intestine, trachea, heart, testicles, prostate, brain, and kidneys. SGLT1 is characterized as a metabotropic receptor, coupled to transmembrane G proteins, with a secondary structure consisting of 664 amino acid residues, arranged in 14 transmembrane helices with both the NH₂ and COOH terminals facing the extracellular side of the plasma membrane. The receptor contains only one N-glycosylation site, at Asn248 [56–58].

The SGLT2 isoform is encoded by the SLC5A2 gene and is found in the kidneys, brain, liver, thyroid, muscle, and heart. The SGLT2 structure is highly similar to that for the SGLT1 receptor and appears to be involved in diabetes and kidney disease mechanisms [54].

Studies have demonstrated the involvement of the factor SGLT1 in Alzheimer's disease, as it is related to cellular mediators of vascular injury [58]. Its activation is associated with a reduction in the levels of epidermal growth factor (EGFR), and its expression can be linked to food and control of insulin release by inhibiting the enzymes α -amylase and α -glucosidase [59–61].

1.8. Factor DJ-1. DJ-1 protein acts as an oxidative stress sensor and eliminates peroxide by self-oxidation [61]. This receptor is also related to cancer pathogenesis and may act as a potential tumor marker [62, 63]. DJ-1 participates in several signaling pathways, including mitochondrial quality control and the reaction to oxidative stress. Cells with high levels of DJ-1 have been shown to be resistant to oxidative stress and neurotoxins, such as 6-OHDA, whereas lower levels of DJ-1 make cells vulnerable to oxidative stress [64, 65].

The DJ-1 receptor was reported to have anti-Parkinson's disease activity, by Dolgacheva and collaborators [66]. The mechanisms addressed included the protection of dopaminergic neurons against neurodegeneration in Parkinson's disease. The authors stated that the wild-type DJ-1 receptor can act as an oxidative stress sensor and as an antioxidant. DJ-1 regulates transcription and protects mitochondria from oxidative stress, in addition to increasing uncoupling protein (UCP)4 and UCP5 levels, which are responsible for mitochondrial decoupling and the consequent decrease in mitochondrial membrane potential. DJ-1 also suppresses the production of EROS and acts on redox factors, such as NF- κ B, which acts on anti-inflammatory factors [67].

1.9. Cyclooxygenase (COX). Prostaglandins (PGs) are produced by prostaglandin-endoperoxide via synthase/cyclooxygenase (COX), which plays important roles in the etiology and inflammation of autoimmune diseases. COX has 2 isoforms: COX-1, which is permanently expressed in most tissues and organs, and COX-2, which is an inflammation-inducible enzyme that is essential during the inflammation process and in autoimmune disease [68–72]. In addition, COX-2 plays a significant role in aging and skin cancer. PGE₂ is a fundamental product of the COX synthesis pathway [70].

COX-2, also known as prostaglandin H synthase 2 (PGHS-2), catalyzes the conversion from arachidonic acid and O₂ to PGs, which are important lipid mediators involved in numerous physiological aspects and pathophysiological processes. Under normal physiological conditions, COX-2 most often has a low level of expression, but this gene is highly induced in response to inflammation [71–73]. COX-1 is a constitutive enzyme, responsible for maintaining a basic level of PGs, to maintain physiological homeostasis, such as gastrointestinal integrity [73, 74]. COX-1 and COX-2 catalyze the biosynthesis of prostaglandins, prostacyclins,

and thromboxanes [68]. COX-1 and COX-2 share a very high degree of sequence identity and very similar active site topologies [75].

Neurodegenerative diseases, such as AD, are sometimes treated with nonsteroidal anti-inflammatory drugs (NSAIDs), which target COX-1 and COX-2 [76].

1.10. Nitric Oxide Synthase (NOS). NOS is formed by a group of three enzymes (*e*NOS, *n*NOS, and *i*NOS), which are responsible for the generation of nitric oxide (NO) from the amino acid *L*-arginine [77, 78]. NO is a free radical gas and is associated with several biological functions, playing key roles in the regulation of blood flow, blood pressure, and oxygen delivery [79–81].

NOS includes endothelial NOS (*e*NOS or NOS1) [81, 82], inducible NOS (*i*NOS or NOS2), and neuronal NOS (*n*NOS or NOS3) [83]. *e*NOS and *n*NOS are characteristically expressed, whereas *i*NOS expression is induced exclusively by appropriate stimuli, such as cytokines, TNF- α , infections, chronic inflammation, tumors, interferon γ , or hypoxia [83]. During *i*NOS induction, the production of large amounts of NO occurs, in contrast with the other two isoforms [79, 84].

The generalized expression of *i*NOS in the CNS is pathological and is often observed during neurological diseases, such as multiple sclerosis, stroke, and Parkinson’s disease [85]. In patients with AD, studies have shown that the number of *i*NOS-positive neurons significantly increases in the brain and is associated with neuronal damage [86].

*e*NOS acts directly on the NO formation rate and acts as a limiting enzyme for this process, based on its expression levels and biological activity [78, 87]. *e*NOS activity also influences the maintenance of vascular and endothelial homeostasis [88–90], in addition to the structure and function of the vascular endothelium [90].

*n*NOS produces NO in both the CNS and the peripheral nervous system, where it acts as a neurotransmitter [91, 92]. Although *n*NOS is the enzyme responsible for NO synthesis in neurons, not all neurons express *n*NOS [93]. However, the excessive activation of *n*NOS can result in neuronal death due to the harmful production of NO [94].

1.11. Lipoxygenases (LOXs). LOXs are a group of dioxygenase enzymes that contain iron and catalyze the stereoselective addition of oxygen to arachidonic acid (AA), docosahexaenoic acid (DHA), and other polyunsaturated fatty acids (PUFAs) [95]. The basic nomenclature of LOXs (except LOX-3) is based on the position of oxygen insertion in a substrate [95, 96]. Five types of LOXs have been identified in mammals, referred to as 5-, 8-, 12-, and 15-LOX and LOX-3 [97, 98].

Although 5-LOX is known primarily as a modulator of oxidation and inflammation [99], according to Chu et al. [100], this pathway can directly influence the pathogenesis of AD. The 5-LOX- γ -secretase pathway acts on the formation of A β peptides and other molecular diseases, including neuroinflammation, synaptic integrity, and cognitive function, which can contribute to new treatments for AD and associated neurodegenerative problems. High levels of 5-

TABLE 1: Set of molecules from the ChEMBL databases for each enzyme selected in the study.

Database	Active molecules	Inactive molecules	Total
JNK-3	580 (pIC ₅₀ \geq 6.0)	642 (pIC ₅₀ < 6.0)	1.222
PTP1B	1.446 (pIC ₅₀ \geq 5.0)	1.354 (pIC ₅₀ < 5.0)	2.800
NFR2	163 (activity)	85 (no activity)	248
NOX1	85 (pIC ₅₀ \geq 4.75)	60 (pIC ₅₀ < 4.75)	145
PDE5	873 (pIC ₅₀ \geq 7.0)	869 (pIC ₅₀ < 7.0)	1742
COX2	2.018 (pIC ₅₀ \geq 5.50)	1.702 (pIC ₅₀ < 5.50)	3.720
<i>i</i> NOS	396 (pIC ₅₀ \geq 5.50)	367 (pIC ₅₀ < 5.50)	763

LOX in the nuclear envelope are associated with the release of leukotrienes to attract inflammatory cells [101].

5-LOX is widely distributed in the CNS and has been shown to be positively regulated in the postmortem brain of patients with AD, playing a functional role in the pathogenesis [102], as well as its activation influencing synapses and memory impairment [103]. According to Di Mecco et al. [104], 5-LOX is a key enzyme for AD because it is involved in inflammatory responses and is expressed at higher levels in the hippocampi of AD patients compared with healthy adults [105].

Observing that several enzymes are directly and indirectly involved through oxidative stress mechanisms and that their activation and inactivation can contribute to neuroprotection or disease progression, the objective of the research was to explore new targets through virtual screening of lignans to identify molecules with potential anti-AD [106, 107].

2. Materials and Methods

2.1. Data Collection and Curation. Several enzymes with available biological activity and 3D structure data were selected and investigated in this study. Chemical compounds were selected with known activity against the following enzymes: JNK-3 (ChEMBL2637), PTP1B (ChEMBL335), NFR2 (ChEMBL1075094), NOX1 (ChEMBL1287628), PDE5 (ChEMBL1827), COX-2 (ChEMBL230), and *i*NOS (ChEMBL4EM1). These compounds were used in the bank of images used to construct predictive models (<https://www.ebi.ac.uk/chembl/>) [108]. The details of the banks can be found in Table 1. The compounds were classified based on the pIC₅₀ ($-\log$ IC₅₀ (mol/l)). The IC₅₀ value represents the concentration required for 50% inhibition. However, for the enzyme Nrf2, activation data was used because the activation of this protein would obtain the desired effect. In addition, 159 ChEMBL lignans (Table S1) were assessed by virtual screening to identify molecules with potential activity against enzymes involved in AD progression, according to the workflows presented by Fourches et al. [109]. Three-dimensional structures were generated by ChemaxonStandardiser v.18.17.0, (<http://www.chemaxon.org>).

2.2. Quantitative Structure-Activity Relationship (QSAR) Modeling. The Knime 3.5.3 software (KNIME 3.5.3, Konstanz Information Miner Copyright, 2018, <https://www.knime.org>) was used to perform the analyses and to generate

the *in silico* models. Given the success of our previous studies [110, 111], we opted to perform a 3D QSAR analysis for each bank of enzymes. All studied compounds with a solved chemical structure were saved in special data file (SDF) format and imported into the Dragon 7.0 software [112], to generate descriptors.

The banks of molecules and their calculated descriptors were imported from the Dragon software, and the data were divided into a "Partitioning" tool, using the "Stratified sample" option, which separated the data into Training and Testing sets, which represented 80% and 20% of all compounds, respectively. The sets were randomly selected, but the proportions of active and inactive substances were maintained in both databases.

The Random Forest (RF) algorithm, using WEKA nodes [113], was used to build predictive models. The parameters selected for RF for all models were as follows: the total number of forests was 250, and 1 seed was used for the generation of random numbers. Cross-validation was performed to estimate the predictive power of the developed models.

The external performances of the selected models were analyzed for sensitivity (true-positive rate, or active rate), specificity (true-negative rate, or inactive rate), and accuracy (general predictability). In addition, the sensitivity and specificity of the receiver operating characters (ROC) curve were used because these describe actual performance more clearly than accuracy.

The models were also analyzed using the Matthews correlation coefficient (MCC), which can evaluate the model globally, based on the results obtained in the confusion matrix. The MCC is a correlation coefficient between the observed and predictive binary classifications, resulting in values between -1 and +1, where a coefficient of +1 represents a perfect prediction, 0 represents a random prediction, and -1 indicates the total disagreement between the prediction and the observation [114].

MCC can be calculated using the following formula:

$$\text{MCC} = \frac{\text{VP} \times \text{VN} - \text{FP} \times \text{FN}}{\sqrt{(\text{VP} + \text{FP})(\text{VP} + \text{FN})(\text{VN} + \text{FP})(\text{VN} + \text{FN})}}, \quad (1)$$

where VP represents true positives, VN represents true negatives, FP represents false positives, and FN represents false negatives.

The applicability domain (APD) was used to analyze the compounds in the test sets, to evaluate whether the predictions are reliable. The APD is a theoretical chemical space that encompasses the model's descriptors and the modeled response, allowing the estimation of uncertainty when predicting the activity of a compound in the training set used during the development of the model. This technique is important for verifying the reliability of QSAR models by comparing predicted values with observed values [115]. APD is calculated using the following formula:

$$\text{APD} = d + Z\sigma, \quad (2)$$

where d and σ are the Euclidean distances and the mean standard deviation, respectively, for the compounds in the train-

ing set. Z is an empirical cutoff value, which was set to 0.5 in this study.

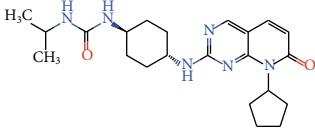
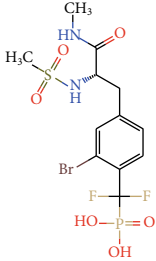
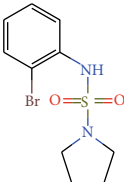
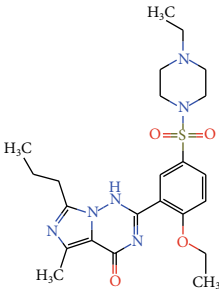
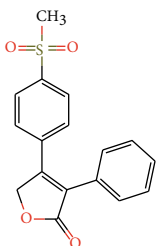
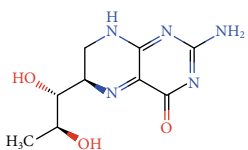
2.3. Molecular Docking. Molecular docking was performed using the Molegro Virtual Docker v6.0.1 (MVD) software [116], and six targets were selected for anchorage studies (Table 2). The 3D structures of the enzymes used in this study were obtained from Protein Data Bank (PDB) [117], using the following codes: PDB ID 4Y46 for JNK-3; PDB ID 4Y14 for PTPB1; PDB ID 6FY4 for NQO1; PDB ID 3B2R for PDE5; PDB ID 5KIR for COX-2; and PDB ID 4NOS for *i*NOS. We did not dock the enzymes Nrf2 and NOX1 because 3D structures were not available in PDB for the human species. Initially, all water molecules were removed from the crystalline structure, and the root-mean-square deviation (RMSD) was calculated from the poses, which indicates the degree of reliability for the fit. The RMSD provides for the connection mode close to the experimental structure and is considered successful if the value is below 2.0 Å. The MolDock score algorithm was used as a scoring function, to predict the best interactions between the ligand and the receptor. Then, the anchor assistant was generated, in which the enzyme and ligands were inserted to analyze the stability of the system based on the interactions identified with the active site of the enzyme.

2.4. Prediction of ADMET Properties. ADME parameters were calculated using the SwissADME open-access web tool (<http://www.swissadme.ch>) [118], which offers a set of rapid predictive models for the assessment of physicochemical, pharmacokinetic, and pharmacological properties. The toxicity prediction was performed in OSIRIS Property Explorer (<https://www.organic-chemistry.org/prog/peo/>) [119], based on the following parameters: mutagenicity, tumorigenicity, reproductive effects, and irritability. For absorption, factors included membrane permeability, intestinal absorption, and substrate or inhibitor of P glycoprotein. Thus, we investigated compounds that did not exceed more than two violations of Lipinski's rule and for which the log P consensus was not greater than 4.15. In addition, compounds were not substrates for the permeability glycoprotein enzyme (P-gp). The distribution was assessed by factors that include the blood-brain barrier (logBB) and the permeability of the CNS. Metabolism was predicted based on the CYP substrate or inhibition models (CYP1A2, CYP2C19, CYP2C9, CYP2D6, and CYP3A4).

3. Results and Discussion

3.1. QSAR Modelling. The metrics mentioned are the most commonly used metrics for chemoinformatics, although others can be used to guarantee the high predictability of the model, such as ROC curves [120]. The results of the ROC curve and MCC analyses revealed excellent results. The models achieved ROC curves greater than 0.78 during cross-validation, and the MCC values were also greater than 0.52 during the cross-validation, revealing a model with excellent classification, performance, and robustness (Table 3, Figure S1). Only the model for the Nrf2 enzyme

TABLE 2: Information regarding the selected enzymes, obtained from the PDB database and used for docking.

PDB ID	Enzyme	Class	PDB ligand	Resolution
4Y46	c-Jun N-terminal kinase	Transferase		2.04 Å
4Y14	Tyrosine phosphatase 1B	Hydrolase		1.89 Å
6FY4	NAD(P)H:quinone oxidoreductase	Oxidoreductase		2.76 Å
3B2R	Phosphodiesterase-5	Hydrolase		2.07 Å
5KIR	Cyclooxygenase-2	Oxidoreductase		2.69 Å
4NOS	Inducible nitric oxide synthase	Oxidoreductase		2.25 Å

achieved an MCC below 0.5. Table 4 shows the ROC curve values for each protein.

Using the models created, with excellent performance, the lignan set was screened to select compounds that are potentially active against the studied enzymes. Lignans with a probability of biological activity above 0.5 and that passed the applicability domain were considered active.

The results showed that no lignans were considered active for the JNK-3, PDE5, and COX-2 targets. However, 22 compounds were potentially active against the PTPB1 enzyme with a probability ranging from 50 to 74%, 111 compounds active against Nfr2 with a probability ranging from 50 to 64%, six compounds active against NOX1 with a probability ranging between 63 and 78%, and 27

TABLE 3: Performance summary corresponding with the results obtained for all Random Forest models.

Enzyme	Validation	Accuracy	Sensitivity	Specificity	PPV	NPV	MCC
JNK-3	Test	0.89	0.91	0.87	0.86	0.91	0.78
	Cross	0.83	0.85	0.82	0.81	0.85	0.67
PTP1B	Test	0.81	0.81	0.81	0.82	0.80	0.62
	Cross	0.82	0.82	0.82	0.83	0.81	0.64
NFR2	Test	0.76	0.75	0.76	0.86	0.61	0.50
	Cross	0.73	0.78	0.63	0.80	0.60	0.41
NOX1	Test	0.82	0.76	0.91	0.92	0.73	0.67
	Cross	0.80	0.89	0.66	0.92	0.73	0.58
PDE5	Test	0.87	0.9	0.84	0.85	0.9	0.75
	Cross	0.86	0.88	0.85	0.85	0.87	0.73
COX2	Test	0.78	0.83	0.71	0.77	0.78	0.55
	Cross	0.76	0.81	0.7	0.76	0.76	0.52
iNOS	Test	0.81	0.87	0.74	0.78	0.84	0.62
	Cross	0.8	0.85	0.74	0.78	0.82	0.60

TABLE 4: Values for the ROC curves, during the test and cross-validation, for each RF model.

Enzyme	ROC curve	
	Test	Cross
JNK-3	0.96	0.91
PTP1B	0.87	0.89
NFR2	0.82	0.81
NOX1	0.90	0.78
PDE5	0.95	0.94
COX2	0.84	0.84
iNOS	0.87	0.87

compounds active against iNOS with probability varying between 52 and 79%.

3.2. Docking Molecular. The molecular docking study was performed for six enzymes that were targeted for the AD treatment. The ligand set was analyzed to select molecules with good probabilities for potential inactivation and activation activity against the enzymes targeted for AD treatment. Docking was not performed for Nrf2 and NOX1, due to the unavailability of human 3D protein structures.

In this study, the docking results were validated by the redocking of the crystallographic ligand and by the RMSD of the poses. Redocking consists of positioning and predicting the binding affinity of the crystallographic ligand in the region of the active site of the enzyme. The RMSD compares and calculates the mean deviation of the square root of the poses obtained by redocking and the structure of the ligand obtained experimentally. For the fit to be reliable, the RMSD value must be 2.0 Å or less. The results showed that the targets JNK-3, PTP1B, NQO1, PDE5, COX-2, and iNOS obtained RMSD values of 0.56, 0.25, 0.18, 0.47, 0.19, and 0.16 Å, respectively.

The Molegro software is capable of generating interaction energies for lignans, by producing a MoldockScore for each studied protein. Then, calculations were performed to iden-

TABLE 5: MoldockScore scores for the top ten lignans with the best energy values relative to the energy value of the crystallographic ligand for each protein.

ID	JNK-3	PTP1B	NQO1	PDE5	COX2	iNOS
1	-183	-177	-137	-204	-203	-178
2	-175	-156	-137	-192	-193	-153
3	-164	-154	-136	-182	-191	-147
4	-159	-153	-124	-169	-190	-144
5	-155	-153	-120	-167	-187	-143
6	-148	-152	-116	-166	-176	-143
7	-148	-152	-116	-164	-175	-143
8	-146	-151	-114	-164	-174	-141
9	-146	-151	-112	-164	-172	-139
10	-144	-150	-108	-162	-170	-139
Ligand PDB	-134	-156	-36	-139	-142	-59

tify the lignans with the best active potential probabilities for each analyzed protein, using the following formula:

$$\text{Prob} = \frac{E_{\text{Lig}}}{E_{\text{MLig}}}, \text{ se } E_{\text{Lig}} < E_{\text{Inib}}, \quad (3)$$

where E_{Lig} is the energy of the analyzed ligand, E_{MLig} is the lowest energy obtained from the tested lignans, and E_{Inib} is the energy of the inhibitor ligand, obtained from the crystallography data for the tested protein. Only molecules that obtained binding energies below the binding energy for the crystallographic inhibitor ligand were considered to be potentially active.

Table 5 shows the interaction energies of the inhibitor ligand for each protein, and the top ten lignans with the best energy values for each protein.

Among the 159 lignans analyzed by molecular docking, 21 were found to be potentially active against JNK-3, 1 was identified for PTP1B, 157 were identified for NQO1, 34 were

identified for PDE5, 53 were identified for COX-2, and 156 were identified for *i*NOS. These results indicated that lignans, in general, are more likely to activate the NQO1 and *i*NOS proteins and are not selective for the PTP1B enzyme.

3.3. Combined Analysis Based on Ligand and Structure. A second consensus analysis was performed to identify potential multitarget lignans, which demonstrate active potential probabilities for more than one protein, based on the RF model and docking. In this case, we use all the results of prediction of biological activity of the lignans and combine them with the results of docking. For this analysis, the following formula was used:

$$\text{Prob}_{\text{Comb}} = \frac{(\text{Prob}_{\text{Dc}} + (1 + \text{ESP}) \times P_{\text{Activity}})}{2 + \text{ESP}}, \text{Se Prob}_{\text{Comb}} > 0.5, \quad (4)$$

where Prob_{Dc} is the active potential probability from the molecular coupling analysis, ESP is the average specific value of the RF model, and P_{Activity} is the active potential probability value of the RF model. This combined probability was conditioned, as only molecules with values greater than 0.5 were considered likely to be active. Combined probability values were calculated for the lignans identified for each target enzyme, and we analyzed which molecules were multitarget.

After performing the combined analysis, based on the ligand and structure, and using the formula to identify multitarget molecules, we identified 139 molecules that were potentially active for two or five target enzymes, out of the entire lignan set analyzed. For Nrf2 and NOX1, we only used the biological activity probability data, and for NQO1, we only used the docking data not enough data was available for these enzymes to construct the necessary models.

The combined probability ($\text{Prob}_{\text{Comb}}$), based on both ligand and structure, can increase the predictive power of the models and decrease the number of false positives. Combined probability analyses could be performed for five enzymes (JNK-3, PTP1B, PDE5, COX-2, and *i*NOS). For enzymes without sufficient data to build both models, only model was used. For molecules to be considered potentially active, the probability values should be equal to or greater than 0.5. However, for Prob_{Dc} , the probability value should also be greater than that for the crystallographic ligand.

After the combined probability analysis, we selected the multitarget compounds that passed the applicability domain for all enzymes in this study. Using $\text{Prob}_{\text{Comb}}$, we were able to select three compounds with probabilities of activity ranging from 50% to 61% for JNK-3, 43 compounds with a 52–72% probabilities for PTP1B, 57 compounds with 51–72% probabilities for PDE5, 27 compounds with probabilities between 50% and 61% for COX-2, and 27 compounds with probabilities between 50% and 81% for *i*NOS (Table 6). The number of compounds with excellent combined probabilities was reduced when compared with the results of the docking probabilities; however, the combined probabilities increased the numbers of true positives.

Based on the biological activity probability data, 111 compounds, with probabilities ranging from 50% to 64%, were identified for Nrf2, and nine compounds, with probabilities ranging from 51% to 78%, were identified for NOX1. Based on the docking probability data, 156 compounds were selected, with probabilities ranging from 27% to 100%, for NQO1. For this enzyme, compounds with probabilities above 0.27 were considered, as these were greater than the probability of the crystallographic ligand, which was 0.26.

We observed that although the results of QSAR do not indicate active compounds for JNK-3, PDE5, and COX-2, after the application of the formula that combines prediction values of biological activity and docking ($\text{Prob}_{\text{Comb}}$), we were able to identify active compounds for all targets of the study.

3.4. Prediction of ADMET Properties. The set of 139 potentially active and multitarget lignans were submitted to several predictive parameters to identify the compounds with the best ADMET profiles. Using physical-chemical properties, we attempted to verify compounds with good absorption, considering the lipid rule as a parameter.

According to Shimohama et al. [42, 43], molecules with molecular weights below 500 Da, calculated $\log P$ ($\text{Clog}P$) values less than five, less than five hydrogen bond donors, no more than ten hydrogen bond acceptors, and ≤ 10 rotating bonds have excellent absorption and bioavailability. Molecules that violate two or more of these rules do not show good absorption. We observed that 66% (92) of our lignans set showed solubility values that varied between soluble and moderately soluble.

Factors such as lipophilicity and solubility contribute to drug distribution *in vivo*, which is a requirement for advancing to preclinical and clinical tests. The most common descriptor for lipophilicity is the partition coefficient between *n*-octanol: water ($\log P$). Ideal $\log P$ values are below 5.0. The results showed that 87% (121) of our lignan compounds had ideal $\log P$ values.

Metabolism can affect drug activity by changing the half-life, promoting the generation of toxic metabolites, or disrupting therapeutic potential. Pharmacokinetics are essential for understanding drug metabolism in the body. For a compound to display the desired effect during AD treatment, the drug must be able to cross the blood-brain barrier. Many compounds that have been developed fail at the preclinical and clinical testing stage due to metabolism effects and poor absorption in the brain. Currently, the prediction and selection of compounds that act on nervous system tissues can be performed through *in silico* tests. The results showed that among lignans that target three or more enzymes, nine lignans would likely cross the blood-brain barrier.

Toxicity was also evaluated, and among the compounds that appeared likely to cross the blood-brain barrier, compounds 6, 11, 19, 64, 116, and 135 had no predicted mutagenicity or tumorigenesis effects or negative effects on the reproductive system and irritability. Therefore, these molecules were considered to have the best ADMET properties because they do not present any toxicity risks. Tables S2 and S3 show the ADMET profiles of compounds with potential activity and multitargeting effects against four or

TABLE 6: Potentially active lignans, multitarget for four or more enzymes, based on the RF and docking model. In bold are the active enzymes that walk in the applicability domain.

ID	Prob _{Comb}		Prob _{Activity}		Prob _{Dc}		Multitarget		
	JNK-3	PTP1B	PDE5	COX-2	iNOS	NFR2		NOX1	NQO1
05	0.39	0.68	0.52	0.41	0.62	0.54	0.17	0.47	5
06	0.38	0.67	0.49	0.43	0.59	0.57	0.51	0.35	4
07	0.45	0.66	0.56	0.53	0.70	0.59	0.25	0.49	4
11	0.35	0.64	0.48	0.46	0.53	0.53	0.63	0.38	4
12	0.37	0.62	0.51	0.48	0.60	0.60	0.25	0.64	4
13	0.32	0.62	0.59	0.46	0.57	0.51	0.45	0.72	4
14	0.51	0.62	0.54	0.45	0.62	0.60	0.25	0.45	5
19	0.31	0.59	0.48	0.49	0.56	0.56	0.51	0.35	4
33	0.41	0.53	0.51	0.50	0.51	0.58	0.41	0.39	5
34	0.35	0.53	0.50	0.43	0.54	0.56	0.45	0.40	5
35	0.27	0.52	0.59	0.46	0.49	0.61	0.70	0.56	5
38	0.54	0.52	0.69	0.51	0.66	0.52	0.31	1.00	5
39	0.54	0.52	0.68	0.61	0.65	0.61	0.33	0.81	4
41	0.59	0.52	0.61	0.60	0.54	0.58	0.33	0.67	4
42	0.52	0.52	0.64	0.59	0.62	0.57	0.36	0.78	4
44	0.35	0.51	0.52	0.45	0.58	0.54	0.43	0.50	4
45	0.45	0.51	0.52	0.49	0.55	0.54	0.35	0.47	4
47	0.39	0.50	0.56	0.47	0.54	0.56	0.36	0.56	4
52	0.45	0.48	0.49	0.50	0.69	0.54	0.45	0.38	4
104	0.42	0.40	0.55	0.51	0.31	0.59	0.30	0.50	4
106	0.48	0.40	0.58	0.57	0.52	0.56	0.25	0.63	4
108	0.53	0.40	0.56	0.45	0.64	0.50	0.38	0.66	4
115	0.31	0.39	0.52	0.51	0.61	0.52	0.28	0.52	4
134	0.26	0.36	0.50	0.40	0.51	0.56	0.71	0.38	5
141	0.40	0.35	0.54	0.50	0.50	0.62	0.52	0.40	5
142	0.37	0.35	0.50	0.51	0.65	0.55	0.30	0.40	4
146	0.40	0.33	0.57	0.56	0.66	0.55	0.27	0.60	4
153	0.49	0.32	0.60	0.50	0.63	0.52	0.39	0.74	4

more enzymes. In addition, Table S4 and Figure 1 show the compounds that did not present toxicity for these evaluated parameters.

Due to the antioxidant properties of lignans, the present study sought to perform a virtual screening among diverse structural lignans to identify potential molecules for the treatment of AD. Lignans represent a huge class of pharmacologically active compounds that exhibit various functionalities, which are worth exploring by pharmaceutical industries [121].

According to a review by Zálešák et al. [122], several researchers have identified the antioxidant activity and neuroprotective properties of lignans. Lignans isolated from *Schisandra bicolor* var. were assayed for their neuroprotective effects against SH-SY5Y cell damage induced by A β 25–35. Among the active compounds, both new lignans (esquibitubina B (L1-4), F (L1-7), H (L4-1), and I) and previously isolated lignans (galgravine, (-)-nectandrin A, (-)-futocadsurine A, (+)-9'-hydroxigalbelgin, austrobailignan-6, oleiferin-F,

(+)-dihydro-guaiaretic acid, and (-)-isotobafenol) increased the cell viability in SH-SY5Y cells, following the induction of cellular injury by 3.25 nM A β 25–35 compared with the negative control group. Furthermore, 25 μ M dibenzocyclooctadiene lignans (L6-14 and NL5-10) from *Schisandra chinensis* exhibited protective activity against A β 1–42 neurotoxicity induced in PC12 cells, increasing cell viability to 84.1% \pm 5.4% and 82.1% \pm 4.3%, respectively, compared with the control (52.0% \pm 3.2%) [122].

Lignans are a large group of naturally occurring phenols widespread in the plant kingdom. In addition, notable advances have been made in the isolation and identification of lignans the last few years, which has already led to around 500 new congeners [121]. In addition, several studies have reported the synthesis of different lignans successfully and which have been tested for various biological activities.

3.5. Interaction Analysis. We analyzed the interactions of six lignans through molecular docking that obtained the highest

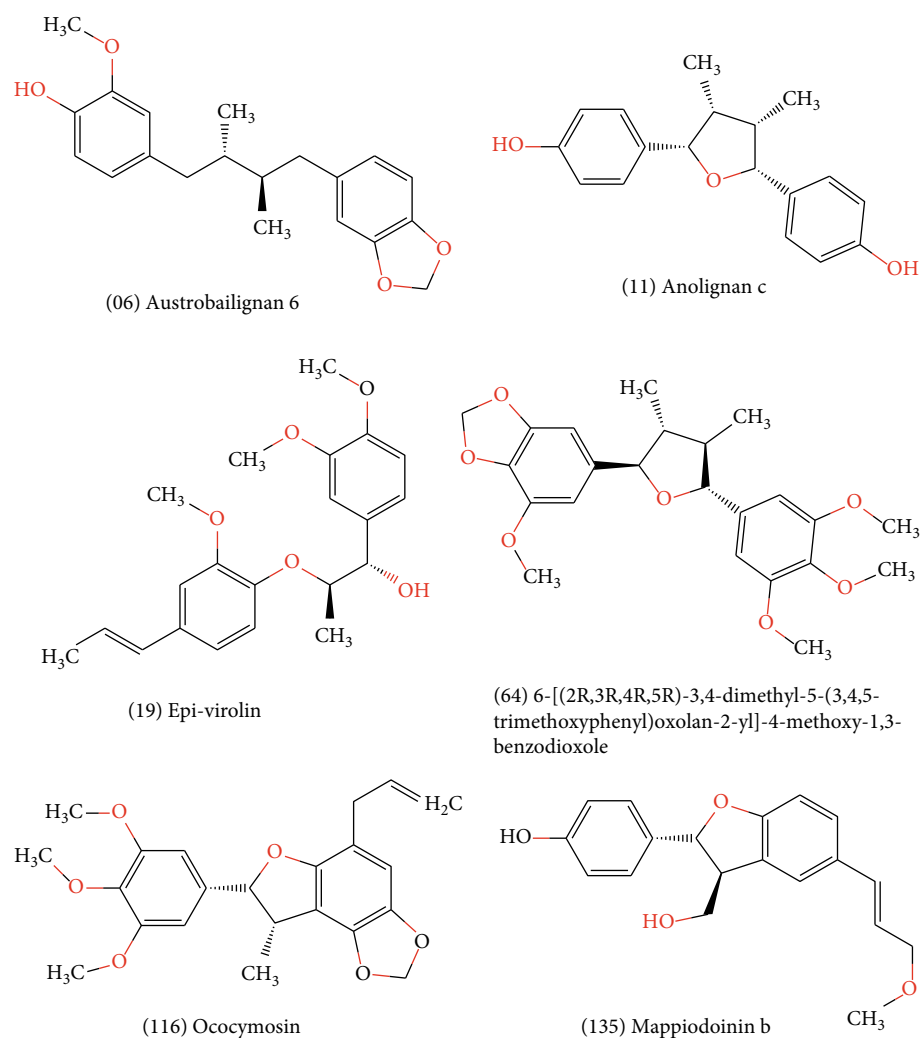


FIGURE 1: Lignans considered to be potentially active according to the Random Forest model, with multitarget effects and no predicted toxicity.

probability of activity, multitarget, and with low toxicity. In addition, we consider analyzing the targets on which these compounds were most active.

The compounds austrobailignan 6 (06), anolignan c (11), and 7-Epi-virolin (19) formed several interactions with the PTP1B active site. Austrobailignan 6 formed hydrophobic interactions with residues Ile219 and Arg221, steric interactions with the amino acids Phe182, Cys215, and Ala217, an electrostatic bond with Arg181, and a hydrogen bond with Tyr46, stabilizing the bond. Anolignan c formed four hydrophobic interactions with the amino acids Tyr26, Cys215, Ala217, and Arg221. In addition, it formed an electrostatic and a steric interaction. 7-Epi-virolin formed several hydrophobic interactions with Tyr46, Phe182, Ala217, and Arg221. Three important hydrogen bonds were also observed with the residues Arg47, Arg45, and Glu262 (Figure 2).

According to the study carried out by Krishnan et al. [123], the inhibitor CPT157633 managed to form electrostatic interactions with the PTP1B active site. In that study, interactions with the amino acids Cys215, Arg221, and

Gln262 were reported. We observed that these amino acids are also interacting with lignans, forming more stable bonds.

These same lignans were also investigated for their interactions with the NQO1 target. We found that 6-[(2R, 3R, 4R, 5R) -3,4-dimethyl-5-(3,4,5-trimethoxyphenyl) oxolan-2-yl] -4-methoxy-1,3-benzodioxole (64) formed hydrogen bonds with the amino acids Tyr129, Gly175, and Ile176, and a hydrophobic interaction with the amino acid Tyr127. Oocymosin (116) showed hydrophobic interactions with Tyr127 and Phe179. In addition, it formed a hydrogen bond with the Tyr129 residue. Mappiodoinin b (135) formed hydrogen bonds with Gly175 and Ile176 and a hydrophobic interaction with Tyr127. All compounds formed interactions with the same amino acids (Figure 3).

NQO1 must be activated to display antioxidant activity. According to Strandback et al. [124], the addition of N-(2-bromophenyl)pyrrolidine-1-sulfonamide (BPPSA) stabilized the flexible C-terminal region of the protein, resulting in the slower incorporation of deuterium. The amino acids involved in the bond were Tyr127, Thr128, and the catalytic residues Tyr156 and His162.

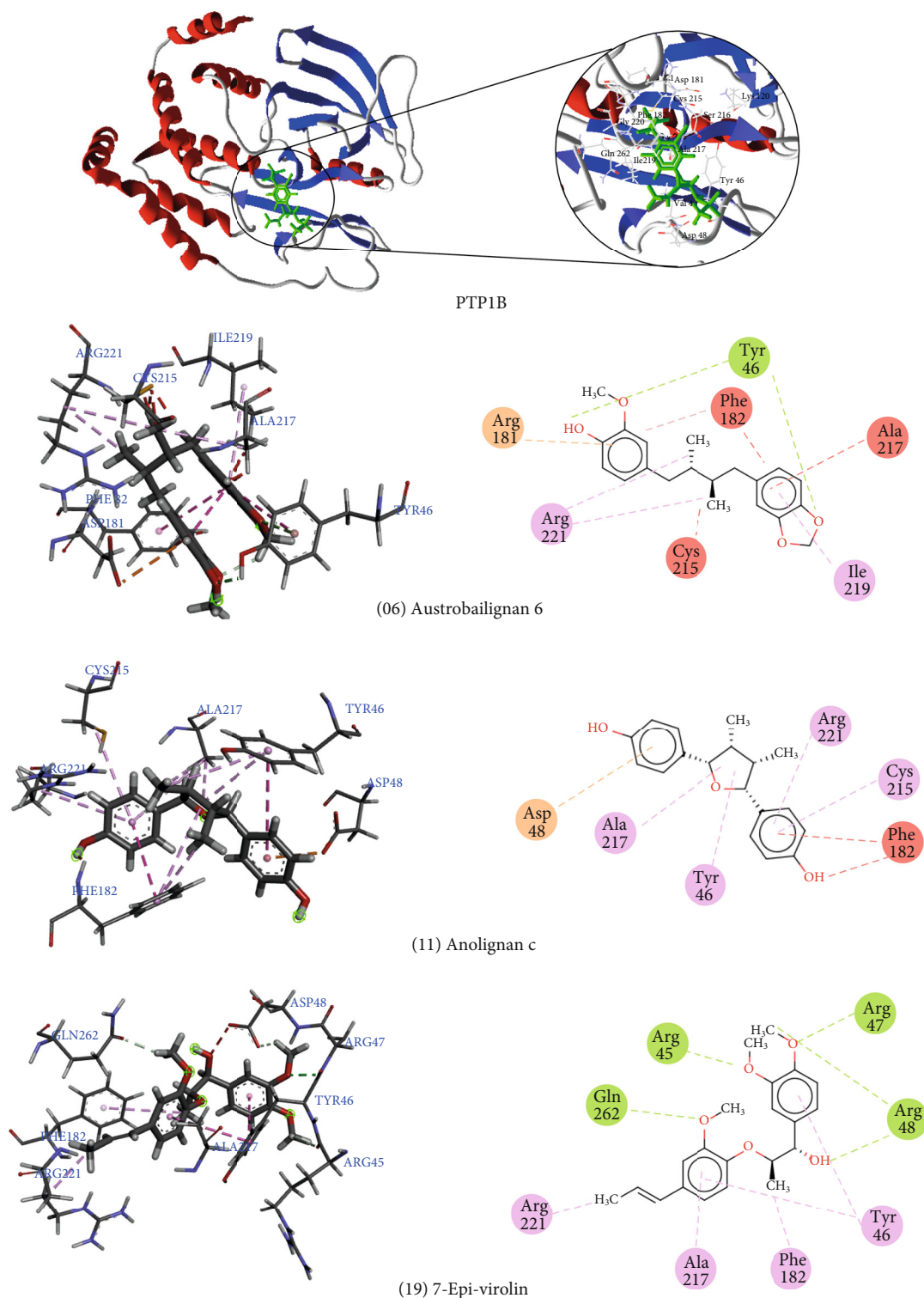


FIGURE 2: 3D and 2D interactions between lignans and PTP1B. Hydrogen bonds are highlighted in green, hydrophobic interactions are highlighted in pink, steric interactions are highlighted in red, and electrostatic interactions are highlighted in orange.

Compounds 6-[(2*R*,3*R*,4*R*,5*R*)-3,4-dimethyl-5-(3,4,5-trimethoxyphenyl)oxolan-2-yl]-4-methoxy-1,3-benzodioxole (64) and Ococymosin (116) interacted well with PDE5. Compound 64 was able to form three hydrogen bonds with Met816, Tyr612, and Gln817 and four hydrophobic interac-

tions with the amino acids Cys677, Val782, Phe786, and Phe820. It also formed a steric interaction with Ile680. Ococymosin formed two hydrogen bonds with Tyr612 and Cys677 and five hydrophobic interactions with Ile680, Ala779, Val782, Phe786, and Phe820 (Figure 4).

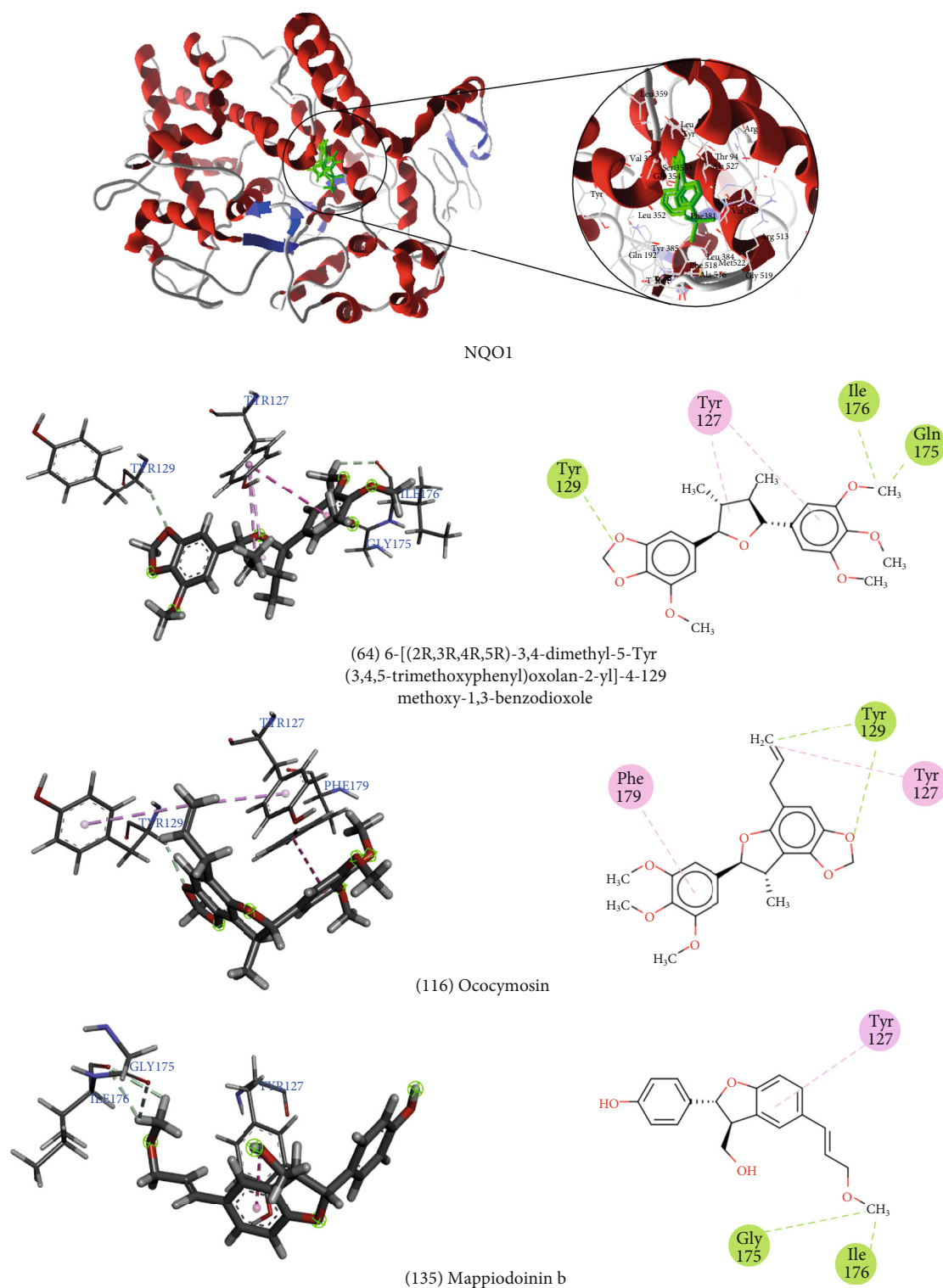


FIGURE 3: 3D and 2D interactions between lignans and NQO1. Hydrogen bonds are highlighted in green, and hydrophobic interactions are highlighted in pink.

Experimental studies carried out by Wang et al. [125] showed that the drug vardenafil is a potent PDE5 inhibitor, binding to several amino acids in the active site. The amino acids

that interacted with vardenafil are Tyr612, Leu765, Ile768, Ala767, Ile680, Cys677, Tyr676, Ile813, Met816, Gln817, and Phe820. Most of these amino acids also interacted with lignans.

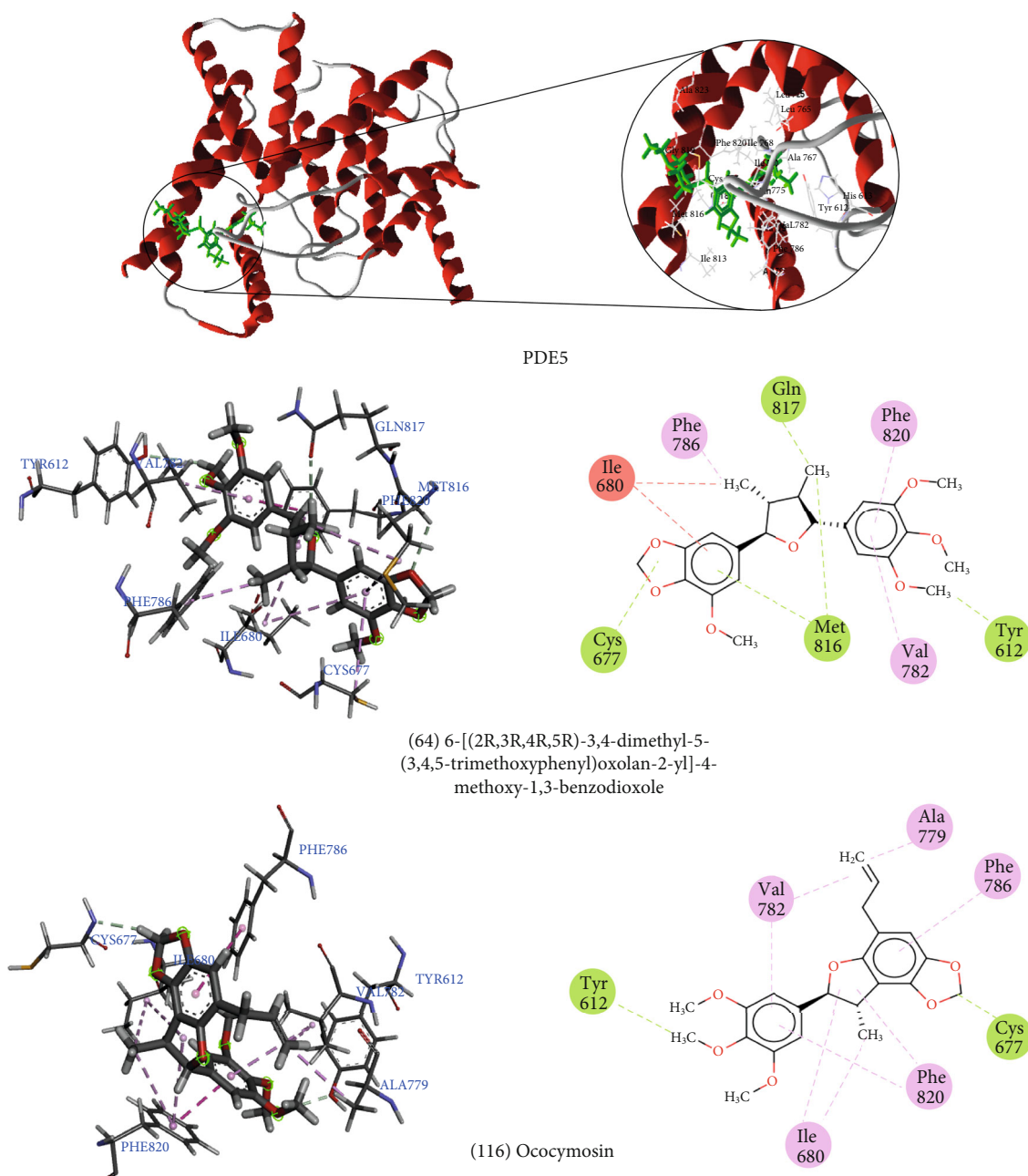


FIGURE 4: 3D and 2D interactions between lignans and PDE5. Hydrogen bonds are highlighted in green, hydrophobic interactions are highlighted in pink, and steric interactions are highlighted in red.

4. Conclusions

AD is a complex and multifactorial disease, comprising a variety of aberrant cellular and molecular processes in different cell types and brain regions. The activation and inactivation of a variety of enzymes can contribute to neuroprotection or disease progression. Therefore, AD therapy must be able to block or compensate for various abnormal pathological events [38].

Few drugs are available for AD treatment. In addition, AD pathophysiology is not well-understood, and the identification of targets for disease treatment remains a major chal-

lenge for drug discovery. Therefore, in this study, we investigated several potential targets that are directly and indirectly involved in the development and progression of AD, through oxidative stress mechanisms, aiming to explore new targets and to design effective drugs, with minimal side effects, for AD treatment. We examined a set of lignans and used virtual screening to select compounds with potential multitargeting effects for the treatment of AD.

The predictive models built in this study obtained excellent performance results, with accuracies greater than 73%. To increase the predictive power and decrease the number of false positives generated by these models, a combined

analysis was used, based on both ligand and structure. The combined analysis was able to identify potentially active molecules, based on the Random Forest and multitargeting models.

Out of 159 total lignans, several potentially active compounds were identified: three compounds with probabilities of activity ranging from 50% to 61% for JNK-3, 43 compounds with a 52–72% probabilities for PTP1B, 57 compounds with 51%–72% probabilities for PDE5, 27 compounds with probabilities between 50% and 61% for COX-2, and 27 compounds with probabilities between 50% and 81% for iNOS; 111 compounds with probabilities ranging from 50% to 64% were identified for Nrf2; nine compounds with probabilities ranging from 51% to 78% were identified for NOX1, and 156 compounds were selected, with probabilities ranging from 27% to 100%, for NQO1. We also identified 139 potentially active molecules for two to five target enzymes, from the entire lignan set analyzed.

Among the 139 lignans that were considered to be potentially active and multitargeting, 92 showed good absorption, bioavailability, and solubility, ranging from soluble to moderately soluble. Among the compounds that were considered to be multitargeting, we selected those likely to cross the blood-brain barrier, through an *in silico* evaluation, resulting in the identification of nine lignans, which were then evaluated for toxicity. The compounds austrobailignan (06), anolignan c (11), 7-epi-virolin (19), 6-[(2R,3R,4R,5R)-3,4-dimethyl-5-(3, 4,5-trimethoxyphenyl)oxolan-2-yl]-4-methoxy-1, 3-benzodioxole (64), ococymosin (116), and mappidoinin b (135) were considered to have no toxicity risks for the evaluated parameters.

We suggest that lignans, especially austrobailignan (06), anolignan c (11), 7-epi-virolin (19), 6-[(2R,3R,4R,5R)-3,4-dimethyl-5-(3,4,5-trimethoxyphenyl)oxolan-2-yl]-4-methoxy-1, 3-benzodioxole (64), ococymosin (116), and mappidoinin b (135), have high probability of activity against several enzymes that may be involved in AD pathogenesis and may confer neuroprotective effects, with low toxicity. The proposed compounds are projected as possible solutions that need to be validated experimentally.

Data Availability

The data used to support the findings of this study are available from the corresponding author upon request.

Conflicts of Interest

The authors declare that there is no conflict of interest regarding the publication of this paper.

Acknowledgments

The authors wish to acknowledge the Conselho Nacional de Desenvolvimento Científico e Tecnológico (CNPq). This study was financed in part by the Coordenação de Aperfeiçoamento de Pessoal de Nível Superior—Brasil (CAPES)—Finance Code 001.

Supplementary Materials

Table S1: smiles of the lignans used in the study. Figure S1: ROC curves generated from the RF models, for each studied enzyme. Table S2: the physical and chemical properties of lignans that are considered to be potentially active against Alzheimer's disease and have multitargeting effects against four or more enzymes. Table S3: pharmacokinetic properties of the lignans that are considered to be potentially active against Alzheimer's disease and have multitargeting effects against four or more enzymes. Lignans that are predicted to cross the blood-brain barrier are highlighted in bold. Table S4: toxicity evaluations for lignans with the best ADMET profiles that are potentially active and that have multitarget effects against four or more enzymes. Lignans that did not present toxicity for any of the analyzed parameters are highlighted in bold. (*Supplementary Materials*)

References

- [1] M. Rosini, E. Simoni, R. Caporaso, and A. Minarini, "Multitarget strategies in Alzheimer's disease: benefits and challenges on the road to therapeutics," *Future Medicinal Chemistry*, vol. 8, no. 6, pp. 697–711, 2016.
- [2] R. Alvariño, E. Alonso, R. Lacret et al., "Streptocyclinones A and B ameliorate Alzheimer's disease pathological processes *in vitro*," *Neuropharmacology*, vol. 141, pp. 283–295, 2018.
- [3] S. Li, X. Zhao, P. Lazarovici, and W. Zheng, "Artemether Activation of AMPK/GSK3 β (ser9)/Nrf2 Signaling Confers Neuroprotection towards β -Amyloid-Induced Neurotoxicity in 3xTg Alzheimer's Mouse Model," *Oxidative Medicine and Cellular Longevity*, vol. 2019, Article ID 1862437, 24 pages, 2019.
- [4] F. Sivandzade, A. Bhalerao, and L. Cucullo, "Cerebrovascular and Neurological Disorders: Protective Role of NRF2," *International Journal of Molecular Sciences*, vol. 20, no. 14, p. 3433, 2019.
- [5] T. Suzuki and M. Yamamoto, "Molecular basis of the Keap1-Nrf2 system," *Free Radical Biology and Medicine*, vol. 88, pp. 93–100, 2015.
- [6] D. Zekry, T. Kay Epperson, and K. H. Krause, "A role for NOX NADPH oxidases in Alzheimer's disease and other types of dementia?," *IUBMB Life*, vol. 55, no. 6, pp. 307–313, 2003.
- [7] S. Manoharan, G. J. Guillemin, R. S. Abiramasundari, M. M. Essa, M. Akbar, and M. D. Akbar, "The role of reactive oxygen species in the pathogenesis of Alzheimer's disease, Parkinson's disease, and Huntington's disease: a mini review," *Oxidative Medicine and Cellular Longevity*, vol. 2016, Article ID 28116038, 15 pages, 2016.
- [8] D. Kumar, A. Ganeshpurkar, D. Kumar, G. Modi, S. K. Gupta, and S. K. Singh, "Secretase inhibitors for the treatment of Alzheimer's disease: long road ahead," *European Journal of Medicinal Chemistry*, vol. 148, pp. 436–452, 2018.
- [9] Y. Tang and W. Le, "Differential roles of M1 and M2 microglia in neurodegenerative diseases," *Molecular Neurobiology*, vol. 53, no. 2, pp. 1181–1194, 2016.
- [10] N. Asimwe, S. G. Yeo, M. S. Kim, J. Jung, and N. Y. Jeong, "Nitric oxide: exploring the contextual link with Alzheimer's disease," *Oxidative Medicine and Cellular Longevity*, vol. 2016, Article ID 7205747, 10 pages, 2016.

- [11] M. T. Islam, "Oxidative stress and mitochondrial dysfunction-linked neurodegenerative disorders," *Neurological Research*, vol. 39, no. 1, pp. 73–82, 2017.
- [12] J. Chhetri, A. E. King, and N. Gueven, "Alzheimer's disease and NQO1: is there a link?," *Current Alzheimer Research*, vol. 15, no. 1, pp. 56–66, 2017.
- [13] R. X. Santos, S. C. Correia, X. Zhu et al., "Nuclear and mitochondrial DNA oxidation in Alzheimer's disease," *Free Radical Research*, vol. 46, no. 4, pp. 565–576, 2012.
- [14] A. Kumar and A. Singh, "A review on Alzheimer's disease pathophysiology and its management: an update," *Pharmacological Reports*, vol. 67, no. 2, pp. 195–203, 2015.
- [15] S. O. Bachurin, E. V. Bovina, and A. A. Ustyugov, "Drugs in clinical trials for Alzheimer's disease: the major trends," *Medicinal Research Reviews*, vol. 37, no. 5, pp. 1186–1225, 2017.
- [16] J. Q. Kwong and J. D. Molkenkin, "Physiological and pathological roles of the mitochondrial permeability transition pore in the heart," *Cell Metabolism*, vol. 21, no. 2, pp. 206–214, 2015.
- [17] P. Albrecht, J. Lewerenz, S. Dittmer, R. Noack, P. Maher, and A. Methner, "Mechanisms of oxidative glutamate toxicity: the glutamate/cystine antiporter system xc⁻; as a neuroprotective drug target," *CNS & Neurological Disorders - Drug Targets*, vol. 9, no. 3, pp. 373–382, 2012.
- [18] T. H. Murphy, M. Miyamoto, A. Sastre, R. L. Schnaar, and J. T. Coyle, "Glutamate toxicity in a neuronal cell line involves inhibition of cystine transport leading to oxidative stress," *Neuron*, vol. 2, no. 6, pp. 1547–1558, 1989.
- [19] R. Briggs, S. P. Kennelly, and D. O'Neill, "Drug treatments in Alzheimer's disease," *Clinical Medicine*, vol. 16, no. 3, pp. 247–253, 2016.
- [20] M. C. Lu, X. Zhang, F. Wu et al., "Discovery of a potent Kelch-like ECH-associated protein 1-nuclear factor erythroid 2-related factor 2 (Keap1-Nrf2) protein-protein interaction inhibitor with natural proline structure as a cytoprotective agent against acetaminophen-induced hepatotoxicity," *Journal of Medicinal Chemistry*, vol. 62, no. 14, pp. 6796–6813, 2019.
- [21] A. Chaudhary, P. K. Maurya, B. S. Yadav, S. Singh, and A. Mani, "Current therapeutic targets for Alzheimer's disease," *Journal of Biomedical*, vol. 3, pp. 74–84, 2018.
- [22] A. García-Osta, M. Cuadrado-Tejedor, C. García-Barroso, J. Oyarzábal, and R. Franco, "Phosphodiesterases as therapeutic targets for Alzheimer's disease," *ACS Chemical Neuroscience*, vol. 3, no. 11, pp. 832–844, 2012.
- [23] L. Liu, H. Xu, S. Ding, D. Wang, G. Song, and X. Huang, "Phosphodiesterase 5 inhibitors as novel agents for the treatment of Alzheimer's disease," *Brain Research Bulletin*, vol. 153, pp. 223–231, 2019.
- [24] C. A. Peixoto, A. K. S. Nunes, and A. Garcia-Osta, "Phosphodiesterase-5 inhibitors: action on the signaling pathways of neuroinflammation, neurodegeneration, and cognition," *Mediators of Inflammation*, vol. 2015, Article ID 940207, 17 pages, 2015.
- [25] A. F. Teich, M. Sakurai, M. Patel et al., "PDE5 exists in human neurons and is a viable therapeutic target for neurologic disease," *J. Alzheimer's Dis.*, vol. 52, no. 1, pp. 295–302, 2016.
- [26] S. Gourmaud, C. Paquet, J. Dumurgier et al., "Increased levels of cerebrospinal fluid JNK3 associated with amyloid pathology: links to cognitive decline," *Journal of Psychiatry & Neuroscience*, vol. 40, no. 3, pp. 151–161, 2015.
- [27] X. Antoniou, M. Falconi, D. Di Marino, and T. Borsello, "JNK3 as a therapeutic target for neurodegenerative diseases," *Journal of Alzheimer's Disease*, vol. 24, no. 4, pp. 633–642, 2011.
- [28] R. Yarza, S. Vela, M. Solas, and M. J. Ramirez, "c-Jun N-terminal kinase (JNK) signaling as a therapeutic target for Alzheimer's disease," *Frontiers in Pharmacology*, vol. 6, p. 321, 2016.
- [29] A. Flemming, "JNK3 as new target in AD?," *Nature Reviews Drug Discovery*, vol. 11, no. 11, p. 829, 2012.
- [30] Y. Wang, J. F. Li, Y. T. Wang et al., "Curcumin reduces hippocampal neuron apoptosis and JNK-3 phosphorylation in rats with A β -induced Alzheimer's disease: protecting spatial learning and memory," *Journal of Neurorestoratology*, vol. - Volume 5, pp. 117–123, 2017.
- [31] J. Fiorito, J. Vendome, F. Saeed et al., "Identification of a novel 1, 2, 3, 4-tetrahydrobenzo [b][1, 6] naphthyridine analogue as a potent phosphodiesterase 5 inhibitor with improved aqueous solubility for the treatment of Alzheimer's disease," *Journal of Medicinal Chemistry*, vol. 60, no. 21, pp. 8858–8875, 2017.
- [32] V. Tell, I. Hilbrich, M. Holzer et al., "Drug development of small-molecule inhibitors of AD-relevant kinases as novel perspective multitargeted approach," *Current Alzheimer Research*, vol. 13, no. 12, pp. 1330–1336, 2016.
- [33] J. Prickaerts, P. R. A. Heckman, and A. Blokland, "Investigational phosphodiesterase inhibitors in phase I and phase II clinical trials for Alzheimer's disease," *Expert Opinion on Investigational Drugs*, vol. 26, no. 9, pp. 1033–1048, 2017.
- [34] S. M. Nabavi, S. Talarek, J. Listos et al., "Phosphodiesterase inhibitors say NO to Alzheimer's disease," *Food and Chemical Toxicology*, vol. 134, article 110822, 2019.
- [35] W. Gulisano, M. R. Tropea, O. Arancio, A. Palmeri, and D. Puzzo, "Sub-efficacious doses of phosphodiesterase 4 and 5 inhibitors improve memory in a mouse model of Alzheimer's disease," *Neuropharmacology*, vol. 138, pp. 151–159, 2018.
- [36] P. G. Través, V. Pardo, M. Pimentel-Santillana et al., "Pivotal role of protein tyrosine phosphatase 1B (PTP1B) in the macrophage response to pro-inflammatory and anti-inflammatory challenge," *Cell Death & Disease*, vol. 5, no. 3, article e1125, 2014.
- [37] G. J. Song, M. Jung, J. H. Kim et al., "A novel role for protein tyrosine phosphatase 1B as a positive regulator of neuroinflammation," *Journal of Neuroinflammation*, vol. 13, no. 1, article 86, 2016.
- [38] M. N. N. Vieira, N. M. Lyra e Silva, S. T. Ferreira, and F. G. de Felice, "Protein tyrosine phosphatase 1B (PTP1B): a potential target for Alzheimer's therapy?," *Frontiers in Aging Neuroscience*, vol. 9, p. 7, 2017.
- [39] K. M. Ricke, S. A. Cruz, Z. Qin et al., "Neuronal protein tyrosine phosphatase 1B hastens amyloid β -associated Alzheimer's disease in mice," *The Journal of Neuroscience*, vol. 40, no. 7, pp. 1581–1593, 2020.
- [40] S. Sorce, R. Stocker, T. Seredenina et al., "NADPH oxidases as drug targets and biomarkers in neurodegenerative diseases: what is the evidence?," *Free Radical Biology and Medicine*, vol. 112, pp. 387–396, 2017.

- [41] M. W. Ma, J. Wang, Q. Zhang et al., "NADPH oxidase in brain injury and neurodegenerative disorders," *Molecular Neurodegeneration*, vol. 12, no. 1, 2017.
- [42] S. Shimohama, H. Tanino, N. Kawakami et al., "Activation of NADPH oxidase in Alzheimer's disease brains," *Biochemical and Biophysical Research Communications*, vol. 273, no. 1, pp. 5–9, 2000.
- [43] M. A. Ansari and S. W. Scheff, "NADPH-oxidase activation and cognition in Alzheimer disease progression," *Free Radical Biology and Medicine*, vol. 51, no. 1, pp. 171–178, 2011.
- [44] D. Ross and D. Siegel, "Functions of NQO1 in cellular protection and CoQ₁₀ metabolism and its potential role as a redox sensitive molecular switch," *Frontiers in Physiology*, vol. 8, p. 595, 2017.
- [45] A. K. Raina, D. J. Templeton, J. C. Deak, G. Perry, and M. A. Smith, "Quinone reductase (NQO1), a sensitive redox indicator, is increased in Alzheimer's disease," *Redox Report*, vol. 4, no. 1–2, pp. 23–27, 2013.
- [46] K. S. Santa Cruz, E. Yazlovitskaya, J. Collins, J. Johnson, and C. DeCarli, "Regional NAD(P)H:quinone oxidoreductase activity in Alzheimer's disease," *Neurobiology of Aging*, vol. 25, no. 1, pp. 63–69, 2004.
- [47] P. Moi, K. Chan, I. Asunis, A. Cao, and Y. W. Kan, "Isolation of NF-E2-related factor 2 (Nrf2), a NF-E2-like basic leucine zipper transcriptional activator that binds to the tandem NF-E2/AP1 repeat of the beta-globin locus control region," *Proceedings of the National Academy of Sciences of the United States of America*, vol. 91, no. 21, pp. 9926–9930, 1994.
- [48] T. W. Kensler, N. Wakabayashi, and S. Biswal, "Cell survival responses to environmental stresses via the Keap1-Nrf2-ARE pathway," *Annual Review of Pharmacology and Toxicology*, vol. 47, no. 1, pp. 89–116, 2007.
- [49] M. Abdalkader, R. Lampinen, K. M. Kanninen, T. M. Malm, and J. R. Liddell, "Targeting Nrf2 to suppress ferroptosis and mitochondrial dysfunction in neurodegeneration," *Frontiers in Neuroscience*, vol. 12, p. 466, 2018.
- [50] J. W. Kaspar, S. K. Niture, and A. K. Jaiswal, "Nrf2:Keap1 signaling in oxidative stress," *Free Radical Biology and Medicine*, vol. 47, no. 9, pp. 1304–1309, 2009.
- [51] D. A. Johnson and J. A. Johnson, "Nrf2—a therapeutic target for the treatment of neurodegenerative diseases," *Free Radical Biology and Medicine*, vol. 88, Part B, pp. 253–267, 2015.
- [52] J. D. Hayes and A. T. Dinkova-Kostova, "The Nrf2 regulatory network provides an interface between redox and intermediary metabolism," *Trends in Biochemical Sciences*, vol. 39, no. 4, pp. 199–218, 2014.
- [53] Y. Huang, W. Li, Z. Su, and A.-N. T. Kong, "The complexity of the Nrf2 pathway: beyond the antioxidant response," *The Journal of Nutritional Biochemistry*, vol. 26, no. 12, pp. 1401–1413, 2015.
- [54] E. M. Wright, D. F. LOO, and B. A. Hirayama, "Biology of human sodium glucose transporters," *Physiological Reviews*, vol. 91, no. 2, pp. 733–794, 2011.
- [55] K. Shah, S. DeSilva, and T. Abbruscato, "The role of glucose transporters in brain disease: diabetes and Alzheimer's disease," *International Journal of Molecular Sciences*, vol. 13, no. 12, pp. 12629–12655, 2012.
- [56] L. Szablewski, "Distribution of glucose transporters in renal diseases," *Biomedical Science*, vol. 24, no. 1, p. 64, 2017.
- [57] M. Sopjani, *The AMP activated protein kinase in the regulation of sodium coupled transporters (SGLT1, EAAT3 & EAAT4) and eryptosis, [Ph.D thesis]*, Eberhard Karls Universität Tübingen, Germany, 2010.
- [58] Z. Li, V. Agrawal, M. Ramratnam et al., "Cardiac sodium-dependent glucose cotransporter 1 is a novel mediator of ischaemia/reperfusion injury," *Cardiovascular Research*, vol. 115, no. 11, pp. 1646–1658, 2019.
- [59] Y. J. Lee, J. S. Heo, H. N. Suh, M. Y. Lee, and H. J. Han, "Interleukin-6 stimulates α -MG uptake in renal proximal tubule cells: involvement of STAT3, PI3K/Akt, MAPKs, and NF- κ B," *American Journal of Physiology-Renal Physiology*, vol. 293, no. 4, pp. F1036–F1046, 2007.
- [60] Z. A. Jigheh, A. G. Haghjo, H. Argani et al., "Empagliflozin alleviates renal inflammation and oxidative stress in streptozotocin-induced diabetic rats partly by repressing HMGB1-TLR4 receptor axis," *Iranian Journal of Basic Medical Sciences*, vol. 22, no. 4, pp. 384–390, 2019.
- [61] A. Mitsumoto and Y. Nakagawa, "DJ-1 is an indicator for endogenous reactive oxygen species elicited by endotoxin," *Free Radical Research*, vol. 35, no. 6, pp. 885–893, 2009.
- [62] D. Yu, H. Pan, R. Zhang, Y. Li, and X. Nie, "Nucleus DJ-1/Park 7 acts as a favorable prognostic factor and involves mucin secretion in invasive breast carcinoma in Chinese population," *International Journal of Clinical and Experimental Medicine*, vol. 10, no. 4, pp. 6558–6567, 2017.
- [63] J. Fan, H. Yu, Y. Lv, and L. Yin, "Diagnostic and prognostic value of serum thioredoxin and DJ-1 in non-small cell lung carcinoma patients," *Tumor Biology*, vol. 37, no. 2, pp. 1949–1958, 2016.
- [64] T. Taira, Y. Saito, T. Niki, S. M. M. Iguchi-Ariga, K. Takahashi, and H. Ariga, "DJ-1 has a role in antioxidative stress to prevent cell death," *EMBO Reports*, vol. 5, no. 2, pp. 213–218, 2004.
- [65] M. Inden, Y. Kitamura, K. Takahashi et al., "Protection against dopaminergic neurodegeneration in Parkinson's disease-model animals by a modulator of the oxidized form of DJ-1, a wild-type of familial Parkinson's disease-linked PARK7," *Journal of Pharmacological Sciences*, vol. 117, no. 3, pp. 189–203, 2011.
- [66] L. P. Dolgacheva, A. V. Berezhnov, E. I. Fedotova, V. P. Zinchenko, and A. Y. Abramov, "Role of DJ-1 in the mechanism of pathogenesis of Parkinson's disease," *Journal of Bioenergetics and Biomembranes*, vol. 51, no. 3, pp. 175–188, 2019.
- [67] R. Xue, J. Jiang, B. Dong et al., "DJ-1 activates autophagy in the repression of cardiac hypertrophy," *Archives of Biochemistry and Biophysics*, vol. 633, pp. 124–132, 2017.
- [68] C. R. del Mundo, A. L. Castillo, S. S. A. An, and M. A. Tan, "In vivo COX-2 modulation and metabolite profiling of *Pandanus tectorius* leaves extracts," *3 Biotech*, vol. 10, no. 3, article 90, 2020.
- [69] B. K. Baothman, J. Smith, L. J. Kay, S. K. Suvarna, and P. T. Peachell, "Prostaglandin D₂ generation from human lung mast cells is catalysed exclusively by cyclooxygenase-1," *European Journal of Pharmacology*, vol. 819, pp. 225–232, 2018.
- [70] M. Sandoughi, M. Saravani, M. Rokni, M. Nora, M. Mehrabani, and A. Dehghan, "Association between COX-2 and 15-PGDH polymorphisms and SLE susceptibility," *International Journal of Rheumatic Diseases*, vol. 23, no. 5, pp. 627–632, 2020.

- [71] R. He, K. Hua, S. Zhang et al., "COX-2 mediated crosstalk between Wnt/ β -catenin and the NF- κ B signaling pathway during inflammatory responses induced by Haemophilus parasuis in PK-15 and NPTr cells," *Developmental & Comparative Immunology*, vol. 105, no. 1, pp. 1–7, 2020.
- [72] H. Wang, J. Wang, J. Wang, W. Cui, M. Sun, and Y. Liu, "Relationships of pain in pancreatic cancer patients with pathological stage and expressions of NF- κ B and COX-2," *Journal of BUON*, vol. 25, no. 1, pp. 448–453, 2020.
- [73] A. Jorda, M. Aldasoro, C. Aldasoro et al., "Action of low doses of aspirin in inflammation and oxidative stress induced by $\alpha\beta_{1-42}$ on astrocytes in primary culture," *International Journal of Medical Sciences*, vol. 17, no. 6, pp. 834–843, 2020.
- [74] A. González-Barnadas, O. Camps-Font, P. Martín-Fatás, R. Figueiredo, C. Gay-Escoda, and E. Valmaseda-Castellón, "Efficacy and safety of selective COX-2 inhibitors for pain management after third molar removal: a meta-analysis of randomized clinical trials," *Clinical Oral Investigations*, vol. 24, no. 1, pp. 79–96, 2020.
- [75] E. M. Gedawy, A. E. Kassab, and A. M. El Kerdawy, "Design, synthesis and biological evaluation of novel pyrazole sulfonamide derivatives as dual COX-2/5-LOX inhibitors," *European Journal of Medicinal Chemistry*, vol. 189, p. 112066, 2020.
- [76] A. Buzharevski, S. Paskaš, M. B. Sárosi et al., "Carboranyl derivatives of rofecoxib with cytostatic activity against human melanoma and colon cancer cells," *Scientific Reports*, vol. 10, no. 1, article 4827, p. 1, 2020.
- [77] C. Brookes, W. J. Ribbans, L. Y. El Khoury, and S. M. Raleigh, "Variability within the human iNOS gene and Achilles tendon injuries: evidence for a heterozygous advantage effect," *Journal of Science and Medicine in Sport*, vol. 23, no. 4, pp. 342–346, 2020.
- [78] J. Li, H. Wang, J. Li, Y. Liu, and H. Ding, "LC-MS analysis of Myrica rubra extract and its hypotensive effects via the inhibition of GLUT 1 and activation of the NO/Akt/eNOS signaling pathway," *RSC Advances*, vol. 10, no. 9, pp. 5371–5384, 2020.
- [79] V. Wilmes, S. Scheiper, W. Roehr et al., "Increased inducible nitric oxide synthase (iNOS) expression in human myocardial infarction," *International Journal of Legal Medicine*, vol. 134, no. 2, pp. 575–581, 2020.
- [80] C. Chen, L. Sun, W. Zhang et al., "Limb ischemic preconditioning ameliorates renal microcirculation through activation of PI3K/Akt/eNOS signaling pathway after acute kidney injury," *European Journal of Medical Research*, vol. 25, no. 1, pp. 10–19, 2020.
- [81] M. O. Kseibati, G. S. G. Shehatou, M. H. Sharawy, A. E. Eladl, and H. A. Salem, "Nicorandil ameliorates bleomycin-induced pulmonary fibrosis in rats through modulating eNOS, iNOS, TXNIP and HIF-1 α levels," *Life Sciences*, vol. 246, p. 117423, 2020.
- [82] Y. Le, R. Wei, K. Yang et al., "Liraglutide ameliorates palmitate-induced oxidative injury in islet microvascular endothelial cells through GLP-1 receptor/PKA and GTPCH1/eNOS signaling pathways," *Peptides*, vol. 124, article 170212, 2020.
- [83] N. Ahmad, M. Y. Ansari, and T. M. Haqqi, "Role of iNOS in osteoarthritis: pathological and therapeutic aspects," *Journal of Cellular Physiology*, vol. 235, 2020.
- [84] S. S. Soskic, "Regulation of inducible nitric oxide synthase (iNOS) and its potential role in insulin resistance, diabetes and heart failure," *Open Cardiovascular Medicine Journal*, vol. 5, no. 1, pp. 153–163, 2011.
- [85] Q. Wang, H. Sun, X. Qi, and M. Zhou, "eNOS rs 2070744 polymorphism might influence predisposition to hemorrhagic cerebral vascular diseases in East Asians: a meta-analysis," *Brain and Behavior*, vol. 10, no. 5, article e01538, 2020.
- [86] P. Jiang, C. Li, Z. Xiang, and B. Jiao, "Tanshinone IIA reduces the risk of Alzheimer's disease by inhibiting iNOS, MMP-2 and NF- κ Bp65 transcription and translation in the temporal lobes of rat models of Alzheimer's disease," *Molecular Medicine Reports*, vol. 10, no. 2, pp. 689–694, 2014.
- [87] J. F. Gielis, L. Quirynen, J. J. Briedé, E. Roelant, P. Cos, and P. E. Y. Van Schil, "Pathogenetic role of endothelial nitric oxide synthase uncoupling during lung ischaemia-reperfusion injury†," *European Journal of Cardio-Thoracic Surgery*, vol. 52, no. 2, pp. 256–263, 2017.
- [88] C. Schirra, N. Xia, A. Schüffler et al., "Phosphorylation and activation of endothelial nitric oxide synthase by red fruit (*Pandanus conoideus* Lam) oil and its fractions," *Journal of Ethnopharmacology*, vol. 251, p. 112534, 2020.
- [89] S. A. Sonar and G. Lal, "The iNOS activity during an immune response controls the CNS pathology in experimental autoimmune encephalomyelitis," *Frontiers in Immunology*, vol. 10, p. 710, 2019.
- [90] X. Chen, H. Li, Z. Wang et al., "Quercetin protects the vascular endothelium against iron overload damages via ROS/ADMA/DDAH II/eNOS/NO pathway," *European Journal of Pharmacology*, vol. 868, article 172885, 2020.
- [91] Z. Chen, J. M. Haus, L. Chen et al., "CCL28-induced CCR10/eNOS interaction in angiogenesis and skin wound healing," *The FASEB Journal*, vol. 34, no. 4, pp. 5838–5850, 2020.
- [92] L. J. Zhu, C. Xu, J. Ren et al., "Dentate nNOS accounts for stress-induced 5-HT_{1A} receptor deficiency: implication in anxiety behaviors," *CNS Neuroscience & Therapeutics*, vol. 26, no. 4, pp. 453–464, 2020.
- [93] S. Choi, J. S. Won, S. L. Carroll, B. Annamalai, I. Singh, and A. K. Singh, "Pathology of nNOS-expressing GABAergic neurons in mouse model of Alzheimer's disease," *Neuroscience*, vol. 384, pp. 41–53, 2018.
- [94] J. Murciano-Calles, A. Coello, A. Cámara-Artigas, and J. C. Martínez, "PDZ/PDZ interaction between PSD-95 and nNOS neuronal proteins: a thermodynamic analysis of the PSD95-PDZ2/nNOS-PDZ interaction," *Journal of Molecular Recognition*, vol. 33, no. 4, article e2826, 2020.
- [95] G. A. Czapski, K. Czubowicz, J. B. Strosznajder, and R. P. Strosznajder, "The lipoxygenases: their regulation and implication in Alzheimer's disease," *Neurochemical Research*, vol. 41, no. 1–2, pp. 243–257, 2016.
- [96] M. Walther, I. Ivanov, G. Myagkova, and H. Kuhn, "Alterations of lipoxygenase specificity by targeted substrate modification and site-directed mutagenesis," *Chemistry & Biology*, vol. 8, no. 8, pp. 779–790, 2001.
- [97] H. Kuhn and B. J. Thiele, "The diversity of the lipoxygenase family," *FEBS Letters*, vol. 449, no. 1, pp. 7–11, 1999.
- [98] Y. B. Joshi, P. F. Giannopoulos, and D. Praticò, "The 12/15-lipoxygenase as an emerging therapeutic target for Alzheimer's disease," *Trends in Pharmacological Sciences*, vol. 36, no. 3, pp. 181–186, 2015.
- [99] I. Ivanov, A. di Venere, T. Horn et al., "Tight association of N-terminal and catalytic subunits of rabbit 12/15-

- lipoxygenase is important for protein stability and catalytic activity,” *Biochimica et Biophysica Acta (BBA) - Molecular and Cell Biology of Lipids*, vol. 1811, no. 12, pp. 1001–1010, 2011.
- [100] J. Chu, P. F. Giannopoulos, C. Ceballos-Diaz, T. E. Golde, and D. Praticò, “5-Lipoxygenase gene transfer worsens memory, amyloid, and tau brain pathologies in a mouse model of Alzheimer disease,” *Annals of Neurology*, vol. 72, no. 3, pp. 442–454, 2012.
- [101] Y. B. Joshi and D. Praticò, “The 5-lipoxygenase pathway: oxidative and inflammatory contributions to the Alzheimer’s disease phenotype,” *Frontiers in Cellular Neuroscience*, vol. 8, p. 436, 2015.
- [102] S. S. Karuppagounder, L. Alin, Y. Chen et al., “N-acetylcysteine targets 5 lipoxygenase-derived, toxic lipids and can synergize with prostaglandin E2 to inhibit ferroptosis and improve outcomes following hemorrhagic stroke in mice,” *Annals of Neurology*, vol. 84, no. 6, pp. 854–872, 2018.
- [103] O. Firuzi, J. Zhuo, C. M. Chinnici, T. Wisniewski, and D. Praticò, “5-Lipoxygenase gene disruption reduces amyloid- β pathology in a mouse model of Alzheimer’s disease,” *The FASEB Journal*, vol. 22, no. 4, pp. 1169–1178, 2007.
- [104] A. Di Meco, J. G. Li, and D. Praticò, “Dissecting the role of 5-lipoxygenase in the homocysteine-induced Alzheimer’s disease pathology,” *Journal of Alzheimer’s Disease*, vol. 62, no. 3, pp. 1337–1344, 2018.
- [105] E. D. Alfadly, P. A. Elzahhar, A. Tramarin et al., “Tackling neuroinflammation and cholinergic deficit in Alzheimer’s disease: multi-target inhibitors of cholinesterases, cyclooxygenase-2 and 15-lipoxygenase,” *European Journal of Medicinal Chemistry*, vol. 167, pp. 161–186, 2019.
- [106] M. Estrada Valencia, C. Herrera-Arozamena, L. de Andrés et al., “Neurogenic and neuroprotective donepezil-flavonoid hybrids with sigma-1 affinity and inhibition of key enzymes in Alzheimer’s disease,” *European Journal of Medicinal Chemistry*, vol. 156, pp. 534–553, 2018.
- [107] D. Schweiger, G. Fürstenberger, and P. Krieg, “Inducible expression of 15-lipoxygenase-2 and 8-lipoxygenase inhibits cell growth via common signaling pathways,” *Journal of Lipid Research*, vol. 48, no. 3, pp. 553–564, 2007.
- [108] A. Gaulton, L. J. Bellis, A. P. Bento et al., “ChEMBL: a large-scale bioactivity database for drug discovery,” *Nucleic Acids Research*, vol. 40, no. D1, pp. D1100–D1107, 2011.
- [109] D. Fourches, E. Muratov, and A. Tropsha, “Trust, but verify: on the importance of chemical structure curation in cheminformatics and QSAR modeling research,” *Journal of Chemical Information and Modeling*, vol. 50, no. 7, pp. 1189–1204, 2010.
- [110] M. M. Dos Santos, N. F. de Sousa, G. C. S. Rodrigues, A. F. M. Monteiro, M. T. Scotti, and L. Scotti, “Lignans and neolignans anti-tuberculosis identified by QSAR and molecular modeling,” *Combinatorial Chemistry & High Throughput Screening*, vol. 23, 2020.
- [111] V. P. Lorenzo, J. M. B. Filho, L. Scotti, and M. T. Scotti, “Combined structure- and ligand-based virtual screening to evaluate caulerpin analogs with potential inhibitory activity against monoamine oxidase B,” *Revista Brasileira de Farmacognosia*, vol. 25, no. 6, pp. 690–697, 2015.
- [112] A. Mauri, V. Consonni, M. Pavan, and R. Todeschini, “DRAGON software: an easy approach to molecular descriptor calculations,” *Match*, vol. 56, no. 2, pp. 237–248, 2006.
- [113] M. Hall, E. Frank, G. Holmes, B. Pfahringer, P. Reutemann, and I. H. Witten, “The WEKA data mining software,” *ACM SIGKDD Explorations Newsletter*, vol. 11, no. 1, pp. 10–18, 2009.
- [114] B. W. Matthews, “Comparison of the predicted and observed secondary structure of T4 phage lysozyme,” *Biochimica et Biophysica Acta*, vol. 405, no. 2, pp. 442–451, 1975.
- [115] K. Roy, S. Kar, and P. Ambure, “On a simple approach for determining applicability domain of QSAR models,” *Chemo-metrics and Intelligent Laboratory Systems*, vol. 145, pp. 22–29, 2015.
- [116] W. F. J. Bitencourt-Ferreira, “Molegro virtual docker for docking,” in *Docking Screens for Drug Discovery*, W. Azevedo Jr., Ed., vol. 2053 of *Methods in Molecular Biology*, pp. 149–167, Humana, New York, NY, 2019.
- [117] F. C. Bernstein, T. F. Koetzle, G. J. Williams et al., “The protein data bank: a computer-based archival file for macromolecular structures,” *European Journal of Biochemistry*, vol. 80, no. 2, pp. 319–324, 1977.
- [118] A. Daina, O. Michielin, and V. Zoete, “SwissADME: a free web tool to evaluate pharmacokinetics, drug-likeness and medicinal chemistry friendliness of small molecules,” *Scientific Reports*, vol. 7, no. 1, 2017.
- [119] S. Mandal, M. Moudgil, and S. K. Mandal, “Rational drug design,” *European Journal of Pharmacology*, vol. 625, no. 1–3, pp. 90–100, 2009.
- [120] V. M. Alves, R. C. Braga, E. N. Muratov, and C. Horta, “Quimioinformática: Uma Introdução,” *Química Nova*, vol. 41, no. 2, pp. 202–212, 2018.
- [121] R. B. Teponno, S. Kusari, and M. Spiteller, “Recent advances in research on lignans and neolignans,” *Natural Product Reports*, vol. 33, no. 9, pp. 1044–1092, 2016.
- [122] F. Zálešák, D. J. Y. D. Bon, and J. Pospíšil, “Lignans and neolignans: plant secondary metabolites as a reservoir of biologically active substances,” *Pharmacological Research*, vol. 146, p. 104284, 2019.
- [123] N. Krishnan, K. Krishnan, C. R. Connors et al., “PTP1B inhibition suggests a therapeutic strategy for Rett syndrome,” *The Journal of Clinical Investigation*, vol. 125, no. 8, pp. 3163–3177, 2015.
- [124] E. Strandback et al., “A small molecule chaperone rescues the stability and activity of a cancer-associated variant of NAD(P)H: quinone oxidoreductase 1 *in vitro*,” *FEBS Letters*, vol. 594, no. 3, pp. 424–438, 2019.
- [125] H. Wang, M. Ye, H. Robinson, S. H. Francis, and H. Ke, “Conformational variations of both phosphodiesterase-5 and inhibitors provide the structural basis for the physiological effects of vardenafil and sildenafil,” *Molecular Pharmacology*, vol. 73, no. 1, pp. 104–110, 2008.

Research Article

The Effects of Alpha-Linolenic Acid on the Secretory Activity of Astrocytes and β Amyloid-Associated Neurodegeneration in Differentiated SH-SY5Y Cells: Alpha-Linolenic Acid Protects the SH-SY5Y cells against β Amyloid Toxicity

Anna Litwiniuk ¹, Anita Domańska,^{1,2} Magdalena Chmielowska,¹ Lidia Martyńska,¹ Wojciech Bik,¹ and Małgorzata Kalisz¹

¹Department of Neuroendocrinology, Centre of Postgraduate Medical Education, Marymoncka 99/103, 01-813 Warsaw, Poland

²Department of Physiological Sciences, Institute of Veterinary Medicine, Warsaw University of Life Sciences (SGGW), Nowoursynowska 159, 02-776 Warsaw, Poland

Correspondence should be addressed to Anna Litwiniuk; alitwiniuk@cmkp.edu.pl

Received 24 April 2020; Revised 16 June 2020; Accepted 6 July 2020; Published 7 August 2020

Guest Editor: Francisco Jaime B. Mendonça Junior

Copyright © 2020 Anna Litwiniuk et al. This is an open access article distributed under the Creative Commons Attribution License, which permits unrestricted use, distribution, and reproduction in any medium, provided the original work is properly cited.

Alzheimer's disease (AD) is the most common neurodegenerative disorder. Amyloid β - ($A\beta$ -) induced mitochondrial dysfunction may be a primary process triggering all the cascades of events that lead to AD. Therefore, identification of natural factors and endogenous mechanisms that protect neurons against $A\beta$ toxicity is needed. In the current study, we investigated whether alpha-linolenic acid (ALA), as a natural product, would increase insulin and IGF-I (insulin-like growth factor I) release from astrocytes. Moreover, we explored the protective effect of astrocytes-derived insulin/IGF-I on $A\beta$ -induced neurotoxicity, with special attention paid to their impact on mitochondrial function of differentiated SH-SY5Y cells. The results showed that ALA induced insulin and IGF-I secretion from astrocytes. Our findings demonstrated that astrocyte-derived insulin/insulin-like growth factor I protects differentiated SH-SY5Y cells against $A\beta_{1-42}$ -induced cell death. Moreover, pretreatment with conditioned medium (CM) and ALA-preactivated CM (ALA-CM) protected the SH-SY5Y cells against $A\beta_{1-42}$ -induced mitochondrial dysfunction by reducing the depolarization of the mitochondrial membrane, increasing mitochondrial biogenesis, restoring the balance between fusion and fission processes, and regulation of mitophagy and autophagy processes. Our study suggested that astrocyte-derived insulin/insulin-like growth factor I suppresses $A\beta_{1-42}$ -induced cytotoxicity in the SH-SY5Y cells by protecting against mitochondrial dysfunction. Moreover, the neuroprotective effects of CM were intensified by preactivation with ALA.

1. Introduction

Alzheimer's disease (AD) is the most common neurodegenerative disorder being the principal cause of dementia among the elderly. The major pathological hallmarks of AD are senile plaques and neurofibrillary tangles (NFTs) along with the loss of neurons and synapse in the AD brains [1]. Most of these changes appear in the brains of patients long before the onset of clinical symptoms of cognitive decline [2]. A recent study demonstrated that besides these known hallmarks, mitochondrial malfunctions may play a distinct role in AD [3].

Mitochondria are highly dynamic organelles with morphology and numbers being regulated by fission and fusion proteins [4]. The balance between fusion and fission processes is essential to maintain the health of the neuronal cells. Both processes are largely regulated by the guanosine triphosphatase (GTPase) enzymes. Mitochondrial fusion is regulated by the GTPases including mitofusin 1 (Mfn1), mitofusin 2 (Mfn2), and optic atrophy protein 1 (OPA1), and helps to maintain tubular mitochondrial network and optimal mitochondrial functions. Whereas the fission process is regulated by dynamin-related protein-1 (Drp1)

and mitochondrial fission 1 protein (Fis1). Excessive mitochondrial fission leads to impaired mitochondrial function and neuronal death in AD [5]. The fusion/fission process is a part of the mitochondrial biogenesis in which the cells increase their mitochondrial mass. However, the mitochondrial biogenesis, another key mitochondrial function, is also impaired in AD. The level of proteins regulating the mitochondrial biogenesis such as peroxisome proliferator-activated receptor gamma coactivator 1-alpha (PGC-1 α), nuclear respiratory factor 1 and 2 (NRF1, NRF2), and mitochondrial transcription factor A (mTFA) was found to be significantly reduced in human AD hippocampus and cellular models overexpressing APP Swedish mutation [6]. Due to the hypothesis that Amyloid β - ($A\beta$ -) induced mitochondrial dysfunction may be the primary process triggering all the cascades of events that lead to AD, identification of the natural factors and the endogenous mechanisms that protect neurons against $A\beta$ toxicity is needed. It has been suggested that neurons may be protected against $A\beta$ -induced damage through activation of the insulin and insulin-like growth factor I (IGF-I) signaling pathways [7, 8]. In recent years, it has been reported that physiological protection against $A\beta$ -induced damage can be mediated by astrocyte-derived insulin and IGF-I [8]. Moreover, the protective role of IGF-I and insulin has been confirmed in animal models of AD [9, 10].

Additionally, growing attention has been paid to the search for compounds from natural sources that can protect neurons against $A\beta$ -induced mitochondrial and synaptic toxicities. Alpha-linolenic acid (ALA) is the plant-derived ω -3 fatty acid. Previous studies showed that consumption of dietary ALA reduced the risk of cardiovascular disease and stroke [11, 12]. Gao et al. demonstrated that long-term dietary intake of ALA improved the cognitive function through the activation of extracellular signal-regulated kinases (ERK) and Akt signaling in the aged-rat model [13]. However, the direct effect of ALA on the secretory activity of astrocytes has not been studied yet. Moreover, very little data have been reported on the effects of astrocytes-derived insulin/IGF-I on $A\beta$ -induced mitochondrial dysfunction.

Therefore, in the current study, we investigated whether ALA would increase insulin and IGF-I secretion from astrocytes. Moreover, we explored the protective effect of astrocytes-derived insulin/IGF-I on $A\beta$ -induced neurotoxicity, with special attention paid to their impact on mitochondrial function of differentiated SH-SY5Y cells.

2. Materials and Methods

2.1. Reagents and Antibodies. Alpha-linolenic acid (ALA), Human Beta Amyloid 1-42 ($A\beta_{1-42}$), All-trans retinoic acid (RA), Insulin, Human Insulin ELISA Kit, Human IGF-I ELISA Kit, 3-(4,5-dimethylthiazol-2-yl)-2-5-diphenyltetrazolium bromide (MTT), bovine serum albumin (BSA), and acridine orange (AO) were purchased from Sigma Aldrich, Saint Louis, MO, USA. Insulin Degrading Enzyme (IDE) was purchased from Abcam Inc., USA. Antibodies to the following targets were used: rabbit anti-TOMM20 antibody (Abcam Inc.), mouse anti-PARKIN (Abcam Inc.), rabbit anti-Synaptophysin (GeneTex, Inc., Alton Pkwy Irvine, CA,

USA), mouse anti- β 3-Tubulin (TUJ 1; Santa Cruz Biotechnology, Dallas, CO, USA), horseradish peroxidase- (HRP-) conjugated goat anti-rabbit IgG antibodies (Abcam Inc.), HRP-conjugated goat anti-mouse IgG antibodies (Abcam Inc.), Alexa Fluor™488-labeled chicken anti-mouse IgG (Thermo Fisher Scientific, Waltham, MA, USA), Alexa Fluor™568-conjugated goat anti-rabbit IgG (Thermo Fisher Scientific).

2.2. $A\beta$ Preparation. Amyloid β_{1-42} ($A\beta_{1-42}$) was prepared as described previously [14]. Dried synthetic $A\beta_{1-42}$ peptide (Sigma Aldrich) was first dissolved in dimethylsulfoxide (DMSO) and then diluted in phosphate buffer saline (PBS) to obtain a 250 mM stock solution. This solution was incubated at 4°C for at least 24 h and stored at -80°C. Before use, the solution was centrifuged at 12 000 g for 10 min, and the supernatant was used as an oligomeric $A\beta_{1-42}$.

2.3. Cell Cultures

2.3.1. Human Astrocyte Cells Cultures. The Normal Human Astrocytes (NHA) were obtained from the Lonza Basel, Switzerland. The cells were cultured in ABM™ Basal Medium (NHA medium, Lonza Basel) supplemented with AGM™ SingleQuots™ Supplements (Lonza Basel) required for growth of Astrocytes.

2.3.2. Preparation of Astrocyte-Conditioned Medium (CM) and ALA-Preactivated CM (ALA-CM). After seeding, the NHA cells were allowed to grow for 24–48 hours or until 60–70% confluence in six-well plates. Next, NHA cultures were grown in the medium containing NHA-Medium and neurobasal medium (the phase II differentiation medium DM II) (1:1). After 24 h, the medium was replaced with DM II medium. The NHA cells were grown in medium without or with ALA at different doses (10 nM, 50 nM, 100 nM, 250 nM) for 24 h to obtain ALA-activated CM (ALA-CM) and control CM, respectively. A dose of 10 nM ALA was used for the following experiments (Figures 1).

2.3.3. Human Neuroblastoma SH-SY5Y Cell Cultures. The human SH-SY5Y cells were purchased from the European Collection of Cell Cultures (ECAAC, cat.94030304, passage 11). The cells were initially cultured in growth media (GM), constituted by Minimum Essential Medium Eagle (MEM, Sigma Aldrich) supplemented with 15% (v/v) heat-inactivated fetal bovine serum (hiFBS), 2 mM L-glutamine (Sigma Aldrich), 50 IU/mL/50 μ g/mL penicillin/streptomycin (Sigma Aldrich), 20 μ g/mL gentamicin sulphate (Biowest, Nuaille, France); and 1 μ g/mL Fungizone/amphotericin B (Biowest), at 37°C in a humidified atmosphere containing 5% CO₂, and kept below ECAAC passage +15 to avoid cell senescence [15].

(1) Differentiation and Treatments. The differentiation of the SH-SY5Y cells was carried out in two steps using phase 1 (DM I) and phase 2 (DM II) media. The presented differentiation protocol was modified from Forster et al. [15] and Mackenzie et al. [16]. The DM I medium was MEM (Sigma Aldrich) containing 2.5% (v/v) hiFBS, 2 mM L-glutamine

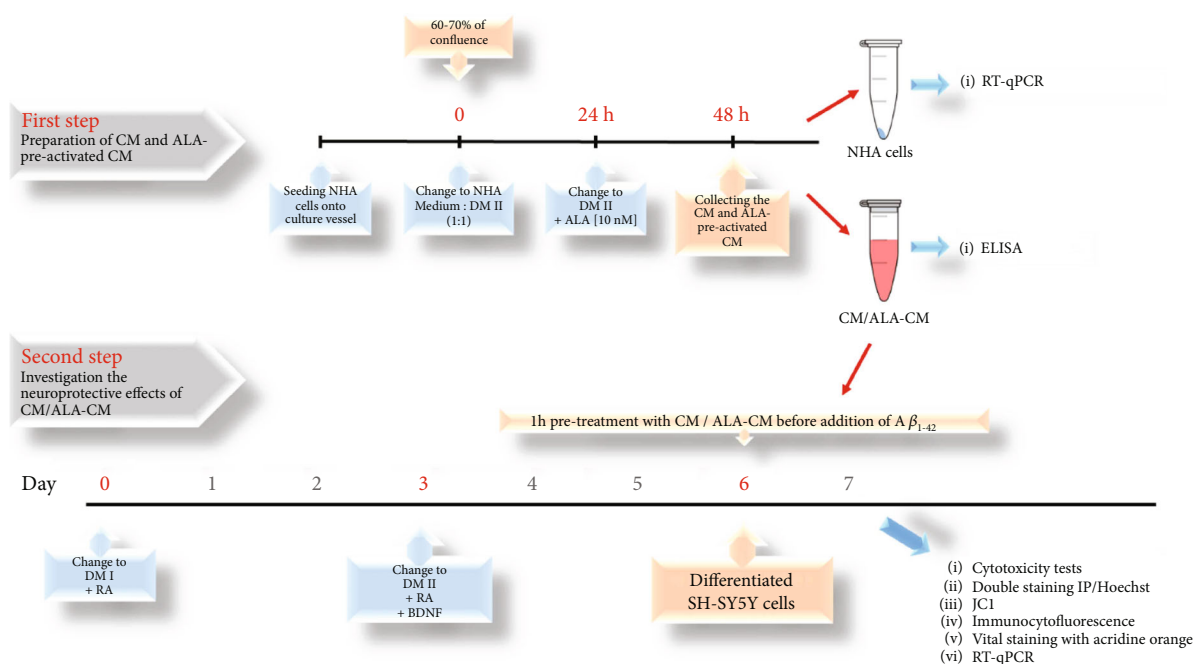


FIGURE 1: Scheme of the experimental procedures. The first step of the research involved the preparation of astrocyte-conditioned medium (CM) and Alpha-linolenic acid-preactivated CM (ALA-CM). The Normal Human Astrocytes (NHA) cells were allowed to grow until 60-70% confluence. Then, NHA cells were grown in the medium containing NHA-Medium and neurobasal medium (the phase II differentiation medium DM II) (1 : 1). After 24 h, the medium was replaced with DM II medium alone or with 10 nM ALA for the next 24 h incubation to obtain CM and ALA-preactivated-CM. The second step included the evaluation of the neuroprotective effect of CM and ALA-CM on Amyloid β_{1-42} - ($A\beta_{1-42}$) induced neurodegeneration of differentiated SH-SY5Y cells. On the day 6th, the SH-SY5Y cells (differentiated) were pretreated for 1 h with CM or ALA-CM before the addition of $5 \mu\text{M } A\beta_{1-42}$.

(Sigma Aldrich), 50 IU/mL/50 $\mu\text{g/mL}$ penicillin/streptomycin (Sigma Aldrich). The DM I was supplemented with 10 μM RA (Sigma Aldrich) immediately before adding the medium to the cells. The DM II medium was Neurobasal medium minus phenol red (Invitrogen, Life Technologies, Saint Aubin, France), supplemented with 2 mM Glutamax I (Invitrogen, Life Technologies), 1x B-27 supplement (50x, Invitrogen, Life Technologies), 20 mM KCl (Sigma Aldrich), and 50 IU/mL/50 $\mu\text{g/mL}$ penicillin/streptomycin (Sigma Aldrich). The DM II was supplemented with 10 μM RA (Sigma Aldrich) and 50 ng/mL Human BDNF (PeproTech EC, Ltd, London, UK) immediately before adding the medium to the cells. On the day 6th, the SH-SY5Y cells (differentiated) were pretreated for 1 h with CM or ALA-CM before the addition of $5 \mu\text{M } A\beta_{1-42}$ for the next 24 h. Preliminary experiments were carried out with increasing concentrations of $A\beta$ to choose the respective half-maximal inhibitory concentrations—IC50.

2.4. Cell Viability and Cytotoxicity Assay. Cell viability was based on the ability of viable cells to convert soluble MTT [3-(4,5n-dimethylthiazol-2-yl)-2-5-diphenyltetrazolium bromide] (Sigma Aldrich) into an insoluble purple formazan. Cells were seeded in 96-well plates. Briefly, cells grown and differentiated as described above were incubated for 4 h at 37°C with MTT (0.5 mg/mL in Neurobasal medium without phenol red). Then, the MTT solution was removed and water-insoluble formazan was immediately dissolved in

DMSO (100 μL per well). The amount of formazan was measured at 570 nm with SpectraMax iD3 Multi-Mode Microplate Reader with a version of SoftMaxPro7.1 Setup Software (Molecular Devices, LLC., San Jose, CA, USA).

Cytotoxicity was determined by measuring the release of LDH using the Pierce LDH Cytotoxicity Assay Kit (Thermo Fisher Scientific) according to the manufacturer's instructions. The absorbance was measured at 490 nm and 680 nm by SpectraMax iD3 Multi-Mode Microplate Reader with a version of SoftMaxPro7.1 Setup Software (Molecular Devices, LLC.). To determine LDH activity, we subtracted the 680 nm absorbance value (background) from the 490 nm absorbance value before calculation of % cytotoxicity [(LDH at 490 nm)—(LDH at 680 nm)]. The percentage of the LDH release was normalized to the condition with the least amount of cell death and divided by a maximum lysis control.

2.5. Hoechst Dye 33342 and Propidium Iodide (PI) Double Staining. The SH-SY5Y cells were seeded onto 24-well culture plates (Corning-Costar, Sigma Aldrich, Saint Louis, MO, USA) and were differentiated as described above. On the day 6th, the SH-SY5Y cells (differentiated) were pretreated for 1 h with CM or ALA-CM before the addition of $5 \mu\text{M } A\beta_{1-42}$ for the next 24 h. Following 24 h incubation, the SH-SY5Y cells were subjected to vital double staining with PI/Hoechst 33342 and evaluated for nuclear morphological changes. Briefly, the SH-SY5Y cells were incubated for 30 min at 37°C (humidified 5% CO_2 /95% air incubator)

with PI (1 $\mu\text{g}/\text{mL}$) and HO33342 (5 $\mu\text{g}/\text{mL}$) (Thermo Fisher Scientific), both dissolved in Neurobasal Medium without phenol red. Before measurement, the staining medium was replaced with fresh Neurobasal Medium. Hoechst 33342 is a cell-permeant nuclear counterstain emitting blue fluorescence when bound to DNA, and PI is a membrane impermeant nuclear dye that emits red fluorescence in dead cells, as previously described [17]. The fluorescence of stained SH-SY5Y cells was measured using excitation/emission wavelengths for Hoechst 33342 350/461 nm and 535/617 nm for PI, respectively, by SpectraMax iD3 Multi-Mode Microplate Reader with SoftMaxPro7.1Setup Software (Molecular Devices, LLC.). The stained cells were also analysed in inverted fluorescence microscopy (Olympus IX73, Japan).

2.6. Mitochondrial Membrane Potential ($\Delta\Psi_m$). Mitochondrial depolarization was evaluated using JC-1 Mitochondrial Membrane Potential Assay Kit (Cayman Chemical Company, Ann Arbor, Michigan USA) according to the manufacturer's protocol. The SH-SY5Y cells were seeded in 96-well black plates (Corning-Costar, Sigma Aldrich) and were differentiated as above. On the day 6th, the SH-SY5Y cells (differentiated) were pretreated for 1 h with CM or ALA-CM before the addition of 5 μM $\text{A}\beta_{1-42}$ for the next 24 h. Following incubation for 24 h, 10 μL JC-1 Staining Solution (JC-1 Staining Solution was prepared by diluting the reagent 1:10 in the culture medium used to culture) was added to each well, and the cells were cultured in the CO_2 incubator for 30 min at 37°C. Then, the plate was centrifuged for 5 min at 400 g at room temperature. The supernatant was removed, and the plate was rinsed with assay buffer and centrifuged again (the cycle was repeated 5 times). Properly, in healthy cells, JC-1 forms J-aggregates, which display strong fluorescence intensity with excitation and emission at 535 nm and 595 nm, respectively. In apoptotic or unhealthy cells, JC-1 exists as a monomer, which shows a strong fluorescence intensity with excitation and emission at 485 nm and 535 nm, respectively. Fluorescence of J-aggregates and J-monomers was measured using excitation/emission wavelengths of 535/595 nm and 485/535 nm, respectively, by SpectraMax iD3 Multi-Mode Microplate Reader with SoftMaxPro7.1Setup Software (Molecular Devices, LLC.) and inverted fluorescence microscopy (Olympus IX73). The ratio of fluorescence intensity of J-aggregates to the fluorescence intensity of monomers was used to measure the $\Delta\Psi_m$ of the SH-SY5Y cells. Mitochondrial depolarization was indicated by an increase in the proportion of cells emitting green fluorescence.

2.7. Immunocytofluorescence. The SH-SY5Y cells were seeded onto 8-chamber slides (0.8 cm^2/well ; Lab-Tek, Thermo Fisher Scientific) and were differentiated as described above. On the day 6th, the SH-SY5Y cells (differentiated) were pretreated for 1 h with CM or ALA-CM before the addition of 5 μM $\text{A}\beta_{1-42}$ for the next 24 h. Following 24 h incubation, the SH-SY5Y cells were fixed (4% paraformaldehyde, 15 min, RT) and permeabilized by subsequent incubation with 0.5% Triton X-100 (10 min, RT) and nonspecific sites blocked with 1% BSA and 5% normal donkey serum (NDS;

30 min, RT). Next, the cells were incubated with mouse monoclonal anti- β_3 Tubulin antibody (TUJ 1; Santa Cruz Biotechnology, Inc.; 1:50 in 1% BSA-PBS, for 1 h, RT), rabbit anti-Synaptophysin (GeneTex, Inc.; 1:500 in 1% BSA-PBS, for 1 h, RT), mouse anti-PARKIN (Abcam Inc.; 1:200 in 1% BSA-PBS, for 1 h, RT), rabbit anti-TOMM20 antibody (Abcam Inc.; 1:500 in 1% BSA-PBS, for 1 h, RT), and Alexa Fluor™488-conjugated donkey anti-mouse IgG or Alexa Fluor™568-conjugated goat anti-rabbit IgG (Invitrogen, Life Technologies; 1:200 in 1% BSA-PBS, for 1 h, RT). The nuclei were visualized by staining with Hoechst 33342 (Thermo Fisher Scientific; 5 $\mu\text{g}/\text{mL}$, 30 min, RT). In all cases, slides were mounted with Mowiol (Calbiochem-Novabiochem Co. La Jolla, CA, USA) and fluorescence was evaluated in the fluorescence microscope (Olympus IX73). Quantification of fluorescent intensity of TUJ 1, Synaptophysin, TOMM20, and PARKIN in untreated and treated cells was calculated according to the following formula:

Fluorescence intensity = Integrated Density – (Sum area of selected cells x Mean fluorescence of background readings).

Fluorescence intensity was quantitated using the cellSens Entry Version 1 software platform (Olympus Camera, Japan) and Fiji (ImageJ) open-source image processing package [20].

2.8. Assessment of Insulin and Insulin-Like Growth Factor I by Enzyme-Linked Immunosorbent Assay. NHA cell culture supernatants were collected and centrifuged at 10 000 g, 4°C for 5 min to remove cell debris. Levels of secreted insulin and IGF-I in cell culture supernatants were measured using a commercially available ELISA kit, (Sigma Aldrich) according to the manufacturer's instructions.

2.9. Detection and Quantification of Autophagic Cells by Vital Staining with Acridine Orange. The SH-SY5Y cells were seeded onto 24-well culture plates (Corning-Costar, Sigma Aldrich) and differentiated as mentioned above. On the day 6th, the SH-SY5Y cells (differentiated) were pretreated for 1 h with CM or ALA-CM before the addition of 5 μM $\text{A}\beta_{1-42}$ for the next 24 h. Following the 24 h incubation, the SH-SY5Y cells were subjected to vital staining with acridine orange (AO). The SH-SY5Y cells were incubated with AO (1 $\mu\text{g}/\text{mL}$) for 10 min. Before measurement, the staining medium was replaced with fresh Neurobasal Medium without phenol red and analysed in the Olympus IX-73 inverted fluorescence microscope. Quantification of acidic vesicular organelles (AVOs) was calculated as red to green fluorescence intensity ratio (R/G-FIR) in each microscopic field, as described previously [18, 19]. At least 10 replicates for each treatment as well as untreated control cells were quantitated using the cellSens Entry Version 1 software platform (Olympus Camera) and Fiji (ImageJ) open-source image processing package [20].

2.10. Quantitative Reverse Transcriptase PCR (RT-qPCR). Total RNA was extracted from NHA and the SH-SY5Y cells using the Universal RNA Purification Kit (EURX, Poland) according to the manufacturer's protocol. One microgram of total RNA was reverse transcribed to cDNA using High Capacity cDNA Reverse Transcription Kit with RNase Inhibitor (Invitrogen, Life Technologies). For RT-qPCR, the

TABLE 1: Primers and their sequences used to identify genes in the quantitative real-time reverse-transcription-polymerase chain reaction (RT-qPCR).

Gene name	Forward primer sequences	Reverse primer sequences
Mitophagy genes		
<i>PINK1</i>	GGACGCTGTTCTCGTTA	ATCTGCGATCACCAGCCA
<i>PARKIN</i>	CCCACCTCTGACAAGGAAACA	TCGTGAACAAACTGCCGATCA
Autophagy genes		
<i>ATG5</i>	ATGATAATGGCAGATGACAAGG	TCAGTCACTCGGTGCAGG
<i>LC3β</i>	AAAGGAGGACATTTGAGCAG	AATGTCTCCTGGGAAGCGTA
Mitochondrial biogenesis genes		
<i>TFAM</i>	GTGGGAGCTTCTCACTCTGG	TAGGGCTTTTTCTCCTGCAA
<i>PGC1α</i>	CACCAGCCAACACTCAGCTA	GTGTGAGGAGGGTTCATCGT
Mitochondrial dynamics genes		
<i>MFN2</i>	AATCTGAGGCGACTGGTGA	CTCCTCTGTTTCGACAGTCA
<i>OPA1</i>	GGCCAGCAAGATTAGCTACG	ACAATGTCAGGCACAATCCA
<i>DRP1</i>	GGCAACTGGAGAGGAATGC	CTTTTTGTGGACT
Synaptic genes		
<i>PSD95</i>	CTTCATCCTTGCTGGGGGTC	TTGCGGAGGTCAACACCATT
<i>Synaptophysin</i>	CTGCGTTAAAGGGGGCACTA	ACAGCCACGGTGACAAAGAA
Reference gene		
<i>GAPDH</i>	GAAGGTGAAGGTCGGAGT	GAAGATGGTGATGGGATTC

quantification of expression changes was performed 5x HOT FIREPol Eva Green qPCR Mix Plus (Solis BioDyne, Tartu, Estonia) and CFX Connect (Bio-Rad, Hercules, California, USA). Data were normalized to the housekeeping gene and displayed as fold-change compared to the control (DM) using the $2^{-\Delta\Delta C_t}$ method. Primers are listed in Table 1.

2.11. Statistical Analysis. Data from at least three independent experiments were expressed as the mean \pm standard error (SEM). Statistical analyses were performed using the one-way analysis of variance (ANOVA) followed by Tukey's multiple comparison post-test and with P value being adjusted for multiple comparisons. P values of less than 0.05 were considered statistically significant. Statistical differences between the treated cells and untreated control cells were indicated by asterisks (* for $P < 0.05$; ** for $P < 0.01$; *** for $P < 0.001$; **** versus the control group). Statistical analyses were performed using GraphPad PrismTM version 5.0 software (GraphPad Software Inc., San Diego, CA, USA).

3. Results

3.1. Effect of Alpha-Linolenic Acid on the Viability and Secretory Activity of the NHA Cells. To determine the optimal dose of ALA, which would stimulate astrocytes to secrete insulin and IGF-I, the NHA cells were treated for 24 h with ALA at different doses (10 nM, 50 nM, 100 nM, and 250 nM). First, we checked the effect of ALA on the viability of the NHA cells by MTT assay. As illustrated in Figure 2, 10 nM and 50 nM ALA treatments increased the NHA cells viability to 120% compared with the control group (100%; $P < 0.05$). When the dose of ALA was increased to 250 nM, the viability decreased to 86% (Figure 2).

Then, we assessed by RT-qPCR the effect of different doses of ALA on IGF-I and insulin mRNA production in the NHA cells (Figures 3(a) and 3(b)). We found that 10 nM ALA treatment significantly increased the mRNA expression of *IGF-I* (Figure 3(a); $P < 0.001$) and insulin (Figure 3(b); $P < 0.01$). Likewise, 10 nM ALA treatment-induced astrocytes to secrete IGF-I (Figure 3(c); $P < 0.05$) and insulin (Figure 3(d); $P < 0.001$) into the culture medium.

Based on the above results, a dose of 10 nM ALA was used for the experiments.

3.2. Effect of CM and ALA-CM on Cell Viability of Differentiated SH-SY5Y Cells. We hypothesized that compound secreted by astrocytes might exert protective effects against $A\beta$ -induced cytotoxicity. To investigate the potential neuroprotective effects of CM and ALA-CM, differentiated SH-SY5Y cells were pretreated with CM and ALA-CM for 1 h before $A\beta_{1-42}$ treatment.

We observed that $A\beta_{1-42}$ treatment effectively inhibited the cell viability of differentiated SH-SY5Y cells in a dose-dependent manner as compared with the control (Figure 4; $P < 0.001$). When the SH-SY5Y cells were exposed to 5 μ M of $A\beta_{1-42}$ for 24 hours, cell viability was reduced to approximately 50% of the control (Figure 4; $P < 0.001$). Thus, the concentration of 5 μ M of $A\beta_{1-42}$ was used for further investigations.

As shown on Figure 5, the CM pretreatment significantly increased the cell viability ($P < 0.001$), and restored the cell viability (to 79.16%) compared to control system (64%; DM + $A\beta_{1-42}$) ($P < 0.01$). Moreover, the ALA-CM pretreatment intensified the neuroprotective effect of CM (Figure 5; $P < 0.01$). A similar effect was observed after treatment of the SH-SY5Y cells with insulin (Figure 5(c); $P < 0.01$).

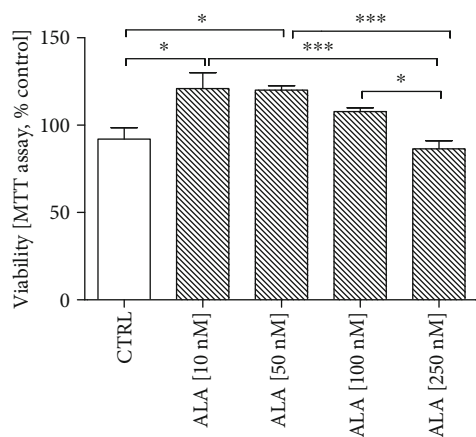


FIGURE 2: Effect of Alpha-linolenic acid (ALA) on the viability of the Normal Human Astrocytes (NHA). The viability of the NHA cells was increased in 10 nM and 50 nM ALA treatments. The NHA cells were exposed for 24 h to ALA at different doses (10 nM, 50 nM, 100 nM, and 250 nM). The obtained results are presented as a percentage of the control value. One-way ANOVA test for viability followed by Tukey's multiple comparisons was used to analyse the data. Results are presented as means \pm SEM ($n = 6 - 12$). Statistical differences between the treated cells and untreated control cells are indicated by asterisks (* for $P < 0.05$; ** for $P < 0.01$; *** for $P < 0.001$).

Additionally, the insulin pretreatment significantly increased the SH-SY5Y cell viability compared to the control model (DM + $A\beta_{1-42}$) (Figure 5(c); $P < 0.01$).

Next, to check whether insulin and IGF-I presence in CM and ALA-CM was responsible for the neuroprotective effect, we treated CM and ALA-CM with the insulin-degrading enzyme (IDE), which degrades both insulin and IGF-I. Cotreatment of CM and ALA-CM with IDE significantly decreased the cell viability to 90.53% and 93.3%, compared to CM and ALA-CM groups, respectively (Figure 5; $P < 0.01$).

3.3. The CM and ALA-CM Pretreatment Reversed the $A\beta_{1-42}$ -Induced Cytotoxicity in Differentiated SH-SY5Y Cells. The inhibitory effects of CM and ALA-CM on $A\beta_{1-42}$ -induced cytotoxicity were evaluated by measuring LDH levels and double-stained with Hoechst 33342 and propidium iodide.

Differentiated SH-SY5Y cells treated with $A\beta_{1-42}$ for 24 h expressed 12.25% LDH release as compared to the control group (4%) (Figure 6(a); $P < 0.001$). However, the CM and ALA-CM pretreatment attenuated LDH activity. The CM-pretreatment markedly decreased LDH release to 8.08% (Figure 6(a); $P < 0.001$). In addition, the ALA-CM pretreatment showed a stronger cytoprotective effect than CM as LDH release was decreased to 4.6% (Figure 6(a); $P < 0.001$).

Similar to the LDH release results, the cytoprotective effect of CM and ALA-CM was confirmed by using double-stained with Hoechst 33342 and propidium iodide (Figures 6(a) and 6(b)). Data indicated that $A\beta_{1-42}$ treated cells (DM + $A\beta_{1-42}$) had a significantly increased ($P < 0.001$) ratio of PI/Hoechst fluorescence signal (Figure 6(b)), which resulted from the increase in cell death. The CM and ALA-CM pretreatment decreased ($P < 0.001$) the ratio

of PI/Hoechst fluorescence signal as compared to the control group (Figure 6(b)). Moreover, the CM pretreatment decreased cell death in the SH-SY5Y cells treated with $A\beta_{1-42}$ when compared with DM + $A\beta_{1-42}$ group (Figure 6(b); $P < 0.05$). Interestingly, ALA preactivated CM significantly intensified the protective effect of CM (Figure 6(b); $P < 0.001$). In contrast, IDE significantly attenuated the protective effect of CM and ALA-CM (Figures 6(a) and 6(b), $P < 0.001$).

A similar effect was observed after the treatment of differentiated SH-SY5Y cells with insulin (Figure 6(c); $P < 0.05$; Figure 6(d); $P < 0.001$, Figure 6(e)). Moreover, the insulin pretreatment reversed the $A\beta_{1-42}$ -induced cytotoxicity in differentiated SH-SY5Y cells. (Figure 6(c); $P < 0.001$, Figure 6(d); $P < 0.01$, Figure 6(c)).

These results indicated that astrocyte-derived insulin/insulin-like growth factor I protect differentiated SH-SY5Y cells against $A\beta_{1-42}$ -induced cell death.

3.4. The CM and ALA-CM Pretreatment Reversed the $A\beta_{1-42}$ -Induced Synaptic Toxicity in Differentiated SH-SY5Y Cells.

To elucidate the effect of CM and ALA-CM on $A\beta_{1-42}$ -induced synaptic toxicity in differentiated SH-SY5Y cells, we measured the expression of synaptic markers through RT-qPCR and immunocytofluorescence methods. RT-qPCR results indicated that pretreatment with CM increased mRNA levels of *Synaptophysin* and *PSD95* (Figures 7(a) and 7(b); $P < 0.001$) in comparison to the control group. Moreover, ALA preactivated CM significantly intensified this effect ($P < 0.001$). However, the $A\beta_{1-42}$ treatment markedly decreased mRNA levels of *Synaptophysin* (Figure 7(a); $P < 0.001$) and *PSD95* (Figure 7(b); $P < 0.05$) when compared to the control group. In contrast, the CM and ALA-CM pretreatment increased levels of *PSD95* in the SH-SY5Y cells treated with $A\beta_{1-42}$ as compared with DM + $A\beta_{1-42}$ group (Figure 7(b); $P < 0.001$). Cotreatment of CM and ALA-CM with IDE significantly attenuated their effect on mRNA expression of synaptic markers.

Further evaluation of the effect of CM and ALA-CM on $A\beta_{1-42}$ -induced synaptic toxicity and neuronal phenotype of differentiated SH-SY5Y cells was established by using immunocytofluorescence staining with antibodies against Synaptophysin and microtubule component β_3 -tubulin TUJ 1 (Figures 7(c)–7(f)). Similar to RT-qPCR results, the $A\beta_{1-42}$ treated cells (DM + $A\beta_{1-42}$) had a decreased Synaptophysin (Figures 7(c) and 7(e); $P < 0.001$) and TUJ 1 (Figures 7(d) and 7(f); $P < 0.001$) fluorescence intensity. Moreover, the $A\beta_{1-42}$ treatment induced fragmentation of neuritis (Figure 7(d)). In contrast, the CM and ALA-CM pretreatment reversed $A\beta_{1-42}$ -induced synaptic toxicity in differentiated SH-SY5Y cells (Figures 7(c)–7(f); $P < 0.05$). Moreover, the insulin pretreatment reversed the $A\beta_{1-42}$ -induced decrease of TUJ 1 fluorescence intensity and fragmentation of neuritis in differentiated SH-SY5Y cells (Figures 7(d) and 7(f); $P < 0.001$). Cotreatment of CM and ALA-CM with IDE attenuated these effects.

3.5. The CM and ALA-CM Pretreatment Protected the SH-SY5Y Cells against $A\beta_{1-42}$ -Induced Mitochondrial Dysfunction. Mitochondrial dysfunction is proposed to participate in cellular

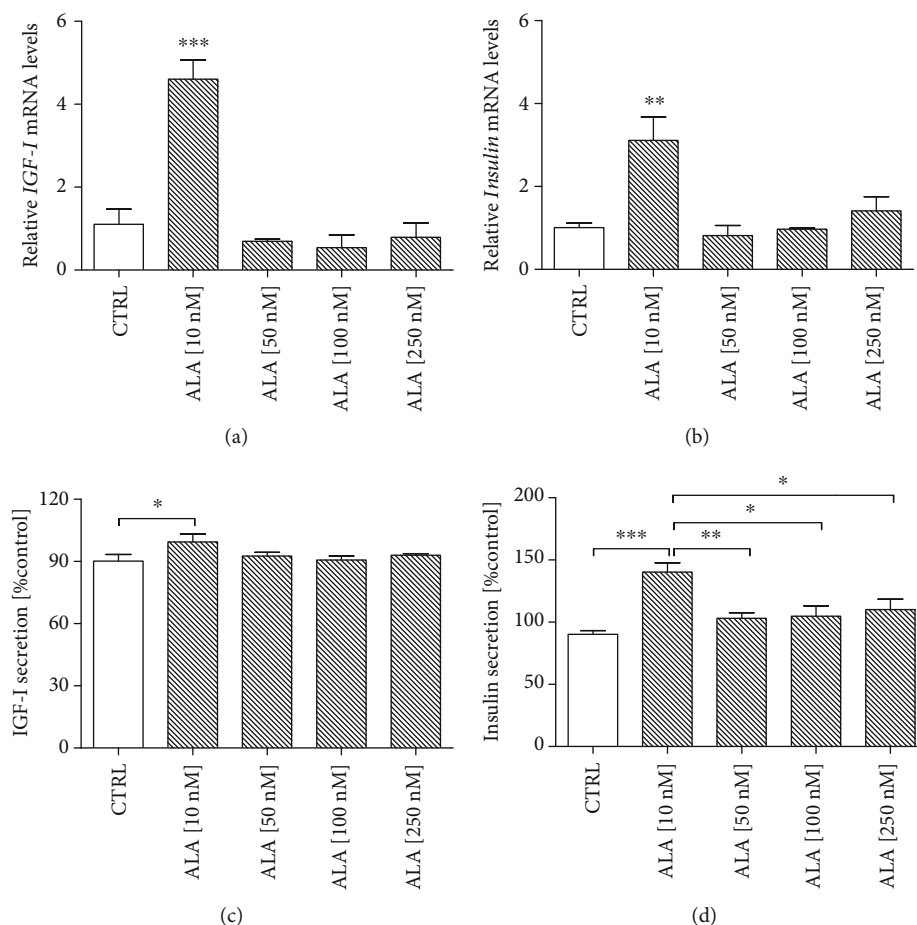


FIGURE 3: Effect of Alpha-linolenic acid (ALA) on mRNA and protein expression of Insulin and Insulin-Like Growth Factor I (IGF-I). Quantitative reverse transcriptase PCR (RT-qPCR) results indicated that 10 nM ALA treatment significantly increased the mRNA expression of IGF-I and Insulin in the NHA cells (a, b). Moreover, the ELISA analysis showed that 10 nM ALA significantly increased the release of IGF-I and insulin from the NHA cells to the medium (c, d). The NHA cells were exposed for 24 h to ALA at different doses (10 nM, 50 nM, 100 nM, and 250 nM). One-way ANOVA followed by Tukey's multiple comparisons test at the 0.05 level was used to determine differences between treated cells and untreated control cells. Results are presented as means \pm SEM ($n = 3 - 8$). RT-qPCR fold increase was calculated according to the formula described in the Materials and Methods section. Statistical differences between treated cells and untreated control cells are indicated by asterisks (* for $P < 0.05$; ** for $P < 0.01$; *** for $P < 0.001$).

apoptosis. Depolarization of the mitochondrial membrane is a sensitive indicator of mitochondrial function. Therefore, the $\Delta\psi_m$ in the SH-SY5Y cells was evaluated by detecting the red/green fluorescence intensity ratio of JC-1 staining (Figures 8(a)–8(c) and 9(b)). The positive control was the SH-SY5Y cells treated with carbonyl-cyano-*m*-chlorophenyl-hydrazone-CCCP (10 μM). CCCP causes uncoupling of the electron transport of the respiratory chain, reducing the mitochondrial membrane potential, which consequently induces cell death. As shown in Figures 8(a) and 8(b), treatment with $A\beta_{1-42}$ significantly increased green fluorescence intensity in the SH-SY5Y cells ($P < 0.001$). The $A\beta_{1-42}$ exposure has a similar effect to CCCP suggesting that $A\beta_{1-42}$ significantly reduced $\Delta\psi_m$. Whereas pretreatment with CM and ALA-CM remarkably reduced green fluorescence intensity and increased red fluorescence intensity in the SH-SY5Y cells treated with $A\beta_{1-42}$ as compared with DM + $A\beta_{1-42}$ treated group ($P < 0.001$). However,

cotreatment of CM and ALA-CM with IDE significantly decreased $\Delta\psi_m$ ($P < 0.001$).

Similarly, the insulin treatment increased red fluorescence intensity in differentiated SH-SY5Y cells (Figure 8(c); $P < 0.01$). Additionally, the insulin pretreatment significantly increased $\Delta\psi_m$ when compared to DM + $A\beta_{1-42}$ treated group (Figure 8(c); $P < 0.05$).

This finding indicates that astrocyte-derived insulin/insulin-like growth factor I inhibits $A\beta_{1-42}$ -induced depolarization of the mitochondrial membrane in differentiated SH-SY5Y cells.

Then, we examined the effect of CM and ALA-CM on mRNA expression of mitochondrial biogenesis and dynamics genes. First, we analysed mRNA levels of the *PGC-1 α* gene and its target gene *mTFA*, which is directly involved in mitochondrial biogenesis. As shown in Figures 10(a) and 10(b), treatment with $A\beta_{1-42}$ significantly decreased mRNA transcripts

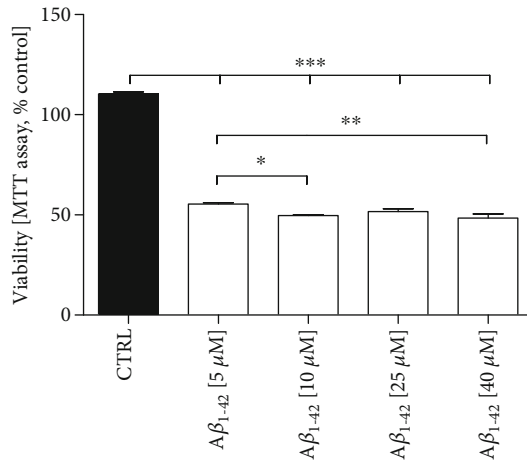


FIGURE 4: Effect of Amyloid β_{1-42} ($A\beta_{1-42}$) treatment on differentiated SH-SY5Y cell viability. $A\beta_{1-42}$ treatment significantly inhibited the cell viability of differentiated SH-SY5Y cells in a dose-dependent manner as compared with the control. Differentiated SH-SY5Y cells (on the day 6th) were exposed for 24 h to $A\beta_{1-42}$ at different doses (5 μ M, 10 μ M, 25 μ M, 40 μ M). The obtained results are presented as a percentage of the control value. One-way ANOVA test for viability followed by Tukey's multiple comparisons was used to analyse the data. Results are presented as means \pm SEM ($n = 7 - 8$). Statistical differences between the treated and untreated control cells are indicated by asterisks (* for $P < 0.05$; ** for $P < 0.01$; *** for $P < 0.001$).

levels of *PGC-1 α* ($P < 0.05$) and its downstream target gene *mTFA* ($P < 0.001$). The pretreatment with CM and ALA-CM increased mRNA levels of *PGC-1 α* and *mTFA* ($P < 0.001$) compared to the control. Moreover, pretreatment with CM and ALA-CM reversed the inhibition of *PGC-1 α* ($P < 0.05$) and *mTFA* ($P < 0.001$) mRNA expression caused by $A\beta_{1-42}$. Cotreatment of CM and ALA-CM with IDE significantly decreased mRNA expression of genes involved in the mitochondrial biogenesis.

Mitochondria are highly dynamic organelles with morphology and numbers regulated by fission and fusion proteins. Excessive mitochondrial fragmentation leads to impaired mitochondrial function and neuronal death in AD. Therefore, in the next step, we also investigated the regulating signals in mitochondrial fission and fusion processes. Mitofusins 2 (*Mfn2*) in the outer mitochondrial membrane and optic atrophy 1 (*Opa1*) in the inner mitochondrial membrane regulate the fusion process, and dynamin-related protein 1 (*Drp1*) regulates the mitochondrial fission. The SH-SY5Y cells exposed to $A\beta_{1-42}$ showed reduced mRNA transcripts levels of *Mfn2* and *Opa1*, and increased levels of mRNA of *Drp1* (Figures 10(c)–10(e)); $P < 0.001$). Whereas pretreatment with CM and ALA-CM of the SH-SY5Y cells exposed to $A\beta_{1-42}$ rescued the levels of these transcripts to values similar to those of the untreated cells. Also, cotreatment of CM and ALA-CM with IDE significantly increased mRNA expression of *Drp1* (Figure 10(e); $P < 0.001$).

To determine the mitochondrial content in the SH-SY5Y cells, we probed for the mitochondrial outer membrane protein TOMM20 (translocase of outer mitochondrial membrane 20) by using the immunocytofluorescence method.

As shown in Figures 9(a) and 9(b), TOMM20 fluorescence intensity was decreased in $A\beta_{1-42}$ -treated SH-SY5Y cells (DM + $A\beta_{1-42}$) ($P < 0.001$). Whereas pretreatment with CM of the SH-SY5Y cells exposed to $A\beta_{1-42}$ increased the immunoreactivity of TOMM20-positive mitochondrial in comparison with DM + $A\beta_{1-42}$ group ($P < 0.05$). Furthermore, pretreatment with ALA-CM increased TOMM20 fluorescence intensity in comparison with CM + $A\beta_{1-42}$ group ($P < 0.05$). However, the SH-SY5Y cells exposed to cotreatment of CM and ALA-CM with IDE showed a decrease in fluorescence intensity of TOMM20 when compared to CM and ALA-CM groups (Figures 9(a) and 9(b); $P < 0.001$). Likewise, we observed that the insulin treatment increased TOMM20 fluorescence intensity (Figures 9(a) and 9(b); $P < 0.05$). Similarly, pretreatment with insulin increased TOMM20 fluorescence intensity in comparison with DM + $A\beta_{1-42}$ group (Figures 9(a) and 9(b); $P < 0.05$).

In agreement with the above results, astrocyte-derived insulin/insulin-like growth factor I restored the $A\beta_{1-42}$ -damaged of mitochondrial biogenesis and dynamic processes.

3.6. The CM and ALA-CM Pretreatment Modulates $A\beta_{1-42}$ -Induced Effects on Mitophagy and Autophagy. As observed above, decreased levels of mitochondrial profusion genes and increased levels of mitochondrial profission genes may result in autophagic clearance of damaged mitochondria. As CM and ALA-CM rescued the $A\beta_{1-42}$ -induced mitochondrial dysfunction, we further investigated these effects on subsequent mitophagy. Autophagy (mitophagy) process has been suggested to remove damaged and dysfunctional mitochondria, which has been implicated in the progression of AD [21]. In this experiment, the potent depolarizing agent CCCP was used as a positive control to chemically induce mitophagy and autophagy. We determined mitophagy by monitoring expression levels of *PINK-1* and *PARKIN*, well-known markers of this process. As shown in Figures 11(a) and 11(b), $A\beta_{1-42}$ treatment markedly increased mRNA levels of *PINK-1* ($P < 0.001$) and *PARKIN* ($P < 0.01$) in comparison to the control group. $A\beta_{1-42}$ exposure had a similar effect to CCCP, suggesting that $A\beta_{1-42}$ significantly increased mitophagy. Whereas pretreatment with CM of the SH-SY5Y cells exposed to $A\beta_{1-42}$ significantly decreased the level of mitophagy markers when compared to DM + $A\beta_{1-42}$ group (Figure 11(a); $P < 0.001$, Figure 11 (b); $P < 0.01$). Interestingly, ALA preactivated CM significantly intensified this effect (Figure 11(a); $P < 0.01$, Figure 11(b); $P < 0.001$).

Similarly, immunofluorescence staining results showed that the $A\beta_{1-42}$ treated cells had an increased PARKIN fluorescence intensity (Figures 11(e) and 11(f); $P < 0.01$). Whereas pretreatment with CM and ALA-CM of the SH-SY5Y cells exposed to $A\beta_{1-42}$ significantly decreased PARKIN fluorescence intensity (Figures 11(e) and 11(f); $P < 0.01$). Similarly, the pretreatment with insulin decreased PARKIN fluorescence intensity in comparison with DM + $A\beta_{1-42}$ group (Figures 11(e) and 11(f); $P < 0.001$). However, the SH-SY5Y cells exposed to cotreatment of CM and ALA-CM with IDE showed an increased PARKIN fluorescence intensity in comparison to CM (Figures 11(e) and 11(f); $P < 0.01$) and ALA-CM groups (Figures 11(e) and 11(f); $P < 0.05$).

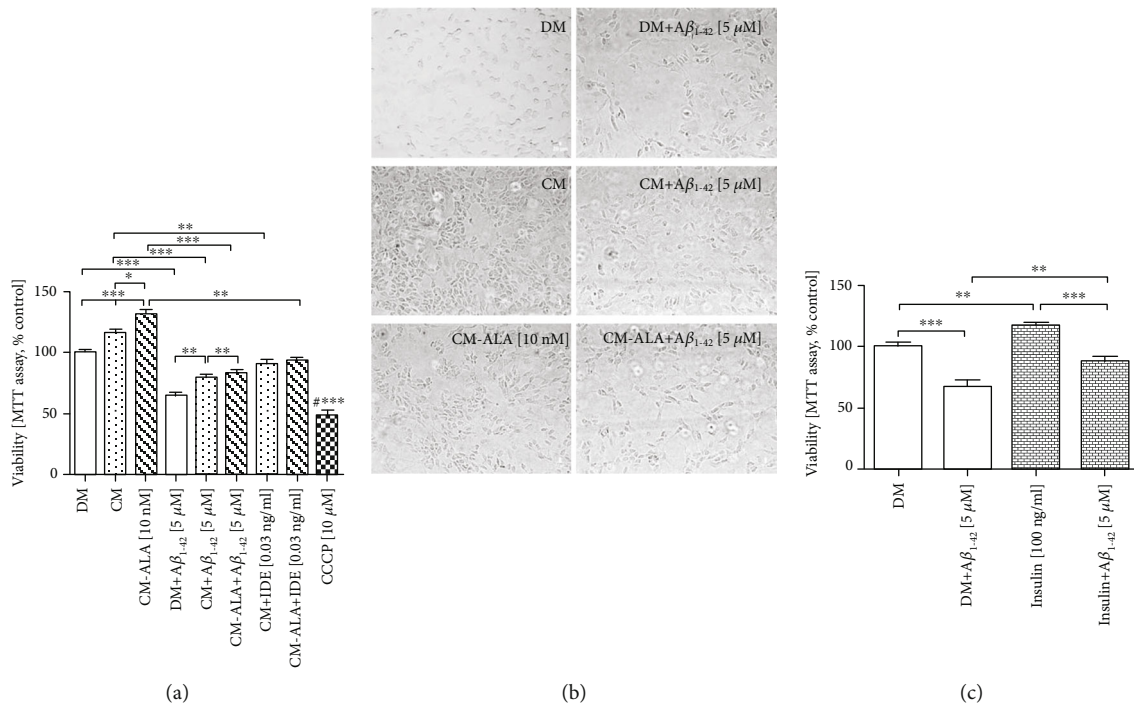


FIGURE 5: CM and ALA-CM reversed the effects of Amyloid β_{1-42} ($A\beta_{1-42}$) treatment on differentiated SH-SY5Y cell viability. The results showed that the CM and ALA-CM pretreatment significantly increased the viability of differentiated SH-SY5Y cells and restored $A\beta_{1-42}$ -induced reduction of the cell viability (a). Insulin Degrading Enzyme (IDE) treatment of CM and ALA-CM reduced this effect. On the day 6th, the SH-SY5Y cells (differentiated) were pretreated for 1 h with CM or ALA-CM before the addition of $5 \mu\text{M}$ $A\beta_{1-42}$ for the next 24 h. The SH-SY5Y cells were also exposed to cotreatment of CM and ALA-CM with IDE to check whether insulin and IGF-I presence in CM and ALA-CM was responsible for the neuroprotective effect. Positive controls were the SH-SY5Y cells treated with insulin (c) and carbonyl-cyano-m-chlorophenylhydrazone-CCCP ($10 \mu\text{M}$). The obtained results are presented as a percentage of the control value. One-way ANOVA test for viability followed by Tukey's multiple comparisons was used to analyse data. Statistical differences between the treated cells and untreated control cells are indicated by asterisks (* for $P < 0.05$; ** for $P < 0.01$; *** for $P < 0.001$; #*** versus the control group). Results are means \pm SEM of three independent experiments. Cell morphology was observed under a microscope (b). Scale bar is $20 \mu\text{m}$.

Removal of damaged mitochondria requires also the induction of general autophagy [22]. Therefore, we assessed expression levels of ATG5 and LC3 β , well-known markers of autophagy. The RT-qPCR results revealed that $A\beta_{1-42}$ exposure resulted in elevated mRNA levels of ATG5 and LC3 β (Figures 11(c) and 11(d); $P < 0.001$). Whereas pretreatment with CM of the SH-SY5Y cells exposed to $A\beta_{1-42}$ significantly decreased expression of ATG5 (Figure 11(c); $P < 0.01$) and LC3 β (Figure 11(d); $P < 0.001$) in comparison with DM + $A\beta_{1-42}$ group.

Interestingly, ALA preactivated CM significantly intensified this effect (Figure 11(c); $P < 0.01$, Figure 11(d); $P < 0.001$).

Besides, the SH-SY5Y cells exposed to the cotreatment of CM and ALA-CM with IDE showed increased expression of mitophagy and autophagy markers (Figures 11(a)–11(d); $P < 0.001$).

The late state of autophagy is characterized by the development of acidic vesicular organelles (AVOs), which include lysosomes as well as autophagosomes. Therefore, to determine the late state of autophagy, the SH-SY5Y cells were stained with acridine orange (AO). The formation of punctate staining was monitored with fluorescence microscopy. As shown in Figures 12(a) and 12(b), $A\beta_{1-42}$ treatment mark-

edly increased AVO production ($P < 0.001$). Whereas pretreatment with CM and ALA-CM remarkably reduced AVO production in the SH-SY5Y cells treated with $A\beta_{1-42}$ to similar values of untreated cells ($P < 0.05$). Increased AVO production was also observed in the SH-SY5Y cells exposed to the cotreatment of CM and ALA-CM with IDE.

4. Discussion

The main purpose of the present study was to explore indicated a new alpha-linolenic acid- (ALA-) induced mechanism of neuroprotection during $A\beta$ -associated neuronal damage, with special regard to astrocyte involvement. Herein, we reported that ALA stimulated the secretory activity of astrocytes. Moreover, our results showed that ALA preactivated astrocytes conditioned medium reversed $A\beta_{1-42}$ -induced mitochondrial dysfunction and neuronal death.

ω -3 (n-3) polyunsaturated fatty acids (PUFAs) are fatty acids that are important for human health, especially for brain development and function. Alpha-linolenic acid, the most abundant n-3 PUFA, is an essential fatty acid in the human diet and is present in green leaves, oil, seeds (flaxseed, canola, perilla), and nuts. Various studies have suggested that

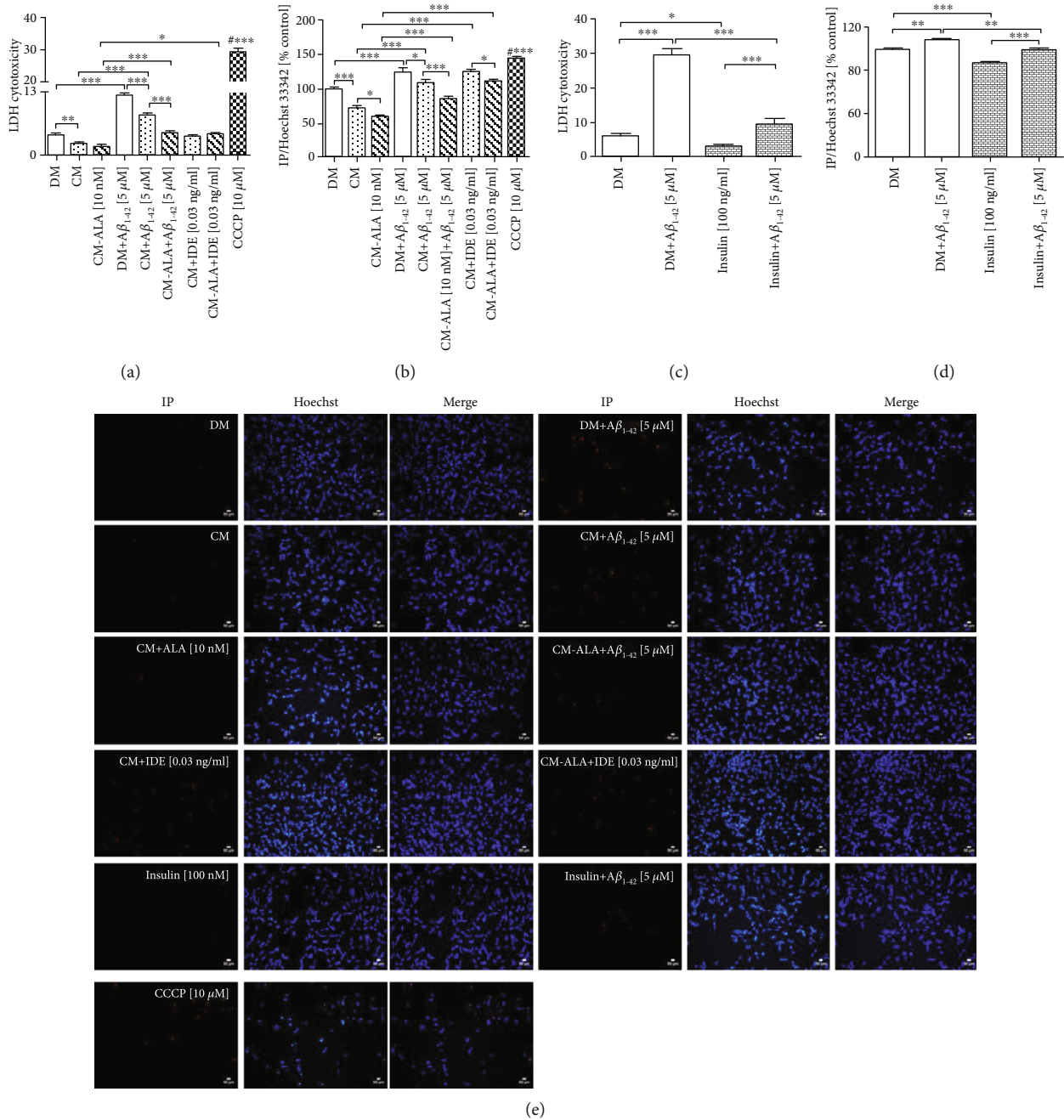


FIGURE 6: The CM and ALA-CM pretreatment reversed the Amyloid β_{1-42} - ($A\beta_{1-42}$ -) induced cytotoxicity in differentiated SH-SY5Y cells. The LDH assay (a, c) and double-stained with Hoechst 33342 and propidium iodide (PI) (b, d, e) results indicated that $A\beta_{1-42}$ significantly increased cell death of differentiated SH-SY5Y cells. Whereas, the CM pretreatment decreased cell death in the SH-SY5Y cells treated with $A\beta_{1-42}$. Besides, ALA preactivated CM significantly intensified the protective effect of CM. In contrast, Insulin Degrading Enzyme (IDE) significantly attenuated the protective effect of CM and ALA-CM. The insulin pretreatment reversed the $A\beta_{1-42}$ -induced cytotoxicity in differentiated SH-SY5Y cells. On the day 6th, the SH-SY5Y cells (differentiated) were pretreated for 1 h with CM or ALA-CM before the addition of $5 \mu\text{M}$ $A\beta_{1-42}$ for the next 24 h. The SH-SY5Y cells were also exposed to cotreatment of CM and ALA-CM with IDE to check whether insulin and IGF-I presence in CM and ALA-CM was responsible for the neuroprotective effect. Positive controls were the SH-SY5Y cells treated with Insulin and carbonyl-cyano-m-chlorophenylhydrazone-CCCP ($10 \mu\text{M}$). Next, cells were subjected to vital double staining with PI and Hoechst 33342 (see Materials and Methods section). The PI/Hoechst ratio was calculated by dividing the PI by Hoechst Relative fluorescence units (RFUs). One-way ANOVA test for cytotoxicity followed by Tukey's multiple comparisons was used to analyse data. Statistical differences between the treated cells and untreated control cells are indicated by asterisks (* for $P < 0.05$; ** for $P < 0.01$; *** for $P < 0.001$; **** versus the control group). Results are means \pm SEM of three independent experiments. The vital double staining cells were also analyzed in inverted fluorescence microscopy (see Materials and Methods section). Scale bar is $50 \mu\text{m}$.

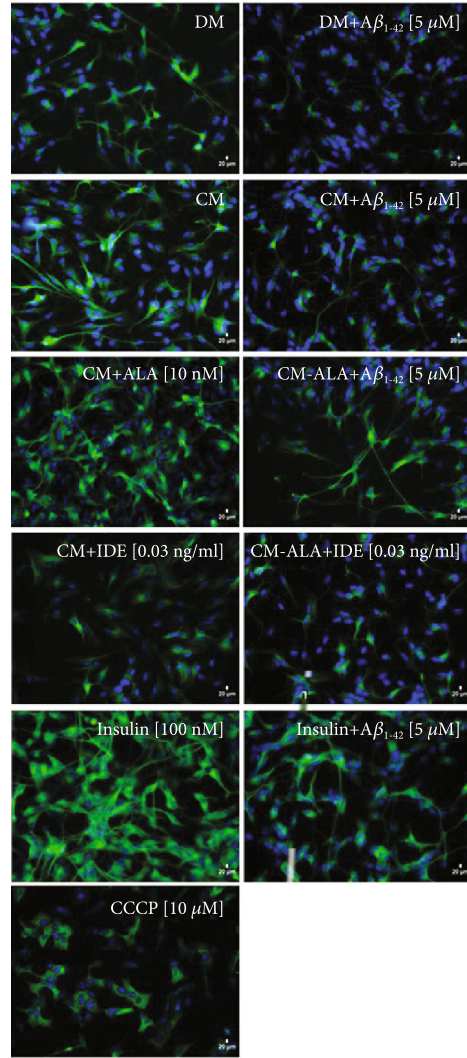
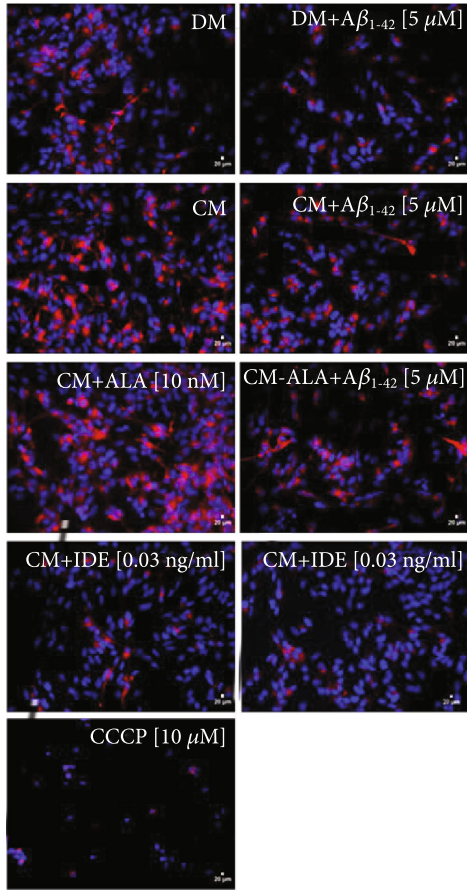
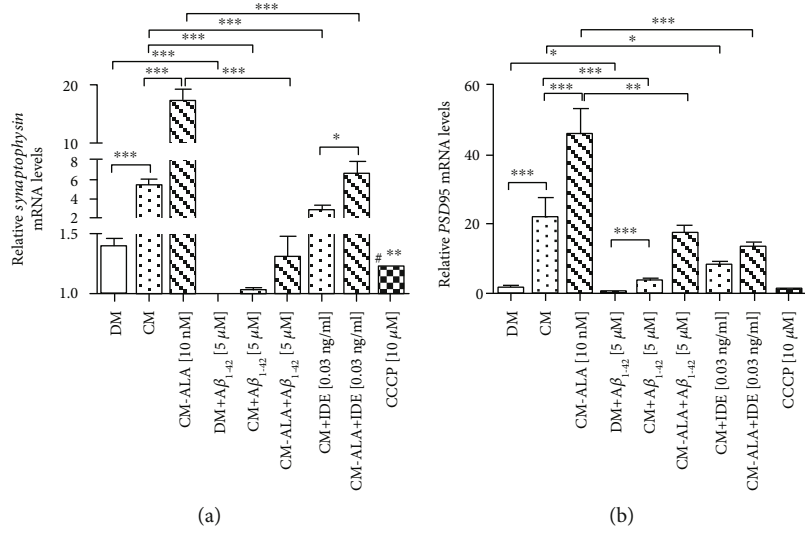


FIGURE 7: Continued.

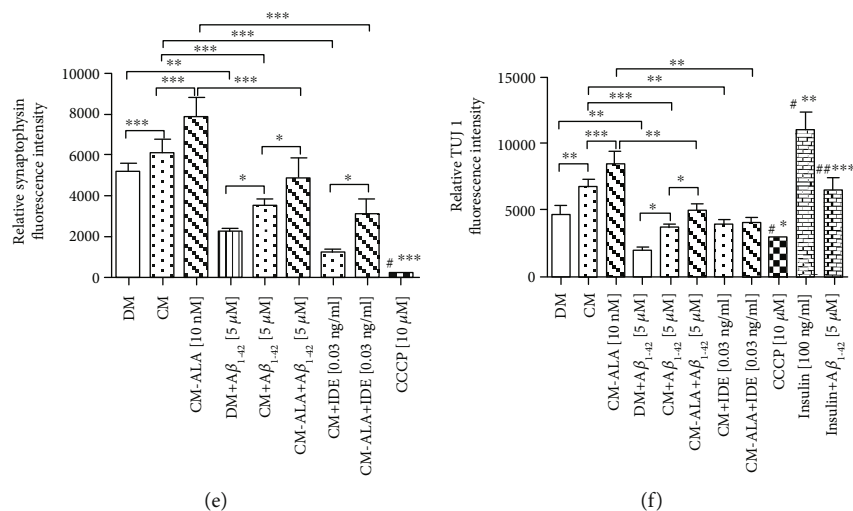


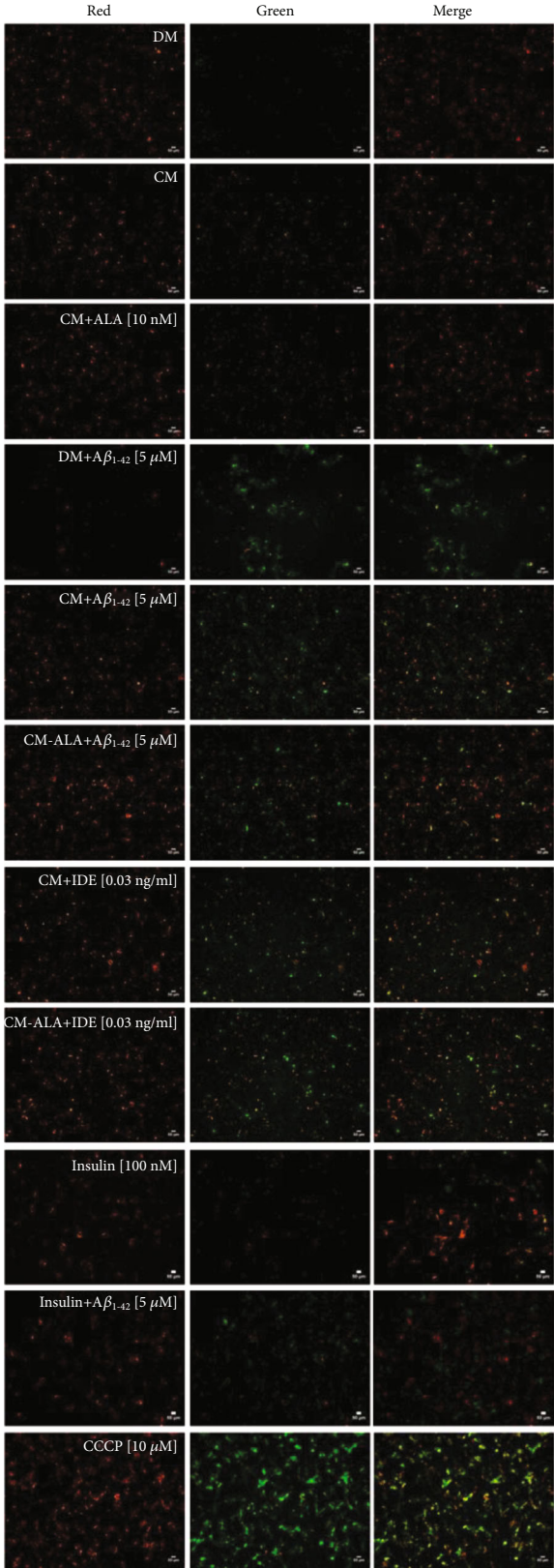
FIGURE 7: The CM and ALA-CM pretreatment reversed Amyloid β - ($A\beta_{1-42}$ -) induced synaptic toxicity in differentiated SH-SY5Y cells. On the day 6th, the SH-SY5Y cells (differentiated) were pretreated for 1 h with CM or ALA-CM before the addition of $5 \mu\text{M}$ $A\beta_{1-42}$ for the next 24 h. The SH-SY5Y cells were also exposed to the cotreatment of CM and ALA-CM with Insulin Degrading Enzyme (IDE) to check whether insulin and IGF-I presence in CM and ALA-CM was responsible for the neuroprotective effect. Positive controls were the SH-SY5Y cells treated with insulin and carbonyl-cyano-m-chlorophenylhydrazone-CCCP ($10 \mu\text{M}$). RT-qPCR results indicated that $A\beta_{1-42}$ significantly decreased mRNA levels of *Synaptophysin* (a) and *PSD95* (b), well-known synaptic markers. The CM and ALA-CM pretreatment reversed the effect of $A\beta_{1-42}$ when compared with DM + $A\beta_{1-42}$ group. The IDE treatment of CM and ALA-CM reduced this effect. The immunocytofluorescence staining showed that the $A\beta_{1-42}$ treated cells had a decreased Synaptophysin (c, e) and TUJ 1 (β -Tubulin) (d, f) fluorescence intensity and increased neurites fragmentation. Moreover, results showed that the CM and ALA-CM pretreatment reversed the $A\beta_{1-42}$ -induced synaptic toxicity in differentiated SH-SY5Y cells. A similar effect of TUJ 1 fluorescence intensity was observed after the treatment of differentiated SH-SY5Y cells with insulin (d, f). The IDE treatment of CM and ALA-CM reduced this effect. The cells were subjected to immunocytofluorescence staining with antibodies against Synaptophysin and TUJ 1. TUJ 1 was used as a marker to stain differentiated SH-SY5Y cells (show as green signals). Synaptophysin was used to stain synaptic in differentiated SH-SY5Y cells (show as red signals). Hoechst 33342 was used to stain nuclei (show as blue signals) (see Materials and Methods section). Bar graphs (e, f) showed the relative fluorescence intensity of Synaptophysin and TUJ 1. Scale bar is $20 \mu\text{m}$. One-way ANOVA followed by Tukey's multiple comparisons test at the 0.05 level was used to determine differences between the treated cells and untreated control cells. Results are presented as means \pm SEM ($n = 3 - 8$). RT-qPCR fold increase and the fluorescence intensity were calculated according to the formula described in the Materials and Methods section. Statistical differences between the treated group and untreated control cells are indicated by asterisks (* for $P < 0.05$; ** for $P < 0.01$; *** for $P < 0.001$; **** versus the control group; ##**** versus DM + $A\beta_{1-42}$ group).

ALA exerts neuroprotective and anti-inflammatory effects [11–13]. However, the direct effect of ALA on the trophic activity of astrocytes has not been studied yet.

In the current study, we focused on astrocytes because it is widely accepted now that they play a key role in the central nervous system. Astrocytes produce and release multiple proteins that impact the survival, migration, differentiation, and function of neurons. Importantly, these proteins can serve as neurotrophic agents against $A\beta$ toxicity [7, 8, 23]. In this study, we focused our interest on insulin and IGF-I as likely candidates for neuroprotection, taking into account their involvement in synaptic and mitochondrial function, as seen also in AD. It seems that insulin and IGF-I production in the brain may be a controversial topic. For many years, it has been thought that brain insulin was derived from pancreatic β cells and permeated through the blood-brain barrier [24]. However, in the last few years, this hypothesis has been abolished. Nowadays, it is believed that astrocytes may be the source of local insulin and IGF-I in the brain. More recently, insulin and IGF-I secretion was also confirmed in cultured astrocytes [8, 25, 26]. Therefore it seems that the identification of astrocytes as an insulin and IGF-I source in the brain would allow us to better understand the importance of these

factors in brain physiology, and it could also point to a new therapeutic target for dementia and age-related cognitive disorders. Interestingly, in the present study, we demonstrated for the first time that ALA stimulates astrocytes to express and release insulin and IGF-I to the medium (Figures 3(c) and 3(d)). However, we also observed that ALA at higher concentrations reduces the viability and thus the secretory activity of astrocytes, which could be due to the excessive oxidation of ALA which generates various metabolites as well as reactive oxygen species. Demar et al. described that radiolabelled ALA entering the brain is almost completely metabolized to its β -oxidation products [27]. Recently, it has been suggested that the oxidation of polyunsaturated fatty acids could be associated with induced cell death. For example, Liu et al. indicated that DHA hydroperoxide is a potential inducer of apoptosis via mitochondrial dysfunction in human neuroblastoma SH-SY5Y cells [28]. Probably, the effect of ALA on astrocytes, similarly to the impact of another PUFA, could be dose-dependent. Therefore, these results indicate that ALA in lower concentrations may regulate the trophic activity of astrocytes.

The next aim of our study was to investigate whether pretreatment with CM and ALA-pretreated CM modulates



(a)

FIGURE 8: Continued.

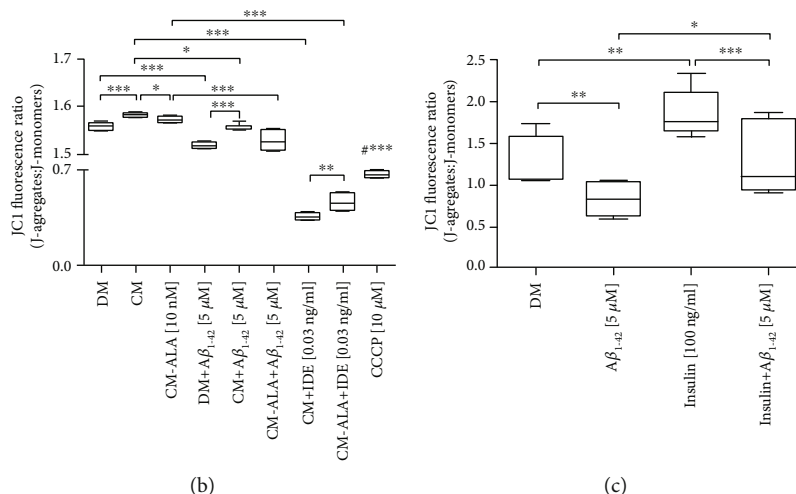


FIGURE 8: The CM and ALA-CM pretreatment inhibits Amyloid β - ($A\beta_{1-42}$) induced depolarization of the mitochondrial membrane in differentiated SH-SY5Y cells. Representative fluorescence microscopy images of 5,5,6,6'-tetrachloro-1,1',3,3' tetraethylbenzimidazolcarbocyanine iodide (JC-1) staining (a) and the ratio of fluorescence intensity of J-aggregates to the fluorescence intensity of monomers (b, c) was used to measure mitochondrial membrane potential ($\Delta\psi_m$) of differentiated SH-SY5Y cells. Results showed that $A\beta_{1-42}$ treatment decreased the $\Delta\psi_m$ of differentiated SH-SY5Y cells. The CM and ALA-CM pretreatment reversed the effect of $A\beta_{1-42}$ compared with DM + $A\beta_{1-42}$ group. The Insulin Degrading Enzyme (IDE) treatment of CM and ALA-CM reduced this effect. On the day 6th, the SH-SY5Y cells (differentiated) were pretreated for 1 h with CM or ALA-CM before the addition of $5 \mu\text{M}$ $A\beta_{1-42}$ for the next 24 h. The SH-SY5Y cells were also exposed to cotreatment of CM and ALA-CM with IDE to check whether insulin and IGF-I presence in CM and ALA-CM was responsible for the neuroprotective effect. Carbonyl cyanide 3-chlorophenylhydrazone (CCCP) was used as a mitochondrial membrane potential disruptor. Insulin was used as a positive control. Next, cells were subjected to JC-1 staining (see Materials and Methods section). Fluorescence of JC-1 was measured by a fluorescence microscope and microplate reader. One-way ANOVA followed by Tukey's multiple comparisons test at the 0.05 level was used to determine differences between the treated cell and untreated control cells. Results are presented as means \pm SEM ($n = 4 - 6$). The ratio of fluorescence intensity of J-aggregates (shown as red signals) to the fluorescence intensity of monomers (shown as green signals) was calculated according to the formula described in the Materials and Methods section. Statistical differences between the treated cells and untreated control cells are indicated by asterisks (* for $P < 0.05$; ** for $P < 0.01$; *** for $P < 0.001$; **** versus the control group). Scale bar is $50 \mu\text{m}$.

$A\beta_{1-42}$ -induced cytotoxicity in differentiated SH-SY5Y cells. $A\beta$ is a key molecular factor in the etiology of AD [29]. Previous *in vitro* studies have shown that $A\beta$ is toxic to neurons, which is manifested by cell death [8, 29–31]. In agreement with the previous findings, our results showed that $A\beta_{1-42}$ was highly toxic to differentiated SH-SY5Y cells what was exemplified by the reduction of MTT values in a dose-dependent manner (Figure 4). Moreover, $A\beta_{1-42}$ probably induced apoptosis of differentiated SH-SY5Y cells. It was evidenced by morphological and biochemical alterations associated with apoptosis including condensed chromatin (Figure 6(e)) increased LDH release and increased ratio fluorescence of PI/Hoechst (Figures 6(a) and 6(b)). However, we are aware that further research is needed to determine which apoptosis pathways are activated in $A\beta_{1-42}$ -treated differentiated SH-SY5Y cells. Nonetheless, our results showed that pretreatment with CM and ALA-CM was able to attenuate the toxic effect of $A\beta_{1-42}$. Additionally, the protective effect of CM was intensified by pre-activation with ALA.

The presented protective action of CM and ALA-CM could also effect through the regulation of synaptic proteins and rescue of synaptic function. The pathogenesis of AD correlates with neuronal dysfunction and loss of functional synapses caused by changes in neurite morphology. *In vitro* studies indicated that mechanisms of synapse deterioration

in AD result from the toxic activity of $A\beta$ [8, 32]. In our study, the addition of $A\beta_{1-42}$ reduced levels of synaptic markers (Figures 7(a)–7(f)) and induced the fragmentation of neuritis (Figures 7(d) and 7(f)) in differentiated SH-SY5Y cells. Whereas treatment with CM and ALA-CM was able to attenuate the synaptotoxic effect of $A\beta_{1-42}$.

Mitochondria are organelles that may activate apoptosis when their function is damaged. A recent study demonstrated that mitochondrial dysfunction is a hallmark of $A\beta$ -induced neuronal toxicity in AD [3, 33]. Therefore, in the next step, we investigated whether mitochondria were involved in the protective effect of CM and ALA-CM against $A\beta_{1-42}$. In our study, we demonstrated that $A\beta_{1-42}$ disrupted the function of mitochondria. Our results, in concordance with previously reported data, showed that $A\beta_{1-42}$ significantly reduced $\Delta\psi_m$ (Figures 8(a) and 8(b)) when compared to the control group [34, 35]. However, pretreatment with CM and ALA-CM reversed the $A\beta_{1-42}$ -induced depolarization of the mitochondrial membrane in differentiated SH-SY5Y cells.

Moreover, we observed the reduced mitochondrial mass in $A\beta_{1-42}$ -treated SH-SY5Y cells (Figure 9). The reduced mitochondrial mass has already been found in brains from AD when compared to a healthy brain in a mouse model of AD as well as in AD cellular models [36, 37]. A reduction

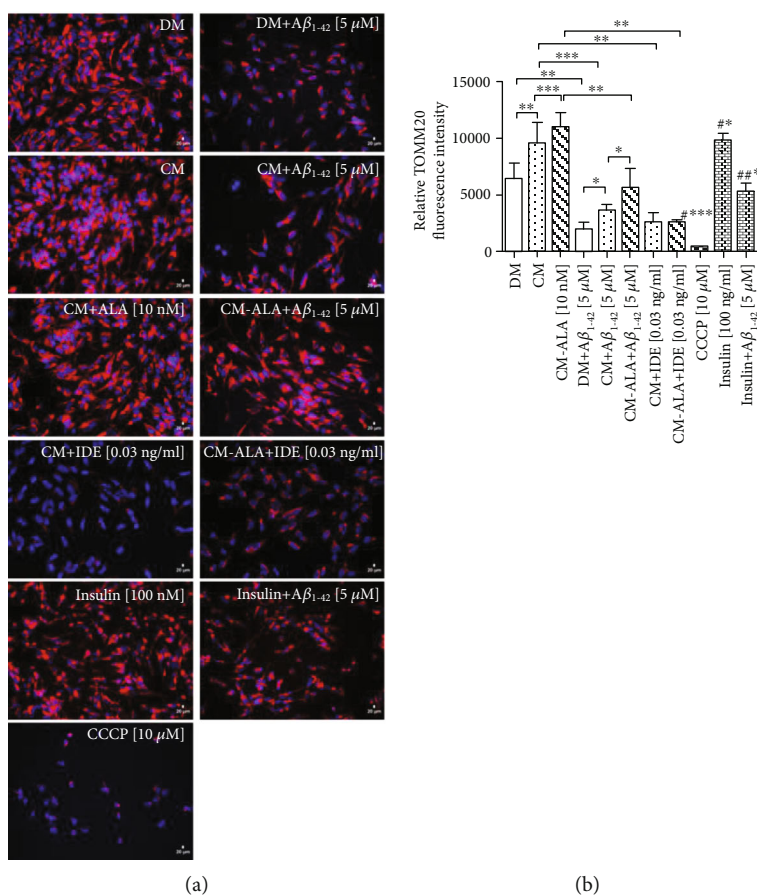


FIGURE 9: The CM and ALA-CM pretreatment reversed Amyloid β ($A\beta_{1-42}$) induced a reduction in mitochondrial mass in differentiated SH-SY5Y cells. The fluorescence intensity indicating mitochondrial mass was calculated by immunocytofluorescence staining of the translocase of outer mitochondrial membrane 20 (TOMM20) in differentiated SH-SY5Y cells. Representative fluorescence images (a) and the relative fluorescence intensity of TOMM20 (b) showed that $A\beta_{1-42}$ induced a reduction of TOMM20 fluorescence intensity. However, the decrease in TOMM20 fluorescence intensity was improved by the CM pretreatment of differentiated SH-SY5Y cells before $A\beta_{1-42}$ exposure. Besides, ALA-pretreated CM intensified this effect. In contrast, cotreatment of CM and ALA-CM with Insulin Degrading Enzyme (IDE) markedly decreased the immunoreactivity of TOMM20-positive mitochondrial. On the day 6th, the SH-SY5Y cells (differentiated) were pretreated for 1 h with CM or ALA-CM before the addition of 5 μ M $A\beta_{1-42}$ for the next 24 h. The SH-SY5Y cells were also exposed to cotreatment of CM and ALA-CM with IDE to check whether insulin and IGF-I presence in CM and ALA-CM was responsible for the neuroprotective effect. Carbonyl cyanide 3-chlorophenylhydrazone (CCCP) was used as a mitochondrial membrane potential disruptor. Insulin was used as a positive control. Next, cells were subjected to immunocytofluorescence staining with antibodies against TOMM20 (see Materials and Methods section). TOMM20 was used to stain mitochondria in differentiated SH-SY5Y cells (shown as red signals). Hoechst 33342 was used to stain nuclei (shown as blue signals). Bar graph showed the relative fluorescence intensity of TOMM20. The fluorescence intensity of TOMM20 was calculated according to the formula described in the Materials and Methods section. Statistical differences between the treated cells and untreated control cells are indicated by asterisks (* for $p < 0.05$; ** for $p < 0.01$; *** for $p < 0.001$; #***, #* versus the control group; ###; versus DM + $A\beta_{1-42}$ group). Scale bar is 20 μ m.

in the number of mitochondria may result from impairment of the mitochondrial biogenesis or increased mitochondrial-specific autophagy clearance known as mitophagy. Our results showed that $A\beta_{1-42}$ suppressed mRNA levels of *PGC-1 α* and *mTFA*, key regulators of mitochondrial biogenesis (Figures 10(a) and 10(b)). Whereas pretreatment with CM and ALA-CM increased *PGC-1 α* and *mTFA* mRNA levels (Figures 10(a) and 10(b)), reversing the $A\beta_{1-42}$ -mediated reduction of the mitochondrial biogenesis.

Another key mitochondrial functions, the mitochondrial dynamics such as fusion and fission processes, were found to be unbalanced in AD. Several findings indicate that $A\beta$ might play a role in impaired mitochondrial dynamics [38]. In the

present study, we showed that the SH-SY5Y cells incubated with $A\beta_{1-42}$ presented alterations in the mitochondrial dynamics towards more fission rather than fusion events. The CM and ALA-CM pretreatment restored $A\beta_{1-42}$ -reduced mRNA levels of the mitochondrial profusion genes *Mfn2* (Figure 10(c)) and *Opa1* (Figure 10(d)), and, conversely, it rescued $A\beta_{1-42}$ -increased mRNA levels of the fission gene *Drp1* (Figure 10(e)). The balance between fusion and fission processes is essential to maintain the health of the neuronal cells. Moreover, *Mfn2*, whose expression is induced by *PGC-1 α* , regulates not only the mitochondrial fusion but also mitochondrial biogenesis and mitochondrial function through changes in the mitochondrial membrane

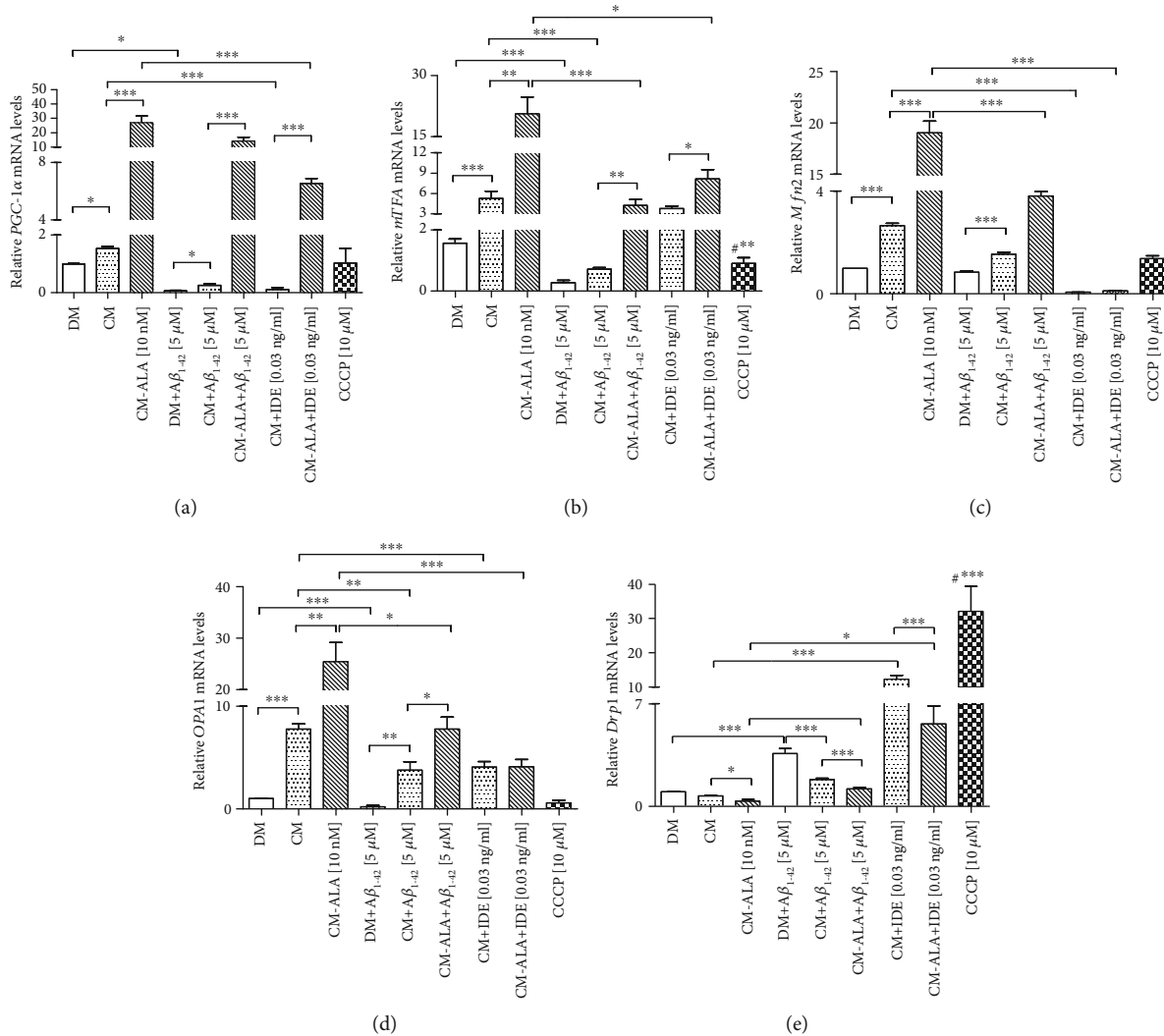


FIGURE 10: The CM and ALA-CM pretreatment regulated the mitochondrial biogenesis and dynamics in differentiated SH-SY5Y cells. RT-qPCR results indicated that Amyloid β ($A\beta_{1-42}$) significantly decreased mRNA levels of PGC-1 α (a), mTFA (b), Mfn2 (c), and OPA1 (d), and increased levels of Drp1 (e). Amyloid β ($A\beta_{1-42}$)-induced reduction on mitochondrial biogenesis was restored by CM and ALA-pretreated CM. Moreover, the CM and ALA-CM pretreatment regulated the balance between fission and fusion processes. Cotreatment of CM and ALA-CM with Insulin Degrading Enzyme (IDE) decreased mRNA expression of genes involved in mitochondrial biogenesis and promoted the elevation of mRNA levels of Drp1, a fission gene. On the day 6th, the SH-SY5Y cells (differentiated) were pretreated for 1 h with CM or ALA-CM before the addition of 5 μ M $A\beta_{1-42}$ for the next 24 h. The SH-SY5Y cells were also exposed to cotreatment of CM and ALA-CM with IDE to check whether insulin and IGF-I presence in CM and ALA-CM was responsible for the neuroprotective effect. The positive control was the SH-SY5Y cells treated with carbonyl-cyano-m-chlorophenylhydrazone-CCCP (10 μ M). One-way ANOVA followed by Tukey's multiple comparisons test at the 0.05 level was used to determine differences between the treated cells and untreated control cells. Results are presented as means \pm SEM ($n = 3 - 8$). RT-qPCR fold increase was calculated according to the formula described in the Materials and Methods section. Statistical differences between the treated cells and untreated control cells are indicated by asterisks (* for $p < 0.05$; ** for $p < 0.01$; *** for $p < 0.001$; ### versus the control; #### versus the control group).

potential and the expression of mitochondrial oxidative phosphorylation subunits [39].

As observed above, decreased levels of mRNA of mitochondrial profusion genes and increased mRNA levels of mitochondrial profission genes may result in the mitophagy of damaged mitochondria. Under physiological conditions, mitophagy plays an essential role in the basal mitochondrial turnover and maintenance. The PTEN-induced putative kinase protein 1- (PINK1-) Parkin-mediated mitophagy is the most extensively studied and the best-understood mito-

phagy pathway [40, 41]. It has been reported that acute depolarization of mitochondrial $\Delta\psi_m$ *in vitro* with $\Delta\psi_m$ dissipation reagents induces Parkin-mediated mitophagy and subsequently eliminates depolarized mitochondria within the autophagy-lysosomal system. Our results showed that $A\beta_{1-42}$ significantly increased mRNA levels of PINK-1 (Figure 11(a)) and PARKIN (Figure 11(b)) in comparison to the control group. Parkin-mediated mitophagy induction has been associated with reduced levels of mitochondrial outer membrane proteins including TOMM20 [42], and

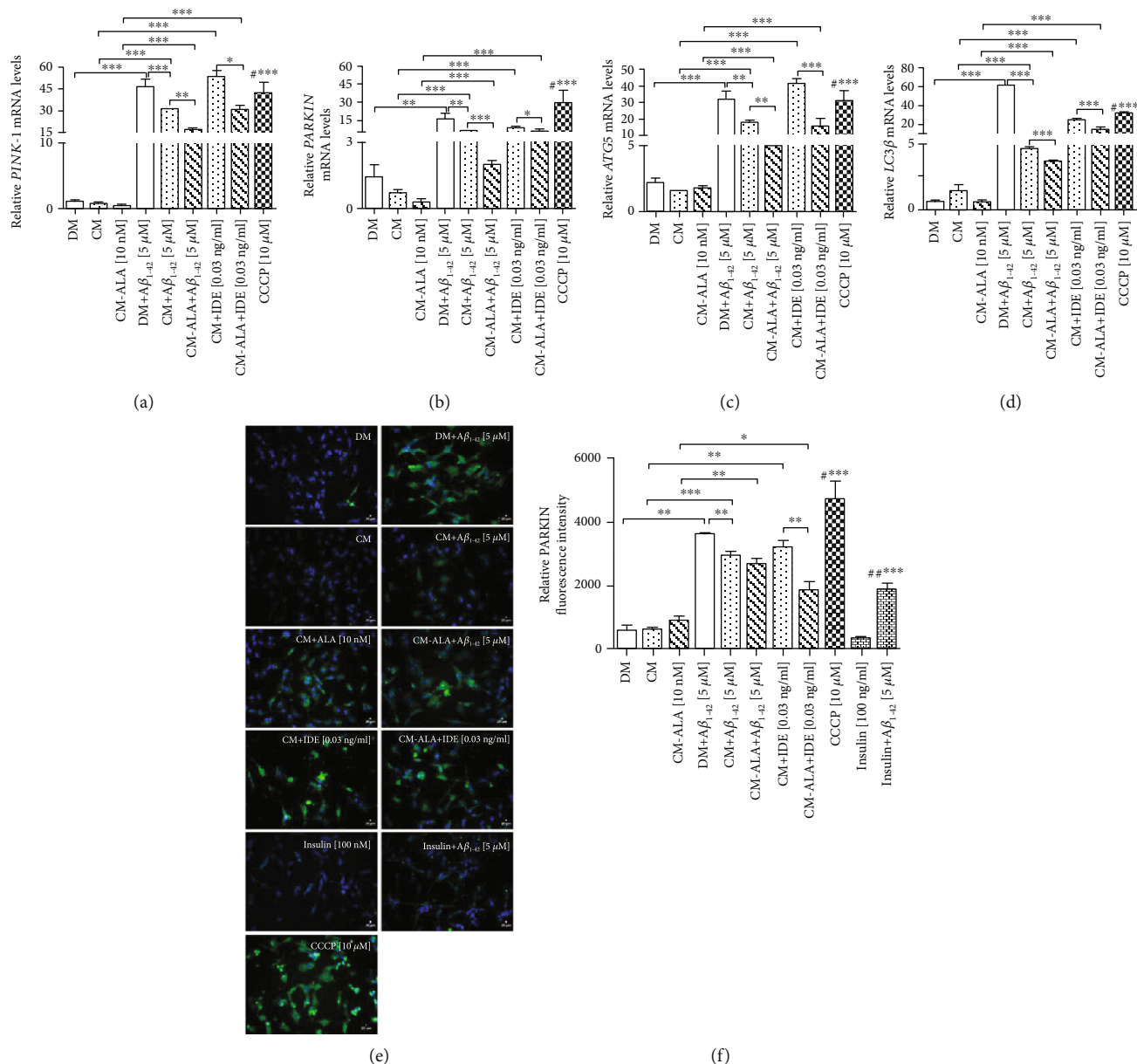


FIGURE 11: The CM and ALA-CM pretreatment modulates Amyloid β - ($A\beta_{1-42}$ -) induced effects on mitophagy and autophagy. On the day 6th, the SH-SY5Y cells (differentiated) were pretreated for 1 h with CM or ALA-CM before the addition of $5 \mu\text{M}$ $A\beta_{1-42}$ for the next 24 h. The SH-SY5Y cells were also exposed to the cotreatment of CM and ALA-CM with Insulin Degrading Enzyme (IDE) to check whether insulin and IGF-I presence of CM and ALA-CM was responsible for the neuroprotective effect. Positive controls were the SH-SY5Y cells treated with insulin and carbonyl-cyano-m-chlorophenylhydrazone-CCCP ($10 \mu\text{M}$). RT-qPCR results showed that $A\beta_{1-42}$ significantly increased mRNA levels of markers of mitophagy (*PINK-1* (a), *PARKIN* (b)), and autophagy (*ATG5* (c) and *LC3 β* (d)). Whereas pretreatment with CM of the SH-SY5Y cells exposed to $A\beta_{1-42}$ significantly decreased expression of mitophagy and autophagy markers. IDE increased levels of mitophagy and autophagy markers. The immunocytofluorescence staining showed that the $A\beta_{1-42}$ treated cells had an increased PARKIN fluorescence intensity, a well-known marker of mitophagy (e, f). Whereas pretreatment with CM and ALA-CM of the SH-SY5Y cells exposed to $A\beta_{1-42}$ significantly decreased PARKIN fluorescence intensity. A similar effect was observed after the insulin treatment. IDE increased PARKIN fluorescence intensity. Bar graph showed the relative fluorescence intensity of PARKIN. Antibody against PARKIN was used to stain marker of mitophagy in differentiated SH-SY5Y cells (shown as green signals). Hoechst 33342 was used to stain nuclei (shown as blue signals). Scale bar is $20 \mu\text{m}$. The results showed that $A\beta_{1-42}$ exposure has a similar effect to CCCP suggesting that $A\beta_{1-42}$ induce mitophagy and autophagy. One-way ANOVA followed by Tukey's multiple comparisons test at the 0.05 level was used to determine differences between the treated cells and untreated control cells. Results are presented as means \pm SEM ($n = 3 - 8$). RT-qPCR fold increase and the fluorescence intensity were calculated according to the formula described in the Materials and Methods section. Statistical differences between the treated cells and untreated control cells are indicated by asterisks (* for $P < 0.05$; ** for $P < 0.01$; *** for $P < 0.001$; **** versus the control group; ***** versus DM + $A\beta_{1-42}$ group).

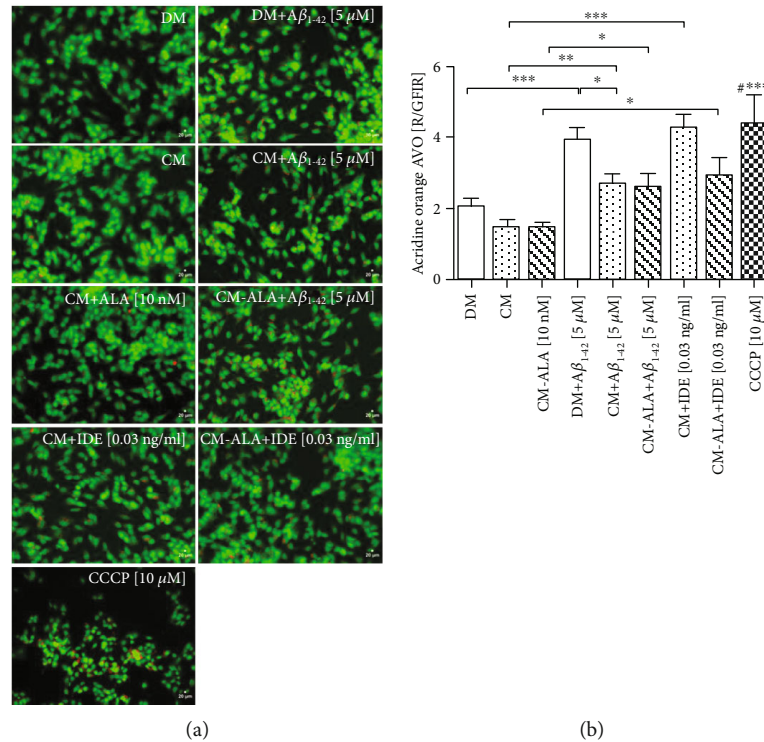


FIGURE 12: The CM and ALA-CM pretreatment reduced acidic vesicular organelles (AVOs) production in the SH-SY5Y cells treated with Amyloid β ($A\beta_{1-42}$). Representative fluorescence microscopy images of acridine orange (AO) staining (a) and the ratio of red to green fluorescence intensity ratio (R/GFIR) (b) were used to measure the late state of autophagy, which is characterized by AVOs production. On the day 6th, the SH-SY5Y cells (differentiated) were pretreated for 1 h with CM or ALA-CM before the addition of 5 μ M $A\beta_{1-42}$ for the next 24 h. The SH-SY5Y cells were also exposed to the cotreatment of CM and ALA-CM with Insulin Degrading Enzyme (IDE) to check whether insulin and IGF-I presence in CM and ALA-CM was responsible for the neuroprotective effect. The positive control was the SH-SY5Y cells treated with carbonyl-cyano-m-chlorophenylhydrazone-CCCP (10 μ M). Next, the SH-SY5Y cells were subjected to vital staining with AO (see Materials and Methods section). Red to green fluorescence intensity ratio (R/GFIR) was calculated in at least 10 replicates for each treatment and nontreated controls. One-way ANOVA followed by Tukey's multiple comparisons test at the 0.05 level was used to determine differences between the treated cells and untreated control cells. Results are presented as means \pm SEM. Statistical differences between the treated cells and untreated control cells are indicated by asterisks (* for $P < 0.05$; ** for $P < 0.01$; *** for $P < 0.001$; **** versus the control group).

this observation is consistent with our results (Figures 9(a) and 9(b)). Enhanced mitophagy has been also confirmed in AD patient brains, and it has been accompanied by depletion of cytosolic PARKIN over disease progression [43]. In the recent study, we demonstrated that CM and ALA-CM abolished $A\beta_{1-42}$ -induced mitophagy by reduction in *PINK1* and *PARKIN* levels to similar values to the control.

Removal of damaged mitochondria requires also the induction of general autophagy [22]. $A\beta_{1-42}$ has been also reported as an autophagy inducer accompanied by increased LC3-II expression [44]. Our results also confirmed that $A\beta_{1-42}$ increased mRNA levels of *ATG5* (Figure 11(c)) and *LC3 β* (Figure 11(d)), well-known markers of autophagy, as well as increased acidic vesicular organelles production (Figures 12(a) and 12(b)). Whereas pretreatment with CM and ALA-CM abolished $A\beta_{1-42}$ -induced autophagy by reduction of *ATG5* and *LC3 β* levels to similar values to the control.

Finally, to check whether insulin and IGF-I presence in CM and ALA-CM was responsible for the above described neuroprotective effects, we treated CM and ALA-CM with

the insulin-degrading enzyme, which degrades both insulin and IGF-I [8]. Our results showed that IDE attenuated neuroprotective effects of CM and ALA-CM by increasing cell death (Figures 5, 6(a), 6(b), and 6(e)), decreasing $\Delta\psi_m$ (Figures 8(a) and 8(b)), increasing mitochondrial dysfunctions and consequently increasing mitophagy and autophagy processes. Besides, we examined the direct neuroprotective effect of insulin on differentiated SH-SY5Y cells untreated or treated with $A\beta_{1-42}$. Our results confirm its neuroprotective effect. Moreover, our results are consistent with previously published results which have shown that both IGF-I and insulin were involved in the pathogenesis of AD. Lower serum levels of IGF-I were associated with an increased risk of developing AD [45]. Moreover, it has been reported that physiological protection against synaptotoxic $A\beta$ can be mediated by astrocyte-derived insulin/IGF-I [8]. Besides, insulin resistance results in mitochondrial dysfunction and excessive autophagy, and in extreme cases, mitochondrial dysfunction can even lead to neuronal cell death as previously described in cases of age-associated neurodegenerative diseases like Alzheimer's disease [46].

To conclude, the present study showed that astrocyte-derived insulin/insulin-like growth factor I suppresses $A\beta_{1-42}$ -induced cytotoxicity in the SH-SY5Y cells by protecting against mitochondrial dysfunction. Moreover, the neuroprotective effects of CM are intensified by preactivation with ALA. Our study suggests that ALA may be a very promising AD-modifying drug candidate.

5. Conclusions

- (1) Alpha-linolenic acid stimulates the release of insulin and IGF-I from astrocytes
- (2) Astrocyte-derived insulin/IGF-I protects differentiated SH-SY5Y cells against $A\beta_{1-42}$ -induced cell death
- (3) Astrocyte-derived insulin/IGF-I protect against $A\beta_{1-42}$ -induced mitochondrial dysfunction in differentiated SH-SY5Y cells via:
 - (i) reducing depolarization of the mitochondrial membrane
 - (ii) increasing mitochondrial biogenesis and restoring the balance between fusion and fission processes
 - (iii) regulation of mitophagy and autophagy processes

Data Availability

Please contact with the main author of the work by email. alitwiniuk@cmkp.edu.pl.

Conflicts of Interest

The authors declare no conflicts of interest.

Acknowledgments

We would like to thank Professor Agnieszka Baranowska-Bik for her expert advice and support. This work was supported by the National Science Centre of Poland (grant No. 2018/02/X/NZ3/00825) and CMKP grants No. 501-1-031-22-19 and No. 501-1-031-22-20.

References

- [1] D. J. Selkoe and J. Hardy, "The amyloid hypothesis of Alzheimer's disease at 25 years," *EMBO Molecular Medicine*, vol. 8, no. 6, pp. 595–608, 2016.
- [2] V. L. Villemagne, S. Burnham, P. Bourgeat et al., "Amyloid β deposition, neurodegeneration, and cognitive decline in sporadic Alzheimer's disease: a prospective cohort study," *The Lancet Neurology*, vol. 12, no. 4, pp. 357–367, 2013.
- [3] M. Obulesu and M. J. Lakshmi, "Apoptosis in Alzheimer's disease: an understanding of the physiology, pathology and therapeutic avenues," *Neurochemical Research*, vol. 39, no. 12, pp. 2301–2312, 2014.
- [4] K. Itoh, K. Nakamura, M. Iijima, and H. Sesaki, "Mitochondrial dynamics in neurodegeneration," *Trends in Cell Biology*, vol. 23, no. 2, pp. 64–71, 2013.
- [5] C. Cadonic, M. G. Sabbir, and B. C. Albensi, "Mechanisms of mitochondrial dysfunction in Alzheimer's disease," *Molecular Neurobiology*, vol. 53, no. 9, pp. 6078–6090, 2016.
- [6] B. Sheng, X. Wang, B. Su et al., "Impaired mitochondrial biogenesis contributes to mitochondrial dysfunction in Alzheimer's disease," *Journal of Neurochemistry*, vol. 120, no. 3, pp. 419–429, 2012.
- [7] J. Pitt, M. Thorner, D. Brautigam, J. Larner, and W. L. Klein, "Protection against the synaptic targeting and toxicity of Alzheimer's-associated $A\beta$ oligomers by insulin mimetic chiro-inositols," *The FASEB Journal*, vol. 27, pp. 199–207, 2012.
- [8] J. Pitt, K. C. Wilcox, V. Tortelli et al., "Neuroprotective astrocyte-derived insulin/insulin-like growth factor 1 stimulates endocytic processing and extracellular release of neuron-bound $A\beta$ oligomers," *Molecular Biology of the Cell*, vol. 28, no. 20, pp. 2623–2636, 2017.
- [9] C. L. Bitel, C. Kasinathan, R. H. Kaswala, W. L. Klein, and P. H. Frederikse, "Amyloid- β and Tau Pathology of Alzheimer's Disease Induced by Diabetes in a Rabbit Animal Model," *Journal of Alzheimers Disease*, vol. 32, no. 2, pp. 291–305, 2012.
- [10] P. Zheng and W. Tong, "IGF-1: an endogenous link between traumatic brain injury and Alzheimer disease?," *Journal of Neurosurgical Sciences*, vol. 61, no. 4, pp. 416–421, 2017.
- [11] G. Zhao, T. D. Etherton, K. R. Martin, S. G. West, P. J. Gillies, and P. M. Kris-Etherton, "Dietary α -linolenic acid reduces inflammatory and lipid cardiovascular risk factors in hypercholesterolemic men and women," *Journal of Nutrition*, vol. 134, no. 11, pp. 2991–2997, 2004.
- [12] C. Nguemni, B. Delplanque, C. Rovère et al., "Dietary supplementation of alpha-linolenic acid in an enriched rapeseed oil diet protects from stroke," *Pharmacological Research*, vol. 61, no. 3, pp. 226–233, 2010.
- [13] H. Gao, P. Yan, S. Zhang et al., "Long-term dietary alpha-linolenic acid supplement alleviates cognitive impairment correlate with activating hippocampal CREB signaling in natural aging rats," *Molecular Neurobiology*, vol. 53, no. 7, pp. 4772–4786, 2016.
- [14] M. S. Tan, L. Tan, T. Jiang et al., "Amyloid- β induces NLRP1-dependent neuronal pyroptosis in models of Alzheimer's disease," *Cell Death and Disease*, vol. 5, no. 8, p. e1382, 2014.
- [15] J. I. Forster, S. Köglberger, C. Trefois et al., "Characterization of differentiated SH-SY5Y as neuronal screening model reveals increased oxidative vulnerability," *Journal of Biomolecular Screening*, vol. 21, no. 5, pp. 496–509, 2016.
- [16] M. M. Shipley, C. A. Mangold, and M. L. Szpara, "Differentiation of the SH-SY5Y human neuroblastoma cell line," *Journal of Visualised Experiments*, vol. 108, no. 108, p. 53193, 2016.
- [17] K. J. Bode, S. Mueller, M. Schweinlin, M. Metzger, and T. Brunner, "A fast and simple fluorometric method to detect cell death in 3D intestinal organoids," *BioTechniques*, vol. 67, no. 1, pp. 23–28, 2019.
- [18] M. P. Thomé, E. C. Filippi-Chiela, E. S. Villodre et al., "Ratio-metric analysis of acridine orange staining in the study of acidic organelles and autophagy," *Journal of Cell Science*, vol. 129, no. 24, pp. 4622–4632, 2016.
- [19] A. Jaśkiewicz, B. Pająk, A. Litwiniuk, K. Urbańska, and A. Orzechowski, "Geranylgeraniol prevents statin-dependent

- myotoxicity in C2C12 muscle cells through RAB1 GTPase prenylation and cytoprotective autophagy,” *Oxidative Medicine and Cellular Longevity*, vol. 2018, Article ID 6463807, 22 pages, 2018.
- [20] J. Schindelin, I. Arganda-Carreras, E. Frise et al., “Fiji: an open-source platform for biological-image analysis,” *Nature Methods*, vol. 9, no. 7, pp. 676–682, 2012.
- [21] I. Kim, S. Rodriguez-Enriquez, and J. J. Lemasters, “Selective degradation of mitochondria by mitophagy,” *Archives of Biochemistry and Biophysics*, vol. 462, no. 2, pp. 245–253, 2007.
- [22] H. Li, A. Ham, T. C. Ma et al., “Mitochondrial dysfunction and mitophagy defect triggered by heterozygous GBA mutations,” *Autophagy*, vol. 15, no. 1, pp. 113–130, 2019.
- [23] L. P. Diniz, V. Tortelli, M. N. Garcia et al., “Astrocyte transforming growth factor beta 1 promotes inhibitory synapse formation via CaM kinase II signaling,” *Glia*, vol. 62, no. 12, pp. 1917–1931, 2014.
- [24] W. A. Banks, “The source of cerebral insulin,” *European Journal of Pharmacology*, vol. 490, no. 1–3, pp. 5–12, 2004.
- [25] W. Chen, B. He, W. Tong, J. Zeng, and P. Zheng, “Astrocytic insulin-like growth factor-1 protects neurons against excitotoxicity,” *Frontiers in Cellular Neuroscience*, vol. 13, p. 298, 2019.
- [26] K. Takano, K. Koarashi, K. Kawabe et al., “Insulin expression in cultured astrocytes and the decrease by amyloid β ,” *Neurochemistry International*, vol. 119, pp. 171–177, 2018.
- [27] J. C. DeMar, K. Ma, L. Chang, J. M. Bell, and S. I. Rapoport, “ α -Linolenic acid does not contribute appreciably to docosahexaenoic acid within brain phospholipids of adult rats fed a diet enriched in docosahexaenoic acid,” *Journal of neurochemistry*, vol. 94, no. 4, pp. 1063–1076, 2005.
- [28] X. Liu, T. Shibata, S. Hisaka, Y. Kawai, and T. Osawa, “DHA hydroperoxides as a potential inducer of neuronal cell death: a mitochondrial dysfunction-mediated pathway,” *Journal of Clinical Biochemistry and Nutrition*, vol. 43, no. 1, pp. 26–33, 2008.
- [29] J. J. Palop and L. Mucke, “Amyloid- β -induced neuronal dysfunction in Alzheimer’s disease: from synapses toward neural networks,” *Nature Neuroscience*, vol. 13, no. 7, pp. 812–818, 2010.
- [30] H. Li, L. Cao, Y. Ren, Y. Jiang, W. Xie, and D. Li, “GLP-1 receptor regulates cell growth through regulating IDE expression level in A β 1-42-treated PC12 cells,” *Bioscience Reports*, vol. 38, no. 4, 2018.
- [31] Z. Wang, L. Xiong, G. Wang, W. Wan, C. Zhong, and H. Zu, “Insulin-like growth factor-1 protects SH-SY5Y cells against β -amyloid-induced apoptosis via the PI3K/Akt-Nrf2 pathway,” *Experimental Gerontology*, vol. 87, no. Part A, pp. 23–32, 2017.
- [32] S. Petratos, Q. X. Li, A. J. George et al., “The β -amyloid protein of Alzheimer’s disease increases neuronal CRMP-2 phosphorylation by a rho-GTP mechanism,” *Brain*, vol. 131, no. 1, pp. 90–108, 2008.
- [33] J. X. Chen and S. D. Yan, “Pathogenic role of mitochondrial [correction of mitochondrial] amyloid-beta peptide,” *Expert Review of Neurotherapeutics*, vol. 7, pp. 1517–1525, 2014.
- [34] A. L. Sereia, M. T. de Oliveira, A. Baranoski et al., “In vitro evaluation of the protective effects of plant extracts against amyloid-beta peptide-induced toxicity in human neuroblastoma SH-SY5Y cells,” *PLoS One*, vol. 14, no. 2, article e0212089, 2019.
- [35] T. F. Chen, M. C. Tang, C. H. Chou, M. J. Chiu, and R. F. S. Huang, “Dose-dependent folic acid and memantine treatments promote synergistic or additive protection against A β (25–35) peptide-induced apoptosis in SH-SY5Y cells mediated by mitochondria stress-associated death signals,” *Food and Chemical Toxicology*, vol. 62, pp. 538–547, 2013.
- [36] G. Amadoro, V. Corsetti, F. Florenzano et al., “AD-linked, toxic NH2 human tau affects the quality control of mitochondria in neurons,” *Neurobiology of Disease*, vol. 62, pp. 489–507, 2014.
- [37] M. J. Calkins, M. Manczak, P. Mao, U. Shirendeb, and P. H. Reddy, “Impaired mitochondrial biogenesis, defective axonal transport of mitochondria, abnormal mitochondrial dynamics and synaptic degeneration in a mouse model of Alzheimer’s disease,” *Human Molecular Genetics*, vol. 20, no. 23, pp. 4515–4529, 2011.
- [38] X. Wang, B. Su, S. L. Siedlak et al., “Amyloid-overproduction causes abnormal mitochondrial dynamics via differential modulation of mitochondrial fission/fusion proteins,” *Proceedings of the National Academy of Sciences of the United States of America*, vol. 105, no. 49, pp. 19318–19323, 2008.
- [39] S. Pich, D. Bach, P. Briones et al., “The Charcot-Marie-Tooth type 2A gene product, Mfn2, up-regulates fuel oxidation through expression of OXPHOS system,” *Human Molecular Genetics*, vol. 14, no. 11, pp. 1405–1415, 2005.
- [40] S. Kawajiri, S. Saiki, S. Sato et al., “PINK1 is recruited to mitochondria with parkin and associates with LC3 in mitophagy,” *FEBS Letters*, vol. 584, no. 6, pp. 1073–1079, 2010.
- [41] N. Matsuda, S. Sato, K. Shiba et al., “PINK1 stabilized by mitochondrial depolarization recruits Parkin to damaged mitochondria and activates latent Parkin for mitophagy,” *Journal of Cell Biology*, vol. 189, no. 2, pp. 211–221, 2010.
- [42] S. R. Yoshii, C. Kishi, N. Ishihara, and N. Mizushima, “Parkin mediates proteasome-dependent protein degradation and rupture of the outer mitochondrial membrane,” *Journal of Biological Chemistry*, vol. 286, no. 22, pp. 19630–19640, 2011.
- [43] X. Ye, X. Sun, V. Starovoytov, and Q. Cai, “Parkin-mediated mitophagy in mutant hAPP neurons and Alzheimer’s disease patient brains,” *Human Molecular Genetics*, vol. 24, no. 10, pp. 2938–2951, 2015.
- [44] M. Guglielmotto, D. Monteleone, A. Piras et al., “A β 1-42 monomers or oligomers have different effects on autophagy and apoptosis,” *Autophagy*, vol. 10, no. 10, pp. 1827–1843, 2014.
- [45] A. J. Westwood, A. Beiser, C. DeCarli et al., “Insulin-like growth factor-1 and risk of Alzheimer dementia and brain atrophy,” *Neurology*, vol. 82, no. 18, pp. 1613–1619, 2014.
- [46] G. E. Gibson, A. Starkov, J. P. Blass, R. R. Ratan, and M. F. Beal, “Cause and consequence: mitochondrial dysfunction initiates and propagates neuronal dysfunction, neuronal death and behavioral abnormalities in age-associated neurodegenerative diseases,” *Biochimica et Biophysica Acta*, vol. 1802, no. 1, pp. 122–134, 2010.

Research Article

Honeybush Extracts (*Cyclopia* spp.) Rescue Mitochondrial Functions and Bioenergetics against Oxidative Injury

Anastasia Agapouda ^{1,2}, Veronika Butterweck ³, Matthias Hamburger ⁴,
Dalene de Beer ^{5,6}, Elizabeth Joubert ^{5,6} and Anne Eckert ^{1,2}

¹University of Basel, Transfaculty Research Platform, Molecular and Cognitive Neuroscience, Neurobiology Lab for Brain Aging and Mental Health, Basel, Switzerland

²Psychiatric University Clinics, Basel, Switzerland

³University of Applied Sciences and Arts Northwestern Switzerland (FHNW), School of Life Sciences, Institute of Pharmaceutical Technology, Gründenstrasse 40, 4132 Muttenz, Switzerland

⁴Division of Pharmaceutical Biology, Department of Pharmaceutical Sciences, University of Basel, Basel, Switzerland

⁵Plant Bioactives Group, Post-Harvest and Agro-Processing Technologies, Agricultural Research Council (ARC) Infruitec-Nietvoorbij, Private Bag X5026, Stellenbosch 7599, South Africa

⁶Department of Food Science, Stellenbosch University, Private Bag XI, Matieland, Stellenbosch, South Africa

Correspondence should be addressed to Anne Eckert; anne.eckert@unibas.ch

Received 23 April 2020; Accepted 9 June 2020; Published 7 August 2020

Guest Editor: Francisco Jaime B. Mendonça Junior

Copyright © 2020 Anastasia Agapouda et al. This is an open access article distributed under the Creative Commons Attribution License, which permits unrestricted use, distribution, and reproduction in any medium, provided the original work is properly cited.

Mitochondrial dysfunction plays a major role not only in the pathogenesis of many oxidative stress or age-related diseases such as neurodegenerative as well as mental disorders but also in normal aging. There is evidence that oxidative stress and mitochondrial dysfunction are the most upstream and common events in the pathomechanisms of neurodegeneration. *Cyclopia* species are endemic South African plants and some have a long tradition of use as herbal tea, known as honeybush tea. Extracts of the tea are gaining more scientific attention due to their phenolic composition. In the present study, we tested not only the *in vitro* mitochondria-enhancing properties of honeybush extracts under physiological conditions but also their ameliorative properties under oxidative stress situations. Hot water and ethanolic extracts of *C. subternata*, *C. genistoides*, and *C. longifolia* were investigated. Pretreatment of human neuroblastoma SH-SY5Y cells with honeybush extracts, at a concentration range of 0.1–1 ng/ml, had a beneficial effect on bioenergetics as it increased ATP production, respiration, and mitochondrial membrane potential (MMP) after 24 hours under physiological conditions. The aqueous extracts of *C. subternata* and *C. genistoides*, in particular, showed a protective effect by rescuing the bioenergetic and mitochondrial deficits under oxidative stress conditions (400 μ M H₂O₂ for 3 hours). These findings indicate that honeybush extracts could constitute candidates for the prevention of oxidative stress with an impact on aging processes and age-related neurodegenerative disorders potentially leading to the development of a condition-specific nutraceutical.

1. Introduction

Reactive oxygen species (ROS) are oxygen-containing chemical entities of great reactivity that have been in the spotlight as a common feature in many diseases. They are involved in neurodegenerative and cardiovascular diseases, cancer, atherosclerosis, diabetes, and also in normal aging [1–4]. ROS include mainly superoxide anion radical (O₂^{•−}), hydrogen

peroxide (H₂O₂), and the hydroxyl radical (OH[•]) of which superoxide anion and hydrogen peroxide are found in the most abundance in cells [5]. Mitochondria are organelles which are responsible for the majority of adenosine triphosphate (ATP) production through oxidative phosphorylation (OXPHOS) taking place at their electron transport chain (ETC). Neurons are high-energy demanding cells and thus are highly dependent on mitochondria in order to survive

and function. However, mitochondria are also the epicenter of ROS production and metabolism [2, 6]. Despite an estimation of 31 existing ROS (mostly superoxide anion and H_2O_2) production sites in the entire cell versus 12 ROS emission sites in the mitochondria, the majority of cellular endogenous ROS are produced by mitochondria as by-products of OXPHOS [5, 7].

Exposure to oxygen is not only unavoidable but also vital and necessary for organism and cell survival and for energy production [5]. Mitochondrial ROS are mostly generated by complexes I and III of the ETC when leaking electrons that are provided by NADH or $FADH_2$ react with oxygen. Interestingly, the two high-production sites releasing $O_2^{\cdot -}$ and H_2O_2 directly into the intermembrane space are the enzyme sn-glycerol-3-phosphate dehydrogenase and complex III of the ETC [5]. As a result, the presence of ROS in the intermembrane space may cause depolarization of the membranes and hinder the free motion of electrons through complexes I-IV, thereby directly affecting the proton gradient and the mitochondrial membrane potential (MMP) and ultimately preventing the production of ATP [8].

As mitochondria are the main superoxide anion and hydrogen peroxide producers, they largely affect redox homeostasis [9]. For their protection, cells are equipped with antioxidant defense systems (superoxide dismutases, glutathione peroxidases, thioredoxin, catalase, and glutathione GSH) in order to fend off ROS [10–12]. The redox state of the cells is dynamic and depends on the production of ROS and the functionality of the antioxidant defense systems. At normal nonelevated concentrations, ROS act as signaling molecules and they participate in the regulation of senescence, cell death, and proliferation. When there is an overproduction of ROS, the antioxidant defense systems are overwhelmed and they are not able to diffuse them. Therefore, oxidative stress is the overaccumulation of ROS (mainly superoxide anion and H_2O_2) due to their overproduction or overburdened antioxidant defense systems [1, 5]. ROS react with and damage many cellular and mitochondrial biomolecules. Of note, they cause lipid peroxidation and membrane damage, protein misfolding, as well as DNA damage [3]. Mitochondrial DNA (mtDNA) is located in the matrix of mitochondria and encodes for 13 proteins which are structural components of the ETC. MtDNA is in very close proximity to the ROS production sites and is therefore directly affected and mutated, leading to faulty ETC components which leads back to impaired OXPHOS and more production of ROS [10, 13]. When the ROS levels surpass a certain threshold, then they become mitochondria-damaging and disease-causing agents [14]. Aging is characterized by an increase in ROS and a decrease in antioxidant defenses leading to mitochondrial damage and ultimately to cellular dysfunction, senescence, and apoptosis. Normal aging and neurodegenerative disorders have these characteristics in common although to a different extent. In neurodegeneration, the damaging effects are even more profound [3, 5, 9, 15].

Hydrogen peroxide, which is endogenously produced in mitochondria, is considered the ROS with the most impact on the fate of the cell. It can easily diffuse through mem-

branes and has the greatest life span [9]. Therefore, hydrogen peroxide was used as an oxidative stressor in this study.

Cyclopia species, belonging to the Fabaceae family, are endemic to South Africa. Old records describe the traditional use of several species including *C. subternata*, *C. genistoides*, and *C. longifolia* as herbal teas [16]. At present, these *Cyclopia* species form the bulk of cultivated plant material supplementing plant material harvested in the wild and crucial to meet the growing demand of international markets. The main product is “fermented” (oxidised) honeybush tea, while the green (unoxidised) herbal tea is preferred for nutraceutical extract production due to a higher phenolic content and antioxidant capacity. The phenolic profile of honeybush varies qualitatively and quantitatively depending on the *Cyclopia* species. Major phenolic constituents belong to xanthone, benzophenone, flavanone, flavone, and dihydrochalcone subclasses [17]. Increased consumption and popularity of honeybush came along with increasing research interest in order to reveal new bioactivities and to examine its potential use as a nutraceutical and functional food [16, 18]. Quite predictably due to their phenolic composition, honeybush extracts have been shown to possess antioxidant activities which are of great importance and interest in the research of oxidative stress-related diseases [19–22]. Considering on the one hand the evidence of its antioxidant capacity and on the other hand the need for mitochondria-targeting antioxidant substances for use in the prevention of oxidative damage or the amelioration of increased oxidative stress levels, we hypothesized that honeybush could possess some beneficial mitochondria-enhancing properties. For this reason, this study is aimed at examining the protective effects of honeybush extracts against H_2O_2 -induced oxidative stress in SH-SY5Y neuronal cells with a focus on mitochondria. To our knowledge, this is the first study that evaluates the effects of honeybush extracts on mitochondrial function in a neuronal cell model.

2. Materials and Methods

2.1. Chemicals and Reagents. Dulbecco’s modified Eagle medium (DMEM), phosphate-buffered saline (PBS), fetal calf serum (FCS), Hanks’ balanced salt solution (HBSS), penicillin/streptomycin, pyruvate, dihydrorhodamine 123 (DHR), 2',7'-dichlorodihydrofluorescein diacetate (DCF), dihydroethidium (DHE), tetramethylrhodamine methyl ester (TMRM), gelatin, and H_2O_2 were from Sigma-Aldrich (St. Louis, MO, USA). MitoSOX and GlutaMAX were from Gibco Invitrogen (Waltham, MA, USA), ATPlite1step kit from PerkinElmer (Waltham, Massachusetts, USA), and XF Cell Mitostress kit from Seahorse Bioscience (North Billerica, MA, USA). Folin-Ciocalteu reagent was purchased from Merck (Darmstadt, Germany). Authentic reference standards (purity > 95%) for identification and quantification of phenolic compounds were obtained from Sigma-Aldrich (hesperidin), Extrasynthese (Genay, France; mangiferin, eriocitrin), Chemos (Regenstauf, Germany; isomangiferin), and Phytolab (Vestenbergsgreuth, Germany; vicenin-2, 3- β -D-glucopyranosylriflophenone). Compounds from the Plant Bioactives Group library included 3- β -D-

glucopyranosyl-4-O- β -D-glucopyranosylriflophenone, 3- β -D-glucopyranosylmaclurin and (2S)-5-O-[α -L-rhamnopyranosyl-(1 \rightarrow 2)- β -D-glucopyranosyl] naringenin isolated from *C. genistoides*, and scolymoside and 3',5'-di- β -D-glucopyranosylphloretin isolated from *C. subternata*. HPLC gradient grade "far UV" acetonitrile was supplied by Merck.

2.2. Plant Material and Extract Preparation. Harvesting of aerial parts (shoots and leaves) occurred in March 2017. *Cyclopia subternata* was harvested on Elsenburg research farm (-34.30267, 19.13809), while *C. longifolia* and *C. genistoides* were harvested on Nietvoorbij research farm (-33.90619, 18.87031), both located in the Western Cape Province of South Africa. The fresh plant material was mechanically cut into small pieces (<3 mm) and dried at 40°C in a cross-flow, temperature-controlled drying tunnel to a moisture content < 7% as for green honeybush tea production. The dried plant material was coarsely milled using a rotary mill equipped with a 1 mm sieve (Retsch, GmbH, Haan, Germany).

Hot water extracts were prepared from each batch of milled plant material by extracting 70 g plant material with 700 ml deionised water at 93°C for 30 min followed by filtration and freeze drying of the filtrate as previously described [23]. Similarly, 40% EtOH-water (v/v) extracts were prepared by extracting the milled plant material at 70°C for 30 min. Ethanol was removed under vacuum using rotary evaporation, and the remaining aqueous layer was freeze-dried. Prior to extraction using 70% EtOH-water (v/v), the plant material was subjected to exhaustive Soxhlet extraction with dichloromethane to remove chlorophyll. The defatted plant material was air-dried and further treated as for the 40% EtOH-water (v/v) extracts. The freeze-dried extracts (>15 g/extract) were coded, aliquoted into glass vials (for testing and retention samples), sealed, and stored under desiccation in the dark.

2.3. Quantification and Identification of Phenolic Compounds. The major phenolic compounds in the extracts were quantified using the respective species-specific validated HPLC-DAD method for *C. subternata* [23], *C. longifolia* [24], and *C. genistoides* [25]. Samples were dissolved in water or 10% DMSO and filtered using 0.45 μ m pore size PVDF syringe filters (Merck) for *C. subternata*, while 0.22 μ m pore size filters were used for *C. genistoides* and *C. longifolia*. Ascorbic acid was added to prevent compound degradation during analysis (final concentration ca 9 mg/ml). Peak areas at the appropriate wavelength together with external calibration curves were used for quantification (benzophenones, flavanones, and dihydrochalcones at 288 nm; xanthenes and flavones at 320 nm). In cases where authentic reference standards were not available, quantification was in equivalents of a similar compound.

Total polyphenol content of extracts was determined using the Folin-Ciocalteu assay as adapted for microplate by Arthur et al. [26]. Values were expressed as g gallic acid equivalents per 100 g extract.

Extracts selected for further study after initial testing were also analyzed by LC-MS using a Waters Acquity ultra-

performance liquid chromatography (UPLC) instrument coupled to a Synapt G2 quadrupole time-of-flight (Q-TOF) MS detector equipped with an electrospray ionization (ESI) source (Waters, Milford, USA). Mass calibration was performed using a sodium formate solution, and leucine enkephalin was used as the lockspray solution. Analysis was first performed in the MS^E mode with negative ionization: scanning range, 150–1500 am; capillary voltage, -2.5 kV; sampling cone voltage, 15.0 V; source temperature, 120°C; desolvation temperature, 275°C; cone gas flow (N₂), 650 l/h; desolvation gas flow (N₂), 50 l/h. For the MS/MS experiments, a collision energy of 30.0 V was used. Peaks were identified by comparing UV-Vis spectra, relative retention time, MS characteristics (molecular formula predicted by accurate mass), and MS/MS fragmentation spectra with those of authentic standards or literature data.

2.4. Cell Culture. The human neuroblastoma SH-SY5Y cell line was selected as our cellular model in this study as it is a well-established and widely used neuronal model in biochemical studies in general. The cell line behaves as human neuronal network in a dish and has been largely used in research as it expresses neuronal receptors. The SH-SY5Y cells were kept and grown at 37°C in a humidified incubator chamber under an atmosphere of 7.5% CO₂ in DMEM supplemented with 10% (v/v) heat-inactivated FCS, 2 mM GlutaMAX, and 1% (v/v) penicillin/streptomycin. Cells were passaged 1–2 times per week, and the cells used for the experiments did not exceed passage 20. The cells were plated when they reached 80–90% confluence.

2.5. Treatment of Cells. Evaluation of ATP production was conducted on SH-SY5Y neuroblastoma cells to determine the potential toxic concentration range of the nine honeybush extracts. Two screenings were performed. Initially, aqueous, 70% ethanolic and 40% ethanolic extracts of the species *C. subternata*, *C. genistoides*, and *C. longifolia* were screened at a very broad concentration range of 0.1 ng/ml to 1 mg/ml (data not shown). Of note, all dry extracts were dissolved in DMSO for our experiments (final concentration of DMSO < 0.005%, no effect of the vehicle solution alone compared to the untreated condition). The first screening revealed that the extracts were not toxic for the neuroblastoma cells up to a concentration of 10 μ g/ml. According to the results of the first screening, the concentration range was reduced down to that of 0.1 ng/ml to 1 μ g/ml and the number of extracts was reduced from nine down to four (according to the capacity of the extracts in increasing the ATP levels of the cells) and a second screening cycle was performed. The screening was conducted by using an ATP detection assay (ATPlite 1step kit was from PerkinElmer). For the experiments, cells were plated and treated 1 day after plating for 24 h either with DMEM (untreated cells—control condition) or with a final concentration of 0.1 ng/ml to 1 μ g/ml of the extracts.

Because vehicle treatment was without any effect in our assays, we evaluated the effects of the honeybush extract concentrations in comparison to the untreated control condition in the following experiments. Cellular sensitivity of SH-SY5Y

cells was confirmed by using the positive control estradiol as previously described in Grimm et al. 2014 [27].

Hydrogen peroxide (H_2O_2) which belongs to the reactive oxygen species produced by mitochondria was used as a stressor at the concentration $400 \mu M$ which was able to decrease mitochondrial and cellular functions. The H_2O_2 concentration was selected based on screening experiments conducted on SH-SY5Y cells. For the stress experiments, cells were firstly pretreated for 24 h with the honeybush extracts and then treated for 3 h with $400 \mu M H_2O_2$. Each assay was conducted and repeated at least in triplicate.

2.6. ATP Levels. Total ATP content was determined using a bioluminescence assay (ATPlite 1step) according to the instructions of the manufacturer and as previously described [28–30]. Cells were plated in 6 replicates into white 96-well cell culture plates at a density of 1×10^4 cells/well. The ATP was extracted from the cells upon lysis and it was transformed into light. The method measures the formation of light from ATP and luciferin catalyzed by the enzyme luciferase. The emitted light was linearly correlated to the ATP concentration and was measured using the multimode plate reader Cytation 3 (BioTek instruments, Winooski, Vermont, United States).

2.7. Determination of Mitochondrial Membrane Potential (MMP). The MMP was measured using the fluorescent dye TMRM, since its transmembrane distribution depends on the MMP. As previously described [31, 32], the cells were plated in 6 replicates into black 96-well cell culture plates at a density of 1×10^4 cells/well and were incubated with the dye at a concentration of $0.4 \mu M$ for 20 min. After washing three times with HBSS, fluorescence was measured at 548 nm (excitation)/574 nm (emission), using a Cytation 3 multimode plate reader (BioTek instruments).

2.8. Mitochondrial Respiration. Mitochondrial respiration and cellular glycolysis were measured using the Seahorse Bioscience XF24 analyser as described before [28, 29, 33]. Briefly, XF24 cell culture microplates were coated with 0.1% gelatin and cells were plated at a density of 2.5×10^4 cells/well in treatment medium ($100 \mu l$) containing 1 g/l glucose, 4 mM pyruvate, and 10% FCS. After treatment with honeybush extracts for 24 h, the cells were washed once with PBS and then $500 \mu l$ of assay medium (DMEM containing 1 g/l of glucose and 4 mM of pyruvate) was added to each well. The oxygen consumption rate (OCR) and extracellular acidification rate (ECAR) were measured concurrently under basal respiration. The data were extracted from the Seahorse XF24 software, and bioenergetic parameters (basal respiration, ATP production, maximal respiration, spare respiratory capacity, and glycolytic reserve) were calculated according to the guidelines of the manufacturer.

2.9. Determination of ROS Levels. Mitochondrial and cytosolic ROS levels and the specific levels of mitochondrial $O_2^{\cdot -}$ superoxide anion radicals and the total levels of $O_2^{\cdot -}$ superoxide anion radicals levels were assessed using the fluorescent dyes dihydrorhodamine 123 (DHR), 2',7'-dichlorodihydrofluorescein diacetate (DCF), the Red Mitochondrial

Superoxide Indicator (MitoSOX), and dihydroethidium (DHE), respectively, as described before [30, 34]. SH-SY5Y cells were plated in 6 replicates into black 96-well cell culture plates at a density of 1×10^4 cells/well. After treatment with honeybush extracts alone or after pretreatment with honeybush extracts, followed by treatment with H_2O_2 , cells were treated with $10 \mu M$ of one of the dyes: DCF, DHR, or DHE for 20 min or $5 \mu M$ of MitoSOX for 90 min at room temperature in the dark on an orbital shaker. After washing the cells three times with HBSS, the formation of green fluorescent products triggered by DCF and DHR, respectively, was detected at 485 nm (excitation)/535 nm (emission). MitoSOX triggers the formation of red fluorescent products which were detected at 531 nm (excitation)/595 nm (emission). DHE, which is permeable to cells, is used as a total $O_2^{\cdot -}$ superoxide anion detector as it is oxidised to the impermeable red fluorescent product ethidium, detected at 531 nm (excitation)/595 nm (emission). The intensity of fluorescence was proportional to mitochondrial ROS, cytosolic ROS, and $O_2^{\cdot -}$ levels (total and mitochondrial). The fluorescence was measured using the Cytation 3 multimode plate reader.

2.10. Statistical Analysis. Data are given as the mean \pm SEM. Statistical analyses were performed using GraphPad Prism software (version 5.02 for Windows, San Diego, California, USA). For statistical comparisons of more than two groups, one-way ANOVA was used, followed by a Dunnett's multiple comparison tests versus the control for physiological conditions and versus H_2O_2 for stress conditions. $P < 0.05$ was considered statistically significant.

3. Results

Two cycles of screenings were conducted with regard to the ability of each extract in increasing the ATP production of SH-SY5Y cells. The nine *Cyclopia* extracts produced by extraction of *C. subternata*, *C. genistoides*, and *C. longifolia* with hot water and two ethanol-water mixtures were screened (data not shown), and the four most promising extracts in terms of increased ATP production were selected for all subsequent experiments: the water extracts of all three *Cyclopia* species and the 70% ethanolic extract of *C. genistoides*. Table 1 gives the content of the major phenolic compounds present in the selected extracts. Qualitative and quantitative differences in the phenolic profile are evident, notably the absence or presence of only trace levels of dihydrochalcones in *C. longifolia* and *C. genistoides* but substantial xanthone levels compared to *C. subternata*. Mangiferin followed by isomangiferin was the predominant compound in the *C. longifolia* and *C. genistoides* extracts. Scolymoside, a flavone rutinoside, followed by 3- β -D-glucopyranosyl-4-O- β -D-glucopyranosyliriflophenone, a benzophenone, was the main phenolic compound in *C. subternata* water extract. Scolymoside was not detected in the two *C. genistoides* extracts, but these extracts had substantially higher levels of the flavone di-glucoside, vicenin-2, compared to the *C. subternata* and *C. longifolia* extracts. Overall, the total phenolic content, based on the sum of individual phenolic compound content, was highest in the 70% EtOH-water extract of *C.*

TABLE 1: Phenolic composition (g/100 g extract) of aqueous extracts of *Cyclopia subternata*, *Cyclopia longifolia*, and *Cyclopia genistoides* and a 70% ethanolic extract of *C. genistoides*.

Compounds	<i>C. subternata</i>	<i>C. longifolia</i>	<i>C. genistoides</i>	
	Water	Water	Water	70% EtOH
Benzophenones				
Maclurin-di-O,C-hexoside (MDH) ^a	nd	nd	0.079	0.061
3-β-D-Glucopyranosyl-4-O-β-D-glucopyranosylriflophenone (IDG)	1.67	0.700	1.78	1.41
3-β-D-Glucopyranosylmaclurin (MMG)	nd	nd	0.400	0.373
3-β-D-Glucopyranosylriflophenone (IMG)	0.536	0.076	1.52	1.12
Total benzophenones	2.21	0.776	3.77	2.97
Xanthonnes				
Tetrahydroxyxanthone-di-O,C-hexoside A (THXA) ^b	nq	0.168	nq	nq
Tetrahydroxyxanthone-di-O,C-hexoside B (THXB) ^b	nq	0.133	nq	nq
Mangiferin	1.16	6.38	6.86	9.66
Isomangiferin	0.458	1.84	1.97	2.36
Total xanthonnes	1.62	8.53	8.83	12.0
Flavones				
Vicenin-2	0.182	0.192	0.498	0.524
Scolymoside	1.84	0.497	nq	nq
Total flavones	2.02	0.690	0.498	0.524
Dihydrochalcones				
3-Hydroxyphloretin-di-C-hexoside (HPDH) ^c	0.458	nq	nq	nq
3',5'-Di-β-D-glucopyranosylphloretin (PDG)	1.22	nq	nq	nq
Total dihydrochalcones	1.67	0.000	0.000	0.000
Flavanones				
Eriodictyol-O-hexoside-O-deoxyhexoside (EHD) ^d	nd	0.186	0.297	0.195
(2R)-5-O-[α-L-Rhamnopyranosyl-(1 → 2)-β-D-glucopyranosyl]naringenin (2RNAR) ^e	nd	0.028	0.146	0.051
(2S)-5-O-[α-L-Rhamnopyranosyl-(1 → 2)-β-D-glucopyranosyl]naringenin (2SNAR)	nd	0.087	0.397	0.444
Eriocitrin	0.536	0.310	nq	nq
Hesperidin	1.43	0.839	0.988	1.73
Total flavanones	1.96	1.45	1.83	2.42
Total quantified phenolics	9.48	11.5	14.9	17.9
Total polyphenols (Folin-Ciocalteu) ^f	25.5	23.7	25.3	27.8

^aExpressed as MMG equivalents. ^bExpressed as mangiferin equivalents. ^cExpressed as PDG equivalents. ^dExpressed as eriocitrin equivalents. ^eExpressed as 2SNAR equivalents. ^fExpressed as g gallic acid equivalents/100 g extract. nd: not detected using LC-MS; nq: present in extract, but not quantified due to coelution of very low content.

genistoides and lowest in the water extract of *C. subternata*. The total polyphenol content determined using the Folin-Ciocalteu assay was highest in the 70% EtOH-water extract of *C. genistoides* and lowest in the water extract of *C. longifolia* with similar values for the water extracts of *C. subternata* and *C. genistoides* (Table 1).

3.1. Honeybush Extracts Increase ATP Production under Physiological Conditions and under H₂O₂-Induced Stress. ATP is the end product not only of mainly oxidative phosphorylation but also of glycolysis and is thus an indicator of mitochondrial and cellular viability and proper functioning. Therefore, we assessed the effect of the honeybush extracts on the ATP production of neuroblastoma cells. The concentration range of 0.1-1000 ng/ml for each extract was first tested under physiological conditions. The results indicated

that the lower concentrations (0.1-1 ng/ml), but not the higher ones (50 ng/ml-100 mg/ml, data not shown), of the water extracts of the three *Cyclopia species* and of the 70% ethanolic extract of *C. genistoides* significantly increased ATP production up to 4% after treatment for 24 h under physiological conditions (Figures 1(a)–1(d)).

Regarding ATP levels under oxidative stress, H₂O₂ at 400 μM caused a 39.1% decrease in ATP production. According to the experimental design under physiological conditions, we tested the same broad concentration range for each extract under oxidative stress (data not shown). Again, the concentrations 0.1 and 1 ng/ml significantly protected against oxidative stress. Therefore, these concentrations were used in the following oxidative stress experiments. The harmful effect of H₂O₂ was partially but significantly ameliorated by all the extracts up to 13.5% (Figure 2).

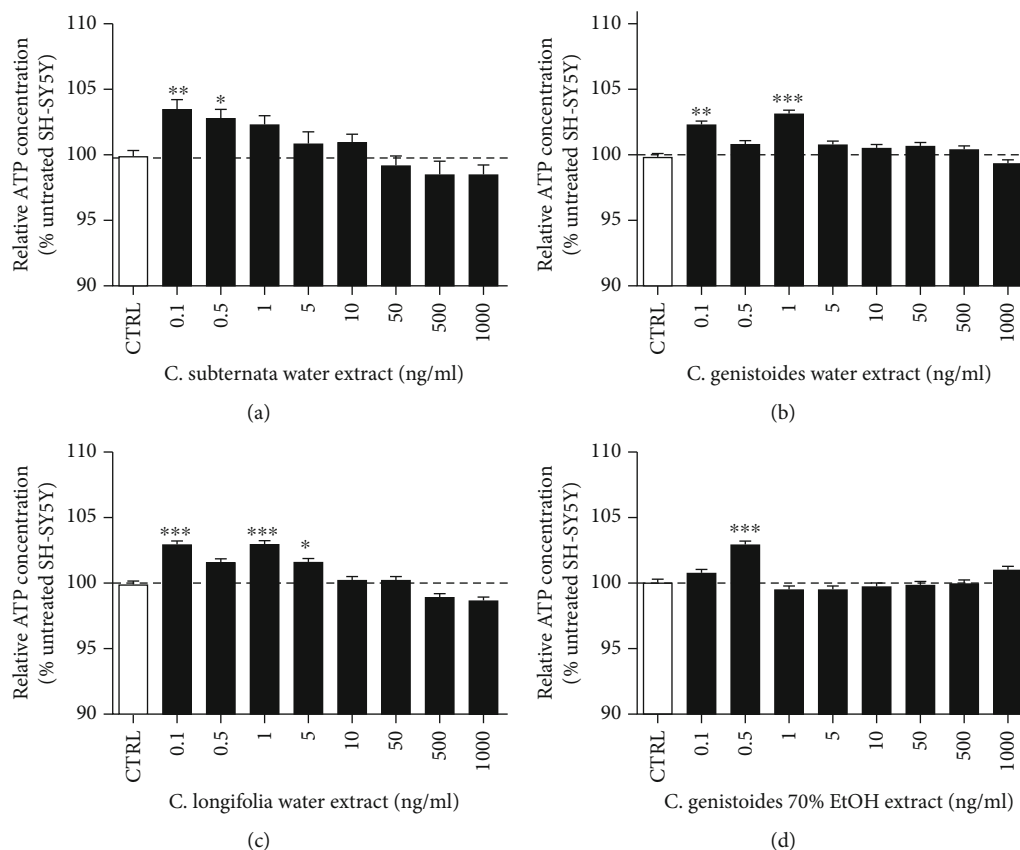


FIGURE 1: (a–d) The water extracts of *Cyclopia subternata*, *C. genistoides*, and *C. longifolia*, and the 70% ethanolic extract of *C. genistoides* significantly increased the ATP levels up to 4%. The cells were treated for 24 h with the extracts. Values represent as the mean \pm SEM of three independent experiments and were normalized to the untreated (CTRL) group (=100%). One-way ANOVA and post hoc Dunnett's multiple comparison test versus CTRL cells. * $P < 0.05$; ** $P < 0.01$; *** $P < 0.001$.

3.2. Honeybush Extracts Increase Mitochondrial Respiration under Physiological Conditions and under H_2O_2 -Induced Stress. Mitochondria consume oxygen to perform respiration and oxidative phosphorylation. Thus, for an assessment of mitochondrial respiration, the oxygen consumption rate of the cells was measured live under basal conditions. The results indicated that the water extracts of *C. subternata* and *C. genistoides* and the 70% ethanolic extract of *C. genistoides* increased the respiration under physiological conditions at baseline. However, upon closer analysis of data, it was found that only the water extracts of *C. subternata* and *C. genistoides* at 1 ng/ml significantly increased the respiration by 33.2% and 40.7%, respectively (Figure 3(a)). The extracts that significantly increased the other pathway leading to the production of ATP, glycolysis, were *C. genistoides* (1 ng/ml) and *C. longifolia* (at 0.1 and 1 ng/ml). This increase was up to 51.7% (Figure 3(b)). Upon correlation of the respiration with the glycolysis, an “energy map” was obtained (Figure 3(c)) which allows a visual representation of where each individual extract acted. Thus, *C. subternata* and *C. genistoides* increased the oxygen consumption rate of the cells (respiration), while *C. longifolia* increased the glycolysis.

H_2O_2 caused a significant decrease of 41.7% in respiration (Figure 4(a), red bar). All extracts increased the oxygen consumption rate, bringing it closer to the levels of the

untreated cells. However, only the water extract of *C. subternata* was able to significantly enhance respiration at baseline (increase of 25.9%) (Figure 4(a)). Regarding glycolysis, H_2O_2 caused a significant decrease of 38.9% which was completely rescued by the water extract of *C. genistoides* (1 ng/ml) (Figure 4(b)). The “energy map” confirmed that the most effective extract in rescuing the respiration under H_2O_2 stress was the aqueous extract of *C. subternata* (Figure 4(c)).

3.3. Honeybush Extracts Increase Mitochondrial Membrane Potential (MMP) under Physiological Conditions and under H_2O_2 -Induced Stress. The aqueous extracts of *C. genistoides* (1 ng/ml) and *C. longifolia* (0.1 and 1 ng/ml) significantly increased MMP up to 24% under physiological conditions after a treatment of 24 h (Figure 5(a)).

H_2O_2 at 400 μM caused a significant reduction of 55.1% in MMP which was increased by up to 67.9% by the extracts. In this case, all extracts completely rescued the MMP (Figure 5(b)).

Overall, all extracts acted on the mitochondrial membrane potential by increasing it both under physiological condition and under H_2O_2 -induced oxidative stress.

3.4. Honeybush Extracts Decrease Different Types of ROS under H_2O_2 -Induced Stress. H_2O_2 at 400 μM caused an

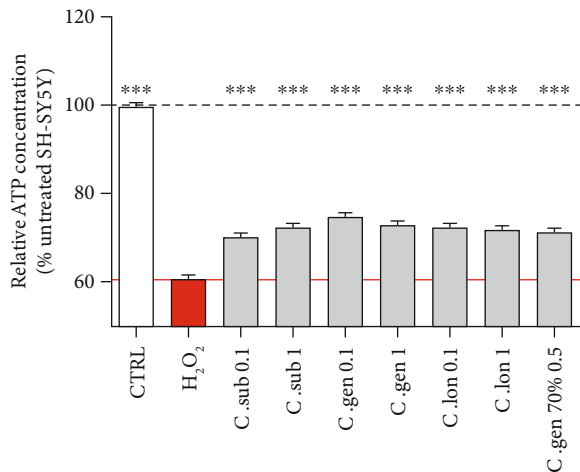


FIGURE 2: H₂O₂ treatment at 400 μ M for 3 h caused a 39.1% decrease in ATP production which was significantly increased up to 13.5% by a 24 h pretreatment with each of the extracts. The red bar represents the H₂O₂-treated cells, and the grey bars represent cells that were pretreated for 24 h with the indicated honeybush extract and then treated for 3 h with H₂O₂. Values represent as the mean \pm SEM of three independent experiments and were normalized on the untreated group (=100%). One-way ANOVA and post hoc Dunnett's multiple comparison test versus H₂O₂-treated cells. * $P < 0.05$; ** $P < 0.01$; *** $P < 0.001$.

increase of 29.5% in mitochondrial ROS which was detected using the dye DHR (dihydrorhodamine 123). This increase was significantly ameliorated up to 23.1% by *C. subternata* water extract. *C. genistoides* also brought the ROS levels down but not significantly (Figure 6(a)).

Cytosolic ROS were detected using the dye DCF (2',7'-dichlorodihydrofluorescein diacetate). H₂O₂ at 400 μ M caused an elevation of 31.2%. All extracts lowered cytosolic ROS levels, but the water extract of *C. subternata* at 1 ng/ml (28.9% reduction of cytosolic ROS) and the 70% ethanolic extract of *C. genistoides* at 0.5 ng/ml (26.2% reduction of cytosolic ROS) were the most effective (Figure 6(b)).

H₂O₂ at 400 μ M increased the mitochondrial superoxide anion levels by 43%. All extracts, except the ethanolic extract of *C. genistoides*, significantly lowered the mitochondrial superoxide anion levels. However, the water extracts of *C. subternata*, *C. genistoides*, and *C. longifolia* at a concentration of 1 ng/ml completely neutralized the mitochondrial superoxide anion levels (reduction of 42%, 42.6%, and 42.6%, respectively) (Figure 6(c)).

The total superoxide anion levels were elevated by 67.9% in the H₂O₂-treated cells. All four extracts ameliorated this increase, but only the water extracts of *C. subternata* and *C. longifolia* at 1 ng/ml and the ethanolic extract of *C. genistoides* at 0.5 ng/ml significantly reduced the superoxide anion levels by 48.8%, 50.9%, and 50.3%, respectively (Figure 6(d)).

4. Discussion

In this study, we hypothesized that honeybush extracts might exert a beneficial effect on mitochondria of neuronal cells under physiological conditions as well as under oxidative

stress due to their phenolic compound content. Neurons have high energy demands and are thus particularly dependent on functional mitochondria. For this reason, we assessed the effects of four different honeybush extracts in a well-characterized neuronal model, the neuroblastoma SH-SY5Y cells. The four extracts were the hot water extracts of *C. subternata*, *C. genistoides*, and *C. longifolia* as well as the 70% ethanolic extract of *C. genistoides*. These extracts were selected after screening the water, 40% ethanolic and 70% ethanolic extracts of these *Cyclopia* species. Hydrogen peroxide (H₂O₂) was used as an oxidative stressor as it is one of the most abundant and reactive endogenous ROS.

The beneficial effect of honeybush extracts on mitochondrial functions under physiological conditions and a protective effect under oxidative stress could be demonstrated. The four extracts showed different beneficial properties in different mitochondrial and cellular sites. ATP is the energy that is required for the survival and functionality of cells and especially of neurons which have high energy demands. At the lowest concentrations (0.1-1 ng/ml), all extracts improved the production of ATP under physiological conditions. This increase amounted up to 4% (Figure 1). Also, all extracts were able to significantly increase the ATP levels under H₂O₂-induced oxidative stress. This improvement was not a complete rescue but a partial increase of up to 13.5% (Figure 2).

Mitochondrial respiration is an intrinsic function of mitochondria and is essential for the survival of the cells as it results in the production of the majority of ATP. Respiration is taking place at the ETC which is located on the inner mitochondrial membrane (IMM). Glycolysis is the secondary pathway leading to production of ATP. The aqueous extracts of *C. subternata* and *C. genistoides* (both at 1 ng/ml) significantly increased the basal respiration of the mitochondria by up to 40.7%, while those of *C. genistoides* and *C. longifolia* significantly increased glycolysis up to 51.7% under physiological conditions (Figure 3). However, only *C. subternata* aqueous extract (1 ng/ml) could significantly rescue the impaired respiration and only *C. genistoides* aqueous extract (1 ng/ml) could rescue the impaired glycolysis caused by H₂O₂ (Figure 4). The aqueous extracts of *C. subternata* and *C. genistoides* specifically acted on respiration. In addition, the *C. subternata* aqueous extract enhanced respiration under oxidative stress. This could be explained by the fact that this extract was the only one that neutralized all four types of tested ROS and particularly the mitochondrial ROS and the mitochondrial superoxide anion which directly affect OXPHOS and respiration (Figure 6). This could be the reason why it was also the only extract to act on respiration under stress.

The aqueous extracts of *C. genistoides* and *C. longifolia* increased the MMP under physiological conditions, while all four extracts completely rescued the MMP under oxidative stress (Figure 5), in addition to partly ameliorating ATP production (Figure 2). During OXPHOS at the ETC of mitochondria, electrons provided by NADH and FADH₂ are transferred through complexes I-IV. This motion of electrons drives the complexes I, III, and IV to pump protons into the intermembrane space where they are finally used

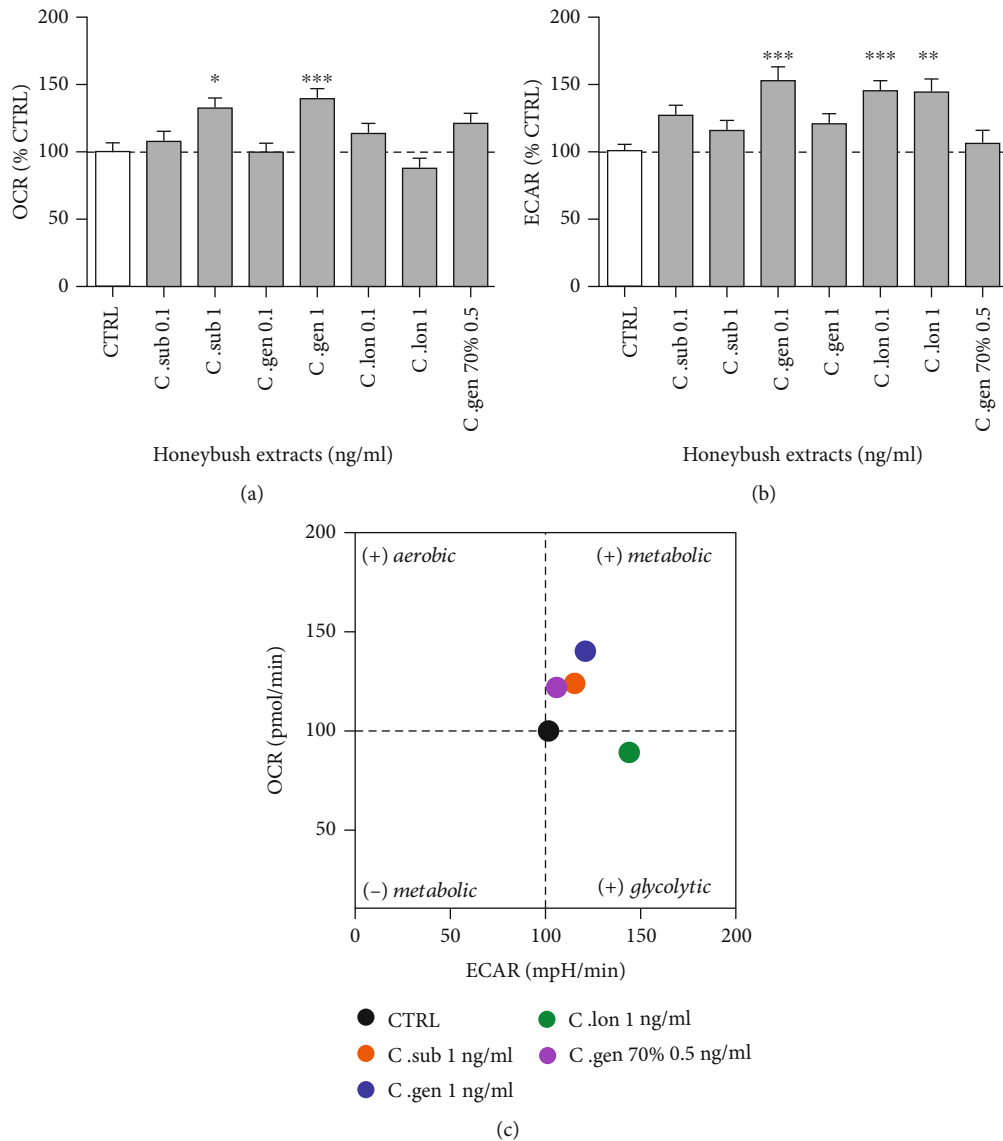


FIGURE 3: Respiration under physiological condition. (a) 24 h pretreatment with the water extracts of *C. subternata* and *C. genistoides* (both at 1 ng/ml) significantly increased the oxygen consumption rate of the cells and therefore the respiration. (b) The water extracts of *C. genistoides* (0.1 ng/ml) and *C. longifolia* (0.1 and 1 ng/ml) significantly increased the glycolysis in the SH-SY5Y cells. (c) Energy map created after correlation of the OCR (respiration— y -axis) with the ECAR (glycolysis— x -axis). The aqueous extracts of *C. subternata* and *C. genistoides* acted on respiration (displayed as + metabolic in the figure), while the water extract of *C. longifolia* increased the glycolytic activity. Values represent as the mean \pm SEM of three independent experiments and were normalized on the comparison test versus H_2O_2 -treated cells. * $P < 0.05$; ** $P < 0.01$; *** $P < 0.001$.

by ATP synthase (complex V) to produce ATP via the phosphorylation of ADP. MMP is an indicator for polarized mitochondrial membranes and therefore an indicator that the pumping of protons in the intermembrane space is not hindered so that they can drive the ATP production by complex V [35, 36]. Amelioration of ATP production under oxidative stress by the extracts could be as a result of their capacity to completely rescue the MMP under oxidative stress and supports this interdependence of MMP and ATP production.

In terms of ROS (Figure 6), pretreatment with the aqueous extract of *C. subternata* (mostly at 1 ng/ml) decreased the four types of tested ROS and it was the only extract of those tested to significantly reduce the mitochondrial ROS

(detected with the dye DHR). The result that *C. subternata* extract acted both on mitochondrial superoxide anion levels (detected with the dye MitoSOX) and on all other mitochondrial ROS, such as H_2O_2 (detected with the dye DHR), could mean that it either additionally scavenges them or it enhances the activity of the antioxidant defenses that neutralize them (e.g., glutathione, catalase) [21]. The aqueous extract of *C. longifolia* lowered cytosolic ROS, total superoxide anion levels, and mitochondrial superoxide anion levels. The two *C. genistoides* extracts differed, i.e., its aqueous extract neutralized cytosolic ROS and mitochondrial superoxide anion, while its 70% ethanolic extract decreased cytosolic ROS and total superoxide anion levels but had no

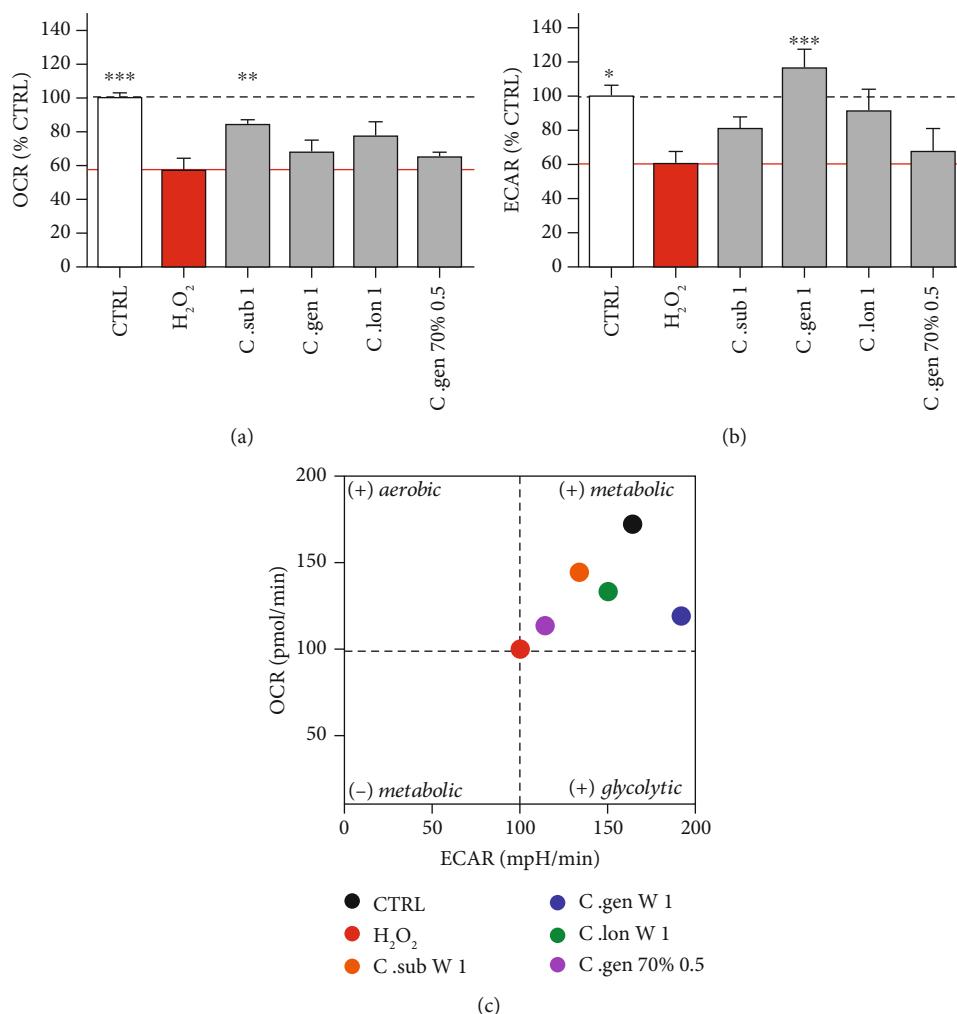


FIGURE 4: Respiration under oxidative stress condition. (a) 3 h treatment with H₂O₂ reduced the oxygen consumption rate by 41.7% (red bars). 24 h pretreatment with the water extract of *C. subternata* (at 1 ng/ml) significantly ameliorated the oxygen consumption rate of the cells and therefore the respiration (grey bars). (b) 3 h treatment with H₂O₂ reduced the glycolysis by 38.9% (red bars). The aqueous extract of *C. genistoides* (1 ng/ml) significantly increased the glycolysis in SH-SY5Y cells. The red bar represents the H₂O₂-treated cells, and the grey bars represent cells that were pretreated for 24 h with the indicated honeybush extract and then treated for 3 h with H₂O₂. (c) Energy map created after correlation of the OCR (respiration—y-axis) with the ECAR (glycolysis—x-axis). This map helps in visually recognizing whether an extract predominantly increased the respiration (displayed as + metabolic in the figure) or the glycolytic activity compared to the H₂O₂-treated cells. Values represent as the mean ± SEM of three independent experiments and were normalized on the untreated group (=100%). One-way ANOVA and post hoc Dunnett's multiple comparison test versus H₂O₂-treated cells. **P* < 0.05; ***P* < 0.01; ****P* < 0.001.

significant effect on the specific mitochondrial ROS. All extracts had thus a minimizing effect on ROS levels, though at different degrees and on different ROS types (Figure 6). This might be explained by different bioactive components in the specific extract depending on *Cyclopia* species and extraction solvent. While all the water extracts (*C. subternata*, *C. genistoides*, *C. longifolia*) act on mitochondrial superoxide anion levels, the ethanolic extract of *C. genistoides* only affects the cytosolic ROS and total superoxide anion levels. It is assumed that the latter extract acted specifically on cytosolic superoxide anions.

The most beneficial concentrations of the honeybush extracts in this study were found to be as low as 0.1 and 1 ng/ml. Plant extracts are complex mixtures of a multitude

of compounds of diverse chemistries and pharmacological activities at different concentrations. The different constituents in the plant extracts could have antagonistic, synergistic, or allosteric effects [37]. For example, an active substance at the higher concentration could have blunted the activity of another bioactive constituent. Possibly, there is one or several constituents that are effective at a low concentration and a gradual increase in concentrations may gradually reduce the efficacy and might explain the observed effect at very low concentrations.

Considering the phenolic profiles of the different extracts, it is clear that no pattern emerged that could explain differential activity. The total polyphenol content often highly correlates with the antioxidant activity *in vitro* but was similar in

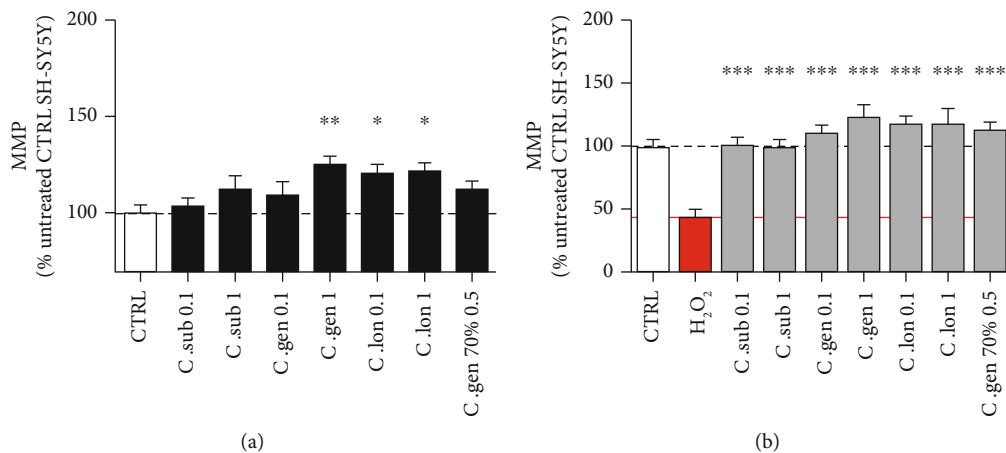


FIGURE 5: (a) Honeybush extracts significantly increased the mitochondrial membrane potential (MMP) up to 24% under physiological conditions (black bars). (b) 3 h treatments with H₂O₂ at 400 μM caused a reduction of 55.1% in MMP which was rescued by the different honeybush extracts. The red bar represents the H₂O₂-treated cells, and the grey bars represent cells that were pretreated for 24 h with the indicated honeybush extract and then treated for 3 h with H₂O₂. Values represent as the mean ± SEM of three independent experiments and were normalized on the untreated group (=100%). One-way ANOVA and post hoc Dunnett's multiple comparison test versus (a) untreated (CTRL) or (b) H₂O₂. **P* < 0.05; ***P* < 0.01; ****P* < 0.001.

the aqueous extracts of *C. subternata*, *C. genistoides*, and *C. longifolia* (~26, 25, and 24 g gallic acid equivalents per 100 g extract, respectively). In the ethanolic extract of *C. genistoides*, the phenolic content was slightly increased (~28 g gallic acid equivalents per 100 g extract). However, the phenolic content does not differ substantially between the different extracts to provide an explanation to our findings. In fact, mangiferin, shown to have beneficial effects in *in vitro* and *in vivo* models of neurodegeneration, as well as of oxidative stress [38–43], was lowest in the *C. subternata* water extract and highest in the 70% ethanolic extract of *C. genistoides*. According to these studies, we expected that the *C. genistoides* 70% ethanolic extract would exert the most potent neuroprotective properties, while the aqueous extract of *C. subternata* would exert the least. Interestingly, the results of our experiments proved our assumption wrong as the opposite effect was observed with the aqueous extract of *C. subternata* being the most beneficial extract. A closer observation at the composition of the extracts (Table 1) reveals that the aqueous extract of *C. subternata* contains higher concentrations of flavones and dihydrochalcones. Scolymoside, present in the highest concentration in the *C. subternata* water extract and absent in detectable quantities in the two *C. genistoides* extracts, is a glycoside of luteolin, a flavone aglycone demonstrated to inhibit the production of neuronal mitochondrial superoxide anion O₂^{•−} [44]. While glycosylation of position C-7 of the A-ring of the flavonoid structure as for scolymoside would decrease its radical scavenging potency compared to luteolin, it does not abolish the activity [45]. Dihydrochalcones related to those in *C. subternata* not only act as radical scavengers [46] but also demonstrated neuroprotective effects [47, 48]. The flavanone, hesperidin, present in the highest level in the 70% ethanolic extract of *C. genistoides* could alleviate oxidative stress [49] and act as neuroprotective agent, amongst others by enhancing endogenous antioxidant defense functions [50].

Regarding the bioavailability of the plant extract, it depends on the bioavailability of the single compounds contained in each extract. Extracts from different honeybush species vary in chemical composition. However, the main active constituents of honeybush have been reported to be mangiferin and hesperidin and there are some data available with regard to their bioavailability and their ability to cross the blood-brain barrier (BBB). Of note, trace amounts of mangiferin were found in the rat brain after an acute oral treatment with a single dose of a plant extract containing mangiferin indicating that the compound can cross the BBB [51], whereas in another study, mangiferin was not detected in the brain of rats after a single dose via intraperitoneal administration [52]. However, one has to take into consideration that different assays of different sensitivities were used in the two studies. In the study from Li et al. (2008), a validated highly sensitive HPLC method was developed and applied to detect mangiferin after a single oral dose of *Rhizoma Anemarrhenae* extract, while in the study of Zajac et al. (2012), a much less sensitive detection method (a simple TLC method) was used. Similarly, the bioavailability of the therapeutically active constituents of *Ginkgo biloba* extract (GBE) in the brain was formerly questioned until recent studies demonstrated the distribution of GBE in the brain of rats after single and repeated oral administration of GBE [53, 54]. The compounds in this case were also successfully detected with an HPLC method. Hesperidin or its aglycone hesperetin seems to be able to traverse the BBB and directly exerts their neuroprotective effect in the brain [55–57].

Furthermore, bioavailability in the brain might be affected by the route of administration and by whether the pure compound is administered or contained in a plant extract but we can assume that mangiferin and hesperidin exert neuroprotective effects on the brain and peripheral neurons.

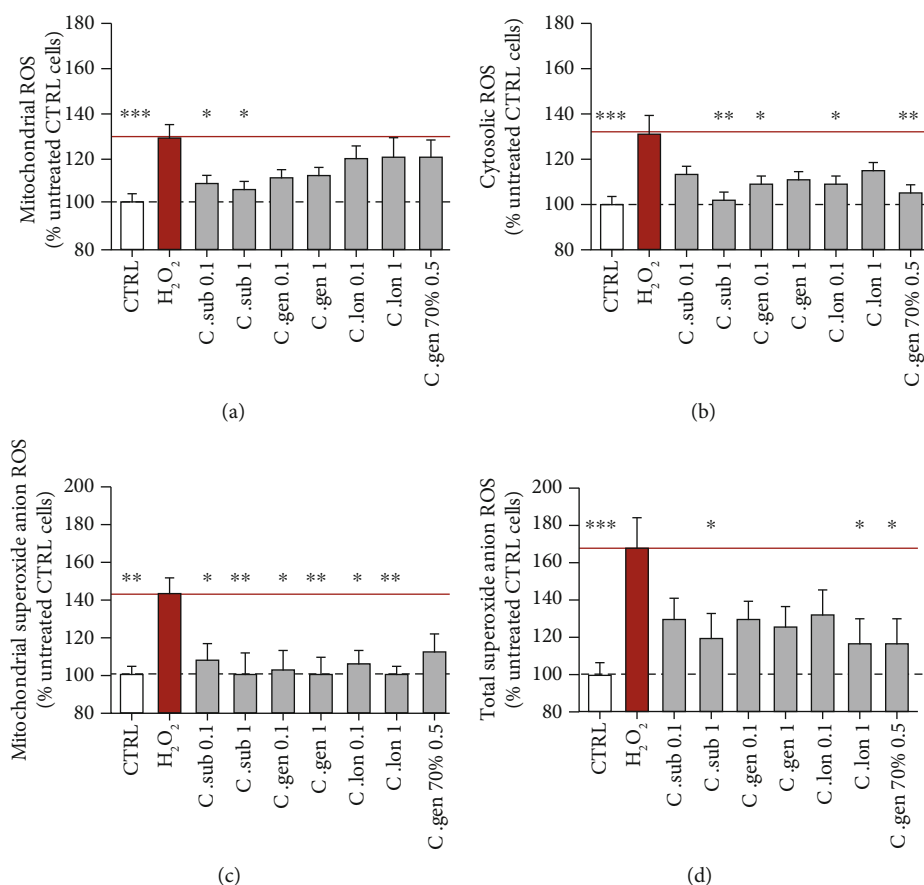


FIGURE 6: Effect of honeybush extracts on ROS levels under H₂O₂-induced oxidative stress. (a) H₂O₂ treatment at 400 μ M caused an increase of 29.5% in mitochondrial ROS which were detected using the dye DHR. This increase was significantly ameliorated up to 23.1% by *C. subternata* aqueous extract. (b) H₂O₂ caused an elevation of 31.2% in cytosolic ROS (detected with the dye DCF). All the extracts could bring the cytosolic ROS levels down, but the ones that reduced them significantly and most effectively were the aqueous extract of *C. subternata* at 1 ng/ml and the 70% ethanolic extract of *C. genistoides* at 0.5 ng/ml. (c) H₂O₂ increased the mitochondrial superoxide anion levels by 43%. All the extracts, except the ethanolic extract of *C. genistoides*, significantly reduced the mitochondrial superoxide anion levels. The aqueous extracts of *C. subternata*, *C. genistoides*, and *C. longifolia* at the concentration of 1 ng/ml each completely neutralized the mitochondrial superoxide anion levels. (d) The total superoxide anion levels were elevated by 67.9% in the H₂O₂-treated cells. All 4 extracts could ameliorate this increase but only the aqueous extracts of *C. subternata* at 1 ng/ml, *C. longifolia* at 1 ng/ml, and the ethanolic extract of *C. genistoides* at 0.5 ng/ml significantly reduced the superoxide anion levels. The red bar represents the H₂O₂-treated cells, and the grey bars represent cells that were pretreated for 24 h with the indicated honeybush extract and then treated for 3 h with H₂O₂. Values represent as the mean \pm SEM of three independent experiments and were normalized on the untreated group (=100%). One-way ANOVA and post hoc Dunnett's multiple comparison test versus (a) untreated (CTRL) or (b) H₂O₂. * $P < 0.05$; ** $P < 0.01$; *** $P < 0.001$.

To sum up, the results obtained from this study indicate that *C. subternata* aqueous extract is the most effective in enhancing mitochondrial functions especially under oxidative stress situations. It was the only one to act on respiration under oxidative stress and the only one to lower all four types of ROS measured in this study. These findings are particularly relevant for the establishment of honeybush tea as nutraceutical as the species that is mostly cultivated for the production of the tea is currently *C. subternata*. The other two aqueous extracts (*C. genistoides* and *C. longifolia*) also exert a beneficial effect. *C. genistoides* acted more on respiration under physiological conditions, while *C. longifolia* was more effective in neutralizing ROS (active against three types of ROS). Interestingly, in the tea industry, honeybush tea is often prepared after blending of different species. Therefore,

evaluating the activity of a mixture of different species extracts will be very interesting.

5. Conclusion

In this study, the effects of honeybush extracts on enhancing mitochondrial and neuronal functions and on preventing the detrimental effects of oxidative stress were examined. The aqueous extract of *C. subternata* was superior to the other extracts in increasing mitochondrial functions and bioenergetics, especially under H₂O₂-induced oxidative stress. The aqueous extracts of *C. genistoides* and *C. longifolia* came next in terms of efficacy on mitochondrial functions. Lower extract concentrations (0.1-1 ng/ml) were also more effective. Overall, our data are in line with existing literature reporting

an antioxidant effect of honeybush [19–22]. However, the effects of honeybush extracts on neuronal cells and specifically on mitochondrial function have been investigated here for the first time. Further research is ongoing by our team in order to study more in depth the effect of honeybush in combatting stress and in enhancing neuronal function. These findings make honeybush a potential candidate for prevention of oxidative stress, laying the foundation for further research aimed at the development of a condition-specific nutraceutical.

Abbreviations

ADP:	Adenosine diphosphate
ATP:	Adenosine triphosphate
BBB:	Blood-brain barrier
DCF:	2',7'-Dichlorodihydrofluorescein diacetate
DHE:	Dihydroethidium
DHR:	Dihydrorhodamine 123
DMEM:	Dulbecco's modified Eagle medium
DMSO:	Dimethyl sulfoxide
ECAR:	Extracellular acidification rate
ESI:	Electrospray ionization
ETC:	Electron transport chain
FADH ₂ :	Reduced form of flavin adenine dinucleotide (FAD)
FCCP:	Carbonyl cyanide-4-(trifluoromethoxy)phenylhydrazine
FCS:	Fetal calf serum
GBE:	<i>Ginkgo biloba</i> extract
GSH:	Glutathione(γ -glutamylcysteinylglycine)
GSH: GSSG:	Reduced glutathione to oxidised glutathione ratio
HBSS:	Hanks' balanced salt solution
HPLC-DAD:	High-performance liquid chromatography with diode array detector
IMM:	Inner mitochondrial membrane
LC-MS:	Liquid chromatography-mass spectrometry
MMP:	Mitochondrial membrane potential
MS/MS:	Tandem mass spectrometry
MtDNA:	Mitochondrial DNA
NADH:	Reduced form of nicotinamide adenine dinucleotide
OCR:	Oxygen consumption rate
OXPPOS:	Oxidative phosphorylation
PBS:	Phosphate-buffered saline
Q-TOF:	Synapt G2 quadrupole time-of-flight
ROS:	Reactive oxygen species
SEM:	Standard error of the mean
SH-SY5Y:	Human neuroblastoma cell line
TMRM:	Tetramethylrhodamine methyl ester
UPLC:	Ultra-performance liquid chromatography
UV-Vis:	Ultraviolet-visible.

Data Availability

The data used to support the findings of this study are available from the corresponding author upon request.

Conflicts of Interest

The authors declare no conflict of interest.

Acknowledgments

This study was supported by a bilateral grant from the Swiss National Science Foundation (grant no. IZLSZ3_170858 to GIAE) and the NRF of South Africa (grant no. 107805 to EJ) between Switzerland and South Africa.

References

- [1] A. Grimm, A. G. Mensah-Nyagan, and A. Eckert, "Alzheimer, mitochondria and gender," *Neuroscience and Biobehavioral Reviews*, vol. 67, pp. 89–101, 2016.
- [2] A. Grimm and A. Eckert, "Brain aging and neurodegeneration: from a mitochondrial point of view," *Journal of Neurochemistry*, vol. 143, no. 4, pp. 418–431, 2017.
- [3] I. Lejri, A. Agapouda, A. Grimm, and A. Eckert, "Mitochondria- and Oxidative Stress-Targeting Substances in Cognitive Decline- Related Disorders: From Molecular Mechanisms to Clinical Evidence," *Oxidative Medicine and Cellular Longevity*, vol. 2019, Article ID 9695412, 26 pages, 2019.
- [4] N. Nissanka and C. T. Moraes, "Mitochondrial DNA damage and reactive oxygen species in neurodegenerative disease," *FEBS Letters*, vol. 592, no. 5, pp. 728–742, 2018.
- [5] N. Kuskal, J. Chalker, and R. J. Mailloux, "Progress in understanding the molecular oxygen paradox - function of mitochondrial reactive oxygen species in cell signaling," *Biological Chemistry*, vol. 398, no. 11, pp. 1209–1227, 2017.
- [6] W. E. Müller, A. Eckert, G. P. Eckert et al., "Therapeutic efficacy of the Ginkgo special extract EGb761® within the framework of the mitochondrial cascade hypothesis of Alzheimer's disease," *The World Journal of Biological Psychiatry*, vol. 20, no. 3, pp. 173–189, 2017.
- [7] J. Dan Dunn, L. A. J. Alvarez, X. Zhang, and T. Soldati, "Reactive oxygen species and mitochondria: a nexus of cellular homeostasis," *Redox Biology*, vol. 6, pp. 472–485, 2015.
- [8] D. B. Zorov, M. Juhaszova, and S. J. Sollott, "Mitochondrial ROS-induced ROS release: an update and review," *Biochimica et Biophysica Acta*, vol. 1757, no. 5-6, pp. 509–517, 2006.
- [9] D. Q. Tan and T. Suda, "Reactive oxygen species and mitochondrial homeostasis as regulators of stem cell fate and function," *Antioxidants & Redox Signaling*, vol. 29, no. 2, pp. 149–168, 2018.
- [10] A. Grimm, K. Friedland, and A. Eckert, "Mitochondrial dysfunction: the missing link between aging and sporadic Alzheimer's disease," *Biogerontology*, vol. 17, no. 2, pp. 281–296, 2016.
- [11] X. Ren, L. Zou, X. Zhang et al., "Redox signaling mediated by thioredoxin and glutathione systems in the central nervous system," *Antioxidants & Redox Signaling*, vol. 27, no. 13, pp. 989–1010, 2017.
- [12] E. B. Kurutas, "The importance of antioxidants which play the role in cellular response against oxidative/nitrosative stress: current state," *Nutrition Journal*, vol. 15, no. 1, p. 71, 2016.
- [13] P. Mecocci, V. Boccardi, R. Cecchetti et al., "A long journey into aging, brain aging, and Alzheimer's disease following the oxidative stress tracks," *Journal of Alzheimer's Disease*, vol. 62, no. 3, pp. 1319–1335, 2018.

- [14] C. Giorgi, S. Marchi, I. C. M. Simoes et al., "Mitochondria and reactive oxygen species in aging and age-related diseases," *International Review of Cell and Molecular Biology*, vol. 340, pp. 209–344, 2018.
- [15] I. Lejri, A. Grimm, and A. Eckert, "Mitochondria, estrogen and female brain aging," *Frontiers in Aging Neuroscience*, vol. 10, p. 124, 2018.
- [16] E. Joubert, M. E. Joubert, C. Bester, D. de Beer, and J. H. de Lange, "Honeybush (*Cyclopia* spp.): from local cottage industry to global markets — the catalytic and supporting role of research," *South African Journal of Botany*, vol. 77, no. 4, pp. 887–907, 2011.
- [17] E. Joubert, W. C. A. Gelderblom, A. Louw, and D. de Beer, "South African herbal teas: *Aspalathus linearis*, *Cyclopia* spp. and *Athrixia phylicoides*—a review," *Journal of Ethnopharmacology*, vol. 119, no. 3, pp. 376–412, 2008.
- [18] D. L. McKay and J. B. Blumberg, "A review of the bioactivity of South African herbal teas: rooibos (*Aspalathus linearis*) and honeybush (*Cyclopia intermedia*)," *Phytotherapy Research*, vol. 21, no. 1, pp. 1–16, 2007.
- [19] P. Dube, S. Meyer, and J. L. Marnewick, "Antimicrobial and antioxidant activities of different solvent extracts from fermented and green honeybush (*Cyclopia intermedia*) plant material," *South African Journal of Botany*, vol. 110, pp. 184–193, 2017.
- [20] A. O. Lawal, L. M. Davids, and J. L. Marnewick, "Rooibos (*Aspalathus linearis*) and honeybush (*Cyclopia species*) modulate the oxidative stress associated injury of diesel exhaust particles in human umbilical vein endothelial cells," *Phytomedicine*, vol. 59, p. 152898, 2019.
- [21] J. D. van der Merwe, D. de Beer, S. Swanevelder, E. Joubert, and W. C. A. Gelderblom, "Dietary exposure to honeybush (*Cyclopia*) polyphenol-enriched extracts altered redox status and expression of oxidative stress and antioxidant defense-related genes in rat liver," *South African Journal of Botany*, vol. 110, pp. 230–239, 2017.
- [22] J. L. Marnewick, E. Joubert, P. Swart, F. van der Westhuizen, and W. C. Gelderblom, "Modulation of hepatic drug metabolizing enzymes and oxidative status by rooibos (*Aspalathus linearis*) and Honeybush (*Cyclopia intermedia*), green and black (*Camellia sinensis*) teas in rats," *Journal of Agricultural and Food Chemistry*, vol. 51, no. 27, pp. 8113–8119, 2003.
- [23] D. de Beer, A. Schulze, E. Joubert, A. de Villiers, C. Malherbe, and M. Stander, "Food ingredient extracts of *Cyclopia subternata* (Honeybush): variation in phenolic composition and antioxidant capacity," *Molecules*, vol. 17, no. 12, pp. 14602–14624, 2012.
- [24] A. E. Schulze, T. Beelders, I. S. Koch, L. M. Erasmus, D. de Beer, and E. Joubert, "Honeybush herbal teas (*Cyclopia* spp.) contribute to high levels of dietary exposure to xanthenes, benzophenones, dihydrochalcones and other bioactive phenolics," *Journal of Food Composition and Analysis*, vol. 44, pp. 139–148, 2015.
- [25] T. Beelders, D. de Beer, M. Stander, and E. Joubert, "Comprehensive phenolic profiling of *Cyclopia genistoides* (L.) Vent. by LC-DAD-MS and -MS/MS reveals novel xanthone and benzophenone constituents," *Molecules*, vol. 19, no. 8, pp. 11760–11790, 2014.
- [26] H. Arthur, E. Joubert, D. de Beer, C. J. Malherbe, and R. C. Witthuhn, "Phenylethanoid glycosides as major antioxidants in *Lippia multiflora* herbal infusion and their stability during steam pasteurisation of plant material," *Food Chemistry*, vol. 127, no. 2, pp. 581–588, 2011.
- [27] A. Grimm, K. Schmitt, U. E. Lang, A. G. Mensah-Nyagan, and A. Eckert, "Improvement of neuronal bioenergetics by neurosteroids: Implications for age-related neurodegenerative disorders," *Biochim Biophys Acta*, vol. 1842, no. 12, pp. 2427–2438, 2014.
- [28] A. Grimm, E. E. Biliouris, U. E. Lang, J. Götz, A. G. Mensah-Nyagan, and A. Eckert, "Sex hormone-related neurosteroids differentially rescue bioenergetic deficits induced by amyloid- β or hyperphosphorylated tau protein," *Cellular and Molecular Life Sciences*, vol. 73, no. 1, pp. 201–215, 2016.
- [29] I. Lejri, A. Grimm, M. Miesch, P. Geoffroy, A. Eckert, and A. G. Mensah-Nyagan, "Allopregnanolone and its analog BR 297 rescue neuronal cells from oxidative stress-induced death through bioenergetic improvement," *Biochimica et Biophysica Acta - Molecular Basis of Disease*, vol. 1863, no. 3, pp. 631–642, 2017.
- [30] K. Schmitt, A. Grimm, R. Dallmann et al., "Circadian control of DRP1 activity regulates mitochondrial dynamics and bioenergetics," *Cell Metabolism*, vol. 27, no. 3, pp. 657–666.e5, 2018, e5.
- [31] A. Grimm, I. Lejri, F. Hallé et al., "Mitochondria modulatory effects of new TSPO ligands in a cellular model of tauopathies," *Journal of Neuroendocrinology*, vol. 32, no. 1, article e12796, 2020.
- [32] Y. Poirier, A. Grimm, K. Schmitt, and A. Eckert, "Link between the unfolded protein response and dysregulation of mitochondrial bioenergetics in Alzheimer's disease," *Cellular and Molecular Life Sciences*, vol. 76, no. 7, pp. 1419–1431, 2019.
- [33] A. Grimm, K. Schmitt, and A. Eckert, "Advanced mitochondrial respiration assay for evaluation of mitochondrial dysfunction in Alzheimer's disease," *Methods in Molecular Biology*, vol. 1303, pp. 171–183, 2016.
- [34] K. Schmitt, A. Grimm, and A. Eckert, "Amyloid- β -Induced changes in molecular clock properties and cellular bioenergetics," *Frontiers in Neuroscience*, vol. 11, p. 124, 2017.
- [35] S. Papa, P. L. Martino, G. Capitanio et al., "The oxidative phosphorylation system in mammalian mitochondria," *Advances in Experimental Medicine and Biology*, vol. 942, pp. 3–37, 2012.
- [36] P. Dimroth, G. Kaim, and U. Matthey, "Crucial role of the membrane potential for ATP synthesis by F(1)F(o) ATP synthases," *The Journal of Experimental Biology*, vol. 203, Part 1, pp. 51–59, 2000.
- [37] L. K. Caesar and N. B. Cech, "Synergy and antagonism in natural product extracts: when 1 + 1 does not equal 2," *Natural Product Reports*, vol. 36, no. 6, pp. 869–888, 2019.
- [38] Z. Wang, S. Guo, J. Wang, Y. Shen, J. Zhang, and Q. Wu, "Nrf2/HO-1 mediates the neuroprotective effect of mangiferin on early brain injury after subarachnoid hemorrhage by attenuating mitochondria-related apoptosis and neuroinflammation," *Scientific Reports*, vol. 7, no. 1, p. 11883, 2017.
- [39] S. Siswanto, W. Arozal, V. Juniantito, A. Grace, F. D. Agustini, and Nafrialdi, "The effect of mangiferin against brain damage caused by oxidative stress and inflammation induced by doxorubicin," *HAYATI Journal of Biosciences*, vol. 23, no. 2, pp. 51–55, 2016.
- [40] S. Das, B. Nageshwar Rao, and B. S. Satish Rao, "Mangiferin attenuates methylmercury induced cytotoxicity against IMR-32, human neuroblastoma cells by the inhibition of oxidative stress and free radical scavenging potential," *Chemico-Biological Interactions*, vol. 193, no. 2, pp. 129–140, 2011.

- [41] C. Infante-Garcia, J. J. Ramos-Rodriguez, I. Delgado-Olmos et al., "Long-term mangiferin extract treatment improves central pathology and cognitive deficits in APP/PS1 mice," *Molecular Neurobiology*, vol. 54, no. 6, pp. 4696–4704, 2017.
- [42] M. Kavitha, J. Nataraj, M. M. Essa, M. A. Memon, and T. Manivasagam, "Mangiferin attenuates MPTP induced dopaminergic neurodegeneration and improves motor impairment, redox balance and Bcl-2/Bax expression in experimental Parkinson's disease mice," *Chemico-Biological Interactions*, vol. 206, no. 2, pp. 239–247, 2013.
- [43] S. T. Feng, Z. Z. Wang, Y. H. Yuan, H. M. Sun, N. H. Chen, and Y. Zhang, "Mangiferin: a multipotent natural product preventing neurodegeneration in Alzheimer's and Parkinson's disease models," *Pharmacological Research*, vol. 146, p. 104336, 2019.
- [44] Y. Y. Tan, J. Xu, P. Zhang et al., "Luteolin exerts neuroprotection via modulation of the p62/Keap1/Nrf2 pathway in intracerebral hemorrhage," *Frontiers in Pharmacology*, vol. 10, p. 1551, 2020.
- [45] O. Farkas, J. Jakus, and K. Heberger, "Quantitative structure-antioxidant activity relationships of flavonoid compounds," *Molecules*, vol. 9, no. 12, pp. 1079–1088, 2004.
- [46] X. Li, B. Chen, H. Xie, Y. He, D. Zhong, and D. Chen, "Antioxidant structure(-)activity relationship analysis of five dihydrochalcones," *Molecules*, vol. 23, no. 5, p. 1162, 2018.
- [47] D. Barreca, M. Currò, E. Bellocco et al., "Neuroprotective effects of phloretin and its glycosylated derivative on rotenone-induced toxicity in human SH-SY5Y neuronal-like cells," *BioFactors*, vol. 43, no. 4, pp. 549–557, 2017.
- [48] Y. Liu, L. Zhang, and J. Liang, "Activation of the Nrf2 defense pathway contributes to neuroprotective effects of phloretin on oxidative stress injury after cerebral ischemia/reperfusion in rats," *Journal of the Neurological Sciences*, vol. 351, no. 1-2, pp. 88–92, 2015.
- [49] D. Wang, L. Liu, X. Zhu, W. Wu, and Y. Wang, "Hesperidin alleviates cognitive impairment, mitochondrial dysfunction and oxidative stress in a mouse model of Alzheimer's disease," *Cellular and Molecular Neurobiology*, vol. 34, no. 8, pp. 1209–1221, 2014.
- [50] M. Hajialyani, M. Hosein Farzaei, J. Echeverría, S. Nabavi, E. Uriarte, and E. Sobarzo-Sánchez, "Hesperidin as a neuroprotective agent: a review of animal and clinical evidence," *Molecules*, vol. 24, no. 3, p. 648, 2019.
- [51] Y.-J. Li, Y. J. Sui, Y. H. Dai, and Y. L. Deng, "LC determination and pharmacokinetics study of mangiferin in rat plasma and tissues," *Chromatographia*, vol. 67, no. 11-12, pp. 957–960, 2008.
- [52] D. Zajac, A. Stasinska, R. Delgado, and M. Pokorski, "Mangiferin and its traversal into the brain," *Advances in Experimental Medicine and Biology*, vol. 756, pp. 105–111, 2013.
- [53] L. Rangel-Ordóñez, M. Nöldner, M. Schubert-Zsilavec, and M. Wurglics, "Plasma levels and distribution of flavonoids in rat brain after single and repeated doses of Standardized-Ginkgo biloba Extract EGb 761®," *Planta Medica*, vol. 76, no. 15, pp. 1683–1690, 2010.
- [54] C. Ude, M. Schubert-Zsilavec, and M. Wurglics, "Ginkgo biloba extracts: a review of the pharmacokinetics of the active ingredients," *Clinical Pharmacokinetics*, vol. 52, no. 9, pp. 727–749, 2013.
- [55] K. A. Youdim, M. S. Dobbie, G. Kuhnle, A. R. Proteggente, N. J. Abbott, and C. Rice-Evans, "Interaction between flavonoids and the blood-brain barrier: in vitro studies," *Journal of Neurochemistry*, vol. 85, no. 1, pp. 180–192, 2003.
- [56] A. Roohbakhsh, H. Parhiz, F. Soltani, R. Rezaee, and M. Iranshahi, "Neuropharmacological properties and pharmacokinetics of the citrus flavonoids hesperidin and hesperetin—a mini-review," *Life Sciences*, vol. 113, no. 1-2, pp. 1–6, 2014.
- [57] U. Z. Said, H. N. Saada, M. S. Abd-Alla, M. E. Elsayed, and A. M. Amin, "Hesperidin attenuates brain biochemical changes of irradiated rats," *International Journal of Radiation Biology*, vol. 88, no. 8, pp. 613–618, 2012.

Review Article

Foods with Potential Prooxidant and Antioxidant Effects Involved in Parkinson's Disease

Alejandra Guillermina Miranda-Díaz , **Andrés García-Sánchez** ,
and **Ernesto Germán Cardona-Muñoz** 

Department of Physiology, University Health Sciences Center, University of Guadalajara, Guadalajara, Jalisco, Mexico

Correspondence should be addressed to Alejandra Guillermina Miranda-Díaz; kindalex1@outlook.com

Received 20 April 2020; Revised 2 July 2020; Accepted 18 July 2020; Published 4 August 2020

Guest Editor: Francisco Jaime B. Mendonça Junior

Copyright © 2020 Alejandra Guillermina Miranda-Díaz et al. This is an open access article distributed under the Creative Commons Attribution License, which permits unrestricted use, distribution, and reproduction in any medium, provided the original work is properly cited.

Oxidative stress plays a fundamental role in the pathogenesis of Parkinson's disease (PD). Oxidative stress appears to be responsible for the gradual dysfunction that manifests via numerous cellular pathways throughout PD progression. This review will describe the prooxidant effect of excessive consumption of processed food. Processed meat can affect health due to its high sodium content, advanced lipid oxidation end-products, cholesterol, and free fatty acids. During cooking, lipids can react with proteins to form advanced end-products of lipid oxidation. Excessive consumption of different types of carbohydrates is a risk factor for PD. The antioxidant effects of some foods in the regular diet provide an inconclusive interpretation of the environment's mechanisms with the modulation of oxidation stress-induced PD. Some antioxidant molecules are known whose primary mechanism is the neuroprotective effect. The melatonin mechanism consists of neutralizing reactive oxygen species (ROS) and inducing antioxidant enzyme's expression and activity. N-acetylcysteine protects against the development of PD by restoring levels of brain glutathione. The balanced administration of vitamin B3, ascorbic acid, vitamin D and the intake of caffeine every day seem beneficial for brain health in PD. Excessive chocolate intake could have adverse effects in PD patients. The findings reported to date do not provide clear benefits for a possible efficient therapeutic intervention by consuming the nutrients that are consumed regularly.

1. Introduction

Parkinson's disease (PD) is the second most common chronic progressive neurodegenerative disorder. PD is characterized by the selective loss of dopaminergic neurons of the substantia nigra (SN) pars compacta, which conditions deficiency of dopamine secretion in the basal ganglia of the midbrain with the ability to produce classic motor symptoms: bradykinesia, tremor, rigidity, posterior postural instability, gait disturbances, smell, memory, and dementia [1]. PD involves genetic, environmental, and toxicological factors [2, 3]. PD is associated with oxide-reduction processes through excessive production of reactive oxygen species (ROS) [4]. The hallmark of PD is the appearance of insoluble inclusions in neurons called Lewy bodies. Lewy bodies mainly consist of α -synuclein deposition [5]. α -Synuclein is a 140 kDa protein encoded via the SNCA gene. α -Synuclein

plays an essential role in the pathogenesis of PD. Duplication, triplication, and point mutations in the N-terminal region (A30P, A53T, and E46K) are linked to familial PD [6]. A recent study suggests that α -synuclein monomers and tetramers are the physiological forms, while oligomers and fibrils are the pathogenic forms [7]. Abnormal accumulation of soluble α -synuclein monomers may lead to the formation of oligomers and fibrils as a key pathogenic event in the early stages of PD [8]. The first clinical signs and symptoms of PD appear after the loss of 50-70% of SN [9, 10]. Based on PD's progressive nature, oxidation might be responsible for gradual dysfunction as a continuous process that manifests itself through many cellular pathways throughout the disease. ROS are normally produced in the cell during the mitochondrial electron transfer chain or by redox reactions [11].

ROS are necessary components for cellular homeostasis. However, when ROS are produced in excess, they induce

transcription errors that cause dysfunction in the expression of different proteins, including C-terminal α -synuclein, parkin, and ubiquitin hydrolase which are directly related to PD [12]. A recent study reported the propensity of oligomers to cause ROS production and significant reduction in the presence of metal chelators such as deferoxamine. This evidence indicates that α -synuclein oligomers produce superoxide (O_2^-) radicals that bind to transition metal ions such as copper and iron [13]. α -Synuclein toxicity may contribute to elevated cellular oxidative stress. Oxidative stress may trigger α -synuclein toxicity [9]. In PD, α -synuclein oligomers cause the impairment of proteasomes and lysosomes' degradation activity, increasing protein accumulation and aggregation. The accumulation of α -synuclein is associated with a decrease of dopamine release [14]. The mitochondrial respiratory chain can produce oxidative stress by generating ROS and reactive nitrogen species (RNS). Excessive production of ROS and RNS can damage the cell, especially the mitochondrial system. Oxidative stress can trigger apoptosis signaling in nerve cells (Figure 1) [15].

In this review article, we will briefly discuss the role of lipoperoxidation, oxidative damage, DNA repair, mitochondria, endogenous antioxidants, and the anti- and prooxidant effects of some natural foods for daily consumption and some food alternatives with antioxidant potential in PD. These dietary alternatives at low or increased levels can have beneficial or detrimental effects to increase or decrease the signs and symptoms of PD.

1.1. Lipoperoxidation in Parkinson's Disease. Oxidative stress induces toxicity in the cell by the oxidation of lipids. Lipid oxidation leads to the accumulation of intracellular aggregates, mitochondrial dysfunction, excitotoxicity, and apoptosis. Oxidative damage is a common phenomenon in neurodegenerative diseases. However, it is unclear whether oxidative stress is a cause or a consequence. The formation of modified lipids via oxidation can produce postmitotic cellular dysfunction, and the dysfunction is capable of leading to necrosis or apoptosis of neurons. Lipoperoxidation of polyunsaturated fatty acids (PUFAs) in cell membranes initiates the cumulative deterioration of cell membrane functions by causing decreased fluidity, reduced electrochemical potential, and increased permeability of the cell membrane [16]. Postmortem studies have shown that the effect of chronic oxidative stress is lipoperoxidation of PUFAs in the SN cell membranes [11]. Malondialdehyde (MDA) and glycosylation end-product levels increase in PD, resulting in impaired oxidation of glucose. The increase of MDA and glycation end-products leads to irreversible oxidation of proteins in the SN and the cerebral cortex. The SN has a high risk of aggressive oxidative attacks via lipoperoxides. It has been previously reported that the distribution of transition metals in the brain showed remarkable regional differences [17]. 4-Hydroxy-2-nonenal is a lipid peroxidation product capable of preventing the fibrillar formation of α -synuclein by promoting the formation of secondary β -sheets and toxic soluble oligomers in a dose-dependent manner. Therefore, oxidative stress can also influence α -synuclein toxicity and mediate the pathogenesis of PD [18]. In the

postmortem brains of PD patients, increased carbonylated proteins and TBAR markers have been detected [19]. Lipoperoxidation markers were increased in plasma and cerebrospinal fluid (CSF) in PD patients compared to controls without the disease [20].

1.2. Oxidative DNA Damage in Parkinson's Disease. PD is characterized by defects in the ability to repair acute or chronic oxidative damage to neurons [21]. The 8-hydroxy-2'-deoxyguanosine (8-OHdG) marker is an indicator of nucleic acid oxidation; in particular, it is a marker of oxidative damage to nuclear and mitochondrial DNA. In patients with PD, the marker has been found to increase in the CSF coupled with increased levels of oxidized coenzyme Q10 [22]. Oxidative DNA damage leads to genomic instability and cellular dysfunction. More than 100 oxidative modifications to DNA are identified; many of these are mutagenic, while others interrupt replication or transcription, leading to cancer or cell death in PD [23]. Oxidative damage can arise from external sources, such as chemical agents and ionizing radiation. However, most of the oxidative damage is caused by ROS produced through normal cellular respiration and metabolism [24]. Oxidative damage to DNA in the brain is particularly frequent since it is produced by endogenous metabolic activity. The continuous electrochemical transmission between brain cells requires a large amount of energy. Brain tissue maintains a high basal metabolic rate to meet high energy demands, resulting in brain cells that produce high levels of ROS [25]. The oxidative stress imbalance amplifies the level of damage within brain cells, increasing the demand for DNA repair activity, requiring additional energy, and creating a perpetual state of oxidative stress. Differentiated postmitotic brain cells lack a robust DNA repair and detection machinery associated with replication [26]. However, brain cells have highly efficient base excision repair (BER) mechanisms to cope with the high oxidative stress involved in neurodegenerative disorders. Emerging research suggests that specific BER pathway deficiencies perpetuate neuronal dysfunction [5, 22]. Injuries that occur in DNA include base modifications, abasic sites, and single- and double-strand breaks of DNA. The injuries that occur are mostly repaired via BER [27]. The first step of BER is the recognition and removal of damaged DNA bases. DNA base modifications are recognized first and removed by glycosylase enzymes. Abasic sites are removed by apurinic enzymes/aprimidinic endonucleases [28]. DNA glycosylases are the first DNA repair enzymes recruited for oxidative damage [29]. Eleven glycosylases are known in humans [30]. The three central glycosylases that recognize oxidative damage are 8-oxoguanin DNA glycosylase (OGG1), endonuclease III, and endonuclease VIII [29]. OGG1 shows specificity for lesions caused by the oxidative damage marker to DNA 8-oxoguanin. The mutY homolog (MYH) can cleave a mismatched adenine throughout the 8-oxoguanin injury to suppress mutagenicity [31]. In the brain, the most abundant oxidative lesions produced by the 8-oxoguanin and formamidopyrimidine (FAPY G) markers are derived from the oxidation and reduction of 8-hydroxyguanine injuries [32].

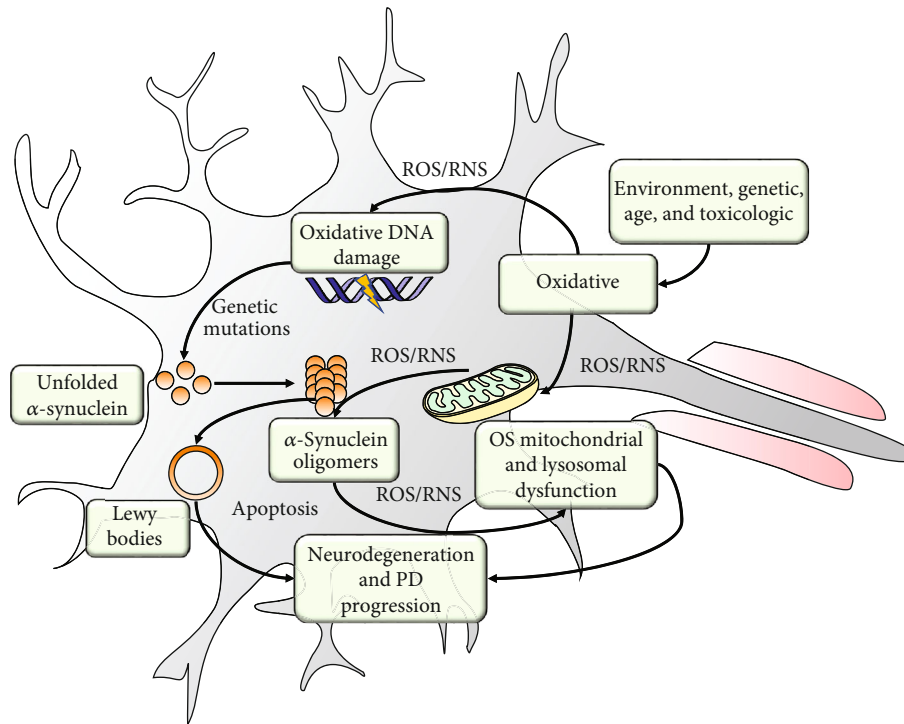


FIGURE 1: Schematic representation of the oxidative stress mechanism in the development of Parkinson's disease in dopaminergic neurons. Oxidative stress from aging or exogenous sources causes damage to vulnerable cellular structures such as mitochondria and DNA. α -Synuclein gene mutations can promote the formation of α -synuclein oligomers and Lewis bodies. Oxidative stress causes mitochondrial dysfunction that converts the mitochondria into a source of ROS/RNS. ROS/RNS increases α -synuclein aggregate formation, and these, in turn, damage mitochondrial function. Both mitochondrial dysfunction and Lewis bodies lead to a loss of dopaminergic neurons and thus neurodegeneration

1.3. Mitochondria in Parkinson's Disease. Mitochondria are organelles that produce ATP (chemical energy) and play a critical role in energy metabolism, the redox state, and Ca^{2+} homeostasis. Therefore, mitochondria are crucial to cell survival. Intracellular Ca^{2+} stimulates the electron transport chain in the mitochondria producing ATP and ROS as sub-products. The endoplasmic reticulum is a quality control organelle that organizes protein synthesis, folding, and transport. Crosstalk between the endoplasmic reticulum and mitochondria increases with oxidative stress and mitochondrial stress, which can cause endoplasmic reticulum dysfunction. Research in the postmortem brain tissue has previously reported impaired mitochondrial function and elevated oxidative stress caused by α -synuclein aggregates, autooxidation, and degradation of dopamine in the SN [33]. Chronic oxidative stress is characterized by altered levels of iron and antioxidant defenses (enzyme superoxide dismutase (SOD) and glutathione (GSH)) in brain cells in PD [34]. Antioxidant enzymes, SOD, and GSH prevent ROS levels from rising [35]. When antioxidant defenses fail to regulate ROS levels, there is an increase in OS capable of producing harmful effects [36]. Random oxidation of macromolecules within the cell can damage cell structures and even cause cell death [37]. OS increases the possibility of spontaneous cellular mutations. The appearance of mutations conditions the vulnerability of cells to dysfunction [38].

1.4. Prooxidant Foods. Prooxidant foods are compounds that promote oxidative stress by increasing ROS generation or by decreasing antioxidant systems [39]. Diet can participate in OS production processes depending on the quantity or quality of micro- or macronutrients [40]. Some characteristics and mechanisms of different types of prooxidant foods that have the ability to favor the clinical manifestations of PD are described below (Figure 2).

1.5. Processed Meat Containing Oxidized Proteins in Parkinson's Disease. Meat products are the primary source of protein, amino acids, vitamins (niacin, vitamin B6, and vitamin B12), and minerals such as iron and zinc [41]. However, meat also contains products that, in excess, can be harmful to human health such as sodium, advanced glycation end-products, cholesterol, and free fatty acids [42, 43]. Currently, most meat products undergo processing stages that involve modification of their structure, changes in aggregation, or fragmentation that can cause protein oxidation [44]. Protein carbonylation determination is a useful marker to measure oxidative damage in different foods with high protein content [45]. Carbonylation is common in some processed foods, such as fermented sausages, dry-cured loins, chicken thigh meat, and pork or beef patties [46]. These products accumulate oxidized molecules during their process, and when ingested, they come into contact with the intestinal mucosa, internal organs, and the bloodstream after

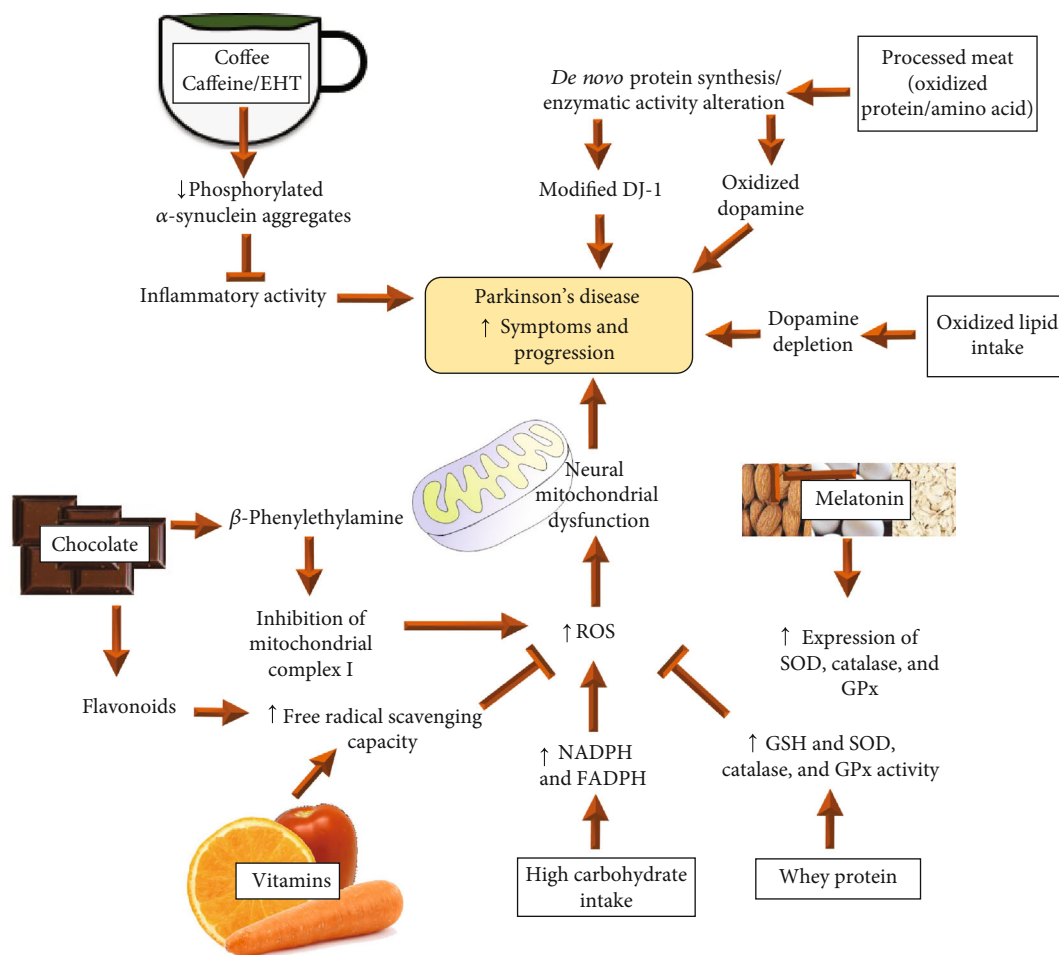


FIGURE 2: Proposed mechanism of food with pro- and antioxidant properties in the development of PD. Description of how the excessive intake of oxidized proteins and lipids causes the synthesis of oxidized molecules that worsens the symptoms of PD. A diet rich in carbohydrates can increase oxidative stress and cause oxidative neuronal damage. Food products can help to neutralize mediators of PD progression.

intestinal absorption [47]. Various studies have reported that oxidative protein modifications can accumulate in the body and damage specific tissues. For example, protein carbonyls correlated with the severity of damage in inflammatory bowel disease [48], and oxidized thyroxines are associated with dysfunction of insulin secretion [49]. Besides, the proteolytic damage of tissue releases 2-amino adipic acid, which is a risk marker for diabetes mellitus (DM) [50]. Intake of products with these structural modifications is also associated with aging and age-related diseases like PD [51–53]. There are different pathological mechanisms in which the intake of peptides or modified amino acids in PD is involved. One mechanism depends on the incorporation of oxidized amino acids into *de novo* protein synthesis, resulting in enzyme dysfunction with the ability to cause cellular damage [54]. One of the examples is the oxidative modification of the DJ-1 protein. The DJ-1 protein, which contains 189 amino acids, has been linked to PD because the loss of its functions causes disease with parkinsonian characteristics [55]. The oxidative modifications in a single amino acid of the DJ-1 protein are sufficient to favor PD development. Oxidative modifications of dopamine have been linked to PD [56].

Oxidized dopamine accumulates in the dopaminergic neurons of patients with sporadic or genetic PD, resulting in mitochondrial and lysosomal dysfunction [57].

1.6. Oxidized Lipids in Parkinson's Disease. Lipids are a necessary part of nutrition, providing large amounts of energy and essential fatty acids and promoting food acceptance [58]. Lipids provide important quality characteristics to meat products such as flavor and juiciness [59]. Lipids are highly prone to oxidation and represent the leading nonmicrobial cause of decomposition of meat products [60, 61]. During the oxidation of lipids in food, nutrient quality is lost due to the decrease of some macro- and micronutrients such as PUFAs, tocopherols, and amino acids or proteins that react with oxidized lipids [62]. Oxidized cholesterol products can be found in beef, *mortadella*, and anchovies [63–65]. Lipid oxysterols and hydroperoxides can be found in butter, corn oil, or olive oil [66, 67]. During food processing or cooking, lipids can react with proteins to form advanced lipid oxidation end-products (ALE) [68]. The health effects of ALEs in food are controversial. Some authors describe that oxidized fats can activate the inflammatory response and damage

organs such as the intestine, liver, and kidney [69, 70]. Baynes reported that enzyme systems can neutralize oxidized fats during metabolism and that harmful metabolic processes can occur in people with compromised cellular functions [71]. The effect of the high-fat diet on PD is not entirely clear. Mouse studies showed that high-fat diets could increase dopamine depletion in the nervous system and promote the progression of PD [72, 73]. Human studies associate the consumption of animal fat with an increased risk of developing PD [74, 75]. However, results were not replicated in other more extensive recent studies [76–78]. The contradictory findings may be due to different types of fat used in the diet that are not always described. Some studies indicate that high cholesterol or a keto diet may lower the risk of developing PD or improve the motor and nonmotor symptoms of the disease [79]. Also, the consumption of PUFAs contributes to the neuroprotective anti-inflammatory capacity [80–82].

1.7. The Effect of a Diet Rich in Carbohydrates in Parkinson's Disease. Eating a diet rich in carbohydrates can promote cellular signaling of inflammatory effects [83]. High carbohydrate consumption increases the glycemic index. A high glycemic index is associated with cancer risk and comorbidities due to overweight or obesity [84, 85]. In the Asian population, high consumption of rice or total carbohydrates is positively related to type 2 DM [86, 87]. Additionally, consuming refined carbohydrates, such as fructose-rich syrups, may lead to metabolic problems such as DM, obesity, and cardiovascular disease [88, 89]. High caloric intake can induce oxidative stress by increasing the substrates of mitochondrial respiration [90]. The high level of glucose metabolism increases NADPH and FADPH, which are capable of increasing O_2 production [91]. High glucose concentrations increase the activity of the thioredoxin-interacting protein that favors the generation of ROS [92]. The increased consumption of fructose products plays an important role as a trigger for oxidative stress. Animal studies showed that increased fructose in the diet causes metabolic and endocrine changes that affect different organs and tissues [93, 94]. Some retrospective studies report risk factors for developing PD due to high carbohydrate intake, but the effects of high carbohydrate intake on PD are still inconclusive. Consumption of dairy products is a risk factor in men, but not in women [74]. It has been previously reported that carbohydrates, monosaccharides, refined sugar, lactose, and other carbohydrate-rich foods such as bread and cereals are risk factors for PD [95]. However, cohort studies have not confirmed that total carbohydrate intake is associated with the risk of developing PD [76]. Diet with a high glycemic index or high carbohydrate intake found in a case-control study reduces the risk of PD [96]. A diet rich in carbohydrates could link DM to the risk of developing PD [97, 98]. PD and DM share common pathogenic mechanisms involving mitochondrial dysfunction, inflammation, and metabolic disturbances [99]. There is evidence between the association of DM with PD risk by increasing postural instability and difficulty walking [100]. However, further confirmatory studies are still needed [101, 102].

1.8. Parkinson's Disease Management Alternatives. Due to the increase in life expectancy and generational change, PD has become a common health problem and care of a PD patient has become a treatment challenge. PD is a costly disease for health services characterized by the accelerated appearance of clinical manifestations. PD becomes devastating for patients and their families. In the field of neurodegenerative diseases, the existing therapies only limit the activity of the disease. Alternative treatments need to be evaluated for both their beneficial and harmful properties (Table 1). A combination of therapies is recommended, which could condition the real delay in the evolution of PD as a possibility to improve the symptomatology of the disease or improve the quality of life of patients [103].

1.9. Antioxidants in Parkinson's Disease. Cells have developed antioxidant defense systems to protect themselves against their destructive products. The antioxidant defense system consists of enzymes that involve BER, SOD, glutathione peroxidase (GPx), peroxiredoxins, and GSH [26]. Due to the brain's high metabolic rate, there may be a decreased ratio of antioxidant to prooxidant enzymes [104]. The SN's antioxidant defenses are relatively low compared to other regions of the central nervous system (CNS). Low levels of GSH are produced during the early stages of PD. Extravesicular dopamine and its breakdown products can act as GSH depleting agents [105]. N-acetylcysteine (NAC) shows antioxidant properties by restoring cellular GSH and participating in important endogenous antioxidant systems. In experimental studies, NAC has been reported to protect against the development of PD [106]. The antioxidant characteristics of GSH have been demonstrated in oxidative stress models, including models that use buthionine-sulfoximine to deplete GSH. GSH depletion increases oxidative stress in all cells and mitochondrial fractions. Most of the antioxidant functions of GSH are exerted as a cofactor of the GPx enzyme family [107]. The GPx family forms a group of selenium-containing enzymes with the ability to reduce toxic peroxides [108]. Under neurotoxicity conditions, the overexpression of the antioxidant enzyme GPx can decrease the number of neurons lost [109]. An immunocytochemical study of GPx1 expression showed that dopaminergic neurons in SN express low levels of the enzyme. In contrast, in other regions not affected by PD, they express high levels of the enzyme [110]. GPx is an enzyme involved in the elimination of peroxides in the brain. The enzymatic activity of GPx reduces the probability that the hydroxyl radical (OH) will be produced by transition metals [44]. One of the major cellular defense systems for oxidative attacks is the antioxidant enzyme SOD. Three types of SOD have been identified in mammalian cells: copper-zinc SOD (Cu/ZnSOD or SOD1), manganese SOD (MnSOD or SOD2), and extracellular SOD (ECSOD or SOD3). SOD1 is a 32 kDa homodimer of a 153-residue polypeptide with one copper and one zinc-binding site per subunit [111]. Specifically, each monomer possesses a β -barrel motif and two functionally important large loops, called zinc and electrostatic loops that coat the metal-binding region. SOD1 catalyzes the reaction of the O_2 anion in molecular oxygen (O_2) and hydrogen peroxide

TABLE 1: Antioxidant and prooxidant properties of nutrients used in Parkinson's disease.

Nutrient	Antioxidant/benefit effects in PD	Prooxidant/side effects in PD
<i>Melatonin</i>	Increases the expression of GPx, SOD, and catalase [134] Improves sleep disturbances in PD patients [139, 140]	Melatonin can promote ROS production at a concentration of 10-1000 μ M [143]
<i>Vitamins</i>	The low singular form of vitamin B (10 mM) can induce differentiation of embryonic stem neuron cells [153] Vitamin C has antioxidant properties and it is well distributed in the brain [155] Vitamin D protects dopaminergic neurons [159]	The high singular form of vitamin B3 (>20 mM) can induce cytotoxicity and cell death [153] Vitamin C can induce OS in the presence of free transition metals and H ₂ O ₂ [156]
<i>Whey protein supplements</i>	20 g/day increases GSH in PD patients but does not improve the severity of disease [176]	High protein intake decreases the absorption of levodopa and increases the symptoms of PD [177]
<i>Chocolate</i>	Chocolate rich in flavonoids has free radical scavenging capacity and neuroprotective effects [180] No improvement was found in motor function after administration of 200 g of cocoa chocolate in PD patients [188]	Cocoa chocolate contains β -phenylethylamine which can promote OH formation and psychomotor dysfunction [192]
<i>Berberine</i>	Administration of 50 mg/kg prevents loss of dopaminergic neurons and improves motor balance and coordination in a rat PD model [219]	Long-term administration of berberine increases loss of dopaminergic neuronal mass <i>in vitro</i> and <i>in vivo</i> [220] Berberine along with chronic L-DOPA administration causes degeneration of dopaminergic cells in the substantia nigra in a rat model of PD [221]
<i>Curcumin</i>	Decreases ROS and the neurodegenerative severity and improves locomotor symptoms in <i>Drosophila</i> PD model [226]	
<i>Quercetin</i>	Administration of quercetin and piperine decreases the neurotoxicity in rat PD model [230]	
<i>Coffee</i>	Components in coffee have antioxidant, anti-inflammatory, and neuroprotective effects [204, 206]	

GSH: glutathione; GPx: glutathione peroxidase; SOD: superoxide dismutase; PD: Parkinson's disease; ROS: reactive oxygen species.

(H₂O₂) in a bonded copper ion [112]. The intracellular concentration of SOD1 is high (between 10 and 100 μ M) [113]. SOD1 represents 1% of the total protein content in the CNS. SOD1 is located in the cytoplasm, nucleus, lysosomes, peroxisomes, and intermitochondrial membrane spaces of eukaryotic cells [114]. Reports suggest that SOD1 is a crucial antioxidant enzyme whose mutations are a significant target of oxidative damage to brains with PD [115, 116]. SOD1 and mitochondrial SOD2 are among the most abundant antioxidant proteins in the brain and are fundamental in protecting neurons from oxidative stress. SOD enzymes eliminate toxic O₂⁻ converting it catalytically into oxygen and H₂O₂. Some studies suggest that abnormalities in SOD1 or SOD2 may contribute to the development of PD [117].

1.10. Melatonin in Parkinson's Disease. Melatonin is a natural hormone mainly secreted by the pineal gland that regulates different physiological functions. Melatonin is also synthesized by other organisms, such as bacteria, invertebrate animals, and plants [118]. The consumption of foods rich in melatonin such as pineapple, orange, and banana, can increase the antioxidant capacity of the organism [119]. Melatonin has also been identified in vegetables, meats, and sprouts [120, 121]. Meng et al. evaluated that eggs, fish, nuts,

cereals, and some seeds are the foods with the highest melatonin content [122]. Melatonin is known for its antioxidant properties and anti-inflammatory and cardiovascular effects. Melatonin has properties that inhibit tumor proliferation in the autoimmune system and provide a neuroprotective effect [123–127]. The main interest in the investigation of the effects of melatonin on PD arises from the relationship between the decrease in the activity of the pineal gland and melatonin in these patients [128]. MT1 and MT2 melatonin receptors are also decreased in PD [129]. Melatonin neutralizes ROS and induces the expression and activity of antioxidant enzymes [130, 131]. In mice, the effect of melatonin counteracts the progression of dopamine by increasing the activity of the mitochondrial complex I by decreasing the levels of lipoperoxides and nitrites in the cytosol and mitochondria of brain cells [132]. Other studies have shown anti-apoptotic, neuroprotective, and antidepressant activity in mouse models with PD [133–135]. Other studies have shown that melatonin treatment can help improve sleep disorder and increase neuroprotection in PD patients [136, 137]. However, the consumption of melatonin has not been able to improve the motor symptoms of PD [138]. Some studies reported that melatonin could promote ROS generation. *In vitro* studies showed that melatonin has prooxidant effects

mainly at lipids and proteins [139]. However, high concentrations of melatonin (10–1000 μM) are reported to promote ROS production by inducing cytotoxicity and apoptosis in human leukemia cells [140]. Similar effects were found in an Alzheimer's disease model culture, where melatonin concentrations of 1 mM increased oxidative stress markers, while concentrations < 0.1 mM reduced oxidative damage [141]. The prooxidant mechanisms of melatonin have not been fully described. Leukocyte studies show that melatonin has little interaction affinity for calmodulin and that this phenomenon seems to favor ROS production [142]. The benefits and risks of melatonin supplementation in PD patients require more clinical evidence to support the previously described findings.

1.11. Vitamins in Parkinson's Disease. Complementary to the usual pharmacological therapy for PD, it is suggested to add some other natural compounds as adjuvants. Vitamins are natural bioactive products with antioxidant properties [135]. Vitamins are necessary to maintain normal body functions; since essential vitamins cannot be synthesized endogenously by the body, they must be obtained through the diet. Vitamin deficiency is common in the elderly. Vitamins A, D, E, and K are fat-soluble. Fat-soluble vitamins bind primarily to nuclear receptors and affect the expression of specific genes [143]. Vitamins B and C are soluble in water and are cofactor constituents that affect enzyme activity [144]. The antioxidant properties of vitamins and their biological functions to regulate gene expression may be beneficial for the treatment of PD. Recent clinical evidence indicates that adequate supplementation of different vitamins can reduce PD incidence and improve the clinical symptoms of patients. Vitamin supplementation may be a beneficial adjuvant treatment for PD [145]. The members of the vitamin B family which are soluble in water include thiamine (vitamin B1), riboflavin (vitamin B2), niacin (vitamin B3), pantothenic acid (vitamin B5), pyridoxine (vitamin B6), biotin (vitamin B7), folic acid (vitamin B9), and cobalamin (vitamin B12) [146]. B vitamins play an important role as enzyme cofactors in multiple biochemical pathways in all tissues, such as regulating metabolism, improving the immune system and nervous system function, and promoting growth and cell division. Recently, the association between vitamin B and PD is receiving increasing attention [147]. Fukushima suggests that excess vitamin B3 (nicotinamide) is related to PD development [148]. Excess nicotinamide can induce the overproduction of 1-methyl nicotinamide (MNA) in PD patients [149]. Griffin et al. found that the singular form of nicotinamide (10 mM) has a significant effect in inducing the differentiation of embryonic stem cells in neurons. However, high singular forms (>20 mM) of nicotinamide cause cytotoxicity and cell death [150].

Vitamin C (ascorbic acid) is an essential water-soluble vitamin that is widely distributed in various tissues. Vitamin C is abundant in vegetables, fresh fruits, and animal livers. Vitamin C contains two molecular subforms in the body. The reduced form of vitamin C is ascorbic acid and the oxidized form of dehydroascorbic acid. Vitamin C is essential for the nervous system's physiological function and antioxi-

dant function by inhibiting oxidative stress, reducing lipoperoxidation, and eliminating free radicals [151]. Vitamin C has the potential for the treatment of PD because it is mainly distributed in areas rich in neurons [152]. Vitamin C deficiency can cause scurvy. However, ascorbic acid exhibits prooxidant properties in the presence of free transition metals because it reduces ferric ions to ferrous ions in a Fenton-type reaction. Ascorbic acid in the presence of H_2O_2 stimulates the formation of OH radicals [153]. Therefore, the final prooxidant or antioxidant effect depends on the relationship between ascorbic acid concentration and the available ferrions [38]. At sufficiently high levels, ascorbic acid reduces and destroys the radicals formed [154]. Postmortem studies have shown that vitamin D receptors are present in dopaminergic neurons in the human SN. Vitamin D administration has been suggested to protect dopaminergic neurons, and its deficiency is associated with increased motor severity, postural instability, worsening verbal fluency, and memory [155, 156]. In early PD, patients have been reported to have significantly lower serum 25-(OH)-D concentrations than controls of the same age, which may have implications for bone health and fracture risk. Sleeman et al. reported a small significant association between vitamin D status at baseline and worsening PD motor function at 36-month follow-up [157]. 25-Hydroxyvitamin-D deficiency and reduced exposure to sunlight are significantly associated with an increased risk of PD. However, vitamin D supplementation does not produce significant benefits to improve motor function in PD patients [158].

1.12. Whey Protein Supplementation in Parkinson's Disease. In addition to the protein obtained from food, there is also whey protein (WP) supplements used to treat some metabolic disorders [159]. WP is a soluble by-product obtained from the separation of casein during cheesemaking [160]. WP is mainly rich in globulins, albumin, and amino acids [161, 162]. Some studies have shown that specific WP preparations can reduce proinflammatory cytokine levels (TNF- α , IL-6) and work as a hepatoprotective agent in hepatitis and liver fibrosis in rat models [163]. Other studies evaluated the antioxidant effect of (WP) supplementation on oxidative stress [164]. Rat studies reported that WP supplementation increases the antioxidant enzyme activity of catalase, SOD, and GPx and reduces the effect of TBAR [165]. Falim et al. evaluated the effect of WP supplementation on oxidative stress in subjects with overweight/obesity and DM. The authors found no significant effect on oxidative stress markers (TBAR, AOPP, and 8-OHdG) [166]. Reyes et al. and Katz et al. demonstrated that supplementation of the amino acid NAC contributes to raising GSH levels in mice and patients with PD [167, 168]. PD patients are generally malnourished and have decreased muscle strength. In these patients, the use of WP may be recommended [169–171], although there is little clinical evidence in this regard. Tosukhowong et al. conducted a double-blind, placebo-controlled clinical trial of 38 patients with PD, and they also conducted a six-month follow-up to assess WP's clinical effects. The authors found that 20 g/day increased the levels of reduced GSH and decreased homocysteine levels. These

results did not impact the severity of PD measured according to the unified PD classification scale (UPDRS) [172]. Clinical studies involving a larger number of patients with long-term follow-up are required to establish the possible beneficial effects of WP supplementation in PD patients. WP supplementation must be monitored because high protein intake decreases the therapeutic effects of levodopa, increasing the symptoms of PD [173].

1.13. Chocolate in Parkinson's Disease. Chocolate is produced from the cocoa bean of the *Theobroma cacao* tree. Polyphenols, especially flavonoids, are the main components of health interest in cocoa and its derivatives [174]. Currently, research on the potential health benefits of consuming PD cocoa is attractive due to their high content of antioxidant polyphenols [175]. The antioxidant capacity of flavonoids has been previously reported due to their free radical scavenging capacity, chelation of transition metal ions, and the mediation of some cell signaling cascades [176]. *In vitro* studies have shown the beneficial antioxidant effects of cocoa [177, 178]. However, these effects are not always extrapolated to *in vivo* studies [179]. It is difficult to establish the recommended amount of chocolate intake to obtain any specific health benefit because the bioavailability characteristics and polyphenol contents are different in each type of chocolate [180]. Dark chocolate, unlike white or milk chocolate, has been used in studies to evaluate its health effects due to its high flavonoid content close to 50% [181]. Dark chocolate shows potential benefits in DM [182], cancer [183], cardiovascular disease [184], and neuroprotective effects [185]. The study on the effects of chocolate in PD patients could be of great importance because the intake of chocolate and other sweets is frequent. A study reported that PD patients consume more chocolate (100 g weekly) than a control group without the disease. PD patients increase chocolate intake by 22% during the disease [186]. A single-dose crossover study evaluated the immediate effect of 200 g of cocoa chocolate on motor function in PD patients. Contrary to expectations, no significant differences in motor function were found in this study at 1-3 h after the ingestion of cocoa chocolate compared to cocoa-free chocolate [187]. An important factor to consider in addition to the flavonoid content is that cocoa contains β -phenylethylamine, traces of a type of amine with neurotransmitter activity [188, 189]. Studies suggest that the distribution of β -phenylethylamine in the brain reaches its maximum concentration in dopaminergic regions [190]. Studies in mice show that β -phenylethylamine causes inhibition of mitochondrial complex I favoring the generation of OH and psychomotor dysfunction [191]. Furthermore, the intake of β -phenylethylamine in mice causes alterations of akinesia, catalepsy, and other motor disorders found in PD [192, 193]. Due to this, it has been reported that long-term intake of cocoa chocolate can promote neurodegeneration and dopamine complications due to its content of β -phenylethylamine [194]. There is still insufficient clinical evidence to support the benefits of the chocolate diet in PD patients. It is necessary to know the singular form and composition of cocoa-derived products that can help improve PD symptoms safely.

1.14. Coffee in Parkinson's Disease. Normally, soluble α -synuclein in PD is intrinsically disordered. This protein erroneously folds and forms distinctive amyloid fibrils in neuropathological inclusions. Initial oligomerization and eventual fibrillation are believed to be critical steps leading to neuronal dysfunction and death [195]. Postmortem brain studies show that α -synuclein in aggregates is hyperphosphorylated in serine 129, and antibodies to phospho-Ser129- α -synuclein (p- α -syn) are useful in detecting these inclusions [196]. The phosphorylation of α -synuclein in serine 129 accelerates its oligomerization and fibrillation *in vitro*. Consequently, this posttranslational modification is of pathogenic and therapeutic interest in α -synucleinopathies [197]. Dephosphorylation of the protein is carried out by a specific isoform of protein phosphatase 2A (PP2A). Serine/threonine phosphatase is the primary brain enzyme consisting of a structural A subunit, a catalytic C subunit, and one of the multiple regulatory B subunits that determine substrate specificity [198]. Carboxyl PP2A methylation is regulated by different PP2A-specific leucine carboxyl methyltransferase 1 (LCMT-1) and a PP2A-specific methyl-esterase (PME-1). The levels of these methylation regulatory enzymes are disturbed in the brains in PD, with low regulation of LCMT-1 and high regulation of PME-1, associated with reduced relative levels of methylated PP2A (methyl-PP2A), which is the enzymatically more active form [199]. In addition to the antioxidant effects present in the components of coffee [200], caffeine has shown protective effects on altered α -synuclein activity in PD [201]. In 2013, the treatment of transgenic mice with PD was reported; these mice were administered eicosanoyl-5-hydroxytryptamide (EHT), an inhibitor of PME-1 methyl esterase activity present in many types of coffee. The authors found increased brain methylation and PP2A phosphatase activity with reduced accumulation of phosphorylated α -synuclein aggregates with improved neuronal integrity and suppression of the neuroinflammatory response [202]. The study results suggest that EHT and caffeine have synergistic effects in protecting the brain against α -synuclein-mediated toxicity by maintaining active PP2A [203]. Decaffeinated coffee has even been found to have a protective effect in PD models in *Drosophila* [204]. Caffeine is one of the widely consumed purines (phytochemicals) that can contribute beneficial effects to the brain. Among the purines, caffeine is the most studied, theobromine and theophylline have been studied less, and other methylxanthines have been mostly unexplored. While caffeine's neurological effects are well established, it is unknown whether this purine alone is responsible for the beneficial effects of coffee consumption on cognition and resistance to neurodegenerative disorders. Emerging evidence suggests that other classes of phytochemicals present in large quantities in coffee may improve neuroplasticity and protect neurons against dysfunction and degeneration. Among the many nonpurine phytochemicals in coffee, flavonoids such as epicatechins have been shown to promote synaptic plasticity [205]. Growing evidence indicates that regular coffee consumption results in better cognitive performance during stressful conditions [206]. Acute caffeine intake improves performance on memory tasks [207]. A 150 mg dose of

caffeine was previously reported to improve cognitive performance for at least 10h, and caffeine is recommended in military rations [208]. Extensive longitudinal clinical studies have established an inverse relationship between coffee consumption and decreased memory during aging [209].

1.15. Other Phytochemicals in Parkinson's Disease. Interest in scientific research on the properties of natural antioxidants in chronic degenerative diseases has been steadily increasing over the past two decades [210]. Medicinal plants are the source of a wide variety of bioactive components with antioxidant and anti-inflammatory properties that can be useful as neuroprotective agents [211]. The neuroprotective molecular mechanisms of plant extracts include the elimination of toxins, antioxidant activity, and antiapoptotic effects [212, 213]. Berberine is one of the active components of different Chinese medicinal herbs, including *Hydrastis canadensis*, *Coptis chinensis*, *Berberis aquifolium*, and *Berberis vulgaris* [214]. Berberine has been used as a natural remedy to treat diarrhea, stomatitis [215], hepatitis [216], and hypoglycemic effect [217]. Studies have shown that berberine also has neuroprotective effects by regulating neurotrophin levels [218, 219]. Experimental PD models report that berberine prevents the loss of dopaminergic neurons and enhances motor balance and coordination with maximum effect at 50 mg/kg [220]. However, the long-term treatment with berberine has been associated with decreased dopamine levels and increased degeneration of dopaminergic neuronal cells and its loss in experimental models of PD in rats [221, 222].

Curcumin is a compound derived from the *Curcuma longa* plant that has been extensively researched for its antioxidant and anti-inflammatory properties [223]. *In vitro* studies report that the antioxidant properties of curcumin contribute to its neuroprotective effects [224]. Cognitive deficiencies have improved after the administration of curcumin due to increased levels of the brain-derived neurotrophic factor [225]. Curcumin also has beneficial effects on PD by destabilizing the α -synuclein protein [226]. A study in the *Drosophila* model of PD has shown that the administration of curcumin decreases ROS and neurodegenerative severity and improves motor skills [227].

Another bioactive molecule of natural products is quercetin. Quercetin is one of the main flavonoids widely distributed in apples, berries, onions, tea, tomatoes, and other plant products [228]. The antioxidant and anti-inflammatory properties of quercetin administration have been demonstrated in rat models [229, 230]. The administration of quercetin and piperine (a natural alkaloid) has potent neuroprotective effects against neurotoxicity in rat PD models [231].

2. Conclusions

PD is a common neurodegenerative disorder. PD incidence generally increases with age. Potential risk factors in developing PD include environmental toxins, drugs, pesticides, brain microtrauma, focal cerebrovascular damage, and genomic defects. Previous studies suggest that the intake of certain products may be associated with an increased risk of PD.

Many foods for daily consumption have benefits because of their content of amino acids, vitamins, minerals, and micronutrients. However, increased use of some prooxidant foods may increase the risk of developing or increasing PD symptoms. Processed meat is characterized by high sodium content, advanced glycation end-products, cholesterol, and free fatty acids. The overconsumption of meat conditions a prooxidant effect. The alteration or fragmentation of the structure of meat products can cause oxidation of proteins by carbonylation. On the other hand, fruits and vegetables stand out for their antioxidant effect due to their amounts of vitamins and minerals. The evidence about the beneficial effect of coffee intake and the health risk by consuming large amounts of chocolate in PD patients is noteworthy. Short-term, medium-term, and long-term follow-up clinical studies are required to establish the useful quantities of the food substances, alone or in combination, to determine the bioavailability and nutritional content of each type of food in PD.

Conflicts of Interest

The authors declare that they have no conflicts of interest.

References

- [1] J. C. Mayo, R. M. Sainz, D. X. Tan, I. Antolín, C. Rodríguez, and R. J. Reiter, "Melatonin and Parkinson's disease," *Endocrine*, vol. 27, no. 2, pp. 169–178, 2005.
- [2] F. N. Emamzadeh and A. Surguchov, "Parkinson's disease: biomarkers, treatment, and risk factors," *Frontiers in Neuroscience*, vol. 12, p. 612, 2018.
- [3] H. Ahmed, A. I. Abushouk, M. Gabr, A. Negida, and M. M. Abdel-Daim, "Parkinson's disease and pesticides: A meta-analysis of disease connection and genetic alterations," *Biomedicine & Pharmacotherapy*, vol. 90, pp. 638–649, 2017.
- [4] S. García, B. López, M. DEG, V. OAJ, and V. R. Coral, "Breve reseña histórica de la enfermedad de Parkinson. De la descripción precipitada de la enfermedad en el siglo XIX, a los avances en biología molecular del padecimiento," *Medicina Interna de México*, vol. 26, pp. 350–373, 2010.
- [5] A. Bellucci, N. B. Mercuri, A. Venneri et al., "Review: Parkinson's disease: from synaptic loss to connectome dysfunction," *Neuropathology and Applied Neurobiology*, vol. 42, no. 1, pp. 77–94, 2016.
- [6] A. Bellucci, M. Zaltieri, L. Navarria, J. Grigoletto, C. Missale, and P. Spano, "From α -synuclein to synaptic dysfunctions: New insights into the pathophysiology of Parkinson's disease," *Brain Research*, vol. 1476, pp. 183–202, 2012.
- [7] T. Bartels, J. G. Choi, and D. J. Selkoe, " α -Synuclein occurs physiologically as a helically folded tetramer that resists aggregation," *Nature*, vol. 477, no. 7362, pp. 107–110, 2011.
- [8] M. J. Volles and P. T. Lansbury, "Zeroing in on the pathogenic form of alpha-synuclein and its mechanism of neurotoxicity in Parkinson's disease," *Biochemistry*, vol. 42, no. 26, pp. 7871–7878, 2003.
- [9] A. Barzilai and E. Melamed, "Molecular mechanisms of selective dopaminergic neuronal death in Parkinson's disease," *Trends in Molecular Medicine*, vol. 9, no. 3, pp. 126–132, 2003.
- [10] S. D. Tabbal, L. Tian, M. Karimi, C. A. Brown, S. K. Loftin, and J. S. Perlmutter, "Low nigrostriatal reserve for motor

- parkinsonism in nonhuman primates," *Experimental Neurology*, vol. 237, no. 2, pp. 355–362, 2012.
- [11] L. Puspita, S. Y. Chung, and J. W. Shim, "Oxidative stress and cellular pathologies in Parkinson's disease," *Molecular Brain*, vol. 10, no. 1, p. 53, 2017.
- [12] G. G. Ortiz, F. P. Pacheco-Moisés, V. M. Gómez-Rodríguez, E. D. González-Renovato, E. D. Torres-Sánchez, and A. C. Ramírez-Anguiano, "Fish oil, melatonin and vitamin E attenuates midbrain cyclooxygenase-2 activity and oxidative stress after the administration of 1-methyl-4-phenyl-1,2,3,6-tetrahydropyridine," *Metabolic Brain Disease*, vol. 28, no. 4, pp. 705–709, 2013.
- [13] D. T. Dexter, F. R. Wells, F. Agid et al., "Increased Nigral Iron Content in Postmortem Parkinsonian Brain," *The Lancet*, vol. 2, no. 8569, pp. 1219–1220, 1987.
- [14] T. Q. Melo, S. J. C. V. M. Copray, and M. F. R. Ferrari, "Alpha-synuclein toxicity on protein quality control, mitochondria and endoplasmic reticulum," *Neurochemical Research*, vol. 43, no. 12, pp. 2212–2223, 2018.
- [15] G. G. Ortiz, M. E. Crespo-López, C. Morán-Moguel, J. J. García, R. J. Reiter, and D. Acuña-Castroviejo, "Protective role of melatonin against MPTP-induced mouse brain cell DNA fragmentation and apoptosis in vivo," *Neuroendocrinology letters*, vol. 22, no. 2, pp. 101–108, 2001.
- [16] D. T. Dexter, C. J. Carter, F. R. Wells et al., "Basal lipid peroxidation in substantia nigra is increased in Parkinson's disease," *Journal of Neurochemistry*, vol. 52, no. 2, pp. 381–389, 1989.
- [17] G. G. Ortiz, F. P. Pacheco-Moisés, M. A. Mireles-Ramírez et al., "Oxidative stress and Parkinson's disease: effects on environmental toxicology," in *Free Radicals and Diseases*, R. Ahmad, Ed., pp. 139–151, InTech, Rijeka, 2016.
- [18] Z. Qin, D. Hu, S. Han, S. H. Reaney, D. A. Di Monte, and A. L. Fink, "Effect of 4-hydroxy-2-nonenal modification on alpha-synuclein aggregation," *The Journal of Biological Chemistry*, vol. 282, no. 8, pp. 5862–5870, 2007.
- [19] A. Navarro, A. Boveris, M. J. Báñez et al., "Human brain cortex: mitochondrial oxidative damage and adaptive response in Parkinson disease and in dementia with Lewy bodies," *Free Radical Biology and Medicine*, vol. 46, no. 12, pp. 1574–1580, 2009.
- [20] C. Buhmann, S. Arlt, A. Kontush et al., "Plasma and CSF markers of oxidative stress are increased in Parkinson's disease and influenced by antiparkinsonian medication," *Neurobiology of Disease*, vol. 15, no. 1, pp. 160–170, 2004.
- [21] C. H. Canugovi, M. Misiak, L. K. Ferrarelli, D. L. Croteau, and V. A. Bohr, "The role of DNA repair in brain related disease pathology," *DNA Repair*, vol. 12, no. 8, pp. 578–587, 2013.
- [22] C. Isobe, T. Abe, and Y. Terayama, "Levels of reduced and oxidized coenzymeQ-10 and 8-hydroxy-2'-deoxyguanosine in the cerebrospinal fluid of patients with living Parkinson's disease demonstrate that mitochondrial oxidative damage and/or oxidative DNA damage contributes to the neurodegenerative process," *Neuroscience Letters*, vol. 469, no. 1, pp. 159–163, 2010.
- [23] M. Dizdaroglu, "Base-excision repair of oxidative DNA damage by DNA glycosylases," *Mutation Research/Fundamental and Molecular Mechanisms of Mutagenesis*, vol. 591, no. 1–2, pp. 45–59, 2005.
- [24] J. H. J. Hoeijmakers, "Genome maintenance mechanisms for preventing cancer," *Nature*, vol. 411, no. 6835, pp. 366–374, 2001.
- [25] R. Floyd and K. Hensley, "Oxidative stress in brain aging: Implications for therapeutics of neurodegenerative diseases," *Neurobiology of Aging*, vol. 23, no. 5, pp. 795–807, 2002.
- [26] D. E. Barnes and T. Lindahl, "Repair and genetic consequences of endogenous DNA base damage in mammalian cells," *Annual Review of Genetics*, vol. 38, no. 1, pp. 445–476, 2004.
- [27] D. M. Wilson 3rd and V. A. Bohr, "The mechanics of base excision repair, and its relationship to aging and disease," *DNA Repair*, vol. 6, no. 4, pp. 544–559, 2007.
- [28] G. L. Dianov, K. M. Sleeth, I. I. Dianova, and S. L. Allinson, "Repair of abasic sites in DNA," *Mutation Research/Fundamental and Molecular Mechanisms of Mutagenesis*, vol. 531, no. 1–2, pp. 157–163, 2003.
- [29] M. L. Hegde, T. K. Hazra, and S. Mitra, "Early steps in the DNA base excision/single-strand interruption repair pathway in mammalian cells," *Cell Research*, vol. 18, no. 1, pp. 27–47, 2008.
- [30] J. Hu, N. C. de Souza-Pinto, K. Haraguchi et al., "Repair of formamidopyrimidines in DNA involves different glycosylases: role of the OGG1, NTH1, and NEIL1 enzymes," *The Journal of Biological Chemistry*, vol. 280, no. 49, pp. 40544–40551, 2005.
- [31] H. Ide and M. Kotera, "Human DNA glycosylases involved in the repair of oxidatively damaged DNA," *Biological & Pharmaceutical Bulletin*, vol. 27, no. 4, pp. 480–485, 2004.
- [32] M. A. Kalam, K. Haraguchi, S. Chandani et al., "Genetic effects of oxidative DNA damages: comparative mutagenesis of the imidazole ring-opened formamidopyrimidines (Fapy lesions) and 8-oxo-purines in simian kidney cells," *Nucleic Acids Research*, vol. 34, no. 8, pp. 2305–2315, 2006.
- [33] W. Dauer and S. Przedborski, "Parkinson's Disease: Mechanisms and Models," *Neuron*, vol. 39, no. 6, pp. 889–909, 2003.
- [34] G. Benzi and A. Moretti, "Are reactive oxygen species involved in Alzheimer's disease?," *Neurobiology of Aging*, vol. 16, no. 4, pp. 661–674, 1995.
- [35] H. P. Indo, H. C. Yen, I. Nakanishi et al., "A mitochondrial superoxide theory for oxidative stress diseases and aging," *Journal of Clinical Biochemistry and Nutrition*, vol. 56, no. 1, pp. 1–7, 2015.
- [36] A. C. Rego and C. R. Oliveira, "Mitochondrial dysfunction and reactive oxygen species in excitotoxicity and apoptosis: implications for the pathogenesis of neurodegenerative diseases," *Neurochemical Research*, vol. 28, no. 10, pp. 1563–1574, 2003.
- [37] H. Wiseman and B. Halliwell, "Damage to DNA by reactive oxygen and nitrogen species: role in inflammatory disease and progression to cancer," *Biochemical Journal*, vol. 313, no. 1, pp. 17–29, 1996.
- [38] E. Floor and M. G. Wetzel, "Increased protein oxidation in human substantia nigra pars compacta in comparison with basal ganglia and prefrontal cortex measured with an improved dinitrophenylhydrazine assay," *Journal of Neurochemistry*, vol. 70, no. 1, pp. 268–275, 1998.
- [39] A. Rahal, A. Kumar, V. Singh et al., "Oxidative Stress, Prooxidants, and Antioxidants: The Interplay," *BioMed Research International*, vol. 2014, Article ID 761264, 19 pages, 2014.
- [40] B. L. Tan, M. E. Norhaizan, and W.-P.-P. Liew, "Nutrients and oxidative stress: friend or foe?," *Oxidative Medicine and Cellular Longevity*, vol. 2018, Article ID 9719584, 24 pages, 2018.

- [41] P. M. de Castro Cardoso and P. A. F. dos Reis Baltazar Vicente, "Meat nutritional composition and nutritive role in the human diet," *Meat Science*, vol. 93, no. 3, pp. 586–592, 2013.
- [42] J. T. Willerson and P. M. Ridker, "Inflammation as a cardiovascular risk factor," *Circulation*, vol. 109, 21_supplement_1, pp. II-2–II-10, 2004.
- [43] K. Nowotny, D. Schröter, M. Schreiner, and T. Grune, "Dietary advanced glycation end products and their relevance for human health," *Ageing Research Reviews*, vol. 47, pp. 55–66, 2018.
- [44] L. Kaur, E. Maudens, D. R. Haisman, M. J. Boland, and H. Singh, "Microstructure and protein digestibility of beef: the effect of cooking conditions as used in stews and curries," *LWT - Food Science and Technology*, vol. 55, no. 2, pp. 612–620, 2014.
- [45] M. Fedorova, R. C. Bollineni, and R. Hoffmann, "Protein carbonylation as a major hallmark of oxidative damage: update of analytical strategies," *Mass Spectrometry Reviews*, vol. 33, no. 2, pp. 79–97, 2014.
- [46] O. P. Soladoye, M. L. Juarez, J. L. Aalhus, P. Shand, and M. Estevez, "Protein oxidation in processed meat: mechanisms and potential implications on human health," *Comprehensive Reviews in Food Science and Food Safety*, vol. 14, no. 2, pp. 106–122, 2015.
- [47] M. Estévez and C. Luna, "Dietary protein oxidation: a silent threat to human health?," *Critical Reviews in Food Science and Nutrition*, vol. 57, no. 17, pp. 3781–3793, 2017.
- [48] A. Keshavarzian, A. Banan, A. Farhadi et al., "Increases in free radicals and cytoskeletal protein oxidation and nitration in the colon of patients with inflammatory bowel disease," *Gut*, vol. 52, no. 5, pp. 720–728, 2003.
- [49] Y.-Y. Ding, Z.-Q. Li, X.-R. Cheng et al., "Dityrosine administration induces dysfunction of insulin secretion accompanied by diminished thyroid hormones T₃ function in pancreas of mice," *Amino Acids*, vol. 49, no. 8, pp. 1401–1414, 2017.
- [50] T. J. Wang, D. Ngo, N. Psychogios et al., "2-Amino adipic acid is a biomarker for diabetes risk," *Journal of Clinical Investigations*, vol. 123, no. 10, pp. 4309–4317, 2013.
- [51] E. Shacter, "Quantification and significance of protein oxidation in biological samples," *Drug Metabolism Reviews*, vol. 32, no. 3-4, pp. 307–326, 2000.
- [52] D. A. Butterfield and C. M. Lauderback, "Lipid peroxidation and protein oxidation in Alzheimer's disease brain: potential causes and consequences involving amyloid β -peptide-associated free radical oxidative stress 1, 2," *Free Radical Biology and Medicine*, vol. 32, no. 11, pp. 1050–1060, 2002.
- [53] E. R. Stadtman, "Protein oxidation and aging," *Free radical research*, vol. 40, no. 12, pp. 1250–1258, 2009.
- [54] H. Gurer-Orhan, N. Ercal, S. Mare, S. Pennathur, H. Orhan, and J. W. Heinecke, "Misincorporation of free *m*-tyrosine into cellular proteins: a potential cytotoxic mechanism for oxidized amino acids," *Biochemical Journal*, vol. 395, no. 2, pp. 277–284, 2006.
- [55] M. Repici and F. Giorgini, "DJ-1 in Parkinson's disease: clinical insights and therapeutic perspectives," *Journal of Clinical Medicine*, vol. 8, no. 9, 2019.
- [56] J. Choi, M. C. Sullards, J. A. Olzmann et al., "Oxidative damage of DJ-1 is linked to sporadic Parkinson and Alzheimer diseases," *Journal of Biological Chemistry*, vol. 281, no. 16, pp. 10816–10824, 2006.
- [57] L. F. Burbulla, P. Song, J. R. Mazzulli et al., "Dopamine oxidation mediates mitochondrial and lysosomal dysfunction in Parkinson's disease," *Science*, vol. 357, no. 6357, pp. 1255–1261, 2017.
- [58] A. Meynier and C. Genot, "Molecular and structural organization of lipids in foods: their fate during digestion and impact in nutrition," *OCL, Oilseeds Fats Crops and Lipids*, vol. 24, no. 2, 2017.
- [59] J. D. Wood, R. I. Richardson, G. R. Nute et al., "Effects of fatty acids on meat quality: a review," *Meat Science*, vol. 66, no. 1, pp. 21–32, 2004.
- [60] B. Min and D. U. Ahn, "Mechanism of lipid peroxidation in meat and meat products—a review," *Food Science Biotechnology*, vol. 14, pp. 152–163, 2005.
- [61] J. M. Lorenzo and M. Gómez, "Shelf life of fresh foal meat under MAP, overwrap and vacuum packaging conditions," *Meat Science*, vol. 92, no. 4, pp. 610–618, 2012.
- [62] K. Eder and R. Ringseis, "Health aspects of oxidized dietary fats," in *Oxidation in Foods and Beverages and Antioxidant Applications. Understanding Mechanisms of Oxidation and Antioxidant Activity*, E. A. Decker, R. J. Elias, and D. J. McClements, Eds., vol. 1, pp. 143–180, Woodhead Publishing Ltd, Cambridge, UK, 2010.
- [63] E. Boselli, M. T. Rodriguez-Estrada, G. Fedrizzi, and M. F. Caboni, "Cholesterol photosensitized oxidation of beef meat under standard and modified atmosphere at retail conditions," *Meat Science*, vol. 81, no. 1, pp. 224–229, 2009.
- [64] E. Novelli, E. Zanardi, G. P. Ghiretti et al., "Lipid and cholesterol oxidation in frozen stored pork, salame milano and mortadella," *Meat Science*, vol. 48, no. 1-2, pp. 29–40, 1998.
- [65] K. Shozen, T. Ohshima, H. Ushio, A. Takiguchi, and C. Koizumi, "Effects of antioxidants and packing on cholesterol oxidation in processed anchovy during storage," *LWT - Food Science and Technology*, vol. 30, no. 1, pp. 2–8, 1997.
- [66] J. E. Pie, K. Spahis, and C. Seillan, "Evaluation of oxidative degradation of cholesterol in food and food ingredients: identification and quantification of cholesterol oxides," *Journal of Agricultural and Food Chemistry*, vol. 38, no. 4, pp. 973–979, 1990.
- [67] N. Udilova, D. Jurek, B. Marian, L. Gille, R. Schulte-Hermann, and H. Nohl, "Induction of lipid peroxidation in biomembranes by dietary oil components," *Food and Chemical Toxicology*, vol. 41, no. 11, pp. 1481–1489, 2003.
- [68] R. Pamplona, "Advanced lipoxidation end-products," *Chemico-Biological Interactions*, vol. 192, no. 1-2, pp. 14–20, 2011.
- [69] T. Koschinsky, C. J. He, T. Mitsuhashi et al., "Orally absorbed reactive glycation products (glycotoxins): an environmental risk factor in diabetic nephropathy," *Proceedings of the National Academy of Sciences*, vol. 94, no. 12, pp. 6474–6479, 1997.
- [70] J. Kanner, "Dietary advanced lipid oxidation end-products are risk factors to human health," *Molecular Nutrition & Food Research*, vol. 51, no. 9, pp. 1094–1101, 2007.
- [71] J. W. Baynes, "Dietary ALEs are a risk to human health—NOT!," *Molecular Nutrition & Food Research*, vol. 51, no. 9, pp. 1102–1106, 2007.
- [72] J. K. Morris, G. L. Bomhoff, J. A. Stanford, and P. C. Geiger, "Neurodegeneration in an animal model of Parkinson's disease is exacerbated by a high-fat diet," *American Journal of*

- Physiology-Regulatory, Integrative and Comparative Physiology*, vol. 299, no. 4, pp. R1082–R1090, 2010.
- [73] M. Bousquet, I. St-Amour, M. Vandal, P. Julien, F. Cicchetti, and F. Calon, “High-fat diet exacerbates MPTP-induced dopaminergic degeneration in mice,” *Neurobiology of Disease*, vol. 45, pp. 529–538, 2012.
- [74] C. Anderson, H. Checkoway, G. M. Franklin, S. Beresford, T. Smith-Weller, and P. D. Swanson, “Dietary factors in Parkinson’s disease: the role of food groups and specific foods,” *Movement Disorders*, vol. 14, no. 1, pp. 21–27, 1999.
- [75] H. Chen, S. M. Zhang, M. A. Hernan, W. C. Willett, and A. Ascherio, “Diet and Parkinson’s disease: a potential role of dairy products in men,” *Annals of Neurology*, vol. 52, no. 6, pp. 793–801, 2002.
- [76] K. M. Powers, T. Smith-Weller, G. M. Franklin, W. T. Longstreth, P. D. Swanson, and H. Checkoway, “Parkinson’s disease risks associated with dietary iron, manganese, and other nutrient intakes,” *Neurology*, vol. 60, no. 11, pp. 1761–1766, 2003.
- [77] H. Chen, S. M. Zhang, M. A. Hernán, W. C. Willett, and A. Ascherio, “Dietary intakes of fat and risk of Parkinson’s disease,” *American Journal of Epidemiology*, vol. 157, no. >11, pp. 1007–1014, 2003.
- [78] J. Dong, J. D. Beard, D. M. Umbach et al., “Dietary fat intake and risk for Parkinson’s disease,” *Movement Disorders*, vol. 29, no. 13, pp. 1623–1630, 2014.
- [79] M. C. L. Phillips, D. K. J. Murtagh, L. J. Gilbertson, F. J. S. Asztely, and C. D. P. Lynch, “Low-fat versus ketogenic diet in Parkinson’s disease: a pilot randomized controlled trial,” *Movement Disorders*, vol. 33, no. 8, pp. 1306–1314, 2018.
- [80] S. Hernando, C. Requejo, E. Herran et al., “Beneficial effects of n-3 polyunsaturated fatty acids administration in a partial lesion model of Parkinson’s disease: The role of glia and Nrf2 regulation,” *Neurobiology of Disease*, vol. 121, pp. 252–262, 2019.
- [81] H. Y. Kim, M. Akbar, and K. Y. Kim, “Inhibition of neuronal apoptosis by polyunsaturated fatty acids,” *Journal of Molecular Neuroscience*, vol. 16, no. 2-3, pp. 223–228, 2001.
- [82] M. A. Mori, A. M. Delattre, B. Carabelli et al., “Neuroprotective effect of omega-3 polyunsaturated fatty acids in the 6-OHDA model of Parkinson’s disease is mediated by a reduction of inducible nitric oxide synthase,” *Nutritional Neuroscience*, vol. 21, no. 5, pp. 341–351, 2017.
- [83] M. K. Piya, P. G. McTernan, and S. Kumary, “Adipokine inflammation and insulin resistance: the role of glucose, lipids and endotoxin,” *Journal of Endocrinology*, vol. 216, no. 1, pp. T1–T15, 2013.
- [84] F. Turati, C. Galeone, S. Gandini et al., “High glycemic index and glycemic load are associated with moderately increased cancer risk,” *Molecular Nutrition & Food Research*, vol. 59, no. 7, pp. 1384–1394, 2015.
- [85] L. Schwingshackl and G. Hoffmann, “Long-term effects of low glycemic index/load vs. high glycemic index/load diets on parameters of obesity and obesity-associated risks: a systematic review and meta-analysis,” *Nutrition, Metabolism and Cardiovascular Diseases*, vol. 23, no. 8, pp. 699–706, 2013.
- [86] E. A. Hu, A. Pan, V. Malik, and Q. Sun, “White rice consumption and risk of type 2 diabetes: meta-analysis and systematic review,” *BMJ*, vol. 344, no. mar15 3, article e1454, 2012.
- [87] A. Nanri, T. Mizoue, M. Noda et al., “Rice intake and type 2 diabetes in Japanese men and women: the Japan Public Health Center-based prospective study,” *American Journal of Clinical Nutrition*, vol. 92, no. 6, pp. 1468–1477, 2010.
- [88] J. J. DiNicolantonio, J. H. O’Keefe, and S. C. Lucan, “Added Fructose: A Principal Driver of Type 2 Diabetes Mellitus and Its Consequences,” *Mayo Clinic Proceedings*, vol. 90, no. 3, pp. 372–381, 2015.
- [89] F. B. Hu and V. S. Malik, “Sugar-sweetened beverages and risk of obesity and type 2 diabetes: epidemiologic evidence,” *Physiology & Behavior*, vol. 100, no. 1, pp. 47–54, 2010.
- [90] J. S. Teodoro, F. V. Duarte, A. P. Gomes et al., “Berberine reverts hepatic mitochondrial dysfunction in high-fat fed rats: a possible role for Sirt3 activation,” *Mitochondrion*, vol. 13, no. 6, pp. 637–646, 2013.
- [91] M. Brownlee, “The pathobiology of diabetic complications: a unifying mechanism,” *Diabetes*, vol. 54, no. 6, pp. 1615–1625, 2005.
- [92] A. Shah, L. Xia, H. Goldberg, K. W. Lee, S. E. Quaggin, and I. G. Fantus, “Thioredoxin-interacting protein mediates high glucose-induced reactive oxygen species generation by mitochondria and the NADPH oxidase, Nox4, in mesangial cells,” *Journal of Biological Chemistry*, vol. 288, no. 10, pp. 6835–6848, 2013.
- [93] A. Alzamendi, A. Giovambattista, A. Raschia et al., “Fructose-rich diet-induced abdominal adipose tissue endocrine dysfunction in normal male rats,” *Endocrine*, vol. 35, no. 2, pp. 227–232, 2009.
- [94] F. Francini, M. C. Castro, G. Schinella et al., “Changes induced by a fructose-rich diet on hepatic metabolism and the antioxidant system,” *Life Sciences*, vol. 86, no. 25-26, pp. 965–971, 2010.
- [95] L. Ishihara and C. Brayne, “A systematic review of nutritional risk factors of Parkinson’s disease,” *Nutrition Research Reviews*, vol. 18, no. 2, pp. 259–282, 2005.
- [96] K. Murakami, Y. Miyake, S. Sasaki et al., “Dietary glycemic index is inversely associated with the risk of Parkinson’s disease: A case-control study in Japan,” *Nutrition*, vol. 26, no. 5, pp. 515–521, 2010.
- [97] H. B. AlEsa, S. N. Bhupathiraju, V. S. Malik et al., “Carbohydrate quality and quantity and risk of type 2 diabetes in US women,” *The American Journal of Clinical Nutrition*, vol. 102, no. 6, pp. 1543–1553, 2015.
- [98] S. Oba, For the Japan Public Health Center-based Prospective Study Group, A. Nanri et al., “Dietary glycemic index, glycemic load and incidence of type 2 diabetes in Japanese men and women: the Japan Public Health Center-based prospective study,” *Nutrition Journal*, vol. 12, no. 1, p. 165, 2013.
- [99] J. A. Santiago and J. A. Potashkin, “Shared dysregulated pathways lead to Parkinson’s disease and diabetes,” *Trends in Molecular Medicine*, vol. 19, no. 3, pp. 176–186, 2013.
- [100] V. Kotagal, R. L. Albin, M. L. T. M. Müller, R. A. Koeppe, K. A. Frey, and N. I. Bohnen, “Diabetes is associated with postural instability and gait difficulty in Parkinson disease,” *Parkinsonism & Related Disorders*, vol. 19, no. 5, pp. 522–526, 2013.
- [101] N. Palacios, X. Gao, M. L. McCullough et al., “Obesity, diabetes, and risk of Parkinson’s disease,” *Movement Disorders*, vol. 26, no. 12, pp. 2253–2259, 2011.
- [102] K. C. Simon, H. Chen, M. Schwarzschild, and A. Ascherio, “Hypertension, hypercholesterolemia, diabetes, and risk of

- Parkinson disease," *Neurology*, vol. 69, no. 17, pp. 1688–1695, 2007.
- [103] G. G. Ortiz, E. W. Moráles-Sánchez, F. P. Pacheco-Moisés et al., "Effect of melatonin administration on cyclooxygenase-2 activity, serum levels of nitric oxide metabolites, lipoperoxides and glutathione peroxidase activity in patients with Parkinson's disease," *Gaceta medica de Mexico*, vol. 153, Supplement 2, pp. S72–S81, 2017.
- [104] B. Halliwell, "Reactive oxygen species and the central nervous system," *Journal of Neurochemistry*, vol. 59, no. 5, pp. 1609–1623, 1992.
- [105] R. K. B. Pearce, A. Owen, S. Daniel, P. Jenner, and C. D. Marsden, "Alterations in the distribution of glutathione in the substantia nigra in Parkinson's disease," *Journal of Neural Transmission*, vol. 104, no. 6-7, pp. 661–677, 1997.
- [106] A. Rahimmi, F. Khosrobakhsh, E. Izadpanah, M. R. Moloudi, and K. Hassanzadeh, "N-acetylcysteine prevents rotenone-induced Parkinson's disease in rat: An investigation into the interaction of parkin and Drp1 proteins," *Brain Research Bulletin*, vol. 113, pp. 34–40, 2015.
- [107] U. Wüllner, P.-A. Löschmann, J. B. Schulz et al., "Glutathione depletion potentiates MPTP and MPP+ toxicity in nigral dopaminergic neurones," *NeuroReport*, vol. 7, no. 4, pp. 921–923, 1996.
- [108] J. T. Rotruck, A. L. Pope, H. E. Ganther, A. B. Swanson, D. G. Hafeman, and W. G. Hoekstra, "Selenium: biochemical role as a component of glutathione peroxidase," *Science*, vol. 179, no. 4073, pp. 588–590, 1973.
- [109] H. Wang, E. Cheng, S. Brooke, P. Chang, and R. Sapolsky, "Over-expression of antioxidant enzymes protects cultured hippocampal and cortical neurons from necrotic insults," *Journal of Neurochemistry*, vol. 87, no. 6, pp. 1527–1534, 2003.
- [110] G. Trépanier, D. Furling, J. Puymirat, and M. E. Mirault, "Immunocytochemical localization of seleno-glutathione peroxidase in the adult mouse brain," *Neuroscience*, vol. 75, no. 1, pp. 231–243, 1996.
- [111] S. H. Kim, S. H. Kim, J. H. Lee et al., "Superoxide dismutase gene (SOD1, SOD2, and SOD3) polymorphisms and anti-tuberculosis drug-induced hepatitis," *Allergy Asthma & Immunology Research*, vol. 7, no. 1, pp. 88–91, 2015.
- [112] J. M. McCord and I. Fridovich, "Superoxide dismutase. An enzymic function for erythrocuprein (hemocuprein)," *The Journal of biological chemistry*, vol. 244, no. 22, pp. 6049–6055, 1969.
- [113] J. Lindenau, H. Noack, H. Possel, K. Asayama, and G. Wolf, "Cellular distribution of superoxide dismutases in the rat CNS," *Glia*, vol. 29, no. 1, pp. 25–34, 2000.
- [114] N. Kurobe, F. Suzuki, K. Okajima, and K. Kato, "Sensitive enzyme immunoassay for human Cu/Zn superoxide dismutase," *Clinica Chimica Acta*, vol. 187, no. 1, pp. 11–20, 1990.
- [115] P. Milani, G. Ambrosi, O. Gammoh, F. Blandini, and C. Cereda, "SOD1 and DJ-1 converge at Nrf2 pathway: a clue for antioxidant therapeutic potential in neurodegeneration," *Oxidative Medicine and Cellular Longevity*, vol. 2013, Article ID 836760, 12 pages, 2013.
- [116] J. Choi, H. D. Rees, S. T. Weintraub, A. I. Levey, L. S. Chin, and L. Li, "Oxidative modifications and aggregation of Cu,Zn-superoxide dismutase associated with Alzheimer and Parkinson diseases," *Journal of Biological Chemistry*, vol. 280, no. 12, pp. 11648–11655, 2005.
- [117] E. Belluzzi, M. Bisaglia, E. Lazzarini, L. C. Tabares, M. Beltramini, and L. Bubacco, "Human SOD2 modification by dopamine quinones affects enzymatic activity by promoting its aggregation: possible implications for Parkinson's disease," *PLoS One*, vol. 7, no. 6, article e38026, 2012.
- [118] R. Hardeland and B. Poeggeler, "Non-vertebrate melatonin," *J Pineal Res.*, vol. 34, no. 4, pp. 233–241, 2003.
- [119] M. Sae-Teaw, J. Johns, N. P. Johns, and S. Subongkot, "Serum melatonin levels and antioxidant capacities after consumption of pineapple, orange, or banana by healthy male volunteers," *Journal of Pineal Research*, vol. 55, no. 1, pp. 58–64, 2013.
- [120] D. X. Tan, B. M. Zanghi, L. C. Manchester, and R. J. Reiter, "Melatonin identified in meats and other food stuffs: potentially nutritional impact," *Journal of Pineal Research*, vol. 57, no. 2, pp. 213–218, 2014.
- [121] Y. Aguilera, T. Herrera, V. Benitez et al., "Estimation of scavenging capacity of melatonin and other antioxidants: contribution and evaluation in germinated seeds," *Food Chemistry*, vol. 170, pp. 203–211, 2015.
- [122] X. Meng, Y. Li, S. Li et al., "Dietary sources and bioactivities of melatonin," *Nutrients*, vol. 9, no. 4, p. 367, 2017.
- [123] A. Carrillo-Vico, R. J. Reiter, P. J. Lardone et al., "The modulatory role of melatonin on immune responsiveness," *Current Opinion in Investigational Drugs*, vol. 7, no. 5, pp. 423–431, 2006.
- [124] F. Li, S. Li, H. B. Li et al., "Antiproliferative activity of peels, pulps and seeds of 61 fruits," *Journal of Functional Foods*, vol. 5, no. 3, pp. 1298–1309, 2013.
- [125] E. Sewerynek, "Melatonin and the cardiovascular system," *Neuroendocrinology Letters*, vol. 23, no. 1, pp. 79–83, 2002.
- [126] E. Sofic, Z. Rimpapa, Z. Kundurovic et al., "Antioxidant capacity of the neurohormone melatonin," *Journal of Neural Transmission*, vol. 112, no. 3, pp. 349–358, 2005.
- [127] V. Srinivasan, S. R. Pandi-Perumal, D. P. Cardinali, B. Poeggeler, and R. Hardeland, "Melatonin in Alzheimer's disease and other neurodegenerative disorders," *Behavioral and Brain Functions*, vol. 2, no. 1, p. 15, 2006.
- [128] R. Sandyk, "Pineal melatonin functions: possible relevance to Parkinson's disease," *International Journal of Neuroscience*, vol. 50, no. 1-2, pp. 37–54, 2009.
- [129] N. Adi, D. C. Mash, Y. Ali, C. Singer, L. Shehadeh, and S. Papapetropoulos, "Melatonin MT₁ and MT₂ receptor expression in Parkinson's disease," *Medical Science Monitor*, vol. 16, no. 2, pp. BR61–BR67, 2010.
- [130] R. J. Reiter, D. X. Tan, and A. Galano, "Melatonin: exceeding expectations," *Physiology*, vol. 29, no. 5, pp. 325–333, 2014.
- [131] C. Rodriguez, J. C. Mayo, R. M. Sainz et al., "Regulation of antioxidant enzymes: a significant role for melatonin," *Journal of Pineal Research*, vol. 36, no. 1, pp. 1–9, 2004.
- [132] V. Tapias, G. Escames, L. C. López et al., "Melatonin and its brain metabolite N¹-acetyl-5-methoxykynuramine prevent mitochondrial nitric oxide synthase induction in parkinsonian mice," *Journal of Neuroscience Research*, vol. 87, no. 13, pp. 3002–3010, 2009.
- [133] J. C. Mayo, R. M. Sainz, H. Uria, I. Antolin, M. M. Esteban, and C. Rodriguez, "Melatonin prevents apoptosis induced by 6-hydroxydopamine in neuronal cells: implications for Parkinson's disease," *Journal of Pineal Research*, vol. 24, no. 3, pp. 179–192, 1998.

- [134] B. K. Jin, D. Y. Shin, M. Y. Jeong et al., "Melatonin protects nigral dopaminergic neurons from 1-methyl-4-phenylpyridinium (MPP⁺) neurotoxicity in rats," *Neuroscience Letters*, vol. 245, no. 2, pp. 61–64, 1998.
- [135] T. B. Bassani, R. W. Gradowski, T. Zaminelli et al., "Neuroprotective and antidepressant-like effects of melatonin in a rotenone-induced Parkinson's disease model in rats," *Brain Research*, vol. 1593, pp. 95–105, 2014.
- [136] G. A. Dowling, J. Mastick, E. Colling, J. H. Carter, C. M. Singer, and M. J. Aminoff, "Melatonin for sleep disturbances in Parkinson's disease," *Sleep Medicine*, vol. 6, no. 5, pp. 459–466, 2005.
- [137] V. Srinivasan, D. De Berardis, T. Partonen, R. Zakaria, and Z. Othman, "The use of melatonin for treating sleep disorders in patients with Parkinson's disease," *ChronoPhysiology and Therapy*, vol. 4, pp. 51–57, 2014.
- [138] C. A. M. Medeiros, P. F. C. de Bruin, L. A. Lopes, M. C. Magalhães, M. de Lourdes Seabra, and V. M. S. de Bruin, "Effect of exogenous melatonin on sleep and motor dysfunction in Parkinson's disease," *Journal of Neurology*, vol. 254, no. 4, pp. 459–464, 2007.
- [139] R. Medina-Navarro, G. Duran-Reyes, and J. J. Hicks, "Pro-oxidating properties of melatonin in the in vitro interaction with the singlet oxygen," *Endocrine Research*, vol. 25, no. 3–4, pp. 263–280, 2009.
- [140] M. Buyukavci, O. Ozdemir, S. Buck, M. Stout, Y. Ravindranath, and S. Savasan, "Melatonin cytotoxicity in human leukemia cells: relation with its pro-oxidant effect," *Fundamental and Clinical Pharmacology*, vol. 20, no. 1, pp. 73–79, 2006.
- [141] K. L. Clapp-Lilly, M. A. Smith, G. Perry, P. L. Harris, X. Zhu, and L. K. Duffy, "Melatonin acts as antioxidant and pro-oxidant in an organotypic slice culture model of Alzheimer's disease," *Neuroreport*, vol. 12, no. 6, pp. 1277–1280, 2001.
- [142] F. Radogna, L. Paternoster, M. De Nicola et al., "Rapid and transient stimulation of intracellular reactive oxygen species by melatonin in normal and tumor leukocytes," *Toxicology and Applied Pharmacology*, vol. 239, no. 1, pp. 37–45, 2009.
- [143] D. Sánchez-Hernández, G. H. Anderson, A. N. Poon et al., "Maternal fat-soluble vitamins, brain development, and regulation of feeding behavior: an overview of research," *Nutrition Research*, vol. 36, no. 10, pp. 1045–1054, 2016.
- [144] J. Chawla and D. Kvarnberg, "Hydrosoluble vitamins," *Neurologic Aspects of Systemic Disease Part II*, vol. 120, pp. 891–914, 2014.
- [145] X. Zhao, M. Zhang, C. Li, X. Jiang, Y. Su, and Y. Zhang, "Benefits of vitamins in the treatment of Parkinson's disease," *Oxidative Medicine and Cellular Longevity*, vol. 2019, Article ID 942686, 14 pages, 2019.
- [146] H. E. Sauberlich, "Implications of nutritional status on human biochemistry, physiology, and health," *Clinical Biochemistry*, vol. 17, no. 2, pp. 132–142, 1984.
- [147] K. Mikkelsen, L. Stojanovska, K. Tangalakis, M. Bosevski, and V. Apostolopoulos, "Cognitive decline: a vitamin B perspective," *Maturitas*, vol. 93, pp. 108–113, 2016.
- [148] T. Fukushima, "Niacin metabolism and Parkinson's disease," *Environmental Health and Preventive Medicine*, vol. 10, no. 1, pp. 3–8, 2005.
- [149] K. Aoyama, K. Matsubara, M. Kondo et al., "Nicotinamide-N-methyltransferase is higher in the lumbar cerebrospinal fluid of patients with Parkinson's disease," *Neuroscience Letters*, vol. 298, no. 1, pp. 78–80, 2001.
- [150] S. M. Griffin, M. R. Pickard, R. P. Orme, C. P. Hawkins, and R. A. Fricker, "Nicotinamide promotes neuronal differentiation of mouse embryonic stem cells *in vitro*," *NeuroReport*, vol. 24, no. 18, pp. 1041–1046, 2013.
- [151] H. M. Oudemans-van Straaten, A. M. Spoelstra-de Man, and M. C. de Waard, "Vitamin C revisited," *Critical Care*, vol. 18, no. 4, 2014.
- [152] G. Grosso, R. Bei, A. Mistretta et al., "Effects of vitamin C on health: a review of evidence," *Frontiers in Bioscience*, vol. 18, no. 3, 2013.
- [153] N. Smirnoff, "Ascorbic acid metabolism and functions: a comparison of plants and mammals," *Free Radical Biology and Medicine*, vol. 122, pp. 116–129, 2018.
- [154] S. K. Jaiswal, V. K. Gupta, M. D. Ansari, N. J. Siddiqi, and B. Sharma, "Vitamin C acts as a hepatoprotectant in carbofuran treated rat liver slices *in vitro*," *Toxicology Reports*, vol. 4, no. 4, pp. 265–273, 2017.
- [155] A. L. Peterson, M. Mancini, and F. B. Horak, "The relationship between balance control and vitamin D in Parkinson's disease—a pilot study," *Movement Disorders*, vol. 28, no. 8, pp. 1133–1137, 2013.
- [156] D. W. Eyles, S. Smith, R. Kinobe, M. Hewison, and J. J. McGrath, "Distribution of the Vitamin D receptor and 1 α -hydroxylase in human brain," *Journal of Chemical Neuroanatomy*, vol. 29, no. 1, pp. 21–30, 2005.
- [157] I. Sleeman, T. Aspray, R. Lawson et al., "The role of vitamin D in disease progression in early Parkinson's disease," *Journal of Parkinson's Disease*, vol. 7, no. 4, pp. 669–675, 2017.
- [158] Z. Zhou, R. Zhou, Z. Zhang, and K. Li, "The association between vitamin D status, vitamin D supplementation, sunlight exposure, and Parkinson's disease: a systematic review and meta-analysis," *Medical Science Monitor*, vol. 25, pp. 666–674, 2019.
- [159] S. Graf, S. Egert, and M. Heer, "Effects of whey protein supplements on metabolism: evidence from human intervention studies," *Current Opinion in Clinical Nutrition and Metabolic Care*, vol. 14, no. 6, pp. 569–580, 2011.
- [160] S. Svanborg, A. G. Johansen, R. K. Abrahamsen, and S. B. Skeie, "The composition and functional properties of whey protein concentrates produced from buttermilk are comparable with those of whey protein concentrates produced from skimmed milk," *Journal of Dairy Science*, vol. 98, no. 9, pp. 5829–5840, 2015.
- [161] A. Haug, A. T. Høstmark, and O. M. Harstad, "Bovine milk in human nutrition—a review," *Lipids in Health and Disease*, vol. 6, no. 1, p. 25, 2007.
- [162] Y. W. Park and M. S. Nam, "Bioactive peptides in milk and dairy products: a review," *Korean Journal for Food Science of Animal Resources*, vol. 35, no. 6, pp. 831–840, 2015.
- [163] H. Ebaid, A. Salem, A. Sayed, and A. Metwalli, "Whey protein enhances normal inflammatory responses during cutaneous wound healing in diabetic rats," *Lipids in Health and Disease*, vol. 10, no. 1, p. 235, 2011.
- [164] H. Kume, K. Okazaki, and H. Sasaki, "Hepatoprotective effects of whey protein on D-galactosamine-induced hepatitis and liver fibrosis in rats," *Bioscience, biotechnology, and biochemistry*, vol. 70, no. 5, pp. 1281–1285, 2014.
- [165] S. Athira, B. Mann, R. Sharma, and R. Kumar, "Ameliorative potential of whey protein hydrolysate against paracetamol-



- induced oxidative stress," *Journal of Dairy Science*, vol. 96, no. 3, pp. 1431–1437, 2013.
- [166] C. Flaim, M. Kob, A. M. Di Pierro, M. Herrmann, and L. Lucchin, "Effects of a whey protein supplementation on oxidative stress, body composition and glucose metabolism among overweight people affected by diabetes mellitus or impaired fasting glucose: a pilot study," *The Journal of Nutritional Biochemistry*, vol. 50, pp. 95–102, 2017.
- [167] R. C. Reyes, G. F. Cittolin-Santos, J. E. Kim et al., "Neuronal glutathione content and antioxidant capacity can be normalized in situ by N-acetyl cysteine concentrations attained in human cerebrospinal fluid," *Neurotherapeutics*, vol. 13, no. 1, pp. 217–225, 2016.
- [168] M. Katz, S. J. Won, Y. Park et al., "Cerebrospinal fluid concentrations of N-acetylcysteine after oral administration in Parkinson's disease," *Parkinsonism & Related Disorders*, vol. 21, no. 5, pp. 500–503, 2015.
- [169] J. M. Sheard, S. Ash, G. D. Mellick, P. A. Silburn, and G. K. Kerr, "Malnutrition in a sample of community-dwelling people with Parkinson's disease," *PLoS ONE*, vol. 8, no. 1, article e53290, 2013.
- [170] J. M. Sheard, S. Ash, P. A. Silburn, and G. K. Kerr, "Prevalence of malnutrition in Parkinson's disease: a systematic review," *Nutrition Reviews*, vol. 69, no. 9, pp. 520–532, 2011.
- [171] R. Cano-de-la-Cuerda, M. Pérez-de-Heredia, J. C. Miangolarra-Page, E. Muñoz-Hellín, and C. Fernández-de-las-Peñas, "Is there muscular weakness in Parkinson's disease?," *American Journal of Physical Medicine & Rehabilitation*, vol. 89, no. 1, pp. 70–76, 2010.
- [172] P. Tosukhowong, C. Boonla, T. Dissayabutra et al., "Biochemical and clinical effects of Whey protein supplementation in Parkinson's disease: A pilot study," *Journal of the Neurological Sciences*, vol. 367, pp. 162–170, 2016.
- [173] L. Wang, N. Xiong, J. Huang et al., "Protein-restricted diets for ameliorating motor fluctuations in Parkinson's disease," *Frontiers in Aging Neuroscience*, vol. 9, p. 206, 2017.
- [174] A. T. Borchers, C. L. Keen, S. M. Hannum, and M. E. Gershwin, "Cocoa and chocolate: composition, bioavailability, and health implications," *Journal of Medicinal Food*, vol. 3, no. 2, pp. 77–105, 2000.
- [175] M. H. Carlsen, B. L. Halvorsen, K. Holte et al., "The total antioxidant content of more than 3100 foods, beverages, spices, herbs and supplements used worldwide," *Nutrition Journal*, vol. 9, no. 1, p. 3, 2010.
- [176] R. J. Williams, J. P. Spencer, and C. Rice-Evans, "Flavonoids: antioxidants or signalling molecules?," *Free Radical Biology and Medicine*, vol. 36, no. 7, pp. 838–849, 2004.
- [177] K. E. Heim, A. R. Tagliaferro, and D. J. Bobilya, "Flavonoid antioxidants: chemistry, metabolism and structure-activity relationships," *The Journal of Nutritional Biochemistry*, vol. 13, no. 10, pp. 572–584, 2002.
- [178] M. Ferrali, C. Signorini, B. Caciotti et al., "Protection against oxidative damage of erythrocyte membrane by the flavonoid quercetin and its relation to iron chelating activity," *FEBS Letters*, vol. 416, no. 2, pp. 123–129, 1997.
- [179] R. Latif and A. A. Alsunni, "Effects of chocolate intake on oxidative stress/oxidant-antioxidant balance in medical students: a controlled clinical trial," *Saudi Journal of Medicine and Medical Sciences*, vol. 4, no. 3, pp. 178–182, 2016.
- [180] K. A. Cooper, E. Campos-Giménez, D. Jiménez-Alvarez, K. Nagy, J. L. Donovan, and G. Williamson, "Rapid reversed Phase Ultra-Performance liquid chromatography analysis of the Major cocoa polyphenols and inter-relationships of their concentrations in chocolate," *Journal of Agricultural and Food Chemistry*, vol. 55, no. 8, pp. 2841–2847, 2007.
- [181] C. Vlachopoulos, N. Alexopoulos, and C. Stefanadis, "Effect of dark chocolate on arterial function in healthy individuals: cocoa instead of ambrosia?," *Current Hypertension Reports*, vol. 8, no. 3, pp. 205–211, 2006.
- [182] D. Grassi, C. Lippi, S. Necozione, G. Desideri, and C. Ferri, "Short-term administration of dark chocolate is followed by a significant increase in insulin sensitivity and a decrease in blood pressure in healthy persons," *The American Journal of Clinical Nutrition*, vol. 81, no. 3, pp. 611–614, 2005.
- [183] G. Maskarinec, "Cancer protective properties of cocoa: a review of the epidemiologic evidence," *Nutrition and Cancer*, vol. 61, no. 5, pp. 573–579, 2009.
- [184] O. Khawaja, J. M. Gaziano, and L. Djoussé, "Chocolate and coronary heart disease: a systematic review," *Current Atherosclerosis Reports*, vol. 13, no. 6, pp. 447–452, 2011.
- [185] E. Ramiro-Puig, G. Casadesús, H. G. Lee et al., "Neuroprotective effect of cocoa flavonoids on in vitro oxidative stress," *European Journal of Nutrition*, vol. 48, no. 1, pp. 54–61, 2009.
- [186] M. Wolz, A. Kaminsky, M. Löhle, R. Koch, A. Storch, and H. Reichmann, "Chocolate consumption is increased in Parkinson's disease. Results from a self-questionnaire study," *Journal of Neurology*, vol. 256, no. 3, pp. 488–492, 2009.
- [187] M. Wolz, C. Schleiffer, L. Klingelhöfer et al., "Comparison of chocolate to cacao-free white chocolate in Parkinson's disease: a single-dose, investigator-blinded, placebo-controlled, crossover trial," *Journal of Neurology*, vol. 259, no. 11, pp. 2447–2451, 2012.
- [188] M. Irsfeld, M. Spadafore, and B. M. Prüß, "β-Phenylethylamine, a small molecule with a large impact," *Webmedcentral*, vol. 4, no. 9, 2013.
- [189] P. Pastore, G. Favaro, D. Badocco, A. Tapparo, S. Cavalli, and G. Saccani, "Determination of biogenic amines in chocolate by ion chromatographic separation and pulsed integrated amperometric detection with implemented wave-form at Au disposable electrode," *Journal of Chromatography A*, vol. 1098, no. 1-2, pp. 111–115, 2005.
- [190] M. D. Berry, "Mammalian central nervous system trace amines. Pharmacologic amphetamines, physiologic neuro-modulators," *Journal of Neurochemistry*, vol. 90, no. 2, pp. 257–271, 2004.
- [191] T. Sengupta and K. P. Mohanakumar, "2-Phenylethylamine, a constituent of chocolate and wine, causes mitochondrial complex-I inhibition, generation of hydroxyl radicals and depletion of striatal biogenic amines leading to psychomotor dysfunctions in Balb/c mice," *Neurochemistry International*, vol. 57, no. 6, pp. 637–646, 2010.
- [192] R. Ortmann, M. Schaub, A. Felner, J. Lauber, P. Christen, and P. C. Waldmeier, "Phenylethylamine-induced stereotypies in the rat: a behavioral test system for assessment of MAO-B inhibitors," *Psychopharmacology*, vol. 84, no. 1, pp. 22–27, 1984.
- [193] I. P. Lapin, "Antagonism by CPP, (±)-3-(2-carboxypiperazin-4-yl)-propyl-1-phosphonic acid, of β-phenylethylamine (PEA)-induced hypermotility in mice of different strains," *Pharmacology Biochemistry and Behavior*, vol. 55, no. 2, pp. 175–178, 1996.

- [194] A. Borah, R. Paul, M. K. Mazumder, and N. Bhattacharjee, "Contribution of β -phenethylamine, a component of chocolate and wine, to dopaminergic neurodegeneration: implications for the pathogenesis of Parkinson's disease," *Neuroscience bulletin*, vol. 29, no. 5, pp. 655–660, 2013.
- [195] M. Goedert, "Alpha-synuclein and neurodegenerative diseases," *Nature Reviews Neuroscience*, vol. 2, no. 7, pp. 492–501, 2001.
- [196] A. Oueslati, "Implication of alpha-synuclein phosphorylation at S129 in synucleinopathies: what have we learned in the last decade?," *Journal of Parkinson's disease*, vol. 6, no. 1, pp. 39–51, 2016.
- [197] H. Fujiwara, M. Hasegawa, N. Dohmae et al., " α -Synuclein is phosphorylated in synucleinopathy lesions," *Nature cell biology*, vol. 4, no. 2, pp. 160–164, 2002.
- [198] J. Wu, T. Tolstykh, J. Lee, K. Boyd, J. B. Stock, and J. R. Broach, "Carboxyl methylation of the phosphoprotein phosphatase 2A catalytic subunit promotes its functional association with regulatory subunits in vivo," *The EMBO journal*, vol. 19, no. 21, pp. 5672–5681, 2000.
- [199] H. J. Park, K. W. Lee, E. S. Park et al., "Dysregulation of protein phosphatase 2A in Parkinson disease and dementia with Lewy bodies," *Annals of clinical and translational neurology*, vol. 3, no. 10, pp. 769–780, 2016.
- [200] D. Martini, C. del Bo', M. Tassotti et al., "Coffee consumption and oxidative stress: a review of human intervention studies," *Molecules*, vol. 21, no. 8, p. 979, 2016.
- [201] Y. Luan, X. Ren, W. Zheng et al., "Chronic caffeine treatment protects against α -synucleinopathy by reestablishing autophagy activity in the mouse striatum," *Frontiers in neuroscience*, vol. 12, p. 301, 2018.
- [202] K. W. Lee, J. Y. Im, J. M. Woo et al., "Neuroprotective and anti-inflammatory properties of a coffee component in the MPTP model of Parkinson's disease," *Neurotherapeutics*, vol. 10, no. 1, pp. 143–153, 2013.
- [203] R. Yan, J. Zhang, H. J. Park et al., "Synergistic neuroprotection by coffee components eicosanoyl-5-hydroxytryptamide and caffeine in models of Parkinson's disease and DLB," *Proceedings of the National Academy of Sciences*, vol. 115, no. 51, pp. E12053–E12062, 2018.
- [204] K. Trinh, L. Andrews, J. Krause et al., "Decaffeinated coffee and nicotine-free tobacco provide neuroprotection in Drosophila models of Parkinson's disease through an NRF2-dependent mechanism," *Journal of Neuroscience*, vol. 30, no. 16, pp. 5525–5532, 2010.
- [205] N. Jia, K. Han, J. J. Kong et al., "(–)-Epigallocatechin-3-gallate alleviates spatial memory impairment in APP/PS1 mice by restoring IRS-1 signaling defects in the hippocampus," *Molecular and cellular biochemistry*, vol. 380, no. 1–2, pp. 211–218, 2013.
- [206] W. L. Kelemen and C. E. Creeley, "State-dependent memory effects using caffeine and placebo do not extend to metamemory," *The Journal of general psychology*, vol. 130, no. 1, pp. 70–86, 2003.
- [207] M. E. Arnold, T. V. Petros, B. E. Beckwith, G. Coons, and N. Gorman, "The effects of caffeine, impulsivity, and sex on memory for word lists," *Physiology & behavior*, vol. 41, no. 1, pp. 25–30, 1987.
- [208] Institute of Medicine Committee on Military Nutrition Research, "Caffeine for the sustainment of mental task performance: formulations for military operations," *Nutrition Today*, vol. 37, no. 1, pp. 26–27, 2002.
- [209] J. Corley, X. Jia, J. A. M. Kyle et al., "Caffeine consumption and cognitive function at age 70: the Lothian Birth Cohort 1936 study," *Psychosomatic medicine*, vol. 72, no. 2, pp. 206–214, 2010.
- [210] A. W. K. Yeung, N. T. Tzvetkov, O. S. El-Tawil, S. G. Bungău, M. M. Abdel-Daim, and A. G. Atanasov, "Antioxidants: scientific literature landscape analysis," *Oxidative medicine and cellular longevity*, vol. 2019, Article ID 8278454, 11 pages, 2019.
- [211] M. S. Uddin, M. F. Hossain, A. A. Mamun et al., "Exploring the multimodal role of phytochemicals in the modulation of cellular signaling pathways to combat age-related neurodegeneration," *Science of The Total Environment*, vol. 725, article 138313, 2020.
- [212] A. I. Abushouk, A. Negida, H. Ahmed, and M. M. Abdel-Daim, "Neuroprotective mechanisms of plant extracts against MPTP induced neurotoxicity: Future applications in Parkinson's disease," *Biomedicine & Pharmacotherapy*, vol. 85, pp. 635–645, 2017.
- [213] M. A. Rahman, M. R. Rahman, T. Zaman et al., "Emerging potential of naturally occurring autophagy modulators against neurodegeneration," *Current Pharmaceutical Design*, vol. 26, no. 7, pp. 772–779, 2020.
- [214] A. Kumar, Ekavali, K. Chopra, M. Mukherjee, R. Pottabathini, and D. K. Dhull, "Current knowledge and pharmacological profile of berberine: an update," *European Journal of Pharmacology*, vol. 761, pp. 288–297, 2015.
- [215] X. W. Jiang, Y. Zhang, Y. L. Zhu et al., "Effects of berberine gelatin on recurrent aphthous stomatitis: a randomized, placebo-controlled, double-blind trial in a Chinese cohort," *Oral Surgery, Oral Medicine, Oral Pathology and Oral Radiology*, vol. 115, no. 2, pp. 212–217, 2013.
- [216] H. L. Li, T. Han, R. H. Liu, C. Zhang, H. S. Chen, and W. D. Zhang, "Alkaloids from *Corydalis saxicola* and their anti-hepatitis B virus activity," *Chemistry & Biodiversity*, vol. 5, no. 5, pp. 777–783, 2008.
- [217] H. Wang, C. Zhu, Y. Ying, L. Luo, D. Huang, and Z. Luo, "Metformin and berberine, two versatile drugs in treatment of common metabolic diseases," *Oncotarget*, vol. 9, no. 11, pp. 10135–10146, 2018.
- [218] H. F. Ji and L. Shen, "Berberine: a potential multipotent natural product to combat Alzheimer's disease," *Molecules*, vol. 16, no. 8, pp. 6732–6740, 2011.
- [219] S. S. K. Durairajan, L.-F. Liu, J.-H. Lu et al., "Berberine ameliorates β -amyloid pathology, gliosis, and cognitive impairment in an Alzheimer's disease transgenic mouse model," *Neurobiology of Aging*, vol. 33, no. 12, pp. 2903–2919, 2012.
- [220] M. Kim, K.-H. Cho, M.-S. Shin et al., "Berberine prevents nigrostriatal dopaminergic neuronal loss and suppresses hippocampal apoptosis in mice with Parkinson's disease," *International Journal of Molecular Medicine*, vol. 33, no. 4, pp. 870–878, 2014.
- [221] I. H. Kwon, H. S. Choi, K. S. Shin et al., "Effects of berberine on 6-hydroxydopamine-induced neurotoxicity in PC12 cells and a rat model of Parkinson's disease," *Neuroscience Letters*, vol. 486, no. 1, pp. 29–33, 2010.
- [222] K. S. Shin, H. S. Choi, T. T. Zhao et al., "Neurotoxic effects of berberine on long-term L-DOPA administration in 6-hydroxydopamine-lesioned rat model of Parkinson's disease," *Archives of Pharmacological Research*, vol. 36, no. 6, pp. 759–767, 2013.

- [223] S. Hewlings and D. Kalman, "Curcumin: a review of its effects on human health," *Foods*, vol. 6, no. 10, 2017.
- [224] V. Zbarsky, K. P. Datla, S. Parkar, D. K. Rai, O. I. Aruoma, and D. T. Dexter, "Neuroprotective properties of the natural phenolic antioxidants curcumin and naringenin but not quercetin and fisetin in a 6-OHDA model of Parkinson's disease," *Free Radical Research*, vol. 39, no. 10, pp. 1119–1125, 2009.
- [225] S. M. Nam, J. H. Choi, D. Y. Yoo et al., "Effects of curcumin (*Curcuma longa*) on learning and spatial memory as well as cell proliferation and neuroblast differentiation in adult and aged mice by upregulating brain-derived neurotrophic factor and CREB signaling," *Journal of Medicinal Food*, vol. 17, no. 6, pp. 641–649, 2014.
- [226] D. Liu, Z. Wang, Z. Gao et al., "Effects of curcumin on learning and memory deficits, BDNF, and ERK protein expression in rats exposed to chronic unpredictable stress," *Behavioural Brain Research*, vol. 271, pp. 116–121, 2014.
- [227] T. T. Nguyen, M. D. Vuu, M. A. Huynh, M. Yamaguchi, L. T. Tran, and T. P. T. Dang, "Curcumin effectively rescued Parkinson's disease-like phenotypes in a novel *Drosophila melanogaster* model with dUCH knockdown," *Oxidative Medicine and Cellular Longevity*, vol. 2018, Article ID 2038267, 12 pages, 2018.
- [228] Y. Li, J. Yao, C. Han et al., "Quercetin, inflammation, and immunity," *Nutrients*, vol. 8, no. 3, 2016.
- [229] L. K. Stewart, J. L. Soileau, D. Ribnicky et al., "Quercetin transiently increases energy expenditure but persistently decreases circulating markers of inflammation in C57BL/6J mice fed a high-fat diet," *Metabolism*, vol. 57, 7 Supplement 1, pp. S39–S46, 2008.
- [230] Y. S. Dong, J. L. Wang, D. Y. Feng et al., "Protective effect of quercetin against oxidative stress and brain edema in an experimental rat model of subarachnoid hemorrhage," *International Journal of Medical Sciences*, vol. 11, no. 3, pp. 282–290, 2014.
- [231] S. Singh, S. Jamwal, and P. Kumar, "Neuroprotective potential of quercetin in combination with piperine against 1-methyl-4-phenyl-1,2,3,6-tetrahydropyridine-induced neurotoxicity," *Neural Regeneration Research*, vol. 12, no. 7, pp. 1137–1144, 2017.

Research Article

A Dihydroflavonoid Naringin Extends the Lifespan of *C. elegans* and Delays the Progression of Aging-Related Diseases in PD/AD Models via DAF-16

Qing Zhu,¹ Yuan Qu,¹ Xiao-Gang Zhou,¹ Jian-Ning Chen,¹ Huai-Rong Luo ^{1,2,3}
and Gui-Sheng Wu ^{1,2}

¹Key Laboratory for Aging and Regenerative Medicine, Department of Pharmacology School of Pharmacy, Southwest Medical University, Luzhou, Sichuan 646000, China

²Key Laboratory of Medical Electrophysiology, Ministry of Education, Institute of Cardiovascular Research of Southwest Medical University, Luzhou, Sichuan 646000, China

³Central Nervous System Drug Key Laboratory of Sichuan Province, Luzhou, Sichuan 646000, China

Correspondence should be addressed to Huai-Rong Luo; lhr@swmu.edu.cn and Gui-Sheng Wu; wgs@swmu.edu.cn

Received 20 April 2020; Revised 20 June 2020; Accepted 14 July 2020; Published 3 August 2020

Guest Editor: Francisco Jaime B. Mendonça Junior

Copyright © 2020 Qing Zhu et al. This is an open access article distributed under the Creative Commons Attribution License, which permits unrestricted use, distribution, and reproduction in any medium, provided the original work is properly cited.

Naringin is a dihydroflavonoid, which is rich in several plant species used for herbal medicine. It has a wide range of biological activities, including antineoplastic, anti-inflammatory, antiphotaging, and antioxidative activities. So it would be interesting to know if naringin has an effect on aging and aging-related diseases. We examined the effect of naringin on the aging of *Caenorhabditis elegans* (*C. elegans*). Our results showed that naringin could extend the lifespan of *C. elegans*. Moreover, naringin could also increase the thermal and oxidative stress tolerance, reduce the accumulation of lipofuscin, and delay the progress of aging-related diseases in *C. elegans* models of AD and PD. Naringin could not significantly extend the lifespan of long-lived mutants from genes in insulin/IGF-1 signaling (IIS) and nutrient-sensing pathways, such as *daf-2*, *akt-2*, *akt-1*, *eat-2*, *sir-2.1*, and *rsk-1*. Naringin treatment prolonged the lifespan of long-lived *glp-1* mutants, which have decreased reproductive stem cells. Naringin could not extend the lifespan of a null mutant of the fox-head transcription factor DAF-16. Moreover, naringin could increase the mRNA expression of genes regulated by *daf-16* and itself. In conclusion, we show that a natural product naringin could extend the lifespan of *C. elegans* and delay the progression of aging-related diseases in *C. elegans* models via DAF-16.

1. Introduction

Aging is accompanied by constant changes in morphology and gradual decline in function. Aging is a major risk factor for human diseases including cancer, diabetes, cardiovascular diseases, and neurodegenerative diseases [1–3]. Aging could be slowed by getting rid of unhealthy habits, including smoking, bad diet, alcohol consumption, lack of sleep, stress, and sun exposure, and by treating signs of aging with various esthetic methods or food supplements such as antioxidants [4]. Many epidemiological studies have shown that natural bioactive products could reduce the risk of aging-related diseases [5–7]. A number of natural bioactive products, including phosvitin [8], royal jelly-collagen peptide [9],

Alaskan berry extracts [10], walnut protein hydrolysate [11], and tea extracts [12], exhibit longevity extension abilities.

Naringin, also known as citrus or isohesperidin, is a kind of dihydroflavonoid (Figure 1(a)), which is a natural pale yellow pigment that exists in the peel and fruit of *Citrus grandis*, *Citrus paradisi*, and *Citrus (Rutaceae) aurantium* [13]. Naringin exhibits multiple biological activities and pharmacological effects, including antitumor [14], anti-hypercholesterolemic [15], desensitization [16], antiallergy, antiphotaging [17], cytoprotective [18], anti-inflammatory, heart-protective [7, 13, 19, 20], and neuroprotective activities [21–23]. Naringin could also regulate glucose and lipid metabolism [24] and oxidative stress [25]. Given the various biological activities reported, we are wondering if naringin

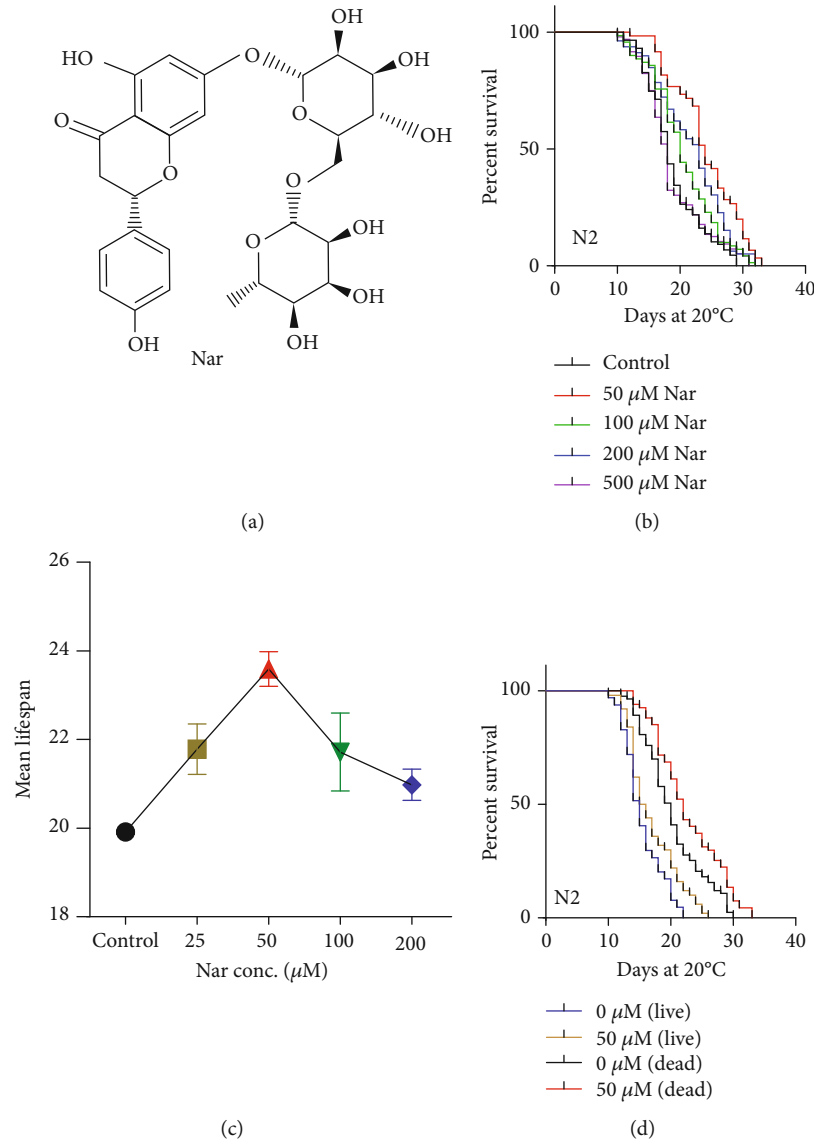


FIGURE 1: Naringin extended adult lifespan in *C. elegans*. (a) Chemical structure of naringin. (b) Survival curves of wild-type (N2) animals raised at 20°C on NGM plates containing 50, 100, 200, and 500 μM of naringin or control plates without naringin. (c) Dose-response analysis of naringin. Wild-type (N2) animals were treated with 25, 50, 100, and 200 μM of naringin at least two independent experiments, plotting the mean changes of lifespan. Error bars represent the standard deviation (SD). (d) Effects of naringin on the lifespan of wild-type (N2) animals raised at 20°C on NGM plates in the absence (0 μM) or presence (50 μM) of naringin with two different feeding procedures including live bacteria (*E. coli* OP50) and dead OP50 (65°C 30 min).

has an effect on aging and aging-related diseases. We found that naringin could significantly extend the lifespan of *C. elegans* and delay aging-related degeneration in body movement and delay the progression of aging-related diseases in models of Alzheimer's and Parkinson's diseases.

2. Materials and Methods

2.1. Chemicals and Strains of *C. elegans*. All strains were from *Caenorhabditis* Genetics Center (CGC) and maintained (unless otherwise stated) at 20°C on nematode growth medium (NGM) agar plates carrying a lawn of *Escherichia coli* OP50 as described previously [26]. The strains used in this study were Bristol N2 (wild-type), DA1116 *eat-*

2(ad1116)II, CL4176 *smg-1(cc546)I*, PS3551 *hsf-1(sy441)I*, CF1903 *glp-1(e2141)III*, TJ356 *zIs356 [Pdaf-16::daf-16-gfp; rol-6]IV*, CB4876 *clk-1(e2519)III*, VC204 *akt-2(ok393)X*, CF1553 *muIs84 [Psod-3::GFP]*, CF1038 *daf-16(mu86)I*, CB1370 *daf-2(e1370)III*, RB759 *akt-1(ok525)V*, VC199 *sir-2.1(ok434)IV*, and BZ555 (*P^{dat-1}::gfp*). CL4176 *smg-1(cc546)I* was temperature-sensitive [27] and was maintained at 15°C and shifted to 25°C at the L3 stage in lifespan experiments. For CF1903 *glp-1(e2141)III*, L1 larvae were cultured at 25°C until they develop into L4 larvae or young adults, then switched to 20°C for the lifespan test [28]. Naringin was purchased from Sigma and completely dissolved in PBS and then added to the top of the prepared plates. NGM plates containing naringin were equilibrated overnight

before use. Synchronized late L4 larvae or young adult worms (wild-type) were transferred to NGM plates containing naringin and maintained at 20°C.

2.2. Lifespan Assay. All strains were cultured on fresh NGM plates at least for 2-3 generations without starvation, and lifespan analyses were performed in the same manner at 20°C, unless otherwise stated. Late L4 larvae or young adults were transferred to NGM plates containing inactive OP50 (65°C for 30 min) and 40 μ M of 5-fluoro-2'-deoxyuridine (FUDR, Sigma) to prevent progeny growth [29]. The time L4 larvae or young adults were transferred to a NGM plate was defined as test day 0. Live and dead animals were counted each day until all individuals have died. The worms that were not active when gently prodded using a platinum wire were scored as dead [29]. Besides, the worms were transferred to fresh plates every other day. Worms suffering from internal hatch and crawling off the NGM plate were not included in the lifespan counts. The lifespan assays were repeated for at least three independent trials. At least 60 animals were included in each group of lifespan experiment.

2.3. Aging-Related Phenotype Analysis. The body movement assay was conducted as previously described [29]. Late L4 larvae or young adults were transferred to NGM plates and treated as described in the lifespan assay. The bending behavior in a coordinated sinusoidal manner was counted.

Lipofuscin accumulation assay was conducted as previously reported [30–32]. Wild-type animals at L4 larvae or young adults were treated with naringin; then, the intestinal autofluorescence of lipofuscin was analyzed on the 2nd and 5th days of adulthood. The intestinal autofluorescence of lipofuscin was captured with a Leica epifluorescence microscope using the GFP filter set (with excitation at 340–380 nm and emission at 435–485 nm) and analyzed by using the image processing software ImageJ. The total number of worms in each group of the aging-related phenotype analysis was at least 20.

2.4. Stress Resistance Assays. Wild-type N2 worms were pretreated with naringin, followed by oxidation and heat stress treatment. For the oxidative stress experiment, larvae and early adults of stage L4 were treated with 50 μ M of naringin for 7 days, then exposed to paraquat (20 mM) and cultured at 20°C, and their death rate was calculated every day [29]. For the heat stress resistance experiment, stage L4 larvae and young adults were treated with 50 μ M of naringin for 7 days. Then, the NGM plates were incubated at 35°C. The death rate was calculated every 2 hours [29]. For the pathogenic stress induced by *Pseudomonas*, stage L4 larvae and young adults were treated with 50 μ M of naringin for 7 days. Then, the worms were transferred to a new NGM containing *Pseudomonas* and the death of animals was monitored every day. The dead animals of the stress resistance assays were counted the same way as in the lifespan assay. The experiments were repeated independently at least twice. The number of worms in each group of experiments was at least 60.

2.5. Aging-Related Disease Analysis. The CL4176 (*dvIs27(myo-3/A beta 1-42/let UTR)+pRF4(rol-6(su1006))*) worms

were incubated at 15°C until the L3 stage [27, 33], then transferred to NGM plates containing 50 μ M of naringin and incubated at 25°C. Paralyzed nematodes were counted every 2 hours. This experiment was independently repeated for at least twice. The total number of worms in each group of experiment was at least 60.

Transgenic nematode strain NL5901 expresses human α -synuclein gene fused with yellow fluorescent protein (YFP) [34]. Worms of NL5901 were treated with 50 μ M of naringin for 7 days; then, the aggregation of α -synuclein was captured with a Leica epifluorescence microscope and analyzed by using the image processing software ImageJ. The experiments were independently repeated at least three times. The number of worms in each group of experiment was at least 30.

The transgenic strain BZ555 (*P^{dat-1}::gfp*) has GFP expressed specifically in dopaminergic neurons, which could be induced to degeneration by 6-OHDA [34, 35]. To induce selective degeneration of DA neurons, the L3 stage larvae of strain BZ555 (*P^{dat-1}::gfp*) were transferred to the OP50/medium containing 50 μ M of 6-OHDA and 10 mM of ascorbic acid, incubated at 20°C for 1 h, and gently shaken every 10 minutes [33]. Then, the worms were washed with an M9 buffer three times and cultured in OP50/NGM plates containing 50 μ M of naringin for 72 hours [34]. After that, fluorescent photos of head neurons were taken using a Leica epifluorescence microscope (DFC 7000T) and analyzed by using the image processing software ImageJ. The experiments were repeated independently at least twice. The number of worms in each group of experiment was at least 30.

2.6. DAF-16::GFP Location and SOD-3::GFP Assay. The subcellular locations of DAF-16::GFP were determined using the transgenic strain TJ356 *daf-16(zls356IV)*. L4 larvae were transferred to the plates containing 50 μ M of naringin and cultured for 48 h at 20°C [29, 32]. The image of DAF-16::GFP signal was captured by using a fluorescence microscope system (Leica, DFC 7000T) and analyzed by using the image processing software ImageJ. The experiments were repeated independently at least twice. The total number of worms in each group of experiment was at least 30.

The *C. elegans* transgenic strain CF1553 *muIs84 [Psod-3::GFP]* expresses GFP fused with SOD-3. The worms of CF1553 were treated with 50 μ M naringin for 7 days for lifespan assays [32]. Then, intensity of fluorescence of worms was observed by using a fluorescence microscope system (Leica, DFC 7000T). All fluorescent photos of at least 30 animals in each group were scored by ImageJ, and the experiment was repeated independently at least twice.

2.7. ROS Assay. For intracellular ROS accumulation, age-synchronized N2 worms (L4 stage) were treated with 50 μ M of naringin at 20°C for 7 days. The positive control group was treated with 2 mM of hydrogen peroxide (H₂O₂) solution while the negative control group was treated with 5 mM of antioxidants *N*-acetylcysteine (NAC) [36]. ROS formation was quantified with H2DCF-DA. After being treated with naringin, worms were collected by washing off the plate with an M9 buffer to a centrifuge tube. OP50 was removed by

washing the plate three times. Then, 50 μM of H2DCF-DA was added and the worms were incubated for 1 h in the dark at 20°C. After that, the worms were mounted on a glass slide and paralyzed by the addition of tetramisole hydrochloride, and at least 20 worms were randomly photographed using a fluorescence microscope (Leica, DFC 7000T) using a DAPI filter set (with excitation at 488 nm and emission at 525 nm) [32]. ImageJ software was then used to measure the relative fluorescence intensity of the full body. The experiment was repeated at least twice in independent trials with 20 worms per plot.

2.8. Reproduction Assay. Individual worms from synchronized L4 larvae were transferred to NGM plates containing 50 μM naringin. Then, the worms from each plate were transferred into a fresh NGM plate at almost the same time every day. The number of progeny was counted each day [37]. The number of worms in each group was more than 20. The experiments were repeated independently at least twice.

2.9. Quantitative RT-PCR Assay. About 3,000 synchronized young adult wild-type worms were transferred to 4 NGM plates containing 50 μM of naringin or control plates and cultured at 20°C for 48 h. The RNA was extracted using RNAiso Plus (Takara) and converted to cDNA using a High-Capacity cDNA Reverse Transcription Kit (Applied Biosystems). The qRT-PCR was performed in Power SYBR Green PCR Master Mix (Applied Biosystems) and run by the QuantStudio 6 Flex system. The relative expression of genes was calculated using the $2^{-\Delta\Delta\text{CT}}$ method and normalized to the expression of gene *cdc-42* [29]. All the primers used in this research are listed in Table S12.

2.10. Statistical Analyses. Lifespan statistical analyses were performed using the SPSS package. Kaplan-Meier lifespan analysis was performed, and *p* values were calculated using the log-rank test. Other results are expressed as the mean \pm SEM, and *p* values were calculated by two-tailed *t*-test. *p* < 0.05 was considered significant.

3. Results

3.1. Naringin Extends the Lifespan of *C. elegans*. To investigate if naringin could extend the lifespan of *C. elegans*, the wild-type *C. elegans* N2 was treated with naringin from stage L4 larva or early adult till their death. Our results showed that naringin increased the lifespan of *C. elegans* in a dose-dependent manner (Figure 1(b), Table S1). The 50 μM of naringin had the greatest effect on longevity, extending adult mean lifespan by up to 23% at 20°C (*p* < 0.001) (Figure 1(b), Table S1). Worms exposed to either higher or lower concentrations of naringin showed a smaller or an insignificant lifespan extension (Figure 1(c), Table S1).

The metabolites produced by live bacteria proliferation could significantly shorten the lifespan of *C. elegans* [38]. To test if the effect of naringin on the lifespan extension could be affected by live bacteria, worms were fed with live and heat-killed bacteria when treated with 50 μM of naringin. We observed that the mean lifespan of worms fed by

heat-killed (nonproliferating) bacteria *E. coli* and live bacteria were both significantly increased under the treatment of naringin (Figure 1(d), Table S1), suggesting naringin did not exert on bacteria to extend the lifespan of *C. elegans*. Therefore, the dead bacteria were used throughout the experiments.

3.2. Naringin Delayed Aging-Related Decline of Phenotypes. The body bending behavior of *C. elegans* declines with aging [39]. In order to test if naringin could delay the decline of body bending with aging, the body movement of nematodes was analyzed. Our results showed that although both treated and nontreated animals showed a tendency of movement slowing down with aging, the treatment of naringin significantly slowed the declining of body movement with aging (Figure 2(a), Table S2). In addition, the level of lipofuscin, an endogenous intestinal autofluorescent, accumulates during the aging of *C. elegans* [3, 40]. Our results showed that the fluorescence intensity of intestinal lipofuscin in worms treated with naringin was reduced by 46.8% and 15.1% on the second day and fifth day, respectively (Figure 2(b), Table S3), indicating that naringin treatment suppressed lipofuscin accumulation.

3.3. Naringin Promotes the Stress Resistance of *C. elegans*. There is a strong correlation between stress resistance and lifespan of *C. elegans*. Several studies have shown that the lifespan of *C. elegans* is affected by oxidative stress or high temperatures [41, 42]. In order to study whether naringin affects stress resistance of *C. elegans*, wild-type N2 worms were pretreated with naringin, followed by oxidative stress or heat stress treatment. Our results showed that pretreatment with naringin increased the survival rate of worms under oxidative stress by 18.1% (Figure 2(c), Table S4). The treatment of naringin increased the survival rate of worms under thermal stress by 31.2% (Figure 2(d), Table S5). In addition, we used *Pseudomonas aeruginosa* (PA14), a pathogenic bacterium, to test if naringin affected the resistance of worms to pathogenic stress. Our results showed that naringin could not extend the lifespan of nematodes fed by *Pseudomonas aeruginosa* (Figure 2(e), Table S1).

HSF-1 is a transcriptional regulator of stress-induced gene expression and protein-folding homeostasis [43]. Therefore, we tested the effect of naringin on the deletion mutant *hsf-1(sy441)I*. Our results showed that naringin could not extend the lifespan of *hsf-1(sy441)I* (Figure 2(f), Table S1).

3.4. Naringin Delays the Progression of Aging-Related Diseases in *C. elegans* Models of AD and PD. Misfolded proteins accumulate with aging and lead to chronic toxic stress for cells [27, 34], which causes a variety of aging-related neurodegenerative diseases, such as Parkinson's disease, Alzheimer's disease, and Huntington's disease. Since naringin could extend the lifespan of *C. elegans*, we are wondering if naringin could also ameliorate protein toxicity stress in nematodes and delay the progression of neurodegenerative diseases.

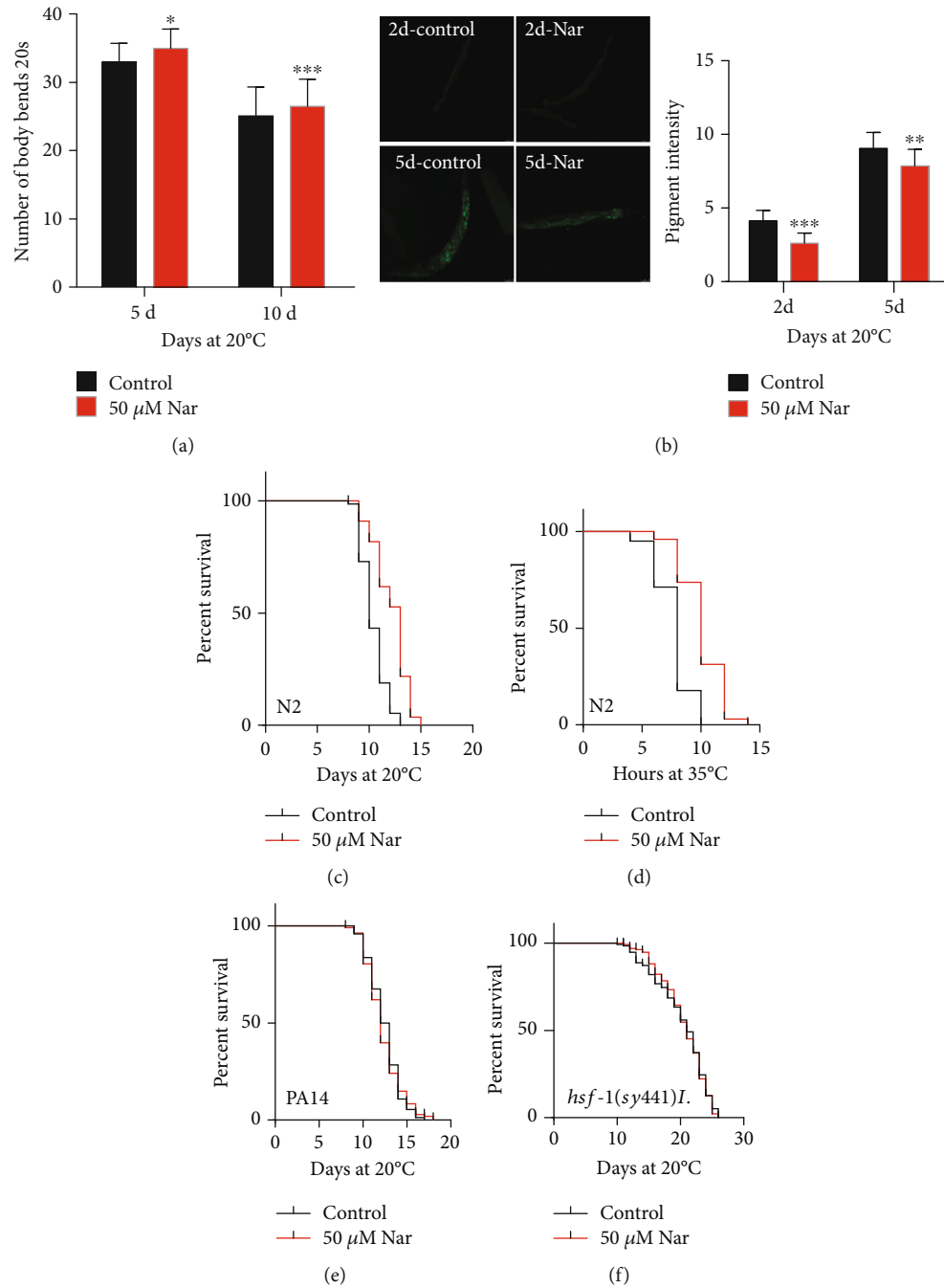


FIGURE 2: Naringin delayed aging-related decline of phenotypes and improved stress resistance. (a) Aging-related movements of worms with nontreated control plates and 50 μ M naringin. The mean body movement speed is found in Table S2 (Supplementary information). (b) The intestinal autofluorescence of lipofuscin was analyzed on the 2nd and 5th days of adulthood. The figures showed the mean lipofuscin aggregated in the intestinal tract at least repeated twice. The statistical details and repeats of these experiments are summarized in Table S3 (Supplementary information). (c) The survival curves of wild-type worms cultured at 20°C in plates with treated 50 μ M and nontreated naringin on the 7th day of adulthood; then, the worms were exposed to paraquat (20 mM) and cultured at 20°C; and their death was calculated every day. Statistical details and repeats of these experiments are summarized in Table S4 (Supplementary information). (d) The survival curves of wild-type worms cultured at 35°C in nontreated control plates and plates treated with 50 μ M naringin. Statistical details and repeats of these experiments are summarized in Table S5 (Supplementary information). (e) Survival curves of wild-type (N2) animals feeding *Pseudomonas aeruginosa* raised at 20°C on NGM plates in the absence (0 μ M) or presence (50 μ M) of naringin. Statistical details and repeats of these experiments are summarized in Table S1 (Supplementary information). (f) Survival curves of *hsf-1* mutants in the control or treated with 50 μ M naringin; naringin could not further extend the mean lifespan of *C. elegans*. Statistical details and repeats of these experiments were summarized in Table S1 (Supplementary information).

Parkinson's disease is characterized by the accumulation of α -synuclein protein and degeneration of dopaminergic neurons in the substantia nigra [33, 34]. *C. elegans* does not have an α -synuclein homolog, so several transgenic *C. elegans* strains with human α -synuclein have been created to study the pathogenicity of α -synuclein. The transgenic strain NL5901 ([*unc-54p:: α -synuclein::YFP+unc-119(+)*]) expresses α -synuclein protein fused with yellow fluorescent protein (YFP) [34] in the body wall muscle cells [33, 34]. We analyzed the aggregation of α -synuclein in worms treated with 50 μ M of naringin for 7 days. We found that naringin treatment significantly decreased the aggregation of α -synuclein ($p < 0.001$) (Figure 3(a), Table S6). In addition, the accumulation of α -synuclein aggregating in NL5901 is associated with locomotion and movement impairments [34]. Our results showed that naringin treatment could also increase the swimming bending behavior of *C. elegans* NL5901 (Figure 3(b), Table S2). Dopaminergic neurodegeneration can easily be induced by neurotoxins such as 6-hydroxydopamine (6-OHDA). Thus, another transgenic strain BZ555 (*P^{dat-1}::gfp*) expressing green fluorescent protein (GFP) in dopaminergic neurons [35] was used to study the degeneration of dopaminergic neurons [33]. Fluorescent photographs of neurons in the head of the nematode BZ555 were taken after being exposed to 6-OHDA for 72 hours. Our results showed that BZ555 treated with 6-OHDA decreased the mean fluorescence intensity from 35.73 ± 2.129 to 18.94 ± 0.757 in the absence of naringin, whereas exposure to 50 μ M of naringin increased the mean fluorescence intensity to 38.82 ± 1.646 (Figure 3(c), Table S6). Our results also showed that BZ555 presents increased neurite blebbing under 6-OHDA treatment, while naringin treatment reduced half of the neurite blebbing caused by 6-OHDA. (Figure S1, Table S7). Above results suggest that naringin treatment slowed the degeneration of head neurons of *C. elegans* BZ555, with the degree of protection comparable to the anti-Parkinson's disease medicine levodopa (Figure 3(c), Table S6).

β -Amyloid is the main component of the extracellular plaques found in the brain of patients with Alzheimer's disease [27]. Temperature-induced expression of human beta-amyloid peptide (A β) in muscles of *C. elegans* CL4176 (*dvIs27 (myo-3/A beta 1-42/let UTR)+pRF4 (rol-6(su1006))*) leads to paralysis [27, 33]. Our results showed that 50 μ M of naringin could delay the temperature-induced paralysis of *C. elegans* CL4176 (Figure 3(d), Table S8), suggesting that naringin could suppress the toxicity of A-beta plaque.

3.5. The Effect of Naringin on the Lifespan Extension in *C. elegans* Depends on FOXO Homologous *daf-16*. In *C. elegans*, the transcription factor FOXO homologous *daf-16* plays a critical role in stress resistance, longevity, development, fat accumulation, and reproductivity [44, 45]. Our results showed that naringin could not extend the lifespan of *daf-16* null mutant *daf-16(mu86)I* (Figure 4(a), Table S1). Upon activation, *daf-16* transferred from the cytoplasm to the nucleus and activates the expression of downstream genes [46]. But our results showed that there was no

significant increase in *daf-16* nuclear translocation in nematodes treated with naringin (Figure 4(b)). So we investigated if naringin could affect the mRNA level of *daf-16* regulated genes *sod-3*, *gst-4*, *dod-3*, *hsp12.6*, *hsp16.1*, and *hsp-16.2* [47, 48]. The mRNA expression level of genes *sod-3*, *hsp12.6*, *hsp16.1*, and *hsp-16.2* was significantly increased in wild-type N2 worms treated with naringin ($p < 0.05$). Among them, the mRNA expression of *sod-3* was increased up to 4-fold. No significant changes were found in the mRNA expression level of genes *gst-4* and *dod-3* in worms treated with naringin ($p > 0.05$) (Figure 4(c), Table S9). In addition, we monitored the fluorescence intensity of SOD-3::GFP in report transgenic strain CF1553; the naringin treatment significantly increased the GFP intensity ($p < 0.001$) (Figure 4(d), Table S10). SOD-3 is a mitochondrial superoxide dismutase which is involved in antioxidative stress [49]. Thus, we use the wild-type nematodes N2 to quantify the ROS in the body. We found that naringin treatment significantly lowered ROS (Figure 4(e), Table S10). These findings showed that naringin extended the lifespan of worms by activating *daf-16*.

In *C. elegans*, the insulin-like ligands interact with DAF-2/insulin receptors to activate the phosphoinositide 3-kinase age-1/PI3K, which regulates the activity of kinases AKT-1, AKT-2, and SGK-1 through phosphorylation of PDK-1. AKT regulates the activity of multiple downstream targets, including DAF-16/FOXO transcription factor [44]. Therefore, we detected the mRNA expression level of genes associated with DAF-16 and itself. The results showed that in naringin-treated groups, the relative expression levels of *daf-2*, *akt-1*, and *akt-2* were downregulated to 0.161 ± 0.014 , 0.472 ± 0.108 , and 0.317 ± 0.150 , respectively. It was worth noticing that the relative expression level of *daf-16* was significantly upregulated to 3.184 ± 0.445 . However, the naringin-treated group did not show significant differences in the expression of *daf-2*, *akt-1*, *akt-2*, as well as *daf-16* in *daf-16* null mutant *daf-16(mu86)I* (Figure 5(a), Table S9). So we studied the effect of naringin on long-lived mutant *daf-2(e1370)III* and loss of function mutants *akt-1(ok525)V* and *akt-2(ok393)X*. Our results showed that naringin could not prolong the lifespan of *daf-2(e1370)III* (Figure 5(b), Table S1), *akt-1(ok525)V*, and *akt-2(ok393)X* (Figures 5(c) and 5(d), Table S1).

3.6. Naringin Does Not Act on the Germline Signaling Pathway. Reduced fertility and slower growth could extend the lifespan of *C. elegans* [50]. To test if naringin could affect the reproduction of *C. elegans*, we measured the oviposition of animals treated with naringin. We found that the number of eggs in the treated group was less than that in the untreated group on the 1st and 2nd days but was more than that in the untreated group on the next three days. The naringin treatment did not significantly change the total number of progenies throughout the spawning cycle (Figure 6(a), Table S11).

To investigate if naringin could extend the lifespan of *C. elegans* by affecting reproduction, we selected the germ-related *glp-1* mutant *glp-1(e2141)III* to determine if naringin acts on the reproductive signaling pathway. Our results

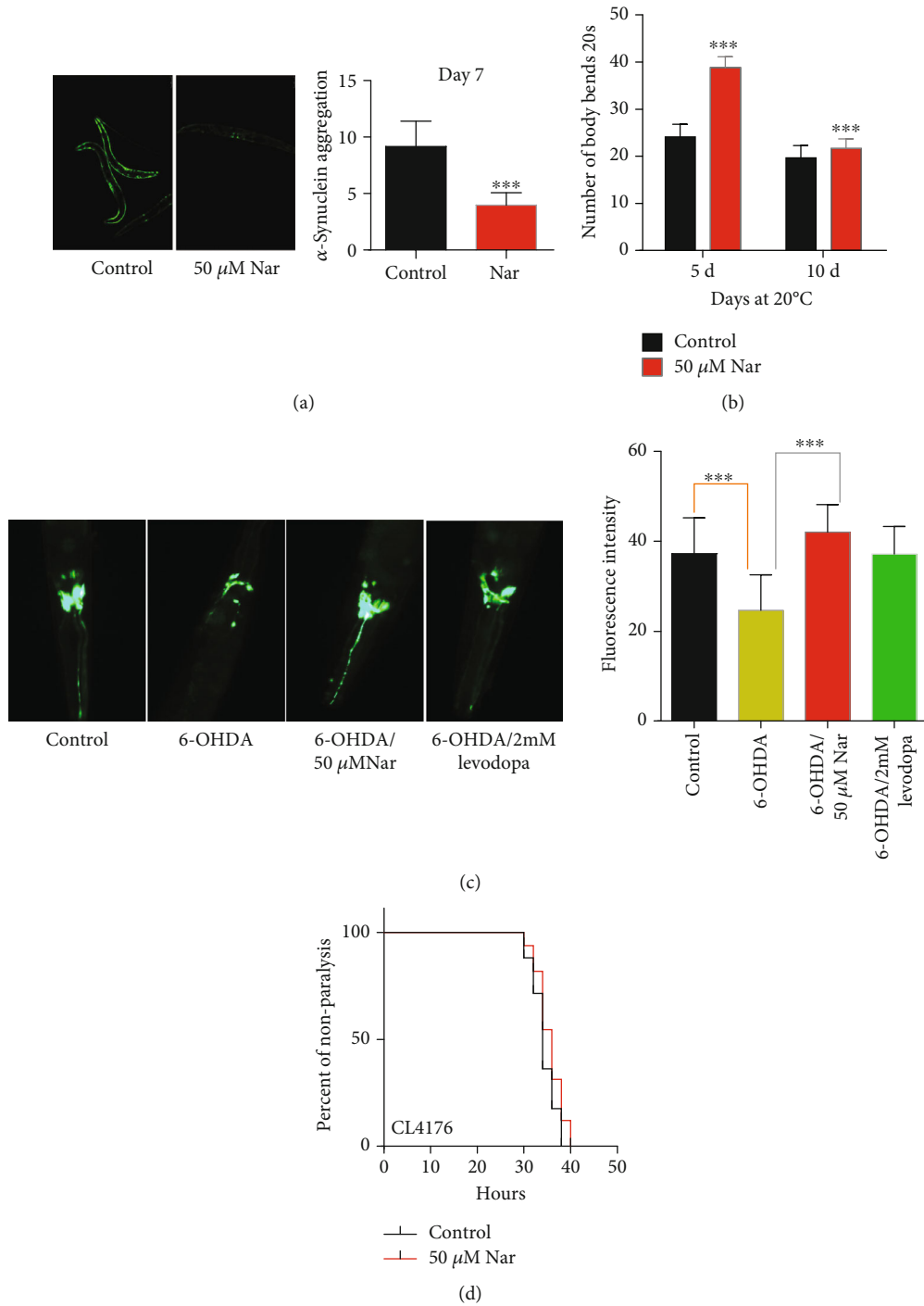


FIGURE 3: Naringin declines the progression of aging-related diseases. (a) Representative images of the α -synuclein in NL5901 treated with or without naringin. The aggregation of α -synuclein in NL5901 treated with or without naringin was captured with a Leica epifluorescence microscope and analyzed by using the image processing software ImageJ. 50 animals of each strain were scored in two independent trials. (b) Aging-related movements of NL5901 with nontreated control plates and 50 μ M naringin. The mean body movement speed is found in Table S2 (Supplementary information). (c) Representative images of the head neurons of BZ555 using different ways of rescue after 6-OHDA induction. After the rescue of 50 μ M naringin, the head neurons showed slow degenerative changes, and the degree of protection was basically consistent with levodopa which is the anti-Parkinson's disease drug. 40 animals of each strain were scored in each independent trial. Statistical details and repeats of these experiments are summarized in Table S6 (Supplementary information). (d) The paralysis phenotype associated with muscle $A\beta$ expression is suppressed by 50 μ M naringin treatment from the L3 stage larvae in the transgenic strain CL4176. Shown is the independent experiment with 70-100 animals in indicated time points after temperature upshift to 25°C. Statistical details and repeats of these experiments are summarized in Table S8 (Supplementary information).

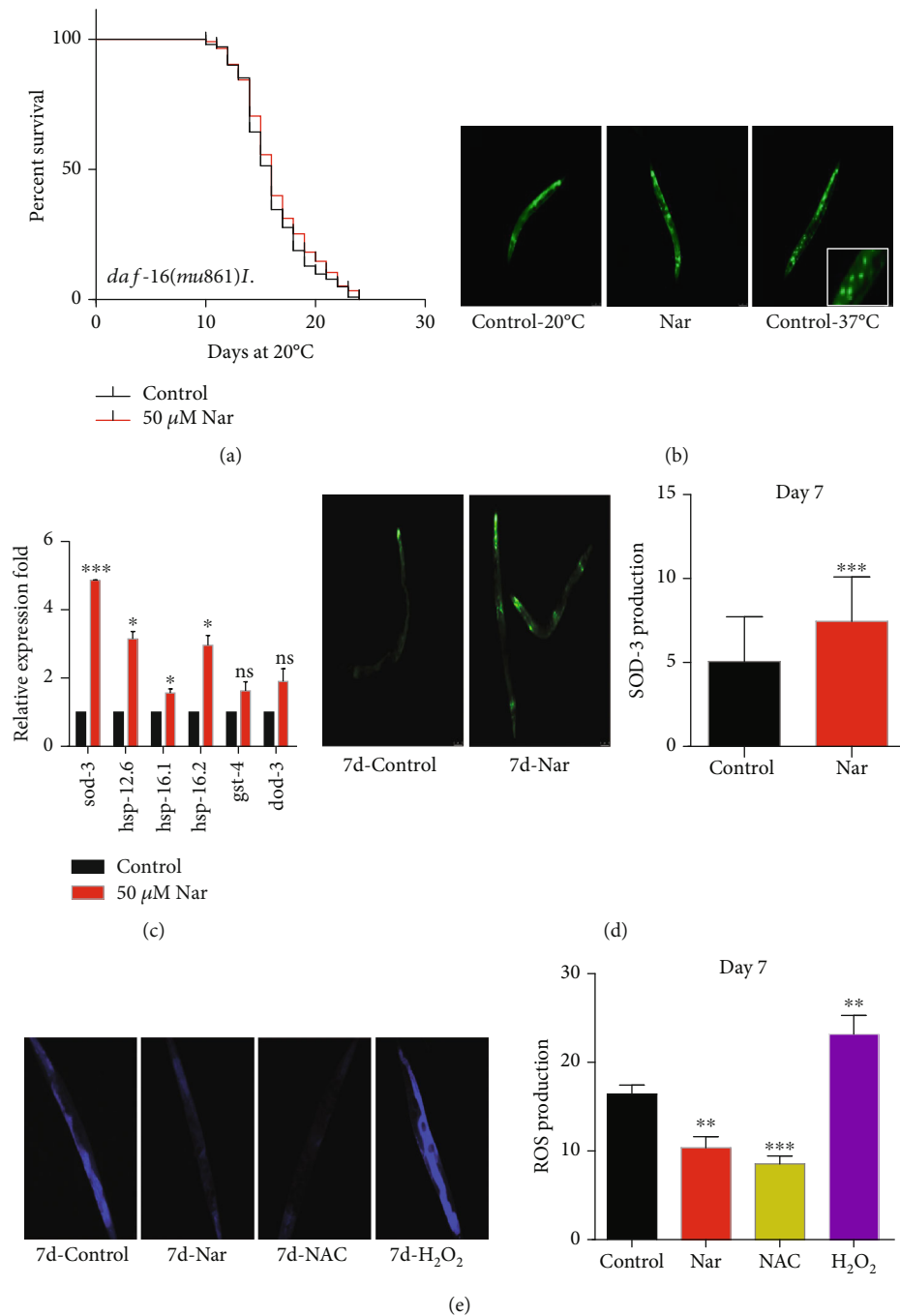


FIGURE 4: The effect of naringin on the lifespan extension in *C. elegans* depends on FOXO homologous *daf-16*. (a) Survival curves of *daf-16* mutants in the control or treated with 50 μ M naringin; naringin could not further extend the mean lifespan of *C. elegans*. (b) 50 μ M naringin could not lead to DAF-16 nuclear localization. DAF-16::GFP expressing worms were placed on the plates with 50 μ M naringin and control plates at 20°C for 48 h. (c) The mRNA level of genes downstream of *daf-16* in worms (N2) treated with or without 50 μ M naringin. The columns showed the mean value of two independent experiments with error bars representing SEM. * represents $p < 0.05$, calculated using two-tailed *t*-test. Statistical details and repeats of these experiments are summarized in Table S9 (Supplementary information). (d) Representative images of the SOD-3::GFP report transgenic CF1553 with naringin or not; naringin enhanced the fluorescence intensity of SOD-3. The aggregation of SOD-3 in N2 treated with or without naringin was captured with a Leica epifluorescence microscope and analyzed by using the image processing software ImageJ. Statistical details and repeats of these experiments are summarized in Table S10 (Supplementary information). (e) Representative images of the degree of ROS in wild-type (N2) animals raised at 20°C on NGM plates via naringin, NAC (5 mM), and H₂O₂ (2 mM) treated; naringin impaired the fluorescence intensity of ROS. The aggregation of ROS in N2 treated with or without naringin was captured with a Leica epifluorescence microscope and analyzed by using the image processing software ImageJ. Statistical details and repeats of these experiments are summarized in Table S10 (Supplementary information).

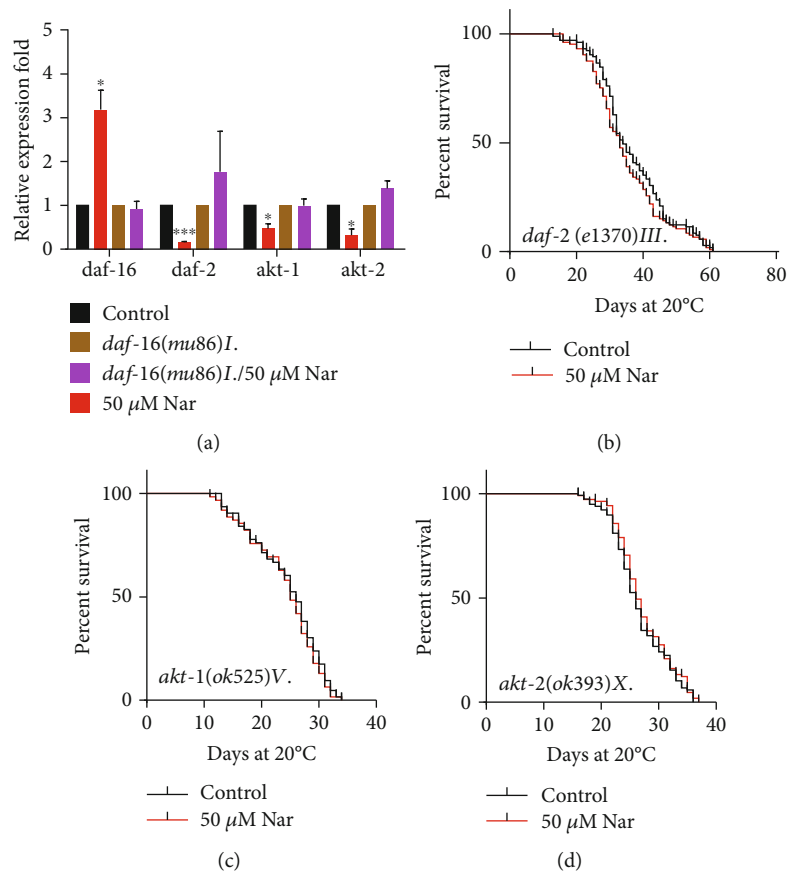


FIGURE 5: Naringin could affect the mRNA expression and not extend the lifespan of *daf-2*, *akt-1*, and *akt-2* mutants in the IIS pathway. (a) The mRNA expression level of genes associated with DAF-16 and itself. The columns showed the mean value of two independent experiments with error bars representing SEM. * represents $p < 0.05$, calculated using two-tailed t -test. Statistical details and repeats of these experiments are summarized in Table S9 (Supplementary information). (b–d) Survival curves of *daf-2*, *akt-1*, and *akt-2* mutants in the control or treated with 50 μM naringin; naringin could not further extend the mean lifespan or control plates without naringin. Statistical details of mutants and repeats of these experiments are summarized in Table S1 (Supplementary information).

showed that naringin treatment further extended the lifespan of the long-lived mutant (Figure 6(b), Table S1), indicating that naringin did not extend the lifespan of nematodes through the germline signaling pathway.

3.7. Naringin Could Not Extend the Lifespan of Long-Lived Mutants in the Nutrition-Sensing Pathway. Dietary restrictions (DR) reduce available nutrients, regulate metabolism, and can extend the lifespan of different organisms, including yeast and mammals [50]. To investigate if the role of naringin in extending the lifespan of *C. elegans* is related to DR, we measured the lifespan of *eat-2(ad1116)II*, a mutant with reduced consumption of food. Our results showed that naringin treatment could not significantly extend the lifespan of *eat-2(ad1116)II* ($p = 0.182$) (Figure 7(a), Table S1).

SIR-2.1 is a member of the Sir-2 family (NAD⁺-dependent protein deacetylases) and regulates nematode aging by interacting with various transcription factors including DAF-16. SIR2 protein has been associated with lifespan regulation in *C. elegans* [51]. We investigated whether naringin could act on SIR2 to extend the lifespan of *C. elegans* by using a null mutant strain *sir-2.1(ok434)IV*. Our results showed

that naringin could not significantly extend the lifespan of *sir-2.1(ok434)IV* ($p = 0.083$) (Figure 7(b), Table S1).

The gene target of rapamycin (TOR) is a highly conserved nutrient-sensing kinase, which plays an important role in DR [52]. RSKS-1 is a homolog of TOR target nuclear subgroup S6 kinase (S6K) in nematodes. Here, our results show that naringin also could not further extend the lifespan of the loss-of-function mutant *rsks-1(ok1255)III* ($p = 0.255$) (Figure 7(c), Table S1).

In addition, mitochondrial involvement in DR-mediated life extension has been reported [52]. The gene *clk-1* encodes a mitochondrial hydroxylase necessary for the biosynthesis of ubiquinone. CLK-1 mutant *clk-1(e2519)III* is a long-lived mutant with mitochondrial respiratory dysfunction [53]. Our results showed that naringin did not significantly extend the lifespan of *clk-1(e2519)III* compared to the control group (Figure 7(d), Table S1).

4. Discussion

The natural product naringin has been reported to have multiple biological activities, such as antineoplastic, anti-

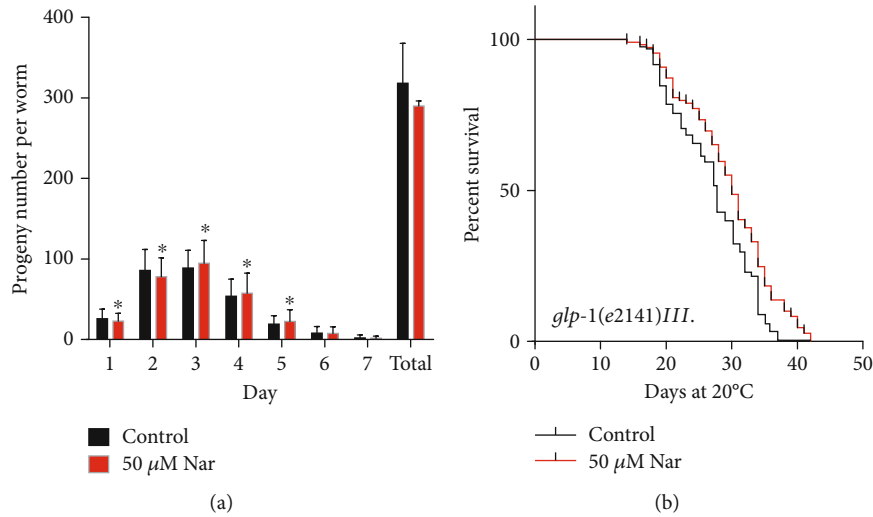


FIGURE 6: Naringin does not act on germline signaling. (a) The offspring of each animal was counted daily at each concentration, and total reproduction outputs were determined by each group. The error bar represent the standard deviation (SD), and no value reached the significance limit of $p < 0.05$ by independent t -test. Statistical details and repeats of these experiments are summarized in Table S11 (Supplementary information). (b) Survival curves of *glp-1* mutants in the control or treated with 50 μ M naringin; naringin could further extend the mean lifespan relative to control plates without naringin. Statistical details and repeats of these experiments are summarized in Table S1 (Supplementary information).

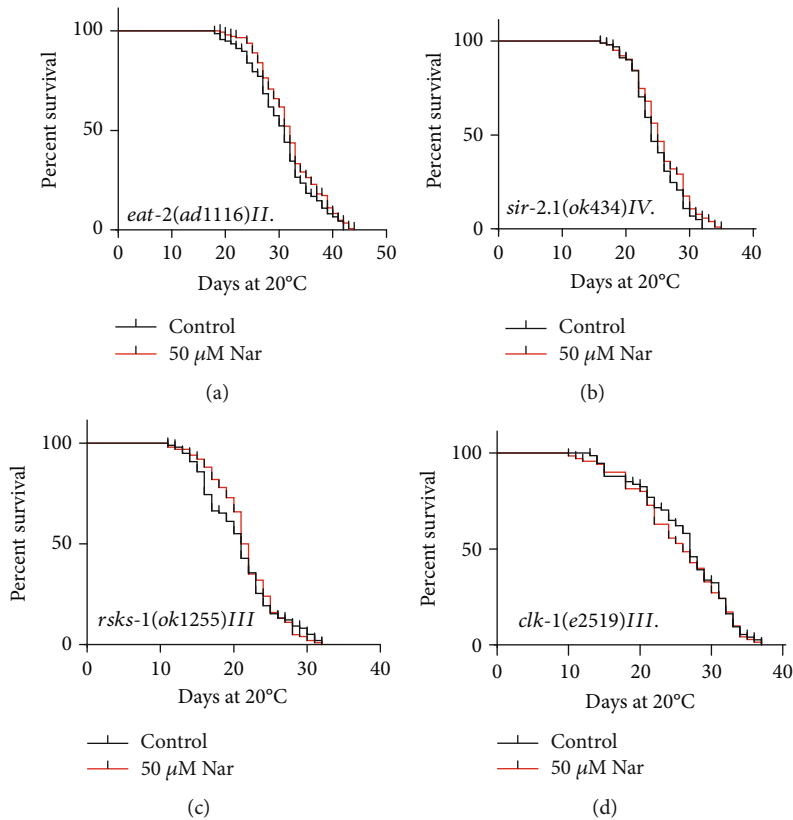


FIGURE 7: Naringin could not extend the lifespan of long-lived mutants in the nutrition-sensing pathway. (a–d) Survival curves of *eat-2*, *sir-2.1*, *rsk-1*, and *clk-1* mutants in the control or treated with 50 μ M naringin; naringin could not further extend the mean lifespan of *C. elegans*. Statistical details and repeats of these experiments are summarized in Table S1 (Supplementary information).

inflammatory, and antioxidative activities [54]. So, we investigated if naringin could influence aging and neurodegenerative diseases. Our results showed that naringin treatment could increase the lifespan of *C. elegans*, delay the aging-related decline of body bending, relieve the accumulation of lipofuscin, enhance the stress resistance, and mitigate the aging-related diseases in models of PD and AD.

Naringin extends the lifespan of *C. elegans* cultured with both live and heat-killed bacteria, suggesting that naringin has biological activity in *C. elegans*. DAF-16 plays a crucial role in stress resistance, longevity, fat accumulation, and reproductive ability in *C. elegans* [47]. Naringin could not extend the lifespan of null mutated *daf-16*. Although no obvious nuclear translocation was observed under treatment of naringin, naringin increased the mRNA expression of *daf-16* and the genes regulated by *daf-16*. Moreover, naringin inhibited the mRNA expression level of the genes upstream of *daf-16* in the IIS pathway. Besides, naringin could not significantly extend the lifespan of long-lived mutants from genes upstream of *daf-16*, including *daf-2*, *akt-1*, and *akt-2*. These results suggest that naringin extends the lifespan of *C. elegans* by regulating the IIS pathway (Figure 8).

We also investigated if naringin could regulate other targets to extend the lifespan of *C. elegans*. It was found that naringin treatment further extended the lifespan of the long-lived *glp-1* mutant (Figure 6(b), Table S1), indicating that naringin did not extend the lifespan of nematodes through the germline signaling pathway.

Dietary restrictions (DR) that reduce available nutrients and regulate metabolism can extend the lifespan of different organisms, including yeast and mammals [50]. Nutrient-sensing pathways play a central role in aging and lifespan. Our results showed that naringin could not significantly extend the lifespan of long-lived mutants from genes in the nutrient-sensing pathway, such as *eat-2*, *sir-2.1*, *rsk-1*, and *clk-1* that modulate mitochondrial respiration. Above results suggest that either the effect of naringin on the lifespan extension is not strong enough to distinguish from the lifespan of the already long-lived mutants or these molecules are required for naringin to extend the lifespan of *C. elegans* (Figure 8). Another possibility is that at the molecular level, the mechanisms of DR appear embedded in the response to reduce energy availability, resulting in the emergence of an altered metabolic state that promotes health and longevity.

Here, we show that naringin could dramatically reduce the α -synuclein aggregation as well as alleviate paralysis in *C. elegans* models of AD and PD. Flavonoids chelate metal ions, preventing formation of free radicals and limiting the onset of PD [55]. Naringin is a kind of dihydroflavonoid. Our results show that naringin could increase the expression of SOD-3 and the scavenging activity of ROS. In addition, several studies showed the link between the IIS pathway and the nervous system. For instance, reduced IGF-1 signaling delays age-associated proteotoxicity in a mouse model of Alzheimer disease [56]. Similarly, attenuated IR substrate of IIS signaling in aging brains extended the lifespan in mice [57]. Likewise, basal IGF-1 activity has been reported to regulate ongoing neuronal activity in hippocampal circuits

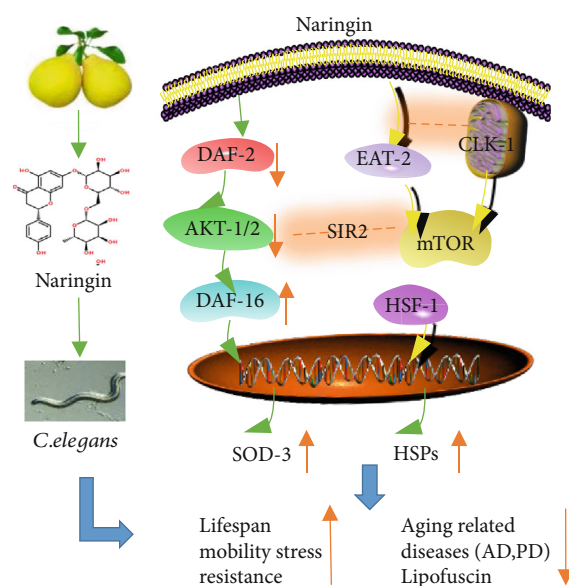


FIGURE 8: A dihydroflavonoid naringin increases stress tolerance, delays progression of aging-related diseases, and extends the lifespan of *C. elegans* via FOXO/DAF-16.

[58]. Interestingly, another study has shown that reduced IGF signaling mediated by FOXO could decrease the proteotoxic activities induced by $A\beta$ hyperaggregation and oxidative stress [56]. Above reports together with our results indicate that naringin might mitigate the aging-related diseases through the IIS pathway.

Data Availability

All the figures and tables used to support the findings of this study are included within the article and supplementary materials.

Conflicts of Interest

The authors declare that there is no conflict of interest.

Authors' Contributions

Qing Zhu and Yuan Qu have contributed equally to this work.

Acknowledgments

We would like to thank *Caenorhabditis* Genetics Center (CGC) for providing the worm strains, which is funded by NIH Office of Research Infrastructure Programs (P40OD010440). Financial support was received from the Natural Science Foundation of China (81771516, 81801398, and 81671405) and the Science and Technology Cooperation Project of Luxian and Southwest Medical University (2019LXXNYKD-04).

Supplementary Materials

Figure S1: the effect of naringin on touch sensory neurons of PD. Table S1: the effect of naringin on lifespan. Table S2: the

effect of naringin on body movement. Table S3: the effect of naringin on intestinal lipofuscin. Table S4: the effect of naringin on oxidative stress resistance. Table S5: the effect of naringin on heat resistance. Table S6: the effect of naringin on aging-related diseases. Table S7: the effect of naringin on touch sensory neurons of PD. Table S8: the effect of naringin on paralysis. Table S9: the effect of naringin on mRNA expression. Table S10: the effect of naringin on SOD-3 and ROS expression. Table S11: the effect of naringin on offspring. Table S12: list of primers used in gene expression assay. (*Supplementary Materials*)

References

- [1] R. Tacutu, D. Thornton, E. Johnson et al., "Human ageing genomic resources: new and updated databases," *Nucleic Acids Research*, vol. 46, no. D1, pp. D1083–D1090, 2018.
- [2] M. Sander, B. Oxlund, A. Jespersen et al., "The challenges of human population ageing," *Age and Ageing*, vol. 44, no. 2, pp. 185–187, 2015.
- [3] C. Lin, X. Zhang, J. Xiao et al., "Effects on longevity extension and mechanism of action of carnosic acid in *Caenorhabditis elegans*," *Food & Function*, vol. 10, no. 3, pp. 1398–1410, 2019.
- [4] A. Godic, "The role of stem cells in anti-aging medicine," *Clinics in Dermatology*, vol. 37, no. 4, pp. 320–325, 2019.
- [5] M. Kozarski, A. Klaus, D. Jakovljevic et al., "Antioxidants of edible mushrooms," *Molecules*, vol. 20, no. 10, pp. 19489–19525, 2015.
- [6] K. B. Pandey and S. I. Rizvi, "Plant polyphenols as dietary antioxidants in human health and disease," *Oxidative Medicine and Cellular Longevity*, vol. 2, no. 5, 278 pages, 2009.
- [7] A. Samoylenko, J. A. Hossain, D. Mennerich, S. Kellokumpu, J. K. Hiltunen, and T. Kietzmann, "Nutritional countermeasures targeting reactive oxygen species in cancer: from mechanisms to biomarkers and clinical evidence," *Antioxidants & Redox Signaling*, vol. 19, no. 17, pp. 2157–2196, 2013.
- [8] H. Yoo, F. Bamdad, N. Gujral, J. W. Suh, and H. Sunwoo, "High hydrostatic pressure-assisted enzymatic treatment improves antioxidant and anti-inflammatory properties of phosvitin," *Current Pharmaceutical Biotechnology*, vol. 18, no. 2, pp. 158–167, 2017.
- [9] W. Qiu, X. Chen, Y. Tian, D. Wu, M. du, and S. Wang, "Protection against oxidative stress and anti-aging effect in *Drosophila* of royal jelly-collagen peptide," *Food and Chemical Toxicology*, vol. 135, article 110881, 2020.
- [10] D. Esposito, J. Overall, M. H. Grace, S. Komarnytsky, and M. A. Lila, "Alaskan berry extracts promote dermal wound repair through modulation of bioenergetics and integrin signaling," *Frontiers in Pharmacology*, vol. 10, article 1058, 2019.
- [11] D. Xu, D. Li, Z. Zhao, J. Wu, and M. Zhao, "Regulation by walnut protein hydrolysate on the components and structural degradation of photoaged skin in SD rats," *Food & Function*, vol. 10, no. 10, pp. 6792–6802, 2019.
- [12] T. Fei, J. Fei, F. Huang et al., "The anti-aging and anti-oxidation effects of tea water extract in *Caenorhabditis elegans*," *Experimental Gerontology*, vol. 97, pp. 89–96, 2017.
- [13] O. M. Ahmed, H. I. Fahim, H. Y. Ahmed et al., "The Preventive Effects and the Mechanisms of Action of Navel Orange Peel Hydroethanolic Extract, Naringin, and Naringenin in N-Acetyl-p-aminophenol- Induced Liver Injury in Wistar Rats," *Oxidative Medicine and Cellular Longevity*, vol. 2019, Article ID 2745352, 19 pages, 2019.
- [14] A. Bernal, E. Zafon, D. Domínguez, E. Bertran, and L. Tusell, "Generation of immortalised but unstable cells after hTERT introduction in telomere-compromised and p53-deficient vHMECs," *International Journal of Molecular Sciences*, vol. 19, no. 7, article 2078, 2018.
- [15] S. M. Jeon, Y. B. Park, and M. S. Choi, "Antihypercholesterolemic property of naringin alters plasma and tissue lipids, cholesterol-regulating enzymes, fecal sterol and tissue morphology in rabbits," *Clinical Nutrition*, vol. 23, no. 5, pp. 1025–1034, 2004.
- [16] S. Ding, J. Hu, J. Yang et al., "The inactivation of JAK2/STAT3 signaling and desensitization of M1 mAChR in minimal hepatic encephalopathy (MHE) and the protection of naringin against MHE," *Cellular Physiology and Biochemistry*, vol. 34, no. 6, pp. 1933–1950, 2014.
- [17] M. I. Prasanth, S. Gayathri, J. P. Bhaskar, V. Krishnan, and K. Balamurugan, "Analyzing the synergistic effects of antioxidants in combating photoaging using model nematode, *Caenorhabditis elegans*," *Photochemistry and Photobiology*, vol. 96, no. 1, pp. 139–147, 2019.
- [18] D. Barreca, G. Laganà, U. Leuzzi, A. Smeriglio, D. Trombetta, and E. Bellocco, "Evaluation of the nutraceutical, antioxidant and cytoprotective properties of ripe pistachio (*Pistacia vera* L., variety Bronte) hulls," *Food Chemistry*, vol. 196, pp. 493–502, 2016.
- [19] F. Chen, G. Wei, J. Xu, X. Ma, and Q. Wang, "Naringin ameliorates the high glucose-induced rat mesangial cell inflammatory reaction by modulating the NLRP3 inflammasome," *BMC Complementary and Alternative Medicine*, vol. 18, no. 1, p. 192, 2018.
- [20] T. P. Hsueh, J. M. Sheen, J. H. Pang et al., "The anti-atherosclerotic effect of naringin is associated with reduced expressions of cell adhesion molecules and chemokines through NF- κ B pathway," *Molecules*, vol. 21, no. 2, p. 195, 2016.
- [21] B. Ben-Azu, E. E. Nwoke, A. O. Aderibigbe et al., "Possible neuroprotective mechanisms of action involved in the neurobehavioral property of naringin in mice," *Biomedicine & Pharmacotherapy*, vol. 109, pp. 536–546, 2019.
- [22] H. Wang, Y. S. Xu, M. L. Wang et al., "Protective effect of naringin against the LPS-induced apoptosis of PC12 cells: implications for the treatment of neurodegenerative disorders," *International Journal of Molecular Medicine*, vol. 39, no. 4, pp. 819–830, 2017.
- [23] S. Ahmed, H. Khan, M. Aschner, M. M. Hasan, and S. T. S. Hassan, "Therapeutic potential of naringin in neurological disorders," *Food and Chemical Toxicology*, vol. 132, article 110646, 2019.
- [24] M. A. Alam, N. Subhan, M. M. Rahman, S. J. Uddin, H. M. Reza, and S. D. Sarker, "Effect of citrus flavonoids, naringin and naringenin, on metabolic syndrome and their mechanisms of action," *Advances in Nutrition*, vol. 5, no. 4, pp. 404–417, 2014.
- [25] F. Chen, N. Zhang, X. Ma et al., "Naringin alleviates diabetic kidney disease through inhibiting oxidative stress and inflammatory reaction," *PLoS One*, vol. 10, no. 11, article e0143868, 2015.
- [26] B. Goldstein, "Sydney Brenner on the genetics of *Caenorhabditis elegans*," *Genetics*, vol. 204, no. 1, pp. 1–2, 2016.

- [27] A. L. Lublin and C. D. Link, "Alzheimer's disease drug discovery: in vivo screening using *Caenorhabditis elegans* as a model for β -amyloid peptide-induced toxicity," *Drug Discovery Today: Technologies*, vol. 10, no. 1, pp. e115–e119, 2013.
- [28] H. Hsin and C. Kenyon, "Signals from the reproductive system regulate the lifespan of *C. elegans*," *Nature*, vol. 399, no. 6734, pp. 362–366, 1999.
- [29] S. Q. Zheng, X. B. Huang, T. K. Xing, A. J. Ding, G. S. Wu, and H. R. Luo, "Chlorogenic acid extends the lifespan of *Caenorhabditis elegans* via insulin/IGF-1 signaling pathway," *The Journals of Gerontology. Series A, Biological Sciences and Medical Sciences*, vol. 72, no. 4, pp. 464–472, 2017.
- [30] S. M. Won, H. U. Cha, S. S. Yi, S. J. Kim, and S. K. Park, "Tenebrio molitor extracts modulate the response to environmental stressors and extend lifespan in *Caenorhabditis elegans*," *Journal of Medicinal Food*, vol. 19, no. 10, pp. 938–944, 2016.
- [31] X. N. Mi, L. F. Wang, Y. Hu et al., "Methyl 3,4-dihydroxybenzoate enhances resistance to oxidative stressors and lifespan in *C. elegans* partially via *daf-2/daf-16*," *International Journal of Molecular Sciences*, vol. 19, no. 6, article 1670, 2018.
- [32] P. Rangsinth, A. Prasansuklab, C. Duangjan et al., "Leaf extract of *Caesalpinia mimosoides* enhances oxidative stress resistance and prolongs lifespan in *Caenorhabditis elegans*," *BMC Complementary and Alternative Medicine*, vol. 19, no. 1, p. 164, 2019.
- [33] X. Chen, J. W. Barclay, R. D. Burgoyne, and A. Morgan, "Using *C. elegans* to discover therapeutic compounds for ageing-associated neurodegenerative diseases," *Chemistry Central Journal*, vol. 9, no. 1, 2015.
- [34] M. Maulik, S. Mitra, A. Bult-Ito, B. E. Taylor, and E. M. Vayndorf, "Behavioral phenotyping and pathological indicators of Parkinson's disease in *C. elegans* models," *Frontiers in Genetics*, vol. 8, 2017.
- [35] C.-W. Tsai, R. T. Tsai, S. P. Liu et al., "Neuroprotective effects of betulin in pharmacological and transgenic *Caenorhabditis elegans* models of Parkinson's disease," *Cell Transplantation*, vol. 26, no. 12, pp. 1903–1918, 2018.
- [36] L. G. Xiong, Y. J. Chen, J. W. Tong, Y. S. Gong, J. A. Huang, and Z. H. Liu, "Epigallocatechin-3-gallate promotes healthy lifespan through mitohormesis during early-to-mid adulthood in *Caenorhabditis elegans*," *Redox Biology*, vol. 14, pp. 305–315, 2018.
- [37] X. B. Huang, X. H. Mu, Q. L. Wan, X. M. He, G. S. Wu, and H. R. Luo, "Aspirin increases metabolism through germline signalling to extend the lifespan of *Caenorhabditis elegans*," *PLoS One*, vol. 12, no. 9, article e0184027, 2017.
- [38] F. Cabreiro, C. Au, K. Y. Leung et al., "Metformin retards aging in *C. elegans* by altering microbial folate and methionine metabolism," *Cell*, vol. 153, no. 1, pp. 228–239, 2013.
- [39] S. Q. Zheng, X. B. Huang, T. K. Xing, A. J. Ding, G. S. Wu, and H. R. Luo, "Chlorogenic acid extends the lifespan of *Caenorhabditis elegans* via insulin/IGF-1 signaling pathway," *The Journals of Gerontology Series A: Biological Sciences and Medical Sciences*, vol. 72, no. 4, pp. 464–464, 2016.
- [40] V. H. C. Liao, C. W. Yu, Y. J. Chu, W. H. Li, Y. C. Hsieh, and T. T. Wang, "Curcumin-mediated lifespan extension in *Caenorhabditis elegans*," *Mechanisms of Ageing and Development*, vol. 132, no. 10, pp. 480–487, 2011.
- [41] S. Deepashree, S. Niveditha, T. Shivanandappa, and S. R. Ramesh, "Oxidative stress resistance as a factor in aging: evidence from an extended longevity phenotype of *Drosophila melanogaster*," *Biogerontology*, vol. 20, no. 4, pp. 497–513, 2019.
- [42] S. M. Won, H. U. Cha, S. S. Yi, S. J. Kim, and S. K. Park, "Tenebrio molitor extracts modulate the response to environmental stressors and extend lifespan in *Caenorhabditis elegans*," *Journal of Medicinal Food*, vol. 19, no. 10, pp. 938–944, 2016.
- [43] C. Kumsta and M. Hansen, "Hormetic heat shock and HSF-1 overexpression improve *C. elegans* survival and proteostasis by inducing autophagy," *Autophagy*, vol. 13, no. 6, pp. 1076–1077, 2017.
- [44] R. Martins, G. J. Lithgow, and W. Link, "Long live FOXO: unraveling the role of FOXO proteins in aging and longevity," *Aging Cell*, vol. 15, no. 2, pp. 196–207, 2016.
- [45] K. Warnhoff, J. T. Murphy, S. Kumar et al., "The DAF-16 FOXO transcription factor regulates *nac-1* to modulate stress resistance in *Caenorhabditis elegans*, linking insulin/IGF-1 signaling to protein N-terminal acetylation," *PLoS Genetics*, vol. 10, no. 10, article e1004703, 2014.
- [46] L. Zhao, Y. Zhao, R. Liu et al., "The Transcription Factor DAF-16 is Essential for Increased Longevity in *C. elegans* Exposed to *Bifidobacterium longum* BB68," *Scientific Reports*, vol. 7, no. 1, article 7408, 2017.
- [47] S. T. Henderson and T. E. Johnson, "*daf-16* integrates developmental and environmental inputs to mediate aging in the nematode *Caenorhabditis elegans*," *Current Biology*, vol. 11, no. 24, pp. 1975–1980, 2001.
- [48] Y. C. Shi, C. W. Yu, V. H. C. Liao, and T. M. Pan, "Monascus-fermented dioscorea enhances oxidative stress resistance via DAF-16/FOXO in *Caenorhabditis elegans*," *PLoS One*, vol. 7, no. 6, article e39515, 2012.
- [49] C. Figueroa-Romero, M. Sadidi, and E. L. Feldman, "Mechanisms of disease: the oxidative stress theory of diabetic neuropathy," *Reviews in Endocrine & Metabolic Disorders*, vol. 9, no. 4, pp. 301–314, 2008.
- [50] W. Mair and A. Dillin, "Aging and survival: the genetics of life span extension by dietary restriction," *Annual Review of Biochemistry*, vol. 77, no. 1, pp. 727–754, 2008.
- [51] J. Lee, G. Kwon, J. Park, J. K. Kim, and Y. H. Lim, "Brief communication: SIR-2.1-dependent lifespan extension of *Caenorhabditis elegans* by oxyresveratrol and resveratrol," *Experimental Biology and Medicine (Maywood, N.J.)*, vol. 241, no. 16, pp. 1757–1763, 2016.
- [52] M. Uno and E. Nishida, "Lifespan-regulating genes in *C. elegans*," *npj Aging and Mechanisms of Disease*, vol. 2, no. 1, article 16010, 2016.
- [53] M. M. Senchuk, D. J. Dues, C. E. Schaar et al., "Activation of DAF-16/FOXO by reactive oxygen species contributes to longevity in long-lived mitochondrial mutants in *Caenorhabditis elegans*," *PLoS Genetics*, vol. 14, no. 3, article e1007268, 2018.
- [54] R. Chen, Q. L. Qi, M. T. Wang, and Q. Y. Li, "Therapeutic potential of naringin: an overview," *Pharmaceutical Biology*, vol. 54, no. 12, pp. 3203–3210, 2016.
- [55] P. Ganesan, H. M. Ko, I. S. Kim, and D. K. Choi, "Recent trends in the development of nanophytoactive compounds and delivery systems for their possible role in reducing oxidative stress in Parkinson's disease models," *International Journal of Nanomedicine*, vol. 10, no. 1, pp. 6757–6772, 2015.

- [56] E. Cohen, J. F. Paulsson, P. Blinder et al., “Reduced IGF-1 signaling delays age-associated proteotoxicity in *mice*,” *Cell*, vol. 140, no. 5, pp. 753–753, 2010.
- [57] A. Taguchi, L. M. Wartschow, and M. F. White, “Brain IRS2 signaling coordinates life span and nutrient homeostasis,” *Science*, vol. 317, no. 5836, pp. 369–372, 2007.
- [58] N. Gazit, I. Vertkin, I. Shapira et al., “IGF-1 receptor differentially regulates spontaneous and evoked transmission via mitochondria at hippocampal synapses,” *Neuron*, vol. 89, no. 3, pp. 583–597, 2016.

Research Article

Amarogentin from *Gentiana rigescens* Franch Exhibits Antiaging and Neuroprotective Effects through Antioxidative Stress

Dejene Disasa , Lihong Cheng , Majid Manzoor , Qian Liu , Ying Wang ,
Lan Xiang , and Jianhua Qi 

College of Pharmaceutical Science, Zhejiang University, 866 Yu Hang Road, Hangzhou, China

Correspondence should be addressed to Jianhua Qi; qijianhua@zju.edu.cn

Dejene Disasa and Lihong Cheng contributed equally to this work.

Received 23 April 2020; Revised 26 June 2020; Accepted 17 July 2020; Published 3 August 2020

Guest Editor: Francisco Jaime B. Mendonça Junior

Copyright © 2020 Dejene Disasa et al. This is an open access article distributed under the Creative Commons Attribution License, which permits unrestricted use, distribution, and reproduction in any medium, provided the original work is properly cited.

In the present study, the replicative lifespan assay of yeast was used to guide the isolation of antiaging substance from *Gentiana rigescens* Franch, a traditional Chinese medicine. A compound with antiaging effect was isolated, and the chemical structure of this molecule as amarogentin was identified by spectral analysis and compared with the reported data. It significantly extended the replicative lifespan of K6001 yeast at doses of 1, 3, and 10 μM . Furthermore, amarogentin improved the survival rate of yeast under oxidative stress by increasing the activities of catalase (CAT), superoxide dismutase (SOD), and glutathione peroxidase (GPx), and these enzymes' gene expression. In addition, this compound did not extend the replicative lifespan of *sod1*, *sod2*, *uth1*, and *skn7* mutants with K6001 background. These results suggested that amarogentin exhibited antiaging effect on yeast via increase of *SOD2*, *CAT*, *GPx* gene expression, enzyme activity, and antioxidative stress. Moreover, we evaluated antioxidant activity of this natural products using PC12 cell system, a useful model for studying the nervous system at the cellular level. Amarogentin significantly improved the survival rate of PC12 cells under H_2O_2 -induced oxidative stress and increased the activities of SOD and SOD2, and gene expression of *SOD2*, *CAT*, *GPx*, *Nrf2*, and *Bcl-x1*. Meanwhile, the levels of reactive oxygen species (ROS) and malondialdehyde (MDA) of PC12 cells were significantly reduced after treatment of the amarogentin. These results indicated that antioxidative stress play an important role for antiaging and neuroprotection of amarogentin. Interestingly, amarogentin exhibited neuritogenic activity in PC12 cells. Therefore, the natural products, amarogentin from *G. rigescens* with antioxidant activity could be a good candidate molecule to develop drug for treating neurodegenerative diseases.

1. Introduction

The number of aging population is rapidly increasing globally [1]. Aging, which is a functional and structural deterioration of cells, tissues, and organs, has been implicated as a risk factor for age-related diseases, such as neurodegenerative disease, cancer, and metabolic diseases [2–5]. Alzheimer's disease (AD) which is the most prevalent neurodegenerative disorder threatens the health of an enormous number of aging populations worldwide. This age-related neurodegenerative disease has no effectively curative drug. Therefore, the discovery of drugs that can effectively delay the inevitable aging process and cure AD is highly desirable. Rapamycin, resveratrol (RES), metformin, and curcumin which exhibit

antiaging effects were also reported to have significant neuroprotective effects in AD models, indicating a strong link between aging and neurodegenerative diseases [6–10]. Thus, antiaging substances may be developed as promising drugs to cure neurodegenerative diseases.

Oxidative stresses play a vital role in aging and neurodegenerative disorders [3, 5]. Gradual accumulation of ROS causes disruption of macromolecules such as proteins, DNA, and lipids which are implicated for progression of neurodegenerative disease and aging processes [5]. The superfluous level of ROS causes several damaging effects such as reduction of ATP production and mitochondrial dysfunction. An excessive or low level of mitochondrial ATP production affects the normal function of nerve cells and its

response to stress during aging and AD development. Mitochondrial permeability transition pore results in hypertrophy of mitochondria and subsequent cell death [11]. Another consequence of oxidative stress is oxidative damage to DNA, which could potentially lead to cellular dysfunction and death [5, 11]. Excessive ROS could be scavenged by antioxidative enzymes such as SOD, CAT, and GPx [5]. SODs are metalloproteinases that catalyze the conversion of ROS into less harmful products to protect cells against oxidative damage [12]. CAT helps cells to survive by breaking down reactive hydrogen peroxide into products such as water and oxygen. It is used as a therapeutic agent for several diseases related to oxidative stress [13]. Cellular GPx system is part of essential constituents in protecting cells against oxidative stress. It detoxifies hydrogen peroxides in cells. It plays an indispensable role to protect cells from oxidative damage exerted by free radicals especially lipid peroxidation [12]. Lipid peroxidation product, MDA, is widely used as a biomarker to examine the level of oxidative damage [14].

The genus *Gentiana*, a major group in the Gentianaceae family, is found in Asia, Europe, and America [15]. Several important molecules, such as iridoids, secoiridoids, essential oils, xanthenes and terpenoids, have been isolated from *Gentiana*. Iridoids and secoiridoids are the major constituents from this genus and are regarded to be responsible for a variety of biological activities [15]. *Gentiana rigescens* Franch (Jian Long Dan in Chinese) is a well-known traditional Chinese medicine (TCM) that is widely distributed in Yunnan Province, Southwest of China. *G. rigescens* is used to treat hepatitis, rheumatism, cholecystitis, and inflammation [16]. “Sheng Nong’s Herbal Classic”, a classic book on TCM material medica, states that *G. rigescens* improves cognition and has antiaging activity. In our previous study, gentisides A–K, which are 11 novel neuritogenic benzoate-type molecules, were isolated from *G. rigescens*; the mixture of gentisides (n-GS) was confirmed to alleviate the impaired memory of the AD model [17–19]. Natural products are important sources of drugs to reduce or prevent oxidative stresses in humans. In our previous studies, 19 molecules were isolated from natural products which were able to extend the replicative lifespan of yeast via antioxidative stress [20–25]. Therefore, searching for effective molecules with antioxidative stress potential should be considered an important strategy to treat aging and neurodegenerative disorders.

Yeast is one of the well-known bioassay models in aging research because of its low cost, genetic tractability, and short generation time. A unique characteristic of K6001 is that only mother cells can produce daughter cells in a glucose medium but not in a galactose medium [26]. In our previous study, K6001, which is a yeast mutant strain, was used as a bioassay system to evaluate the antiaging activity of natural products [20–25]. Furthermore, the PC12 cell line, which was derived from rat pheochromocytoma cells, is one of the useful models for studying the nervous system at the cellular level [27]. Based on the link between aging and neurodegenerative diseases [6–10], PC12 cells were also used to evaluate the neuroprotective activity of antiaging molecules.

In present study, a K6001 yeast bioassay system was employed to guide the isolation of antiaging substances. Amarogentin was discovered as an antiaging natural product. Amarogentin is a kind of secoiridoid-type compound that can be found in *Gentiana lutea*, *Swertia japonica*, *Gentianella nitida*, and *Swertia chirayita* [28–30]. It has been reported to possess various activities, such as anti-inflammatory, immunomodulatory, antioxidative stress, and antidiabetic effects [31–33]. Herein, the antiaging, neuroprotective, and neuritogenic effects and the underlying mechanism of the natural bioactive product, amarogentin, which possesses antioxidative stress potential for treatment neurodegenerative disease, will be reported.

2. Materials and Methods

2.1. General. Silica gel (200–300 mesh, Yantai Chemical Industry Research Institute, Yantai, China) and reversed phase C18 (Octadecylsilyl, ODS) silica gel (Cosmosil 75 C₁₈ OPN, Nacalai Tesque, Japan) were used for column chromatography. Precoated silica gel (0.25 mm) and RP-18 plate (0.25 mm) were used for TLC analysis. Preparative high-performance liquid chromatography (HPLC) was performed using a HPLC equipped with two ELITE P-230 pumps and a UV detector. High-resolution electrospray ionisation mass spectrometry (HR-MS) analysis was performed on Agilent 6224A accurate mass time-of-flight LC/MS system (Agilent Technologies). A Bruker AV III-500 spectrometer (Bruker, Billerica, MA, USA) was operated for NMR measurement. The NMR chemical shifts in δ (ppm) were referred to the solvent peak of δ_C (49.0) for methanol.

2.2. Extraction and Isolation. Dried roots of *G. rigescens* were purchased from HuQingYuTang Pharmacy in Hangzhou City, Zhejiang Province, China. The plant material (1.5 kg dry weight) was smashed and extracted with methanol for 48 h under shaking at room temperature. The extract was filtered, and the supernatant was concentrated to obtain 400 g of crude extract. The crude extract was partitioned between the water and ethyl acetate. The samples from each layer were tested for antiaging activity on the K6001 yeast strain. The active ethyl acetate layer (12 g) was subjected to silica open column and eluted with *n*-hexane/ethyl acetate (100/0, 90/10, 80/20, 70/30, 60/40, 50/50, 30/70, and 0/100 and methanol 100%) to obtain nine fractions. The active fraction (300 mg) obtained from *n*-hexane/ethyl acetate (30/70) was further chromatographed on ODS and eluted with methanol/water (30/70, 40/60, 50/50 70/30, 80/20, 90/10, and 100/0) to obtain six fractions. The active fraction obtained from 50/50 methanol/water (19 mg) was subjected to HPLC purification (Develosil 5C18-MS-II (10 × 250 mm), flow rate of 3 ml/min and 40% aqueous methanol) to obtain the active sample (11 mg, $t_R = 25$ min). In the present study, amarogentin was dissolved in ethanol or DMSO with stock concentration of 10 mM for yeast and PC12 cell experiments, respectively.

2.3. Yeast Strains, Culture Medium, and Lifespan Assay. K6001 yeast with back ground W303, wild-type BY4741

yeast strain, and *uth1*, *skn7*, *sod1*, and *sod2* mutants with K6001 background were used. The liquid culture medium contained yeast extract, peptone, and D-glucose (YPD, 1% yeast extract, 2% peptone and 2% glucose) or galactose (YPG, 1% yeast extract, 2% peptone, 3% galactose) media. Replicative lifespan assays were performed as described in our previous study [20]. In brief, the K6001 yeast strain was inoculated in 5 ml of galactose medium and incubated in a shaking incubator at 180 rpm for 24 h at 28°C. Afterwards, 1 ml of broth containing yeast was centrifuged, and the yeast pellet was washed three times with phosphate buffer solution (PBS). The pellet was then diluted with PBS, and a haemocytometer was used to count cells. Approximately 4,000 cells were smeared on the glucose medium agar plates containing resveratrol (RES) or amarogentin at different concentrations. The agar plates were incubated for 48 h at 28°C, and the microcolonies that formed on the agar plate were observed under a microscope. Forty microcolonies were randomly chosen to count the number of daughter cells produced by one mother cell. The replicative lifespan assay of *uth1*, *skn7*, *sod1*, and *sod2* mutants with K6001 background was the same as that of K6001 yeast strain.

2.4. Antioxidative Stress Assay. Based on the evidence from our previous studies [21, 23], 10 mM H₂O₂ was chosen as the optimum concentration to induce oxidative stress. The wild-type BY4741 yeast was inoculated in YPD medium, placed in a shaker incubator, and cultured for 24 h. The BY4741 yeast at initial 0.1 OD was placed in a liquid glucose medium and treated with RES at 10 μM as positive control or amarogentin (0, 1, 3 and 10 μM) for 24 h at 28°C. Subsequently, 5 μl of the cultured cells with the same OD600 value from each group was dropped on a plate containing 10 mM H₂O₂. The growth of yeast cells on the plate was observed and photographed after 3 days of incubation at 28°C.

The effect of amarogentin on oxidative stress in yeast was quantified using a different approach. Similar to the above antioxidative stress assessment, BY4741 yeast cells were treated with RES (10 μM) or amarogentin (0, 1, 3, and 10 μM). The counted 200 yeast cells from each group were spread on a glucose agar plate with or without 5.5 mM H₂O₂ and incubated at 28°C for 48 h. After 2 days, the colonies that formed on the plate were counted. The survival rate of the yeast cells was analysed from the ratio of the number of colonies in the absence of 5.5 mM H₂O₂ divided by the number of colonies in the presence of 5.5 mM H₂O₂.

2.5. Measurement of SOD, GPx, and CAT Enzymatic Activities in Yeast. Y4741 yeast in the liquid glucose medium was treated with RES (10 μM) or amarogentin (0, 1, 3, and 10 μM) for 48 h at 28°C. The activity assays of total SOD, SOD1, SOD2, GPx, and CAT were performed according to a previous study [23, 24]. The BY4741 yeast cells in the liquid glucose medium was treated with RES (10 μM) or amarogentin (0, 1, 3, and 10 μM) for 24 h at 28°C with the initial OD of 0.1. Yeast cells were collected and sonicated for five minutes (each time lasted for 1 min). The cell lysates were centrifuged to get supernatant. The enzymatic activities of the SOD, GPx, and CAT in the supernatant were measured with corre-

sponding assay kits (Biotime Biotechnology Limited Company, Shanghai, China) following the manufacturer's instructions; the details of assays procedures are shown in supplementary materials.

2.6. Neuroprotection Effect of Amarogentin in PC12 Cells. Approximately 50,000 PC12 cells were seeded in each well of a 24-well plate and cultured in 5% CO₂ at 37°C for 24 h. Then, the medium was replaced by 1 ml serum-free Dulbecco's modified Eagle's medium (DMEM; Thermo Scientific, Shanghai, China) containing different tested samples. In the dose-dependent experiment of H₂O₂, the cells were treated with 0.5% dimethyl sulphoxide (DMSO) for 24 h and cultured with different concentrations of H₂O₂ for 1 h. To investigate the neuroprotection effect of amarogentin, PC12 cells were treated with RES (10 μM) or amarogentin (1, 3, or 10 μM) for 24 h and with 0.9 mM H₂O₂ for 1 h. The medium was replaced with 500 μl of serum-free DMEM containing 200 μg/ml 3-(4,5-dimethylthiazol-2-yl)-2,5-diphenyltetrazolium bromide (MTT) and cultured for another 2 h. The medium was completely removed and replaced by 200 μl of DMSO to each well to solubilise the formed formazan crystal. The resultant formazan was detected at 570 nm by using a plate reader (Bio-Tec instruments Inc., Winooski, VT, USA). The experiment was performed three times, and the result was considered viable compared with negative control.

2.7. ROS, MDA, Total SOD, SOD1, and SOD2 Enzymatic Activity Assays in PC12 Cells. To determine the ROS level in PC12 cells, approximately 50,000 PC12 cells were seeded in each well of a 24-well plate. The cells were treated with RES (10 μM) or amarogentin (1, 3, and 10 μM) for 24 h and then with 0.9 mM H₂O₂ for 1 h. Each well was then added with DCFH-DA (2',7'-dichlorodihydrofluorescein diacetate, final concentration, 10 μM) and incubated for 30 min. The cells were washed with PBS to remove extracellular DCFH-DA, and intercellular ROS was detected by using the Spectra-Max M3 multimode microplate reader (Molecular Devices Corporation, California, USA) under the excitation wavelength of 488 nm and emission wavelength of 525 nm. At the same time, DCF in PC12 cells was observed using a fluorescence microscope (HCS, Thermo Fisher, scientific, Waltham, MA, USA).

To test the MDA content and total SOD, SOD1, and SOD2 enzymatic activities in PC12 cells, approximately 2 × 10⁶ of PC12 cells were seeded in a 60 mm culture dish, containing 5 ml of DMEM medium, and incubated for 24 h. Then, PC12 cells were treated with RES (10 μM) or amarogentin (1, 3, or 10 μM) for 24 h and then with 0.9 mM H₂O₂ for another 1 h to determine MDA content, and total SOD, SOD1, and SOD2 activities. The cells were then collected by centrifugation and three cycles of ultrasonication (1 min for each instance) with PBS. The cell lysates were centrifuged, and the supernatant was removed to assess MDA, total SOD, SOD1, and SOD2 enzymatic activities. MDA quantification and total SOD, SOD1, and SOD2 activities were determined using MDA and SOD enzymatic activity assay kits (Nanjing Jiancheng Bioengineering

Institute, Nanjing, China) following the manufacturer's instructions; the details of assays procedures are shown in supplementary materials.

2.8. RT-PCR Analysis. To get the RNA samples of yeast, BY4741 yeast cells were cultured in glucose medium >following addition of 0, 1, 3, and 10 μM of amarogentin or 10 μM RES. RNA was extracted from yeast cells in the exponential phase through the hot phenol method. For PC12 cells, approximately 2×10^6 of PC12 cells were seeded in a 60 mm culture dish and treated with RES (10 μM) or amarogentin (1, 3, or 10 μM) for 12 h or 24 h. Total RNA was extracted with TRIzol Reagent (Beijing Cowin Biotech Company, Beijing, China). RNA content was determined using Eppendorf Biophotometer Plus (Eppendorf Company, Hamburg, Germany). Transcription was performed using 5 μg of total RNA, Oligo (dT)₂₀ primers, and reverse transcriptase (Beijing Cowin Biotech Company, Beijing, China). Transcript levels were quantified by real-time PCR (AB SCIEX, Massachusetts, USA) and SYBR Premix EX Taq™ (Takara, Otsu, Japan). The primers (Sangon Biotech Co. Ltd., Shanghai, China) used in this study are given in Supplementary Table S1. Thermal recycling parameters for yeast are as follows: *SOD1* and *SOD2*, 95°C for 2 min, followed by 40 cycles, 94°C for 15 seconds, 60°C for 25 seconds, and 72°C for 10 seconds; and *GPx* and *CAT*, 40 cycles, 95°C for 15 seconds, 60°C for 35 seconds. Thermal recycling parameters for PC12 cells are as follows: *SOD1* and *SOD2*: 95°C for 2 min, followed by 40 cycles, 54°C for 35 seconds; *GPx* and *CAT*, 95°C for 2 min, followed by 40 cycles, 55°C for 35 seconds; and *Bcl-x1* and *Nrf2*: 95°C for 2 min, followed by 40 cycles, 95°C for 15 seconds, 60°C for 15 seconds, and 68°C for 20 seconds. All results were normalized to *TUB1* or *GAPDH* RNA levels, and relative mRNA transcript levels were calculated using the $\Delta\Delta\text{Ct}$ formula. All samples were run in triplicate, and the average values were calculated.

2.9. Neuritogenic Activity of Amarogentin in PC12 Cells. The neuritogenic activity of the isolated compound was evaluated according to our previous report [17]. Approximately 50,000 PC12 cells were seeded in each well of a 24-well microplate in 1 ml of DMEM containing 7.5% foetal bovine serum, 10% horse serum, and 1% premixed antibiotics (Invitrogen, Shanghai, China) and cultured under a humidified atmosphere of 5% CO₂ at 37°C. The medium was replaced by serum-free DMEM containing either DMSO (0.5%) or the sample at various concentrations after 24 h. The cells were treated with 40 ng/ml NGF (Recombinant Human β -NGF, Sigma, Shanghai, China) as the positive control. For evaluation of the enhancement of NGF activity, the medium was replaced by serum-free DMEM containing 1 ng/ml NGF in addition to the test sample. Cellular morphological changes were observed under a phase-contrast microscope (Olympus, model CKX41, Tokyo, Japan) after 48 h. Approximately 100 cells were randomly selected from different areas and counted. Cells bearing neuritis outgrowth longer than the diameter of the cell body were considered positive cells.

2.10. Statistical Analysis. Data were evaluated by one-way ANOVA, followed by Tukey's post hoc test by using Graph-Pad Prism software. *p* value < 0.05 was considered statistically significant. Each experiment was repeated three times, and data were expressed as mean \pm SEM.

3. Results

3.1. Extraction and Isolation. The methanol extract of *G. rigescens* was partitioned between ethyl acetate and water to obtain two samples from each layer, respectively. The two samples were tested on the K6001 yeast strain to evaluate their antiaging activity. The active ethyl acetate layer sample was subjected to silica gel and then ODS open column followed by HPLC purification to yield the active molecule (11 mg). The chemical structure of the molecule was identified as amarogentin (AMA) (Figure 1(a)) by comparing spectral data with those reported in literature [34]. ¹³C NMR (125 MHz, methanol-*d*₄): δ 25.8, 28.7, 43.4, 62.4, 69.5, 71.7, 74.6, 74.8, 78.4, 96.8, 97.2, 103.1, 104.0, 105.6, 112.9, 114.5, 116.5, 121.0, 121.2, 129.3, 132.9, 146.5, 148.6, 153.7, 157.5, 163.9, 166.0, 167.6 and 171.5; HRESI-TOF-MS, *m/z* 609.1584, calculated for C₂₉H₃₀O₁₃Na (M+Na)⁺ 609.1579.

3.2. Amarogentin Extended the Replicative Lifespan of Yeast with K6001 Background. The K6001 yeast strain has a unique characteristic; that is, daughter cells produced by mother cells only survive in a galactose medium and not in a glucose medium [23]. Therefore, we utilized this characteristic to perform a replicative lifespan assay. The effect of amarogentin on the replicative lifespan of the K6001 yeast strain is displayed in Figure 1(b). The mean lifespan of the control is 7.8 ± 0.1 generations, 10.4 ± 0.1 in the RES-treated group, and 9.8 ± 2.4 , 10.6 ± 2.0 , 9.8 ± 0.1 , and 8.1 ± 0.2 generations in amarogentin groups at concentrations of 1, 3, 10, and 20 μM , respectively. Amarogentin extended the replicative lifespan of K6001 yeast at concentrations of 1, 3, and 10 μM compared with the control group (*p* < 0.05, *p* < 0.01, and *p* < 0.05, respectively). Hence, 3 μM amarogentin is the best concentration. The result also suggests that amarogentin has antiaging effect on yeasts.

3.3. Amarogentin Improved the Survival Rate of Yeast under Oxidative Stress and SOD, GPx, and CAT Activities. Oxidative stress is one of the major risk factors for aging and age-related pathologies. The elevated level of oxidants or free radicals released from biochemical reactions triggers deleterious effect on macromolecules, such as proteins, nucleic acids, and lipids [11, 12]. Therefore, we focused on the antioxidative stress to do investigation with two methods. The effects of amarogentin on the growth of yeast under oxidative stress induced by 10 mM H₂O₂ are shown in Figure 2(a). The growth of yeast on the agar plate with H₂O₂ in the amarogentin-treated groups was better than negative control and RES-treated groups. To quantify the change induced by amarogentin on oxidative stress, we used another analytical method. The survival rate of yeast under oxidative stress induced by 5.5 mM H₂O₂ in the amarogentin-treated group was significantly increased compared with that in the control

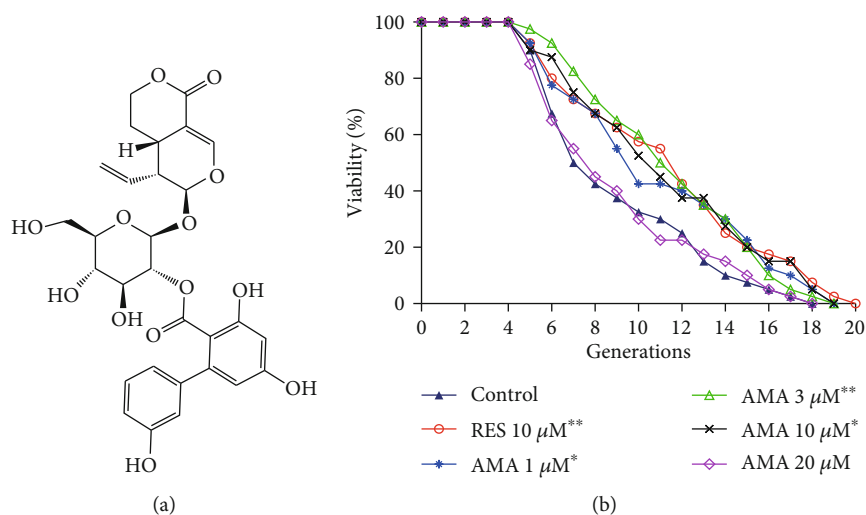


FIGURE 1: Chemical structure of amarogentin (AMA) (a), changes in the replicative lifespan of K6001 yeast after treatment with different concentrations of amarogentin (b). In the replicative lifespan assay, K6001 yeast cultured in galactose medium for 24 h. After that, it was spread on glucose agar plates with different concentrations of amarogentin or 10 μM RES as a positive control and incubated for 48 h. The randomly selected daughter cells produced by 40 mother cells were counted, and the survival curve was plotted for analysis. This process was repeated three times. *, ** indicated significant difference as compared with the control ($p < 0.05$ and 0.01), respectively.

group (Figure 2(b)). The effect of amarogentin on antioxidative stress at a concentration of 3 μM is similar to that of RES at a concentration of 10 μM . These results indicate that amarogentin showed antiaging effect by inhibiting oxidative stress.

Antioxidant enzyme system widely exists in organisms. It can effectively eliminate the active oxygen produced by the metabolism of organisms and protect the biological macromolecules from the oxidative damage of active oxygen radicals. The antioxidant enzyme system is mainly composed of superoxide dismutase, glutathione peroxidase, and catalase [5]. Thus, we evaluated the activities of total SOD, SOD1, SOD2, CAT, and total GPx in yeast after treatment with amarogentin at different concentrations for 24 h. As indicated in Figures 2(c)–2(g), the enzymatic activities of total SOD, SOD2, CAT, and GPx notably increased after treatment with 3 and 10 μM amarogentin. The SOD1 activity was not affected by amarogentin. Therefore, amarogentin exhibited antiaging effect by regulating the total SOD, SOD2, GPx, and CAT enzymatic activities.

3.4. Effect of Amarogentin on Gene Expression of SOD1, SOD2, GPx, and CAT in Yeast. The changes on SOD1, SOD2, GPx, and CAT gene expression of yeast are shown in Figure 3. The gene expression of SOD1 was not affected by amarogentin (Figure 3(a)). The abundance of SOD2 mRNA was significantly increased after treatment of amarogentin at doses of 1 and 3 μM (Figure 3(b), $p < 0.05$, $p < 0.05$). The significant increase of GPx gene expression was observed in all of amarogentin-treated groups (Figure 3(c), $p < 0.01$, $p < 0.01$, and $p < 0.01$). The significant increase of CAT gene expression was only observed in the 3 μM amarogentin-treated group (Figure 3(d), $p < 0.05$). These results suggested that SOD2, GPx, and CAT genes took important roles in antiaging effect of amarogentin.

3.5. Amarogentin Failed to Extend the Replicative Lifespan of *sod1*, *sod2*, *uth1*, and *skn7* Mutants of Yeast with K6001 Background. Several genes are known to be involved in regulating the aging process. *UTH1*, which is an aging gene, is involved in apoptosis. *UTH1* gene intrinsically participates in regulating oxidative stress, and the deletion of this gene leads to extended replicative life span in yeast. *SKN7* is an upstream transcriptional factor for *UTH1*, which is associated in the defence against oxidative stress [35, 36]. SOD is a kind of antioxidant metal enzyme in an organism. This molecule can catalyse the superoxide anion free radical disproportionation to produce oxygen and hydrogen peroxide. SOD plays an important role in the balance of oxidation and antioxidation and is closely related to the occurrence and development of many diseases. To investigate whether these proteins and gene were involved in the anti-aging effect of amarogentin, we used *sod1*, *sod2*, *uth1*, and *skn7* mutants of yeast with K6001 background to perform the replicative lifespan assay. The changes in the replicative lifespan of mutant yeast with K6001 background after treatment with amarogentin are shown in Figures 4(a)–4(d). The replicative lifespan in Δuth1 yeast significantly increased compared with that in K6001 yeast. However, the replicative lifespans of the mutants were not affected by amarogentin and RES. These results indicate that SOD1, SOD2, UTH1, and SKN7 genes were involved in the antiaging effect of amarogentin.

3.6. Amarogentin Exhibited Neuroprotection on the H_2O_2 -Induced Oxidative Damage in PC12 Cells. Antioxidative stress is one of the essential pathways for protecting against neurodegeneration. Based on the significant antioxidative activity of amarogentin in yeast, the PC12 cell line, which was derived from mammalian cells, was employed as a bioassay system to confirm the effects of the antioxidative stress of

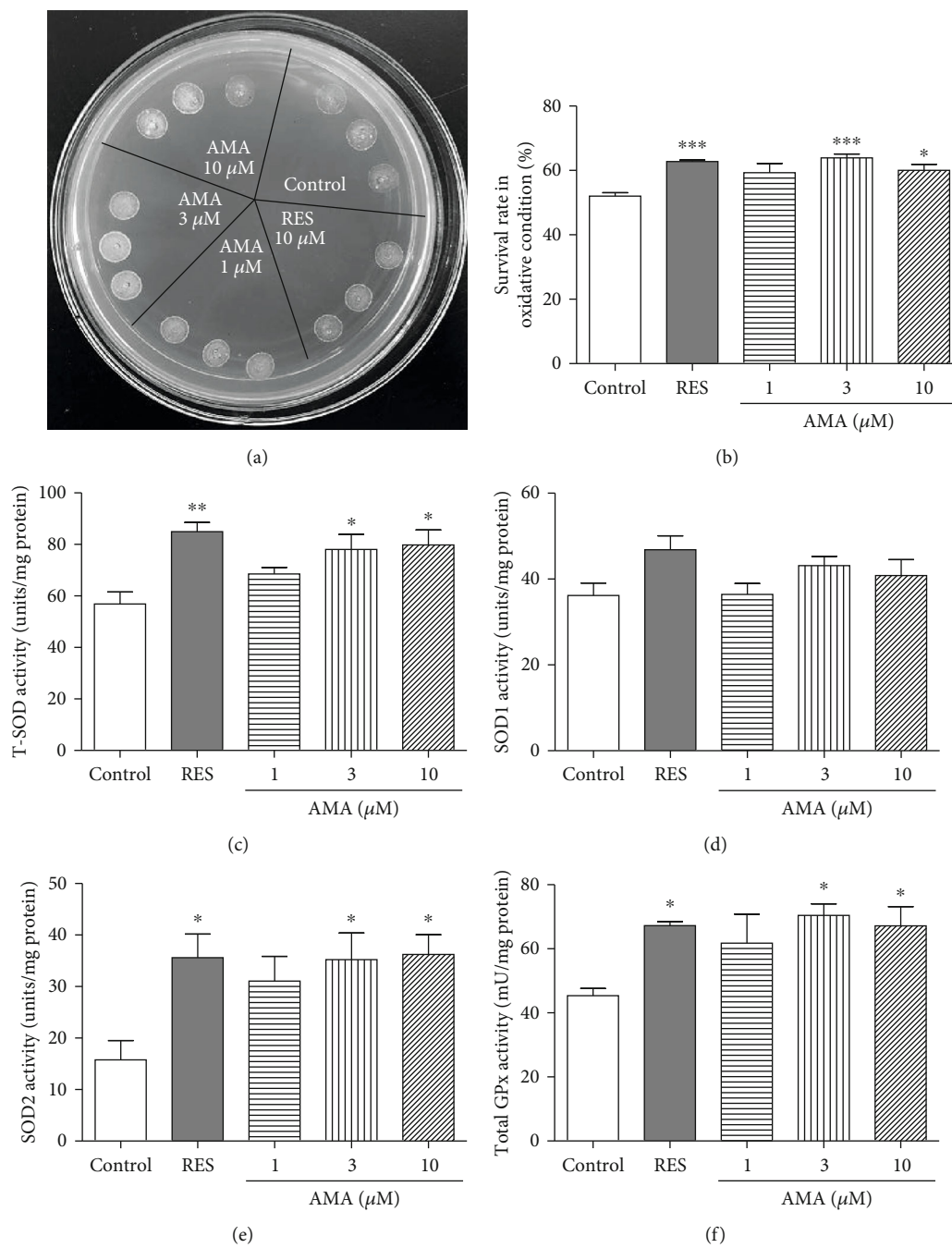


FIGURE 2: Continued.

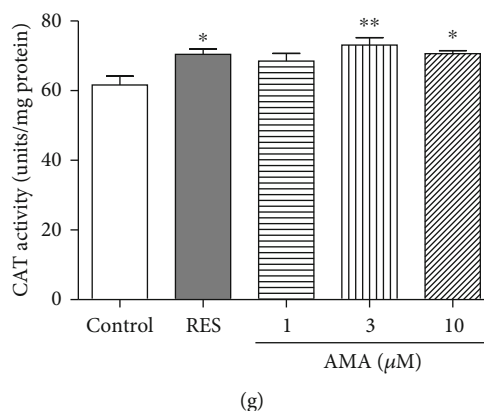


FIGURE 2: Effect of amarogentin on oxidative stress in yeast and the SOD, GPx, and CAT enzymatic activities of yeast. (a) The growth of yeast under oxidative stress induced by 10 mM H_2O_2 after treatment with amarogentin. The wild-type BY4741 yeast was inoculated in YPD medium for 24 h. Then after, initial 0.1 OD of yeast was placed in a liquid glucose medium and treated with RES at 10 μ M as positive control or amarogentin (0, 1, 3, and 10 μ M) for 24 h at 28°C. Subsequently, 5 μ l of the cultured cells with the same OD600 value from each group was dropped on a plate containing 10 mM H_2O_2 . The growth of yeast cells on the plate was observed and photographed after 3 days of incubation at 28°C. (b) Survival rate of the BY4741 yeast strain under 5.5 mM H_2O_2 -induced yeast oxidative stress after adding amarogentin. BY4741 yeast cells were treated with RES (10 μ M) or amarogentin (0, 1, 3, and 10 μ M). The counted 200 yeast cells from each group were spread on a glucose agar plate with or without 5.5 mM H_2O_2 and incubated at 28°C for 48 h. After 2 days, the colonies that formed on the plate were counted. The survival rate of yeast cells was analysed from the ratio of the number of colonies in the absence of 5.5 mM H_2O_2 divided by the number of colonies in the presence of 5.5 mM H_2O_2 . Effect of amarogentin on the total superoxide dismutase (T-SOD) (c), SOD1 (d), SOD2 (e), total glutathione peroxidase (GPx) (f) and catalase (CAT) (g). BY4741 yeast strain cells were incubated with RES as a positive control or amarogentin at concentrations of 1, 3, and 10 μ M for 24 h. Afterwards, the yeast cells were collected by centrifugation and ultrasonicated for five times. The supernatant of the yeast was used to measure the T-SOD, SOD1, SOD2, GPx, and CAT activities according to the manufacturer's instructions. Each experiment was conducted thrice. *, **, and *** indicated significant difference as compared with the control ($p < 0.05$, 0.01, and 0.001), respectively.

amarogentin in higher organisms. H_2O_2 was used to induce oxidative stress in PC12 cells, and the effect of amarogentin on cell viability was assessed by the MTT method. Figure 5(a) shows that the cell viability decreased dose-dependently with increasing concentration of H_2O_2 from 0.2 mM to 1 mM. This result indicates that approximately 50% of the cells were dead or under poor condition after 1 h of treatment with 0.9 mM H_2O_2 . According to the cell viability induced by H_2O_2 , 0.9 mM H_2O_2 was chosen as the optimum concentration to induce oxidative stress in PC12 cells. Amarogentin at 1 μ M and 3 μ M and RES at 10 μ M significantly increase survival rates of PC12 cells (Figure 5(b)). These results demonstrate that amarogentin exhibited a neuroprotective effect on PC12 cells.

3.7. Amarogentin Decreased Intracellular ROS Level and MDA Content under Oxidative Stress Induced by H_2O_2 in PC12 Cells. ROS is one of the main causes of many age-related diseases, such as AD. In addition, ROS is an effector of oxidative stress in cells [37]. Therefore, the protection effect of amarogentin against ROS production induced by H_2O_2 was investigated. The intracellular formation of ROS in the PC12 cells was monitored by using the DCFH-DA assay. The nonfluorescent DCFH-DA can be oxidised to a green fluorescent substance (DCF) when it reacts with ROS [38]. As shown in Figure 5(c), the fluorescence intensity was enhanced after treatment with 0.9 mM H_2O_2 for 1 h. However, the increasing fluorescence intensity by H_2O_2 was diminished after adding 1, 3, and 10 μ M amarogentin. The

photomicrographs of PC12 cells under fluorescence microscope are shown in Figure 5(d). These results suggest that amarogentin is essential to counteract an oxidative insult to cells rendered by the highly reactive ROS induced by H_2O_2 .

Lipids are among the classes of biological macromolecules that are targeted by oxidative substances. Lipid oxidation results in the formation of numerous metabolites, which are mainly aldehydes. Metabolites from lipid peroxidation can interact with other macromolecules, such as nucleic acids and protein; such interaction most often results in irreversible damage to cellular function. MDA, which is the principal and most studied product of polyunsaturated fatty acid peroxidation, is often considered a biomarker of oxidative stress [14]. Therefore, the MDA level in H_2O_2 -induced oxidative damage to PC12 cells was evaluated. The MDA level increased significantly in the H_2O_2 -treated cells compared with the untreated control group. However, the MDA level in the amarogentin-treated group was significantly decreased compared with that in the H_2O_2 -treated group. This result confirms that the pretreatment with amarogentin inhibited lipid peroxidation, reduced the level of MDA formation, and rescued cells from damage (Figure 5(e)).

3.8. Amarogentin Increased the Total SOD and SOD2 Activity under Oxidative Stress Induced by H_2O_2 in PC12 Cells. SOD is an important endogenous free radical scavenger in mammalian cells [39]. Therefore, the level of SOD in the H_2O_2 -induced oxidative damage to PC12 cells was evaluated. The

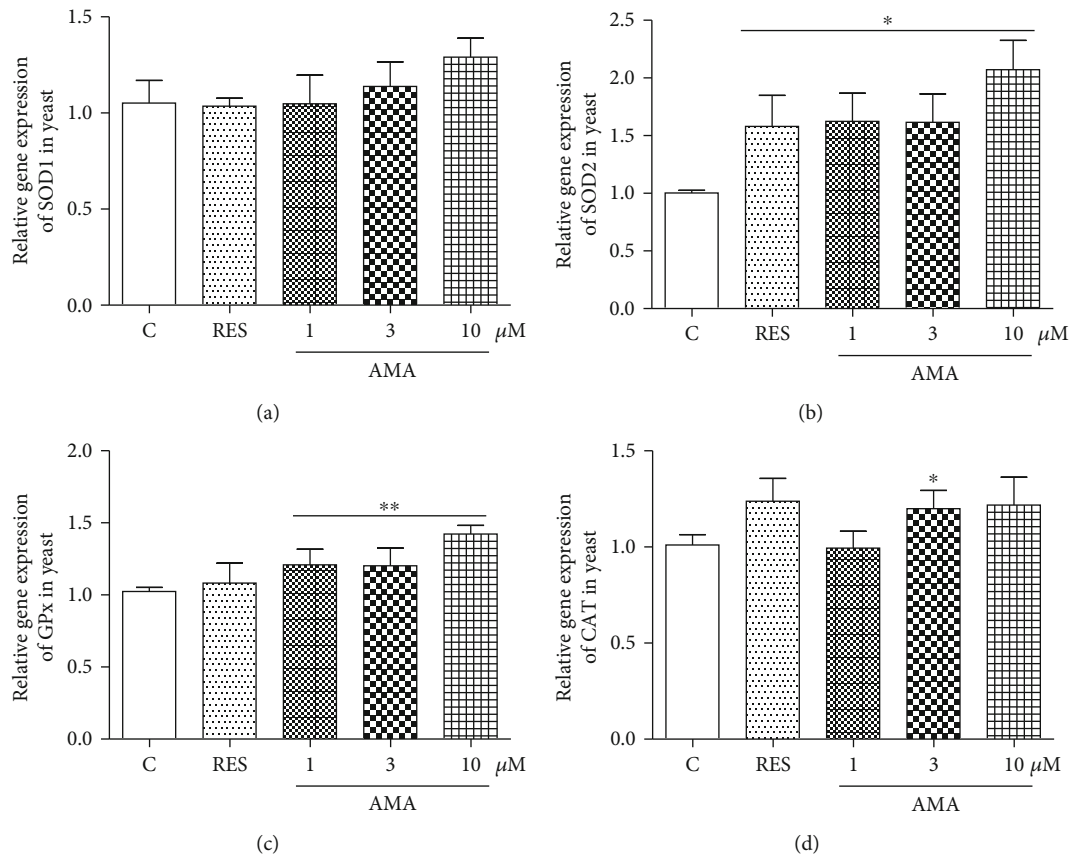


FIGURE 3: Effect of amarogentin on *SOD1*, *SOD2*, *GPx*, and *CAT* gene expression in BY4741 yeast after treatment of amarogentin and RES. Experiments were repeated thrice, and the data were presented as means \pm SEM. * $p < 0.05$ and ** $p < 0.01$ represent significant difference compared with the control group.

total SOD and SOD2 activities were significantly decreased in the H_2O_2 -treated group. The total SOD and SOD2 activities evidently increased in amarogentin-treated cells (Figures 5(f) and 5(g)). However, SOD1 activity in PC12 cells was not affected by amarogentin (Figure 5(h)). Furthermore, amarogentin and RES alone did not affect the cell viability, fluorescence intensity, MDA level, and the total SOD, SOD1, and SOD2 activities in normal condition. These results indicate that amarogentin could significantly reduce the oxidative damage in PC12 cells.

3.9. Effect of Amarogentin on Gene Expression of *SOD1*, *SOD2*, *Bcl-x1*, and *Nrf2* in PC12 Cells. The gene expressions of *SOD1* and *SOD2* in PC12 cells after treatment of RES or amarogentin are shown in Figure 6. The *SOD1* gene expression in all of treatment groups was not affected by RES or amarogentin (Figure 6(a)). However, *SOD2* gene expression in these groups was significantly increased after treatment with RES (10 μ M) or amarogentin (1, 3 μ M) for 12 h (Figure 6(b)). In addition, we detected the gene expression of *GPx* and *CAT*. The abundance of *GPx* and *CAT* mRNA was also significantly increased with RES (10 μ M) or amarogentin (1, 3 μ M) for 12 h or 24 h (Supplementary Figure 1).

Nrf2 plays an important role in protecting against oxidative stress and apoptotic damage [40]. *Bcl-x1*, one of the antiapoptotic proteins, plays a considerable role of resistance in apoptosis and involves neuroprotection [41]. Thus, we conducted qRT-PCR to detect whether *Nrf2* and *Bcl-x1* genes were involved in the protection effect of amarogentin. The abundance of *Bcl-x1* and *Nrf2* mRNA was significantly increased with RES or amarogentin (1, 3, and 10 μ M) for 12 h or 24 h (Figures 6(c) and 6(d)). These results indicated that *SOD2*, *CAT*, *Gpx*, *Bcl-x1*, and *Nrf2* genes were involved in the neuroprotective effects of amarogentin.

3.10. Amarogentin Showed Neuritogenic Activity in PC12 Cells. The neuritogenic activity of amarogentin was evaluated in PC12 cells. Amarogentin induced neurite outgrowth in a dose-dependent manner. The percentage of cells with neurite outgrowth after treatment with 0, 0.3, 1, and 3 μ M amarogentin for 48 h was $6.3\% \pm 0.9\%$, $36.7\% \pm 2.3\%$, $43.0\% \pm 2.3\%$, and $50.0\% \pm 1.5\%$, respectively (Figure 7(a)). Interestingly, amarogentin (3 μ M) combined with NGF (1 ng/ml) remarkably increased the percentage of cells with neurite outgrowth from $50.0\% \pm 1.5\%$ to $80.3\% \pm 1.5\%$ (Figure 7(a)), and the neurite outgrowth interweaved into a network. The morphological changes in PC12 cells after treatment with DMSO, NGF (40 ng/ml), amarogentin (3 μ M), and amarogentin

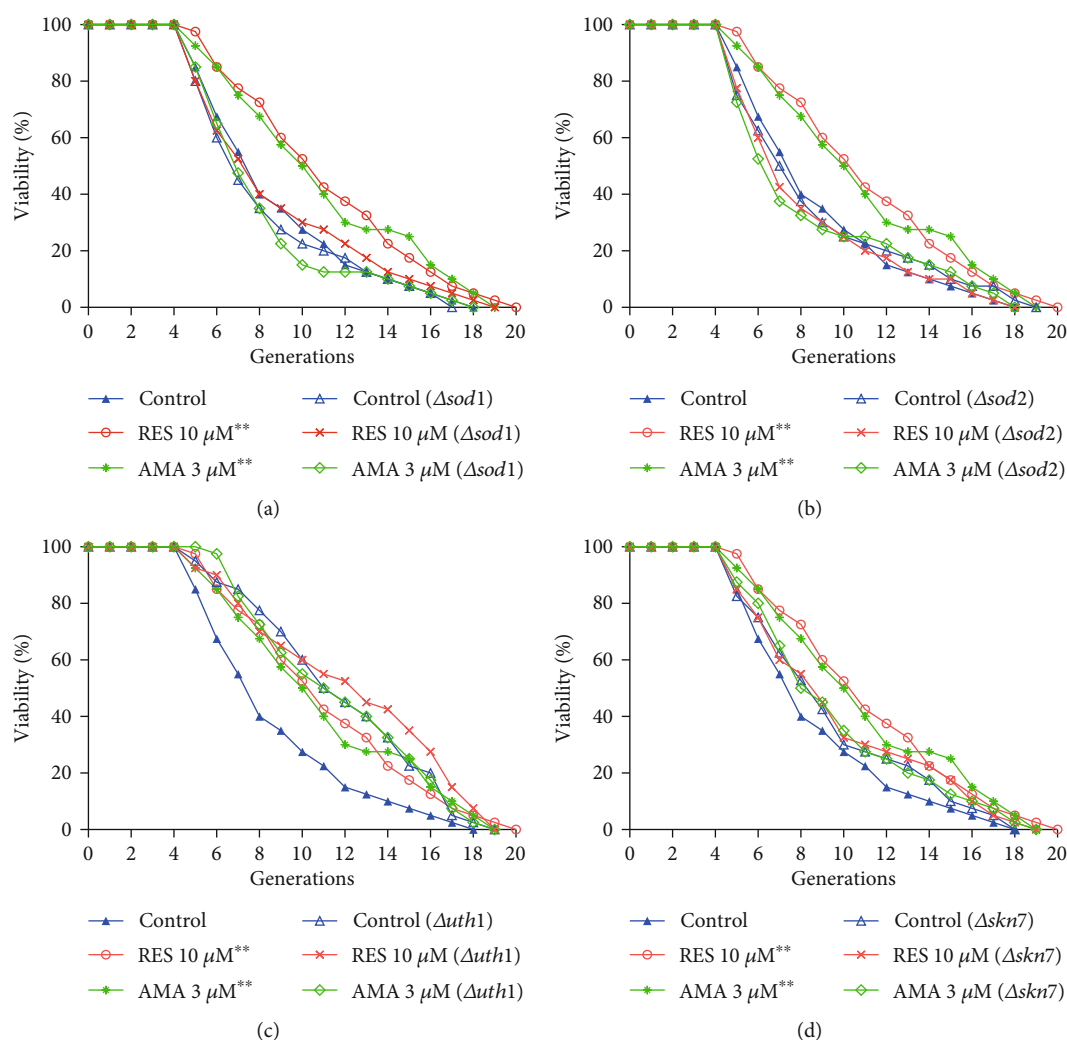


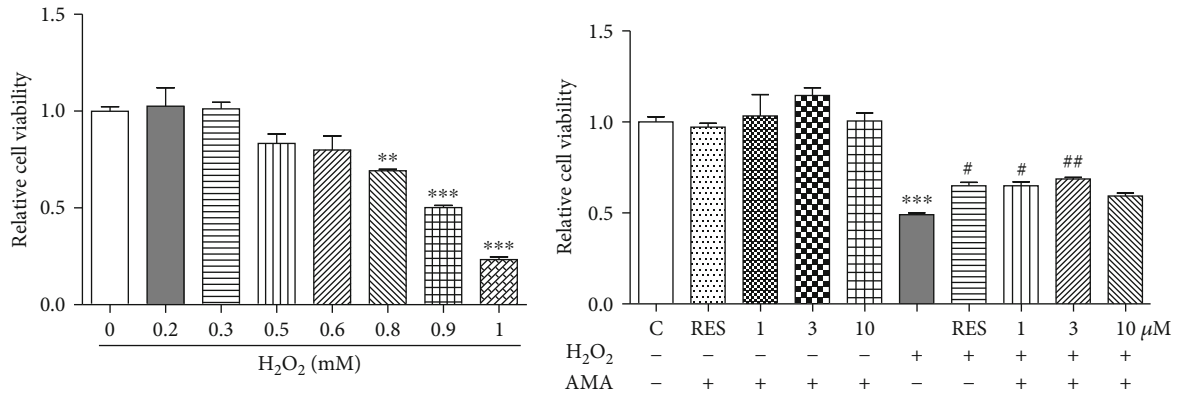
FIGURE 4: Effect of amarogentin on the replicative lifespans of *sod1* (a), *sod2* (b), *uth1* (c), and *skn7* (d) mutant yeast strain with K6001 background. The average replicative lifespans of the wild-type K6001 yeast were 7.0 ± 0.3 generations under the control treatment, 9.0 ± 0.5 generations under the RES treatment, and 9.6 ± 0.5 generations under the $3 \mu\text{M}$ amarogentin treatment. The average replicative lifespans of the *sod1* mutant were 7.5 ± 0.1 generations under the control treatment, 7.6 ± 0.3 generations under the RES treatment, and 7.6 ± 0.2 generations under the $3 \mu\text{M}$ amarogentin treatment. The average replicative lifespans of the *sod2* mutant were 8.1 ± 0.1 generations under the control treatment, 8.1 ± 0.5 generations under the RES treatment, and 7.7 ± 0.2 generations under the $3 \mu\text{M}$ amarogentin treatment. The average replicative lifespans of the *uth1* mutant were 10.8 ± 0.1 generations under the control treatment, 11.3 ± 0.1 generations under the RES treatment, and 11.0 ± 0.1 generations under the $3 \mu\text{M}$ amarogentin treatment. The average replicative lifespans of *skn7* were 8.5 ± 0.7 generations under the control treatment, 8.1 ± 0.6 generations under RES treatment, and 8.0 ± 0.6 generations under $3 \mu\text{M}$ amarogentin treatment.

together with NGF are shown in Figure 7(b). The results suggest that amarogentin possessed NGF-mimic activity and could enhance NGF activity in PC12 cells. Amarogentin should be further studied given that it could be a candidate molecule because of its neurotogenic activity for treatment of neurodegenerative disorders.

4. Discussion

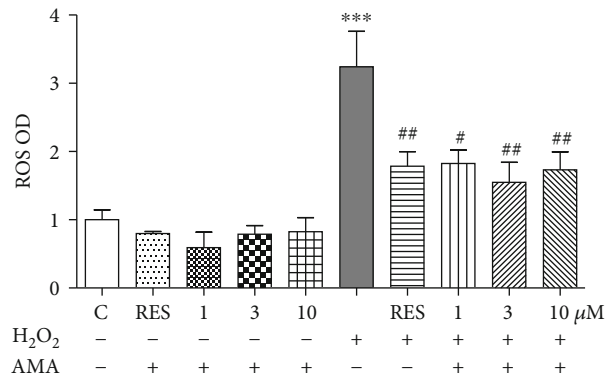
G. rigescens is a traditional Chinese herbal medicine which is used to treat inflammations, hepatitis, rheumatism, cholecystitis, and inflammation in China [16]. To search for the active components and understand the action mechanism of these compounds of *G. rigescens*, we began an intensive study on

this species more than ten years ago. In our previous study, we used PC12 cells as a bioassay system to isolate 11 novel neurotogenic substances from *G. rigescens* and named as gentsides A–K [17, 18]. Furthermore, we used the fraction consisted with gentsides A–K to investigate the neuroprotection effects in AD model mice induced by scopolamine. We found that this fraction could improve the memory function of AD model mice in vivo [19]. In the present study, we focused on the isolation of antiaging molecules from *G. rigescens* by using a yeast replicative lifespan bioassay system. The chemical structure of amarogentin and changes in replicative lifespan of yeast in Figures 1(a) and 1(b) indicated that amarogentin has antiaging effect on yeast.

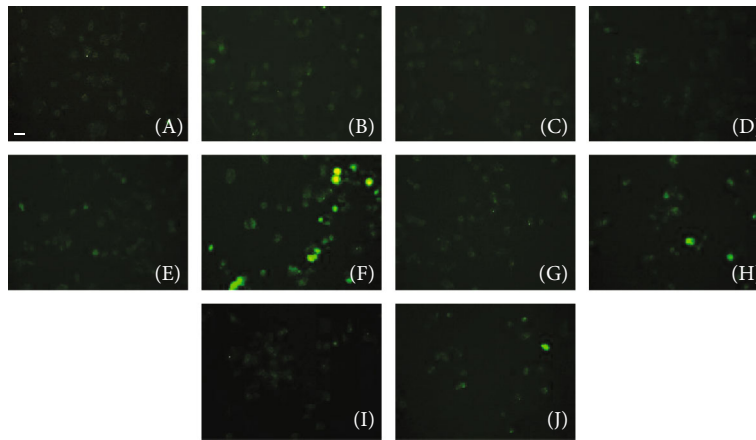


(a)

(b)



(c)



(d)

FIGURE 5: Continued.

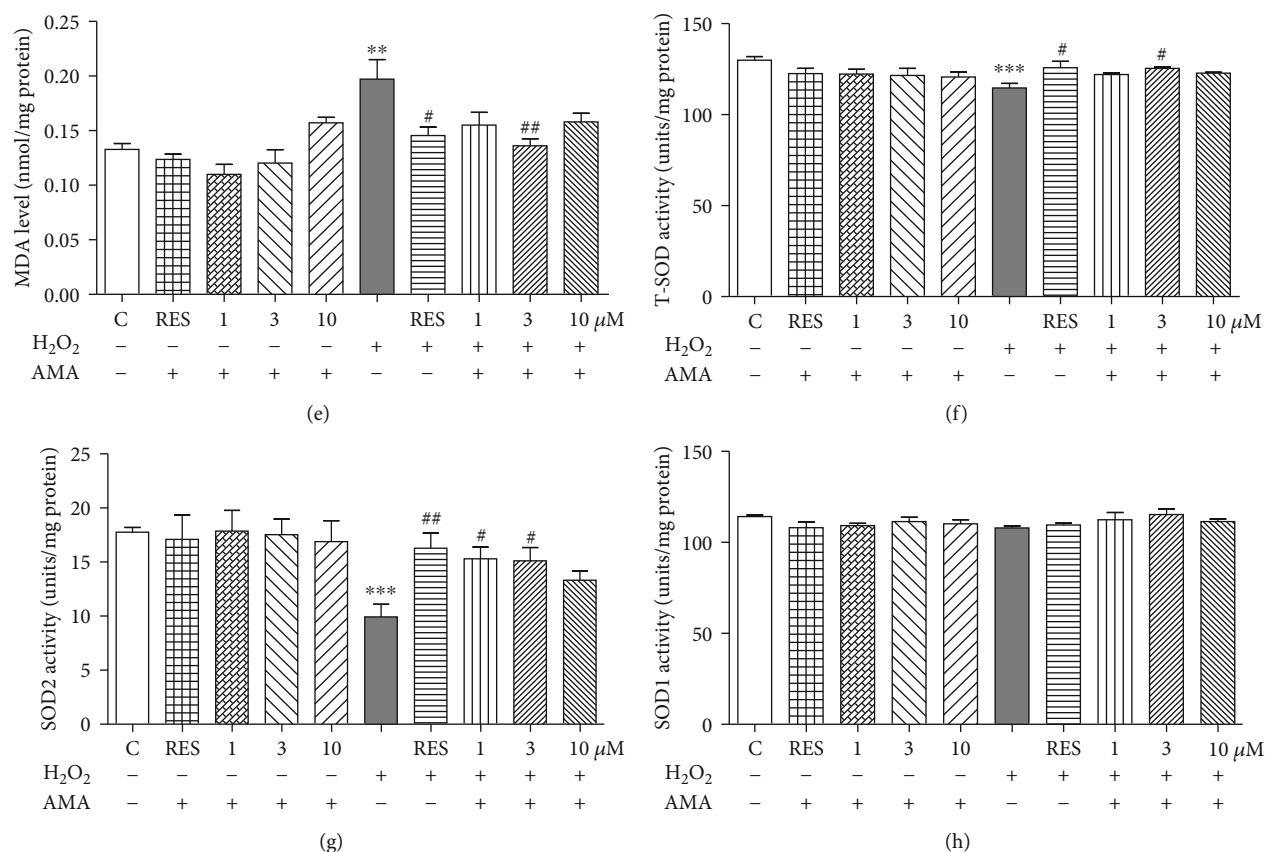


FIGURE 5: Neuroprotection effect of amarogentin on the H₂O₂-induced oxidative damage in the PC12 cells. (a) Relative viability of the PC12 cells after treatment with H₂O₂ at different concentrations for 1 h. With an increase in H₂O₂ concentration, survival rates decreased significantly compared with the control group. (b) Neuronal protection of amarogentin at 1, 3, and 10 μM with or without the H₂O₂ stimulation. (c) Effect of amarogentin with or without H₂O₂-induced on ROS production in PC12 cells as detected by fluorescence microplate reader. (d) Photomicrographs of PC12 cells stained with DCFH-DA under a fluorescence microscope. Control (A), RES (10 μM) (B), amarogentin (1 μM) (C), amarogentin (3 μM) (D), amarogentin (10 μM) (E), H₂O₂-treated control (F), H₂O₂+RES (10 μM) (G), H₂O₂+amarogentin (1 μM) (H), H₂O₂+amarogentin (3 μM) (I), and H₂O₂+amarogentin (10 μM) (J); scale bar, 20 μm. The levels of MDA content (e), total SOD activities (f), SOD2 activities (g), and SOD1 activities (h) were measured by corresponding assay kits. The PC12 cells were pretreated with RES (10 μM) and different concentrations of amarogentin (1, 3, and 10 μM) for 24 h and then subjected to H₂O₂ (0.9 mM) for 1 h or treated with RES (10 μM) and amarogentin (1, 3, and 10 μM) alone for 24 h. Experiments were repeated thrice, and the data were presented as means ± SEM. **p* < 0.05, ***p* < 0.01, and ****p* < 0.001 compared with the control group; #*p* < 0.05, ##*p* < 0.01, compared with the H₂O₂-treated group (grey color bar).

Oxidative stress plays a crucial role in the aging process, and antioxidative stress mechanism is a strategy used to prevent and treat aging-related diseases, such as neurodegenerative diseases [11]. To understand the action mechanism of amarogentin for anti-aging, we firstly examined the effect of amarogentin on the survival rate of yeast under oxidative stress condition and activity of enzymes. The results in Figures 2(a) and 2(b) and the activities of total SOD and SOD2, CAT, and GPx (Figures 2(c)–2(g)) suggested that antioxidative stress and activity increase of enzymes are involved in antiaging effect of amarogentin. To obtain more evidences to support our conclusion, we investigated the gene expression of antioxidative enzyme and constructed *sod1*, *sod2*, *uth1*, and *skn7* mutants of yeast with K6001 background. We conducted replicative lifespan assays of *sod1*, *sod2*, *uth1*, and *skn7* mutants with a K6001 background; all of which had related effects on antioxidative stress. The

results in Figures 3(a)–3(d) and Figures 4(a)–4(d) show that *SOD1*, *SOD2*, *CAT*, *GPX*, *UTH1*, and *SKN7* contribute to the antiaging effect of amarogentin. The results demonstrated that antioxidative stress is an important role for the antiaging effect of amarogentin.

In our research strategy, the yeast biological activity evaluation system has the advantages of low cost, short research period, and easy operation. This system was used for the initial screening and mechanism study. To confirm the effects of the antioxidative stress activity of amarogentin in higher organisms, we employed the PC12 cell line, which was derived from mammalian cells, as a bioassay system. A significant increase of the survival rates of PC12 cells under oxidative conditions as shown in Figure 5(b), significant reduction of ROS and MDA levels (Figures 5(c) and 5(d)), and increase of the total SOD and SOD2 activities (Figures 5(e)–5(g)) implied that amarogentin possessed the neuroprotective

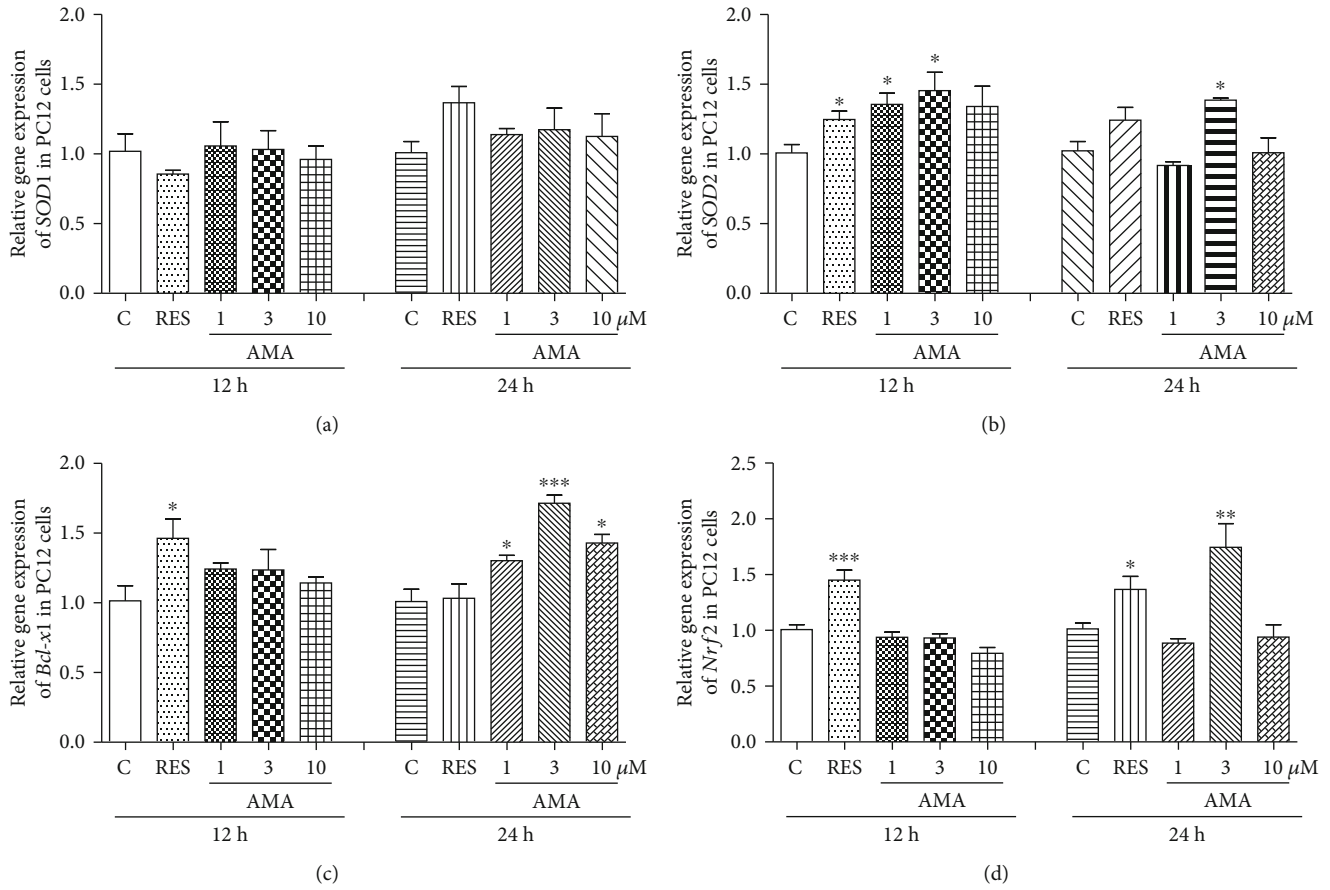


FIGURE 6: Effect of amarogentin on *SOD1*, *SOD2*, *Bcl-x1*, and *Nrf2* gene expression in PC12 cells after treatment of amarogentin and resveratrol for 12 h or 24 h. Experiments were repeated thrice, and the data were presented as mean \pm SEM. * $p < 0.05$, ** $p < 0.01$, and *** $p < 0.001$ compared with the control group.

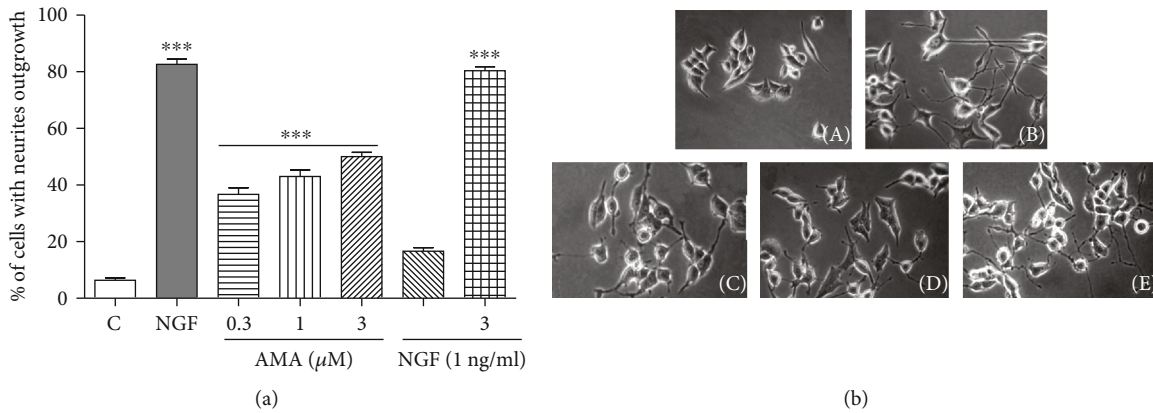


FIGURE 7: Neurogenesis activity of amarogentin in PC12 cells. (a) Percentage of cells with neurite outgrowth after treatment with indicated doses of amarogentin and amarogentin with NGF for 48 h. (b) Morphological changes in the neurite outgrowth of PC12 cells treated with negative control (0.5% DMSO) (A), positive control (40 ng/ml NGF) (B), amarogentin (3 μM) (C), NGF (1 ng/ml) (D), and amarogentin (3 μM) with NGF (1 ng/ml) (E). Each experiment was repeated thrice. The data are presented as mean \pm SEM. *** indicated significant and highly significant differences compared with the negative control group at $p < 0.001$.

effect in PC12 cells via regulation of antioxidative stress. To understand which genes and signalling pathways were involved in antioxidative stress, we investigated both of the genes, *Nrf2* and *Bcl-x1* which are related to oxidative stress

and neuroprotection [40, 41]. The increase of *SOD2*, *Nrf2*, and *Bcl-x1* gene expression after treatment of amarogentin (Figures 6(b)-6(d)) clarified that amarogentin produced neuroprotection via modification of antioxidative stress and

regulation of *SOD2*, *Nrf2*, and *Bcl-xl* gene expression. These results were consistent with other reports [42].

The NGF is the first and best characterized neurotrophic factor [27]. NGF cannot pass through the blood brain barrier (BBB) because of its physical property, resulting in difficulty in using NGF as a drug to treat neurodegenerative diseases. Therefore, a small molecule that mimics or enhances the NGF activity and can pass through BBB can be a promising candidate for treatment of neurodegenerative diseases [43]. In the present study, we found that amarogentin not only significantly induced the neurite outgrowth but also enhanced the neurotogenic activity of NGF (Figures 7(a) and 7(b)). These results suggested that amarogentin has potential for treatment of neurodegenerative diseases, such as AD.

To confirm whether these obtained antiaging compounds have an anti-AD effect, PC12 cells were used to evaluate neurotogenic activity of them. Cucurbitacin B which is a triterpenoid and isolated from *Pedicellus melo*, like amarogentin, not only exerted antiaging effects on yeasts but also induced neurogenesis in PC12 cells and improved the memory of APP/PS1 transgenic mice [20, 44]. Amarogentin, which has a structure that is completely different to that of CuB, exhibits significant antiaging activity and NGF-mimic activity and enhances the NGF activity. The underlying mechanisms of the activities of amarogentin should be elucidated. Comparison of the similarity and difference of mechanisms of two different structures may be important for drug discovery.

5. Conclusion

Amarogentin isolated from *G. rigescens*, which is a TCM, showed a significant antiaging effect on yeasts and neuroprotective and neurotogenic activities in PC12 cells, a mammalian cell line. Amarogentin prolonged the replicative lifespan and neuroprotective activities by antioxidative stress activity. However, the underlying mechanisms of neurotogenic and antiaging activities need to be elucidated, and the relationship between these activities should also be addressed in future studies. Novel leading compounds can be designed and synthesised based on the structure of amarogentin. This study lays an important foundation for development of a novel drug for treatment of aging and neurodegenerative diseases.

Data Availability

All figures and data used to support this study are included within this article.

Conflicts of Interest

The authors declare that there is no conflict of interest regarding publication of this paper.

Authors' Contributions

Dejene Disasa and Lihong Cheng contributed equally to this work.

Acknowledgments

The authors are grateful to professor Akira Matsuura (Chiba University, Japan) for the gifts of BY4741 and all mutations with the K6001 background and grateful to professor Michael Breitenbach (Salzburg University, Austria) for the gifts of K6001. This work was financially supported by the National Key R&D Program of China (Grant Number 2017YFE0117200) and the National Natural Science Foundation of China (Grant numbers 21661140001 and 21877098).

Supplementary Materials

The detailed method of measurement of SOD, GPx, and CAT enzymatic activities in yeast or PC12 cells; primer sequences used in this study; gene expression of *CAT*, and *GPx* in PC12 cells. (*Supplementary Materials*)

References

- [1] W. Lutz, W. Sanderson, and S. Scherbov, "The coming acceleration of global population ageing," *Nature*, vol. 451, no. 7179, pp. 716–719, 2008.
- [2] J. H. Chung, A. Y. Seo, S. W. Chung et al., "Molecular mechanism of PPAR in the regulation of age-related inflammation," *Ageing Research Reviews*, vol. 7, no. 2, pp. 126–136, 2008.
- [3] H. Y. Chung, M. Cesari, S. Anton et al., "Molecular inflammation: underpinnings of aging and age-related diseases," *Ageing Research Reviews*, vol. 8, no. 1, pp. 18–30, 2009.
- [4] M. Kaeblerlein, P. S. Rabinovitch, and G. M. Martin, "Healthy aging: the ultimate preventative medicine," *Science*, vol. 350, no. 6265, pp. 1191–1193, 2015.
- [5] M. Valko, D. Leibfritz, J. Moncol, M. T. D. Cronin, M. Mazur, and J. Telser, "Free radicals and antioxidants in normal physiological functions and human disease," *The International Journal of Biochemistry & Cell Biology*, vol. 39, no. 1, pp. 44–84, 2007.
- [6] D. Kim, M. D. Nguyen, M. M. Dobbin et al., "SIRT1 deacetylase protects against neurodegeneration in models for Alzheimer's disease and amyotrophic lateral sclerosis," *EMBO Journal*, vol. 26, no. 13, pp. 3169–3179, 2007.
- [7] A. Thapa, B. C. Vernon, K. de la Peña et al., "Membrane-mediated neuroprotection by curcumin from amyloid- β -peptide-induced toxicity," *Langmuir*, vol. 29, no. 37, pp. 11713–11723, 2013.
- [8] T. Jiang, J. T. Yu, X. C. Zhu et al., "Acute metformin preconditioning confers neuroprotection against focal cerebral ischemia by pre-activation of AMPK-dependent autophagy," *British Journal of Pharmacology*, vol. 171, no. 13, pp. 3146–3157, 2014.
- [9] M. E. Orr, A. Salinas, R. Buffenstein, and S. Oddo, "Mammalian target of rapamycin hyperactivity mediates the detrimental effects of a high sucrose diet on Alzheimer's disease pathology," *Neurobiology of Aging*, vol. 35, no. 6, pp. 1233–1242, 2014.
- [10] T. Pan, S. Kondo, W. Zhu, W. Xie, J. Jankovic, and W. Le, "Neuroprotection of rapamycin in lactacystin-induced neurodegeneration via autophagy enhancement," *Neurobiology of Disease*, vol. 32, no. 1, pp. 16–25, 2008.

- [11] X. K. Wang and E. K. Michaelis, "Selective neuronal vulnerability to oxidative stress in the brain," *Frontiers in Aging Neuroscience*, vol. 2, 2010.
- [12] J. M. Mates, C. Perez-Gomez, and I. N. De Castro, "Antioxidant enzymes and human diseases," *Clinical Biochemistry*, vol. 32, no. 8, pp. 595–603, 1999.
- [13] A. Nandi, L. J. Yan, C. K. Jana, and N. Das, "Role of catalase in oxidative stress- and age-associated degenerative diseases," *Oxidative Medicine and Cellular Longevity*, vol. 2019, Article ID 9613090, 19 pages, 2019.
- [14] D. Sharma, S. S. Trivedi, and J. Bhattacharjee, "Oxidative stress and eNOS (Glu298Asp) gene polymorphism in preeclampsia in Indian population," *Molecular and Cellular Biochemistry*, vol. 353, no. 1-2, pp. 189–193, 2011.
- [15] Y. Xu, Y. Li, K. Maffucci, L. Huang, and R. Zeng, "Analytical methods of phytochemicals from the genus *Gentiana*," *Molecules*, vol. 22, no. 12, article 2080, 2017.
- [16] M. Xu, D. Wang, Y. J. Zhang, and C. R. Yang, "Dammarane triterpenoids from the roots of *Gentiana rigescens*," *Journal of Natural Products*, vol. 70, no. 5, pp. 880–883, 2007.
- [17] L. Gao, J. Li, and J. Qi, "Gentisides A and B, two new neurotogenic compounds from the traditional Chinese medicine *Gentiana rigescens* Franch," *Bioorganic & Medicinal Chemistry*, vol. 18, no. 6, pp. 2131–2134, 2010.
- [18] L. Gao, L. Xiang, Y. Luo, G. Wang, J. Li, and J. Qi, "Gentisides C-K: Nine new neurotogenic compounds from the traditional Chinese medicine *Gentiana rigescens* Franch," *Bioorganic & Medicinal Chemistry*, vol. 18, no. 19, pp. 6995–7000, 2010.
- [19] J. Li, L. Gao, K. Sun et al., "Benzoate fraction from *Gentiana rigescens* Franch alleviates scopolamine- induced impaired memory in mice model *in vivo*," *Journal of Ethnopharmacology*, vol. 193, pp. 107–116, 2016.
- [20] Y. Lin, Y. Kotakeyama, J. Li et al., "Cucurbitacin B exerts antiaging effects in yeast by regulating autophagy and oxidative stress," *Oxidative Medicine and Cellular Longevity*, vol. 2019, Article ID 4517091, 15 pages, 2019.
- [21] X. Cao, Y. Sun, Y. Lin et al., "Antiaging of cucurbitane glycosides from fruits of *Momordica charantia* L.," *Oxidative Medicine and Cellular Longevity*, vol. 2018, Article ID 1538632, 10 pages, 2018.
- [22] Y. Wang, Y. Lin, L. Xiang, H. Osada, and J. Qi, "Sesquiterpene glucosides from Shenzhou honey peach fruit showed the antiaging activity in the evaluation system using yeasts," *Bioscience, Biotechnology, and Biochemistry*, vol. 81, no. 8, pp. 1586–1590, 2017.
- [23] Y. Lin, Y. Sun, Y. Weng, A. Matsuura, L. Xiang, and J. Qi, "Parishin from *Gastrodia elata* extends the lifespan of yeast via regulation of Sir2/Uth1/TOR signaling pathway," *Oxidative Medicine and Cellular Longevity*, vol. 2016, Article ID 4074690, 11 pages, 2016.
- [24] U. Farooq, Y. Pan, Y. Lin et al., "Structure characterization and action mechanism of an antiaging new compound from *Gastrodia elata* Blume," *Oxidative Medicine and Cellular Longevity*, vol. 2019, Article ID 5459862, 10 pages, 2019.
- [25] Y. Sun, Y. Lin, X. Cao, L. Xiang, and J. Qi, "Sterols from *mytilidae* show anti-aging and neuroprotective effects via anti-oxidative activity," *International Journal of Molecular Sciences*, vol. 15, no. 12, pp. 21660–21673, 2014.
- [26] S. Jarolim, J. Millen, G. Heeren, P. Laun, D. Goldfarb, and M. Breitenbach, "A novel assay for replicative lifespan in *Saccharomyces cerevisiae*," *FEMS Yeast Research*, vol. 5, no. 2, pp. 169–177, 2004.
- [27] L. A. Greene and A. S. Tischler, "Establishment of a noradrenergic clonal line of rat adrenal pheochromocytoma cells which respond to nerve growth factor," *Proceedings of the National Academy of Science of the United States of America*, vol. 73, no. 7, pp. 2424–2428, 1976.
- [28] A. Singh, "Phytochemicals of gentianaceae: a review of pharmacological properties," *International Journal of Pharmaceutical Sciences and Nanotechnology*, vol. 1, no. 1, pp. 33–36, 2008.
- [29] N. Kawahara, K. Masuda, S. Sekita, and M. Satake, "A new secoiridoid glucoside, amaronitidin, from the Peruvian folk medicine "hercampuri" (*Gentianella nitida*)," *Chemical and Pharmaceutical Bulletin*, vol. 49, no. 6, pp. 771–772, 2001.
- [30] G. Brahmachari, S. Mondal, A. Gangopadhyay et al., "*Sweritia* (Gentianaceae): chemical and pharmacological aspects," *Chemistry & Biodiversity*, vol. 1, no. 11, pp. 1627–1651, 2004.
- [31] U. R. Potunuru, K. V. Priya, M. K. N. S. Varsha et al., "Amarogentin, a secoiridoid glycoside, activates AMP- activated protein kinase (AMPK) to exert beneficial vasculo-metabolic effects," *Biochimica et Biophysica Acta-General Subjects*, vol. 1863, no. 8, pp. 1270–1282, 2019.
- [32] K. Dai, X. J. Yi, X. J. Huang et al., "Hepatoprotective activity of iridoids, seco-iridoids and analog glycosides from Gentianaceae on HepG₂ cells via CYP_{3A4} induction and mitochondrial pathway," *Food & Function*, vol. 9, no. 5, pp. 2673–2683, 2018.
- [33] H. S. Niu, P. C. Chao, P. M. Ku, C. S. Niu, K. S. Lee, and J. T. Cheng, "Amarogentin ameliorates diabetic disorders in animal models," *Naunyn-Schmiedeberg's Archives of Pharmacology*, vol. 389, no. 11, pp. 1215–1223, 2016.
- [34] C. Z. Wang, U. H. Maier, W. Eisenreich et al., "Unexpected biosynthetic precursors of amarogentin – a retrobiosynthetic ¹³C NMR study," *European Journal of Organic Chemistry*, vol. 2001, no. 8, pp. 1459–1465, 2001.
- [35] P. D. S. Bandara, J. A. Flattery-O'Brien, C. M. Grant, and I. W. Dawes, "Involvement of the *Saccharomyces cerevisiae* UTH1 gene in the oxidative-stress response," *Current Genetics*, vol. 34, no. 4, pp. 259–268, 1998.
- [36] V. Basso, S. Znaidi, V. Lagage et al., "The two-component response regulator Skn7 belongs to a network of transcription factors regulating morphogenesis in *Candida albicans* and independently limits morphogenesis-induced ROS accumulation," *Molecular Microbiology*, vol. 106, no. 1, pp. 157–182, 2017.
- [37] M. Dumont and M. F. Beal, "Neuroprotective strategies involving ROS in Alzheimer disease," *Free Radical Biology & Medicine*, vol. 51, no. 5, pp. 1014–1026, 2011.
- [38] M. Karlsson, T. Kurz, U. T. Brunk, S. E. Nilsson, and C. I. Frennsson, "What does the commonly used DCF test for oxidative stress really show?," *Biochemical Journal*, vol. 428, no. 2, pp. 183–190, 2010.
- [39] J. Xia, Y. Fang, Y. Shi et al., "Effect of food matrices on the *in vitro* bioavailability and oxidative damage in PC12 cells of lead," *Food Chemistry*, vol. 266, pp. 397–404, 2018.
- [40] Q. Ma, "Role of Nrf₂ in oxidative stress and toxicity," *Annual Review of Pharmacology and Toxicology*, vol. 53, no. 1, pp. 401–426, 2013.
- [41] B. D'Orsi, J. Mateyka, and J. H. M. Prehn, "Control of mitochondrial physiology and cell death by the Bcl-2 family

- proteins Bax and Bok,” *Neurochemistry International*, vol. 109, pp. 162–170, 2017.
- [42] L. Wang, Z. Pu, M. Li, K. Wang, L. Deng, and W. Chen, “Antioxidative and antiapoptosis: neuroprotective effects of dauricine in Alzheimer's disease models,” *Life Sciences*, vol. 243, article 117237, 2020.
- [43] K. J. Park, S. Y. Lee, H. S. Kim, M. Yamazaki, K. Chiba, and H. C. Ha, “The neuroprotective and neurotrophic effects of *Tremella fuciformis* in PC12h cells,” *Mycobiology*, vol. 35, no. 1, pp. 11–15, 2007.
- [44] J. Li, K. Sun, M. Muroi et al., “Cucurbitacin B induces neurogenesis in PC12 cells and protects memory in APP/PS1 mice,” *Journal of Cellular and Molecular Medicine*, vol. 23, no. 9, pp. 6283–6294, 2019.

Research Article

Olive Leaf Polyphenols Attenuate the Clinical Course of Experimental Autoimmune Encephalomyelitis and Provide Neuroprotection by Reducing Oxidative Stress, Regulating Microglia and SIRT1, and Preserving Myelin Integrity

Jasminka Giacometti ¹ and Tanja Grubić-Kezele ^{2,3}

¹Department of Biotechnology, University of Rijeka, Radmile Matečić 2, 51000 Rijeka, Croatia

²Department of Physiology and Immunology, Faculty of Medicine, University of Rijeka, Braće Branchetta 20, 51000 Rijeka, Croatia

³Clinical Department for Clinical Microbiology, Clinical Hospital Center Rijeka, Krešimirova 42, 51000 Rijeka, Croatia

Correspondence should be addressed to Tanja Grubić-Kezele; tanja.grubic@medri.uniri.hr

Received 21 April 2020; Revised 24 June 2020; Accepted 1 July 2020; Published 31 July 2020

Guest Editor: Francisco Jaime B. Mendonça Junior

Copyright © 2020 Jasminka Giacometti and Tanja Grubić-Kezele. This is an open access article distributed under the Creative Commons Attribution License, which permits unrestricted use, distribution, and reproduction in any medium, provided the original work is properly cited.

Numerous evidences suggest that plant polyphenols may have therapeutic benefits in regulating oxidative stress and providing neuroprotection in many neurodegenerative diseases, including multiple sclerosis (MS). However, these mechanisms are not yet completely understood. In this study, we investigated the effect of olive leaf polyphenols on oxidative stress through oxidation marker level and activity (TBARS, SOD, and GPX) and their protein expression (SOD1, SOD2, and GPX1), as well as the protein expression of Sirtuin 1 (SIRT1) and microglia markers (Iba-1, CD206, and iNOS) and myelin integrity (proteolipid protein expression) in the brain of rats with induced experimental autoimmune encephalomyelitis (EAE) and subjected to olive leaf therapy. Experiments were performed in male EAE DA rats, which were randomly divided into 2 main groups: EAE groups treated with the therapy of olive leaf (EAE+TOL) and untreated EAE control groups. The EAE treated groups consumed olive leaf tea instead of drinking water (*ad libitum*) from the beginning to the end of the experiment. In addition, olive leaf extract was injected intraperitoneally (*i.p.*) for the 10 continuous days and started on the 8th day after EAE induction. The clinical course was monitored in both groups until the 30th day after EAE induction. Our results demonstrated that TOL attenuated the clinical course of EAE; reduced the oxidative stress (by decreasing the concentration of MDA); upregulated antioxidant enzymes (SOD1, SOD2, and GPX1), SIRT1 (overall and microglial), and anti-inflammatory M2 microglia; downregulated proinflammatory M1 type; and preserved myelin integrity. These data support the idea that TOL may be an effective therapeutic approach for treating MS and other neurodegenerative diseases.

1. Introduction

A broad range of evidence suggests that oxidative stress plays a major role in the pathogenesis of neurodegenerative diseases, including multiple sclerosis (MS) [1, 2]. Reactive oxygen species (ROS), which if produced in excess during inflammation lead to oxidative stress, have been implicated as mediators of demyelination and axonal damage in both MS and its animal models.

One of the most studied cell populations in the central nervous system (CNS) in the context of ROS-mediated tissue damage in MS are microglia cells. An activated microglia produce ROS [3] and NO radicals in MS lesions, which suggests their role in the demyelination and neurodegeneration process of MS [4–8] and accounts for the features of MS pathological findings [9].

Oligodendrocyte progenitor cells (OPCs) are particularly vulnerable to oxidative stress because they have lower levels

of antioxidant enzymes [8]. The extent of lipid and DNA oxidation correlates significantly with inflammation and oxidative injury of oligodendrocytes and neurons, which is also associated with active demyelination and axonal and neuronal injury [10], together with upregulated expression of oxidative molecules and antioxidant enzymes in MS lesions [11–13].

However, and this aspect is less well understood, the extracellular and intracellular redox milieu is integral to many processes underlying T cell activation, proliferation, and apoptosis and subsequent neuropathological processes. Besides the promotion of demyelination through oxidative damage [14], release of proinflammatory cytokines (IL-1 β , IL-6, and TNF- α), and increased expression of iNOS and ROS [15], microglia contribute to the repair-permissive environment by providing growth factors, such as IGF-1 and FGF-2 [16], and provide myelin debris clearance for adequate oligodendrocyte differentiation and ongoing myelination/remyelination [17–19].

Furthermore, it seems SIRT1, the nicotinamide adenine dinucleotide- (NAD⁺-) dependent deacetylase highly expressed in both neurons and glial cells in the brain [20–22], is a crucial component of multiple interconnected regulatory networks that modulate dendritic and axonal growth, as well as survival against oxidative stress [23].

Moreover, SIRT1 exerts neuroprotective effects in many models of microglial activation-induced neurodegenerative disease [24, 25].

A decrease in SIRT1 levels and activities is related to inflammation-associated diseases, including various neurodegenerative diseases [26, 27]. Moreover, the reduction of SIRT1 expression could contribute to microglial activation and neuroinflammation [28]. Thus, pharmacological activation or upregulation of SIRT1 may be a promising strategy for the treatment of inflammation-related neurodegenerative diseases. Till now, there are already some phytochemical compounds that have been confirmed to have the ability to increase SIRT1 expression and activity, including resveratrol, quercetin, catechin, and protocatechuic acid [29–33].

Numerous evidences reported that olive leaf phenolics have an antioxidant effect [34], and it seems to have a good potential therapeutic effect on the prevention of neurodegenerative diseases; however, further investigation in humans is needed.

Nevertheless, the effect of olive leaf polyphenols (OLP) on SIRT1 during microglial activation is not completely understood. However, there is little data regarding the effect of OLP in MS or its animal models. Here, we examined the effect of OLP on oxidative stress mediators (SOD and GPX), SIRT1, and microglia and integrity of myelin in experimental autoimmune encephalomyelitis (EAE), an animal model of MS, in an attempt to provide further insights into the neuroprotective potential of olive leaf polyphenols.

2. Materials and Methods

2.1. Experimental Animals. Experiments were performed on male Dark Agouti (DA) rats, aged 2–3 months. They were housed under standard conditions of light, temperature,

and humidity with unlimited access to food and water. Experimental procedures involving animals complied with Croatian laws and rules (NN 135/06; NN 37/13; NN 125/13; NN 055/2013) and with the guidelines set by the European Community Council Directive (86/609/EEC). The experimental protocol was approved by the Ethics Committee of the Department of Biotechnology University of Rijeka (2170-57-005-02-17-1).

2.1.1. EAE Induction and Evaluation. Induction of chronic relapsing- (CR-) EAE was performed in male DA rats by bovine brain white matter homogenate emulsion (BBH) in the complete Freund's adjuvant (CFA) (Sigma, St. Louis, Mo., USA), as previously described [35]. To each animal, 0.1 mL emulsion was injected subcutaneously in each hind footpad. The evaluation of the clinical course was assessed daily using the following criteria: 0: no symptoms; 1: flaccid paralysis of the tail; 2: hind leg paresis; 3: hind leg paralysis with incontinence; and 4: the death of the animal.

2.1.2. Preparation of the Olive Leaf Tea and Olive Leaf Extract (OLE). Olive leaf extract (OLE) was prepared from samples of olive tree leaves according to the method of Giacometti et al. [36]. The dry residue was weighed and then dissolved in sterile saline and kept at -20°C until its use as therapy together with olive leaf tea (olive leaf therapy; TOL). In addition, the sample of OLE was analyzed using ultrahigh-pressure liquid chromatography with a diode array detector (UHPLC-DAD) in order to determine the concentration of oleuropein and other major phenolics in the extract according to the method of Giacometti et al. [36]. The administered dose of olive leaf extract (OLE) was 1024 mg/kg, while the concentration of oleuropein was 45.96 mg/kg.

Olive leaf tea was prepared from the dry and ground olive leaf by pouring hot water (at 60–80°C) over plant matter (1.5%, w/v) and infused for 30 min. After then, the plant matter was removed by filtration. Analysis of major phenolics in the water infusion was performed using the UHPLC-DAD method according to the method of Giacometti et al. [36]. The concentration of oleuropein in tea was 1.5 mg/mL.

2.2. Experimental Design. EAE rats were randomly divided into 2 main groups: EAE groups treated with the therapy of olive leaf (EAE+TOL) and untreated EAE control groups. Both main groups are divided into 2 smaller groups sacrificed on different days after EAE induction, i.e., on the 20th day or the 2nd relapse (EAE+TOL 20d and EAE 20d group) and the 30th day or the 2nd remission (EAE+TOL 30d and EAE 30d group). The experimental groups (EAE+TOL 20d and EAE+TOL 30d) were treated with olive leaf tea *ad libitum* from the first day after EAE induction and with OLE injected intraperitoneally (*i.p.*) for 10 continuous days starting from the 8th day after EAE induction (a day before the onset of the first EAE symptoms). This study design was chosen as the design with the highest amelioration of the clinical course symptoms of EAE from the pilot experiments conducted with different olive leaf polyphenol concentrations (see Suppl. Figure 1). Control EAE groups (EAE 20d and EAE 30d) were treated in the same way with physiological saline

solution. The fifth group of rats was untreated or did not get EAE induction nor treatment with olive leaf therapy (untreated). EAE rats were sacrificed by exsanguination on the 20th day after induction ($n=5$) and on the 30th day after induction ($n=5$). EAE rats treated with OLE were sacrificed on the same days as untreated EAE rats (on the 20th and 30th day after EAE induction, $n=5$ each). The exsanguination was done in deep anaesthesia (EAE, EAE+TOL, and untreated rats), induced by a combination of ketamine (80 mg/kg) and xylazine (5 mg/kg), given by intraperitoneal (i.p.) injection, according to the guidance of European Community Council Directive (86/609/EEC) and recommendation of the National Centre for the Replacement, Refinement and Reduction of Animals in Research (<http://www.nc3rs.org.uk>).

2.3. Tissue Preparation for Paraffin Slices. The rat brain hemisphere samples were fixed in 4% buffered paraformaldehyde (Sigma-Aldrich, St. Louis, MD, USA) solution during 24 h. Tissue was then embedded in paraffin wax, and sections were cut at 4 μm using the HM 340E microtome (Microtome, Germany). Heat-induced epitope retrieval was done prior to staining procedure by heating tissue slides in boiled citrate buffer pH 6.0 for four times, each 5 min, using a microwave steamer.

2.4. Immunohistological and Immunofluorescence Staining

2.4.1. Immunohistochemistry. Immunohistochemical labeling of proteolipid protein (PLP) was performed on paraffin-embedded tissues using DAKO EnVision+ System, Peroxidase (DAB) kit, according to the manufacturer's instructions (DAKO Cytomation, USA), as previously described [36, 37]. Briefly, slices were incubated with peroxidase block to eliminate endogenous peroxidase activity.

After washing, rabbit polyclonal anti-myelin PLP IgG antibodies (Abcam, UK, diluted 1:1000 with 1% BSA in PBS) were added to tissue samples and incubated overnight at 4°C in a humid environment, followed by 45 min incubation with peroxidase-labeled polymer conjugated to goat anti-mouse or anti-rabbit immunoglobulins containing carrier protein linked to Fc fragments to prevent nonspecific binding. The immunoreactions' product was visualized by adding substrate chromogen (DAB) solution. Tissues were counterstained with hematoxylin, dehydrated through graded ethanol, and mounted using Entellan (Sigma-Aldrich, Germany). The photomicrographs were taken and examined under an Olympus BX51 light microscope (Olympus, Japan).

2.4.2. Immunofluorescence. Immunofluorescence labeling was also performed on paraffin-embedded tissue sections. Nonspecific binding was blocked by one-hour incubation with 1% BSA in PBS containing 0.001% NaN_3 at room temperature, as previously described [37]. The following primary antibodies were used: rabbit polyclonal anti-SIRT1 IgG (GeneTex, Alton Pkwy, Irvine, CA, USA, 1:200), goat polyclonal anti-Iba-1 IgG (Abcam, Cambridge, UK, 1:200), rabbit polyclonal anti-iNOS IgG (Abcam, Cambridge, UK, 1:200), and rabbit polyclonal anti-CD206/Mannose receptor IgG (Abcam, Cambridge, UK, 1:200). Primary antibodies

were diluted in blocking solution and incubated with tissue sections overnight at 4°C in a humid environment. To visualize immunocomplexes, the following secondary antibodies were used: Alexa Fluor donkey anti-rabbit IgG 594 nm (Molecular Probes, Carlsbad, CA, USA, 1:500) and Alexa Fluor donkey anti-goat IgG 488 nm (Molecular Probes, Carlsbad, CA, USA, 1:300). Secondary antibodies were diluted in blocking solution and incubated with tissue sections in the dark for 1 h at room temperature in a humid environment. Nuclei were visualized by DAPI staining (1:1000 in PBS for 5 min; Molecular Probes, Carlsbad, CA, USA). Slides were afterwards washed in PBS and mounted with Mowiol (Sigma-Aldrich, Germany). The photomicrographs were taken under a fluorescent microscope equipped with DP71CCD camera (Olympus, Japan) and Cell F imaging software.

2.5. Immunohistochemical Staining Quantification and Cell Counting

2.5.1. Quantification. The immunohistochemical staining quantification of protein expression was performed on 4 μm tissue sections from paraffin-embedded tissues of the brain using Cell F v3.1 software (Olympus Soft Imaging Solutions), as previously described [38]. Captured images were subjected to intensity separation. They were subsequently inverted, resulting in grayscale images with different intensity ranges, depending on the strength of immunohistochemical signals. Regions of interest (ROIs) were arranged to cover the area being analyzed, and mean gray values were measured. ROI surface size was always equal for each analyzed area. Twelve ROIs were analyzed per field (400x) on 3 separate microscopic slides of different tissue samples per animal, obtained from 5 animals/group. The data were expressed as the mean gray value \pm SD.

2.5.2. Cell Counting. In the dentate gyrus, subventricular zone, and cortex were estimated the SIRT1⁺, iNOS⁺, and CD206⁺ microglial cells by using antibodies and DAPI staining, respectively. SIRT1⁺ and Iba-1⁺ cells were counted manually in an image surface area of 0.014 mm² and magnification of 1000x. Iba-1⁺ CD206⁺ and Iba-1⁺ iNOS⁺ cells were counted manually in an image surface area of 0.053 mm² and magnification of 400x. Results are expressed as a mean number of cells per mm² [39].

2.6. Tissue Preparation and Homogenization for Western Blot and Biochemical Analyses. Brain tissue for protein isolation was obtained from 5 intact rats (untreated), 10 EAE rats (5 EAE 20d and 5 EAE 30d), and 10 EAE rats treated with olive leaf therapy (5 EAE+TOL 20d and 5 EAE+TOL 30d). The rat brain hemisphere samples were rapidly removed and snap-frozen in liquid nitrogen for protein isolation and stored at -80°C. Bead Ruptor 12 homogenizer (Omni International, Kennesaw GA, USA) was used for the preparation of brain tissue homogenates (10% w/v) from frozen samples. Briefly, one rat cerebral hemisphere was placed into 7 mL tube containing 1.4 mm ceramic beads and suspended with 100 mM Tris-HCl buffer pH 7.6 containing phosphatase and protease inhibitors. The samples were processed at speed 4 for three

cycles; each was 15 sec with Dwell of 30 sec. The homogenates were then centrifuged in an Eppendorf 5427R centrifuge (Eppendorf, Hamburg, Germany) for 10 min at 5000 rpm and 4°C. The obtained supernatants were aliquoted and stored at -80°C until analysis. Protein concentrations in supernatants of brain homogenate were determined according to the manufacturer procedure using a BCA protein assay kit (Pierce, Thermo Scientific, Rockford, IL, USA).

2.7. Biochemical Analyses

2.7.1. Determination of Malondialdehyde. The lipid peroxidation level (as TBARS) was measured spectrophotometrically by the estimation of malondialdehyde concentration (nmol/mg of proteins) based on the reaction with thiobarbituric acid (TBA) according to the modified method by Ohkawa et al. [40]. Briefly, 100 μ L of brain tissue homogenate supernatant was added in the test tube that contained the mixture of 1% *w/v* of TBA dissolved in 10% *w/v* trichloroacetic acid (TCA) and 2% *w/v* butylhydroxytoluene (BHT) dissolved in 10% *w/v* TCA. The test tubes were kept for boiling at 90°C for 20 min. After cooling, the tubes were centrifuged at 10000 rpm for 15 min at RT. Separated supernatant was collected and absorbance read at 532 nm using Eppendorf BioSpectrometer® basic (Eppendorf AG, Hamburg, Germany) against reagent blank. All absorbances were read in triplicate. 1,1,3,3-Tetraethoxypropane (TEP) was used as a standard for calibration curve in the range of 0 to 125 μ M ($y = 0.019x + 0.0102$, $R^2 = 0.99996$).

2.7.2. Glutathione Peroxidase Activity. Glutathione peroxidase (GPX) activity was determined in the brain homogenate supernatants by commercial Ransel kit (Randox, Crumlin, UK) according to the manufacturer's instructions. GPX activity was calculated as U/mg protein/min.

2.7.3. Superoxide Dismutase Activity. The total superoxide dismutase (SOD) activity was determined in the supernatants of brain homogenates using Ransod kit (Randox, Crumlin, UK) according to the manufacturer's instructions. The percent of SOD inhibition was found between 63.98 and 95.36% ($y = 43.238x + 63.984$, $R^2 = 0.9929$). SOD activity was calculated in terms of U/mg protein/min. GPX and SOD activities were measured at room temperature (RT) using BioSpectrometer fluorescence (Eppendorf, Hamburg, Germany).

2.8. Western Blot Analysis. The supernatants were collected and used for the determination of SOD1, SOD2, GPX1, SIRT1, Iba-1, and myelin basic protein (MBP). Briefly, 50 μ g protein was subjected to SDS-PAGE and transferred to a PVDF membrane using a semidry protocol after previous protein determination by the BCA method. Electrophoretic separation was performed using precast 4–15% TGX gels in the Mini-PROTEAN Tetra Vertical Electrophoresis Cell (Bio-Rad, Hercules, CA, USA) according to the manufacturer's procedure. The transfer run was at 275 mA for 30 min in an SD10 semidry blotter (Clever Scientific Ltd., Rugby, Warwickshire, UK). The membranes were blocked in TBST with a 5% *w/v* nonfat dry milk, incubated with pri-

mary rabbit monoclonal antibodies SOD1 (Booster Biological Technology, Pleasanton, CA, 1:1000), SOD2 (Booster Biological Technology, Pleasanton, CA, 1:1000), GPX1 (Booster Biological Technology, Pleasanton, CA, 1:1000), SIRT1 (Cell Signaling, Leiden, Netherlands, 1:1000), MBP (Booster Biological Technology, Pleasanton, CA, 1:1000), and goat polyclonal Iba-1 antibody (Abcam, Cambridge, UK, 1:1000) overnight at 4°C without agitation. After that, membranes were washed five times for 10 minutes with TBST (containing 0.1% *v/v* Tween-20) with agitation and incubated for 2 h at room temperature with the appropriate secondary antibody (peroxidase-conjugated goat anti-rabbit IgG, Booster Biological Technology, Pleasanton, CA, USA, 1:2000), with agitation. Next, they were washed again with TBST, five times for 10 min at room temperature. Protein loading was controlled using a monoclonal rabbit antibody against β -actin (Cell Signaling, Leiden, Netherlands, 1:1000). Chemiluminescent substrate for Horseradish Peroxidase- (HRP-) labeled reporter molecules (Roti®-Lumin, Carl Roth GmbH+ Co. KG) was used for protein detection. The light was detected after then using Image Quant LAS 500 chemiluminescence CCD camera (GE Healthcare UK Ltd., Buckinghamshire, HP7 9NA, UK). The bands were examined densitometrically using ImageJ, an image analysis system (National Institutes of Health, Bethesda, USA) which evaluated the relative amount of protein staining and quantified the results in terms of density. The results of treatment with olive leaf EAE+TOL 20d and EAE+TOL 30d were normalized related to the EAE 20d and EAE 30d, respectively.

2.9. Statistical Analysis. The data were evaluated with Statistica (data analysis software system), version 13 (TIBCO Software Inc., 2017, Palo Alto, CA, USA). The distribution of data was tested for normality using the Kolmogorov–Smirnov test. Differences between groups were assessed with either one-way analysis of variance (ANOVA) followed by the post hoc Scheffé test or Mann–Whitney *U* test. For evaluation of death frequency between the EAE and EAE+TOL groups, we used Fisher's exact test. Pearson correlation (*r*) was used for determining the association between Iba-1 and SIRT1 cerebral protein expressions within immunofluorescence images.

The data are expressed as mean \pm SD and the level of significance is set at $p < 0.05$.

3. Results

EAE was induced in genetically susceptible DA rats, which were then treated with olive leaf therapy. The clinical course and the expression profiles of the following proteins (SIRT1, Iba-1, iNOS, CD206, PLP, SOD1, SOD2, and GPX1), biochemical activity (GPX and SOD), and peroxidation level (as TBARS) were examined in the brain, and the data were compared with the findings in untreated EAE rats and untreated control rats.

3.1. Olive Leaf Therapy Attenuates the Clinical Course and Reduces Death Frequency during EAE. The EAE control group of rats (EAE 30d; $n = 16$) and EAE rats treated with

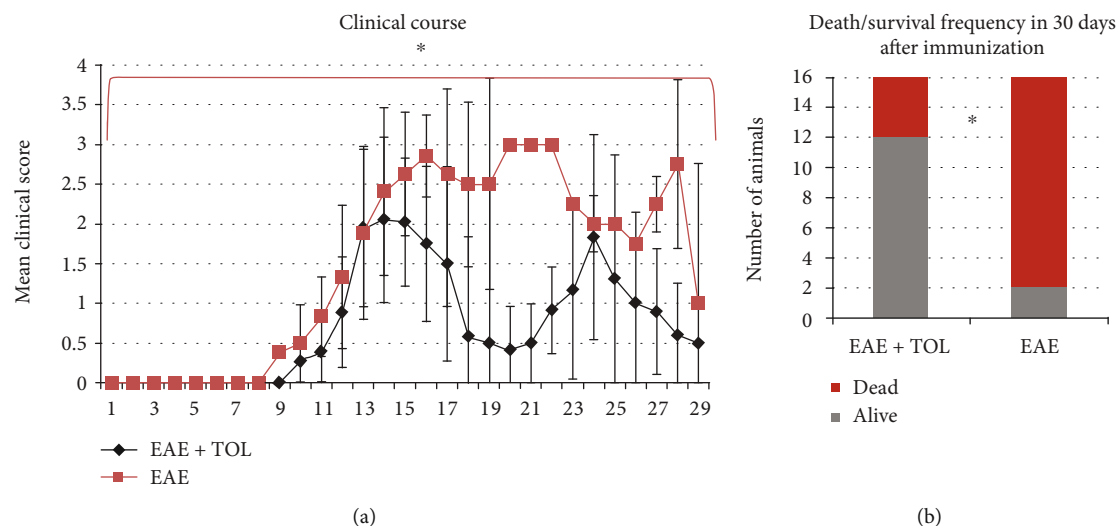


FIGURE 1: Clinical course and death frequency in the EAE and EAE+TOL groups. (a) The clinical course in the EAE ($n = 16$) and EAE+TOL ($n = 16$) rat groups. Values are presented as mean \pm SD (Mann–Whitney U test) using EAE scores of each animal for every day. (b) Death/survival frequency during 30 days after EAE induction. Values are presented as a number of animals per group (Fisher's exact test); $*p < 0.05$.

olive leaf (EAE 30d+TOL; $n = 16$) were monitored daily during the period of 30 days to evaluate the effects of therapy of olive leaf on the clinical course of the disease.

The intensity of the clinical course of EAE was attenuated in a group of animals treated with olive leaf (EAE+TOL) (Figure 1(a)). The onset of clinical symptoms in the EAE+TOL group was one day after the onset in the EAE group. Furthermore, the clinical scores/symptoms were rising faster in the EAE group during the first five days with a maximum mean score of 3.0 ± 0.0 that reached at the peak of disease. The maximum mean score in the EAE+TOL group that reached at the peak of disease was 2.1 ± 0.8 . The first relapse in the EAE group lasted for 3 days with a minimum mean score of 2.5 ± 0.0 , unlike the relapse in the EAE+TOL group that lasted for 7 days with a minimum mean score of 0.4 ± 0.5 (Figure 1(a)). During the 30 days after immunization, death occurred in 14 from 16 rats in the EAE group, unlike in the EAE+TOL group, where only 2 from 16 rats died, with a significant difference of $p = 0.011$ (Figure 1(b)).

3.2. Biochemical Analysis. TBARS level and SOD and GPX activity are presented in Figure 2. The level of lipoperoxidation as TBARS is expressed as nM/mg protein of MDA (Figure 2(a)). The level of MDA changed significantly ($p < 0.001$) in all examined groups. TBARS were significantly higher in the EAE groups according to the duration of the illness ($p < 0.001$ for EAE 20d and $p = 0.001$ for EAE 30d). Therapy with olive leaf (TOL) in the EAE groups significantly decreased TBARS level ($p = 0.009$ for EAE+TOL 20d and $p = 0.001$ for EAE+TOL 30d).

Total SOD activity changed related to all examined groups and increased in EAE treated groups (EAE+TOL 20d and EAE+TOL 30d) compared to the untreated control (EAE 20d and EAE 30d), but not significantly (Figure 2(b)). As presented, in the EAE 20d postimmunization group, SOD activity was significantly lower than that in the EAE

30d ($p = 0.043$). The same trend was found in the EAE groups treated with olive leaf polyphenols ($p = 0.033$).

Total GPX activity changed significantly related to all examined groups ($p < 0.001$) (Figure 2(c)). The EAE groups treated with olive leaf polyphenols showed that GPX activity increased significantly in the group EAE+TOL 20d compared to the EAE 20d group ($p < 0.001$) as well as in the EAE+TOL 30d group ($p < 0.001$) compared to the EAE 30d group. These results showed that therapy with OLP affected the increase of endogenous antioxidants in the rat brain during EAE and also reduced lipoperoxidation. Our results showed significant alterations in the antioxidant defenses, especially in the second remission. In addition, the differences were found also in relation to the duration of illness, where the application of OLP can be beneficial to long therapies.

3.3. Western Blot Analysis of SOD1, SOD2, GPX1, SIRT1, and Iba-1. Although total SOD activity was lower in the EAE groups and higher in the OLP-treated groups with EAE (Figure 3(b)), we believe that the differences in the protein abundance exist in cytosolic SOD1 (Cu-Zn) and mitochondrial SOD2 (MnSOD) in the rat brain. To determine this alteration, rat brain protein extracts were analyzed with western blot analysis (Figures 3(b) and 3(c)). Therapy with OLP significantly changed cytosolic SOD1 only at the 30th day ($p = 0.048$) and in the mitochondrial SOD2 at both the 20th and 30th days after induced EAE ($p < 0.001$ and $p < 0.001$, respectively). All analyzed groups had the SOD2/SOD1 ratio less than 1.0, after normalizing to the sum of the untreated control group for SOD1 and SOD2, except the EAE+TOL 30d group (the ratio is 1.013). On the other hand, the SOD2/SOD1 ratio was lower in the EAE 20d group (the ratio is 0.814). Thus, we suggested that EAE reduced SOD2 abundance (and activity) in the mitochondria, and OLE therapy enhanced SOD2 in the mitochondria, especially in the remission phase (at 30 days postimmunization). We conclude that

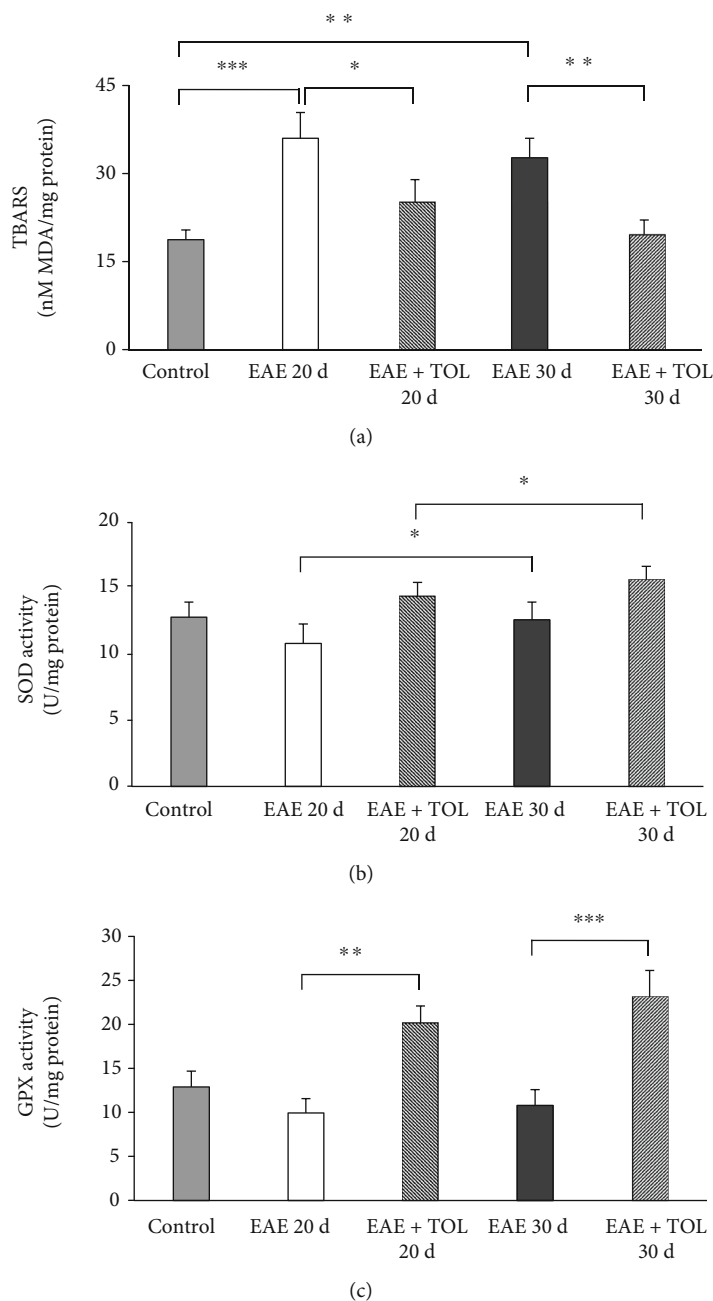


FIGURE 2: Biochemical assays in the rat brain. (a) The concentration of MDA (nM/mg protein), (b) the activity of SOD (U/mg protein), and (c) the activity of GPX (U/mg protein) in the healthy untreated group (control), in the groups induced EAE after 20 days (EAE 20d) and 30 days (EAE 30d) postimmunization and EAE groups with olive leaf therapy (EAE+TOL 20d and EAE+TOL 30d). For each group, values are presented as the mean \pm SD of five rats per group. One-way ANOVA followed by the post hoc Scheffé test was used for the statistical analysis: * $p < 0.05$, ** $p < 0.01$, and *** $p < 0.001$.

EAE progression alters the cytosolic SOD1 and mitochondrial SOD2 protein levels. In addition, OLP therapy effect seems to be compensatory on the mitochondrial SOD2 protein level due to the loss of the specific activity of mitochondrial SOD2 to reduce the deleterious effect of the mitochondrial superoxide.

GPX1 is found in the cytosol and mitochondria to remove a large amount of generated superoxide. We did not find significant changes in the expression of GPX1 in

the EAE+TOL 20d group; however, a significant increase of GPX1 expression was found in the EAE+TOL 30d group ($p = 0.005$) (Figure 3(d)).

The western blotting analysis demonstrated that SOD1, SOD2, and GPX1 expressions in OLP-treated EAE rat brain were higher compared to those in EAE animals without the OLP treatment and even higher than those in the untreated control. These data also suggested that the neuroprotective effect of OLP is carried out through its effect on SOD1,

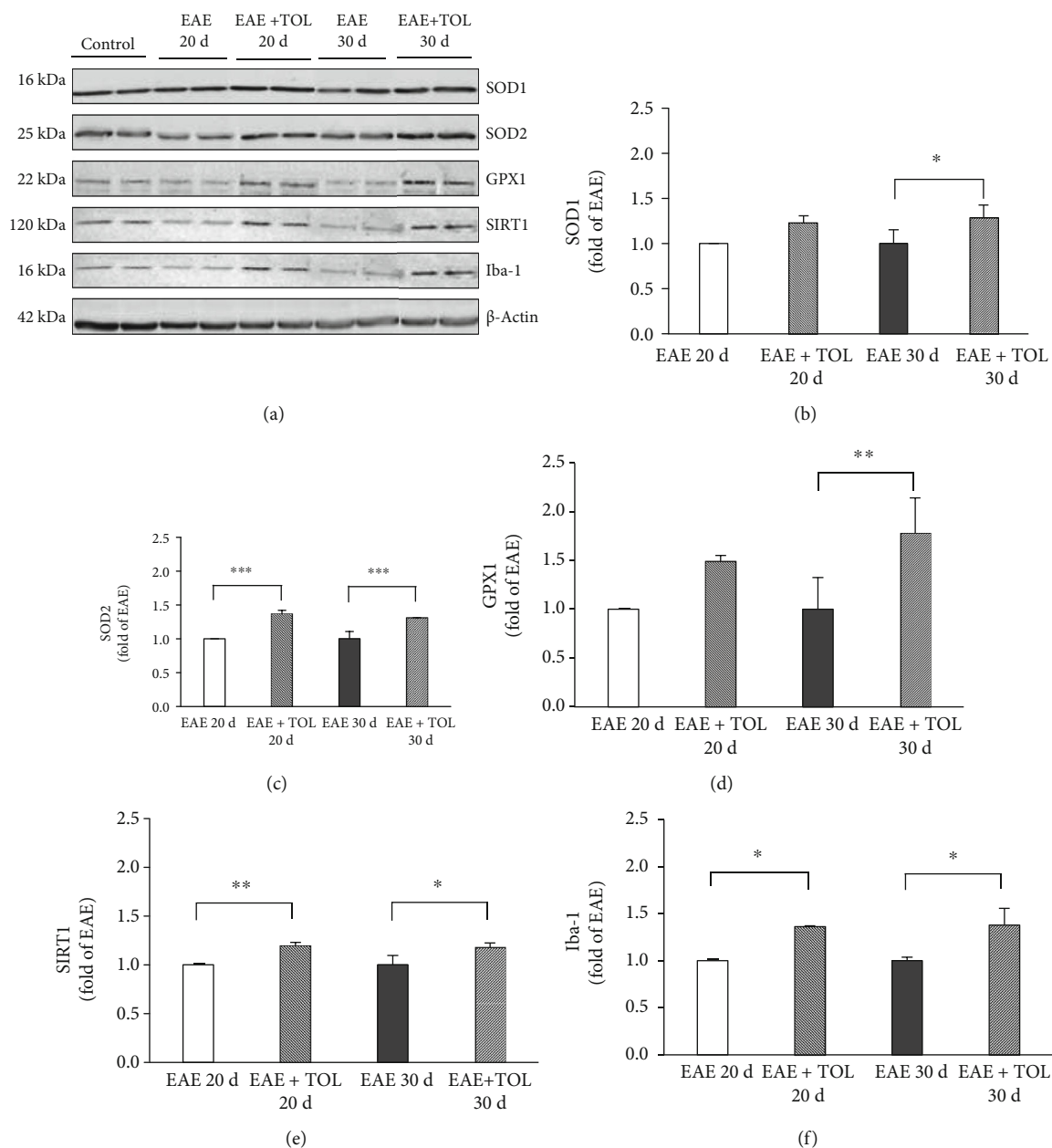


FIGURE 3: Immunoblot of SOD1, SOD2, GPX1, SIRT1, and Iba-1 in the isolated rat brain proteins. Cell lysate proteins (50 μ g) were immunoblotted using β -actin as the loading control. (a) Representative western blot images of the target proteins. The expression of (b) SOD1, (c) SOD2, (d) GPX1, (e) SIRT1, and (f) Iba-1 is shown at the normalized expression level of EAE. For each group, values are presented as the mean \pm SD of five rats per group. One-way ANOVA followed by the post hoc Scheffé test was used for the statistical analysis: * $p < 0.05$, ** $p < 0.01$, and *** $p < 0.001$.

SOD2, and GPX1, not only in the acute phase of the disease (20th day) but in the remission period as well (on the 30th day postimmunization). Therefore, the effectiveness of OLP therapy can be proposed, at least in part, to increase levels of these antioxidant enzymes in the brain *in vivo*.

However, the SOD1 and SOD2 protein expression obtained by immunofluorescence revealed a different pattern at the tissue distribution level. Higher SOD1 cell upregulation, including in neurons and microglia, was found in different brain regions (i.e., cortex, hippocampus, and subventricular zone) in rats without the TOL treatment or EAE control rats

(see Suppl. Figure 2). Furthermore, the SOD2 expression was upregulated in microglia surrounding lesions in the brain stem from rats without the TOL treatment as well (see Suppl. Figure 3), but not elsewhere.

3.4. Olive Leaf Therapy Stimulates Cerebral SIRT1 Expression during EAE. Profiling of cerebral SIRT1 protein by immunohistochemistry and western blot showed significant upregulation at the 20th day after EAE induction in rats treated with olive leaf therapy (Figures 3(e) and 4) and greater than that in untreated EAE rats. The data obtained by

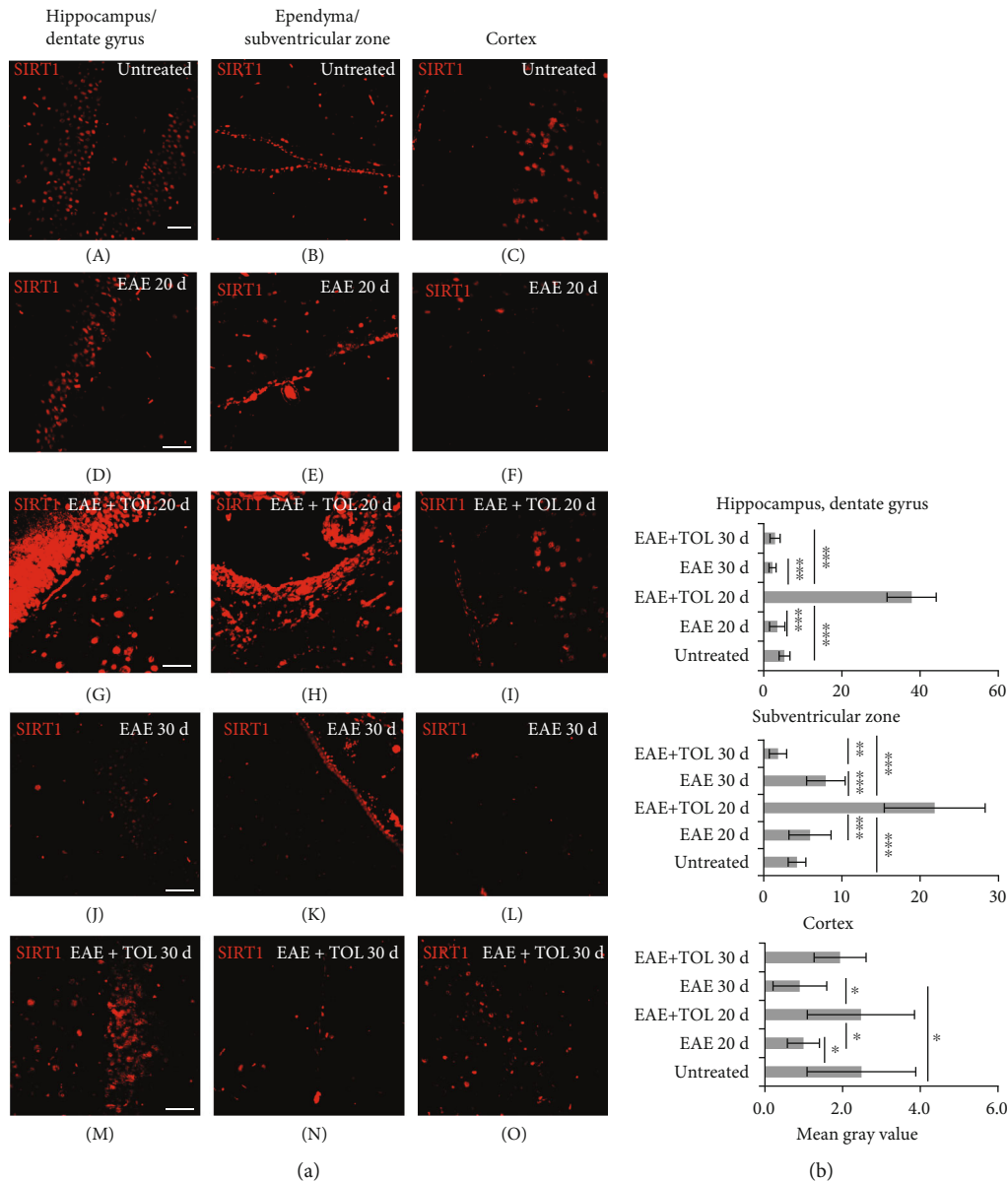


FIGURE 4: Polyphenols from olive leaf extract induce the upregulation of SIRT1 in different brain regions (hippocampus, ependyma, subventricular zone (SVZ), and cortex). (a) Representative immunofluorescent pictures show staining with anti-SIRT1 antibody in paraffin-embedded sections of the brain tissue obtained from DA rats: (A–C) untreated, (D–F) with induced EAE and the second attack (on the 20th day postinduction), (G–I) with induced EAE and treated with the olive leaf therapy (TOL) till the 20th day postinduction, (J–L) with induced EAE and the second remission (on the 30th day postinduction), and (M–O) with induced EAE and treated with TOL on the 30th day postinduction. (b) SIRT1 immunoreactivity in different brain regions. The immunofluorescent staining quantification was performed using Cell F v3.1 software analysis (12 ROI/4 μ m slice \times 3 slices/rat \times 5 rats/group). Values are expressed as mean gray value \pm SD. One-way ANOVA followed by the post hoc Scheffé test: * p < 0.05, ** p < 0.01, and *** p < 0.001. Scale bars indicate 50 μ m.

immunohistochemistry clearly showed that SIRT1 expression was markedly upregulated (Figures 4(a) and 4(b)) in the EAE+TOL 20d group of rats in comparison with findings in the untreated control and untreated EAE group of rats in the following locations: in the hippocampus/dentate gyrus (Figures 4(a) A D, G, J, M and 4(b): p < 0.001, p < 0.001), in the ependymal, subependymal, and subventricular area (Figures 4(a) B, E, H, K, N and 4(b): p < 0.001, p < 0.001), and in the cortex (Figures 4(a) C, F, I, L, O and 4(b): p = 1.000, p = 0.038). The western blot showed, as presented in

Figure 5(e), that therapy of olive leaf activated brain SIRT1 in both relapse (20th day) and remission (30th day) phase of the EAE, compared to the same phases in the untreated EAE groups (p = 0.009 and p = 0.016, respectively). Interestingly, the findings from the relapse phase (20th day) showed higher expression of brain SIRT1 than those from the remission phase (30th day) for normalized values related to untreated control (48% greater for EAE 20d than EAE 30d and 50% greater for EAE+TOL 20d than EAE+TOL 30d) (data not shown). The immunohistochemical findings

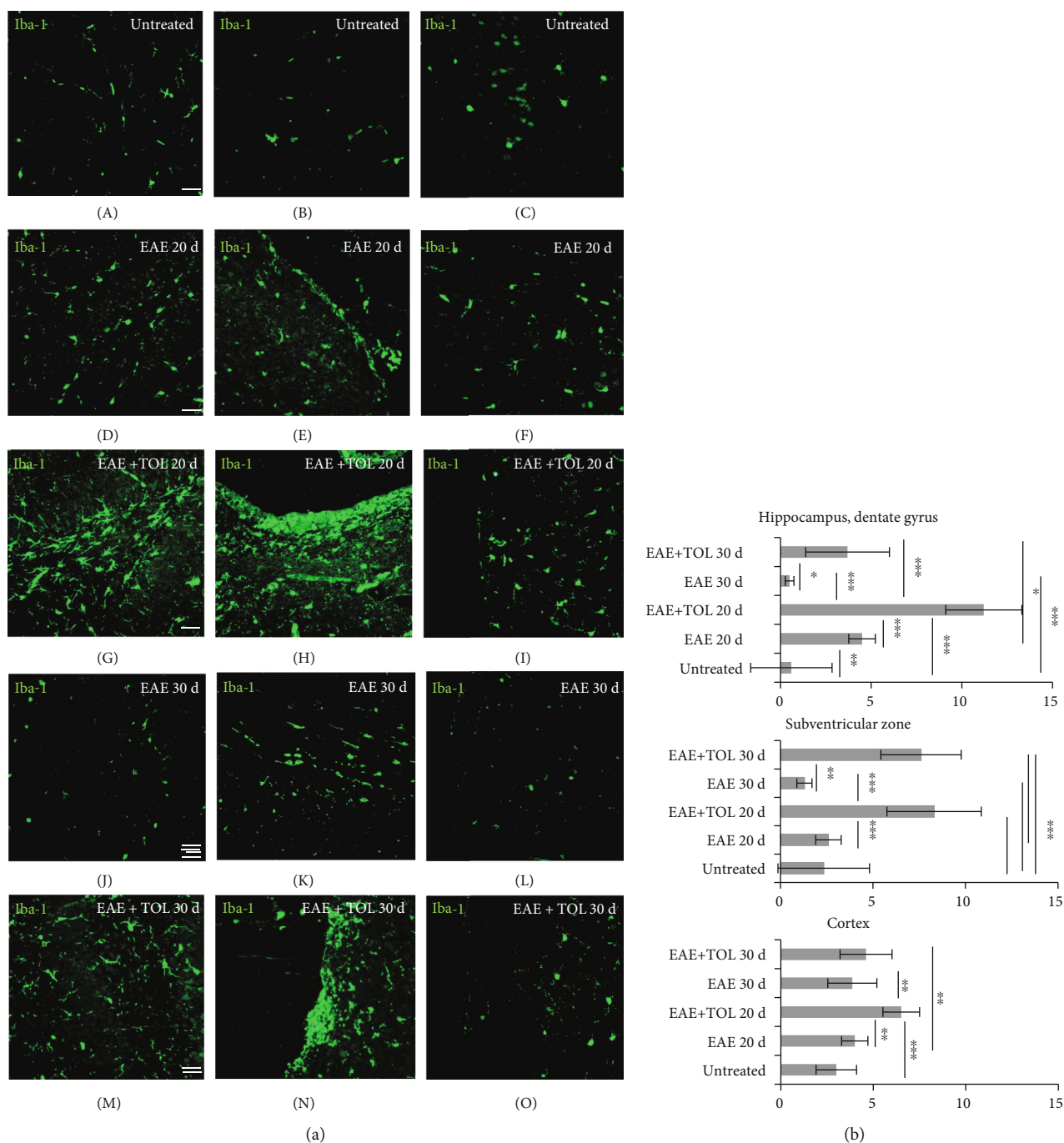


FIGURE 5: Polyphenols from olive leaf induce the upregulation of Iba-1 in different brain regions (hippocampus, ependyma, subventricular zone (SVZ), and cortex). (a) Representative immunofluorescent pictures show staining with anti-Iba-1 antibody in paraffin-embedded sections of the brain tissue obtained from DA rats: (A–C) untreated, (D–F) with induced EAE and second attack (on the 20th day postinduction), (G–I) with induced EAE and treated with the therapy of olive leaf (TOL) till the 20th day postinduction, (J–L) with induced EAE and the second remission (on the 30th day postinduction), and (M–O) with induced EAE and treated with TOL on the 30th day postinduction. (b) Iba-1 immunoreactivity in different brain regions. The immunofluorescent staining quantification was performed using Cell F v3.1 software analysis (12 ROI/4 μm slice and 3 slices/rat × 5 rats/group). Values are expressed as mean gray value ± SD. One-way ANOVA followed by the post hoc Scheffé test: * $p < 0.05$, ** $p < 0.01$, and *** $p < 0.001$. Scale bars indicate 50 μm.

showed the higher expression level of brain SIRT1 in the relapse phase (20th day) as well than that in the remission phase (30th day), especially in the dentate gyrus (Figures 4(a) M and 4(b); $p < 0.001$) and subventricular zone (Figures 4(a) N and 4(b); $p < 0.001$).

3.5. Olive Leaf Therapy Stimulates Cerebral Iba-1 Expression during EAE. To detect the microglia during the olive leaf therapy, a protein marker Iba-1 was used in immunohistochemistry and western blot analyses. The immunohistochemistry showed significant upregulation of Iba-1 on the

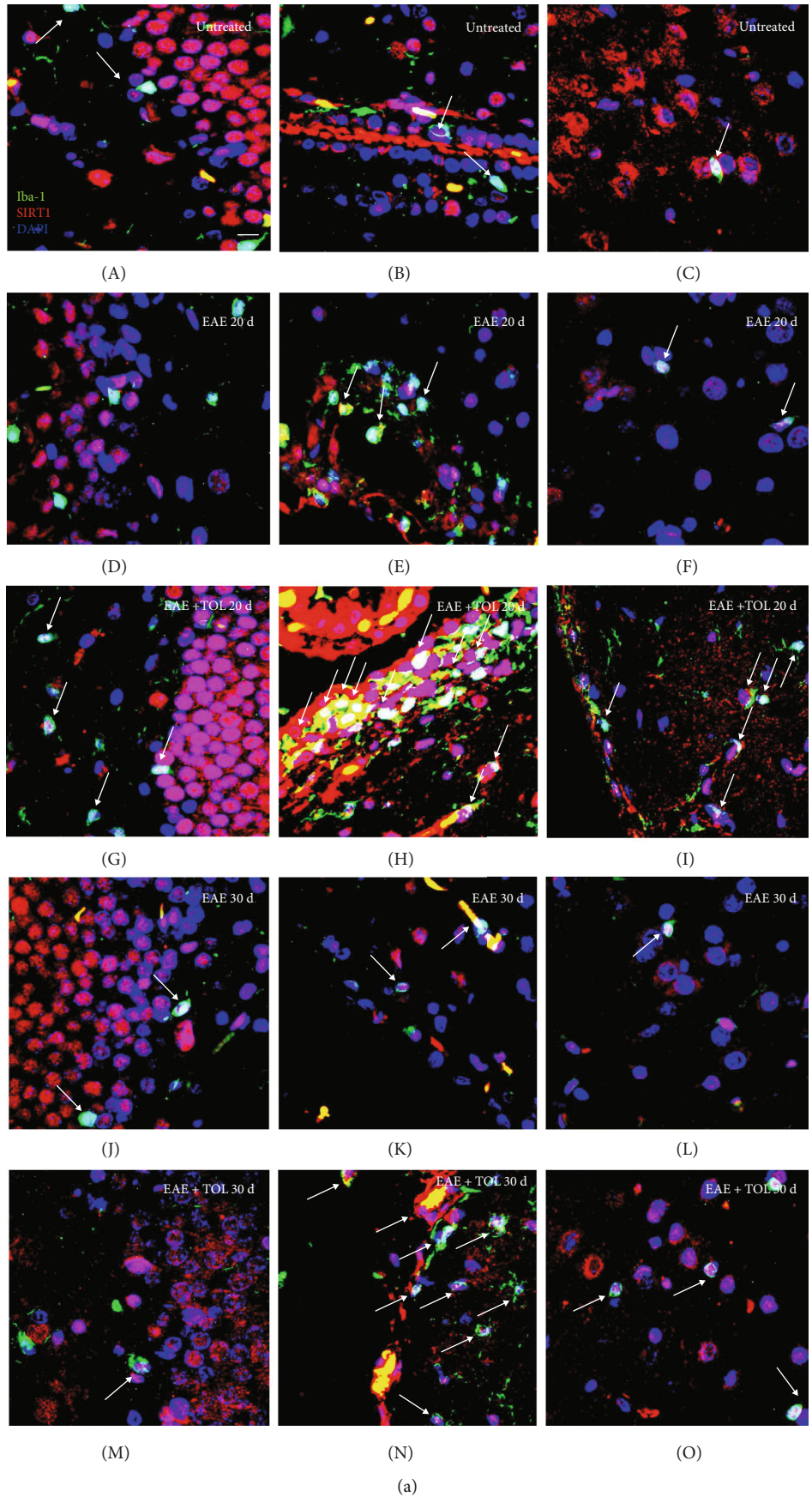


FIGURE 6: Continued.

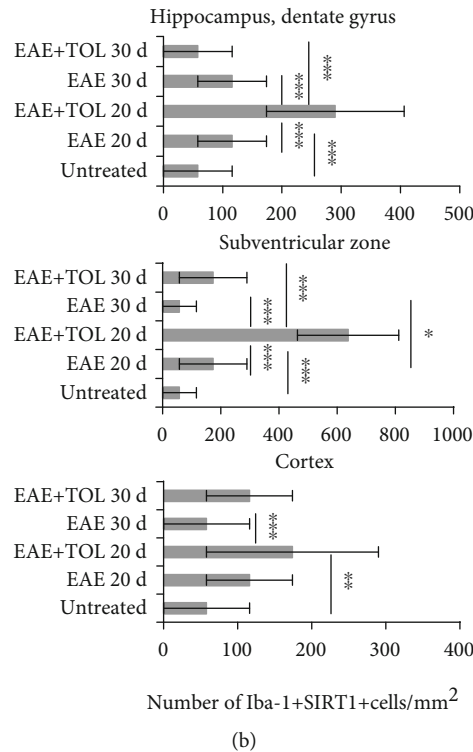


FIGURE 6: In the cerebral hippocampus, subventricular zone (SVZ), and cortex of rats treated with the therapy of olive leaf (TOL), microglia cells that abundantly express SIRT1 are present. (a) Representative immunofluorescent pictures show the relationship between SIRT1⁺ and Iba-1⁺ microglia cells in DA rats: (A–C) untreated, (D–F) with induced EAE and the second attack (on the 20th day postinduction), (G–I) with induced EAE and treated with TOL till the 20th day postinduction, (J–L) with induced EAE and the second remission (on the 30th day postinduction), and (M–O) with induced EAE and treated with TOL on the 30th day postinduction. (b) A number of Iba-1⁺ SIRT1⁺ cells were manually counted in the area of interest (0.014 mm²/4 μm slice × 3 slices/rat × 5 rats/group). Values are expressed as mean gray value ± SD of a number of cells per mm². One-way ANOVA followed by the post hoc Scheffé test: * $p < 0.05$, ** $p < 0.01$, and *** $p < 0.001$. Scale bars indicate 20 μm.

20th and 30th days after EAE induction in rats treated with TOL (Figures 5(a) G, H, I, M, N, and O) and greater than that in untreated EAE rats (Figures 5(a) and 5(b)). The data obtained by immunohistochemistry clearly showed that Iba-1 expression was markedly upregulated in the EAE +TOL 20d group of rats in comparison with the findings in the untreated control and untreated EAE group of rats in the following locations: in the hippocampus/dentate gyrus (Figures 5(a) A, D, G, J, and M and 5(b): $p < 0.001$, $p < 0.001$), in the ependymal, subependymal, and subventricular area (Figures 5(a) B, E, H, K, and N and 5(b): $p < 0.001$, $p < 0.001$), and in the cortex (Figures 5(a) C, F, I, L, and O and 5(b): $p < 0.001$, $p = 0.001$). As shown with WB analysis, therapy of olive leaf activated Iba-1 in the EAE 20d ($p = 0.013$) and EAE 30d groups ($p = 0.010$) (see Figure 3(f)). Compared to the untreated control, Iba-1 was reduced for 1.8% in the EAE 20d group and 32.3% in the EAE 30d group. In addition, therapy with olive leaf polyphenols enhanced Iba-1 expression for 33% in the EAE+TOL 20d and decreased Iba-1 expression for 6.5% in the group EAE+TOL 30d (data not shown). The immunohistochemical findings showed the higher expression level of Iba-1 marker in the relapse phase (20th day) as well than that in the remission phase (30th day), but only in the dentate gyrus (Figures 5(a) M and 5(b); $p < 0.001$).

TABLE 1: Pearson correlations (r) between Iba-1 and SIRT1 cerebral expressions.

Variable	SIRT1 (SVZ)	SIRT1 (hippocampus)	SIRT1 (cortex)
Iba-1 (SVZ)	0.85*	/	/
Iba-1 (hippocampus)	/	0.85*	/
Iba-1 (cortex)	/	/	0.61*

*Denotes statistical significance at $p < 0.05$. Iba-1 and SIRT expressions were correlated using the average gray intensity level of immunofluorescent staining.

3.5.1. Coexpression of Iba-1 and SIRT1 in the Brain. Immunofluorescent analyses confirmed coexpression of Iba-1 with SIRT1 in the different brain regions (Figure 6), especially in EAE rats treated with the therapy of olive leaf (TOL) (Figures 6(a) G, H, I, N, and O). A number of Iba-1⁺SIRT1⁺ cells per mm² of brain tissue are most abundant in EAE rats treated with TOL till the 20th day after EAE induction (Figure 6(b)), especially in the subventricular zone (Figure 6(a) H, arrows) compared to the untreated EAE 20d (hippocampus: $p < 0.001$; SVZ: $p < 0.001$; and cortex: $p = 0.081$) and control groups of rats (hippocampus: $p < 0.001$; SVZ: $p < 0.001$; and cortex: $p = 0.039$) (Figure 6(b)).

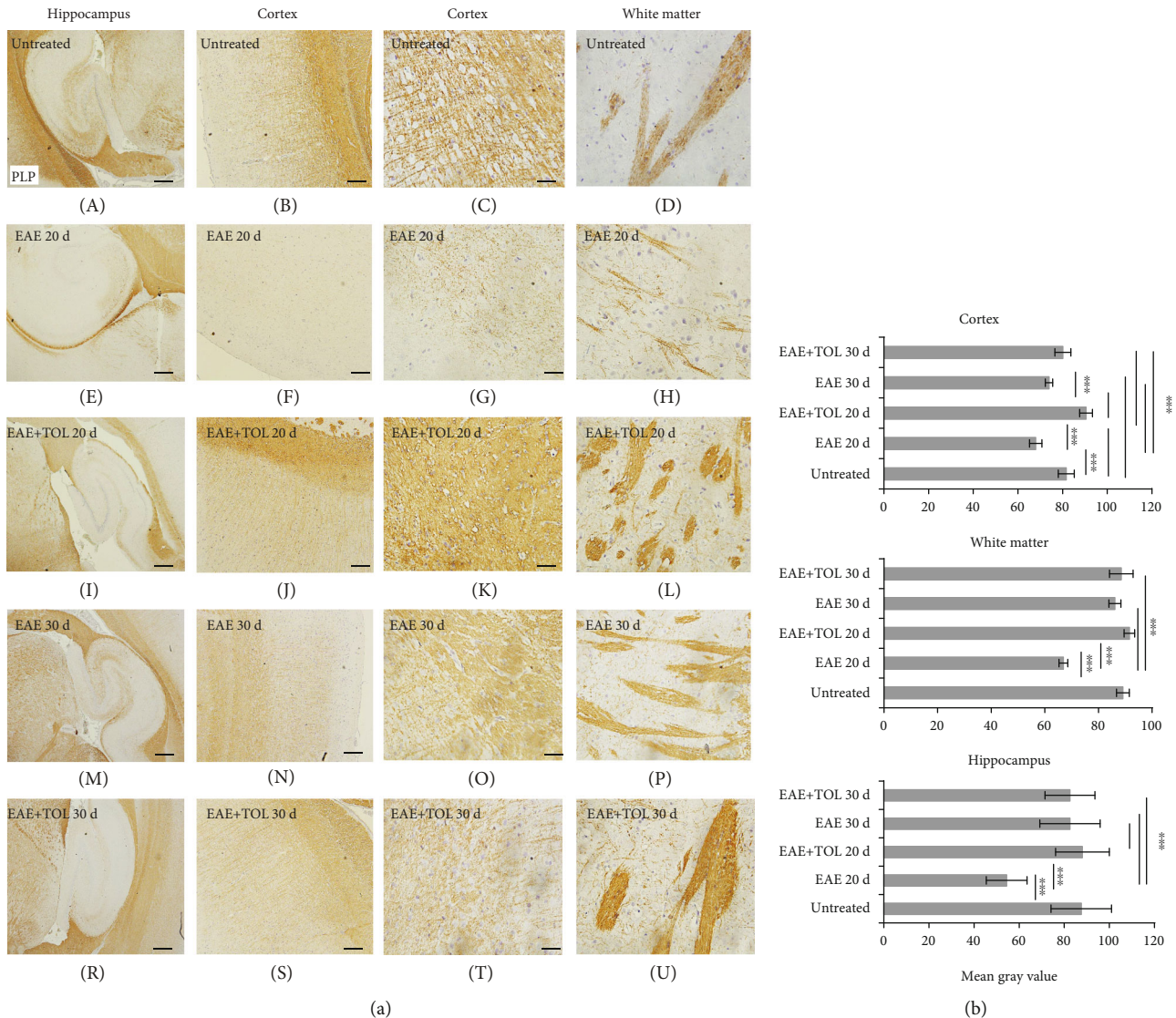


FIGURE 7: Polyphenols from olive leaf extract induce the upregulation of PLP in different brain regions (hippocampus, cortex, and white matter). (a) Representative immunohistochemical pictures show staining with anti-PLP antibody in paraffin-embedded sections of the brain tissue obtained from DA rats: (A–C) untreated, (D–F) with induced EAE and the second attack (on the 20th day postinduction), (G–I) with induced EAE and treated with polyphenols till the 20th day postinduction, (J–L) with induced EAE and the second remission (on the 30th day postinduction), and (M–O) with induced EAE and treated with polyphenols on the 30th day postinduction. (b) PLP immunoreactivity in different brain regions. The immunohistochemical staining quantification was performed using Cell F v3.1 software analysis (12 ROI/4 μm slice × 3 slices/rat × 5 rats/group) of representative cortex photomicrographs (C, G, K, O, T). Values are expressed as mean gray value ± SE. One-way ANOVA followed by the post hoc Scheffé test: ****p* < 0.001. Scale bars in horizontal order indicate 500 μm (for the hippocampus), 200 μm (for the cortex), 50 μm (for the cortex), and 50 μm (for the white matter).

3.5.2. Correlation of Iba-1 and SIRT1 in the Brain. The SIRT1 expression strongly correlated with the Iba-1 expression in the SVZ region ($r = 0.85$, $p < 0.001$), hippocampal region ($r = 0.85$, $p < 0.001$), and cortex region ($r = 0.61$, $p < 0.001$) (Table 1).

3.6. Myelin Integrity Is Reduced in EAE Untreated Rats Compared to EAE Rats Treated with Olive Leaf. Myelin integrity was assessed by PLP immunostaining which differed significantly between the untreated control group, untreated EAE groups, and EAE groups treated with olive leaf (EAE+TOL) when analyzed (mean gray value ± SD; one-way

ANOVA followed by the post hoc Scheffé test PLP; $p < 0.001$). PLP immunostaining was significantly lower in the untreated EAE 20d group vs. the treated EAE+TOL 20d group ($p < 0.001$) and vs. the untreated control group ($p < 0.001$) (Figure 7).

This was accompanied by a corresponding increase in the cellular content of the 18 kDa isoform of MBP at the 30th day compared to the 20th day after inducing EAE (see Suppl. Figure 4B). In addition, MBP expression was significantly greater in rats treated with olive leaf polyphenols at the 20th day of induced EAE. However, we did not find higher MBP after the olive leaf treatment on the 30th day (Suppl.

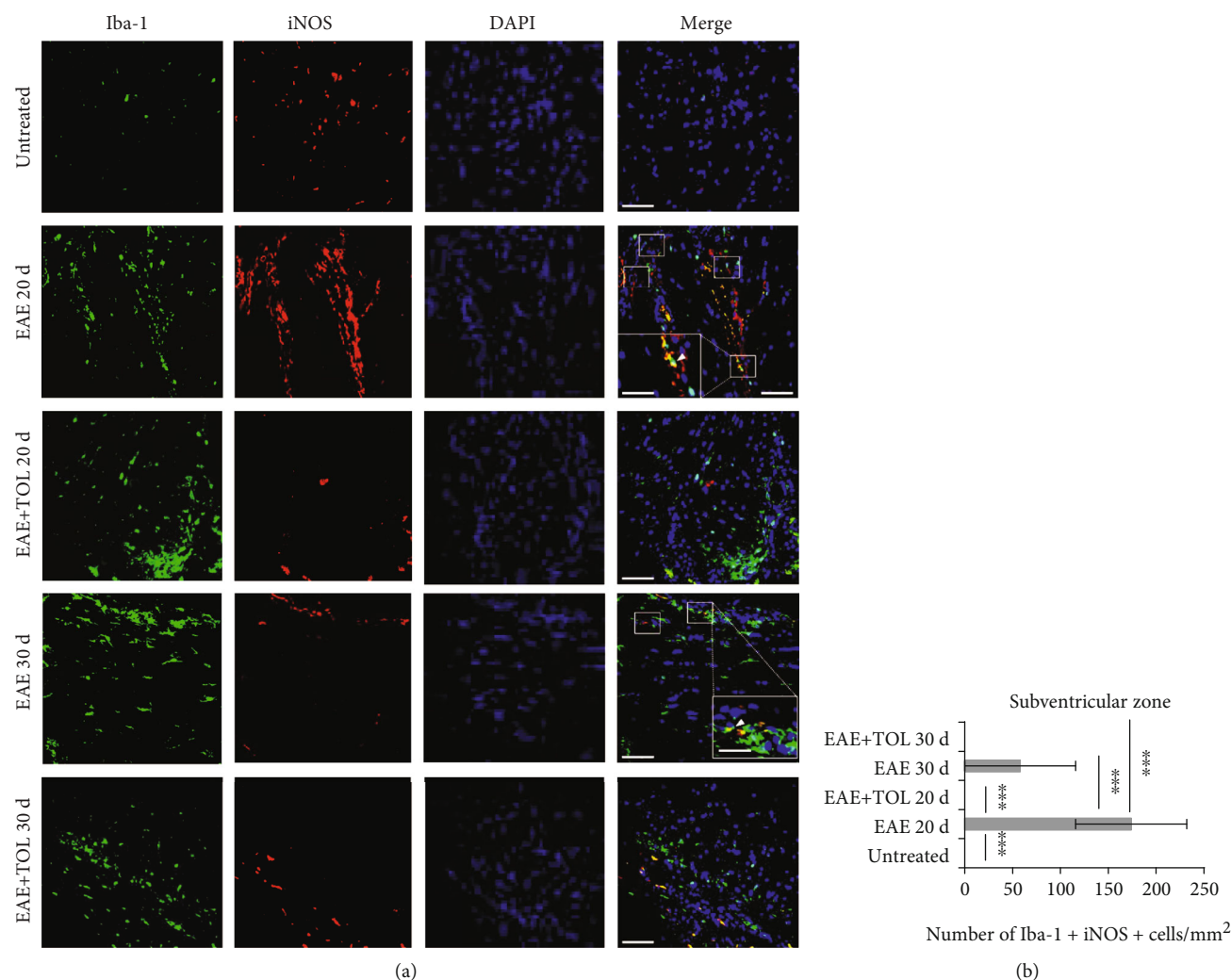


FIGURE 8: (a) Representative immunofluorescent pictures show the relationship between iNOS⁺ and Iba-1⁺ (M1) microglia cells in the subventricular zone: untreated, with induced EAE and the second attack (on the 20th day postinduction), with induced EAE and treated with TOL till the 20th day postinduction, with induced EAE and the second remission (on the 30th day postinduction), and with induced EAE and treated with TOL on the 30th day postinduction. (b) The number of Iba-1⁺ iNOS⁺ was manually counted in the area of interest (0.053 mm²/4 μm slice × 3 slices/rat × 5 rats/group). Values are expressed as mean gray value ± SD of a number of cells per mm². One-way ANOVA followed by the post hoc Scheffé test: *** $p < 0.001$. Scale bars indicate 50 μm and 20 μm (insets).

Figure 4C). Since the content of MBP in the brain tissue is a quantitative indicator of the myelin membrane integrity and that myelin also depends on its characteristic lipid contents, therefore, we assume that olive leaf polyphenols attenuate myelin sheath destruction through suppression of the oxidative changes, as well as affect the regulation of lipogenesis. This was supported by the expression of both myelin proteins (PLP and MBP).

3.7. Olive Leaf Therapy Influences Microglial M1 to M2 Phenotypic Switch in the Subventricular Zone. To investigate the effect of olive leaf therapy on microglial M1 and M2 phenotypes, the immunohistochemical staining and number of Iba⁺ CD206⁺ (M2) and Iba⁺ iNOS⁺ (M1) cells in the subventricular zone were determined and compared to the EAE and untreated control groups. TOL significantly decreased the number of microglial M1 cells in the EAE+TOL 20d group

compared to both EAE groups (EAE 20d and EAE 30d; $p < 0.001$, $p < 0.001$) (Figures 8(a) and 8(b)). Furthermore, TOL significantly increased the number of microglial M2 cells in the EAE+TOL 20d and EAE+TOL 30d groups compared to both EAE groups (EAE 20d and EAE 30d; $p < 0.001$, $p = 0.046$) and untreated group ($p < 0.001$, $p < 0.001$) (Figures 9(a) and 9(b)). Taken together, these results indicate that olive leaf therapy not only reduces M1 cells but also promotes microglial polarization toward the M2 alternative phenotype.

4. Discussion

With this study, we present that therapy with olive leaf polyphenols downregulates the EAE and provides neuroprotection through the attenuation of the clinical course, reduces

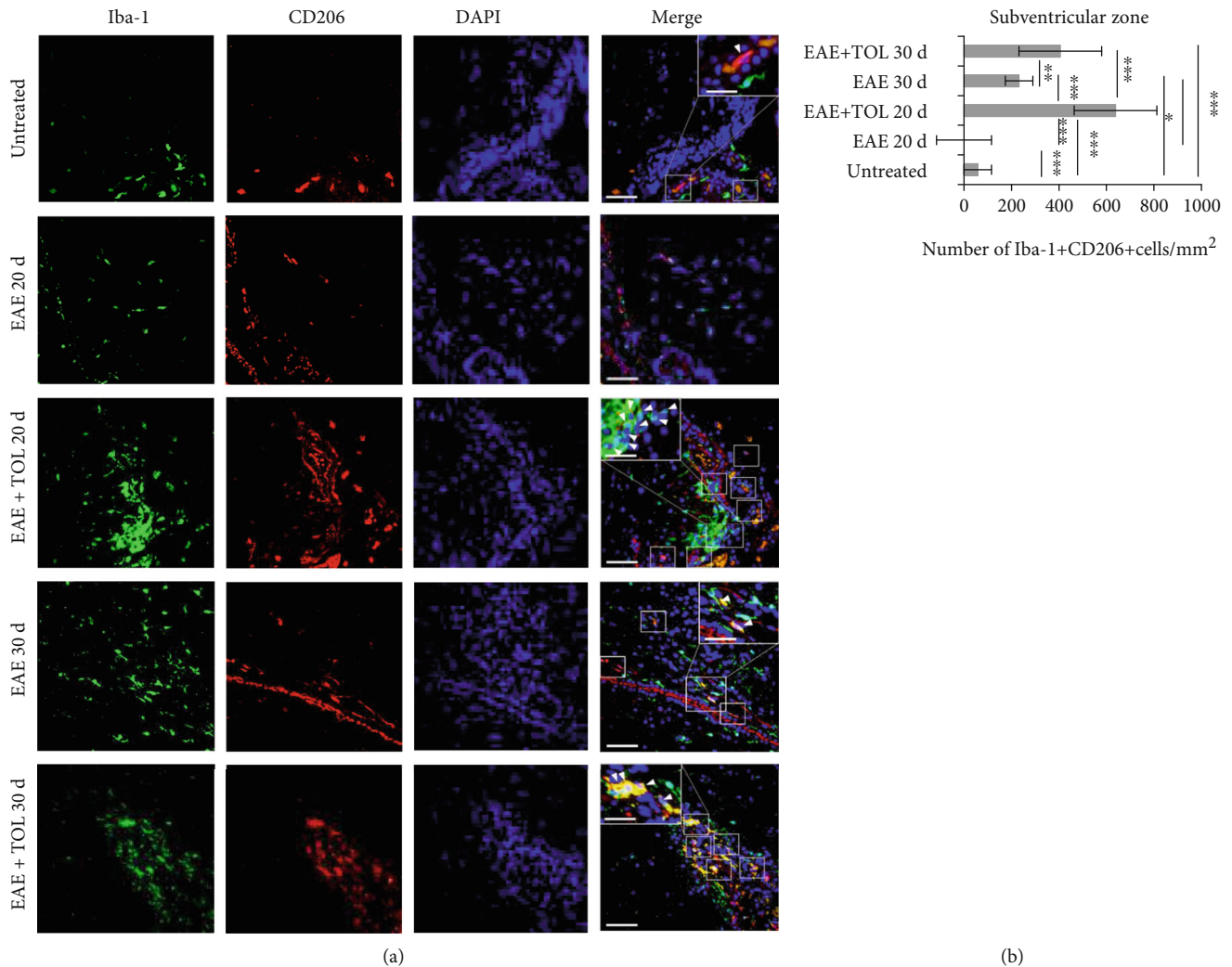


FIGURE 9: (a) Representative immunofluorescent pictures show the relationship between CD206⁺ and Iba-1⁺ (M2) microglia cells in the subventricular zone: untreated, with induced EAE and the second attack (on the 20th day postinduction), with induced EAE and treated with TOL till the 20th day postinduction, with induced EAE and the second remission (on the 30th day postinduction), and with induced EAE and treated with TOL on the 30th day postinduction. (b) The number of Iba-1⁺ CD206⁺ cells was manually counted in the area of interest (0.053 mm²/4 μm slice \times 3 slices/rat \times 5 rats/group). Values are expressed as mean gray value \pm SD of a number of cells per mm². One-way ANOVA followed by the post hoc Scheffé test: * p < 0.05, ** p < 0.01, and *** p < 0.001. Scale bars indicate 50 μm and 20 μm (insets).

oxidative stress, regulates microglia and SIRT1, and preserves myelin in the CNS.

Multiple sclerosis (MS) is a chronic inflammatory and neurodegenerative disease of the brain and spinal cord characterized by focal lesions of inflammation, axonal loss, gliosis, and demyelination that affect the white and gray matter [41, 42]. Studies which include EAE, an animal model of MS, have demonstrated that microglia/macrophages actively participate in the pathogenesis of EAE progression [43, 44]. In MS patients, the destruction of myelin in the CNS is associated with activated microglia, which is thought to be involved in the disease pathogenesis [45]. However, other studies indicate that microglia activation counteracts pathological processes by providing neurotrophic and immunosuppressive factors and promoting recovery [46, 47] since the microglia are highly heterogeneous immune

cells with a continuous spectrum of activation states [48]. The so-called proinflammatory (M1 phenotype) and the anti-inflammatory (M2 phenotype) microglia are at the opposite ends of this spectrum [49]. The proinflammatory microglia by the activation of T-lymphocytes release proteolytic enzymes, cytokines, oxidative products, and ROS, which affect the development of neurodegeneration in MS. Furthermore, the anti-inflammatory microglia secrete anti-inflammatory cytokines and growth factors that promote oligodendrocyte progenitor proliferation, differentiation, and remyelination and protect neurons from damage [50–53]. Finally, a block in the proinflammatory to anti-inflammatory switch has been hypothesized to contribute to remyelination failure in chronic inactive MS lesions [54]. Thus, our interest is related to the investigations of phytochemicals as possible microglia-targeted therapy for

achieving an efficient treatment strategy for MS. As an example for the treatment of relapsing-remitting MS is “Food and Drug Administration-” (FDA-) approved glatiramer acetate which mediates neuroprotective effects by inducing an anti-inflammatory microglial M2 phenotype [55].

However, there are little reports about OLP impact on MS or its animal model EAE. The major bioactive phenolic compound in the olive leaf is oleuropein, while other bioactives are present in the minority [56]. In general, due to the presence of a wide number of bioactive compounds and their synergism, their biological activity is higher than the alone individual.

As described in the study by Miljković et al. [57], the effect of dry olive leaf extract was mediated through the reduction of encephalitogenic cell numbers generated in draining lymph nodes, as well as through inhibition of IFN- γ and IL-17 production by the cells infiltrating the CNS.

The main phenolic compound of the OLP extract oleuropein is able to exert, in an indirect way, its antioxidant action by stimulating the expression of intracellular antioxidant enzymes via the activation of nuclear factor erythroid 2-related factor 2 (Nrf2) transcription, as well as by increasing the level of nonenzymatic antioxidants [58]. In addition, Park et al. [59] suggested a role for oleuropein in controlling microglial cell activation and as a potential drug candidate for inflammation-mediated neurodegenerative disorders. In our study, we investigated the impact of OLP on microglia with its possible polarization and on the cerebral SIRT1 protein expression. In addition, the impact of OLP on myelin integrity and measure oxidative stress parameters (SOD and GPX activity, lipoperoxidation level as TBARS) was studied as a correlation to antioxidative characteristics of OLP.

Investigating the mechanism of action of natural polyphenols has revealed that they modulate the cell response to oxidative stress via oxidative as well as several other cellular signalling pathways, including regulation of microglia and SIRT1 protein expression [30]. ROS, which if produced in excess lead to oxidative stress, have been implicated as mediators of demyelination and axonal and mitochondria damage as well, in both MS and its animal models [2, 30]. Endogenous antioxidant enzymes can counteract to oxidative stress by conferring protection against oxidative damage. Except for the fact that macrophages and microglial cells exhibit high ROS production in EAE compared to control [60], they produce high levels of superoxide as well in all affected brain areas [61]. Some studies reported that oligodendrocytes are more susceptible to ROS-mediated damage than astrocytes or macrophages [62] due to the high levels of iron found in them, which react with hydrogen peroxide and form the highly toxic peroxynitrite. Next, low levels of glutathione in oligodendrocytes reduce the expression of SOD2 (MnSOD) [63, 64]. Hydrogen peroxide, produced in peroxisomes of oligodendrocytes during the period of active remyelination, affects negatively the long-term repair of myelin and thus causes progression of the disease [65].

Here, we showed that antioxidant enzymes, including SOD1 and SOD2, and GPX1 are markedly downregulated in whole EAE brains compared to normal brain tissue from

the control EAE animals. However, by analyzing the tissue distribution of SOD1 and SOD2 proteins, we revealed a different pattern, which is consistent with the study from van Horsen et al. [13, 66]. They reported that antioxidant enzymes, including SOD1 and SOD2, catalase, and heme oxygenase 1, are markedly upregulated in actively demyelinating MS lesions compared to normal-appearing white matter and white matter tissue of the control brains. Hence, they explained that enhanced antioxidant enzymes are due to an adaptive defense mechanism, which reduces ROS-induced cellular damage. Another study reported about impaired antioxidant enzymes in terms of high activity of catalase and decreased activity of MnSOD in peripheral blood mononuclear cells (PBMCs) from patients with relapsing-remitting multiple sclerosis (RRMS) compared to healthy controls [67]. In addition, Stojanović et al. [68] described that in EAE rats, GSH level and SOD activity were decreased in whole encephalitic mass (WEM) and cerebellum homogenates compared to those in untreated control animals.

In our study, the pathological CNS changes in EAE were successfully attenuated by the olive leaf polyphenol application: TBARS were reduced, GPX and SOD activity was enhanced, and in addition, mitochondrial SOD2, cytosolic SOD1, and GPX1 expression levels were increased. Following that, we suggest that the olive leaf polyphenols have the neuroprotective effects and could be successful in the therapy of MS. As reported, SOD2 overexpression, as well as lower immune infiltration, could play a key role in managing underlying pathogenesis of MS and reducing disease severity [69]. Considering that mitochondrial oxidative stress in the CNS affects the modulation of SOD2 function and neurological disorders in neurodegenerative diseases such as stroke, Alzheimer’s disease (AD), Parkinson’s disease (PD), and age-related loss of cognitive function, we suppose that consumption of olive leaf tea and olive leaf supplements could help in slowing the progression of the disease.

Many studies have already proved the potential ability of natural polyphenols to inhibit and prevent both acute and chronic neurodegenerative diseases, including AD and PD, by decreasing neuronal damage or death [30, 34, 70, 71]. These active compounds are able to modulate cell redox state [72] through the direct action on enzymes, proteins, receptors, and different signalling pathways [73, 74], as well as to interfere with biochemical homeostasis [75, 76]. It has been shown that some of these effects are related to epigenetic modifications of the chromatin [30, 77].

It is described how epigenetic effect of certain cell proteins is due to their ability to deacetylate many transcription factors and thus regulate cell survival, inflammation, and immune function, including neurodegeneration as well [78].

Sirtuin 1 is one such protein, a member of the sirtuin superfamily of histone deacetylases (HDACs), and it is now established that it can directly or indirectly influence the redox property of the cell [23] and reduce oxidative stress through regulation of FOXO3a. The deacetylation of FOXO3a leads to the upregulation of catalase and MnSOD [78]. Sirtuins are NAD⁺-dependent epigenetic and metabolic regulators, which have crucial roles in the physiology of the

CNS, immune system, and metabolism. Based on these facts, SIRT1s are crucial candidates of therapeutic targets in MS.

Although a large number of studies have focused on sirtuins' functions in health and diseases, the relevance of sirtuins in MS or its animal models is not clear. There are numerous investigations that used disease protective agents and measured SIRT1 level.

Many previous reports of both *in vitro* and *in vivo* studies have proved that natural polyphenols, including those from olive leaf extract, have antioxidant and anti-inflammatory properties *via* modulating important signalling pathways such as NF kappaB, COX-2, and iNOS [29, 79]. Moreover, recently, it was shown that the upregulation of microglial SIRT1, *via* the phenolic compound protocatechuic acid, inhibited the release of inflammatory mediators and ameliorated microglial activation-induced neuron death [29].

The polyphenols are responsible for many health beneficial effects mediated via epigenetic chromatin modifications [78] and can also activate SIRT1 [30]. Therefore, it is possible that the activation of SIRT1 by polyphenols and the resulting inhibitory effects on NF-kappa B and MAPK signalling pathways with a concomitant decrease in release of inflammatory mediators such as TNF- α and IL-6 are responsible for the claimed beneficial effect of these compounds including neuroprotection [78–82].

Our results show upregulated SIRT1 in different brain regions of EAE rats treated with olive leaf (Figure 4) (cortex, hippocampus, ependymal, and subventricular zone). However, this upregulation is seen not only in microglia (Figure 6 and Table 1) but also in other cells like neurons, glial, ependymal, and endothelial cells (Figure 4), which is in accordance with other studies investigating SIRT1 expression [83–85]. Still, further investigation on SIRT1 expression in certain cell types in different brain regions is needed for better understanding of its role in proliferation or differentiation during the processes of oligodendrogenesis or neurogenesis.

The data presented in our report are generally in line with the updated knowledge about the antioxidant and anti-inflammatory properties of natural polyphenols, including those from olive leaf [86, 87].

Our hypothesis is based on our findings that SIRT1 is upregulated in microglia and that the most abundant microglia in the brain of EAE rats treated with TOL are anti-inflammatory M2 type or Iba-1⁺ CD206⁺ microglia as seen in Figure 9. These data are shown here only in the subventricular zone as this brain region has gone through the most changes regarding microglial upregulation. In opposite, the subventricular zone had downregulation of proinflammatory M1 type or Iba-1⁺ iNOS⁺ microglia (Figure 8). These data are in high agreement with evidence showing that polyphenols may suppress inflammation mediated by M1 phenotype and influence macrophage metabolism by promoting oxidative pathways and M2 polarization of active macrophages [88].

Microglia may also sense signals from the surrounding environment and have regulatory effects on neurogenesis and oligodendrogenesis in the subventricular zone and the subgranular zone of the hippocampal dentate gyrus [89].

However, which exact signals and cytokines are involved in this process during EAE and during the treatment with OLE should be broadly investigated.

Furthermore, our data showed preserved myelin integrity (Figure 7), which is in correlation with the upregulated SIRT1 and increased superoxide dismutase (SOD) and glutathione peroxidase (GPX) activity found in the brain of EAE rats treated with olive leaf (Figure 2). These findings are supported by already known evidence that SIRT1 antioxidant properties are mediated via modulation of SOD and GPX enzymes [90–93], which prevent the generation of free radicals [94] that cause demyelination during EAE [2].

Clinical signs were coincident with the reduction of MBP in the cortex, while in rats receiving OLP the onset of the disease was delayed and clinical signs were reduced. This amelioration of clinical signs was accompanied by sustained levels of MBP. Busto et al. [95] reported that ellagic acid protects from myelin-associated sphingolipid loss in the cortex in EAE, suggesting a neuroprotective effect. Our results showed that OLP significantly increased 18 kDa MBP at the 20th day, while decreased at the 30th day (Supplementary Figure 4C), but not significantly. We assume that therapy with OLP should be constant throughout the course of the disease to reduce MBP loss. The animals did not receive therapy from the 20th to the 30th day, which reflected on the level of MBP.

Finally, our results demonstrate that TOL attenuates the clinical course of EAE, and the possible mechanisms include reduction of oxidative stress, upregulation of SIRT1 in the brain tissue including microglial cells, upregulation of the anti-inflammatory M2 type of microglia, and preservation of the myelin integrity. These data support the idea that OLE may be an effective therapeutic approach for treating MS and other neurodegenerative diseases as well.

Data Availability

The data used to support the findings of this study are available from the corresponding author upon request.

Conflicts of Interest

The authors have declared no conflict of interest.

Authors' Contributions

JG and TGK performed all *in vivo* experiments; TGK performed immunohistochemistry; JG performed western blotting; JG and TGK designed the research study and wrote the paper, analyzed and reviewed the results, and approved the final version of the manuscript. Jasminka Giacometti and Tanja Grubić-Kezele contributed equally to this work.

Acknowledgments

This work has been supported by the University of Rijeka (number: uniri-prirod-18-46).

Supplementary Materials

Supplementary Figure S1: pilot experiments for the best study design. Different concentrations or different kinds of administration, i.e., (1) EAE+TEA: only the olive leaf tea ad libitum (oleuropein 1.5 mg/mL) (light blue line); (2) EAE+EXTRACT×3+TEA: olive leaf extract i.p. (45.96 mg/kg 3 times every second day) together with olive leaf tea ad libitum (yellow line); (3) EAE+EXTRACT×10: olive leaf extract i.p. (45.96 mg/kg/day for 10 days) alone (gray line); and (4) EAE+EXTRACT×10+TEA: olive leaf extract i.p. (45.96 mg/kg/day for 10 days) together with olive leaf tea ad libitum (oleuropein 1.5 mg/mL) (orange line). Dark blue line represents EAE without any treatment. The best results or the highest amelioration of clinical symptoms we get with the fourth option or 45.96 mg/kg/day for 10 days i.p. together with olive leaf tea ad libitum and we decided to use it in further investigation (orange line in the figure). The values are presented as mean of EAE scores of each animal for every day. Supplementary Figure S2: in the cerebral hippocampus, subventricular zone (SVZ), and cortex of rats treated with polyphenols from olive leaf extract, microglia cells that express less SOD1 are present. Representative immunofluorescent pictures show relationship between SOD1⁺ cells and Iba-1⁺ microglia cells in DA rats (arrows point the SOD1⁺Iba-1⁺ cells): (a–c) untreated, (d–f) with induced EAE and second attack on the 20th day postinduction, (g–i) with induced EAE and treated with polyphenols till the 20th day postinduction, (j–l) with induced EAE on the 30th day postinduction, and (m–o) with induced EAE and treated with polyphenols on the 30th day postinduction. Scale bars indicate 20 μ m. Supplementary Figure S3: representative immunofluorescent pictures show the relationship between SOD2 and Iba-1⁺ microglia cells in the inflamed area of the brain stem: untreated, with induced EAE and the second attack (on the 20th day postinduction), with induced EAE and treated with TOL till the 20th day postinduction, with induced EAE and the second remission (on the 30th day postinduction), and with induced EAE and treated with TOL on the 30th day postinduction. Scale bars indicate 50 μ m. Supplementary Figure S4: immunoblot of myelin basic protein (MBP) in the isolated rat brain proteins. Cell lysate proteins (50 μ g) were immunoblotted using β -actin as the loading control. (A) Representative western blot image of the target protein. (B) The expression of mean MBP is shown at the normalized expression level. (C) The expression of MBP is shown at the normalized expression level of the EAE. For each group, values are presented as the mean \pm SD of five rats per group. One-way ANOVA followed by the post hoc Scheffé test was used for the statistical analysis: ** p < 0.01 and *** p < 0.001. (*Supplementary Materials*)

References

[1] B. Adamczyk, N. Niedziela, and M. Adamczyk-Sowa, "Novel approaches of oxidative stress mechanisms in the multiple sclerosis pathophysiology and therapy," in *Multiple Sclerosis: Perspectives in Treatment and Pathogenesis*, I. S. Zagon and

- P. J. McLaughlin, Eds., pp. 155–171, Codon Publications, Brisbane, Australia, 2017.
- [2] K. Ohl, K. Tenbrock, and M. Kipp, "Oxidative stress in multiple sclerosis: central and peripheral mode of action," *Experimental Neurology*, vol. 277, pp. 58–67, 2016.
- [3] E. Miller, B. Wachowicz, and I. Majsterek, "Advances in antioxidative therapy of multiple sclerosis," *Current Medicinal Chemistry*, vol. 20, no. 37, pp. 4720–4730, 2013.
- [4] E. Gray, T. L. Thomas, S. Betmouni, N. Scolding, and S. Love, "Elevated myeloperoxidase activity in white matter in multiple sclerosis," *Neuroscience Letters*, vol. 444, no. 2, pp. 195–198, 2008.
- [5] J. S. Liu, M. Zhao, C. F. Brosnan, and S. C. Lee, "Expression of inducible nitric oxide synthase and nitrotyrosine in multiple sclerosis lesions," *The American Journal of Pathology*, vol. 158, no. 6, pp. 2057–2066, 2001.
- [6] M. T. Fischer, R. Sharma, J. L. Lim et al., "NADPH oxidase expression in active multiple sclerosis lesions in relation to oxidative tissue damage and mitochondrial injury," *Brain*, vol. 135, no. 3, pp. 886–899, 2012.
- [7] M. T. Fischer, I. Wimmer, R. Höftberger et al., "Disease-specific molecular events in cortical multiple sclerosis lesions," *Brain*, vol. 136, no. 6, pp. 1799–1815, 2013.
- [8] T. Zeis, A. Probst, A. J. Steck, C. Stadelmann, W. Brück, and W. N. Schaeren, "Molecular changes in white matter adjacent to an active demyelinating lesion in early multiple sclerosis," *Brain Pathology*, vol. 19, no. 3, pp. 459–466, 2009.
- [9] L. Haider, M. T. Fischer, J. M. Frischer et al., "Oxidative damage in multiple sclerosis lesions," *Brain*, vol. 134, no. 7, pp. 1914–1924, 2011.
- [10] B. D. Butts, C. Houde, and H. Mehmet, "Maturation-dependent sensitivity of oligodendrocyte lineage cells to apoptosis: implications for normal development and disease," *Cell Death and Differentiation*, vol. 15, no. 7, pp. 1178–1186, 2008.
- [11] J. van Horssen, J. A. Drexhage, T. Flor, W. Gerritsen, P. van der Valk, and H. E. de Vries, "Nrf2 and DJ1 are consistently upregulated in inflammatory multiple sclerosis lesions," *Free Radical Biology & Medicine*, vol. 49, no. 8, pp. 1283–1289, 2010.
- [12] J. van Horssen, G. Schreibelt, L. Bö et al., "NAD(P)H: quinone oxidoreductase 1 expression in multiple sclerosis lesions," *Free Radical Biology & Medicine*, vol. 41, no. 2, pp. 311–317, 2006.
- [13] J. van Horssen, G. Schreibelt, J. Drexhage et al., "Severe oxidative damage in multiple sclerosis lesions coincides with enhanced antioxidant enzyme expression," *Free Radical Biology & Medicine*, vol. 45, no. 12, pp. 1729–1737, 2008.
- [14] J. Liu, D. Tian, M. Murugan et al., "Microglial Hv1 proton channel promotes cuprizone-induced demyelination through oxidative damage," *Journal of Neurochemistry*, vol. 135, no. 2, pp. 347–356, 2015.
- [15] A. Di Penta, A. Chiba, I. Alloza et al., "A trifluoromethyl analogue of celecoxib exerts beneficial effects in neuroinflammation," *Plos One*, vol. 8, no. 12, article e83119, 2013.
- [16] E. V. Vofß, J. Škuljec, V. Gudi et al., "Characterisation of microglia during de- and remyelination: can they create a repair promoting environment?," *Neurobiology of Disease*, vol. 45, no. 1, pp. 519–528, 2012.
- [17] Y. Huang and C. F. Dreyfus, "The role of growth factors as a therapeutic approach to demyelinating disease," *Experimental Neurology*, vol. 283, Part B, pp. 531–540, 2016.
- [18] V. E. Miron, A. Boyd, J.-W. Zhao et al., "M2 microglia and macrophages drive oligodendrocyte differentiation during

- CNS remyelination,” *Nature Neuroscience*, vol. 16, no. 9, pp. 1211–1218, 2013.
- [19] T. Kuhlmann, V. Miron, Q. Cuo, C. Wegner, J. Antel, and W. Brück, “Differentiation block of oligodendroglial progenitor cells as a cause for remyelination failure in chronic multiple sclerosis,” *Brain*, vol. 131, no. 7, pp. 1749–1758, 2008.
- [20] Y. Cheng, H. Takeuchi, Y. Sonobe et al., “Sirtuin 1 attenuates oxidative stress via upregulation of superoxide dismutase 2 and catalase in astrocytes,” *Journal of Neuroimmunology*, vol. 269, no. 1-2, pp. 38–43, 2014.
- [21] M. C. Haigis and D. A. Sinclair, “Mammalian sirtuins: biological insights and disease relevance,” *Annual Review of Pathology*, vol. 5, no. 1, pp. 253–295, 2010.
- [22] J.-W. Hwang, H. Yao, S. Caito, I. K. Sundar, and I. Rahman, “Redox regulation of SIRT1 in inflammation and cellular senescence,” *Free Radical Biology & Medicine*, vol. 61, pp. 95–110, 2013.
- [23] F. Ng, L. Wijaya, and B. L. Tang, “SIRT1 in the brain—connections with aging-associated disorders and lifespan,” *Frontiers in Cellular Neuroscience*, vol. 9, p. 64, 2015.
- [24] L. Cartier, O. Hartley, M. Dubois-Dauphin, and K. H. Krause, “Chemokine receptors in the central nervous system: role in brain inflammation and neurodegenerative diseases,” *Brain Research. Brain Research Reviews*, vol. 48, no. 1, pp. 16–42, 2005.
- [25] A. Satoh, S. Imai, and L. Guarente, “The brain, sirtuins, and aging,” *Nature Reviews Neuroscience*, vol. 18, pp. 362–374, 2017.
- [26] Y. Fujita and T. Yamashita, “Sirtuins in neuroendocrine regulation and neurological diseases,” *Frontiers in Neuroscience*, vol. 12, p. 778, 2018.
- [27] J. Xie, X. Zhang, and L. Zhang, “Negative regulation of inflammation by SIRT1,” *Pharmacological Research*, vol. 67, no. 1, pp. 60–67, 2013.
- [28] J. Yan, A. Luo, J. Gao et al., “The role of SIRT1 in neuroinflammation and cognitive dysfunction in aged rats after anesthesia and surgery,” *American Journal of Translational Research*, vol. 11, no. 3, pp. 1555–1568, 2019.
- [29] C. Kaewmool, P. Kongtawelert, T. Phitak, P. Pothacharoen, and S. Udomruk, “Protocatechuic acid inhibits inflammatory responses in LPS-activated BV2 microglia via regulating SIRT1/NF- κ B pathway contributed to the suppression of microglial activation-induced PC12 cell apoptosis,” *Journal of Neuroimmunology*, vol. 341, p. 577164, 2020.
- [30] V. B. Ayissi, A. Ebrahimi, and H. Schluesener, “Epigenetic effects of natural polyphenols: a focus on SIRT1-mediated mechanisms,” *Molecular Nutrition & Food Research*, vol. 58, no. 1, pp. 22–32, 2014.
- [31] F. Sarubbo, S. Esteban, A. Miralles, and D. Moranta, “Effects of resveratrol and other polyphenols on Sirt1: relevance to brain function during aging,” *Current Neuropharmacology*, vol. 16, no. 2, pp. 126–136, 2018.
- [32] M. Martin Brennen, T. Mahfouz, and A. Stockert, “Cooperative binding of cinnamon polyphenols as activators of Sirtuin-1 protein in the insulin signaling pathway,” *The FASEB Journal*, vol. 761, no. 25, 2017.
- [33] D. A. Duarte, M. A. B. Rosales, A. Papadimitriou et al., “Polyphenol-enriched cocoa protects the diabetic retina from glial reaction through the sirtuin pathway,” *The Journal of Nutritional Biochemistry*, vol. 26, no. 1, pp. 64–74, 2015.
- [34] M. Sarbishegi, E. A. Charkhat Gorgich, O. Khajavi, G. Komeili, and S. Salimi, “The neuroprotective effects of hydro-alcoholic extract of olive (*Olea europaea* L.) leaf on rotenone-induced Parkinson’s disease in rat,” *Metabolic Brain Diseases*, vol. 33, no. 1, pp. 79–88, 2018.
- [35] B. Ćurko-Cofek, T. G. Kezele, J. Marinić et al., “Chronic iron overload induces gender-dependent changes in iron homeostasis, lipid peroxidation and clinical course of experimental autoimmune encephalomyelitis,” *Neurotoxicology*, vol. 57, pp. 1–12, 2016.
- [36] J. Giacometti, G. Žauhar, and M. Žuvić, “Optimization of ultrasonic-assisted extraction of major phenolic compounds from olive leaves (*Olea europaea* L.) using response surface methodology,” *Foods*, vol. 7, no. 9, p. 149, 2018.
- [37] H. Jakovac, T. Grubić Kezele, and B. Radošević-Stašić, “Expression profiles of metallothionein I/II and megalin in cuprizone model of de- and remyelination,” *Neuroscience*, vol. 388, pp. 69–86, 2018.
- [38] T. Grubić-Kezele, H. Jakovac, M. Tota et al., “Metallothioneins I/II expression in rat strains with genetically different susceptibility to experimental autoimmune encephalomyelitis,” *Neuroimmunomodulation*, vol. 20, no. 3, pp. 152–163, 2013.
- [39] T. Grubić Kezele, G. Blagojević Zagorac, H. Jakovac, R. Domitrović, and B. Radošević-Stašić, “Hippocampal expressions of metallothionein I/II and glycoprotein 96 in EAE-prone and EAE-resistant strains of rats,” *Histology and Histopathology*, vol. 32, no. 2, pp. 137–151, 2017.
- [40] H. Ohkawa, N. Ohishi, and K. Yagi, “Assay for lipid peroxides in animal tissues by thiobarbituric acid reaction,” *Analytical Biochemistry*, vol. 95, no. 2, pp. 351–358, 1979.
- [41] C. J. De Groot, E. Bergers, W. Kamphorst et al., “Post-mortem MRI-guided sampling of multiple sclerosis brain lesions: increased yield of active demyelinating and (p)reactive lesions,” *Brain*, vol. 124, no. 8, pp. 1635–1645, 2001.
- [42] H. Lassmann, W. Brück, and C. F. Lucchinetti, “The immunopathology of multiple sclerosis: an overview,” *Brain Pathology*, vol. 17, no. 2, pp. 210–218, 2007.
- [43] Z. Jiang, J. X. Jiang, and G. X. Zhang, “Macrophages: a double-edged sword in experimental autoimmune encephalomyelitis,” *Immunology Letters*, vol. 160, no. 1, pp. 17–22, 2014.
- [44] J. Wang, J. Wang, B. Yang, Q. Weng, and Q. He, “Targeting microglia and macrophages: a potential treatment strategy for multiple sclerosis,” *Frontiers in Pharmacology*, vol. 10, p. 286, 2019.
- [45] C. Luo, C. Jian, Y. Liao et al., “The role of microglia in multiple sclerosis,” *Neuropsychiatric Disease and Treatment*, vol. - Volume 13, pp. 1661–1667, 2017.
- [46] V. E. Miron and R. J. Franklin, “Macrophages and CNS remyelination,” *Journal of Neurochemistry*, vol. 130, no. 2, pp. 165–171, 2014.
- [47] A. Lampron, A. Laroche, N. Laflamme et al., “Inefficient clearance of myelin debris by microglia impairs remyelinating processes,” *The Journal of Experimental Medicine*, vol. 212, no. 4, pp. 481–495, 2015.
- [48] J. Xue, S. V. Schmidt, J. Sander et al., “Transcriptome-based network analysis reveals a spectrum model of human macrophage activation,” *Immunity*, vol. 40, no. 2, pp. 274–288, 2014.
- [49] P. J. Murray, J. E. Allen, S. K. Biswas et al., “Macrophage activation and polarization: nomenclature and experimental guidelines,” *Immunity*, vol. 41, no. 1, pp. 14–20, 2014.
- [50] O. Butovsky, G. Landa, G. Kunis et al., “Induction and blockage of oligodendrogenesis by differently activated microglia

- in an animal model of multiple sclerosis,” *The Journal of Clinical Investigation*, vol. 116, no. 4, pp. 905–915, 2006.
- [51] J. Mikita, N. Dubourdiou-Cassagno, M. S. A. Deloire et al., “Altered M1/M2 activation patterns of monocytes in severe relapsing experimental rat model of multiple sclerosis. Amelioration of clinical status by M2 activated monocyte administration,” *Multiple Sclerosis*, vol. 17, no. 1, pp. 2–15, 2011.
- [52] S. C. Starossom, I. D. Mascanfroni, J. Imitola et al., “Galectin-1 deactivates classically activated microglia and protects from inflammation-induced neurodegeneration,” *Immunity*, vol. 37, no. 2, pp. 249–263, 2012.
- [53] Z. Yu, D. Sun, J. Feng et al., “MSX3 switches microglia polarization and protects from inflammation-induced demyelination,” *The Journal of Neuroscience*, vol. 35, no. 16, pp. 6350–6365, 2015.
- [54] A. Zabala, N. Vazquez-Villoldo, B. Rissiek et al., “P2X4 receptor controls microglia activation and favors remyelination in autoimmune encephalitis,” *EMBO Molecular Medicine*, vol. 10, no. 8, 2018.
- [55] C. English and J. J. Aloï, “New FDA-approved disease-modifying therapies for multiple sclerosis,” *Clinical Therapeutics*, vol. 37, no. 4, pp. 691–715, 2015.
- [56] N. Talhaoui, A. M. Gómez-Caravaca, C. Roldán et al., “Chemometric analysis for the evaluation of phenolic patterns in olive leaves from six cultivars at different growth stages,” *Journal of Agricultural and Food Chemistry*, vol. 63, no. 6, pp. 1722–1729, 2015.
- [57] D. Miljković, D. Dekanski, Z. Miljković, M. Momčilović, and M. Mostarica-Stojkovic, “Dry olive leaf extract ameliorates experimental autoimmune encephalomyelitis,” *Clinical Nutrition*, vol. 28, no. 3, pp. 346–350, 2009.
- [58] W. Sun, X. Wang, C. Hou et al., “Oleuropein improves mitochondrial function to attenuate oxidative stress by activating the Nrf2 pathway in the hypothalamic paraventricular nucleus of spontaneously hypertensive rats,” *Neuropharmacology*, vol. 113, no. Part A, pp. 556–566, 2017.
- [59] J. Park, J. S. Min, U. Chae et al., “Anti-inflammatory effect of oleuropein on microglia through regulation of Drp1-dependent mitochondrial fission,” *Journal of Neuroimmunology*, vol. 306, pp. 46–52, 2017.
- [60] S. R. Ruuls, J. Bauer, K. Sontrop, I. Huitinga, B. A. 't Hart, and C. D. Dijkstra, “Reactive oxygen species are involved in the pathogenesis of experimental allergic encephalomyelitis in Lewis rats,” *Journal of Neuroimmunology*, vol. 56, no. 2, pp. 207–217, 1995.
- [61] G. S. Scott, K. I. Williams, and C. Bolton, “Reactive oxygen species in experimental allergic encephalomyelitis,” *Biochemical Society Transactions*, vol. 25, no. 2, p. 166S, 1997.
- [62] C. Griot, M. Vandeveld, A. Richard, E. Peterhans, and R. Stocker, “Selective degeneration of oligodendrocytes mediated by reactive oxygen species,” *Free Radical Research Communications*, vol. 11, pp. 181–193, 2009.
- [63] E. Pinteaux, M. Perrault, and G. Tholey, “Distribution of mitochondrial manganese superoxide dismutase among rat glial cells in culture,” *Glia*, vol. 22, no. 4, pp. 408–414, 1998.
- [64] S. K. Thorburne and B. H. Juurlink, “Low glutathione and high iron govern the susceptibility of oligodendroglial precursors to oxidative stress,” *Journal of Neurochemistry*, vol. 67, no. 3, pp. 1014–1022, 1996.
- [65] S. A. Back, X. Gan, Y. Li, P. A. Rosenberg, and J. J. Volpe, “Maturation-dependent vulnerability of oligodendrocytes to oxidative stress-induced death caused by glutathione depletion,” *The Journal of Neuroscience*, vol. 18, no. 16, pp. 6241–6253, 1998.
- [66] J. van Horsen, M. E. Witte, G. Schreiberl, and H. E. de Vries, “Radical changes in multiple sclerosis pathogenesis,” *Biochimica et Biophysica Acta*, vol. 1812, no. 2, pp. 141–150, 2011.
- [67] S. Emamgholipour, A. Hossein-Nezhad, M. A. Sahraian, and F. Askarisadr, “Expression and enzyme activity of MnSOD and catalase in peripheral blood mononuclear cells isolated from multiple sclerosis patients,” *Archives of Medical Laboratory Sciences*, vol. 1, pp. 23–28, 2015.
- [68] I. Stojanović, S. Ljubišavljević, I. Stevanović et al., “Benefit agmatine effects in experimental multiple sclerosis. CNS nitrosative and oxidative stress suppression / protektivni efekti agmatina u eksperimentalnoj multiploj sklerozi. Supresija nitrozativnog i oksidativnog stresa u CNS-U,” *Acta Facultatis Medicæ Naissensis*, vol. 31, no. 4, pp. 233–243, 2014.
- [69] T. Inoue, T. Majid, A. Quick, R. G. Pautler, and C. Beeton, “The role of SOD-2 in a mouse model of multiple sclerosis,” *The FASEB Journal*, vol. 26, 1_supplement, 2012.
- [70] Y. Porat, A. Abramowitz, and E. Gazit, “Inhibition of amyloid fibril formation by polyphenols: structural similarity and aromatic interactions as a common inhibition mechanism,” *Chemical Biology and Drug Design*, vol. 67, no. 1, pp. 27–37, 2006.
- [71] M. Sarbishegi, “Antioxidant effects of olive leaf extract in prevention of Alzheimer’s disease and Parkinson’s disease,” *Gene, Cell and Tissue*, vol. 5, p. e79847, 2018.
- [72] M. Singh, M. Arseneault, T. Sanderson, V. Murthy, and C. Ramassamy, “Challenges for research on polyphenols from foods in Alzheimer’s disease: bioavailability, metabolism, and cellular and molecular mechanisms,” *Journal of Agricultural and Food Chemistry*, vol. 56, no. 13, pp. 4855–4873, 2008.
- [73] H. S. Kim, M. J. Quon, and J. A. Kim, “New insights into the mechanisms of polyphenols beyond antioxidant properties; lessons from the green tea polyphenol, epigallocatechin 3-gallate,” *Redox Biology*, vol. 2, pp. 187–195, 2014.
- [74] K. Goszcz, G. G. Duthie, D. Stewart, S. J. Leslie, and I. L. Megson, “Bioactive polyphenols and cardiovascular disease: chemical antagonists, pharmacological agents or xenobiotics that drive an adaptive response?,” *British Journal of Pharmacology*, vol. 174, no. 11, pp. 1209–1225, 2017.
- [75] A. H. Abuznait, H. Qosa, B. A. Busnena, K. A. El Sayed, and A. Kaddoumi, “Olive-oil-derived oleocanthal enhances β -amyloid clearance as a potential neuroprotective mechanism against Alzheimer’s disease: in vitro and in vivo studies,” *ACS Chemical Neuroscience*, vol. 4, no. 6, pp. 973–982, 2013.
- [76] C. Grossi, S. Rigacci, S. Ambrosini et al., “The polyphenol oleuropein aglycone protects TgCRND8 mice against A β plaque pathology,” *PLoS ONE*, vol. 8, no. 8, p. e71702, 2013.
- [77] K. Declerck, K. Szarc vel Szic, A. Palagani et al., “Epigenetic control of cardiovascular health by nutritional polyphenols involves multiple chromatin-modifying writer-reader-eraser proteins,” *Current Topics in Medicinal Chemistry*, vol. 16, no. 7, pp. 788–806, 2015.
- [78] C. Angeloni, M. Malaguti, M. C. Barbalace, and S. Hrelia, “Bioactivity of olive oil phenols in neuroprotection,” *International Journal of Molecular Sciences*, vol. 18, no. 11, p. 2230, 2017.
- [79] X. Jin, M. Y. Liu, D. F. Zhang et al., “Natural products as a potential modulator of microglial polarization in

- neurodegenerative diseases,” *Pharmacological Research*, vol. 145, p. 104253, 2019.
- [80] J. Ye, Z. Liu, J. Wei et al., “Protective effect of SIRT1 on toxicity of microglial-derived factors induced by LPS to PC12 cells via the p53-caspase-3-dependent apoptotic pathway,” *Neuroscience Letters*, vol. 553, pp. 72–77, 2013.
- [81] V. K. Nimmagadda, C. T. Bever, N. R. Vattikunta et al., “Over-expression of SIRT1 protein in neurons protects against experimental autoimmune encephalomyelitis through activation of multiple SIRT1 targets,” *Journal of Immunology*, vol. 190, no. 9, pp. 4595–4607, 2013.
- [82] V. K. C. Nimmagadda, T. K. Makar, K. Chandrasekaran et al., “SIRT1 and NAD⁺ precursors: Therapeutic targets in multiple sclerosis a review,” *Journal of Neuroimmunology*, vol. 304, pp. 29–34, 2017.
- [83] G. Ramadori, C. E. Lee, A. L. Bookout et al., “Brain SIRT1: anatomical distribution and regulation by energy availability,” *The Journal of Neuroscience*, vol. 28, no. 40, pp. 9989–9996, 2008.
- [84] S. Hisahara, S. Chiba, H. Matsumoto et al., “Histone deacetylase SIRT1 modulates neuronal differentiation by its nuclear translocation,” *Proceedings of the National Academy of Sciences of the United States of America*, vol. 105, no. 40, pp. 15599–15604, 2008.
- [85] J. Sakamoto, T. Miura, K. Shimamoto, and Y. Horio, “Predominant expression of Sir2 α , an NAD-dependent histone deacetylase, in the embryonic mouse heart and brain¹,” *FEBS Letters*, vol. 556, no. 1-3, pp. 281–286, 2004.
- [86] M. E. Cavet, K. L. Harrington, T. R. Vollmer, K. W. Ward, and J. Z. Zhang, “Anti-inflammatory and anti-oxidative effects of the green tea polyphenol epigallocatechin gallate in human corneal epithelial cells,” *Molecular Vision*, vol. 17, pp. 533–542, 2011.
- [87] G. P. Collett and F. C. Campbell, “Curcumin induces c-Jun N-terminal kinase-dependent apoptosis in HCT116 human colon cancer cells,” *Carcinogenesis*, vol. s, no. 11, pp. 2183–2189, 2004.
- [88] L. Dugo, M. G. Belluomo, C. Fanali et al., “Effect of cocoa polyphenolic extract on macrophage polarization from proinflammatory M1 to anti-inflammatory M2 state,” *Oxidative Medicine and Cellular Longevity*, vol. 2017, Article ID 6293740, 11 pages, 2017.
- [89] K. Sato, “Effects of Microglia on Neurogenesis,” *Glia*, vol. 63, no. 8, pp. 1394–1405, 2015.
- [90] A. Brunet, L. B. Sweeney, J. F. Sturgill et al., “Stress-dependent regulation of FOXO transcription factors by the SIRT1 deacetylase,” *Science*, vol. 303, no. 5666, pp. 2011–2015, 2004.
- [91] S. P. Hussain, P. Amstad, P. He et al., “p53-Induced up-regulation of MnSOD and GPx but not catalase increases oxidative stress and apoptosis,” *Cancer Research*, vol. 64, no. 7, pp. 2350–2356, 2004.
- [92] A. A. Sablina, A. V. Budanov, G. V. Ilyinskaya, L. S. Agapova, J. E. Kravchenko, and P. M. Chumakov, “The antioxidant function of the p 53 tumor suppressor,” *Nature Medicine*, vol. 11, no. 12, pp. 1306–1313, 2005.
- [93] M. Tan, S. Li, M. Swaroop, K. Guan, L. W. Oberley, and Y. Sun, “Transcriptional activation of the human glutathione peroxidase promoter by p 53,” *The Journal of Biological Chemistry*, vol. 274, no. 17, pp. 12061–12066, 1999.
- [94] C. K. Singh, G. Chhabra, M. A. Ndiaye, L. M. Garcia-Peterson, N. J. Mack, and N. Ahmad, “The role of sirtuins in antioxidant and redox signaling,” *Antioxidants & Redox Signaling*, vol. 28, no. 8, pp. 643–661, 2018.
- [95] R. Busto, J. Serna, A. Perianes-Cachero et al., “Ellagic acid protects from myelin-associated sphingolipid loss in experimental autoimmune encephalomyelitis,” *Biochimica et Biophysica Acta (BBA) - Molecular and Cell Biology of Lipids*, vol. 1863, pp. 958–967, 2018.

Research Article

Hydroxy- α -sanshool Possesses Protective Potentials on H_2O_2 -Stimulated PC12 Cells by Suppression of Oxidative Stress-Induced Apoptosis through Regulation of PI3K/Akt Signal Pathway

Ruo-Lan Li , Qing Zhang , Jia Liu , Jia-yi Sun , Li-Ying He , Hu-Xinyue Duan , Wei Peng , and Chun-Jie Wu 

School of Pharmacy, Chengdu University of Traditional Chinese Medicine, Chengdu 611130, China

Correspondence should be addressed to Wei Peng; pengwei@cudtc.edu.cn and Chun-Jie Wu; wucjcdtc@163.com

Received 5 February 2020; Revised 6 June 2020; Accepted 24 June 2020; Published 9 July 2020

Guest Editor: Francisco Jaime B. Mendonça Junior

Copyright © 2020 Ruo-Lan Li et al. This is an open access article distributed under the Creative Commons Attribution License, which permits unrestricted use, distribution, and reproduction in any medium, provided the original work is properly cited.

Zanthoxylum bungeanum pericarp is a commonly used herbal medicine in China with effects of anti-inflammatory and analgesic, improving learning and memory ability, while hydroxy- α -sanshool (HAS) is the most important active ingredient of *Z. bungeanum* pericarps. The purpose of this study was to investigate the neuroprotective effect of HAS and its related possible mechanisms using a H_2O_2 -stimulated PC12 cell model. CCK-8 assay results showed that HAS had a significant protective effect on H_2O_2 -stimulated PC12 cells without obvious cytotoxicity on normal PC12 cells. Flow cytometry and fluorescence microscope (DAPI staining and DCFH-DA staining) indicated that HAS could reduce the H_2O_2 -induced apoptosis in PC12 cells via reduction of intracellular ROS and increase of mitochondrial membrane potential (MMP). Subsequently, results of malondialdehyde (MDA), superoxide dismutase (SOD), catalase (CAT), and glutathione peroxidase (GSH-Px) determination suggested that HAS could increase the enzyme activities of SOD, CAT, and GSH-Px whereas it could decrease the MDA contents in H_2O_2 -stimulated PC12 cells. Furthermore, the western blotting assays showed that HAS could upregulate the expressions of p-PI3k, Akt, p-Akt, and Bcl-2, while it could downregulate the expressions of cleaved caspase-3 and Bax in H_2O_2 -stimulated PC12 cells. Collectively, it could be concluded according to our results that HAS possesses protective potentials on H_2O_2 -stimulated PC12 cells through suppression of oxidative stress-induced apoptosis via regulation of PI3K/Akt signal pathway.

1. Introduction

Increasing evidences have revealed that oxidative stress is closely related to neurodegenerative diseases, such as Parkinson's disease and Alzheimer's disease. In the body, excessive reactive oxygen species (ROS) is commonly considered the main cause corresponding to oxidative stress [1–3]. ROS, such as hydrogen peroxide (H_2O_2), superoxide anions, and hydroxyl radicals, can stimulate cells which cause structural damage including lipid peroxidation and DNA and protein oxidation, promote oxidative stress, and disrupt the redox balance of the body, as well as change the normal function and morphology of cells [4]. There are a variety of antioxidant systems in cells, while the synergistic antioxidant effect is mainly achieved by eliminating intracellular ROS to prevent oxidative damage to the body [5]. In fact, oxidant/antioxidant

levels are critical for neurodegeneration or neuroprotection, in which enzymes such as superoxide dismutase (SOD), catalase (CAT), and glutathione peroxidase (GSH-Px) constitute the key antioxidant defenses [6]. Excessive ROS not only is closely related to mitochondrial dysfunction but also can increase intracellular Ca^{2+} concentration and activate some intracellular apoptotic pathways. Among them, the PI3K/Akt signaling pathway is closely correlated to it, which is also involved in the changes of Bcl-2 family proteins and the activation of caspase family proteins [7].

It is no doubt that herbal medicines are beneficial for treating various diseases with low toxic and side effects. *Zanthoxylum bungeanum*, belonging to the *Rutaceae* family, is a known medicinal plant widely distributed in China. *Z. bungeanum* pericarp is a known spice in China and widely used in cooking because of its unique fragrance and taste

[8, 9]. According to the *Compendium of Materia Medica*, it can be used to treat various diseases such as vomiting, pathogenic wind, and toothache [10, 11]. In addition, modern pharmacological and phytochemical evidences have found that essential oil in *Z. bungeanum* pericarps has a variety of pharmacological effects, including antitumor effects, anti-inflammatory effects, and antibacterial and insecticidal activities [12–16]. In addition, the unsaturated fatty acid amides in *Z. bungeanum* pericarps, such as hydroxy- α -sanshool (HAS), hydroxy- β -sanshool, and hydroxy- γ -sanshool, also have wide-spectrum pharmacological activities, including hypolipidemic and hypoglycemic effects and anti-inflammatory and neurotrophic effects [17, 18]. Further studies have also shown that HAS has an antioxidant effect and can improve scopolamine-induced learning and memory impairments in rats [19, 20]. Consequently, we speculated that HAS may have neuroprotective potentials, and the present study was aimed at investigating the protective effect of HAS and its related possible mechanisms using a H_2O_2 -stimulated PC12 cell model.

2. Materials and Methods

2.1. Materials and Chemicals. Hydroxy- α -sanshool (HAS) (purity was higher than 98%) used in the present study was isolated from the *Z. bungeanum* pericarps and supplied by the PUSH Bio-Technology (Chengdu, China). Fetal bovine serum (FBS) and horse serum (HS) were purchased from the Hyclone Co. (Logan, UT, USA). H_2O_2 was purchased from Chengdu Chron Chemicals Co. Ltd. (Chengdu, China). RPMI-1640 culture medium, phosphate-buffered saline (PBS), and 0.25% trypsin-EDTA (1x) were purchased from Gibco Co. (Grand Island, NY, USA). Dimethyl sulfoxide (DMSO), cell counting kit-8 (CCK-8), BCA protein assay reagents, and primary antibodies for Bcl-2, Bax, and cleaved (C) caspase-3 were purchased from Boster Biol. Tech. (Wuhan, China). Primary antibodies for PI3K, phosphorylation- (p-) PI3K, AKT, and p-AKT were obtained from the ImmunoWay Biotechnology Co. (Suzhou, China). The assay kits for DCFH-DA, MDA, and SOD and horseradish peroxidase- (HRP-) conjugated secondary antibody were purchased from the Beyotime Institute of Biotechnology (Haimen, China). The assay kits for LDH, CAT, and GSH-PX were purchased from the Nanjing Jiancheng Bioengineering Institute (Nanjing, China). The 5,5',6,6'-tetrachloro-1,1',3,3'-tetraethyl-imidacarbocyanine iodide (JC-1) was obtained from the Jiangsu KeyGen Biotech. (Nanjing, China). All other reagents used in the experiments were of analytical grade.

2.2. Cell Culture and Treatment. The PC12 cells were purchased from Wuhan Pu-nuo-sai Life Technology Co. Ltd. (Wuhan, China) and used throughout the study. PC12 cells were cultured in RPMI-1640 medium containing 5% FBS (v/v), 5% horse serum, penicillin (100 units/mL), and streptomycin (100 μ g/mL) at 37°C in a humidified atmosphere of 5% CO_2 . Cells were subcultured twice a week, and only those in the exponential growth phase were used in experiments.

PC12 cells were pretreated with different concentrations of HAS (15, 30, and 60 μ M) for 2 hours and then incubated

with 90 μ M H_2O_2 for another 4 hours. The control group was administered with the same amount of 1640 medium and then stimulated with H_2O_2 . HAS was solubilized with DMSO and subsequently diluted in culture medium with the final concentration of DMSO less than 0.1% (v/v).

2.3. Determination of Cell Viability. Cell counting kit-8 was used to test cell activity. Before the formal experiment, the cytotoxicity of HAS on PC12 cells was first investigated. Briefly, PC12 cells were cultured in 96-well plates with 1×10^4 cells per well and incubated with PC12 cells with 6.5–120 μ M of HAS for 24 hours. Subsequently, CCK-8 solution was added to each well and cells were kept in a humidified atmosphere of 5% CO_2 at 37°C for 1 hour. Finally, the optical density (OD) values at 450 nm were measured by a microplate reader (Bio-Rad, Hercules, CA, USA). After that, PC12 cells were pretreated with different concentrations of HAS (7.5–120 μ M) for 1–4 hours and then incubated with 90 μ M H_2O_2 for another 4 hours to select the optimal working concentration of HAS for the further experiments.

After selecting the optimal time and concentration of HAS, the cells were incubated at 37°C for 24 hours, pretreated with HAS (final concentrations in the well were 15, 30, and 60 μ M) for 2 hours, and then stimulated with H_2O_2 (final concentration was 90 μ M) for 4 hours. The control group was administered with the same amount of 1640 medium, while the positive group was incubated with 100 μ M vitamin C and then stimulated with H_2O_2 .

2.4. Nuclear Staining with DAPI. PC12 cells were seeded in 6-well plates with a density of 1×10^5 per well. The cells were incubated at 37°C for 24 hours and pretreated with HAS (final concentrations in the well were 15, 30, and 60 μ M) or 100 μ M vitamin C for 2 hours and then stimulated with H_2O_2 (final concentration was 90 μ M) for 4 hours. Subsequently, the cells were washed twice with PBS and then fixed with 10% paraformaldehyde in each well. After fixation, the cells were stained with DAPI solution, incubated at room temperature for 5 min, and then washed three times with PBS. Finally, the staining of the cells was observed under a fluorescence microscope (Olympus, IX-83, Tokyo, Japan).

2.5. Apoptosis Assay by Flow Cytometer. For the apoptosis of PC12 cells, the Annexin V/FITC kit was used. The cells were incubated in 6-well plates with a density of 1×10^5 per well and given different concentrations of HAS (final concentrations in well were 15, 30, and 60 μ M) or 100 μ M vitamin C and H_2O_2 as described above. Subsequently, cells were collected and washed twice with PBS at 4°C, while the supernatant was removed by centrifugation. At the final concentration, the cells were suspended with 500 μ L binding buffer and incubated with 5 μ L Annexin V-FITC and 5 μ L PI for 15 minutes at room temperature; then a FACSCanto II Flow cytometer (BD Company, New York, NY, USA) was used to detect cell apoptosis.

2.6. Assessment of Mitochondrial Membrane Potential. The decrease of intracellular mitochondrial membrane potential (MMP, $\Delta\Psi_m$) can be used as an important indicator of mitochondrial dysfunction, JC-1 is commonly considered as an

ideal probe to evaluate $\Delta\Psi_m$. At a hyperpolarized membrane potential, JC-1 aggregates in the mitochondrial matrix to form polymers that emit red fluorescence; while when it is at the depolarized membrane potential, JC-1 only emits green fluorescence as a monomer. Therefore, the fluorescence transformation will directly reflect the $\Delta\Psi_m$ changes. Consequently, in our present study, PC12 cells were seeded in 6-well plates and treated as described in the individual experiment, then incubated with JC-1 at 37°C in the dark for 15 min. After washing the cells twice with PBS, the cells' fluorescence was measured by using a laser confocal microscopy (Leica, SP8 SR, Wetzlar, Germany).

2.7. Detection of Intracellular ROS Accumulation in PC12 Cells. In an oxidized environment, DCFH-DA can be transformed into green fluorescent DCFH in the cell and the intracellular ROS could be monitored by fluorescent probe DCFH-DA. Briefly, cells were incubated in 6-well plates with different pretreatment or stimulation. Subsequently, the supernatant was removed and cells were incubated with DCFH-DA (10 μM) for 20 min at 37°C in a dark environment and followed by washing for three times with PBS. Intracellular ROS was analyzed by measuring the fluorescence intensity of DCF with a FACSCanto II Flow cytometer (BD Company, New York, NY, USA).

2.8. Determination of MDA, SOD, GSH-Px, and CAT in H_2O_2 -Induced PC12 Cells. The cells were incubated in 6-well plates and given different concentrations of HAS and H_2O_2 as described above. The supernatants were removed; then cells were washed with PBS for three times. Subsequently, the cells were lysed by lysis buffer, which was collected and centrifuged to obtain the total cell protein. Protein concentrations, MDA level, and activities of SOD, GSH-Px, and CAT were determined using commercial assay kits according to the manufacturer's instructions.

2.9. Western Blotting Assay. After treating as described in the individual experiment, cells were harvested and total proteins were extracted using RIPA lysis buffer. The protein concentrations were determined using BCA protein assay reagents; subsequently, the total protein (30 μg) was separated by 12% SDS-PAGE, then transferred to the PVDF membrane. After blocking by sealing fluid (5% skimmed milk), the PVDF membrane was incubated overnight with diluted primary antibodies of C-caspase-3, Bax, Bcl-2, PI3K, p-PI3K, Akt, and p-Akt (dilution 1:1000), respectively, at 4°C. Subsequently, the PVDF membrane was incubated with HRP-conjugated secondary antibody (1:5000) at room temperature for 1 hour. Finally, the protein bands were stained with ECL detection kits, and β -actin was used as the internal reference. Image analysis software ImageJ (version 1.51, National Institutes of Health, MD, USA) was used for gray analysis.

2.10. Determination of Cell Viability after the Inhibition of Signaling Pathway. To further examine the role of the PI3K/Akt signaling pathway in HAS protecting PC12 cells from H_2O_2 stimulation, we used a chemical inhibitor LY294002 to inhibit the expression of the PI3K/Akt signaling pathway by CCK-8. In this part, the HAS group was incu-

bated with 60 μM HAS and 90 μM H_2O_2 , and the HAS +LY294002 group was pretreated with 20 μM LY294002 for 1 hour and then incubated 60 μM HAS and 90 μM H_2O_2 , while the LY294002 group was only treated with LY294002 and H_2O_2 .

2.11. Statistical Analysis. Data are presented as the mean \pm standard deviations (SD). Statistical comparisons except the seizure rate were made by Student's *t*-test or one-way analysis of variance (ANOVA) using GraphPad Prism 5 software (GraphPad Software Inc., La Jolla, CA). $P < 0.05$ was considered the significant level.

3. Results

3.1. HAS Protects the Cell Viability of H_2O_2 -Stimulated PC12 Cells. As can be seen from the Figure 1(b), HAS at the concentration ranging from 7.5 to 120 μM had no obvious effects on the viability of PC12 cells and the viability of all groups was approximate. In addition, CCK-8 assay results showed that 90 μM H_2O_2 treatment could significantly decrease the viability of PC12 cells, making them 40% lower than the normal group ($P < 0.01$) (Figures 1(a) and 1(d)). What is more, it can be seen from Figure 1(c) that the optimal working time for HAS was 2 hours. Importantly and interestingly, pretreatment with HAS (15, 30, 60, and 120 μM) for 2 hours could significantly concentration-dependently increase the cell viability of H_2O_2 -stimulated PC12 cells, compared to the control PC12 cells ($P < 0.01$) (Figures 1(a) and 1(d)).

3.2. HAS Suppresses Apoptosis in H_2O_2 -Stimulated PC12 Cells. To evaluate the apoptosis of PC12 cells, DAPI staining and flow cytometric assay with Annexin V-FITC/PI staining were utilized. As shown in Figure 2(a), nuclear morphological changes of the H_2O_2 -stimulated PC12 cells were examined by staining with cell permeable DNA dye DAPI. For normal PC12 cells, PC12 cells were alive and the cell nucleus was round and intact with faint DAPI staining. However, after stimulation with 90 μM H_2O_2 for 2 h, nuclear shrinkage or condensation and improved brightness could be obviously observed in the cell nucleus, indicating characteristic apoptotic features appeared. Interestingly, pretreatment with 100 μM vitamin C or HAS (15, 30, and 60 μM) significantly attenuated the apoptosis induced by H_2O_2 in PC12 cells, compared to the control PC12 cells. Besides that, we also found the protective effect of 60 μM HAS was approximated to 100 μM vitamin C.

Moreover, the further results of flow cytometric assay also confirmed the DAPI staining experiment. After induction with 90 μM H_2O_2 , the apoptosis rate of PC12 cells sharply increased to 48.74% compared with the normal group 2.21% ($P < 0.01$). However, pretreatment with 100 μM vitamin C or different concentrations of HAS (15, 30, and 60 μM) for 2 hours significantly improved the apoptosis induced by H_2O_2 stimulation ($P < 0.01$) with an obvious concentration-dependent manner, compared to the control PC12 cells (Figure 2(b)).

Besides, we also used JC-1 probe to detect the loss of $\Delta\Psi_m$ in PC12 cells exposed to H_2O_2 . $\Delta\Psi_m$ was determined according to the green/red fluorescence ratio in PC12 cells. As shown

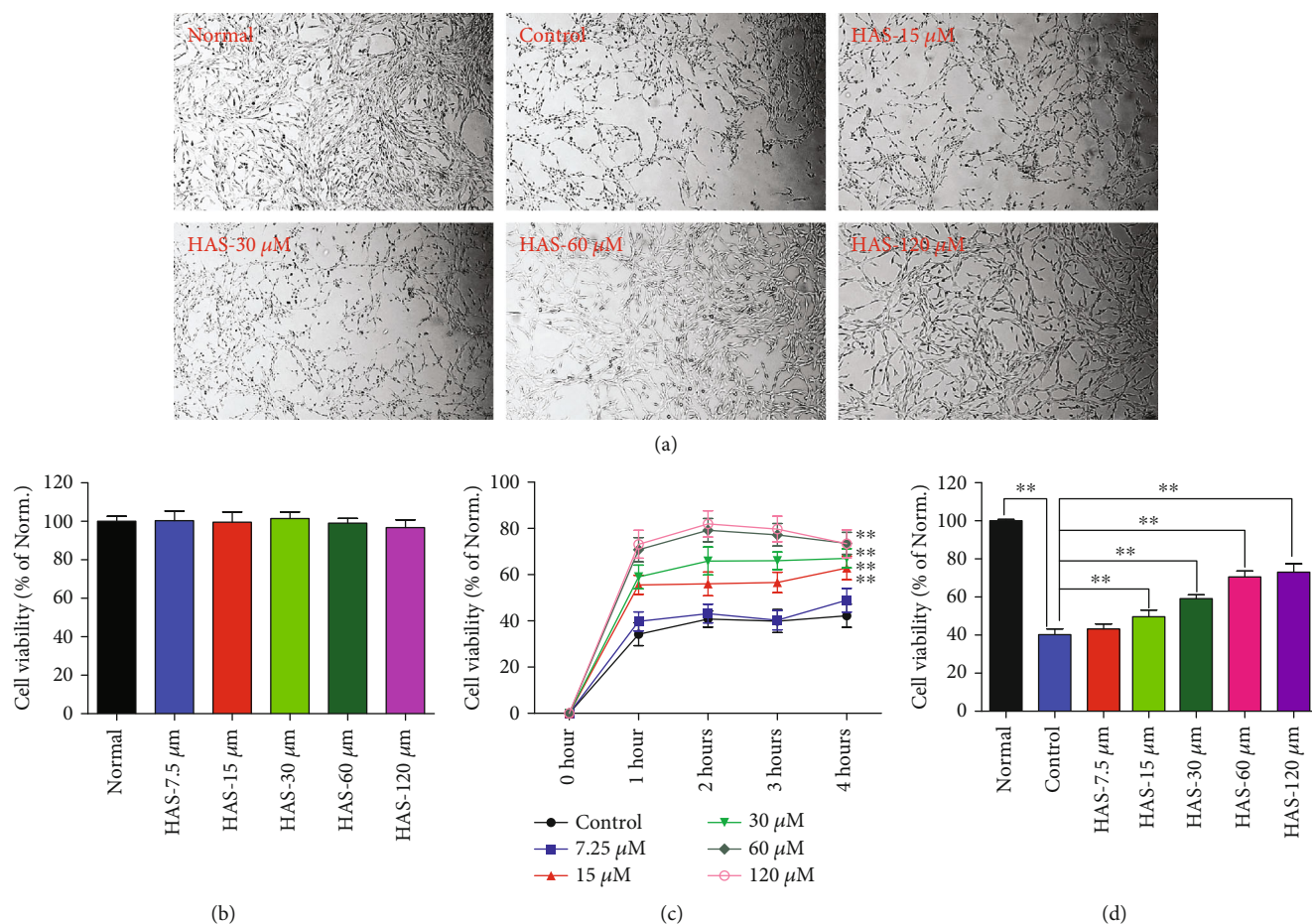


FIGURE 1: Protective effects of HAS on the cell viability of H_2O_2 -stimulated PC12 cells. (a) The represented cell morphology of PC12 cells with different treatment ($\times 100$). (b) Effects of HAS on cell viability of normal PC12 cell. (c) Effects of HAS on cell viability of H_2O_2 -induced PC12 cells under different concentration and time. (d) Effects of HAS pretreatment for 2 hours on cell viability of H_2O_2 -induced PC12 cells. HAS: hydroxy- α -sanshool; Norm.: normal. The values were represented as the mean \pm SD ($n = 3$). ** $P < 0.01$ vs. the control group.

in Figure 3, after incubation with 90 μM H_2O_2 for 2 h, the green fluorescence of the PC12 cells increased sharply, and the ratio of green/red fluorescence became more than 80%. All of these indicated an obvious decline of $\Delta\Psi_m$. However, pretreatment with 100 μM vitamin C or HAS (15, 30, and 60 μM) reversed the green/red ratio significantly, while 60 μM HAS could exploit the advantages to the full (Figure 3). All the above results suggested that HAS could significantly suppress H_2O_2 -stimulated apoptosis in PC12 cells.

3.3. HAS Decreases the H_2O_2 -Stimulated ROS Generation in PC12 Cells. Results of the above studies revealed that HAS could suppress H_2O_2 stimulation-induced apoptosis in PC12 cells. Importantly, cells stimulated by H_2O_2 will produce excessive ROS, which is also an important cause of cell apoptosis [5, 21]. To investigate the possible mechanisms for the antiapoptotic effects of HAS on H_2O_2 -induced PC12 cells, we determined the ROS generation in PC12 cells. We used the fluorescence probe DCFH-DA to further explore whether HAS could prevent H_2O_2 -stimulated ROS generation and resulting oxidative stress. As can be seen from the Figure 4, it was found that when the cells were exposed to 90 μM H_2O_2 , the ROS produced in the cells increased

sharply, compared to the normal cells ($P < 0.01$). However, pretreatment with 100 μM vitamin C or HAS (15, 30, and 60 μM) significantly reduced the intracellular ROS accumulation in H_2O_2 -induced PC12 cells, compared to the control cells ($P < 0.01$).

3.4. HAS Enhances the Activities of ROS Scavenging Enzymes in H_2O_2 -Stimulated PC12 Cells. Intracellular MDA, SOD, GSH-Px, and CAT are commonly used biomarkers for the evaluation of the oxidative stress level of cells or tissues [21–23]. Thus, to clarify whether HAS protects PC12 cells from H_2O_2 induced damage through antioxidant action or not, we studied the effect of HAS on MDA production and activities of ROS scavenging enzymes (SOD, GSH-Px, and CAT) in H_2O_2 -stimulated PC12 cells. As shown in Figure 5, an extremely significant increase in MDA was observed in PC12 cells exposed to 90 μM H_2O_2 for 2 hours ($P < 0.01$), compared to the normal cells. However, this growth trend was greatly alleviated by pretreatment with 100 μM vitamin C or HAS (15, 30, and 60 μM) for 2 hours ($P < 0.01$), compared to the control cells. On the other hand, the amount of antioxidant enzymes including SOD, GSH-Px, and CAT is reduced sharply in H_2O_2 -stimulated PC12 cells

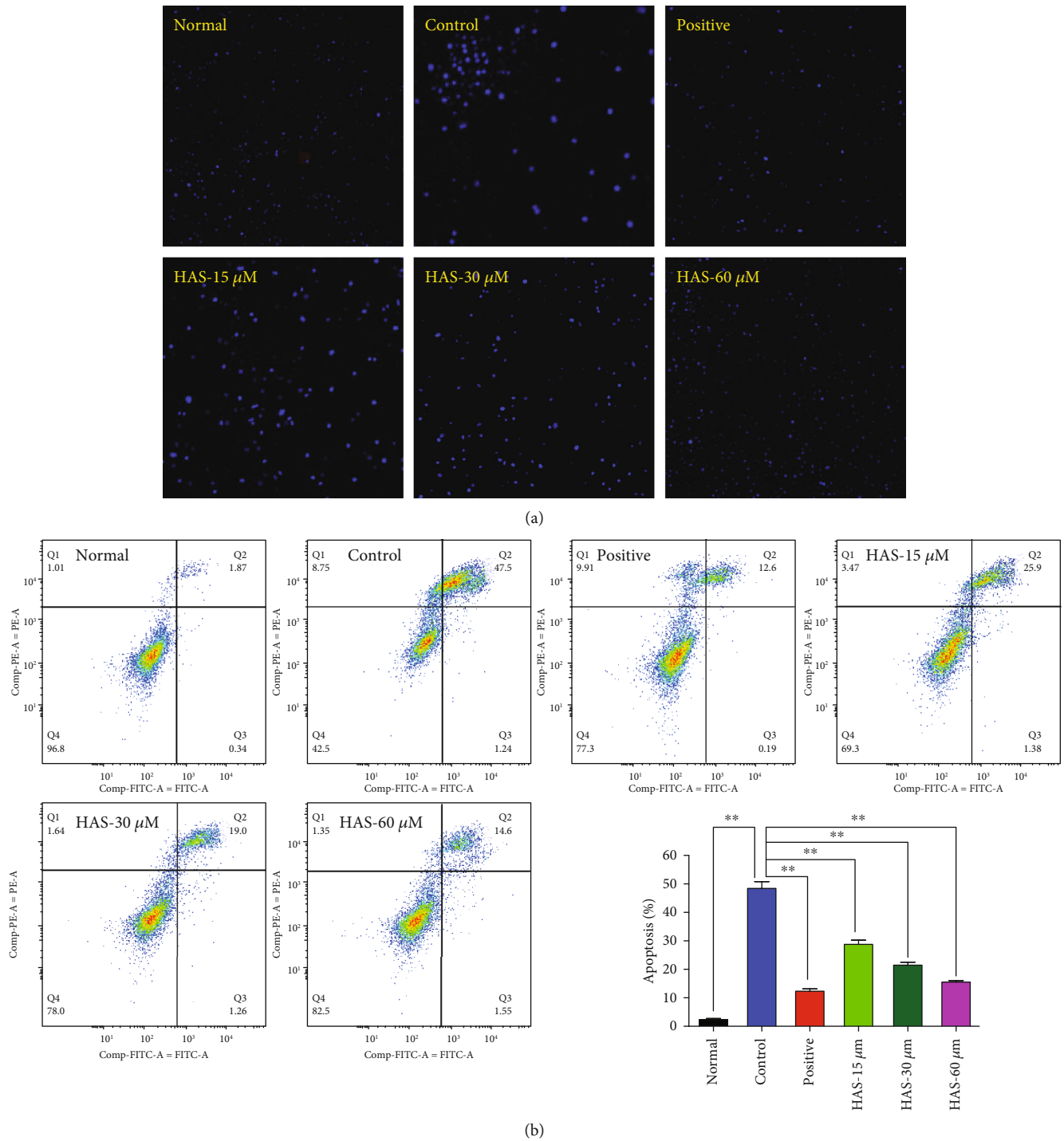


FIGURE 2: Effects of HAS on apoptosis in H_2O_2 -stimulated PC12 cells. (a) Apoptotic assay by DAPI staining and observed under a 100x microscope. (b) Apoptotic assay by flow cytometry. Vitamin C ($100\ \mu\text{M}$) was used as the positive control. The values were represented as the mean \pm SD ($n = 3$). ** $P < 0.01$ vs. the control group.

($P < 0.01$), compared with the normal cells. At the same time, the content of the three enzymes can be increased to different degrees by incubating the cells with HAS for 2 hours ($P < 0.01$). All the above results indicate that HAS treatment might be beneficial for protecting PC12 cells from the H_2O_2 -caused damage through enhancement of activities of ROS scavenging enzymes.

3.5. HAS Regulates the Expressions of Caspase-3, Bax, and Bcl-2 in H_2O_2 -Stimulated PC12 Cells. In order to explore the molecular mechanism for antiapoptotic effects of HAS on H_2O_2 -stimulated PC12 cells, western blotting assays were carried out to detect the expressions of caspase-3, Bax, and Bcl-2 in cells. The Bcl-2 family proteins are key regulatory factors in mitochondrial-mediated apoptosis, which are

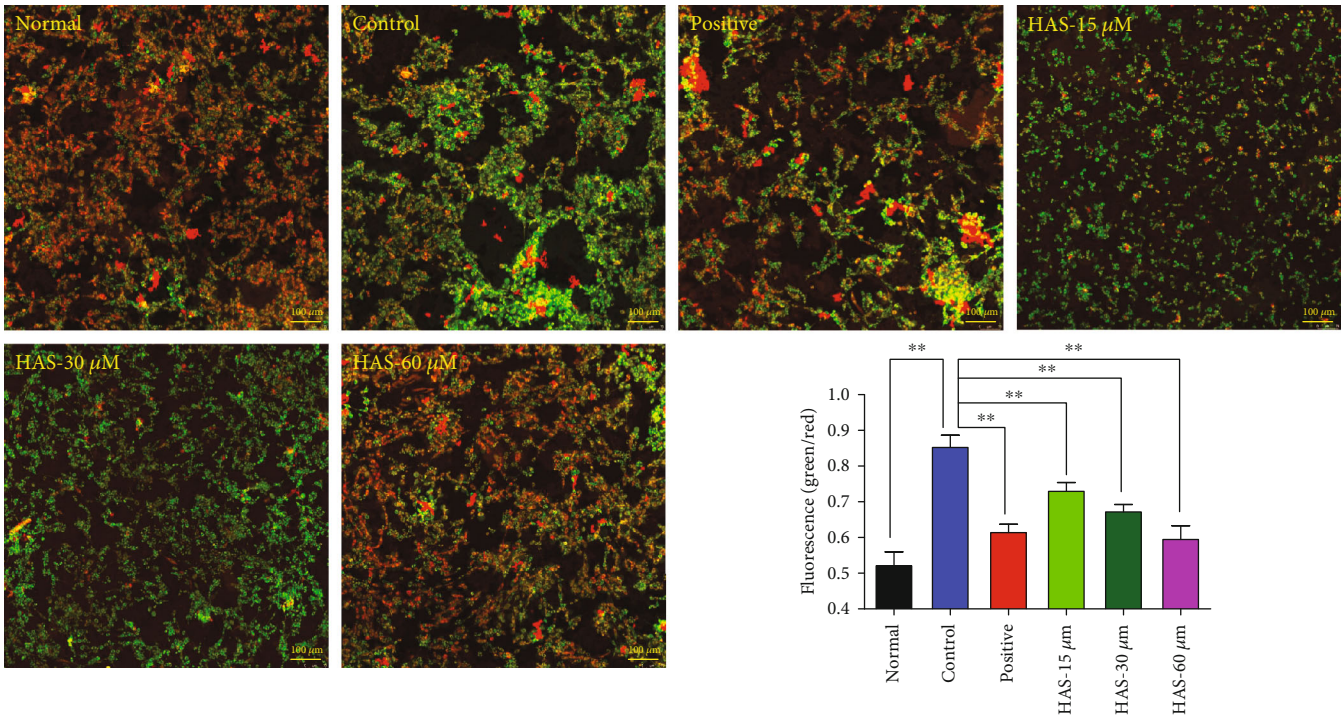


FIGURE 3: Effects of HAS on the $\Delta\Psi_m$ in PC12 cells ($\times 100$). Cells were pretreated with vitamin C ($100 \mu\text{M}$) or HAS ($15, 30, \text{ and } 60 \mu\text{M}$) for 2 h and then incubated in the presence of H_2O_2 ($90 \mu\text{M}$) for 4 h. $\Delta\Psi_m$ was measured using a JC-1 assay kit and observed using a laser confocal microscopy under a $100\times$ microscope. HAS: hydroxy- α -sanshool. The values were represented as the mean \pm SD ($n = 3$). $**P < 0.01$ vs. the control group.

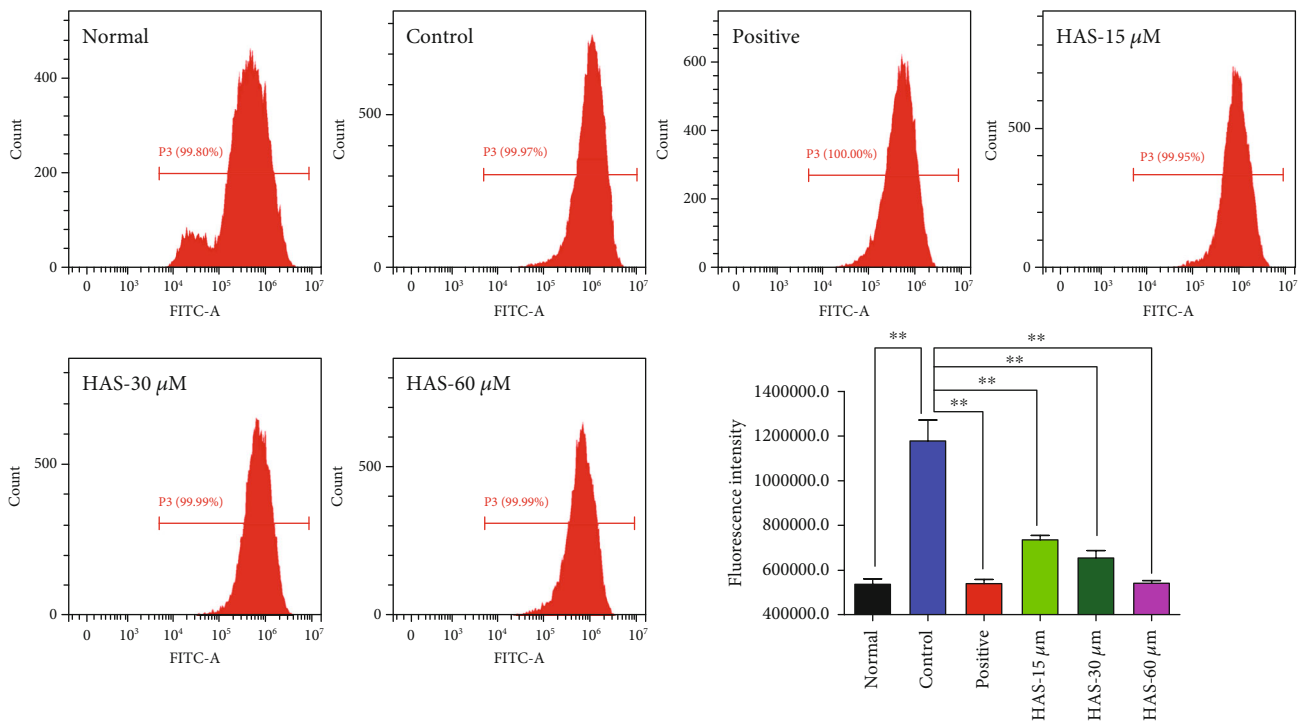


FIGURE 4: Effects of HAS on ROS levels of H_2O_2 -stimulated PC12 cells. PC12 cells were treated with vitamin C ($100 \mu\text{M}$) or HAS ($5, 30, \text{ and } 60 \mu\text{M}$) for 2 h, subsequently subjected to H_2O_2 ($90 \mu\text{M}$) for 4 h. The intracellular ROS level was determined by the flow cytometry (FCM) assay. The values were represented as the mean \pm SD ($n = 3$). $**P < 0.01$ vs. the control group.

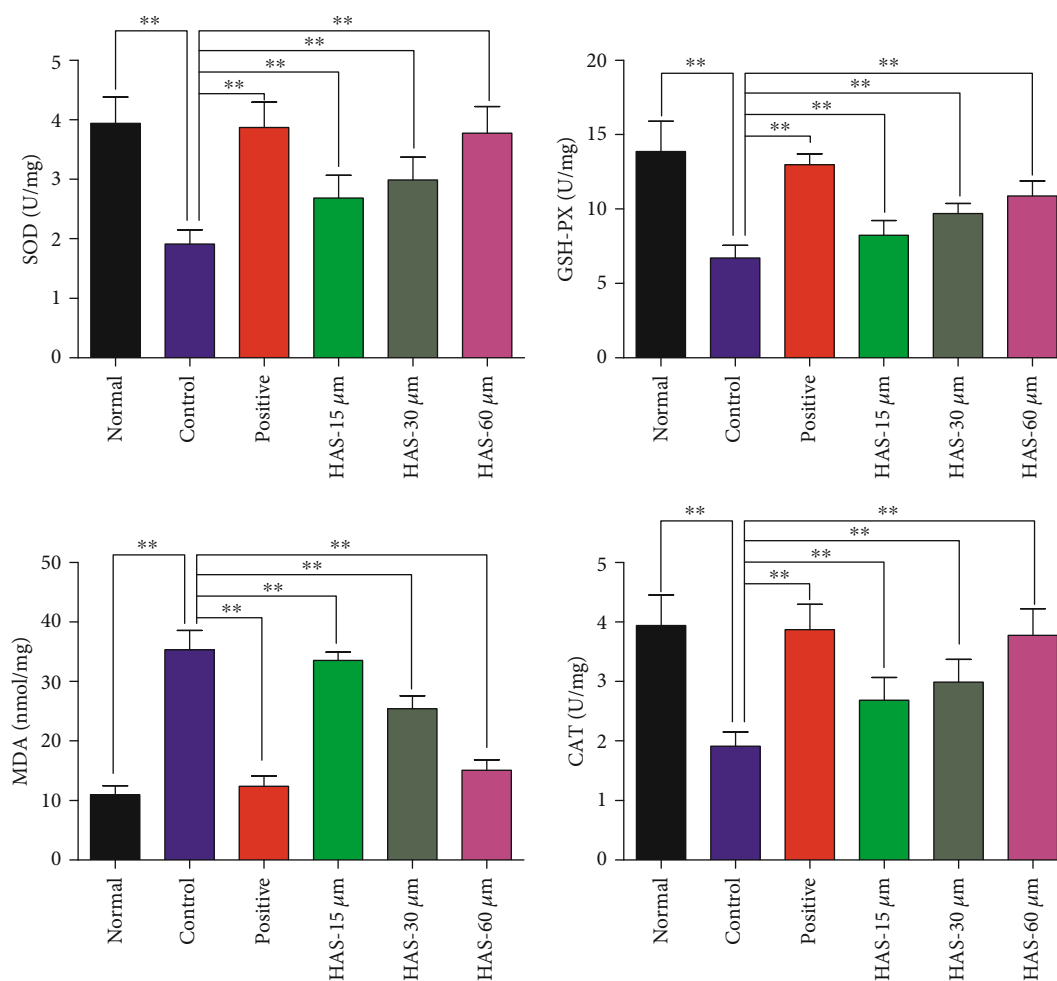


FIGURE 5: Effects of HAS on SOD, GSH-Px, MDA, and CAT in H_2O_2 -stimulated PC12 cells. The levels of MDA and activities of SOD, CAT, and GSH-Px were determined by commercial assay kits. PC12 cells were treated with vitamin C (100 μM) or HAS (15, 30, and 60 μM) for 2 h, subsequently subjected to H_2O_2 (90 μM) for 4 h. The values were represented as the mean \pm SD ($n = 3$). ** $P < 0.01$ vs. the control group.

divided into two categories: proapoptotic proteins (Bax, Bim, Bak, etc.) and antiapoptotic proteins (Bcl-2, Bcl-xl, Mcl-1, etc.) [24]. As shown in Figure 6(a), compared to the normal cells, 90 μM H_2O_2 stimulation significantly downregulated the antiapoptotic protein of Bcl-2 in PC12 cells ($P < 0.01$), while upregulating the proapoptotic proteins of Bax and cleaved caspase-3 ($P < 0.01$). However, the present results also showed that HAS (15, 30, and 60 μM) and 100 μM vitamin C could reverse abovementioned changes and upregulated Bcl-2 ($P < 0.01$) whereas they could downregulate caspase-3 in H_2O_2 -stimulated PC12 cells ($P < 0.01$), compared to the control cells. Besides these, Bax could be downregulated by treatment with 100 μM vitamin C or HAS at the concentrations of 30 and 60 μM in H_2O_2 -stimulated PC12 cells ($P < 0.01$), compared to the control cells.

3.6. HAS Regulates the Expressions of PI3K, p-PI3K, Akt, and p-Akt in H_2O_2 -Stimulated PC12 Cells. The PI3K/Akt signal pathway is essential for the survival of neurons related to suppression of apoptosis [25]. In our present results as shown in Figure 6(b), it was found that expressions of Akt, p-Akt, and p-PI3K in PC12 cells were significantly decreased after stim-

ulation with H_2O_2 for 2 hours ($P < 0.01$), compared to the normal cells. However, pretreatment with HAS (15, 30, and 60 μM) and 100 μM vitamin C significantly upregulated the p-Akt and p-PI3K in PC12 cells ($P < 0.01$), compared to the control cells. Besides, pretreatment with HAS (30 and 60 μM) could also significantly upregulate Akt in H_2O_2 -stimulated PC12 cells ($P < 0.01$), compared to the control PC 12 cells, while PI3K expression difference was not statistically significant. These results suggested that HAS may possess protective potentials on H_2O_2 -stimulated PC12 cells via the PI3K/Akt pathway.

To further explore whether the PI3K/Akt pathway is the key in the protective effect of HAS, we used a chemical inhibitor LY294002 to inhibit the expression of the PI3K/Akt signaling pathway. As shown in Figure 7, after incubation with 90 μM H_2O_2 , the viability of PC12 cells dropped to nearly 40%; the LY294002 group was approximated to it. Besides that, the HAS group could increase the viability of PC12 cells to 60%, while the HAS/LY294002 group just increased a little. All of these data showed that HAS possessed protective potentials on H_2O_2 -stimulated PC12 cells via the PI3K/Akt pathway.

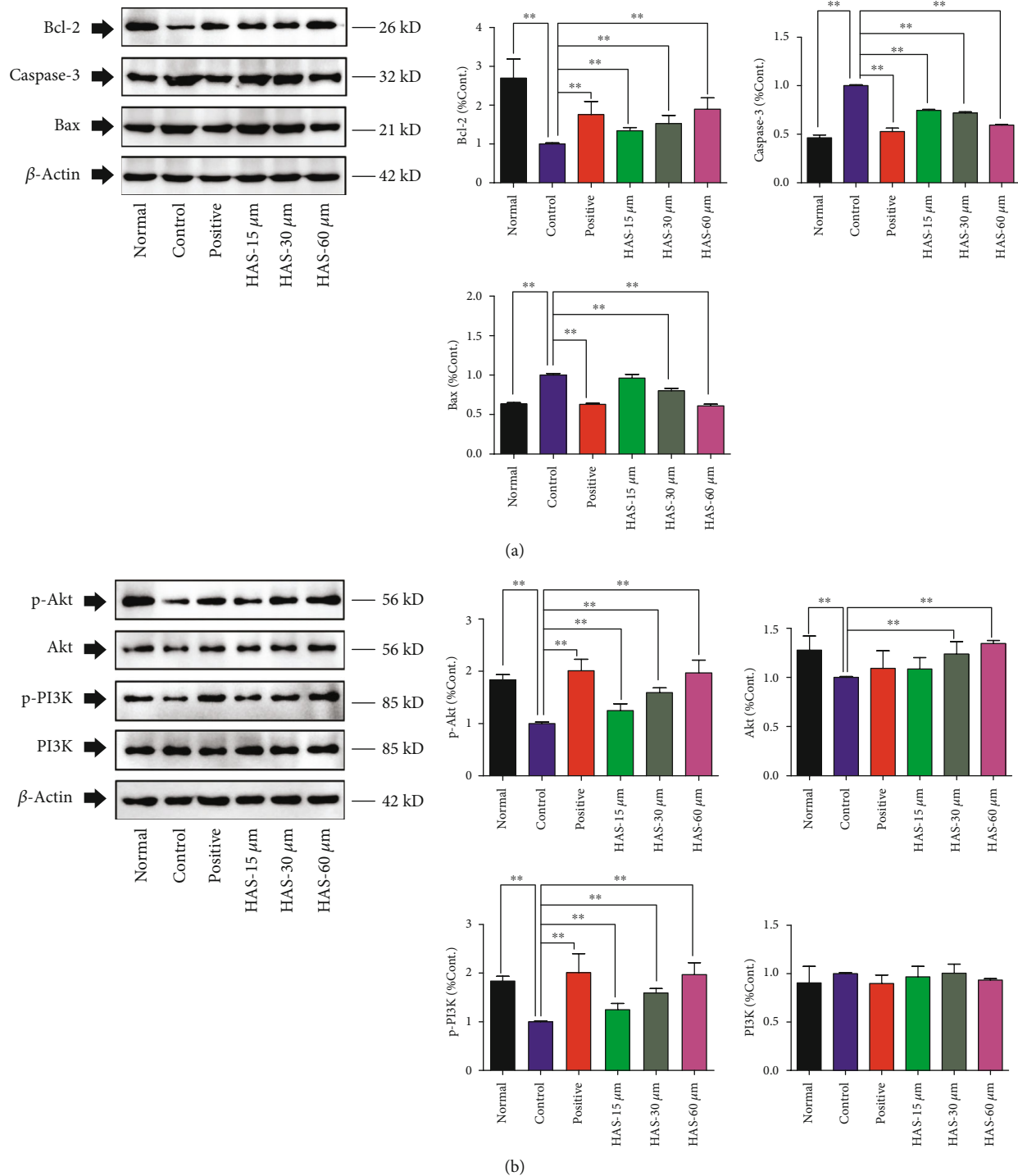


FIGURE 6: Effects of HAS on protein expressions of caspase-3, Bax, Bcl-2, PI3K, p-PI3K, Akt, and p-Akt in H_2O_2 -stimulated PC12 cells. PC12 cells were treated with HAS (15, 30, and 60 μM) or 100 μM vitamin C for 2 h, subsequently subjected to H_2O_2 (90 μM) for 4 h. Protein expressions of caspase-3, Bax, Bcl-2, PI3K, p-PI3K, Akt, and p-Akt were determined by western blotting, and β -actin was used as the internal reference. The values were represented as the mean \pm SD ($n = 3$). ** $P < 0.01$ vs. the control group.

4. Discussion

Hydroxy- α -sanshool (HAS) is a promising natural monomer of unsaturated fatty acid amide isolated from the *Z. bungeanum* pericarps with lots of bioactivities, such as hypolipidemic

and hypoglycemic effects, improving learning and memory effects. As part of our continuing research on this compound, to the best of our knowledge, the present study provides the first evidence that HAS can protect PC12 cells from H_2O_2 -induced damage through the suppression of apoptosis.

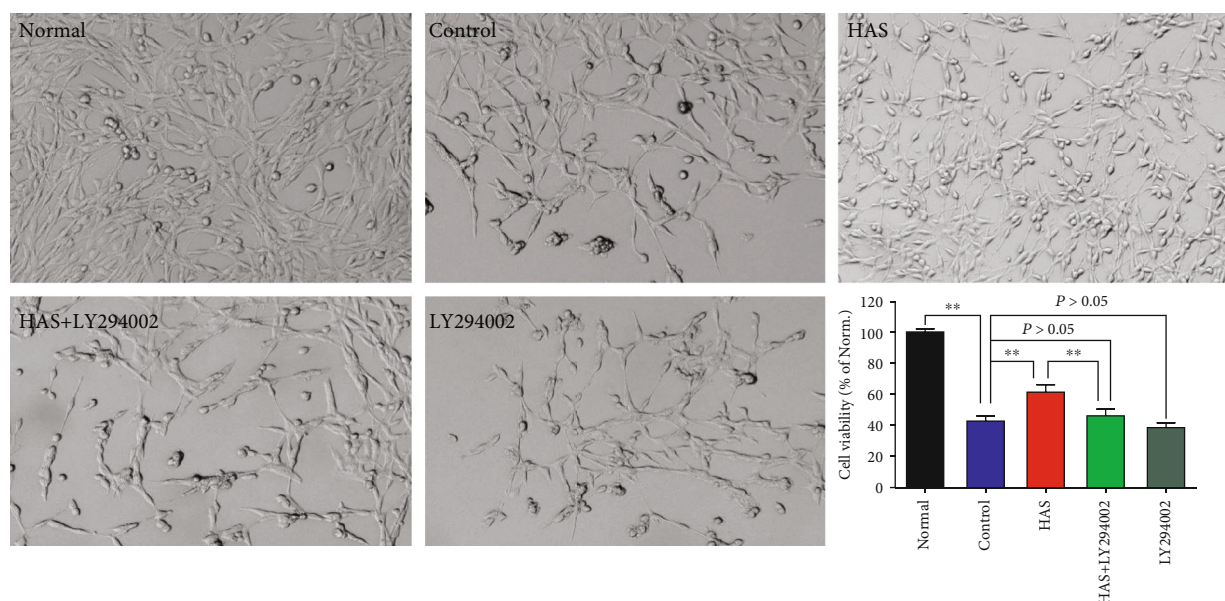


FIGURE 7: Effects of PI3K inhibitor LY294002 on the viability of PC12 cells ($\times 100$). The PC12 cells were pretreated with LY294002 ($20 \mu\text{M}$) or not for 1 hour; then cells were treated with HAS ($60 \mu\text{M}$) for 2 h, subsequently subjected to H_2O_2 ($90 \mu\text{M}$) for 4 h. HAS: hydroxy- α -sanshool; Norm.: normal. The values were represented as the mean \pm SD ($n = 3$). ** $P < 0.01$ vs. the control group.

Previous researches revealed that PC12 cell, a rat photochromogenic cell line, has some neuronal characteristics and similar physiology and pathology of the nerve cells, and in addition, H_2O_2 possesses high cell membrane transmittance; consequently, H_2O_2 -stimulated PC12 cells commonly considered an ideal cell model for studying pathology and screening candidate drugs of neurodegenerative diseases, such as Alzheimer's disease (AD) and epilepsy [26–28]. Thus, the PC12 cell line was selected as the experimental cell model in our present study. According to relevant research, many free radicals are generated during the development of neurodegenerative diseases, and some of the reactive oxygen species (ROS) can cause oxidative damage to nerve tissues and eventually lead to apoptosis or even necrosis of neurons [29, 30]. Therefore, ROS play an important role in the apoptosis caused by oxidative stress. As an important member of the ROS family, H_2O_2 can easily cross cell membranes to generate hydroxyl radicals, which are highly toxic and can cause serious damage to cells and attack biomolecules, ultimately leading to apoptosis or necrosis [31–33]. Therefore, in this study, H_2O_2 was used to stimulate PC12 cells to simulate the occurrence and development of neurodegenerative diseases caused by oxidative stress. According to CCK-8 assay, after stimulation with H_2O_2 , cell viability of the PC12 cells decreased by 60%; however, pretreatment with HAS reversed the decrease of cell viability induced by H_2O_2 .

For the neurodegenerative diseases, the excessive ROS can lead to direct oxidative damage of molecules, followed by cell dysfunction and apoptosis [5, 34]. Our present investigation found that H_2O_2 stimulation resulted in excessive ROS accumulation in PC12 cells, and interestingly, HAS pretreatment could decrease the excessive ROS in PC12 cells caused by H_2O_2 . Malondialdehyde (MDA), a product of lipid peroxidation, would be significantly increased when exposed to oxidative stimulation, which is also considered a biomarker of oxidative stress and also causes damage to the cell

membrane [22, 23]. In addition, there are various ROS scavenging enzymes in living organisms, among which the most important are the superoxide dismutase (SOD), catalase (CAT), and glutathione peroxidase (GSH-Px). Under physiological conditions, they jointly maintain the redox balance in the body [35]. In vivo, SOD can catalyze the conversion of superoxide anions into H_2O_2 , GSH-Px can reduce toxic peroxides to nontoxic hydroxyl compounds, and CAT can promote the further conversion of H_2O_2 into oxygen and water [36, 37]. According to our results, H_2O_2 -stimulated PC12 cells produced excessive MDA, accompanied by significantly decreased activity of SOD, GSH-Px, and CAT. Interestingly, pretreatment with HAS can decrease the MDA level whereas it can increase the activities of SOD, GSH-Px, and CAT in stimulated PC12 cells. In previous reports, excessive intracellular ROS produced by mitochondria could also lead to mitochondrial dysfunction through oxidative stress-induced apoptosis, and MMP is a sensitive indicator of mitochondrial function [38, 39]. In our results, after H_2O_2 stimulation, significant apoptosis and reduced cell survival as well as declined $\Delta\Psi_m$ can be found in PC12 cells. In addition, intracellular ROS accumulation increased after H_2O_2 stimulation, which further promoted the loss of $\Delta\Psi_m$. Besides, as expected, H_2O_2 -induced cell apoptosis events in PC12 cells can be blocked by pretreatment with HAS. All these results suggested that HAS might be beneficial for protecting H_2O_2 -stimulated PC12 cells from ROS-induced apoptosis.

Currently, increasing evidences have suggested that the PI3K/AKT signal pathway plays a crucial role in cell survival and development as well as ROS-induced cell apoptosis [40, 41]. In addition, the PI3K/AKT pathway shows significant antioxidant activity in central and peripheral neurons and can be considered a potential therapeutic target for neurodegenerative diseases, participating in the cellular protective mechanism of ROS-induced cell damage [39]. AKT is a

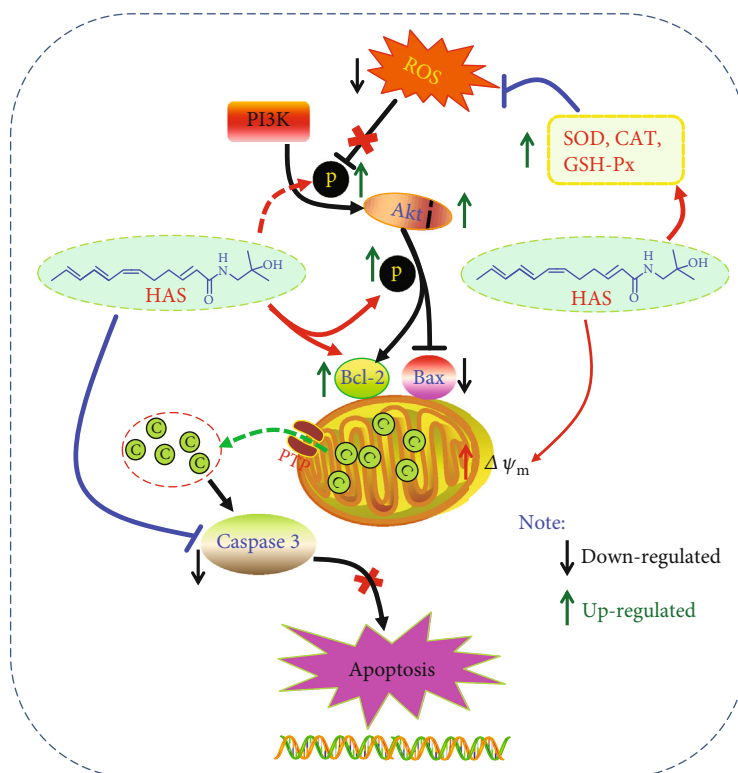


FIGURE 8: Molecular mechanism of the protective effect of HAS. HAS possesses protective potentials on H_2O_2 -stimulated PC12 cells through suppression of oxidative stress-induced apoptosis via regulation of the PI3K/Akt signal pathway.

serine/threonine kinase activated by recruitment to the plasma membrane and is a key mediator of PI3K-mediated signal transduction [42, 43]. As is shown in Figure 8, the direct results of PI3K phosphorylation is the phosphorylation of AKT, which further affects the expression of Bcl-2 and Bax proteins. Bcl-2 and Bax are a group of proteins closely related to mitochondrial mediated apoptosis, among which the anti-apoptotic protein Bcl-2 is a channel protein located on the mitochondrial membrane, which can inhibit the proapoptotic effect of Bax [44]. Activated p-AKT increased the expression of Bcl-2 and decreased the expression of Bax. In normal PC12 cells, these entire proteins in this signal pathway would be in a dynamic balance [45]. Our results showed that HAS pretreatment could upregulate the proteins of PI3K/Akt signaling (p-PI3K, Akt, and p-Akt) and antiapoptotic proteins of Bcl-2, whereas it could downregulate the apoptotic proteins (caspase-3 and Bax), compared to the PC12 without HAS treatment.

5. Conclusion

In summary, our study suggested that the hydroxy- α -sanshool (HAS) possesses protective potentials on H_2O_2 -stimulated PC12 cells by suppression of oxidative stress-induced apoptosis through the regulation of the PI3K/Akt signal pathway. Our results provide scientific evidences that HAS might be considered in the development of a new drug for treating neurodegenerative diseases related to excessive apoptosis induced by oxidative stress.

Data Availability

The data used to support the findings of this study are available from the corresponding author upon request.

Disclosure

Ruo-Lan Li and Qing Zhang should be considered the co-first authors.

Conflicts of Interest

There are no conflicts of interest associated with this paper.

Authors' Contributions

Ruo-Lan Li and Qing Zhang contributed equally to this work.

Acknowledgments

This research was supported by the Project of Administration of Traditional Chinese Medicine of Sichuan Province of China (grant nos. 2018JC001, 2018HJZX004, and 2018HJZX005) and Xinglin Scholar Discipline Promotion Talent Program of Chengdu University of Traditional Chinese Medicine (no. BSH2018006).

References

- [1] L. Ung, U. Pattamatta, N. Carnt, J. L. Wilkinson-Berka, G. Liew, and A. J. R. White, "Oxidative stress and reactive oxygen species: a review of their role in ocular disease," *Clinical Science*, vol. 131, no. 24, pp. 2865–2883, 2017.
- [2] F. Chen, Y. Liu, N. K. Wong, J. Xiao, and K. F. So, "Oxidative stress in stem cell aging," *Cell Transplantation*, vol. 26, no. 9, pp. 1483–1495, 2017.
- [3] S. Gandhi and A. Y. Abramov, "Mechanism of oxidative stress in neurodegeneration," *Oxidative Medicine and Cellular Longevity*, vol. 2012, no. 3, Article ID 428010, 11 pages, 2012.
- [4] K. A. Radermacher, K. Wingler, F. Langhauser et al., "Neuroprotection After Stroke by Targeting NOX4 As a Source of Oxidative Stress," *Antioxidants & Redox Signaling*, vol. 18, no. 12, pp. 1418–1427, 2013.
- [5] M. Liu, Y. Xu, X. Han et al., "Potent effects of flavonoid-rich extract from *Rosa laevigata* Michx fruit against hydrogen peroxide-induced damage in PC12 cells via attenuation of oxidative stress, inflammation and apoptosis," *Molecules*, vol. 19, no. 8, pp. 11816–11832, 2014.
- [6] S. Khoshirat, H. A. Abbaszadeh, M. S. Khoramgah et al., "Protective effect of photobiomodulation therapy and bone marrow stromal stem cells conditioned media on pheochromocytoma cell line 12 against oxidative stress induced by hydrogen peroxide," *Lasers in Medical Science*, vol. 10, no. 3, pp. 163–170, 2019.
- [7] Y. Yu, J. R. Du, C. Y. Wang, and Z. M. Qian, "Protection against hydrogen peroxide-induced injury by Z-ligustilide in PC12 cells," *Experimental Brain Research*, vol. 184, no. 3, pp. 307–312, 2008.
- [8] L. Xiang, Y. Liu, C. Xie et al., "The chemical and genetic characteristics of szechuan pepper (*Zanthoxylum bungeanum* and *Z. armatum*) cultivars and their suitable habitat," *Frontiers in Plant Science*, vol. 7, 2016.
- [9] Y. Gong, Y. Huang, L. Zhou et al., "Chemical composition and antifungal activity of the fruit oil of *Zanthoxylum bungeanum*-Maxim. (Rutaceae) from China," *Journal of Essential Oil Research*, vol. 21, no. 2, pp. 174–178, 2009.
- [10] Y. Lan, Q. Wu, Y. Q. Mao et al., "Cytotoxicity and enhancement activity of essential oil from *Zanthoxylum bungeanum* Maxim. as a natural transdermal penetration enhancer," *Journal of Zhejiang University SCIENCE B*, vol. 15, no. 2, pp. 153–164, 2014.
- [11] S. Huang, L. Zhao, X. L. Zhou, M. Ying, C. J. Wang, and J. Weng, "New alkylamides from pericarps of *Zanthoxylum bungeanum*," *Chinese Chemical Letters*, vol. 23, no. 11, pp. 1247–1250, 2012.
- [12] H. C. Huang, R. Y. Wang, and W. M. Zhou, "Lethal effect of *Zanthoxylum Maxim* volatile oil on Pheochromocytoma cells," *Heilongjiang Medicine Journal*, vol. 23, no. 4, pp. 514–515, 2010.
- [13] Z. Lin, S. Han, J. Jiang, Y. Lin, H. Chen, and H. Yuan, "Antitumor compound identification from *Zanthoxylum bungeanum* essential oil based on composition-activity relationship," *Chemical Research in Chinese Universities*, vol. 29, no. 6, pp. 1068–1071, 2013.
- [14] Y. Tezuka, S. Irikawa, T. Kaneko et al., "Screening of Chinese herbal drug extracts for inhibitory activity on nitric oxide production and identification of an active compound of *Zanthoxylum bungeanum*," *Journal of Ethnopharmacology*, vol. 77, no. 2-3, pp. 209–217, 2001.
- [15] R. X. Zhu, W. C. Zeng, and Z. F. Zhao, "Chemical components and antibacterial activity of Hanyuan *Zanthoxylum bungeanum* seed oil," *Food Science*, vol. 32, no. 17, pp. 85–88, 2011.
- [16] C. F. Wang, K. Yang, H. M. Zhang et al., "Components and insecticidal activity against the maize weevils of *Zanthoxylum schinifolium* fruits and leaves," *Molecules*, vol. 16, no. 4, pp. 3077–3088, 2011.
- [17] Chinese Pharmacopoeia Commission, "Chinese pharmacopoeia," *Science and Technology Press of Shanghai*, vol. 1, pp. 159–160, 2015.
- [18] T. Wu, L. Zhong, Z. Hong et al., "The effects of *Zanthoxylum bungeanum* extract on lipid metabolism induced by sterols," *Journal of Pharmacological Sciences*, vol. 127, no. 3, pp. 251–259, 2015.
- [19] L. Wang, W. Fan, M. Zhang et al., "Antiobesity, regulation of lipid metabolism, and attenuation of liver oxidative stress effects of hydroxy- α -sanshool isolated from *Zanthoxylum bungeanum* on high-fat diet-induced hyperlipidemic rats," *Oxidative Medicine and Cellular Longevity*, vol. 2019, Article ID 5852494, 13 pages, 2019.
- [20] M. Zhang, M. Xie, D. Wei et al., "Hydroxy- α -sanshool isolated from *Zanthoxylum bungeanum* attenuates learning and memory impairments in scopolamine-treated mice," *Food and Function*, vol. 10, no. 11, pp. 7315–7324, 2019.
- [21] M. Hu, Y. Liu, L. He, X. Yuan, W. Peng, and C. Wu, "Antiepileptic effects of protein-rich extract from *Bombyx batryticatus* on mice and its protective effects against H₂O₂-induced oxidative damage in PC12 cells via regulating PI3K/Akt signaling pathways," *Oxidative Medicine and Cellular Longevity*, vol. 2019, Article ID 7897584, 13 pages, 2019.
- [22] W. Peng, X. Q. Qiu, Z. H. Shu et al., "Hepatoprotective activity of total iridoid glycosides isolated from *Paederia scandens* (Lour.) Merr. var. *tomentosa*," *Journal of Ethnopharmacology*, vol. 174, no. 11, pp. 317–321, 2015.
- [23] M. Valko, D. Leibfritz, J. Moncol, M. T. D. Cronin, M. Mazur, and J. Telser, "Free radicals and antioxidants in normal physiological functions and human disease," *The International Journal of Biochemistry & Cell Biology*, vol. 39, no. 1, pp. 44–84, 2007.
- [24] Z. Fu, J. Yang, Y. Wei, and J. Li, "Effects of piceatannol and pterostilbene against β -amyloid-induced apoptosis on the pi3k/akt/bad signaling pathway in pc12 cells," *Food and Function*, vol. 7, no. 2, pp. 1014–1023, 2016.
- [25] L. Zhu, N. Ning, Y. Li et al., "Biatractylolide modulates PI3K-Akt-GSK3 β -dependent pathways to protect against glutamate-induced cell damage in PC12 and SH-SY5Y cells," *Evidence-based Complementary and Alternative Medicine*, vol. 2017, Article ID 1291458, 9 pages, 2017.
- [26] Y. Sai, Q. Wu, W. Le, F. Ye, Y. Li, and Z. Dong, "Rotenone-induced PC12 cell toxicity is caused by oxidative stress resulting from altered dopamine metabolism," *Toxicology In Vitro*, vol. 22, no. 6, pp. 1461–1468, 2008.
- [27] H. Boujrad, O. Gubkina, N. Robert, S. Krantic, and S. A. Susin, "AIF-mediated programmed necrosis: a highly orchestrated way to die," *Cell Cycle*, vol. 6, no. 21, pp. 2612–2619, 2014.
- [28] S. Demirci, S. Kutluhan, M. Naziroğlu, A. C. Uğuz, V. A. Yüreklı, and K. Demirci, "Effects of selenium and topiramate on cytosolic Ca²⁺ influx and oxidative stress in neuronal PC12 cells," *Neurochemical Research*, vol. 38, no. 1, pp. 90–97, 2013.

- [29] I. Solaroglu, T. Tsubokawa, J. Cahill, and J. H. Zhang, "Antiapoptotic effect of granulocyte-colony stimulating factor after focal cerebral ischemia in the rat," *Neuroscience*, vol. 143, no. 4, pp. 965–974, 2006.
- [30] H. Wang, N. Gao, Z. Li, Z. Yang, and T. Zhang, "Autophagy alleviates melamine-induced cell death in PC12 cells via decreasing ROS level," *Molecular Neurobiology*, vol. 53, no. 3, pp. 1718–1729, 2016.
- [31] Z. Gao, K. Huang, and H. Xu, "Protective effects of flavonoids in the roots of *Scutellaria baicalensis* Georgi against hydrogen peroxide-induced oxidative stress in hs-sy5y cells," *Pharmacological Research*, vol. 43, no. 2, pp. 173–178, 2001.
- [32] G. Ren, H. X. Qiao, J. Yang, and C. X. Zhou, "Protective effects of steroids from *Allium chinense* against H₂O₂-induced oxidative stress in rat cardiac H9C2 cells," *Phytotherapy Research*, vol. 24, no. 3, pp. 404–409, 2010.
- [33] A. H. Bhat, K. B. Dar, S. Anees et al., "Oxidative stress, mitochondrial dysfunction and neurodegenerative diseases; a mechanistic insight," *Biomedicine and Pharmacotherapy*, vol. 74, pp. 101–110, 2015.
- [34] G. H. Kim, J. E. Kim, S. J. Rhie, and S. Yoon, "The role of oxidative stress in neurodegenerative diseases," *Experimental Neurobiology*, vol. 24, no. 4, pp. 325–340, 2015.
- [35] B. Chance, H. Sies, and A. Boveris, "Hydroperoxide metabolism in mammalian organs," *Physiological Reviews*, vol. 59, no. 3, pp. 527–605, 1979.
- [36] G. Z. Ao, X. J. Chu, Y. Y. Ji, and J. W. Wang, "Antioxidant properties and PC12 cell protective effects of a novel curcumin analogue (2E,6E)-2,6-bis(3,5-dimethoxybenzylidene)cyclohexanone (MCH)," *International Journal of Molecular Sciences*, vol. 15, no. 3, pp. 3970–3988, 2014.
- [37] H. Stridh, M. Kimland, D. P. Jones, S. Orrenius, and M. B. Hampton, "Cytochrome c release and caspase activation in hydrogen peroxide- and tributyltin-induced apoptosis," *FEBS Letters*, vol. 429, no. 3, pp. 351–355, 1998.
- [38] T. H. Lu, C. C. Su, Y. W. Chen et al., "Arsenic induces pancreatic β -cell apoptosis via the oxidative stress-regulated mitochondria-dependent and endoplasmic reticulum stress-triggered signaling pathways," *Toxicology Letters*, vol. 201, no. 1, pp. 15–26, 2011.
- [39] H. Li, Z. Tang, P. Chu et al., "Neuroprotective effect of phosphocreatine on oxidative stress and mitochondrial dysfunction induced apoptosis in vitro and in vivo: involvement of dual PI3K/Akt and Nrf2/HO-1 pathways," *Free Radical Biology and Medicine*, vol. 120, pp. 228–238, 2018.
- [40] M. Wang, R. Hu, Y. Wang et al., "Atractylenolide III attenuates muscle wasting in chronic kidney disease via the oxidative stress-mediated PI3K/AKT/mTOR pathway," *Oxidative Medicine and Cellular Longevity*, vol. 2019, no. 4, Article ID 1875471, 16 pages, 2019.
- [41] S. Lei, W. Su, Z. Y. Xia et al., "Hyperglycemia-Induced Oxidative Stress Abrogates Remifentanyl Preconditioning-Mediated Cardioprotection in Diabetic Rats by Impairing Caveolin-3-Modulated PI3K/Akt and JAK2/STAT3 Signaling," *Oxidative Medicine and Cellular Longevity*, vol. 2019, no. 9, Article ID 9836302, 19 pages, 2019.
- [42] Q. Zhang, J. Liu, M. Zhang et al., "Apoptosis induction of fibroblast-like synoviocytes is an important molecular-mechanism for herbal medicine along with its active components in treating rheumatoid arthritis," *Biomolecules*, vol. 9, no. 12, p. 795, 2019.
- [43] G. Huang, J. Mao, Z. Ji, and A. Ailati, "Stachyose-induced apoptosis of Caco-2 cells via the caspase-dependent mitochondrial pathway," *Food and Function*, vol. 6, no. 3, pp. 765–771, 2015.
- [44] S. M. Kønig, V. Rissler, T. Terkelsen, M. Lambrugh, and E. Papaleo, "Alterations of the interactome of Bcl-2 proteins in breast cancer at the transcriptional, mutational and structural level," *PLOS Computational Biology*, vol. 15, article e1007485, no. 12, 2019.
- [45] C. Lv, X. Yuan, H. W. Zeng, R. H. Liu, and W. D. Zhang, "Protective effect of cinnamaldehyde against glutamate-induced oxidative stress and apoptosis in PC12 cells," *European Journal of Pharmacology*, vol. 815, pp. 487–494, 2017.

Research Article

Integrated Metabolomic and Lipidomic Analysis Reveals the Neuroprotective Mechanisms of Bushen Tiansui Formula in an A β 1-42-Induced Rat Model of Alzheimer's Disease

Min Yi ¹, Chunhu Zhang ², Zheyu Zhang ¹, Pengji Yi,¹ Panpan Xu,¹ Jianhua Huang,³ and Weijun Peng ¹

¹Department of Integrated Traditional Chinese & Western Medicine, The Second Xiangya Hospital, Central South University, Changsha, Hunan 410011, China

²Department of Integrated Traditional Chinese and Western Medicine, Xiangya Hospital, Central South University, Changsha, Hunan 410008, China

³Hunan Academy of Chinese Medicine, Changsha 410013, China

Correspondence should be addressed to Weijun Peng; pengweijun87@csu.edu.cn

Received 12 March 2020; Accepted 13 May 2020; Published 20 June 2020

Guest Editor: Francisco Jaime B. Mendonça Junior

Copyright © 2020 Min Yi et al. This is an open access article distributed under the Creative Commons Attribution License, which permits unrestricted use, distribution, and reproduction in any medium, provided the original work is properly cited.

Bushen Tiansui Formula (BSTSF) is a traditional Chinese medicine prescription. It has been widely applied to treat Alzheimer's disease (AD) in the clinic; however, the mechanisms underlying its effects remain largely unknown. In this study, we used a rat AD model to study the effects of BSTSF on cognitive performance, and UPLC-MS/MS-based metabolomic and lipidomic analysis was further performed to identify significantly altered metabolites in the cerebral cortices of AD rats and determine the effects of BSTSF on the metabolomic and lipidomic profiles in the cerebral cortices of these animals. The results revealed that the levels of 47 metabolites and 30 lipids primarily associated with sphingolipid metabolism, glycerophospholipid metabolism, and linoleic acid metabolism were significantly changed in the cerebral cortices of AD rats. Among the altered lipids, ceramides, phosphatidylethanolamines, lysophosphatidylethanolamines, phosphatidylcholines, lysophosphatidylcholines, phosphatidylserines, sphingomyelins, and phosphatidylglycerols showed robust changes. Moreover, 34 differential endogenous metabolites and 21 lipids, of which the levels were mostly improved in the BSTSF treatment group, were identified as potential therapeutic targets of BSTSF against AD. Our results suggest that lipid metabolism is highly dysregulated in the cerebral cortices of AD rats, and BSTSF may exert its neuroprotective mechanisms by restoring metabolic balance, including that of sphingolipid metabolism, glycerophospholipid metabolism, alanine, aspartate, and glutamate metabolism, and D-glutamine and D-glutamate metabolism. Our data may lead to a deeper understanding of the AD-associated metabolic profile and shed new light on the mechanism underlying the therapeutic effects of BSTSF.

1. Introduction

Alzheimer's disease (AD) is a common neurodegenerative disorder of the central nervous system characterized by progressive memory loss, cognitive impairment, abnormal behavior, and personality disorders. Dementia, including that related to AD, is the fifth leading cause of death worldwide, and 40–50 million people are thought to be affected by this condition [1], making it a major and increasing global

health challenge. However, an effective treatment for AD remains elusive [2].

Traditional Chinese medicines (TCMs) have been used in the treatment of dementia for thousands of years. The Bushen Tiansui Formula (BSTSF, also known as “Naoling decoction”) is derived from Sagacious Confucius' Pillow Elixir, a classic Chinese medicinal formula mainly used to treat cognitive decline [3]. This formula comprises six herbs, including *Epimedium acuminatum* Franch. (Yinyanghuo),

Fallopia multiflora (Thunb.) Harald. (Heshouwu), *Polygala tenuifolia* Willd. (Yuanzhi), *Acorus tatarinowii* Schott. (Shichangpu), *Plastrum testudinis* (Guiban), and *Ossa draconis* (Longgu). We recently showed that BSTSF could improve learning and memory deficits in AD model rats through regulating serum lipid metabolism and the amino acid metabolic pathway [4]. However, the mechanism underlying the therapeutic effects of BSTSF, especially its effects on metabolic stress and impaired lipid metabolism in brain tissue, is poorly understood.

Senile plaques, neurofibrillary tangles, and lipid granule accumulation were the three defining neuropathological features in the cerebral cortex of AD patients identified in the original analysis by Alois Alzheimer [5]. Subsequently, a large number of studies have shown that beta-amyloid ($A\beta$) plaques accumulate in the cerebral cortex in the early stages of AD [6–8]. These observations highlight that the cerebral cortex is the main pathological region in brain tissue of AD. The prefrontal cortex (PFC) is implicated in cognitive processes including working memory, temporal processing, decision-making, flexibility, and goal-oriented behavior [9]. Alterations in prefrontal cortex (PFC) function and abnormalities in its interactions with other brain areas (i.e., the hippocampus) have been related to Alzheimer's disease (AD) [10]. Several potential biomarkers have been proposed for preclinical AD and are mainly related to lipid metabolism. Perturbations of sphingolipid metabolism in brain tissue are consistently associated with endophenotypes across preclinical and prodromal AD, indicating that sphingolipids may be biologically relevant biomarkers for early AD detection [11]. Moreover, phosphatidylcholine breakdown may be mediated by phospholipase A2, leading to significantly elevated levels of glycerophosphocholine in human cerebrospinal fluid [12], while amino acids such as valine, arginine, and histidine are also associated with AD [13, 14]. These observations suggest that severe metabolic disorder and dysregulated lipid metabolism may have an important role in the pathogenesis of AD.

In this study, an ultra-high-performance liquid chromatography-mass spectrometry- (UHPLC-MS-) based metabolomic and lipidomic analysis was performed in cerebral cortices of control and AD model rats. Furthermore, the therapeutic effects of BSTSF and the mechanism underlying its ameliorating effects on the pathogenesis of AD were also explored for the first time using a metabolomic strategy. This study may provide a basis for a better understanding of the AD metabolic profile and novel insight into the clinical utility of BSTSF.

2. Material and Methods

2.1. Preparation of BSTSF. The six herbs (*H. epimedii*, *P. multiflorum*, tortoise plastron, *O. draconis*, *P. tenuifolia*, and *R. acori graminei*) comprising BSTSF were mixed at a ratio of 3:3:4:4:2:2. To ensure the quality of the herbal medicine, all herbs were obtained from the TCM pharmacy of the Second Xiangya Hospital of Central South University (CSU, Changsha, China) and were authoritatively identified by Professor Suiyu Hu. For details of the preparation and quality

control of lyophilized powder, refer to our previous publication [15].

2.2. Animals and Experimental Design. Adult male Sprague-Dawley rats, weighing 180–220 g, used in our experiments, were purchased from the Laboratory Animal Centre of Central South University (Changsha, China). All animal experiments were performed following guidelines from the Committee on the Ethics of Animal Experiments of Central South University. Rats were housed under standard animal house conditions and randomly allocated into one of three groups: sham, AD, and BSTSF. For the AD and BSTSF groups, rats were injected intracerebroventricularly with oligomeric $A\beta_{1-42}$ to generate a validated AD model, as we previously described [16]. The sham rats were injected bilaterally with the vehicle into the lateral ventricles. According to our previous study, the BSTSF group was intragastrically administered with 27 g/kg BSTSF once daily from 1 to 28 days, whereas the sham and AD groups were intragastrically administered with an equal volume of distilled water. By referring to the calculation formula from the *Experiment Methodology of Pharmacology*, the conversion factor between rats (200 g) and humans (70 kg) is 0.018; therefore, the calculated gavage dose of BSTSF for rats is about 9 g/kg/d. Our previous study explored the efficacy of three doses (9 g/kg/d, 27 g/kg/d, and 54 g/kg/d) of this prescription, and the result demonstrated that BSTSF owns optimal efficacy when it is administered at three times the regular dose; therefore, a dose of 27 g/kg/d was chosen for the experiments in the current study [15].

2.3. Morris Water Maze Test. The Morris water maze (MWM) test was used to assess the hippocampus-dependent learning and memory ability of the rats, as described in our previous study with minor modifications [17]. In brief, a spatial acquisition test was carried out from the 24th to 28th days after $A\beta_{1-42}$ infusion, and animals were subjected to a five-day memory acquisition experiment to assess their spatial learning ability. Subsequent spatial probe experiments were conducted on day 29, to determine rat spatial memory retention ability. We applied SuperMaze video tracking and analysis systems to analyze experimental parameters (XR-XM101, Shanghai Softmaze Information Technology Co. Ltd., China).

2.4. UPLC-TripleTOF/MS-Based Metabolomics

2.4.1. Sample Preparation. After the MWM test, the prefrontal cortices were harvested and immediately washed with pre-cooled physiological saline and stored at -80°C for further analysis. Samples (50 mg) were accurately weighed, and the metabolites extracted using 400 μL of a methanol:water (4:1, v/v) solution. The mixture was allowed to settle at -20°C and treated using a high-throughput Wonbio-96c tissue crusher (Shanghai Wanbo Biotechnology Co., Ltd., China) at 60 Hz for 6 min, vortexed for 30 s, and sonicated at 40 kHz for 10 min at -20°C . This step was performed three times. The samples were placed at -20°C for 30 min to precipitate the proteins. After centrifugation at $13,000 \times g$ at 4°C for 15 min, the supernatants were carefully transferred

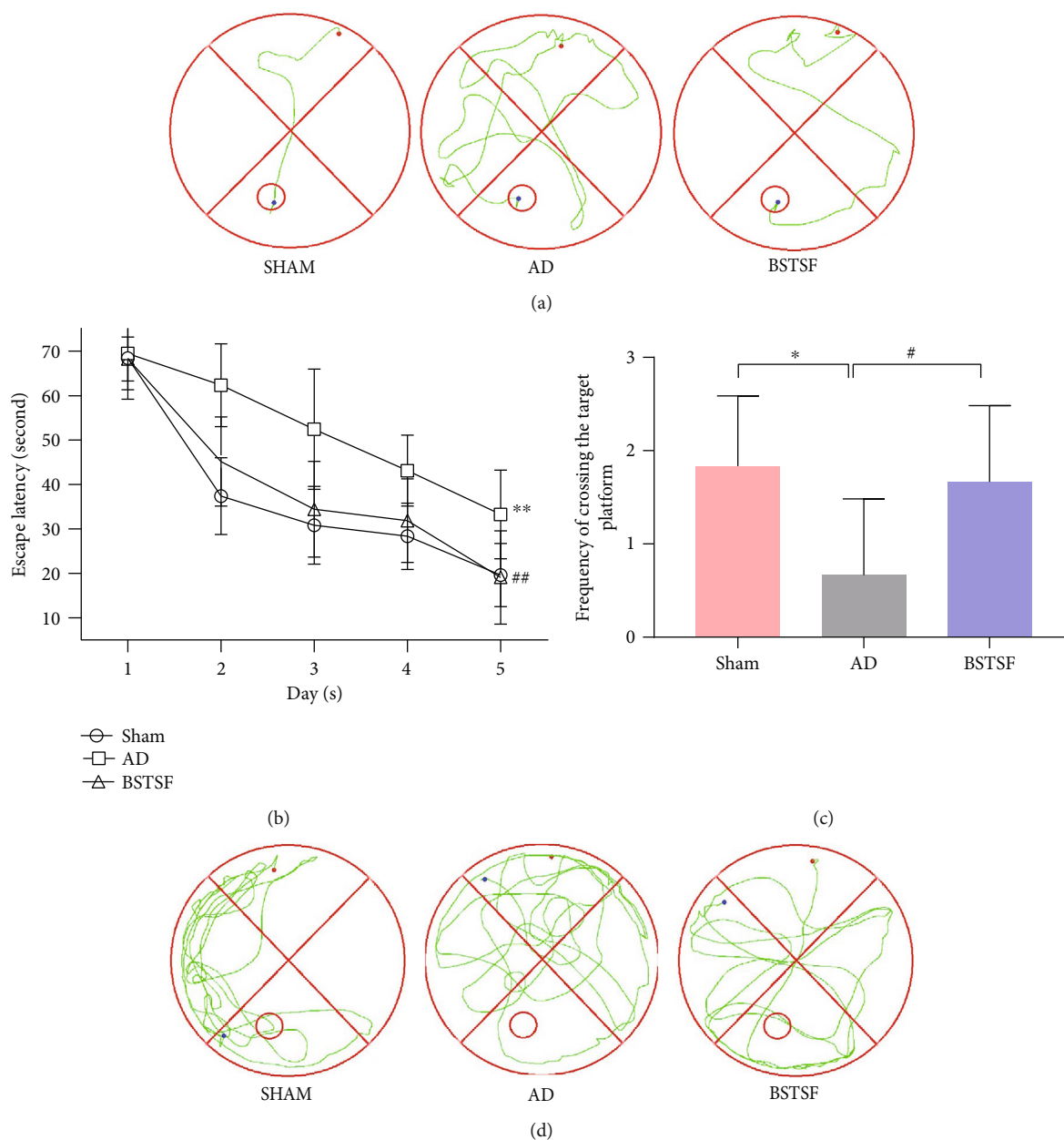


FIGURE 1: Effects of BSTSF on spatial learning and memory deficiency in AD rats. (a) Representative images of the swim paths and (b) time needed to reach the hidden platform. (c) Time spent in the target quadrant was measured for analysis of spatial memory function, and (d) representative images of the frequency of crossing the target platform within 90 seconds are shown. Data are expressed as the mean \pm SD ($n = 5$ per group; escape latency was analyzed by repeated measures analysis of variance (ANOVA); other data were analyzed by one-way ANOVA followed by least significant difference tests). * $p < 0.05$, ** $p < 0.01$ vs. sham group; # $p < 0.05$, ## $p < 0.05$ vs. AD group.

to sample vials for LC-MS/MS analysis. The pooled quality control (QC) sample was prepared by mixing equal volumes of all the samples.

2.4.2. Acquisition of LC-MS/MS Data. Metabolites were profiled using a UPLC-MS/MS-based platform. Chromatographic separation of the metabolites was performed on an ExionLC™ AD system (AB Sciex, USA) equipped with an ACQUITY UPLC BEH C18 column (100 mm \times 2.1 mm i.d., 1.7 μ m) (Waters, Milford, CT, USA). The mobile phase consisted of 0.1% formic acid in water (solvent A) and 0.1% formic acid in acetonitrile:isopropanol (1:1, v/v) (solvent B).

The solvent gradient program was as follows: from 0 to 3 min, 95% (A):5% (B) to 80% (A):20% (B); from 3 to 9 min, 80% (A):20% (B) to 5% (A):95% (B); from 9 to 13 min, 5% (A):95% (B) to 5% (A):95% (B); from 13 to 13.1 min, 5% (A):95% (B) to 95% (A):5% (B); and from 13.1 to 16 min, 95% (A):5% (B) to 95% (A):5% (B). The sample injection volume was 20 μ L, and the flow rate was set to 0.4 mL/min. The column temperature was maintained at 40°C. All these samples were stored at 4°C during the analysis. The UPLC system was coupled to a quadrupole time-of-flight mass spectrometer (TripleTOF™ 5600+; AB Sciex) equipped with an electrospray ionization (ESI) source

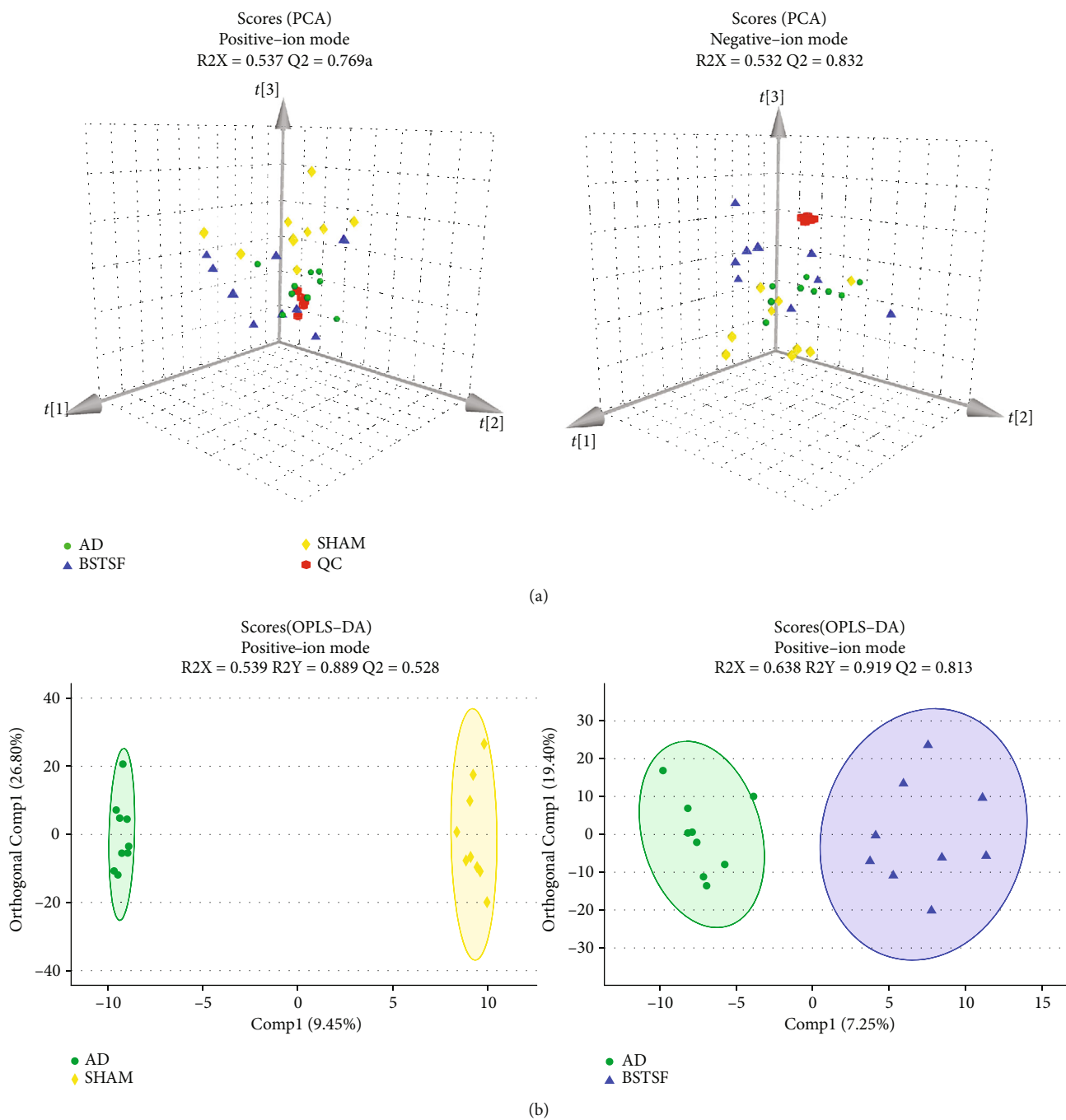


FIGURE 2: Continued.

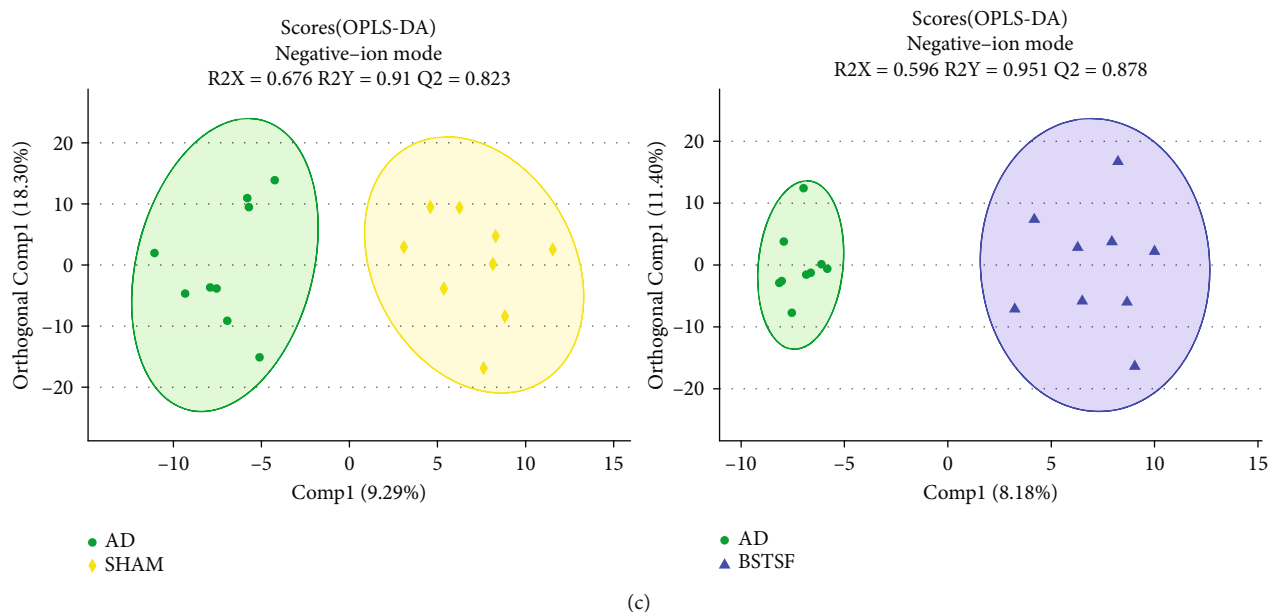


FIGURE 2: Multivariate statistical analysis of cerebral cortex metabolomics: (a) PCA 3D score plots of metabolomic data in the cerebral cortex and (b, c) OPLS-DA score plots between each two groups in positive- and negative-ion modes, respectively.

operating in positive and negative modes. The optimal conditions were set as follows: source temperature, 500°C; curtain gas (CUR), 30 psi; ion sources GS1 and GS2, both 50 psi; ion-spray voltage floating (ISVF), -4000 V in negative mode and 5000 V in positive mode; declustering potential, 80 V; and rolling collision energy (CE), 20–60 V for MS/MS analysis. Data acquisition was performed in the Data-Dependent Acquisition (DDA) mode. The detection was carried out over a mass range of 50–1000 m/z .

2.4.3. Data Processing. After UPLC-MS/MS analysis, the raw data were imported into Progenesis QI 2.3 (Nonlinear Dynamics, Waters) for peak detection and alignment. The preprocessing results generated a data matrix that consisted of the retention time (RT), mass-to-charge ratio (m/z) values, and peak intensity. After filtering, half of the minimum metabolite values were imputed for specific samples in which the metabolite levels fell below the lower limit of quantitation and each metabolic feature was normalized by sum. The internal standard was used for data QC (reproducibility), and metabolic features with a QC relative standard deviation (RSD) > 30% were discarded. Following normalization and imputation, statistical analysis was performed on log-transformed data to identify significant differences in metabolite levels between comparable groups. The mass spectra of these metabolic features were identified by using the accurate mass, MS/MS fragment spectra, and isotope ratio difference searched in reliable metabolite databases such as the Human Metabolome Database (HMDB) (<http://www.hmdb.ca/>) and Metlin Database (<https://metlin.scripps.edu/>). Specifically, the mass tolerance between the measured m/z values and the exact mass of the components of interest was ± 10 ppm. For metabolites confirmed by MS/MS, only those with a MS/MS fragment score above 30 were consid-

ered confidently identified. Otherwise, metabolites were only tentatively assigned.

2.4.4. Statistical Analysis. Multivariate statistical analysis was performed using the ropls (version 1.6.2) R package from Bioconductor on the Majorbio Cloud Platform (<https://cloud.majorbio.com>) and SIMCA-P 14.1 (Umetrics, Umea, Sweden). Unsupervised principal component analysis (PCA) was applied to obtain an overview of the metabolic data, general clustering, trends, and outliers. All the metabolite variables were scaled to unit variances before PCA. Orthogonal partial least squares discriminant analysis (OPLS-DA) was used to determine global metabolic changes between comparable groups. All the metabolite variables were scaled using Pareto scaling before the OPLS-DA. Model validity was evaluated from model parameters R^2 and Q^2 , which provide information for the interpretability and predictability, respectively, of the model and avoid the risk of overfitting. Variable importance in the projection (VIP) was calculated in the OPLS-DA model. p values were estimated with paired Student's t -tests for single-dimensional statistical analysis. Significance among groups was assumed with VIP scores > 1 and p values < 0.05.

2.4.5. Metabolic Pathway Analysis. Significantly altered metabolite data were imported into MetaboAnalyst 3.5 (<https://www.metaboanalyst.ca>) to investigate the therapeutic mechanisms related to BSTSF treatment. The impact value threshold calculated from pathway topology analysis was set to 0.10, and a raw p value < 0.05 was regarded as significant.

2.5. UHPLC-Obitrap/MS-Based Lipidomics

2.5.1. Sample Preparation. Prefrontal cortex tissue (300 mg) was slowly thawed at 4°C and homogenized in 200 μ L of

TABLE 1: Differentially expressed endogenous metabolites between groups sham and AD and their change trends in all groups.

Metabolite	<i>m/z</i>	Rt (min)	HMDB ID	PubChem ID	AD vs. sham			AD ^a	BSTSP ^b
					VIP	<i>p</i>	FC		
ESI+									
Tangeritin	373.1267	5.3139	0030539	68077	2.374	0.001	0.591	↓*	↑
Cer(d18:1/16:0)	538.5199	11.3614	0000790	5283564	1.953	0.004	0.750	↓*	↑
Candicidin	566.289	7.6092	0015283	10079874	1.493	0.031	0.835	↓*	↑
Cer(d18:1/24:1(15Z))	648.6289	13.1778	0004953	5283568	1.468	0.035	0.871	↓*	—
GlcCer(d14:1/20:0)	700.5725	11.005	—	70699223	1.257	0.043	0.883	↓*	↑
Galbeta-Cer(d18:1/20:0)	778.6169	12.1307	—	44260150	1.564	0.012	0.902	↓*	↑
Cer(d18:1/18:0)	566.5511	11.9439	0004950	5283565	2.03	0.004	0.929	↓*	—
Sphinganine	302.3053	7.4398	0000269	91486	1.656	0.014	0.949	↓*	—
LysoPE(16:1(9Z)/0:0)	452.2772	7.6754	0011504	52925129	1.644	0.021	0.976	↓*	↑
PE(18:1(9Z)/16:0)	759.565	8.4109	0009055	9546802	2.422	0.001	0.977	↓*	—
LysoPC(16:1(9Z)/0:0)	494.3241	7.5904	0010383	24779461	1.4	0.041	0.986	↓*	↑
PI(20:4(5Z,8Z,11Z,14Z)/0:0)	621.303	7.8276	—	42607497	1.679	0.023	0.986	↓*	↑
LysoPE(0:0/22:6(4Z,7Z,10Z,13Z,16Z,19Z))	548.2745	7.6944	0011496	53480945	1.603	0.043	0.989	↓*	↑
Oleamide	563.5505	8.9533	0002117	5283387	2.205	0.001	1.003	↑*	—
Cer(d18:0/22:0)	665.6552	10.5332	0011765	5283575	1.564	0.01	1.004	↑*	↓*
Desmethylclomipramine	301.1428	13.9123	0060947	622606	1.551	0.026	1.005	↑*	↓
Phytol	360.3263	13.3117	0002019	5280435	1.649	0.017	1.007	↑*	↓
PE(15:0/14:1(9Z))	680.4797	10.8995	0008888	52924158	1.879	0.014	1.017	↑*	↓*
Cotinine glucuronide	416.1429	0.768	0001013	3398121	1.78	0.025	1.024	↑*	↓
13Z-Docosamide	338.3424	9.7988	—	5365371	1.091	0.05	1.027	↑*	↓
PI(18:0/0:0)	601.3349	9.4901	—	42607495	1.735	0.011	1.027	↑*	—
L-a-Lysophosphatidylserine	526.3142	9.1446	—	28040605	1.827	0.002	1.029	↑*	—
S-Adenosylmethionine	399.1444	0.5786	0001185	34755	1.358	0.033	1.038	↑*	↓
Rollinecin A	663.4538	11.419	0030438	177320	1.881	0.005	1.046	↑*	—
Jubanine B	762.3905	6.2048	0030206	101316795	1.692	0.011	1.052	↑*	↓
Sinapoylspermine	409.2812	6.1949	0033479	131751433	1.891	0.005	1.052	↑*	↓
Latrepirdine	352.2404	12.5435	0240240	197033	1.828	0.002	1.059	↑*	↓
Ecgonine methyl ester	232.1546	12.0323	0006406	104904	2.296	0.001	1.085	↑*	—
Xestoaminol C	230.248	6.1084	—	14756407	1.128	0.044	1.087	↑*	↓
Fasciculic acid B	678.4588	7.1307	0036438	196808	1.434	0.011	1.140	↑*	↓*
ESI-									
Citbismine A	639.1921	3.8775	0041086	131753020	1.875	0.007	0.840	↓*	↑*
Cer(d18:1/20:0)	638.5713	12.6161	0004951	5283566	2.051	0.004	0.916	↓*	↑
Glucosylceramide (d18:1/18:0)	772.5938	11.5561	0004972	11958364	1.543	0.009	0.929	↓*	↑
1-O-Beta-D-glucopyranosyl-2,3-di-O-palmitoylglycerol	775.5571	11.6171	0031680	10462651	1.902	0.005	0.941	↓*	—
PE(16:1(9Z)/P-16:0)	672.4954	11.2227	0008982	53479605	1.331	0.038	0.954	↓*	—
PC(18:1(11Z)/18:2(9Z,12Z))	771.5158	10.4438	0010620	53480619	1.676	0.027	0.962	↓*	↑
PE(15:0/22:0)	806.5909	11.8787	0008907	52924172	1.69	0.025	0.974	↓*	—
PS(20:1(11Z)/18:0)	838.5596	12.6161	0112545	52925649	2.134	0.006	0.977	↓*	—
4-Nitrophenol	138.02	3.6423	0001232	980	1.926	0.015	1.014	↓*	↑*
PC(18:1(11Z)/20:4(5Z,8Z,11Z,14Z))	852.5756	10.6464	0008081	53478741	1.665	0.019	1.019	↑*	↓

TABLE 1: Continued.

Metabolite	<i>m/z</i>	Rt (min)	HMDB ID	PubChem ID	AD vs. sham			AD ^a	BSTSF ^b
					VIP	<i>p</i>	FC		
PE(18:3(9Z,12Z,15Z)/22:1(13Z))	840.5778	10.9036	0009172	53479688	1.712	0.01	1.022	↑*	
GDP	442.0154	0.883	0001201	135398619	1.617	0.006	1.042	↑*	
Luteolin 6-C-glucoside 8-C-arabinoside	655.1563	11.4852	0029258	131750830	1.708	0.046	1.067	↑*	
Digoxigenin bisdigitoxoside	631.3473	10.9633	0060818	92999	1.397	0.045	1.155	↑*	
Blasticidin S	459.1466	4.0897	0030452	170012	1.823	0.016	1.221	↑*	
Cefotaxime	490.0302	4.0897	0014636	5742673	1.656	0.043	1.715	↑*	
Deacetylnomilin	509.1563	3.6723	0035684	90472146	1.548	0.018	0.591	↓*	

Abbreviations: AD: Alzheimer's disease; Rt (min): retention time; VIP: variable importance; FC: fold change. Fold change was calculated as relative intensity obtained from group sham/group AD, and a value less than 1 indicates a decrease in the metabolites of group AD. The levels of potential biomarkers were labeled with "↓" (downregulated) and "↑" (upregulated) ($*p < 0.05$). ^aChange trend compared with the sham group. ^bChange trend compared with the AD group.

water. Then, 240 μL of precooled methanol was added to the homogenate which was then vortexed for 10 s, mixed with 800 μL of MTBE, vortexed again for 10 s, and finally sonicated for 20 min. The mixture was left at room temperature for 30 min and then centrifuged (14,000 $\times g$, 10°C, 10 min). The upper layer was collected and dried using nitrogen. The samples were redissolved in 200 μL of a 90% isopropanol/acetonitrile solution and then centrifuged (14,000 $\times g$, 10°C, 10 min) before MS analysis. The supernatants were transferred into sample vials to be injected and analyzed by UHPLC-Obitrapp/MS. The QC was prepared by mixing equal volumes of all the samples.

2.5.2. Acquisition of LC-MS/MS Data. The UHPLC-Obitrapp/MS analysis was performed in a UHPLC system (Nexera LC-30A, Shimadzu) and with a Q Exactive Plus mass spectrometer (Thermo Scientific). The UPLC autosampler temperature was set at 10°C, and the injection volume for each sample was 3 μL . Column temperature was maintained at 45°C. The velocity was 300 $\mu\text{L}/\text{min}$. The mobile phase consisted of acetonitrile and water (3:2) with 10 mM ammonium formate and 0.1% formic acid (solvent A) and isopropanol and acetonitrile (9:1) with 10 mM ammonium formate and 0.1% formic acid (solvent B). Mass spectrometry was performed in an either positive (ESI+) or negative (ESI-) electrospray ionization mode. The conditions for positive- and negative-ion modes were as follows: heater temperature, 300°C; sheath gas flow rate, 45 arb; auxiliary gas flow rate, 15 arb; sweep gas flow rate, 1 arb; spray voltage, 3.0 kV and 2.5 kV, respectively; capillary temperature, 350°C; S-lens RF level, 50% and 60%, respectively; and MS1 scan range: 200–1800 *m/z*. MS1 spectra were acquired with a target mass resolving power (RP) of 70,000 at *m/z* 200, and MS2 spectra were acquired with a target mass RP of 17,500 at *m/z* 200.

2.5.3. Data Processing. LipidSearch software (version 4.1, Thermo Scientific) was used for peak identification, lipid identification (secondary identification), peak extraction, peak alignment, and quantitative processing. The main parameters were as follows: precursor tolerance, 5 ppm;

product tolerance, 5 ppm; and product ion threshold, 5%. Lipid molecules with RSD > 30% were deleted.

2.6. Statistical Analysis. All data are presented as mean \pm standard error of the mean (SEM) and were analyzed using SPSS 22.0 software (IBM Corp., Armonk, NY, USA). Student's *t*-test was carried out for comparisons between two groups, whereas ANOVA was conducted for comparisons of repeated measures. $p < 0.05$ was defined as indicating a statistically significant difference.

3. Results

3.1. BSTSF Ameliorates Learning and Memory Deficits of $A\beta_{1-42}$ -Induced AD Rats. First, we examined the effects of BSTSF on learning and memory ability in AD model rats using the MWM test. As shown in Figures 1(a) and 1(b), escape latency time gradually decreased in all groups over time; however, rats in the BSTSF group had significantly lower escape latency than those in the AD group during the last three training days. These results indicate that BSTSF can significantly alleviate the impaired learning ability induced by $A\beta_{1-42}$. In the probe test, AD rats crossed the platform fewer times and spent less time in the target quadrant, suggesting that their memory capacity was significantly decreased, while BSTSF treatment significantly reversed these defects in AD rats (Figures 1(c) and 1(d)). Together, these results suggested that BSTSF treatment can ameliorate $A\beta_{1-42}$ -induced spatial learning and memory impairment.

3.2. Cerebral Cortex Metabolomics

3.2.1. Metabolite Identification and Multivariate Statistical Analysis. In this study, we identified 228 metabolites in a positive-ion mode and 287 in a negative-ion mode. An unsupervised PCA recognition model was generated for the whole dataset to evaluate the clustering trend of the samples with multidimensional data. The clustered QC samples confirmed the repeatability and stability of the instrument and the reliability of the data in the current research (Figure 2(a)). The separation between the AD and sham groups could be clearly observed in the PCA 3D patterns in both negative- and

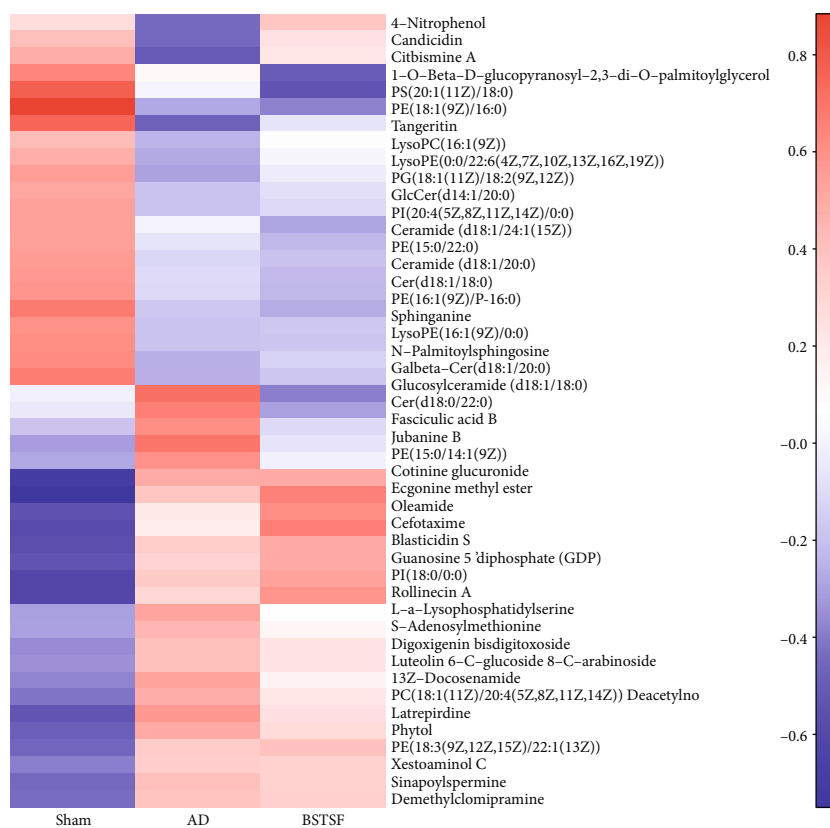
TABLE 2: Differentially expressed endogenous metabolites between groups BSTSF and AD and their change trends in all groups.

Metabolite	<i>m/z</i>	Rt (min)	HMDB ID	PubChem ID	BSTSF vs. AD			AD ^a	BSTSF ^b
					VIP	<i>p</i>	FC		
ESI+									
5'-Methylthioadenosine	342.0866	2.1028	0001173	439176	1.779	0.028	0.962	↑	↓*
1-(Hydroxymethyl)-5,5-dimethyl-2,4-imidazolidinedione	123.0551	1.3183	0031670	67000	1.923	0.031	0.981	↑	↓*
Buddledin A	277.1805	6.8324	—	5281514	2.010	0.022	0.953	↑	↓*
C16 sphinganine	274.2742	5.8082	—	5283572	2.003	0.029	0.981	↑	↓*
D-Glutamine	147.0762	0.7581	0003423	145815	1.907	0.032	0.987	↑	↓*
Cer(d18:0/22:0)	665.6552	10.5332	0011765	5283575	2.332	0.007	0.995	↑*	↓*
Fasciculic acid B	678.4588	7.1307	0036438	196808	1.923	0.021	0.833	↑*	↓*
L-Carnitine	162.1123	0.7298	0000062	10917	2.276	0.005	0.981	↑	↓*
Methyl 10-undecenoate	199.1691	6.5087	0029585	8138	1.762	0.038	0.992	↑	↓*
PE(15:0/14:1(9Z))	680.4797	10.8995	0008888	52924158	2.101	0.017	0.987	↑*	↓*
N-Acetylproline	190.1068	5.3884	0094701	66141	1.920	0.028	0.987	↑	↓*
N-Succinyl-L,L-2,6-diaminopimelate	273.1097	14.0721	0012267	25202447	1.759	0.038	1.007		↑*
Peperinic acid	205.0849	6.1559	0038181	156203	2.192	0.008	1.013	—	↑*
2-Octenyl butyrate	199.1693	7.5996	0038081	124355627	1.989	0.019	1.045	↓	↑*
Glycinoeclepin A	510.2488	5.5944	0037037	19007174	1.914	0.022	1.020	↓	↑*
L-Aspartic acid	134.0446	0.9605	0000191	5960	1.741	0.040	1.008	↓	↑*
Monoisobutyl phthalic acid	205.085	5.9735	0002056	92272	2.182	0.008	1.028	↓	↑*
N-Acetyl-L-aspartic acid	351.1035	0.9605	0000812	65065	2.425	0.003	1.018	↓	↑*
ESI-									
3-Oxo-4,6-choladienoic acid	415.2505	14.0629	0000476	5283992	2.242	0.007	0.981	↑	↓*
Acetyl-DL-leucine	172.0975	2.7628	—	1995	2.152	0.012	0.882	↑	↓*
Camellianin A	655.1471	10.0921	0029908	5487343	2.046	0.020	0.985	↑	↓*
Furanofukinin	293.1751	5.9909	0036640	78385403	1.662	0.042	0.981	↑	↓*
Glycerol 2-(9Z,12Z)-octadecadienoate)			0041511	15607291	1.992	0.025	0.871	—	↓*
Indinavir	648.3376	11.0497	0014369	5362440	1.912	0.029	0.972		↓*
Methylisocitric acid	241.0113	0.73	0006471	5459784	1.897	0.036	0.939	↑	↓*
N-Acetyl-D-phenylalanine	206.0817	3.0047	—	101184	1.863	0.027	0.887	↑	↓*
N-Hexacosanoylglycine	498.4148	9.9473	0062678	91828268	1.704	0.046	0.798	↑	↓*
PS(20:3(5Z,8Z,11Z)/22:4(7Z,10Z,13Z,16Z))	896.518	12.6161	0112616	131819845	1.904	0.031	0.955	—	↓*
Sodium tetradecyl sulfate	275.1677	7.6509	0014607	23665770	1.752	0.032	0.841	↑	↓*
Tetracosahexaenoic acid	393.2201	6.0111	0002007	6439582	1.912	0.033	1.290	↓	↑*
4-Nitrophenol	138.02	3.6423	0001232	980	1.675	0.034	1.028	↓*	↑*
Amphotericin B	922.4847	10.5551	0014819	5280965	2.121	0.016	1.102		↑*
Citbismine A	639.1921	3.8775	0041086	131753020	1.609	0.038	1.710	↓*	↑*
PE-NMe(15:0/18:0)	754.5181	11.0497	0113019	131820134	1.896	0.021	1.051	↓	↑*

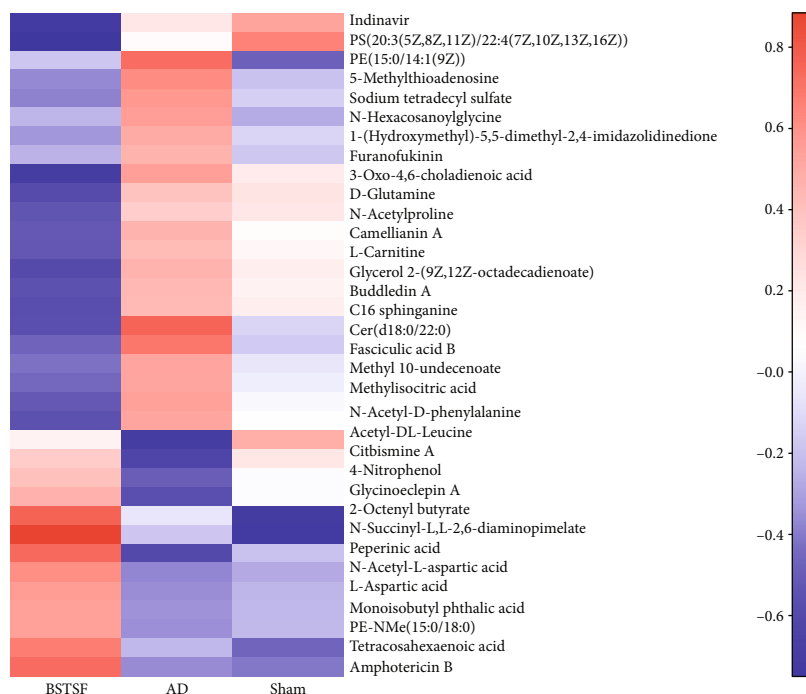
Abbreviations: BSTSF: Bushen Tiansui Formula; AD: Alzheimer's disease; Rt (min): retention time; VIP: variable importance; FC: fold change. Fold change was calculated as average relative quantitation obtained from group BSTSF/group AD, and a value less than 1 indicates a decrease in the metabolites of group BSTSF. The levels of potential biomarkers were labeled with "↓" (downregulated) and "↑" (upregulated) (**p* < 0.05). ^aChange trend compared with the sham group. ^bChange trend compared with the AD group.

positive-ion modes, which demonstrated that the AD model can be successfully induced by Aβ₁₋₄₂ and there was a severe metabolic disorder in the AD model rats. Furthermore, we also noted a trend towards separation between the BSTSF

and AD groups, indicating that metabolism was significantly altered after 28 days of BSTSF administration. A supervised OPLS-DA pattern recognition method was applied to identify the overall metabolic differences between two groups.



(a)



(b)

FIGURE 3: Heatmap of metabolites. (a) Heatmap analysis of the identified metabolites between groups sham and AD. (b) Heatmap analysis of the identified metabolites between groups BSTSF and AD. The blue band indicates a decreased level of metabolite, and the red band indicates an increased level of metabolite.

TABLE 3: Metabolite pathway changes between sham and AD groups.

No.	Pathway	Hits	Total	p	$-\text{Log}(p)$	FDR p	Impact
1	Sphingolipid metabolism	3	21	0.0011		0.0901	0.46248
2	Glycerophospholipid metabolism	3	36	0.0052	5.2518	0.21999	0.21631
3	Linoleic acid metabolism	1	5	0.0506	2.9834	1	0
4	Alpha-linolenic acid metabolism	1	13	0.1266	2.0663	1	0
5	Glycosylphosphatidylinositol (GPI) anchor biosynthesis	1	14	0.1357	1.997	1	0.00399
6	Cysteine and methionine metabolism	1	33	0.2925	1.2293	1	0.05271
7	Arachidonic acid metabolism	1	36	0.3147	1.1562	1	0
8	Arginine and proline metabolism	1	38	0.3291	1.1115	1	0
9	Purine metabolism	1	65	0.4979	0.69746	1	0.02939

Hits represent the matched number of metabolites in one pathway. p represents the original p value calculated from the enrichment analysis. FDR p represents the p value adjusted using the false discovery rate.

TABLE 4: Metabolite pathway changes between BSTSF and AD groups.

No.	Pathway	Hits	Total	p	$-\text{Log}(p)$	FDR p	Impact
1	Alanine, aspartate, and glutamate metabolism	2	28	0.0156	4.157	1	0.3101
2	D-Glutamine and D-glutamate metabolism	1	6	0.0419	3.1725	1	0
3	Arginine biosynthesis	1	14	0.0953	2.3509	1	0
4	Glycosylphosphatidylinositol (GPI) anchor biosynthesis	1	14	0.0953	2.3509	1	0.00399
5	Nicotinate and nicotinamide metabolism	1	15	0.1017	2.2851	1	0
6	Histidine metabolism	1	16	0.1082	2.2238	1	0
7	Pantothenate and CoA biosynthesis	1	19	0.1273	2.0615	1	0
8	Beta-alanine metabolism	1	21	0.1398	1.9678	1	0
9	Cysteine and methionine metabolism	1	33	0.2114	1.554	1	0.02089
10	Glycerophospholipid metabolism	1	36	0.2284	1.4765	1	0.10449
11	Aminoacyl-tRNA biosynthesis	1	48	0.2933	1.2265	1	0

Notes: hits represent the matched number of metabolites in one pathway. p represents the original p value calculated from the enrichment analysis. FDR p represents the p value adjusted using the false discovery rate.

As shown in Figure 2(b) (positive-ion mode) and Figure 2(c) (negative-ion mode), a significant trend towards separation was observed between every two groups.

3.2.2. Potential Metabolite Biomarkers in AD and Effect of BSTSF on AD. Metabolites with VIP scores > 1.0 and p values < 0.05 were defined as potential biomarkers. As shown in Table 1, forty-seven (24 upregulated and 23 downregulated) differential endogenous metabolites were identified between the AD and sham groups. After BSTSF administration, the levels of five metabolites changed significantly, including those of PE(15:0/14:1(9Z)), Cer(d18:0/22:0), fasciculic acid B, citbismine A, and 4-nitrophenol. 14 downregulated metabolites in the AD group compared with the sham group were increased after treatment with BSTSF, and 16 upregulated metabolites were decreased after administration with BSTSF. As shown in Table 2, thirty-four (12 upregulated and 22 downregulated) differential endogenous metabolites were identified between the BSTSF and AD groups. The differential metabolite dataset was imported into R (version 3.4.1) to generate a heatmap. Figures 3(a) and 3(b) show

the 47 differential metabolites between the sham and AD groups and the 34 differential metabolites between the AD and BSTSF groups, as well as the relative changes in the concentration of the metabolites in the different groups.

3.2.3. Analysis of Metabolic Pathways. Metabolic pathway analysis was conducted with MetaboAnalyst 3.5 to further explore the pathogenesis of AD and the possible mechanism by which BSTSF treatment ameliorates this disease. The 47 differential endogenous metabolites between the sham and AD groups were mainly involved in sphingolipid metabolism, glycerophospholipid metabolism, linoleic acid metabolism, and alpha-linolenic acid metabolism (Table 3). The 34 differential endogenous metabolites between the BSTSF and AD groups were primarily associated with alanine, aspartate, and glutamate metabolism, D-glutamine and D-glutamate metabolism, arginine biosynthesis, and glycosylphosphatidylinositol (GPI) anchor biosynthesis (Table 4). Figure 4 illustrates the differential metabolites classified through the HMDB database. The different colors in each pie chart represent different

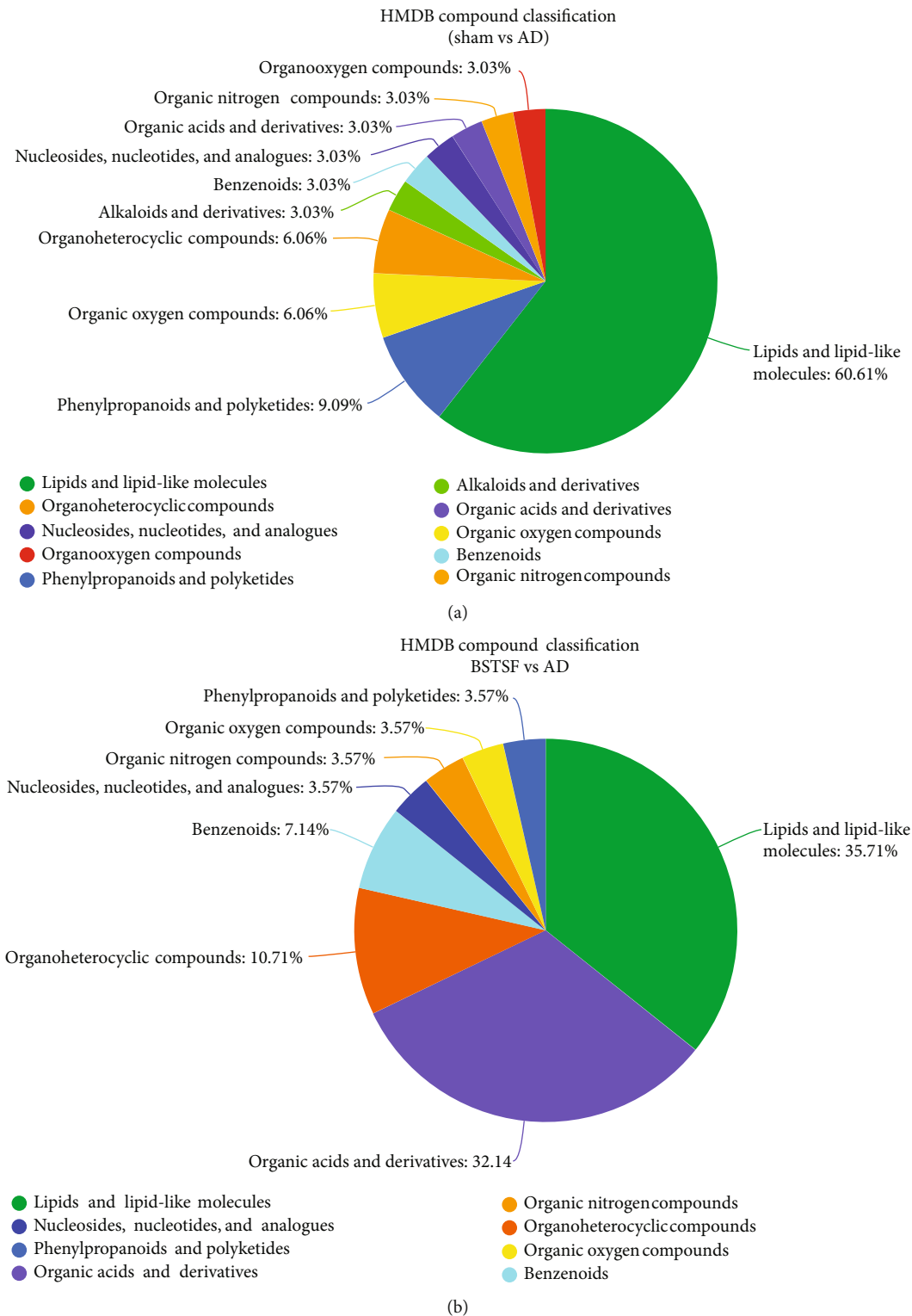


FIGURE 4: HMDB database classification: (a) differential metabolites between groups sham and AD in HMDB database classification and (b) differential metabolites between groups BSTSF and AD in HMDB database classification.

HMDB classifications, and the area represents the relative proportion of metabolites in the classification. The figure further shows that 60.61% of the differential metabolites between the AD and sham groups were lipid metabolites,

indicative of significant changes in the levels of lipid metabolites in the cerebral cortices of AD rats. After BSTSF intervention, 35.71% of the differential metabolites were classified as significantly altered lipids.

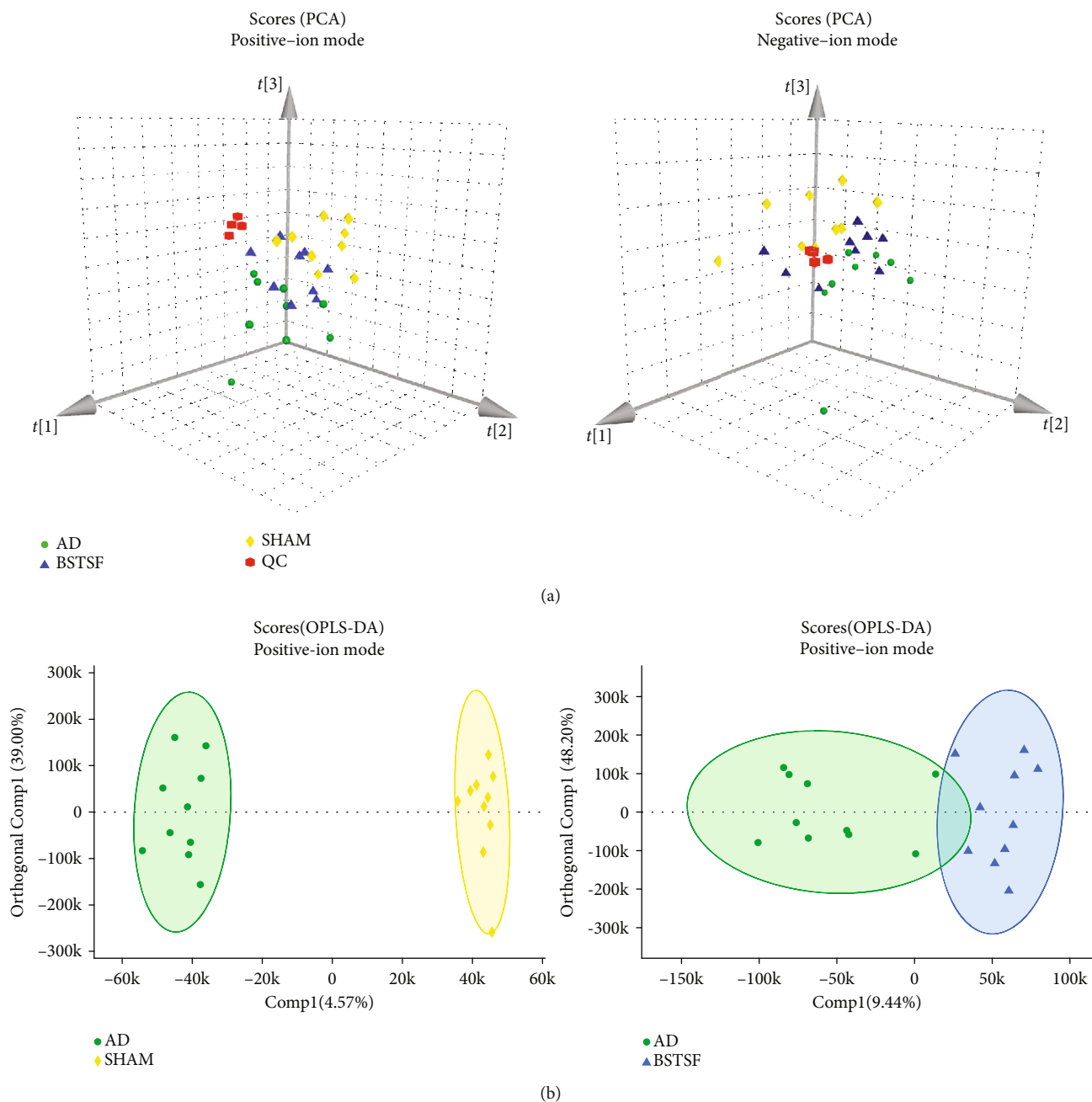


FIGURE 5: Continued.

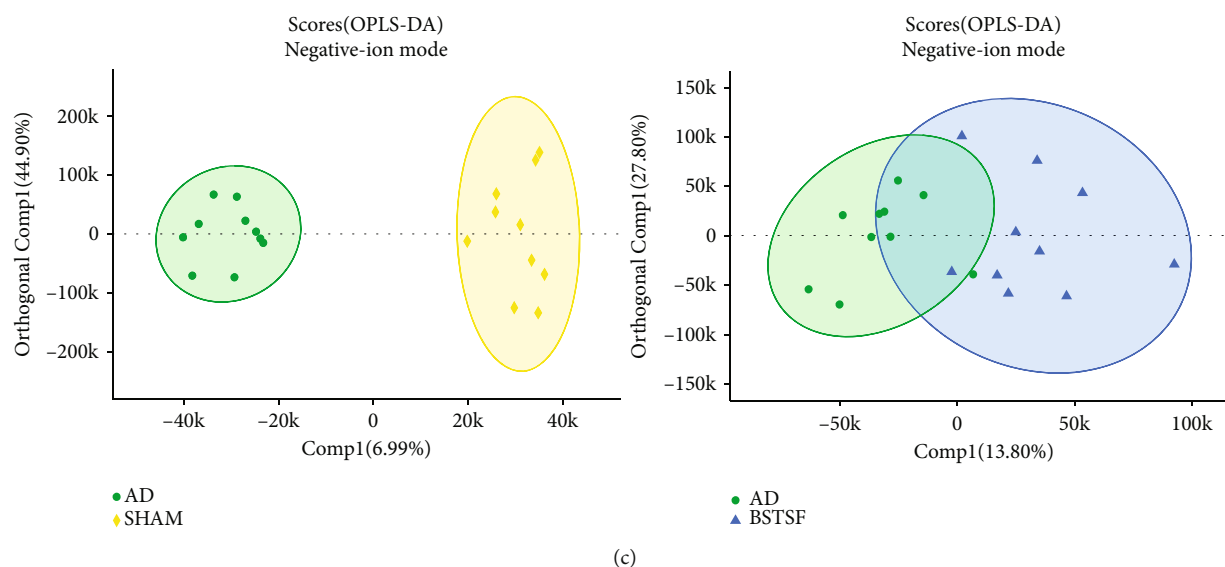


FIGURE 5: Multivariate statistical analysis of cerebral cortex lipidomics: (a) PCA 3D score plots of lipidomic data in the cerebral cortex and (b, c) OPLS-DA score plots between each two groups in positive- and negative-ion modes, respectively.

3.3. Cerebral Cortex Lipidomics

3.3.1. Lipid Identification and Multivariate Statistical Analysis. In this study, we identified 1191 lipid species from 31 lipid subclasses. The PCA 3D score plot chart (Figure 5(a)) shows a trend towards separation between the three groups. The clustered QC samples confirmed the repeatability and stability of the instrument and the reliability of the data. Moreover, OPLS-DA was performed to identify the pattern of separation. As shown in Figure 5(b) (positive-ion mode) and Figure 5(c) (negative-ion mode), there was a clear trend towards separation between the sham and AD groups and between the AD and BSTSF groups. This suggested that lipid metabolism was dysregulated in the cerebral cortices of AD rats, and this dysregulation could be ameliorated by BSTSF administration.

3.3.2. Identification of the Differential Lipid Metabolites in Cerebral Cortex Samples between the Sham and AD Groups and the BSTSF and AD Groups. VIP scores > 1 and p values < 0.05 were used to determine the significantly altered lipid metabolites between the sham and AD groups and the BSTSF and AD groups. As shown in Table 5, the concentrations of 30 lipids changed markedly after being induced by $A\beta_{1-42}$ while those of 21 lipids were altered after BSTSF administration. Interestingly, ceramide levels, including those of Cer(d18:1/18:0), Cer(d18:2/20:2), Cer(d36:0), and Cer(d20:1/18:0), and PC(18:0/20:4) and PE(16:0p/22:6) were substantially higher in the AD group than in the sham group, whereas the levels of all these metabolites were significantly reduced in BSTSF-treated rats. PS(20:3/22:6) was downregulated in the AD group compared with the sham group; however, its level was markedly upregulated with BSTSF treatment (Figure 6).

4. Discussion

In the present study, we found that the cerebral cortex of the AD rats has a distinct metabolomic profile, including the dysregulated sphingolipid metabolism, glycerophospholipid metabolism, linoleic acid metabolism, and alpha-linolenic acid metabolism. The lipidomic analysis indicated that sphingolipids and glycerophospholipids, such as Cer (ceramide), PE (phosphatidylethanolamine), LPE (lysophosphatidylethanolamine), and PC (phosphatidylcholine), are dysregulated in the brain of AD rats. Moreover, the results indicated that BSTSF treatment could restore some dysregulation metabolites and abnormal lipid metabolism in the cerebral cortex of AD rats, especially involving lipid and amino acid metabolism (Figure 7).

Lipid homeostasis plays important roles in the central nervous system, including the maintenance of cell membrane structure, signal transduction, and being components of lipid rafts [18–20]. Our study identified sphingolipids as a class of lipid metabolites that are closely related to the pathology of AD. As the key intermediates in sphingolipid metabolism, we found that the levels of Cer(d18:0/22:0), d18:1/18:0, d18:2/20:2, d36:0, d20:1/18:0) were markedly upregulated in the AD group when compared with the sham-treated group. Some studies demonstrated that elevated Cer levels in reactive astrocytes were associated with neuroinflammation [21] and can promote the overproduction and aggregation of $A\beta$ through their effects on lipid rafts [22]. Interestingly, the Cer levels were significantly reduced after BSTSF administration and may act as a putative therapeutic target of BSTSF in AD. In addition, sphingomyelins (SMs) were a subclass of sphingolipids, and it also enriched in the central nervous system. They are important constituents of lipid rafts [23] and play a critical role in neuronal cell signaling [24].

TABLE 5: Differentially expressed lipids detected by LC-MS/MS.

Lipid ion	Class	Ion formula	<i>m/z</i>	Rt (min)	AD vs. sham			BSTSF vs. AD			
					<i>p</i>	VIP	FC	<i>p</i>	VIP	FC	
ESI+											
Cer(d18:1/24:1)	Cer	C42 H82 O3 N1	648.6289	18.24252	0.016	1.420	1.373	—	—	—	
PE(20:3e)	PE	C25 H46 O7 N1 P1 Na1	526.2904	3.140912	0.004	1.102	1.646	—	—	—	
Cer(d18:1/18:0)	Cer	C36 H72 O3 N1	566.5507	15.29891	0.007	6.805	1.529	0.002	1.724	0.646	
Cer(d20:1/18:0)	Cer	C38 H76 O3 N1	594.582	16.73516	0.003	1.898	1.507	—	—	—	
LPC(16:0)	LPC	C24 H51 O7 N1 P1	496.3398	4.266847	0.041	2.016	1.533	—	—	—	
Cer(d18:2/20:2)	Cer	C38 H70 O3 N1	588.535	15.19771	0.033	3.174	1.304	0.003	2.537	0.747	
LPC(18:0)	LPC	C26 H55 O7 N1 P1	524.3711	5.993806	0.046	1.211	1.417	—	—	—	
PC(32:1e)	PC	C40 H81 O7 N1 P1	718.5745	14.22706	—	—	—	0.007	1.014	0.718	
PC(38:4)	PC	C46 H85 O8 N1 P1	810.6007	13.76129	—	—	—	0.011	3.016	0.872	
PE(16:0p/20:4)	PE	C41 H75 O7 N1 P1	724.5276	13.45675	—	—	—	0.018	2.391	0.778	
Cer(d18:2/18:0)	Cer	C36 H70 O3 N1	564.535	14.0985	—	—	—	0.021	1.147	0.784	
PE(37:1p)	PE	C42 H82 O7 N1 P1 Na1	766.5721	13.06318	—	—	—	0.030	1.838	0.735	
PS(18:1/22:6)	PS	C46 H77 O10 N1 P1	834.528	11.2969	—	—	—	0.033	1.718	0.663	
PC(34:1e)	PC	C42 H85 O7 N1 P1	746.6058	15.56148	—	—	—	0.042	2.541	1.515	
ESI-											
PS(20:3/22:6)	PS	C48 H75 O10 N1 P1	856.5134	11.75541	0.030	1.406	0.815	0.021	1.537	1.279	
SM(d16:1/18:0)	SM	C40 H80 O8 N2 P1	747.5658	11.40332	0.020	1.280	0.817	—	—	—	
Cer(d18:1/16:0)	Cer	C35 H68 O5 N1	582.5103	12.79807	0.009	1.942	1.367	—	—	—	
Cer(d15:0/20:1)	Cer	C36 H70 O5 N1	596.5259	13.38667	0.004	1.052	1.439	—	—	—	
Cer(d36:0)	Cer	C37 H74 O5 N1	612.5572	14.35006	0.002	2.378	1.598	0.002	1.160	0.704	
Cer(d16:0/21:1)	Cer	C38 H74 O5 N1	624.5572	14.49407	0.014	1.254	1.464	—	—	—	
Cer(d20:1/18:0)	Cer	C39 H76 O5 N1	638.5729	15.25846	0.002	4.956	1.382	0.008	2.903	0.811	
Cer(d18:1/22:0)	Cer	C41 H80 O5 N1	666.6042	16.5813	0.000	1.921	1.404	—	—	—	
Cer(d18:1/22:1)	Cer	C41 H78 O5 N1	664.5885	15.15109	0.018	1.171	1.486	—	—	—	
Cer(d18:1/23:0)	Cer	C42 H82 O5 N1	680.6198	17.28717	0.001	1.368	1.431	—	—	—	
Cer(d18:1/24:0)	Cer	C43 H84 O5 N1	694.6355	17.99214	0.002	1.893	1.423	—	—	—	
Cer(d18:1/24:1)	Cer	C43 H82 O5 N1	692.6198	16.51347	0.014	3.881	1.372	—	—	—	
LPC(16:0)	LPC	C25 H51 O9 N1 P1	540.3307	3.236844	0.000	1.157	1.460	—	—	—	
LPC(18:0)	LPC	C27 H55 O9 N1 P1	568.362	4.929942	0.016	1.612	1.386	—	—	—	
LPC(18:1)	LPC	C27 H53 O9 N1 P1	566.3463	3.43383	0.002	1.347	1.474	—	—	—	
LPC(20:4)	LPC	C29 H51 O9 N1 P1	588.3307	2.702941	0.023	1.167	1.610	—	—	—	
LPE(20:4)	LPE	C25 H43 O7 N1 P1	500.2783	2.830786	0.002	1.657	1.552	—	—	—	
LPE(22:6)	LPE	C27 H43 O7 N1 P1	524.2783	2.696826	0.002	2.536	1.640	—	—	—	
PC(18:0/20:4)	PC	C47 H85 O10 N1 P1	854.5917	12.64714	0.004	1.505	1.103	0.007	1.605	0.907	
PC(16:0/22:5)	PC	C47 H83 O10 N1 P1	852.576	12.042	0.046	1.805	1.422	—	—	—	
PE(16:0p/22:6)	PE	C43 H73 O7 N1 P1	746.513	11.99096	0.016	3.248	1.112	0.009	3.056	0.902	
PE(18:1p/22:6)	PE	C45 H75 O7 N1 P1	772.5287	12.0979	0.009	1.202	1.104	—	—	—	
PG(42:6)	PG	C48 H82 O10 N0 P1	849.5651	11.75907	0.022	1.445	1.248	—	—	—	
PC(16:0/20:4)	PC	C45 H81 O10 N1 P1	826.5604	11.53414	—	—	—	0.005	1.825	0.887	
PE(18:0p/20:4)	PE	C43 H77 O7 N1 P1	750.5443	13.11735	—	—	—	0.009	2.226	0.894	
PE(18:0/22:4)	PE	C45 H81 O8 N1 P1	794.5705	13.64911	—	—	—	0.017	1.971	0.905	
PS(18:0/22:6)	PS	C46 H77 O10 N1 P1	834.5291	13.47165	—	—	—	0.027	1.376	2.309	
PE(34:1e)	PE	C39 H77 O7 N1 P1	702.5443	13.497	—	—	—	0.030	1.789	1.250	
PE(18:0/20:4)	PE	C43 H77 O8 N1 P1	766.5392	12.85352	—	—	—	0.038	2.780	0.924	
PS(18:0/18:1)	PS	C42 H79 O10 N1 P1	788.5447	12.64461	—	—	—	0.044	2.484	1.284	

Notes: BSTSF: Bushen Tiansui Formula; AD: Alzheimer's disease; RT (min): retention time; VIP: variable importance; FC: fold change. Fold change was calculated as average relative quantitation obtained from group 1/group 2, and a value less than 1 indicates a decrease in the metabolites of group 1.

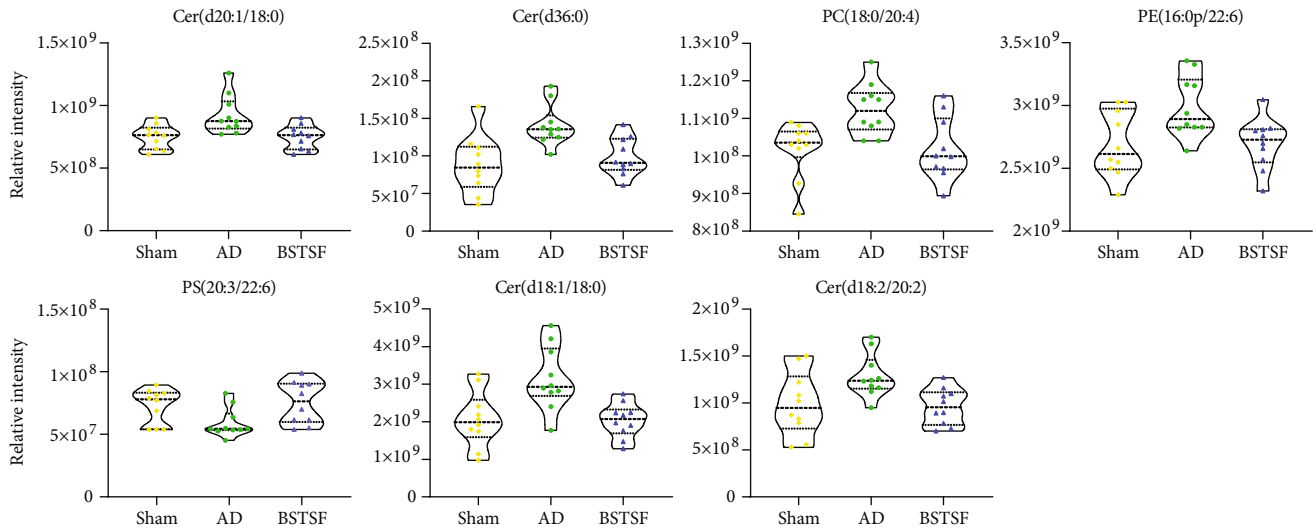


FIGURE 6: Changes in the relative signal intensities of differential lipids in the rat cerebral cortex from different groups.

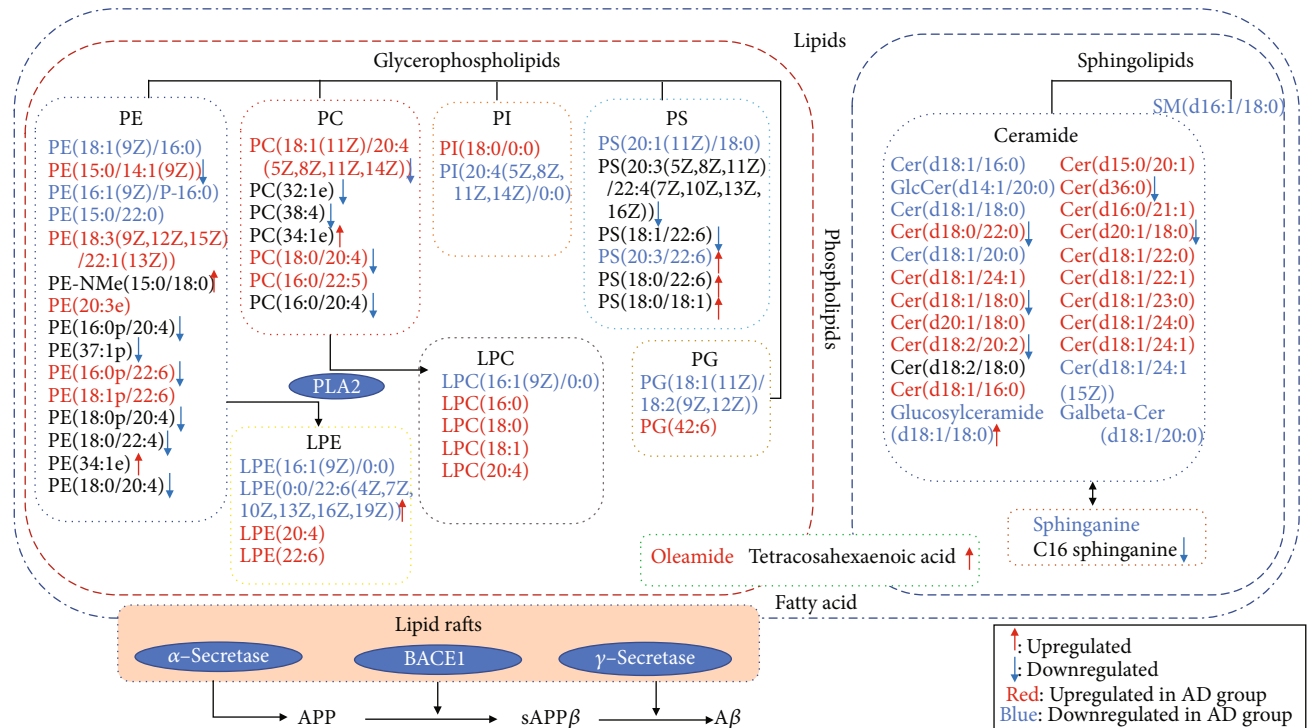


FIGURE 7: Lipid metabolism pathway map depicts the pathomechanism in AD rats and the therapeutic mechanism of BSTSF for AD. Notes: the red and blue letters indicate that the lipids were upregulated or downregulated, respectively, in group AD compared with group sham. The red upward arrow and blue downward arrow indicate that the lipids were upregulated or downregulated, respectively, by BSTSF.

Importantly, SMs have been associated with amyloidogenic processing of the amyloid precursor protein (APP) [25]. Here, we showed that the levels of SM(d16:1/18:0) were downregulated in AD brains when compared with those from the sham-treated group.

Glycerophospholipids were the second major class of lipid metabolites found to be related to AD pathology and BSTSF therapeutic mechanisms in the present study. Concentrations of glycerophospholipids have been associated with the severity of amyloid and neurofibrillary pathology

in AD [26]. In this study, the levels of PE(15:0/14:1(9Z)), PE(16:0p/22:6), LPE(0:0/22:6(4Z,7Z,10Z,13Z,16Z,19Z)), PC(18:1(11Z)/20:4(5Z,8Z,11Z,14Z)), PC(18:0/20:4), and PS(20:3/22:6) were dysregulated in AD rats when compared with those of rats in the sham group; however, this dysregulation was ameliorated after BSTSF treatment. A related study showed that BACE1 silencing restored PE derivatives such as LPE and etherphosphatidylethanolamine and reduced PLA2 phosphorylation, which favored cellular homeostasis and cognitive function recovery in the

hippocampus of triple transgenic AD mice [27]. Similar to our findings, the level of PC was increased in cerebrospinal fluid from AD patients and was associated with aberrant cerebrospinal fluid A β 1–42 values, which may be indicative of loss of membrane function and neurodegeneration in the early stages of cognitive dysfunction [14]. Our data confirmed that the concentrations of PC(18:1(11Z)/20:4(5Z,8Z,11Z,14Z)) and PC(18:0/20:4) were increased in the cerebral cortex of the AD rat, which may facilitate the aggregation of A β . Treatment with BSTSF may reduce A β aggregation through modulation of related PCs. Myelin is enriched in PS in brain tissue, and the docosahexaenoic acid (DHA) content of neuronal PS is of functional importance. Lower PS concentration can reduce the sensitivity of postsynaptic membranes to neurotransmitters such as acetylcholine [28]. PE was also reported to reduce reactive oxygen species levels and protect neuron membranes from oxidative damage [29]. One study found that PS supplementation significantly improved memory, information processing, and the ability to perform daily activities in elderly people [30]. Our data showed that the concentration of PS(20:3/22:6) was markedly upregulated in BSTSF-treated AD rats, which might ameliorate AD pathology by improving sensitivity to neurotransmitters and reducing oxidative damage.

The metabolites of sphingolipids and glycerophospholipids both belonged to phospholipid metabolism. So there was a serious disturbance of phospholipid metabolism in brain tissue of AD. Related research confirmed that ApoE proteins are critical determinants of brain phospholipid homeostasis. The phospholipid dysregulation contributes to ApoE4-associated cognitive deficits in AD pathogenesis [31]. APOE4 has been identified as the most prevalent genetic risk factor for AD [32], and it could exacerbate the intraneuronal accumulation of A β [33] and plaque deposition in the brain parenchyma [34]. Therefore, BSTSF might treat AD through regulating the APOE4 and phospholipid metabolism.

Additionally, we observed that the level of oleamide was upregulated in AD rats while that of tetracosahexaenoic acid was downregulated after BSTSF administration, and both of these lipids have roles in fatty acid metabolism. Oleamide has been found to accumulate in the cerebrospinal fluid of sleep-deprived cats and mice [35] and is an important regulatory lipid in the brain and central nervous system. Oleamide regulates the sleep-wake cycle, memory, locomotion, and pain perception and exhibits anti-inflammatory, anxiolytic, and neuroprotective properties [36]. Oleamide levels were shown to be increased in the plasma of AD patients [37]. A recent study indicated that DHA is both a product and a precursor of tetracosahexaenoic acid [38], while other investigations have shown that dietary DHA administration can exert protective effects against A β production, plaque deposition, and cerebral amyloid angiopathy in an aged mouse model of AD, as well as increasing cerebral blood volume [39, 40]. This indicates that BSTSF might regulate DHA and increase tetracosahexaenoic acid treating AD.

In the current study, the level of S-adenosylmethionine (SAM) was significantly upregulated in the cerebral cortex

of the AD rat, indicative of aberrant amino acid metabolism in AD. S-Adenosylmethionine is generated through the activity of methionine adenosyltransferases, and more than 50 endogenous substances in the body, including phosphatidylcholine, need SAM as the methyl donor. Homocysteine is formed by SAM demethylation. A related study showed that an elevated total homocysteine baseline serum level during six years was associated with an increased risk of dementia and AD, and the putative mechanism was associated with loss of total brain tissue volume and brain atrophy [41, 42]. Therefore, increased SAM concentrations in the AD brain may lead to higher levels of homocysteine, resulting in the loss of total brain tissue volume and brain atrophy. We found that BSTSF ameliorated AD pathology mainly through the alanine, aspartate, and glutamate metabolic pathway and the D-glutamine and D-glutamate metabolic pathway that is involved in regulating amino acid metabolism. N-Acetyl-L-aspartic acid (NAA) and L-aspartic acid are involved in the alanine, aspartate, and glutamate metabolic pathway. NAA is a biomarker for neuronal damage in the human brain during neurodegeneration [43], and reduced cortical levels of NAA were shown to be correlated with clinical scales of dementia severity [44]. L-Aspartic acid also functions as a neurotransmitter. D-Glutamine forms part of the D-glutamate metabolic pathway and is converted from glutamate by astrocytes in the brain [45]. Glutamate, as an excitatory neurotransmitter, is released decarboxylated by neurons to yield the inhibitory neurotransmitter gamma-aminobutyric acid (GABA) [46]. Numerous studies have shown that the level of GABA is closely associated with AD [47, 48]. D-Glutamine and GABA could be putative therapeutic targets of BSTSF in AD.

Through integrated metabolic and lipidomic analyses, we revealed the metabolic dysregulation in the cerebral cortex of the AD rat, as well as the metabolism-related therapeutic effects of BSTSF on AD. However, this study had some limitations. First, we only obtained a relative quantification of metabolite levels based on untargeted metabolomic analysis. Absolute quantitation of critical metabolites performed by targeted metabolomics is needed in future research. Second, numerous metabolites are regulated by BSTSF; however, the associated molecular mechanisms are not well understood and will be the basis of our future research.

5. Conclusions

The metabolic disturbance in the cerebral cortex of the AD rat is primarily associated with sphingolipid metabolism, glycerophospholipid metabolism, linoleic acid metabolism, and fatty acid metabolism. Moreover, BSTSF ameliorates the severity of AD by regulating phospholipid metabolism, maintaining fatty acid metabolism, and balancing amino acid metabolism. Our research highlighted some important mechanisms involved in the pathogenesis of AD and revealed the metabolism-related therapeutic effects of BSTSF on AD.

Data Availability

The necessary data are included within the article. All data are available from the corresponding authors on reasonable request.

Conflicts of Interest

The authors declare that there are no other nonfinancial competing interests.

Authors' Contributions

WP contributed to the design of this study, MY and CZ drafted the main manuscript, PX, ZZ, and PY conducted the experiments, and JH and MY analyzed all data. All the authors participated in the interpretation of results. All the authors have read and approved the final manuscript. Min Yi and Chunhu Zhang contributed equally to this work.

Acknowledgments

This work was financially supported by the National Natural Science Foundation of China (Nos. 81603670, 81873169, and 81673951) and the Hunan Provincial Natural Science Foundation of China (Nos. 2017JJ3459 and 2020JJ4803). We also thank Majorbio Bio-Pharm Technology Co., Ltd. (Shanghai, China) for their technical advice regarding our bioinformatic analysis.

References

- [1] E. Nichols, C. E. I. Szoek, S. E. Vollset et al., "Global, regional, and national burden of Alzheimer's disease and other dementias, 1990–2016: a systematic analysis for the Global Burden of Disease Study 2016," *The Lancet Neurology*, vol. 18, no. 1, pp. 88–106, 2019.
- [2] Alzheimer's Association, "2019 Alzheimer's disease facts and figures," *Alzheimer's & Dementia*, vol. 15, no. 3, pp. 321–387, 2019.
- [3] Z. Hou, F. Li, J. Chen et al., "Beneficial Effects of Sagacious Confucius' Pillow Elixir on Cognitive Function in Senescence-Accelerated P8 Mice (SAMP8) via the NLRP3/Caspase-1 Pathway," *Evidence-based Complementary and Alternative Medicine*, vol. 2019, Article ID 3097923, 13 pages, 2019.
- [4] Z. Zhang, P. Yi, J. Yang et al., "Integrated network pharmacology analysis and serum metabolomics to reveal the cognitive improvement effect of Bushen Tiansui Formula on Alzheimer's disease," *Journal of Ethnopharmacology*, vol. 249, p. 112371, 2020.
- [5] P. Foley, "Lipids in Alzheimer's disease: a century-old story," *Biochimica et Biophysica Acta (BBA) - Molecular and Cell Biology of Lipids*, vol. 1801, no. 8, pp. 750–753, 2010.
- [6] H. Braak and E. Braak, "Neuropathological stageing of Alzheimer-related changes," *Acta Neuropathologica*, vol. 82, no. 4, pp. 239–259, 1991.
- [7] D. R. Thal, U. Rub, C. Schultz et al., "Sequence of Abeta-protein deposition in the human medial temporal lobe," *Journal of Neuropathology and Experimental Neurology*, vol. 59, no. 8, pp. 733–748, 2000.
- [8] D. R. Thal, U. Rub, M. Orantes, and H. Braak, "Phases of A β -deposition in the human brain and its relevance for the development of AD," *Neurology*, vol. 58, no. 12, pp. 1791–1800, 2002.
- [9] E. Flores-Martinez and F. Pena-Ortega, "Amyloid β Peptide-Induced Changes in Prefrontal Cortex Activity and Its Response to Hippocampal Input," *International Journal of Peptide*, vol. 2017, article 7386809, 9 pages, 2017.
- [10] M. Garranzo-Asensio, P. San Segundo-Acosta, J. Martinez-Useros et al., "Identification of prefrontal cortex protein alterations in Alzheimer's disease," *Oncotarget*, vol. 9, no. 13, pp. 10847–10867, 2018.
- [11] V. R. Varma, A. M. Oommen, S. Varma et al., "Brain and blood metabolite signatures of pathology and progression in Alzheimer disease: a targeted metabolomics study," *PLoS Medicine*, vol. 15, no. 1, article e1002482, 2018.
- [12] A. Walter, U. Korth, M. Hilgert et al., "Glycerophosphocholine is elevated in cerebrospinal fluid of Alzheimer patients," *Neurobiology of Aging*, vol. 25, no. 10, pp. 1299–1303, 2004.
- [13] J. Bressler, B. Yu, T. H. Mosley et al., "Metabolomics and cognition in African American adults in midlife: the atherosclerosis risk in communities study," *Translational Psychiatry*, vol. 7, no. 7, article e1173, 2017.
- [14] J. B. Toledo, M. Arnold, G. Kastentmüller et al., "Metabolic network failures in Alzheimer's disease: a biochemical road map," *Alzheimer's & Dementia*, vol. 13, no. 9, pp. 965–984, 2017.
- [15] Z. A. Xia, W. Peng, S. Cheng et al., "Naoling decoction restores cognitive function by inhibiting the neuroinflammatory network in a rat model of Alzheimer's disease," *Oncotarget*, vol. 8, no. 26, pp. 42648–42663, 2017.
- [16] S. Hui, Y. Yang, W. J. Peng et al., "Protective effects of Bushen Tiansui decoction on hippocampal synapses in a rat model of Alzheimer's disease," *Neural Regeneration Research*, vol. 12, no. 10, pp. 1680–1686, 2017.
- [17] B. Yang, Z. A. Xia, B. Zhong et al., "Distinct hippocampal expression profiles of long non-coding RNAs in an Alzheimer's disease model," *Molecular Neurobiology*, vol. 54, no. 7, pp. 4833–4846, 2017.
- [18] X. Han, "Lipidomics for studying metabolism," *Nature Reviews. Endocrinology*, vol. 12, no. 11, pp. 668–679, 2016.
- [19] I. Kaya, E. Jennische, J. Dunevall et al., "Spatial lipidomics reveals region and long chain base specific accumulations of monosialogangliosides in amyloid plaques in familial Alzheimer's disease mice (5xFAD) brain," *ACS Chemical Neuroscience*, vol. 11, no. 1, pp. 14–24, 2020.
- [20] L. Yi, W. Liu, Z. Wang, D. Ren, and W. Peng, "Characterizing Alzheimer's disease through metabolomics and investigating anti-Alzheimer's disease effects of natural products," *Annals of the New York Academy of Sciences*, vol. 1398, no. 1, pp. 130–141, 2017.
- [21] N. M. de Wit, S. den Hoedt, P. Martinez-Martinez, A. J. Roze-muller, M. T. Mulder, and H. E. de Vries, "Astrocytic ceramide as possible indicator of neuroinflammation," *Journal of Neuroinflammation*, vol. 16, no. 1, p. 48, 2019.
- [22] S. M. M. Badawy, T. Okada, T. Kajimoto et al., "Extracellular α -synuclein drives sphingosine 1-phosphate receptor subtype 1 out of lipid rafts, leading to impaired inhibitory G-protein signaling," *The Journal of Biological Chemistry*, vol. 293, no. 21, pp. 8208–8216, 2018.

- [23] B. P. Head, H. H. Patel, and P. A. Insel, "Interaction of membrane/lipid rafts with the cytoskeleton: impact on signaling and function: membrane/lipid rafts, mediators of cytoskeletal arrangement and cell signaling," *Biochimica et Biophysica Acta*, vol. 1838, no. 2, pp. 532–545, 2014.
- [24] Y. A. Hannun and L. M. Obeid, "Principles of bioactive lipid signalling: lessons from sphingolipids," *Nature Reviews Molecular Cell Biology*, vol. 9, no. 2, pp. 139–150, 2008.
- [25] N. Fabelo, V. Martin, R. Marin, D. Moreno, I. Ferrer, and M. Diaz, "Altered lipid composition in cortical lipid rafts occurs at early stages of sporadic Alzheimer's disease and facilitates APP/BACE1 interactions," *Neurobiology of Aging*, vol. 35, no. 8, pp. 1801–1812, 2014.
- [26] L. Whiley, et al. A. Sen, J. Heaton et al., "Evidence of altered phosphatidylcholine metabolism in Alzheimer's disease," *Neurobiology of Aging*, vol. 35, no. 2, pp. 271–278, 2014.
- [27] J. G. Villamil-Ortiz, A. Barrera-Ocampo, D. Piedrahita, C. M. Velásquez-Rodríguez, J. D. Arias-Londoño, and G. P. Cardona-Gómez, "BACE1 RNAi restores the composition of phosphatidylethanolamine-derivates related to memory improvement in aged 3xTg-AD mice," *Frontiers in Cellular Neuroscience*, vol. 10, p. 260, 2016.
- [28] M. J. Glade and K. Smith, "Phosphatidylserine and the human brain," *Nutrition*, vol. 31, no. 6, pp. 781–786, 2015.
- [29] H. C. Chaung, C. D. Chang, P. H. Chen, C. J. Chang, S. H. Liu, and C. C. Chen, "Docosahexaenoic acid and phosphatidylserine improves the antioxidant activities in vitro and in vivo and cognitive functions of the developing brain," *Food Chemistry*, vol. 138, no. 1, pp. 342–347, 2013.
- [30] T. Cenacchi, T. Bertoldin, C. Farina, M. G. Fiori, and G. Crepaldi, "Cognitive decline in the elderly: a double-blind, placebo-controlled multicenter study on efficacy of phosphatidylserine administration," *Aging*, vol. 5, no. 2, pp. 123–133, 1993.
- [31] L. Zhu, M. Zhong, G. A. Elder et al., "Phospholipid dysregulation contributes to ApoE4-associated cognitive deficits in Alzheimer's disease pathogenesis," *Proceedings of the National Academy of Sciences of the United States of America*, vol. 112, no. 38, pp. 11965–11970, 2015.
- [32] M. O. W. Grimm, D. M. Michaelson, and T. Hartmann, "Omega-3 fatty acids, lipids, and apoE lipidation in Alzheimer's disease: a rationale for multi-nutrient dementia prevention," *Journal of Lipid Research*, vol. 58, no. 11, pp. 2083–2101, 2017.
- [33] D. Z. Christensen, T. Schneider-Axmann, P. J. Lucassen, T. A. Bayer, and O. Wirths, "Accumulation of intraneuronal Abeta correlates with ApoE4 genotype," *Acta Neuropathologica*, vol. 119, no. 5, pp. 555–566, 2010.
- [34] Y. Yamazaki, N. Zhao, T. R. Caulfield, C.-C. Liu, and G. Bu, "Apolipoprotein E and Alzheimer disease: pathobiology and targeting strategies," *Nature Reviews Neurology*, vol. 15, no. 9, pp. 501–518, 2019.
- [35] B. F. Cravatt, O. Prospero-Garcia, G. Siuzdak et al., "Chemical characterization of a family of brain lipids that induce sleep," *Science*, vol. 268, no. 5216, pp. 1506–1509, 1995.
- [36] E. K. Farrell and D. J. Merkler, "Biosynthesis, degradation and pharmacological importance of the fatty acid amides," *Drug Discovery Today*, vol. 13, no. 13-14, pp. 558–568, 2008.
- [37] M. Kim, S. Snowden, T. Suvitaival et al., "Primary fatty amides in plasma associated with brain amyloid burden, hippocampal volume, and memory in the European Medical Information Framework for Alzheimer's disease biomarker discovery cohort," *Alzheimer's & Dementia*, vol. 15, no. 6, pp. 817–827, 2019.
- [38] A. H. Metherel, R. J. S. Lacombe, R. Chouinard-Watkins, and R. P. Bazinet, "Erratum: docosahexaenoic acid is both a product of and a precursor to tetraacosahexaenoic acid in the rat," *Journal of Lipid Research*, vol. 60, no. 12, p. 2102, 2019.
- [39] C. R. Hooijmans, C. E. E. M. van der Zee, P. J. Dederen et al., "DHA and cholesterol containing diets influence Alzheimer-like pathology, cognition and cerebral vasculature in APP_{swe}/PS1_{dE9} mice," *Neurobiology of Disease*, vol. 33, no. 3, pp. 482–498, 2009.
- [40] C. I. F. Janssen and A. J. Kiliaan, "Long-chain polyunsaturated fatty acids (LCPUFA) from genesis to senescence: the influence of LCPUFA on neural development, aging, and neurodegeneration," *Progress in Lipid Research*, vol. 53, pp. 1–17, 2014.
- [41] B. Hooshmand, H. Refsum, A. D. Smith et al., "Association of methionine to homocysteine status with brain magnetic resonance imaging measures and risk of dementia," *JAMA Psychiatry*, vol. 76, no. 11, p. 1198, 2019.
- [42] B. Hooshmand, F. Mangialasche, G. Kalpouzos et al., "Association of vitamin B12, folate, and sulfur amino acids with brain magnetic resonance imaging measures in older adults," *JAMA Psychiatry*, vol. 73, no. 6, pp. 606–613, 2016.
- [43] A. Forgacsova, J. Galba, R. M. Garruto, P. Majerova, S. Katina, and A. Kovac, "A novel liquid chromatography/mass spectrometry method for determination of neurotransmitters in brain tissue: application to human tauopathies," *Journal of Chromatography. B, Analytical Technologies in the Biomedical and Life Sciences*, vol. 1073, pp. 154–162, 2018.
- [44] P. F. Kwo-On-Yuen, R. D. Newmark, T. F. Budinger, J. A. Kaye, M. J. Ball, and W. J. Jagust, "Brain N-acetyl-l-aspartic acid in Alzheimer's disease: a proton magnetic resonance spectroscopy study," *Brain Research*, vol. 667, no. 2, pp. 167–174, 1994.
- [45] M. El Hage, J. Masson, A. Conjard-Duplany, B. Ferrier, G. Baverel, and G. Martin, "Brain slices from glutaminase-deficient mice metabolize less glutamine: a cellular metabolic study with carbon 13 NMR," *Journal of Cerebral Blood Flow & Metabolism*, vol. 32, no. 5, pp. 816–824, 2012.
- [46] A. Schousboe and H. S. Waagepetersen, "Glial modulation of GABAergic and glutamate ergic neurotransmission," *Current Topics in Medicinal Chemistry*, vol. 6, no. 10, pp. 929–934, 2006.
- [47] Y. Fu, L. Li, Y. Wang, G. Chu, X. Kong, and J. Wang, "Role of GABAA receptors in EEG activity and spatial recognition memory in aged APP and PS1 double transgenic mice," *Neurochemistry International*, vol. 131, p. 104542, 2019.
- [48] V. Pilipenko, K. Narbutė, I. Amara et al., "GABA-containing compound gammapyrone protects against brain impairments in Alzheimer's disease model male rats and prevents mitochondrial dysfunction in cell culture," *Journal of Neuroscience Research*, vol. 97, no. 6, pp. 708–726, 2019.

Research Article

Antia, a Natural Antioxidant Product, Attenuates Cognitive Dysfunction in Streptozotocin-Induced Mouse Model of Sporadic Alzheimer's Disease by Targeting the Amyloidogenic, Inflammatory, Autophagy, and Oxidative Stress Pathways

Nesrine S. El Sayed ¹ and Mamdooh H. Ghoneum ²

¹Department of Pharmacology and Toxicology, Faculty of Pharmacy, Cairo University, Cairo, Egypt

²Department of Surgery, Charles Drew University of Medicine and Science, Los Angeles, California, USA

Correspondence should be addressed to Nesrine S. El Sayed; nesrine_salah2002@yahoo.com

Received 17 March 2020; Revised 7 April 2020; Accepted 11 April 2020; Published 18 June 2020

Guest Editor: Francisco Jaime B. Mendonça Junior

Copyright © 2020 Nesrine S. El Sayed and Mamdooh H. Ghoneum. This is an open access article distributed under the Creative Commons Attribution License, which permits unrestricted use, distribution, and reproduction in any medium, provided the original work is properly cited.

Background. Many neurodegenerative diseases such as Alzheimer's disease are associated with oxidative stress. Therefore, antioxidant therapy has been suggested for the prevention and treatment of neurodegenerative diseases. **Objective.** We investigated the ability of the antioxidant Antia to exert a protective effect against sporadic Alzheimer's disease (SAD) induced in mice. Antia is a natural product that is extracted from the edible yamabushitake mushroom, the gotsukora and kothala himbutu plants, diosgenin (an extract from wild yam tubers), and amla (Indian gooseberry) after treatment with MRN-100. **Methods.** Single intracerebroventricular (ICV) injection of streptozotocin (STZ) (3 mg/kg) was used for induction of SAD in mice. Antia was injected intraperitoneally (i.p.) in 3 doses (25, 50, and 100 mg/kg/day) for 21 days. Neurobehavioral tests were conducted within 24 h after the last day of injection. Afterwards, mice were sacrificed and their hippocampi were rapidly excised, weighed, and homogenized to be used for measuring biochemical parameters. **Results.** Treatment with Antia significantly improved mice performance in the Morris water maze. In addition, biochemical analysis showed that Antia exerted a protective effect for several compounds, including GSH, MDA, NF- κ B, IL-6, TNF- α , and amyloid β . Further studies with western blot showed the protective effect of Antia for the JAK2/STAT3 pathway. **Conclusions.** Antia exerts a significant protection against cognitive dysfunction induced by ICV-STZ injection. This effect is achieved through targeting of the amyloidogenic, inflammatory, and oxidative stress pathways. The JAK2/STAT3 pathway plays a protective role for neuroinflammatory and neurodegenerative diseases such as SAD.

1. Introduction

Age-related neurodegenerative diseases like Alzheimer's disease (AD) are on the rise. AD is a disorder characterized by progressive deterioration of cognition and memory, and it accounts for 60-80% of all dementia cases [1]. Among the elderly, the most common type of AD is sporadic Alzheimer's disease (SAD), a type that involves the central nervous system's progressive degeneration [2]. Several pathways have been examined as possible targets for SAD, including the oxidative stress, amyloidogenic, inflammatory, and autophagy pathways.

One of the earliest changes in AD brains is the appearance of oxidative stress markers, which precedes the accumulation of neurofibrillary tangles and visible amyloid deposits [3]. Oxidative stress is implicated in many disorders like chronic inflammation, AD, and Parkinson's disease [4]. The brain's neurons have high rates of energy production and oxygen consumption, making them extremely sensitive to excessive generation of reactive oxygen species (ROS) and oxidative damage [5].

In AD brains, normally solid amyloid β ($A\beta$) and tau proteins assemble into amyloid-like filaments called plaques and tangles. The manner by which $A\beta$ accumulates in the

central nervous system and triggers cell disease is currently unresolved, but a suggested mechanism by which $A\beta$ may damage neurons and cause neuronal death includes ROS generation during $A\beta$ self-aggregation. When this process was observed in vitro on neuron membranes, it ultimately led to mitochondrial impairment, excessive calcium influx, and synaptic membrane depolarization [6, 7].

Neurodegenerative diseases like AD are also accompanied by neuroinflammation. The inflammatory response of neurons has been linked with the transcription factor NF- κ B. In normal conditions, NF- κ B forms an inactive cytoplasmic complex with $I\kappa$ B α , its inhibitor. When NF- κ B is stimulated, however, it can induce the transcription of inflammatory target genes such as interleukin-1 β (IL-1 β), interleukin-6 (IL-6), tumor necrosis factor- α (TNF- α), and cyclooxygenase-2 (COX-2). In addition, neuroinflammation has been linked with autophagy in neurodegenerative diseases. Neuroinflammation can result in a deficit of autophagy that exacerbates neurodegeneration and, conversely, a disruption of autophagy during pathological conditions can initiate or intensify neuroinflammation [8]. In human AD and in mouse models of AD, decreased autophagy has been observed and found to contribute to pathological build-up of tau aggregates [9]. Autophagy is known to be regulated by mTOR, rapamycin's mammalian target, and mTOR inhibition has been found to prevent neuroinflammation in a mouse model of cerebral palsy [10]. Moreover, in a study of rat cortices subjected to ischemic brain injury, it has been shown that GSK-3 β inhibition suppresses neuroinflammation through autophagy activation [11].

Pharmacological management of AD has been limited to date. In 2007, long-term use of nonsteroidal anti-inflammatory drugs (NSAIDs) was considered to be linked with a reduced probability of developing AD [12]. NSAIDs were also indicated by evidence to potentially reduce amyloid-plaque-related inflammation, but high adverse events caused a suspension of trials [13]. AD risk has not been found to decrease with any medications or supplements [13], and unfortunately, current treatments for AD that are FDA-approved offer only symptomatic relief and are not able to cure or delay the disease [1].

Recently, antioxidants have received increased attention in preventing the onset of AD by reducing oxidative stress insult [14, 15]. Furthermore, there has been an acceleration in the search for and use of drugs and dietary supplements from plants, due in part to the health benefits that have been found in phytochemicals whose uses have been documented in traditional medicine [16]. Components of the traditional Chinese medicinal mushroom called yamabushitake promote nerve growth factor synthesis in cultured astrocytes [17, 18] as well as improving mild cognitive impairment in humans [19]. The gotukora plant has traditionally been used for dementia and memory improvement [20, 21], and its extracts have been shown to improve memory retention in rodents [22], to alter amyloid beta pathology in the hippocampi of a mouse model of AD, and to modulate the oxidative stress response involved in AD-related neurodegeneration [23]. Diosgenin, a plant-derived steroidal sapogenin, has been

shown to exert anticancer effects [24], improve aging-related cognitive deficits [25], and relieve diabetic neuropathy [26]. Recently, it was proven that diosgenin improves memory function and reduces axonal degeneration in AD mouse models [20, 27]. Amla (*Emblica officinalis*), the Indian gooseberry, has been shown to exert diverse neuroprotective pharmacodynamic actions [28]; to have potent radical scavenging effects [29]; to have a high degree of neuroprotective potential in a panel of bioassays that targeted protein glycation, carbonyl stress, acetylcholinesterase inhibition, oxidative stress, $A\beta$ fibrillation, and neuroinflammation [30]; and to improve the acetylcholinesterase activity, brain antioxidant enzymes, and cognitive functions in a rat model of AD [31]. Finally, kothala himbutu (*Salacia reticulata*) has been shown to protect against deleterious cognitive changes in young streptozotocin-induced diabetic rats [32] and against mercury toxicity in mice hippocampi [33].

In this study, we examine the cogno-protective effects of an antioxidant product called Antia whose components include yamabushitake, gotukora, diosgenin, amla, and kothala himbutu. These components are treated together with the hydroferrate fluid MRN-100 to generate Antia. Long-term administration of MRN-100 revealed its protective effect against age-associated oxidative stress [34] and against oxidative damage in human leukemia cells and in endothelial cells [35]. Recent studies on Antia have shown its ability to reverse mitochondrial dysfunction caused by oxidative stress in human peripheral blood lymphocytes [36]. In light of the above-mentioned neuroprotective effects of Antia's plant components, we hypothesized that Antia would have beneficial effects on the pathways relevant to AD, namely, the oxidative stress, amyloidogenic, inflammatory, and autophagy pathways. We studied the effect of Antia on mice induced with SAD via intracerebroventricular (ICV) injection of streptozotocin (STZ); this is a well-established animal model of SAD based on brain resistance to insulin [37] and imitates the age-related pathology of SAD in humans such as memory impairment, oxidative stress, neuroinflammation, and neurodegeneration [38]. Here, we present behavioral, biochemical, and western blot experiments in support of our hypothesis.

2. Materials and Methods

2.1. Animals. Adult male albino mice 25-30 g in weight were provided by the animal facility of the Faculty of Pharmacy, Cairo University, Egypt. For one week before conducting the study, the mice were allowed to acclimate. Mice were housed in a controlled environment with constant temperature ($25 \pm 2^\circ\text{C}$), relative humidity of $60 \pm 10\%$, and a 12/12 h light/dark cycle. Standard chow diet and water were allowed ad libitum. Every effort was made to minimize mice suffering and to reduce the mice number used. This study was approved by the Ethics Committee for Animal Experimentation and complied with the recommendations of the National Institutes of Health Guide for Care and Use of Laboratory Animals (2011).

2.2. Chemicals. STZ was purchased from Sigma-Aldrich Co. (St Louis, MO, USA). STZ was dissolved in saline solution (0.9% NaCl) and injected ICV at a volume of 10 μ L by the freehand method. Antia was dissolved in saline solution in three doses: 25 mg/kg equivalent to the adult dose (4 tablets/day), 50 mg/kg, and 100 mg/kg. It was then administered intraperitoneally (i.p.) at a volume of 0.1 mL/20 g-mouse. Each day, fresh drug solutions were prepared. Equivalent volumes and administration routes were used for the control group's saline injections. All other chemicals were of the highest analytical grade.

2.3. Antia. Antia is a natural compound derived from a variety of mushrooms and plants, including the edible yamabushitake mushroom, the gotsukora and kothala himbutu plants, diosgenin (an extract from the tubers of *Dioscorea* wild yam), and amla (Indian gooseberry). The ingredients are treated with an iron-based fluid called MRN-100. MRN-100 is made from phytosin and is an iron-based compound derived from bivalent and trivalent ferrates (hydroferrate fluid). The exact chemical composition of Antia is still under active investigation. Antia was provided by ACM Co., Ltd, Japan. Antia was prepared in distilled water (DW) with the concentration of MRN-100 at about 2×10^{-12} mol/L.

2.4. Induction of SAD. SAD was induced by ICV injection of STZ (3 mg/kg) into the lateral ventricle of mice according to the freehand procedure [39] and as updated by Warnock [40] to avoid the probability of cerebral vein penetration. Anesthetization of mice was carried out with thiopental (5 mg/kg, i.p.). Their heads were stabilized with downward pressure above the ears, and a needle was directly inserted through the skin and skull into the lateral ventricle. The bregma was located by visualizing an equilateral triangle between the center of the skull and the eyes, allowing the needle to be inserted approximately 1 mm lateral to this point. Normal behavior was observed one minute after injection.

2.5. Experimental Design. The experimental design is illustrated in Figure 1. Mice were divided randomly into five groups containing 12 animals each. Group I (sham control): mice received ICV injection once and intraperitoneal (i.p.) saline injection for 21 consecutive days and served as the sham control group. Group II (STZ): mice received STZ (3 mg/kg, ICV) once and served as a model for SAD [41]. Group III (STZ+Antia 1): mice received STZ (3 mg/kg, ICV) followed by Antia (25 mg/kg, i.p.) after five hours and then every day for 21 consecutive days. Group IV (STZ+Antia 2): mice received STZ (3 mg/kg, ICV) followed by Antia (50 mg/kg, i.p.) after five hours and then every day for 21 consecutive days. Group V (STZ+Antia 3): mice received STZ (3 mg/kg, ICV) followed by Antia (100 mg/kg, i.p.) after five hours and then every day for 21 consecutive days. 24h after the end of treatments, neurobehavioral tests were carried out, including object recognition and Morris water maze (MWM) tests, sequentially arranged from the least to most stressful. Testing was performed during animals' light cycle under top illumination to minimize circadian variability. No mortality was observed among all

the animals in different groups during the experimental period of 21 days.

2.6. Acute Toxicity Study. The acute toxicity of Antia was evaluated in mice using the up and down procedure according to the Organization for Economic Cooperation and Development (OECD), guideline no. 423, 2001 [42].

Mice received Antia starting at a dose of 2 g/kg. The animals were observed for toxic symptoms continuously for 24 hours and then maintained for additional 20 days with daily observations.

2.7. Behavioral Assessments

2.7.1. Object Recognition Test. Long-term memory and cognition were assessed via the object recognition test [43]. In this study, the performed tests took place over three consecutive days. On day one (the habituation phase), each mouse was individually placed into a wooden box of dimensions $30 \times 30 \times 30$ cm³ for 30 min in order to adapt to the surrounding environment. Day two was designed for familiarization or training, where two wooden cubes identical in shape, color, and size were placed in opposite corners of the box, 2 cm from the walls. Each mouse was placed in the middle of the box and was left to explore these two objects for 10 min. On day three, testing took place. A novel object that was different from the identical cubes in shape, size, and color was used to replace one of the two identical cubes. Each mouse was exposed again to these two objects for 5 min. 70% ethanol was used to clean objects between animal experiments to ensure that odor cues did not guide behavior. All locations and objects were adjusted to decrease biases due to inclinations for particular objects or locations. Mice were always placed in the box confronting the same wall, and mice were unable to physically move the objects. The animals' behavior was video-recorded and the following parameters were calculated:

- (1) Discrimination index: temporal difference between exploring the novel object and the familiar object divided by the total time used to explore both objects. The measurement varies between -1 and +1, where a negative (positive) score indicates that more (less) time was used to explore the familiar object, and a score of zero indicates no preference
- (2) Preference index: time spent by the animal exploring the novel object as a percentage of the total time exploring both objects

2.7.2. Morris Water Maze Test. Spatial learning and memory was assessed via the Morris water maze (MWM) test [44]. The maze consisted of stainless-steel circular tanks (210 cm in diameter, 51 cm high) filled with water ($25 \pm 2^\circ$ C, 35 cm deep) and divided into four quadrants. A submerged black platform (10 cm width, 28 cm height) was placed in a target quadrant 2 cm below the surface of the water. This platform remained at a consistent position during the time of training and the test. A nontoxic purple dye was added to the water to obscure any visible evidence of the platform's position. Trials

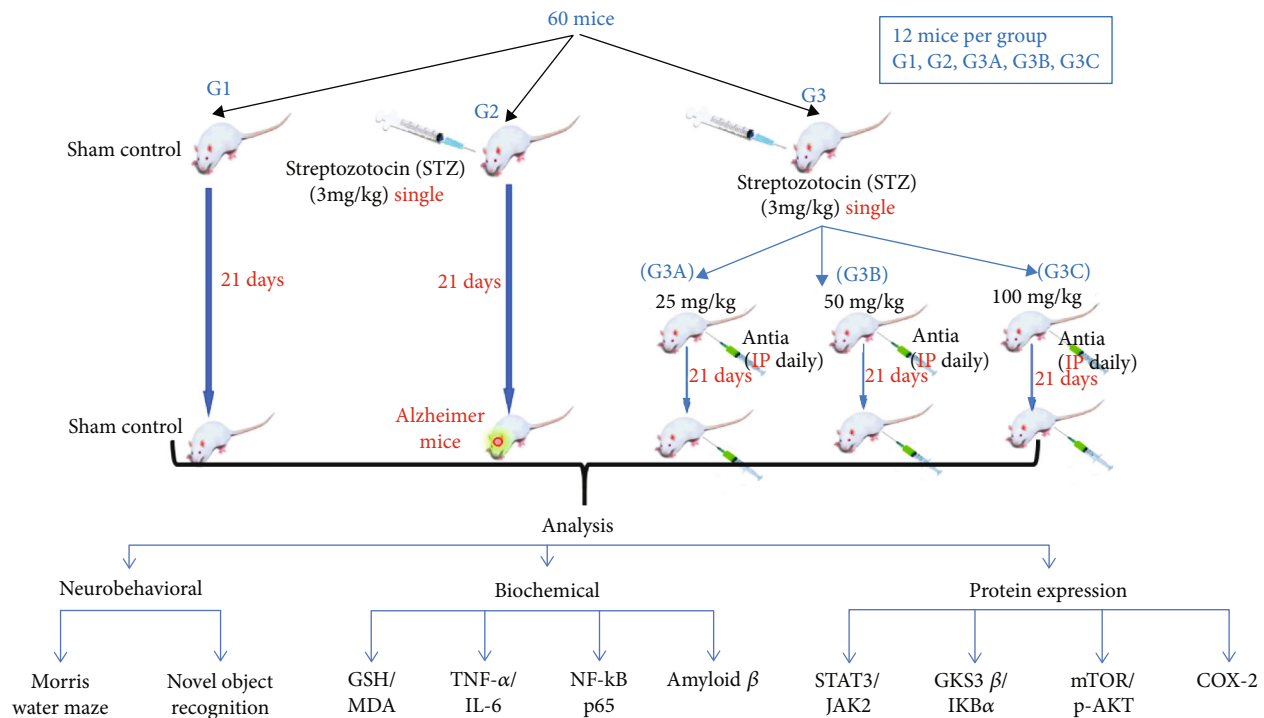


FIGURE 1: Experimental design.

for memory acquisition (120 s/trial) were performed 2x/day over four consecutive days, with a period between trials of at least 15 min. For each acquisition trial, mice were left free to locate the hidden platform in the target quadrant. If a mouse located the platform, it was allowed to rest there for 20 s, while if a mouse failed to locate the platform within 120 s, it was gently guided to the platform and allowed to rest there for 20 s. The mean escape latency was measured as the time taken by each mouse to locate the hidden platform and was used as an index of learning or acquisition. On day five, the mice were given a probe-trial session. The platform was taken out of the pool and each mouse was given 60 s to probe the pool. The time each mouse spent in the target quadrant of the previously placed platform was measured as an indicator of memory or retrieval.

2.8. Brain Processing. After behavioral testing, cervical dislocation was used to euthanize mice and brains were rapidly dissected and washed with ice-cold saline. The hippocampi ($n = 6$) were excised from each brain on an ice-cold glass plate. The hippocampus was homogenized in ice-cold saline to prepare 10% homogenates. These were split into several aliquots and stored at -80°C . The other hippocampus was stored at -80°C to be used for western blot analysis.

2.9. Biochemical Measurements

2.9.1. Determination of Oxidative Stress Biomarkers. Hippocampal lipid peroxidation was estimated by measuring malondialdehyde (MDA) levels. MDA was determined by measuring the thiobarbituric acid reactive substances as

described in [45]. Brain glutathione (GSH) content was measured spectrophotometrically using Ellman's reagent as described in [46]. The results are expressed as mmol/mg protein.

2.9.2. Determination of Inflammatory Biomarkers and Amyloid β_{1-42} . Hippocampal TNF- α , IL-6 levels, NF- κ B p65, and β -amyloid $_{1-42}$ were measured using mouse ELISA kits purchased from RayBiotech Inc. (Norcross, GA, USA) and R&D Systems Inc. (Minneapolis, USA), respectively. The procedures were performed according to the manufacturers' instructions. Results are presented as pg/mg protein for TNF- α , IL-6, NF- κ B p65, and β -amyloid $_{1-42}$.

2.9.3. Western Blot Analysis. Protein solutions were extracted from brain tissues, after which equal protein amounts (20–30 μg of total protein) were separated by SDS-PAGE (10% acrylamide gel) and transferred to polyvinylidene difluoride membranes (Pierce, Rockford, IL, USA) with a Bio-Rad Trans-Blot system. Western blot immunodetection was performed by incubating membranes for 1 h at room temperature with blocking solution comprised of 20 mM Tris-Cl, pH 7.5, 150 mM NaCl, 0.1% Tween 20, and 3% bovine serum albumin. Membranes were incubated overnight at 4°C with one of the following primary antibodies: P-JAK2 (Tyr 1007/1008), P-STAT3 (Tyr 705), I κ B α , GSK-3 β , mTOR, COX-2, or β -actin, obtained from Thermo Fisher Scientific Inc. (Rockford, IL, USA). Peroxidase-labelled secondary antibodies were added after washing, and the membranes were incubated at room temperature for 1 h. ChemiDoc™ imaging system with Image Lab™ software version 5.1 (Bio-Rad Laboratories Inc., Hercules, CA, USA) was used

to analyze the band intensity. Results are presented in arbitrary units after normalization to levels of the β -actin protein.

2.9.4. Determination of Protein Content. The method of Bradford was used to measure protein content. All results are expressed as tissue concentration per mg protein.

2.10. Statistical Analysis. The presented data are mean \pm S.E. One-way analysis of variance (ANOVA) followed by the Tukey-Kramer multiple comparison test was used in data analysis. GraphPad Prism software (version 6; GraphPad Software, Inc., San Diego, CA, USA) was used for statistical analysis and the creation of graphical presentations. Significance levels of all statistical tests are set at $p < 0.05$.

3. Results

The acute toxicities of the tested *Antia* were studied, and the results showed no general behavior changes, toxicity, and mortality in test animals up to the dose level of 2 g/kg during a 24 h period, thus indicating that this substance had no toxicity.

The effects of *Antia* on the behavioral and biochemical functions of ICV-STZ-treated mice were measured with neurobehavioral tests and biochemical analysis of the hippocampal content. The effects of STZ and *Antia* (25, 50, and 100 mg/kg) on neurobehavioral tests were carried out within 24 h after the last day of *Antia* injection. The Morris water maze was used to examine the possible protective effect of *Antia* treatment on ICV-STZ-injected mice. As illustrated in Figure 2(a) for the mean escape latency (MEL), mice in different groups took different times to escape on day 2. STZ-treated mice took 1.63 times as long to escape on day 2 as compared to sham control mice. Treatment of STZ-injected mice with *Antia*, however, took only 1.08 times as long as sham control mice on day 2. These results were further confirmed in the subsequent days 3 and 4. The study of the effect of *Antia* on the time mice spent in the target quadrant of the Morris water maze (Figure 2(b)) showed that STZ-treated mice spent only 25.4% of the time in the quadrant in comparison with sham control mice, while treatment of STZ-injected mice with 25, 50, and 100 mg/kg of *Antia* spent 72.5%, 75.8%, and 85.4% of the time, respectively, in comparison with sham control mice.

The effect of STZ and *Antia* was further examined through the discrimination and preference indices of the novel object recognition test. The discrimination index was decreased in STZ-induced SAD mice when compared to the sham control group, but it was significantly increased after *Antia* administration (25, 50, and 100 mg/kg) as compared to the STZ group in a dose-dependent manner. In addition, the time spent exploring the novel object was lower in ICV-STZ-injected mice by 63% compared to the sham control group, reflecting a lower preference index. *Antia* administration (25, 50, and 100 mg/kg) normalized the preference index, indicating that *Antia*-treated mice preferred the novel object over the familiar object in a dose-dependent manner (Figure 2(c)).

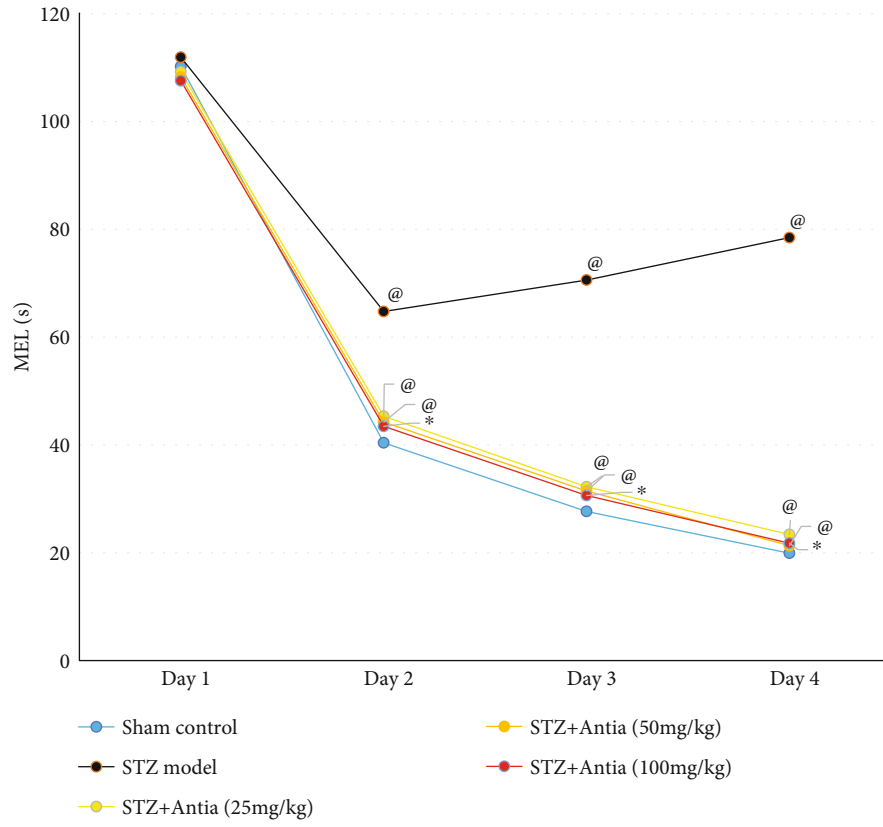
Several biochemical analyses of the hippocampal content in ICV-STZ-treated mice were conducted in order to examine the ability of *Antia* to attenuate the amyloidogenic, inflammatory, autophagy, and oxidative stress pathways. Measurements of the protective effect of *Antia* treatments on the levels of malondialdehyde (MDA) and glutathione (GSH) hippocampal content were carried out. Results in Figure 3(a) show that STZ-treated mice had a GSH level that was 15.5% of the GSH level of sham control mice. On the other hand, treatment of STZ-injected mice with *Antia* showed an elevation in the GSH content in a dose-dependent manner that maximized at 78.7% of the control GSH level for 100 mg/kg *Antia* treatment. Results of the levels of MDA hippocampal content show significantly higher levels of MDA in ICV-STZ-injected mice as compared with sham control mice by a factor of 4.3-fold. On the other hand, Alzheimer's mice with *Antia* showed an elevation in the MDA content of only 3.5-fold, 2.5-fold, and 1.8-fold for mice receiving *Antia* at doses of 25, 50, and 100 mg/kg, respectively (Figure 3(b)).

The effect of ICV-STZ injection on the hippocampal content of anti-inflammatory cytokines was also examined in the presence and absence of *Antia* treatment. Two cytokines were examined: TNF- α and IL-6. Results in Figure 4 show that STZ model mice exhibited a significant increase in TNF- α and IL-6 cytokine expression as compared with sham control, but *Antia* treatment suppressed this induction in a dose-dependent fashion, reaching the control's level at 100 mg/kg. A similar trend can also be seen in the hippocampal content of NF- κ B p65. Results in Figure 4 show increased levels of NF- κ B p65 in STZ-treated mice and its gradual decrease after treatment with *Antia*.

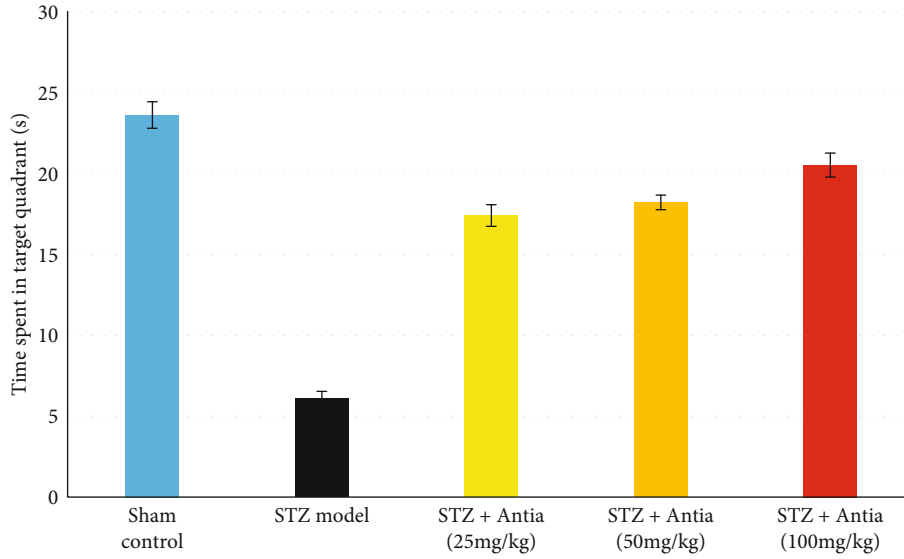
Since amyloid β makes up Alzheimer's disease plaques, we examined the effect of *Antia* on Amyloid β_{1-42} hippocampal content in ICV-STZ-injected mice. Results depicted in Figure 5 show that STZ model mice exhibited an approximately 4-fold increase in the expression of amyloid β as compared with sham control mice. However, amyloid β levels were significantly decreased after treatment with *Antia*. The effect was dose-dependent and reached its lowest levels at 100 mg/kg.

We further examined protein expression. The levels of phosphorylation of STAT and JAK protein expression are a well-established method used in Alzheimer's research. We examined whether treatment with *Antia* suppresses the phosphorylation of STAT expression in STZ mice. As expected, the levels of phosphorylation of STAT protein expression were significantly increased when compared with sham control mice. However, treatment of STZ mice with *Antia* caused a significant inhibition in the phosphorylation level of STAT3 (Figure 6(a)). A similar trend in results was observed with JAK2 protein expression. *Antia* treatment resulted in a significant inhibition in the phosphorylation level of JAK2 due to of STZ injection (Figure 6(a)). These results indicate the protective effect of *Antia* for the JAK2/STAT3 pathway.

Earlier studies have shown that glycogen synthase kinase-3 (GSK-3) phosphorylates tau protein, the primary component of neurofibrillary tangles. GSK-3 β inhibition presents



(a)



(b)

FIGURE 2: Continued.

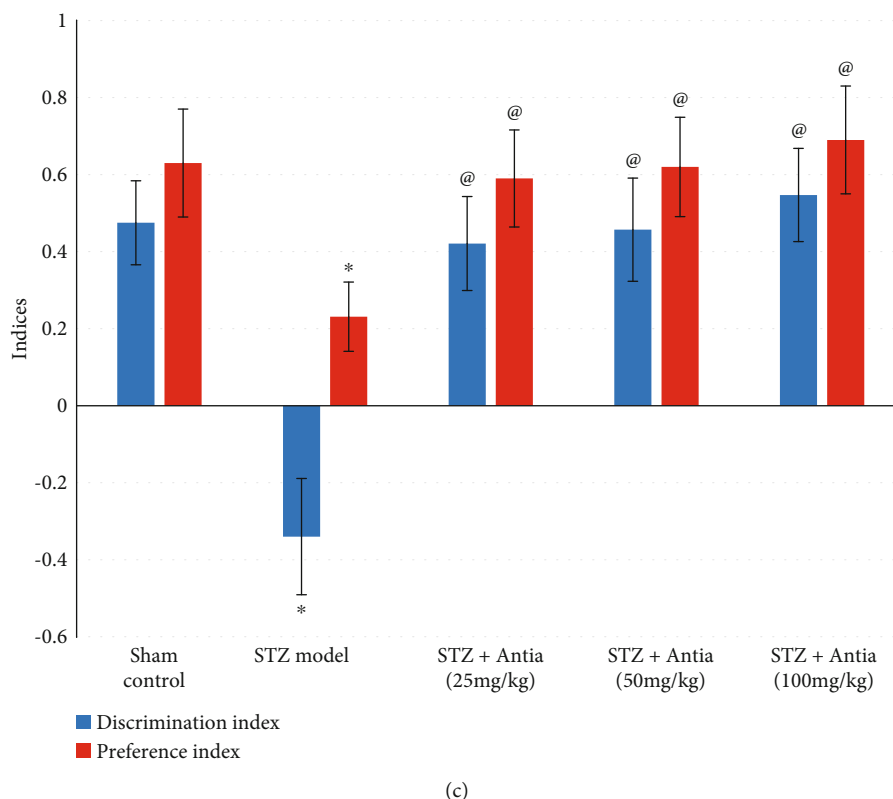


FIGURE 2: (a) Effect of Antia on mean escape latency (MEL) in Morris water maze, (b) effect of Antia on time spent in target quadrant in Morris water maze, and (c) effect of Antia on cognitive function in the novel object recognition test for ICV-STZ-injected mice. *Significantly different from the sham control group at $p < 0.05$. @Significantly different from the ICV-STZ group at $p < 0.05$.

a new method for reducing the formation of both neurofibrillary tangles and amyloid plaques, two of Alzheimer's disease's pathological hallmarks [47]. Results in Figure 6(b) show that STZ-treated mice had a higher expression of GSK-3 β level that was 7-fold larger than the GSK-3 β level of sham control mice. Antia treatment, however, resulted in a dramatic inhibition in the expression of GSK-3 β that was approximately 3-fold of the control. Results in Figure 6(b) also show that STZ-treated mice had an approximately 6.5-fold larger I κ B α level expression than the sham control mice, whereas Antia treatment resulted in a dramatic inhibition in the expression of I κ B α that was approximately 2.8-fold of the control.

Several studies have shown that mTOR, rapamycin's mammalian target, may contribute to amyloid β - and tau-induced neurodegeneration [48]. Earlier studies showed that AD cases had higher levels than the control of mTOR phosphorylated at Ser2481 in the medial temporal cortex [49, 50]. Results in Figure 6(c) showed that STZ-injected mice exhibited significantly increased levels of the p-mTOR and p-AKT protein expression that were 5-6 fold greater than the level of sham control mice, respectively, but treatment with Antia reversed that increase and brought it close to that of the control values.

Finally, COX-2 is an important enzyme in inflammatory processes. Results in Figure 6(d) show that STZ-treated mice exhibited a significant induction in COX-2 expression of about 6-fold compared to sham control mice. Treatment

with Antia, however, significantly reduced the expression of COX-2 to 150%-300%.

4. Discussion

The present study's results demonstrate that the antioxidant Antia exerts protective effects for mice induced with SAD. The constituents of Antia have previously been shown to possess various neuroregenerative and protective properties. Yamabushitake mushrooms have been shown to synthesize nerve growth factor [51–53]; gotsukora extracts reduce the amyloid β levels in the Alzheimer-stricken brains of laboratory animals [23]; diosgenin enhances the cognitive performance of mice [27]; amla acts as a potent antioxidant with strong neuroprotective effects and cognitive enhancement properties [28–31]; and kothala himbutu protects against deleterious cognitive changes in young diabetic rats [32] and against mercury toxicity in mice hippocampi [33]. Here, Antia is shown to attenuate cognitive dysfunction in the mouse model by targeting several linked pathways, including the amyloidogenic, inflammatory, autophagy, and oxidative stress pathways.

In the present study, induction of SAD in mice by STZ induced a significant cognitive decline in the Morris water maze and novel object recognition tests. ICV injection of STZ is an experimental model that mimics the progressive pathology of SAD similar to human brains [38]. STZ-treated mice showed significant memory and learning

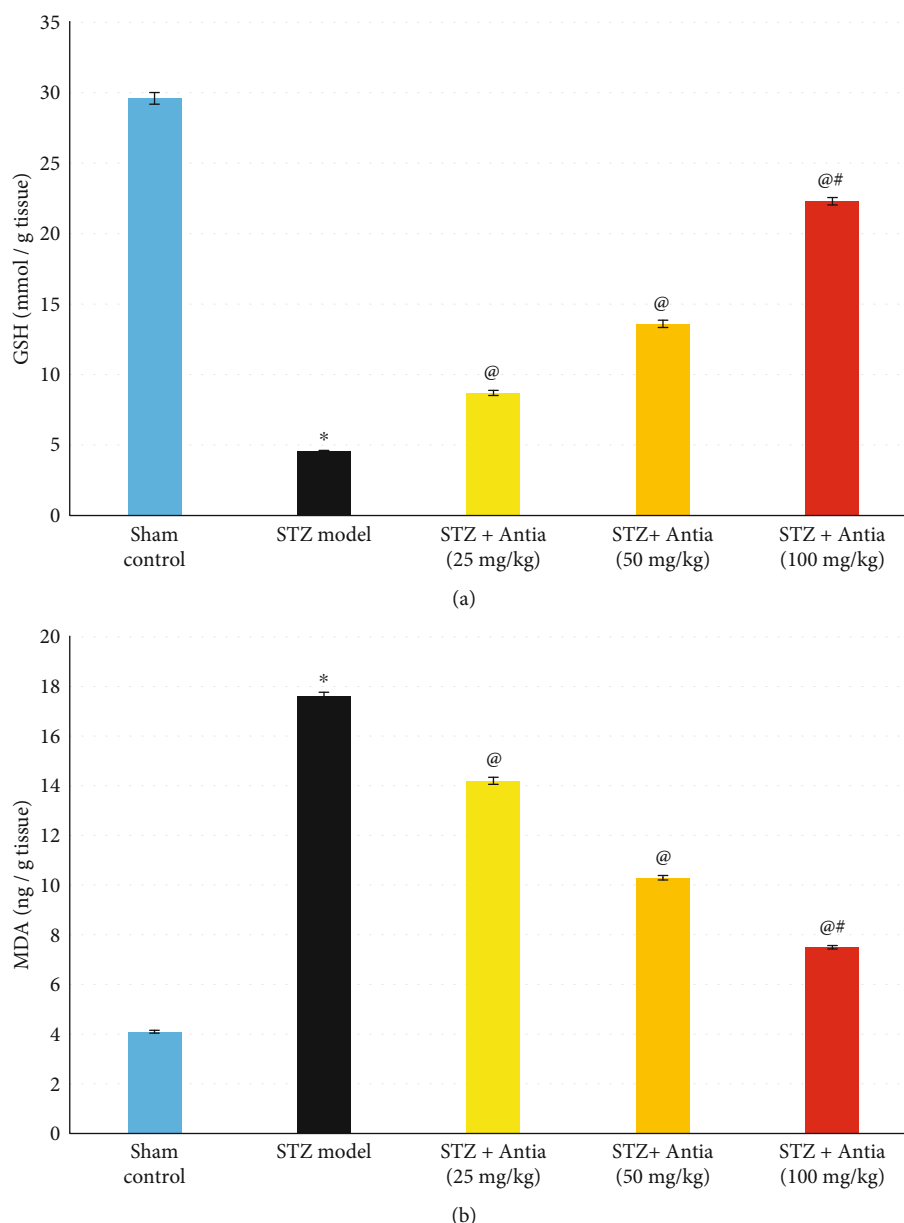


FIGURE 3: (a, b) Effect of Antia on GSH and MDA hippocampal content in ICV-STZ-injected mice. *Significantly different from the sham control group at $p < 0.05$. @Significantly different from the ICV-STZ group at $p < 0.05$. #Significantly different from Antia (25 mg/kg) at $p < 0.05$. §Significantly different from Antia (50 mg/kg) at $p < 0.05$.

deficits, as shown by the mice's noticeable inability to discriminate between novel and familiar objects in the novel object recognition tasks and Morris water maze test. This is in harmony with previous studies [54, 55]. However, the profound elevation in escape latency during the acquisition trial and the time spent in the target quadrant during the probe trail in the Morris water maze test, as well as the increase in discrimination and preference indices in the novel object recognition test, proved that Antia prevented the STZ-induced impairments of spatial and short-term memory. This improvement in the object recognition memory deficit could be attributed to the previously proven effects of several of Antia's ingredients. For example, it has been shown that diosgenin has an anti-amyloidogenic effect [27, 56] and that Her-

icium erinaceus has a strong neuroprotective effect against neuronal loss and dementia in AD [57, 58]. Furthermore, oral administration of dried yamabushitake mushroom powder has been demonstrated to effectively improve mild cognitive impairment in humans [19].

STZ administration significantly increased the hippocampal content expression of NF- κ B and anti-inflammatory cytokines, namely, IL-6 and TNF- α . NF- κ B plays a pivotal role in neurons' inflammatory responses by inducing the transcription of inflammatory target genes, including COX-2, TNF- α , IL-6, and IL-1 β [59]. TNF- α is involved in systemic inflammation, and in particular, it is involved in AD-related brain neuroinflammation as well as amyloidogenesis via β -secretase regulation. Moreover, increased IL-6

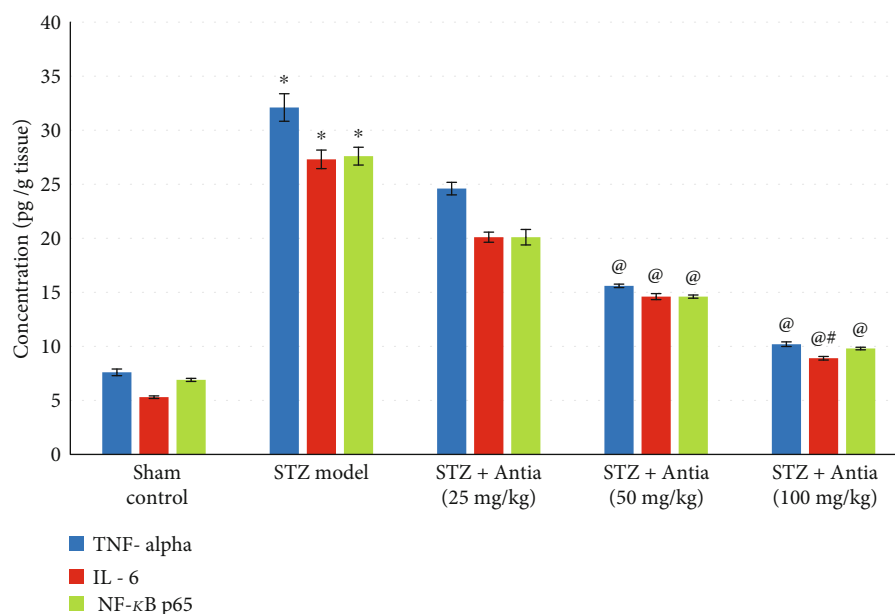


FIGURE 4: Effect of Antia on TNF- α , IL-6, and NF- κ B p65 hippocampal content in ICV-STZ-injected mice. *Significantly different from the sham control group at $p < 0.05$. @Significantly different from the ICV-STZ group at $p < 0.05$. #Significantly different from Antia (25 mg/kg) at $p < 0.05$. §Significantly different from Antia (50 mg/kg) at $p < 0.05$.

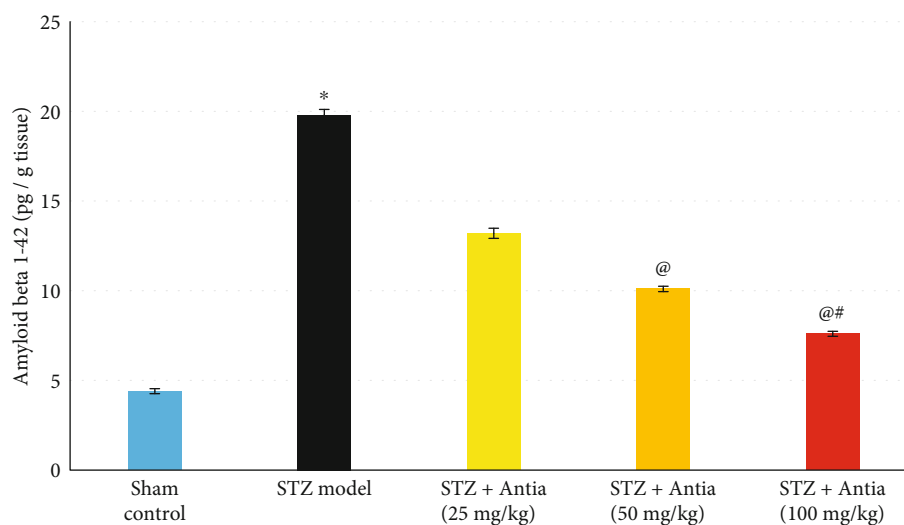
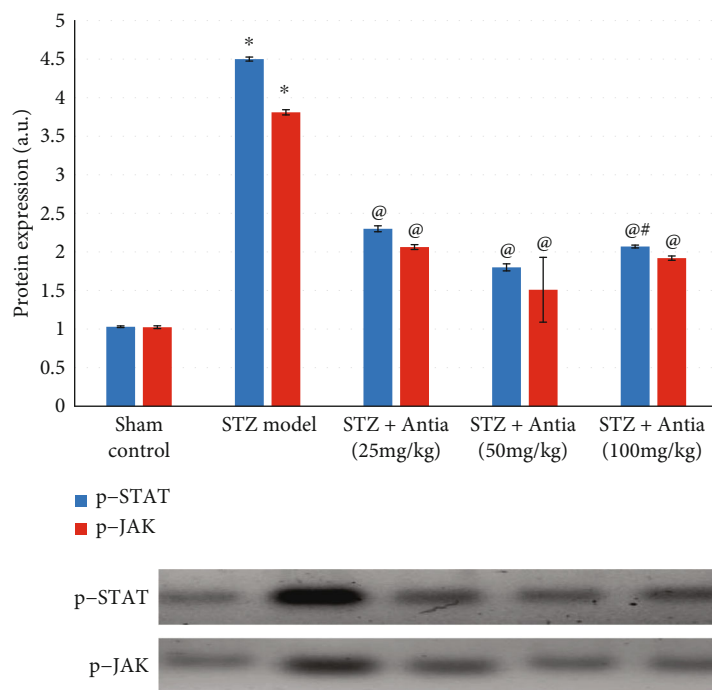


FIGURE 5: Effect of Antia on Amyloid β_{1-42} hippocampal content in ICV-STZ-injected mice. *Significantly different from the sham control group at $p < 0.05$. @Significantly different from the ICV-STZ group at $p < 0.05$. #Significantly different from Antia (25 mg/kg) at $p < 0.05$. §Significantly different from Antia (50 mg/kg) at $p < 0.05$.

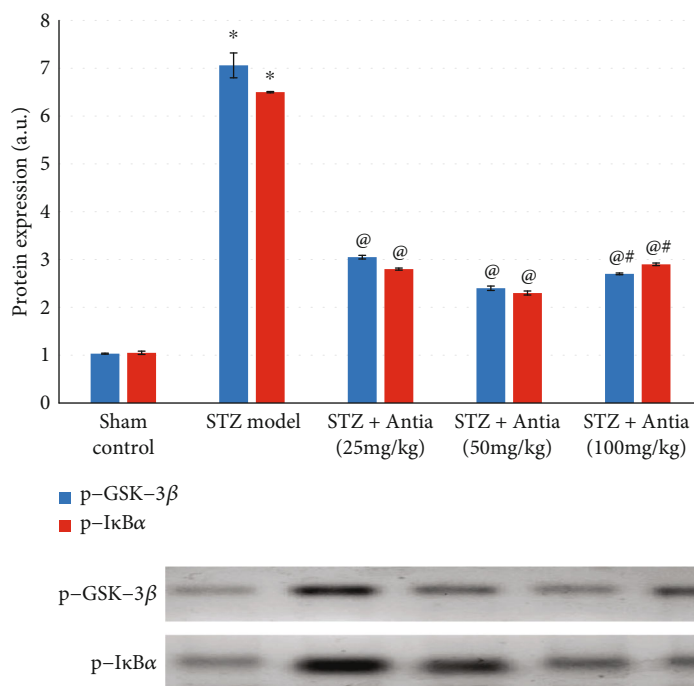
expression in the brain is linked with the profound neuropathological changes found with Alzheimer's and Parkinson's disease [60]. NF- κ B has also been demonstrated to regulate the expression of BACE-1, the rate-limiting enzyme responsible for amyloid β production. The Janus Kinase/Signal Transducers and Activators of Transcription (JAK/STAT) signaling pathway emerged in the 1980s as the pathway mediating interferon signaling. Neuroinflammation is accompanied by diseases, and JAK2/STAT3 pathway activation leads to pathogenic inflammation. Thus, targeting the JAK2/STAT3 pathway can be used as

a protective therapy for neuroinflammatory and neurodegenerative diseases like AD.

In the present study, administration of Antia was shown to have a significant anti-inflammatory effect, as demonstrated by decreasing the levels of all measured inflammatory cytokines as well as dramatically inhibiting the expression of phosphorylated STAT3 and JAK2. The STAT3/JAK2 pathway has been linked to TNF- α production [61, 62]. The significant inhibition of TNF- α and NF- κ B might be caused by the action of *Hericium erinaceus*, known as yamabushitake, which has been demonstrated to contribute to transcriptional



(a)



(b)

FIGURE 6: Continued.

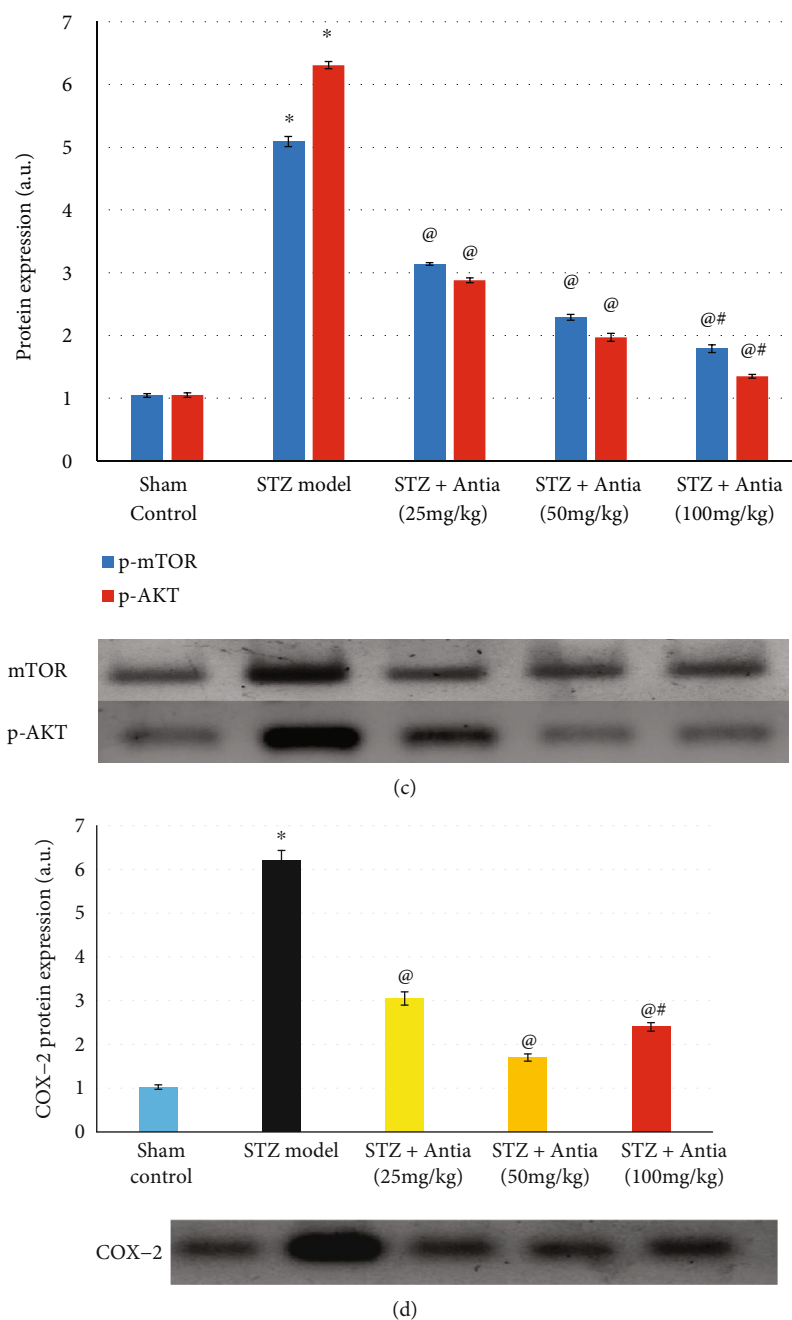


FIGURE 6: Effect of Antia on protein expression in the hippocampi of ICV-STZ-injected mice for (a) phosphorylated STAT and JAK, (b) GSK-3 β and I κ B α , (c) mTOR and p-AKT, and (d) COX-2. *Significantly different from the sham control group at $p < 0.05$. @Significantly different from the ICV-STZ group at $p < 0.05$. #Significantly different from Antia (25 mg/kg) at $p < 0.05$. §Significantly different from Antia (50 mg/kg) at $p < 0.05$.

regulation of adhesion molecules and numerous cytokines including TNF- α and IL-6 [63, 64].

Neuroinflammation has been linked to a deficit of autophagy, which may contribute to neurodegeneration [8]. mTOR, rapamycin's mammalian target, is known to regulate autophagy along with protein kinase B (Akt) [65]. Several studies emphasize the close link between cognitive impairment in AD and mTOR signaling and the presence of amyloid β plaques [66–69]. Furthermore, in human and rat studies of AD, autophagy activation has been linked to

GSK-3 β inhibitors and its deficit has been found to play a role in pathological tau aggregate accumulation [9, 11].

Treatment with Antia reversed the elevated expression of mTOR, Akt, I κ B α , and GSK-3 β levels after STZ injection and brought it closer to that of the control. Recent reports found that increasing neurons' axonal density with diosgenin significantly improved cognitive function. This could be achieved through modulation of the PI3K-Akt pathway, a pathway that plays a key role in axon regeneration by regulating local protein translation via the mTOR pathway [27, 70].

Moreover, it was proven recently that amla, a major constituent of Antia, exerted a significant modulation of the p-AKT/GSK-3 β pathway, resulting in a decline of phosphorylated tau and amelioration of cognitive deficits [71].

Results of this study showed that Antia increases GSH and decreases lipid peroxidation in STZ-treated mice. Previous research showed that the generation of ROS via amyloid β during self-aggregation may damage neurons and cause neuronal death [72]. Lipid peroxidation is considered to be a major outcome of injury mediated by free radicals that directly damages membranes, and increased lipid peroxidation has been found in AD patients' brains [73, 74]. Treatment of STZ-treated mice with Antia improved the oxidative stress parameters. This might be due to its previously known ability to reverse oxidative-stress-induced mitochondrial dysfunction and apoptosis [36]. In addition, Centella asiatica, commonly known as gotsukora, and MRN-100 have been found previously to provide multiple mechanisms for altering Alzheimer's brain pathology such as protection from DNA fragmentation due to oxidative stress, decreased lipid peroxidation, and the exhibition of noticeable free radical scavenging properties [23, 34]. GSH is an antioxidant that can prevent damage caused by ROS and may protect against oxidative and neurotoxic degeneration of oligomeric amyloid β [75, 76].

It could be concluded from the present study that Antia exerts a significant protection against sporadic AD induced by ICV injection of STZ. This effect is achieved through targeting the amyloidogenic, inflammatory, and oxidative stress pathways. The JAK2/STAT3 pathway played a protective role for the induced neuroinflammation, which is mediated through modulation of the Akt/mTOR/GSK-3 β pathway. To our knowledge, this is the first work done to investigate the protective effect of Antia against neurodegenerative diseases such as SAD.

Data Availability

The data of the present study including the figures and western blot analysis, used to support the findings of this study are included within the article.

Conflicts of Interest

The authors declare that they have no conflicts of interest.

Authors' Contributions

N. S. and M. G. designed the research, N. S. conducted the research, and N. S. and M. G. analyzed the data and wrote the paper. N. S. and M. G. had equal responsibility for the final content. Both read and approved the final manuscript.

Acknowledgments

The authors acknowledge ACM Co., Ltd., Japan, for providing Antia and Dr. B. J. Winjum at UCLA for the help in preparing the manuscript.

References

- [1] C. Patterson, *World Alzheimer Report 2018: the state of the art of dementia research: new frontiers*, Alzheimer's Disease International, London, 2018.
- [2] K. Blennow, M. J. de Leon, and H. Zetterberg, "Alzheimer's disease," *Lancet*, vol. 368, no. 9533, pp. 387–403, 2006.
- [3] A. Nunomura, G. Perry, M. A. Pappolla et al., "Neuronal oxidative stress precedes Amyloid- β deposition in Down syndrome," *Journal of Neuropathology and Experimental Neurology*, vol. 59, no. 11, pp. 1011–1017, 2000.
- [4] M. C. Polidori, "Oxidative stress and risk factors for Alzheimer's disease: clues to prevention and therapy," *Journal of Alzheimer's Disease*, vol. 6, no. 2, pp. 185–191, 2004.
- [5] M. Bélanger, I. Allaman, and P. J. Magistretti, "Brain energy metabolism: focus on astrocyte-neuron metabolic cooperation," *Cell Metabolism*, vol. 14, no. 6, pp. 724–738, 2011.
- [6] M. P. Mattson, "Pathways towards and away from Alzheimer's disease," *Nature*, vol. 430, no. 7000, pp. 631–639, 2004.
- [7] P. Flagmeier, S. de, D. C. Wirthensohn et al., "Ultrasensitive measurement of CA²⁺ influx into lipid vesicles induced by protein aggregates," *Angewandte Chemie*, vol. 56, no. 27, pp. 7750–7754, 2017.
- [8] H. F. Zheng, Y. P. Yang, L. F. Hu et al., "Autophagic impairment contributes to systemic inflammation-induced dopaminergic neuron loss in the midbrain," *PLoS One*, vol. 8, no. 8, article e70472, 2013.
- [9] A. Zare-Shahabadi, E. Masliah, G. V. Johnson, and N. Rezaei, "Autophagy in Alzheimer's disease," *Reviews in the Neurosciences*, vol. 26, no. 4, pp. 385–395, 2015.
- [10] I. N. Srivastava, J. Shperdheja, M. Baybis, T. Ferguson, and P. B. Crino, "mTOR pathway inhibition prevents neuroinflammation and neuronal death in a mouse model of cerebral palsy," *Neurobiology of Disease*, vol. 85, pp. 144–154, 2016.
- [11] X. Zhou, J. Zhou, X. Li, C. Guo, T. Fang, and Z. Chen, "GSK-3 β inhibitors suppressed neuroinflammation in rat cortex by activating autophagy in ischemic brain injury," *Biochemical and Biophysical Research Communications*, vol. 411, no. 2, pp. 271–275, 2011.
- [12] C. A. Szekely, T. Town, and P. P. Zandi, "NSAIDs for the chemoprevention of Alzheimer's disease," *Sub-Cellular Biochemistry*, vol. 42, pp. 229–248, 2007.
- [13] D. Hsu and G. A. Marshall, "Primary and secondary prevention trials in Alzheimer disease: looking back, moving forward," *Current Alzheimer Research*, vol. 13, no. 999, pp. 1–440, 2016.
- [14] W. R. Markesbery, "The role of oxidative stress in Alzheimer disease," *Archives of Neurology*, vol. 56, no. 12, pp. 1449–1452, 1999.
- [15] A. Gugliandolo, P. Bramanti, and E. Mazzon, "Role of vitamin E in the treatment of Alzheimer's disease: evidence from animal models," *International Journal of Molecular Sciences*, vol. 18, no. 12, p. 2504, 2017.
- [16] S. Y. Choi, S. H. Lim, J. S. Kim et al., "Evaluation of the estrogenic and antioxidant activity of some edible and medicinal plants," *Korean Journal of Food Science and Technology*, vol. 37, pp. 549–556, 2005.
- [17] H. Kawagishi, M. Ando, and T. Mizuno, "Hericenone A and B as cytotoxic principles from the mushroom *Hericium erinaceum*," *Tetrahedron Letters*, vol. 31, no. 3, pp. 373–376, 1990.
- [18] H. Kawagishi, A. Shimada, R. Shirai et al., "Erinacines A, B and C, strong stimulators of nerve growth factor (NGF)-synthesis,

- from the mycelia of *Herichium erinaceum*,” *Tetrahedron Letters*, vol. 35, no. 10, pp. 1569–1572, 1994.
- [19] K. Mori, S. Inatomi, K. Ouchi, Y. Azumi, and T. Tuchida, “Improving effects of the mushroom Yamabushitake (*Herichium erinaceum*) on mild cognitive impairment: a double-blind placebo-controlled clinical trial,” *Phytotherapy Research*, vol. 23, no. 3, pp. 367–372, 2009.
- [20] K. M. Nadkarni and A. K. Nadkarni, “Dr. K.M,” in *Indian Materia Medica*, Bombay Popular Prakashan, 1954.
- [21] K. R. Kirtikar, B. D. Basu, and E. Blatter, *Indian Medicinal Plants*, International Books Distributors, Dehradun, 1987.
- [22] Y. K. Gupta, M. H. Veerendra Kumar, and A. K. Srivastava, “Effect of *Centella asiatica* on pentylentetrazole-induced kindling, cognition and oxidative stress in rats,” *Pharmacology, Biochemistry, and Behavior*, vol. 74, no. 3, pp. 579–585, 2003.
- [23] M. Dhanasekaran, L. A. Holcomb, A. R. Hitt et al., “*Centella asiatica* extract selectively decreases amyloid beta levels in hippocampus of Alzheimer’s disease animal model,” *Phytotherapy Research*, vol. 23, no. 1, pp. 14–19, 2009.
- [24] P. L. McGeer and E. G. McGeer, “The amyloid cascade-inflammatory hypothesis of Alzheimer disease: implications for therapy,” *Acta Neuropathologica*, vol. 126, no. 4, pp. 479–497, 2013.
- [25] X. Zhu, B. Su, X. Wang, M. A. Smith, and G. Perry, “Causes of oxidative stress in Alzheimer disease,” *Cellular and Molecular Life Sciences*, vol. 64, no. 17, pp. 2202–2210, 2007.
- [26] A. I. Bush, “Drug development based on the metals hypothesis of Alzheimer’s disease,” *Journal of Alzheimer’s Disease*, vol. 15, no. 2, pp. 223–240, 2008.
- [27] C. Tohda, Y. A. Lee, Y. Goto, and I. Nemere, “Diosgenin-induced cognitive enhancement in normal mice is mediated by 1,25D₃-MARAS,” *Scientific Reports*, vol. 3, no. 1, 2013.
- [28] I. Husain, S. Zameer, T. Madaan et al., “Exploring the multifaceted neuroprotective actions of *Emblica officinalis* (Amla): a review,” *Metabolic Brain Disease*, vol. 34, no. 4, pp. 957–965, 2019.
- [29] S. K. Ali, A. R. Hamed, M. M. Soltan et al., “In-vitro evaluation of selected Egyptian traditional herbal medicines for treatment of Alzheimer disease,” *BMC Complementary and Alternative Medicine*, vol. 13, no. 1, 2013.
- [30] W. Liu, H. Ma, N. A. DaSilva et al., “Development of a neuroprotective potential algorithm for medicinal plants,” *Neurochemistry International*, vol. 100, pp. 164–177, 2016.
- [31] M. S. Uddin, A. A. Mamun, M. S. Hossain, F. Akter, M. A. Iqbal, and M. Asaduzzaman, “Exploring the effect of *Phyllanthus emblica* L. on cognitive performance, brain antioxidant markers and acetylcholinesterase activity in rats: promising natural gift for the mitigation of Alzheimer’s disease,” *Annals of Neurosciences*, vol. 23, no. 4, pp. 218–229, 2016.
- [32] R. Rajashree, R. Patil, S. D. Khlokute, and S. S. Goudar, “Effect of *Salacia reticulata* W. and *Clitoria ternatea* L. on the cognitive and behavioral changes in the streptozotocin-induced young diabetic rats,” *Journal of Basic and Clinical Physiology and Pharmacology*, vol. 28, no. 2, pp. 107–114, 2017.
- [33] G. E. Tams, J. N. Kani, C. D. Blessing, and A. S. Peter, “Antidegenerative and neurobehavioral effects of ethanolic root extract of *Salacia reticulata* on mercury chloride induced cellular damage in the hippocampus of adult male mice,” *Journal of Cytology & Histology*, vol. 9, no. 3, p. 3, 2018.
- [34] N. K. Badr El-Din, E. Noaman, S. M. Fattah, and M. Ghoneum, “Reversal of age-associated oxidative stress in rats by MRN-100, a hydro-ferrate fluid,” *In Vivo*, vol. 24, no. 4, pp. 525–533, 2010.
- [35] F. Lin and A. W. Girotti, “Elevated ferritin production, iron containment, and oxidant resistance in hemin-treated leukemia cells,” *Archives of Biochemistry and Biophysics*, vol. 346, no. 1, pp. 131–141, 1997.
- [36] M. H. Ghoneum, “Reversal of oxidative-stress-induced mitochondrial dysfunction and apoptosis in human peripheral blood lymphocytes by Antia, a naturally-derived anti-oxidant,” in *Alzheimer’s Association International Conference (AAIC) 2019*, Los Angeles, California, July 2019.
- [37] M. Salkovic-Petrisic, A. Knezovic, S. Hoyer, and P. Riederer, “What have we learned from the streptozotocin-induced animal model of sporadic Alzheimer’s disease, about the therapeutic strategies in Alzheimer’s research,” *Journal of Neural Transmission (Vienna)*, vol. 120, no. 1, pp. 233–252, 2013.
- [38] P. K. Kamat, A. Kalani, S. Rai, S. K. Tota, A. Kumar, and A. S. Ahmad, “Streptozotocin intracerebroventricular-induced neurotoxicity and brain insulin resistance: a therapeutic intervention for treatment of sporadic Alzheimer’s disease (sAD)-like pathology,” *Molecular Neurobiology*, vol. 53, no. 7, pp. 4548–4562, 2016.
- [39] M. A. Pellemounter, M. Joppa, N. Ling, and A. C. Foster, “Pharmacological evidence supporting a role for central corticotropin-releasing factor(2) receptors in behavioral, but not endocrine, response to environmental stress,” *The Journal of Pharmacology and Experimental Therapeutics*, vol. 302, no. 1, pp. 145–152, 2002.
- [40] G. I. Warnock, *Study of the Central Corticotrophin-Releasing Factor System Using the 2-Deoxyglucose Method for Measurement of Local Cerebral Glucose Utilisation*, University of Bath, Dissertation, 2010.
- [41] J. Mehla, M. Pahuja, and Y. K. Gupta, “Streptozotocin-induced sporadic Alzheimer’s disease: selection of appropriate dose,” *Journal of Alzheimer’s Disease*, vol. 33, no. 1, pp. 17–21, 2012.
- [42] OECD, “Organization for Economic Cooperation and Development (OECD) Guidelines for Testing of Chemicals,” *Acute Oral Toxic. Acute Toxic Class Method*, no. 423, 2001.
- [43] A. Ennaceur, “One-trial object recognition in rats and mice : methodological and theoretical issues,” *Behavioural Brain Research*, vol. 215, no. 2, pp. 244–254, 2010.
- [44] G. M. Morris, “Spatial localization does not require local cues the presence of local cues,” *Learning and Motivation*, vol. 260, pp. 239–260, 1981.
- [45] M. Mihara and M. Uchiyama, “Determination of malonaldehyde precursor in tissues by thiobarbituric acid test,” *Analytical Biochemistry*, vol. 86, no. 1, pp. 271–278, 1978.
- [46] E. Beutler, O. Duron, and B. M. Kelly, “Improved method for the determination of blood glutathione,” *The Journal of Laboratory and Clinical Medicine*, vol. 61, pp. 882–888, 1963.
- [47] C. J. Phiel, C. A. Wilson, V. M. Lee, and P. S. Klein, “GSK-3alpha regulates production of Alzheimer’s disease amyloid-beta peptides,” *Nature*, vol. 423, no. 6938, pp. 435–439, 2003.
- [48] S. Oddo, “The role of mTOR signaling in Alzheimer disease,” *Frontiers in Bioscience*, vol. 4, pp. 941–952, 2012.
- [49] X. Li, I. Alafuzoff, H. Soininen, B. Winblad, and J. J. Pei, “Levels of mTOR and its downstream targets 4E-BP1, eEF2, and eEF2 kinase in relationships with tau in Alzheimer’s disease brain,” *The FEBS Journal*, vol. 272, no. 16, pp. 4211–4220, 2005.

- [50] R. J. Griffin, A. Moloney, M. Kelliher et al., "Activation of Akt/PKB, increased phosphorylation of Akt substrates and loss and altered distribution of Akt and PTEN are features of Alzheimer's disease pathology," *Journal of Neurochemistry*, vol. 93, no. 1, pp. 105–117, 2005.
- [51] K. Mori, Y. Obara, M. Hirota et al., "Nerve growth factor-inducing activity of *Herichium erinaceus* in 1321NI human astrocytoma cells," *Biological & Pharmaceutical Bulletin*, vol. 31, no. 9, pp. 1727–1732, 2008.
- [52] B.-J. Ma, J.-W. Shen, H.-Y. Yu, Y. Ruan, T.-T. Wu, and X. Zhao, "Hericenones and erinacines: stimulators of nerve growth factor (NGF) biosynthesis in *Herichium erinaceus*," *Mycology*, vol. 1, no. 2, pp. 92–98, 2010.
- [53] K. Spelman, E. Sutherland, and A. Bagade, "Neurological activity of lion's mane (*Herichium erinaceus*)," *Journal of Restorative Medicine*, vol. 6, no. 1, pp. 19–26, 2017.
- [54] A. M. E. Halawany, N. S. E. Sayed, H. M. Abdallah, and R. S. E. Dine, "Protective effects of gingerol on streptozotocin-induced sporadic Alzheimer's disease: emphasis on inhibition of β -amyloid, COX-2, alpha-, beta-secretases and A β 1a," *Scientific Reports*, vol. 7, no. 1, p. 2902, 2017.
- [55] N. O. Abdel Rasheed, N. S. El Sayed, and A. S. El-Khatib, "Targeting central β 2 receptors ameliorates streptozotocin-induced neuroinflammation via inhibition of glycogen synthase kinase3 pathway in mice," *Progress in Neuro-Psychopharmacology and Biological Psychiatry*, vol. 86, pp. 65–75, 2018.
- [56] L. Lecanu, G. Rammouz, A. McCourty, E. K. Sidahmed, J. Greeson, and V. Papadopoulos, "Caprospinol reduces amyloid deposits and improves cognitive function in a rat model of Alzheimer's disease," *Neuroscience*, vol. 165, no. 2, pp. 427–435, 2010.
- [57] K. Nagai, A. Chiba, T. Nishino, T. Kubota, and H. Kawagishi, "Dilinoleoyl-phosphatidylethanolamine from *Herichium erinaceum* protects against ER stress-dependent Neuro2a cell death via protein kinase C pathway," *The Journal of Nutritional Biochemistry*, vol. 17, no. 8, pp. 525–530, 2006.
- [58] H. Kawagishi and C. Zhuang, "Compounds for dementia from *Herichium erinaceum*," *Drugs of the Future*, vol. 33, no. 2, pp. 149–155, 2008.
- [59] C. Xiao and S. Ghosh, "NF-kappaB, an evolutionarily conserved mediator of immune and inflammatory responses," *Advances in Experimental Medicine and Biology*, vol. 560, pp. 41–45, 2005.
- [60] Q. Alam, M. Z. Alam, G. Mushtaq et al., "Inflammatory process in Alzheimer's and Parkinson's diseases: central role of cytokines," *Current Pharmaceutical Design*, vol. 22, no. 5, pp. 541–548, 2016.
- [61] C. Huang, R. Ma, S. Sun et al., "JAK2-STAT3 signaling pathway mediates thrombin-induced proinflammatory actions of microglia in vitro," *Journal of Neuroimmunology*, vol. 204, no. 1–2, pp. 118–125, 2008.
- [62] S. Nishiki, F. Hato, N. Kamata et al., "Selective activation of STAT3 in human monocytes stimulated by G-CSF: implication in inhibition of LPS-induced TNF-alpha production," *American Journal of Physiology. Cell Physiology*, vol. 286, no. 6, pp. C1302–C1311, 2004.
- [63] B. Thongbai, S. Rapior, K. D. Hyde, K. Wittstein, and M. Stadler, "*Herichium erinaceus*, an amazing medicinal mushroom," *Mycological Progress*, vol. 14, no. 10, 2015.
- [64] C. Diling, Y. Tianqiao, Y. Jian, Z. Chaoqun, S. Ou, and X. Yizhen, "Docking studies and biological evaluation of a potential β -secretase inhibitor of 3-hydroxyhericenone F from *Herichium erinaceus*," *Frontiers in Pharmacology*, vol. 8, p. 219, 2017.
- [65] C. H. Jung, S. H. Ro, J. Cao, N. M. Otto, and D. H. Kim, "mTOR regulation of autophagy," *FEBS Letters*, vol. 584, no. 7, pp. 1287–1295, 2010.
- [66] M. Paccalin, S. Pain-Barc, C. Pluchon et al., "Activated mTOR and PKR kinases in lymphocytes correlate with memory and cognitive decline in Alzheimer's disease," *Dementia and Geriatric Cognitive Disorders*, vol. 22, no. 4, pp. 320–326, 2006.
- [67] Z. Cai, B. Zhao, K. Li et al., "Mammalian target of rapamycin: a valid therapeutic target through the autophagy pathway for Alzheimer's disease?," *Journal of Neuroscience Research*, vol. 90, no. 6, pp. 1105–1118, 2012.
- [68] J. Pozueta, R. Lefort, and M. L. Shelanski, "Synaptic changes in Alzheimer's disease and its models," *Neuroscience*, vol. 251, pp. 51–65, 2013.
- [69] C. Lafay-Chebassier, M. Paccalin, G. Page et al., "mTOR/p70S6k signalling alteration by A β exposure as well as in APP-PS1 transgenic models and in patients with Alzheimer's disease," *Journal of Neurochemistry*, vol. 94, no. 1, pp. 215–225, 2005.
- [70] P. Verma, S. Chierzi, A. M. Codd et al., "Axonal protein synthesis and degradation are necessary for efficient growth cone regeneration," *The Journal of Neuroscience*, vol. 25, no. 2, pp. 331–342, 2005.
- [71] M. D. Bharathi and A. J. Thenmozhi, "Attenuation of aluminum-induced neurotoxicity by tannoid principles of *Emblca officinalis* in Wistar rats," *The International Journal of Nutrition, Pharmacology, Neurological Diseases*, vol. 8, no. 2, p. 35, 2018.
- [72] W. Ahmad, B. Ijaz, K. Shabbiri, F. Ahmed, and S. Rehman, "Oxidative toxicity in diabetes and Alzheimer's disease: mechanisms behind ROS/ RNS generation," *Journal of Biomedical Science*, vol. 24, no. 1, p. 76, 2017.
- [73] T. J. Montine, M. D. Neely, J. F. Quinn et al., "Lipid peroxidation in aging brain and Alzheimer's disease," *Free Radical Biology & Medicine*, vol. 33, no. 5, pp. 620–626, 2002.
- [74] Q. Liu, M. A. Smith, J. Avilá et al., "Alzheimer-specific epitopes of tau represent lipid peroxidation-induced conformations," *Free Radical Biology & Medicine*, vol. 38, no. 6, pp. 746–754, 2005.
- [75] T. J. Monks, J.-F. Ghersi-Egea, M. Philbert, A. J. L. Cooper, and E. A. Lock, "Symposium overview: the role of glutathione in neuroprotection and neurotoxicity," *Toxicological Sciences*, vol. 51, no. 2, pp. 161–177, 1999.
- [76] J. Lasierra-Cirujeda, P. Coronel, M. J. Aza, and M. Gimeno, "Beta-amyloidolysis and glutathione in Alzheimer's disease," *Journal of Blood Medicine*, vol. 4, pp. 31–38, 2013.

Research Article

Characterization of Polysaccharides Extracted from Pulps and Seeds of *Crataegus azarolus* L. var. *aronia*: Preliminary Structure, Antioxidant, Antibacterial, α -Amylase, and Acetylcholinesterase Inhibition Properties

Ilhem Rjeibi ¹, Rihab Zaabi,² and Warda Jouida²

¹Research Unit of Macromolecular Biochemistry and Genetics, Faculty of Sciences of Gafsa, 2112 Gafsa, Tunisia

²Faculty of Sciences of Gabés, University of Gabés, 6072, Tunisia

Correspondence should be addressed to Ilhem Rjeibi; rjeibii@yahoo.fr

Received 15 February 2020; Revised 14 April 2020; Accepted 5 May 2020; Published 29 May 2020

Guest Editor: Francisco Jaime B. Mendonça Junior

Copyright © 2020 Ilhem Rjeibi et al. This is an open access article distributed under the Creative Commons Attribution License, which permits unrestricted use, distribution, and reproduction in any medium, provided the original work is properly cited.

Polysaccharides from the pulps (CAP) and seeds (CAS) of *Crataegus azarolus* L. var. *aronia* were extracted by hot water method. Both polysaccharides were characterized by scanning electron microscopy (SEM), Congo red test, FT-IR spectroscopy, and their antioxidant, α -amylase, antiacetylcholinesterase, and antibacterial activities were evaluated. CAP showed the highest total carbohydrate (82.35%) and uronic acid (29.39%) contents. The Congo red test revealed the lack of triple-helical conformation for both polysaccharides. The comparison of both infrared spectra indicated similar patterns with the presence of typical bands of polysaccharides. However, the microstructure of both samples indicated differences when analyzed by SEM. CAP displayed higher antioxidant, α -amylase, and acetylcholinesterase inhibitory activities. Besides, CAP showed the strongest antimicrobial effects against seven microorganisms and, notably, the Gram-positive bacteria. Overall, the results suggest that polysaccharides from *C. azarolus* L. var. *aronia* may be considered as novel sources of antioxidants and recommended as enzyme inhibitory agents in food and pharmaceutical industries.

1. Introduction

Polysaccharides are biomacromolecules widely distributed in algae, plants, animals, and microorganisms. Plant polysaccharides have proved to be potential sources of natural antibacterial, antioxidants, immunomodulatory, antitumor, hepato-cardioprotective, and neuroprotective compounds [1–3]. They have been increasingly applied because they are sourced naturally, and they impart less toxicity, biodegradability, and fewer side effects than synthetic ones. Polysaccharides are also widely used as emulsifiers, gelling agents, thickeners, and fat replacers in functional food, cosmetics industries, and biological medicine, including drug delivery and tissue engineering [4]. Over the past decade, there has been a wave of studies into finding new sources of polysaccharides that could hotspot a potential technological interest over existing commercial polysaccharides.

The genus *Crataegus* spp., which belongs to the Rosaceae, is largely distributed in Africa, North Europe, and North America [5]. This genus is commonly known as hawthorn in English and Zaarour in Arabic. The fruits of *Crataegus* spp. are commonly eaten as edible food. In addition, fruits, leaves, and flowers have long been used as a traditional medicine to cure various diseases such as asthma, insomnia, flu, coughs, and bronchitis, and headache, respiratory, and cardiovascular problems [6, 7]. Previous research has shown that hawthorn exerts a variety of pharmacological effects, including antioxidant, antidiabetic, antimicrobial, antiviral, anti-inflammatory, antithrombotic, antihyperlipidemic, cardioactive, hepatoprotective, and hypotensive activities [8]. Numerous biochemical studies have demonstrated that hawthorn is a valuable source of bioactive components (e.g., minerals, sugar alcohols, phenolic acids, essential oil, organic acids, tannins, vitamin, flavonoids, and polysaccharides) [8,

9]. Polysaccharides and oligosaccharides extracted from the fruits and flowers of *Crataegus* spp. possess various human health-promoting effects, such as anticoagulant (for *C. monogyna*) [10] and hypolipidemic activities (for *C. pinnatifida*) [11]. Likewise, several reports have demonstrated the antioxidant and probiotic properties of polysaccharides extracted from *C. pinnatifida* [12, 13].

Among plant species *Crataegus azarolus* L. var. *aronia* (Yellow Azarole) is native to the Mediterranean countries, which have long been used in Tunisian traditional medicines to prevent cancer, diabetes, sexual weakness, and cardiovascular diseases [14]. Previous studies revealed that the leaves, flowers, and fruits of *C. azarolus* had various biological activities including antimicrobial, antioxidant, antihyperglycemic, and antihyperlipidemic activities [15, 16]. These potential health benefits are related to their high content in many natural active compounds, such as flavonoids, minerals, sugar alcohols, carotenoids, polyphenols, amino acids, and tannins [14, 17].

However, to the best of our knowledge, none of the previous studies have focused on the extraction of polysaccharides from *C. azarolus* L. var. *aronia* and the evaluation of their antioxidant, antibacterial, α -amylase, and acetylcholinesterase inhibition properties. In this study, two polysaccharides from *C. azarolus* were extracted and structurally characterized preliminarily. Then, their biological activities *in vitro* were evaluated.

2. Materials and Methods

2.1. Plant Material. Fresh fruits of *Crataegus azarolus* L. var. *aronia* were collected from Gafsa (Northwestern Tunisia, 36° 46' 34" N latitude and 8° 41' 05" E longitude) between October and November 2018. The plant was identified by Professor Elkadri Lefi, at the Department of Biology, Faculty of Sciences of Gafsa, Tunisia. A voucher specimen (MSE 0795) was deposited at the herbarium in the Faculty of Sciences Gafsa, Tunisia. The pulps and seeds of the fruits were separated, dried, and crushed individually to obtain a fine powder.

2.2. Extraction of CAS and CAP. The powdered pulps and seeds (60 g, each) were defatted with 95% ethanol and petroleum ether with continuous stirring for 24 h. The residues were dried and then extracted with hot water at 90°C for 5 h (three-time, 3 × 5 h). Following centrifugation at 4500 rpm for 10 min, the supernatants were mixed with 95% cold ethanol (3:1, *v/v*) at 4°C overnight. Precipitates were dissolved in distilled water and deproteinized using Sevag reagent (chloroform/butanol 4:1, *v/v*). The deproteinized mixture was dialyzed for 3 days (with 3500 Da cut-off, *Spectra/Por*[™], Fisher Scientific, Illkirch, France) and lyophilized to obtain the water-soluble polysaccharides from *C. azarolus* seeds and pulps named, respectively, CAS and CAP.

Finally, the CAP and CAS extraction yields were calculated.

2.3. Characterization of CAS and CAP

2.3.1. Chemical Composition. Total carbohydrates were assessed using the phenol-sulfuric acid method [18], and

concentrations were determined against the glucose standard. The total neutral sugar, total phenolic compounds, and uronic acid contents were estimated using, respectively, the sulfuric resorcinol method [19], Folin-Ciocalteu method [20], and *m*-hydroxydiphenyl test [21]. The protein content was determined using the Bradford method [22], and concentrations were estimated against the bovine serum albumin standard. Ash content was determined according to AOAC methods [23].

2.3.2. Infrared Spectroscopic Analysis (FT-IR). CAP and CAS were individually mixed with potassium bromide powder and pressed into pellets. The spectra were analyzed using Fourier transform infrared spectrophotometer (Shimadzu, FT-IR-8400S spectrophotometer equipped with IR solution version 1.10) in the range of 400–4000 cm⁻¹.

2.3.3. Scanning Electron Microscopy. CAP and CAS were examined by scanning electron microscopy (SEM) model JEOL (JSM-IT100). Each dried polysaccharide was mounted on a metal stub and was sputtered with gold. The images were observed at different magnifications (35x and 250x).

2.3.4. Helix-Coil Transition Analysis. The conformational structure of CAP and CAS was analyzed using the Congo red assay [24]. In brief, the two polysaccharides (2 mg/mL each) were individually mixed with 2 mL of 100 μ M Congo red solution. Different volumes of NaOH solution (2 M) were added to the mixture to achieve a final concentration of 0–0.5 M. Meanwhile, the solution prepared without adding polysaccharides was considered as the control. The maximum UV-vis absorption was measured from 250 to 550 nm using Analytik Jena spectrophotometer.

2.4. Antioxidant Activity

2.4.1. DPPH Radical Scavenging Activity. The scavenging capacity of CAP and CAS against DPPH radical was assayed using the method of Bersuder et al. [25]. Aliquots of polysaccharides (500 μ L) at different concentrations (0.1–4 mg/mL) were mixed with DPPH solution (125 μ L, 0.2 mM) and deionized water (375 μ L), then incubated for 1 h in the dark. The positive standards (butylated hydroxytoluene and vitamin C) were prepared using the same procedure. The absorbance was measured at 517 nm. The scavenging activity of DPPH radicals was calculated according to

$$\text{Scavenging activity (\%)} = \frac{\text{Abs}_{\text{Control}} - \text{Abs}_{\text{Sample}}}{\text{Abs}_{\text{Control}}} \times 100. \quad (1)$$

2.4.2. H₂O₂ Scavenging Activity. The scavenging capacity of CAP and CAS against H₂O₂ radical was conducted according to the modified procedure of Liu et al. [26]. Briefly, 0.5 mL of CAP and CAS at various concentrations (0.1, 0.5, 1.5, 2.5, 3, and 4 mg/mL) were individually mixed with 0.1 M phosphate buffer (1.2 mL, pH 7.4) and 40 mM H₂O₂ solution (0.3 mL), then incubated for 10 min at room temperature. The positive standard in this assay was vitamin C. The absorbance of each sample was measured at 230 nm. The scavenging activity of H₂O₂ radicals was calculated according to Equation (1).

2.4.3. Fe^{2+} -Chelating Activity. The chelating capacity of ferrous ions by CAP and CAS was assessed using ferrozine reagent procedure as described previously with slight modifications [27]. Solution of polysaccharides (500 μ L) at different concentrations (0.1–4 mg/mL) were mixed with 2 mM $FeCl_2$ (100 μ L), 5 mM ferrozine (200 μ L), and deionized water (200 μ L) and incubated for 10 min at 25°C. In the control solution, the sample was replaced by deionized water. The positive standard in this assay was EDTA (ethylenediaminetetraacetic acid). The ferrous ion chelation activity was calculated according to Equation (1).

2.4.4. Lipid Peroxidation Inhibition Activity. The inhibition effect of CAP and CAS on lipid peroxidation was carried out as described by Yen and Hsieh [28] using mice liver homogenate as the lipid-rich media, $FeCl_2-H_2O_2$ as inducer, and ascorbic acid as the standard. The livers of Swiss albinos mice obtained from the departmental animal house at the Faculty of Sciences Gafsa were dissected, washed, and homogenized into ice-cold Tris-HCl buffer (1%, pH 7.4). The resulting reaction mixture was centrifuged for 30 min at 9000 rpm at 4°C. Aliquots (500 μ L) were mixed with solutions of polysaccharides (500 μ L) at different concentrations (0.5–6 mg/mL), then 50 μ L of $FeCl_2$ (0.5 mmol/L) and H_2O_2 (0.5 mmol/L) was added to start lipid peroxidation. After incubation for 30 min at 37°C, the trichloroacetic acid (500 μ L, 20%) was added to precipitate proteins, and the mixture was centrifuged. The thiobarbituric acid (1 mL, 0.8%) was added to the obtained supernatant, then heated in boiling water for 9 min. The absorbance of the supernatant was recorded at 532 nm. The inhibition was calculated using

$$\text{Inhibition rate (\%)} = \frac{1 - (A1 - A2)}{A0} \times 100, \quad (2)$$

where A0 and A1 were, respectively, the absorbance without and with the test sample, and A2 was the absorbance without liver homogenate.

2.5. Enzyme Inhibitory Activity Assays

2.5.1. Acetylcholinesterase Inhibition. The antiacetylcholinesterase effects of CAP and CAS on AChE was analyzed using the modified procedure of Ellman et al. [29]. Briefly, a mixture of 300 μ L (50 mM) Tris-HCl buffer pH 8, 100 μ L of each polysaccharide, and 30 μ L AChE solutions was well shaken and incubated for 15 min. Then, 130 μ L of AChI (acetylthiocholine iodide) and 440 μ L of (3 mM) DTNB (5,5'-Dithiobis-(2-nitrobenzoic acid)) were added. Galantamine was used as the positive control. The absorbance was measured at 412 nm.

The inhibition activity was calculated using

$$\text{Inhibition activity (\%)} = \frac{1 - ES}{E} \times 100. \quad (3)$$

ES and E were the respective activity of enzyme with and without the test sample.

2.5.2. α -Amylase Inhibition. The α -amylase inhibitory activity of CAP and CAS was assessed as described by Oboh et al. [30] with minor modifications. Firstly, 500 μ L of different concentrations (0.1–5 mg/mL) of each polysaccharide prepared in PBS (20 mM) were mixed with α -amylase (500 μ L, 1.0 U/mL) prepared in NaCl (6.0 mM) and incubated for 10 min at 37°C. Then, potato starch solutions (500 μ L, 1%) was added to the mixture and re-incubated for 10 min at 37°C. Finally, the reaction was stopped using 1 mL of dinitrosalicylic acid (DNS) reagent and heated in boiling water for 5 min. The absorbance of the resulting mixture was measured at 520 nm. The acarbose was used as the positive control.

The inhibitory activity was estimated as follows:

$$\text{Inhibition (\%)} = \frac{\text{Abs}_{520\text{control}} - \text{Abs}_{520\text{sample}}}{\text{Abs}_{A1\text{control}}} \times 100. \quad (4)$$

2.6. Antibacterial Activity

2.6.1. Microorganisms. Microorganisms used in this study represent pathogenic species commonly associated with sanitary relevance. These bacterial organisms, including Gram-positive and Gram-negative, are the main source that causes severe infections in humans. Antibacterial activity of polysaccharides was tested against Gram-positive and Gram-negative bacterial strains from the American Type Culture Collection. The test organisms used here are as follows: *Escherichia coli* (ATCC 35218), *Enterococcus faecalis* (ATCC 29212), *Pseudomonas aeruginosa* (ATCC 27853), *Listeria monocytogenes* (ATCC 19117), *Klebsiella pneumoniae* (ATCC 13883), *Staphylococcus aureus* (ATCC 25923), *Bacillus cereus* (ATCC 11778), and *Salmonella typhimurium* (ATCC 23564).

2.6.2. Disc Diffusion Assay. Antibacterial activity of CAP and CAS (15 mg/mL) was performed by disc diffusion method. The suspensions of bacteria (200 μ L, 10^6 CFU/mL, with CFU/mL of bacterial cells estimated by absorbance at 600 nm) were spread on Mueller–Hinton (MH) agar (Sigma-Aldrich) already cast into Petri dishes. Next, impregnated sterile paper discs (6 mm diameter, 1 mm thickness) with 10 μ L of each polysaccharide were deposited individually on Petri dishes, then incubated for 24 h at 37°C. The antimicrobial activity was evaluated by measuring the inhibition zone surrounding the discs (mm) using vernier caliper (accuracy 0.02 mm). Gentamicin at 20 μ g/disc was used as the positive control.

2.6.3. Minimum Inhibitory Concentration (MIC). The MIC of different polysaccharides was performed using the 96-well microdilution method as previously described by Gullon et al. [31]. The microorganism suspension was prepared in order to obtain a final cell density of about 10^6 CFU/mL. Serial dilutions of each polysaccharide from 1.56 to 25 mg/mL were prepared using MH broth. Subsequently, 100 μ L of the diluted samples were distributed into the microplate. To the above dilutions, equal volumes (100 μ L)

TABLE 1: Global composition of CAP and CAS extracted from *Crataegus azarolus*.

	Yield (%, w/w)	Carbohydrate (%, w/w)	Neutral sugar (%, w/w)	Proteins (%, w/w)	Uronic acid (%, w/w)	Polyphenolics (%, w/w)	Ash (%, w/w)
CAP	6.92 ± 0.15 ^b	82.35 ± 0.23 ^b	52.86 ± 0.19 ^b	0.83 ± 0.01 ^b	29.49 ± 0.04 ^b	1.10 ± 0.01 ^b	3.03 ± 0.08 ^a
CAS	2.58 ± 0.05 ^a	64.93 ± 0.41 ^a	45.25 ± 0.31 ^a	5.68 ± 0.05 ^a	19.68 ± 0.10 ^a	2.13 ± 0.16 ^a	3.99 ± 0.04 ^b

Values are means ± SD of three separate experiments. Different letters indicate a comparison between the two polysaccharides at a level of $p < 0.05$.

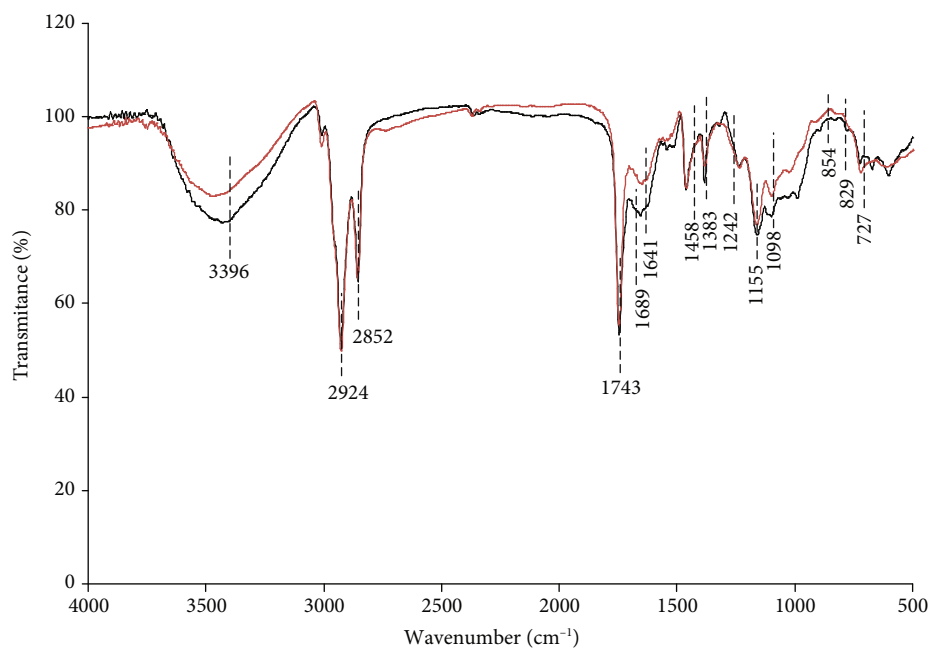


FIGURE 1: Fourier-transform infrared spectroscopy spectra of CAS and CAP.

of the different bacterial suspensions (10^6 CFU/mL) were added. Plates were then incubated at 37°C for 24 h. The MIC was considered as the lowest concentration of drugs or substances able to inhibit any visible microbial growth.

2.7. Statistical Analysis. Statistical analysis was performed using the SPSS version 18.0 software. All data were analyzed using a one-way analysis of variance (ANOVA) (Tukey test). All values are expressed as mean ± standard deviation (SD) and $p < 0.05$ considered significant.

3. Results and Discussion

3.1. Extraction Yields and Physicochemical Property of Polysaccharides. The extraction yields and chemical composition of the crude polysaccharides CAS and CAP obtained from *C. azarolus* seeds and pulps, respectively, are summarized in Table 1. The extraction yield of CAP (6.92%) was higher than that of CAS (2.58%). Pawlaczyk-Graja [10] reported that the extraction yield of polysaccharides from *C. monogyna* flowers and fruits ranged from 16.7 to 4.1%. Our results were in line with previous reports suggesting that the differences in species, conditions, and type of extraction procedure could influence the extraction yield of polysaccharides [32]. CAP and CAS showed relative high ash content

(3.08% in CAP and 3.99% in CAS). This high content could be related to the presence of residual inorganic salt after the purification of polysaccharides. Protein contents were 0.83% and 5.68% for CAP and CAS, respectively. CAP showed 82.35% of carbohydrate and 52.86% of neutral sugar contents, which were higher than those of CAS (64.93% of carbohydrate and 45.25% of neutral sugar). Uronic acid contents were 29.49% for CAP and 19.68% for CAS suggesting the presence of acidic polysaccharides [33].

3.2. FT-IR Spectrometric Analysis. For quick evaluation of the important functional groups and linkage of polysaccharides, the FT-IR spectrum of CAP and CAS was performed, and results are illustrated in Figure 1. The comparison of both spectra indicated similar patterns. Both spectra showed broad peaks at around 3396 cm^{-1} which were ascribed to the stretching vibration of hydroxyl groups in the constituent sugar residues [34]. The peaks at approximately 2924 and 1242 cm^{-1} were related to the C-H asymmetric stretching vibration [35]. The peak located at 1537 cm^{-1} suggested the presence of phenolic groups [36]. The absorbance peaks at about 1743 cm^{-1} , 1689 cm^{-1} , and 1522 cm^{-1} were attributed to carboxyl and carboxylate vibrations, showing the presence of uronic acids [37, 38], which was verified by chemical analysis. The region at around 1000–1200 cm^{-1} indicates the

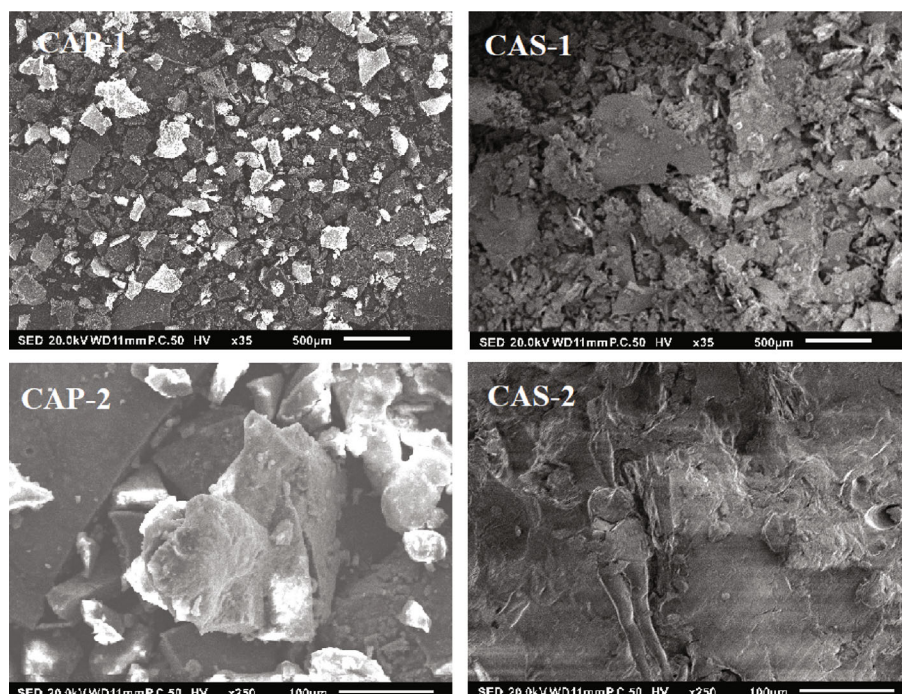


FIGURE 2: Scanning electron micrographs of polysaccharides from CAP and CAS (1: magnification 35x, scale bar 500 μm ; 2: magnification 250x, scale bar 100 μm).

presence of pyranose [39]. The characteristic absorptions at 854 cm^{-1} and 921 cm^{-1} might be attributed to the existence of α and β configurations in CAP and CAS [40].

3.3. SEM Analysis. The microstructure of the two samples indicated differences when analyzed by SEM at different magnifications (35x and 250x) (Figure 2). CAS consisted of many small particles in aggregation with irregular shape and dimensions [41], whereas CAP has a relatively uniform surface with schistose substances. Nep and Conway [42] reported that the method of the preparation of the plant material may affect the shape and surface topology of polysaccharides.

3.4. Triple-Helical Conformation Analysis. The Congo red is a sensitive technique to confirm the conformational structure of the polysaccharides as a triple-helical structure [43]. In general, when a polysaccharide with a triple-helical conformation is mixed with Congo red, the λ_{max} will shift towards a longer wavelength [33]. But this λ_{max} will decrease rapidly with the increase of NaOH concentrations (Figure 3). Our results showed that the λ_{max} of Congo red-CAP complex and Congo red-CAS complex presented a comparable shift trend as Congo red alone once the concentration of NaOH increased from 0 to 0.5 mol/L, suggesting no triple-helical conformation for both polysaccharides.

3.5. In Vitro Antioxidant Activities Analysis

3.5.1. DPPH Radical Scavenging Activity. The scavenging rates of DPPH radicals by both polysaccharides increased with the increase of concentrations ranging from 0.1 to 4 mg/mL (Figure 4(a)). The scavenging effects attained maximum values of 83.2% and 63.74% for CAP and CAS, respec-

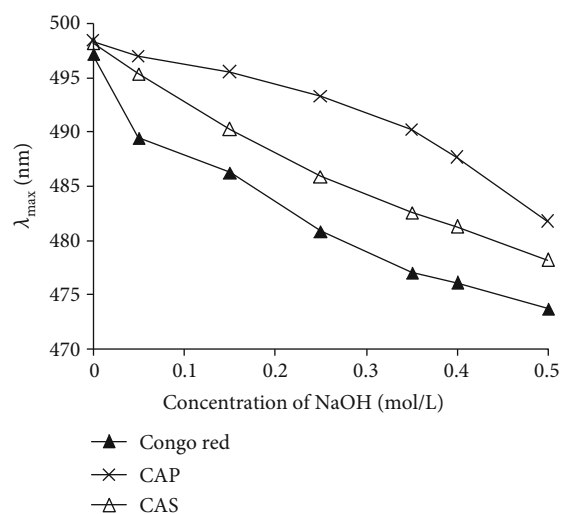


FIGURE 3: Changes in absorption wavelength maximum (λ_{max}) of CAS and CAP Congo red complex at various NaOH concentrations. The maximum absorption wavelength of the mixture was determined by ultraviolet scanning (250–550 nm).

tively, at the concentration of 4 mg/mL. It can be seen that the scavenging capacity of *C. azarolus* polysaccharides to DPPH radicals was similar to other polysaccharides. For example, polysaccharides extracted from *Crataegus pinnatifida* Bunge (CPPu) have been reported to have a DPPH radical scavenging activity of 87.4% at a concentration of 5 mg/mL [44]. CAS had lower efficacy to scavenge DPPH ($\text{SC}_{50} = 2.56\text{ mg/mL}$) than CAP ($\text{SC}_{50} = 1.47\text{ mg/mL}$). However, the free radical scavenging ability of CAP and CAS was lower than that of the positive control (vitamin C, $\text{SC}_{50} = 0.47\text{ mg/mL}$). The

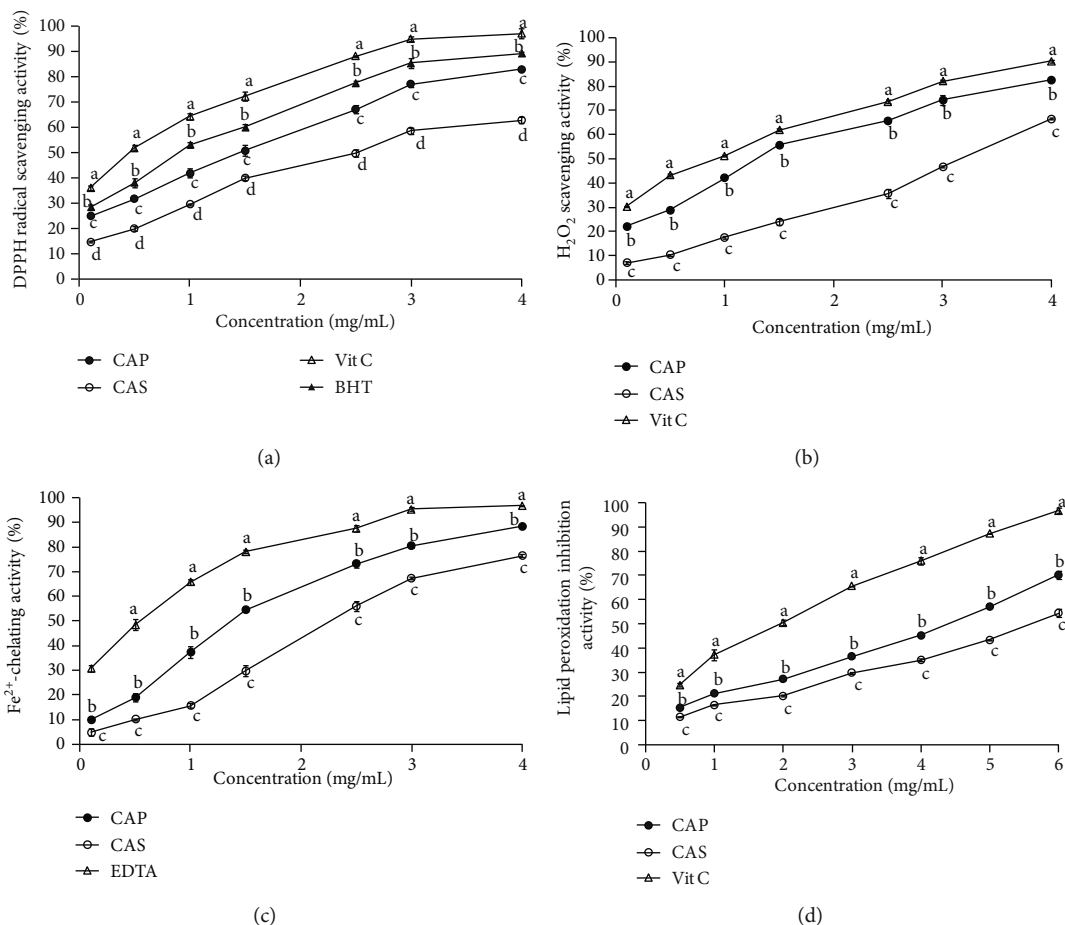


FIGURE 4: Antioxidant activities of CAP and CAS with different methods. (a) DPPH scavenging activity; (b) H₂O₂ scavenging activity; (c) Fe²⁺-chelating activity; (d) lipid peroxidation inhibition activity. Positive controls consisted of Vit C, BHT, and EDTA (vitamin C, butylated hydroxytoluene, and ethylenediaminetetraacetic acid, respectively). Each value is expressed as mean \pm SD of three replicates. Different letters represent the significant difference ($p < 0.05$) at the same concentration for different samples.

DPPH radical scavenging ability of CAP and CAS was higher than that of polysaccharide extracted from the fruits of *Morus nigra* [45] but lower than that from *Nitraria retusa* fruit polysaccharide [3]. Previous studies suggested that the content of uronic acid is a key factor in the antioxidant effects of polysaccharides [46, 47]. Our study showed that CAP and CAS contained 29.49 and 19.68% uronic acid, respectively, which might serve as an important factor in the antioxidant capacity of both polysaccharides. Moreover, Blois [48] has demonstrated that hydroxyl groups are involved in the higher DPPH radical scavenging ability, which was consistent to our study.

3.5.2. H₂O₂ Scavenging Activity. H₂O₂ scavenging effect of CAP and CAS are illustrated in Figure 4(b). Clearly, there was a dose-dependent relationship between each polysaccharide concentrations and the antioxidant activity. The scavenging efficiencies of CAP, CAS, and vitamin C at 4 mg/mL were 82.48%, 66.51%, and 90.25%, respectively. The SC₅₀ value of the CAP was 1.34 mg/mL, which was 2.39-fold lower than that of CAS, indicating that CAP is a more potent radical scavenger than CAS. In the literature, there are no studies on the H₂O₂ scavenging effect of the *Crataegus* species presented in the present study. In comparison with polysaccha-

rides extracted from the fruits of other species, the antiradical activity of CAP was found near to that of *Lycium europaeum* (SC₅₀ = 1.19 mg/mL) [49] and lower than that of *Nitraria retusa* (SC₅₀ = 2.03 mg/mL) [3]. Previous studies reported that the scavenging abilities of polysaccharides might depend on functional groups as COOH and OH present in saccharides structures [50], which was similar to the present study.

3.5.3. Ferrous Ion-Chelating Activity. Metal ions (Cu²⁺, Pb²⁺, and Fe²⁺) are well known to be engaged in the generation of free radicals and indirectly contribute to lipid peroxidation and DNA damage. The Fe²⁺-chelating activity of the CAP and CAS was evaluated, and results are illustrated in Figure 4(c). Both polysaccharides exhibited good concentration-dependent ferrous ion-chelating ability. The chelating potential increased with increasing concentration up to 4 mg/mL and was always stronger for CAP than CAS. This might be due to a stronger chelating ability for CAP compared to CAS. At 4 mg/mL, the chelating potential of CAP, CAS, and EDTA were 88.43%, 76.53%, and 96.76%, respectively. The EC₅₀ values of CAP and CAS were 1.38 and 2.28 mg/mL, respectively, which were higher than that of EDTA (0.51 mg/L). In the literature, there are no studies

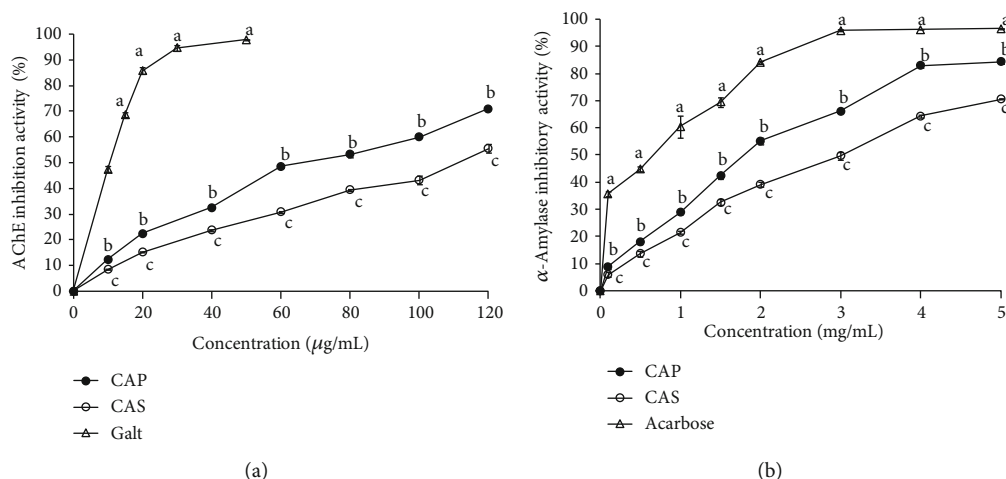


FIGURE 5: Enzyme inhibitory activities of CAP and CAS with various concentrations. (a) AChE inhibitory activity; (b) α -amylase inhibitory activity. Each value is expressed as mean \pm SD of three replicates. Different letters represent the significant difference ($p < 0.05$) at the same concentration for different samples.

on the Fe^{2+} -chelating activity of the *Crataegus* species presented in the present study. The ferrous ion-chelating ability of CAP was found to be close to that of polysaccharides extracted from *Malva aegyptiaca* ($\text{EC}_{50} = 1.15 \text{ mg/mL}$) [51]. It has been reported that biomolecules including some functional groups like COH can easily chelate ferrous (Fe^{2+}) ions. In addition, the substances, which own two or more functional groups of OH, COOH, SH, S, CO, and O, had a structure-function relationship [52]. Accordingly, the chelating activity of CAP and CAS might be in part linked to the presence of the strong Fe^{2+} -chelating groups in their structure.

3.5.4. Liver Lipid Peroxidation Inhibition Activity. Lipid peroxidation is widely recognized as a key process in diverse diseases [26]. In the literature, there are no studies on the lipid peroxidation inhibition activity of the *Crataegus* species presented in the present study. The effects of both polysaccharides on $\text{FeCl}_2\text{-H}_2\text{O}_2$ -induced lipid peroxidation in mice liver are illustrated in Figure 4(d). The result showed that liver lipid peroxidation was effectively inhibited by CAS and CAP at all tested concentrations. At 6 mg/mL, the inhibition effects of CAP, CAS, and vitamin C were 70.07%, 54.32%, and 96.57%, respectively. The EC_{50} values of the CAP and CAS were 4.44 and 5.52 mg/mL, respectively, which were lower than that of vitamin C (2.29 mg/mL). It has been documented that the protective effects of natural antioxidants (like polysaccharides) on lipid peroxidation induced by $\text{Fe}^{2+}/\text{H}_2\text{O}_2$ system might be assigned to their scavenging abilities on H_2O_2 and OH radical [53]. Another report [26] revealed that polysaccharides with high metal ion-chelating activities are able to inhibit peroxidation by interfering with the free radical reaction chains.

3.6. Enzyme Inhibitory Activity Assays

3.6.1. Acetylcholinesterase (AChE) Inhibition. Alzheimer's disease (AD) is an example of a neurodegenerative disease which affects the memory. One of the goals of AD treatment is to increase the level of acetylcholine in the brain by inhibit-

ing the activity of AChE [54]. Due to the lack of effective treatments for AD and the considerable side effects associated with the use of neuroprotective drugs, researchers are constantly looking for new and more effective therapies from medicinal plants to improve the loss of neuronal cells and brain restoration [55, 56]. Natural antioxidants have been often evinced to have beneficial effects in the prevention of memory impairment. Several investigations have demonstrated the neuroprotective and antioxidant effects of phenolic compounds extracted from hawthorn seeds [57, 58]. These properties were explained by their inhibitory effects on lipid peroxidation and free radicals. Other studies have demonstrated the anticholinesterase activity of phenolic compounds isolated from *C. oxyacantha* [59]. However, the enzyme inhibitory effect of polysaccharides from these plants has not yet been reported. In this study, the effects of both polysaccharides extracted from *C. azarolus* on AChE inhibitory activities are presented in Figure 5(a). The inhibitory effect of CAP and CAS was proportional to the concentration (10–120 $\mu\text{g/mL}$). The inhibitory effect of CAS was 55.46% at a concentration of 120 $\mu\text{g/mL}$, which was weaker than the CAP (71.03%) under the same concentration. As summarized in Table 2, CAP displayed important AChE inhibitory activity ($\text{EC}_{50} = 61.56 \mu\text{g/mL}$) as compared to CAS ($\text{EC}_{50} = 115.94 \mu\text{g/mL}$). In this study, the anticholinesterase drug galantamine (an alkaloid isolated from the bulbs and flowers of *Galanthus caucasicus* and FDA-approved drug) was used as a positive control. Results showed that the activity of CAP was less than that of galantamine ($\text{EC}_{50} = 10.53 \mu\text{g/mL}$). AChE inhibitory activity of CAP and CAS were higher than those of *Physalis alkekengi* and *Flammulina velutipes* polysaccharides [60, 61]. This implies that CAS and CAP could be potential inhibitors of AChE and beneficial for human memory. The modulation of the cholinergic system could be one of the pharmacological mechanisms used by *Crataegus* to improve memory problems. In this inhibitory mechanism, polysaccharides

TABLE 2: Inhibition activity (IC₅₀ values) of CAS and CAP on studied enzymes.

	CAP	CAS	Galantamine	Acarbose
AChE (IC ₅₀ , µg/mL)	61.56 ± 0.64 ^b	115.94 ± 4.68 ^c	10.53 ± 0.23 ^a	—
α-Amylase (IC ₅₀ , mg/mL)	1.81 ± 0.03 ^b	3.01 ± 0.08 ^c	—	0.82 ± 0.04 ^a

Values are means ± SD of three separate experiments. Different letters indicate a comparison between the samples at a level of $p < 0.05$.

TABLE 3: The antimicrobial activity and MICs of CAP and CAS.

Microorganism	Diameters of inhibition zone (mm)		MICs (mg/mL)	
	CAP	CAS	CAP	CAS
Gram negative				
<i>Escherichia coli</i> (ATCC 35218)	12.48 ± 0.02	11.25 ± 0.05	3.12	6.25
<i>Klebsiella pneumoniae</i> (ATCC 13883)	10.16 ± 0.04	9.16 ± 0.07	6.25	12.5
<i>Salmonella typhimurium</i> (ATCC 23564)	13.21 ± 0.01	11.62 ± 0.02	1.56	3.12
Gram positive				
<i>Bacillus cereus</i> (ATCC 11778)	14.49 ± 0.01	8.61 ± 0.02	1.56	3.12
<i>Listeria monocytogenes</i> (ATCC 19117)	16.65 ± 0.05	11.4 ± 0.11	<1.56	1.56
<i>Staphylococcus aureus</i> (ATCC 25923)	12.36 ± 0.04	10.15 ± 0.05	3.12	6.25
<i>Enterococcus faecalis</i> (ATCC 29212)	13.95 ± 0.05	11.66 ± 0.04	3.12	1.56

MIC: minimum inhibitory concentration. Values are means ± SD of three separate experiments.

(inhibitors) bind to the same active site as the enzyme substrate, and this implies a nonmetabolizable response [62].

3.6.2. α-Amylase Inhibition. Among the available procedures, inhibition of α-amylase has seemed to be an important therapeutic target for the prevention and management of type 2 diabetes mellitus [63]. When the activity of α-amylase is inhibited, the increase of blood glucose concentrations can be delayed. There were a few researches on the inhibition activity of α-amylase by *Crataegus* sp. extracts [8]. As far as we know, the present study is the first to describe the *in vitro* antidiabetic effects of polysaccharides from *C. azarolus*. As illustrated in Figure 5(b), both polysaccharides displayed α-amylase inhibitory activity in a dose-dependent manner at the range from 0.1 to 5.0 mg/mL. The EC₅₀ value of CAP was about 1.81 mg/mL, which was more effective than that of CAS (EC₅₀ = 3.01 mg/mL) but less effective than that of acarbose (EC₅₀ = 0.82 mg/mL) (Table 2). The inhibitory effects of polysaccharides from *C. azarolus* were similar to that from *Diaphragma juglandis fructus* [64], but also more efficient than that from *Corbicula fluminea* [65] and blackcurrant fruits [66], which have been demonstrated as potent antihyperglycemic agents *in vivo*. Authors have suggested that the high antihyperglycemic capacity of polysaccharides was related to their structure, the configuration of glycosidic bonds, monosaccharide composition, and the high uronic acid content. Other studies have shown that the inhibition mechanism could be that the carboxyl group and the hydroxyl group of polysaccharides could react with the amino acid residues of the digestive enzymes, which caused a reduction in the α-amylase activity [67].

3.7. Antimicrobial Activity. Antimicrobial activity of CAP and CAS tested against seven microorganisms is summarized

in Table 3. The result evidenced that the antibacterial effect of both polysaccharides varied with bacterial species. The inhibition zone diameter of the two polysaccharides against tested bacteria ranged from 10.16 to 16.65 mm and from 8.61 to 11.66 mm for CAP and CAS, respectively. CAP revealed the best antimicrobial effect against *L. monocytogenes* and *B. cereus*. However, CAS displayed the highest inhibition activity toward *E. faecalis*. Moderate antibacterial activity was observed against *K. pneumoniae* with inhibition zones of 10.16 and 9.16 mm for CAP and CAS, respectively. The antimicrobial activity of polysaccharides was also estimated as minimal inhibitory concentration (MIC) (Table 3). Results proved that Gram-positive bacteria were more sensitive to both polysaccharides than Gram-negative. These findings were in accordance with previously published searches [68, 69]. They reported that the outer membrane of Gram (-) bacteria may act as a barrier against hyperacidification, which would result in differences in the resistance of Gram-positive and Gram-negative bacteria to the action of antimicrobial drugs. The mechanisms related to the antimicrobial activity of polysaccharides were still not clear and deserve to be deepened. The broad-spectrum antimicrobial potential of CAP and CAS may be explained by their higher total sugar contents [48]. He et al. [70] reported that the inhibition effect of polysaccharides may be explained by their abilities to induce the disruption of the cell wall of bacteria and to enhance ion permeability leading cell death. Further, DNA might be decomposed into small fragment after the polysaccharide has penetrated into the cell, which can make the bacteria unable to develop resistance. The best activity against *Listeria monocytogenes* was observed with CAP (MIC < 1.56 mg/mL). In the literature, there are no studies on the antimicrobial activity of the *Crataegus* species presented in the present study. The results of MICs denoted that

MIC values of polysaccharides from *C. azarolus* found in this study were lower than those obtained in previous findings, which were on the order of 6.25 and 25 mg/mL for polysaccharide from *Saussurea controversa* and from 3.12 to 100 mg/mL for polysaccharide from *Lallemantia royleana*, respectively [71, 72].

4. Conclusion

In the present study, two polysaccharides (CAP and CAS) were extracted from *C. azarolus* fruits, and their physicochemical properties were characterized using FT-IR, SEM, and Congo red test. Results of FT-IR analysis indicated that CAP and CAS have similar functional groups that are typical of polysaccharides. Both polysaccharides were devoid of helical conformation. CAP had the highest H₂O₂ and DPPH radicals scavenging activities and maximum chelating activity on ferrous ion. *In vitro* CAP remarkably decreased liver lipid peroxidation levels induced by FeCl₂-H₂O₂. Both polysaccharides successfully inhibited AChE and α -amylase activities and exhibited effective antimicrobial properties against seven pathogenic bacteria. Altogether, our studies suggest that *C. azarolus* fruits can be further used in food production as a useful natural antioxidant ingredient. Nevertheless, additional studies deserve to be carried out which will elucidate a clear structure-activity relationship.

Data Availability

All data included in this study are available upon request by contacting the corresponding author.

Conflicts of Interest

The authors declare that there is no conflict of interest.

Acknowledgments

We greatly appreciate the technical support provided by the Unit of Common Services, Faculty of Sciences Gafsa, Tunisia.

References

- [1] J. H. Xie, M. L. Jin, G. A. Morris et al., "Advances on bioactive polysaccharides from medicinal plants," *Critical Reviews in Food Science and Nutrition*, vol. 56, pp. 60–84, 2016.
- [2] D. Wei, T. Chen, M. Yan et al., "Synthesis, characterization, antioxidant activity and neuroprotective effects of selenium polysaccharide from *Radix hedysari*," *Carbohydrate Polymers*, vol. 125, pp. 161–168, 2015.
- [3] I. Rjeibi, A. Feriani, F. Hentati, N. Hfaiedh, P. Michaud, and G. Pierre, "Structural characterization of water-soluble polysaccharides from *Nitraria retusa* fruits and their antioxidant and hypolipidemic activities," *International Journal of Biological Macromolecules*, vol. 129, pp. 422–432, 2019.
- [4] D. Bais, A. Trevisan, R. Lapasin, P. Partal, and C. Gallegos, "Rheological characterization of polysaccharide-surfactant matrices for cosmetic O/W emulsions," *Journal of Colloid and Interface Science*, vol. 290, no. 2, pp. 546–556, 2005.
- [5] K. L. Christensen, "A biometric study of some hybridizing *Crataegus* populations in Denmark," *Nordic Journal of Botany*, vol. 2, no. 6, pp. 537–548, 1983.
- [6] R. Bahri-Sahloul, R. Ben Fredj, N. Boughalleb et al., "Phenolic composition and antioxidant and antimicrobial activities of extracts obtained from *Crataegus azarolus* L. var. *aronia* (Willd.) Batt. ovaries calli," *Journal of Botany*, vol. 2014, 11 pages, 2014.
- [7] M. Hanus, J. Lafon, and M. Mathieu, "Double-blind, randomised, placebo-controlled study to evaluate the efficacy and safety of a fixed combination containing two plant extracts (*Crataegus oxyacantha* and *Eschscholtzia californica*) and magnesium in mild-to-moderate anxiety disorders," *Current Medical Research and Opinion*, vol. 20, pp. 63–71, 2008.
- [8] D. Kumar, V. Arya, Z. A. Bhat, N. A. Khan, and D. N. Prasad, "The genus *Crataegus*: chemical and pharmacological perspectives," *Revista Brasileira de Farmacognosia*, vol. 22, no. 5, pp. 1187–1200, 2012.
- [9] J. E. Edwards, P. N. Brown, N. Talent, T. A. Dickinson, and P. R. Shipley, "A review of the chemistry of the genus *Crataegus*," *Phytochemistry*, vol. 79, pp. 5–26, 2012.
- [10] I. Pawlaczyk-Graja, "Polyphenolic-polysaccharide conjugates from flowers and fruits of single-seeded hawthorn (*Crataegus monogyna* Jacq.): chemical profiles and mechanisms of anticoagulant activity," *International Journal of Biological Macromolecules*, vol. 116, pp. 869–879, 2018.
- [11] R. G. Zhu, Y. D. Sun, T. P. Li et al., "Comparative effects of hawthorn (*Crataegus pinnatifida* Bunge) pectin and pectin hydrolyzates on the cholesterol homeostasis of hamsters fed high-cholesterol diets," *Chemico-Biological Interactions*, vol. 238, pp. 42–47, 2015.
- [12] S. Zhang, C. Zhang, M. Li, X. Chen, and K. Ding, "Structural elucidation of a glucan from *Crataegus pinnatifida* and its bioactivity on intestinal bacteria strains," *International Journal of Biological Macromolecules*, vol. 128, pp. 435–443, 2019.
- [13] S. Jeong, R. Tulasi, and S. Koyyalamudi, "Antioxidant capacities of hot water extracts and endopolysaccharides of selected Chinese medicinal fruits," *Cancers*, vol. 8, no. 3, p. 33, 2016.
- [14] R. Bahri-Sahloul, S. Ammar, S. Grec, and F. Harzallah-Skhiri, "Chemical characterisation of *Crataegus azarolus* L. fruit from 14 genotypes found in Tunisia," *Journal of Horticultural Science and Biotechnology*, vol. 84, pp. 23–28, 2015.
- [15] M. Belkhir, O. Rebai, K. Dhaouadi, B. Sioud, M. Amri, and S. Fattouch, "Antioxidant and antimicrobial activities of Tunisian azarole (*Crataegus Azarolus* L.) leaves and fruit pulp/peel polyphenolic extracts," *International Journal of Food Properties*, vol. 16, no. 6, pp. 1380–1393, 2013.
- [16] E. Abu-Gharbieh and N. G. Shehab, "Therapeutic potentials of *Crataegus azarolus* var. *eu-azarolus* Maire leaves and its isolated compounds," *BMC Complementary and Alternative Medicine*, vol. 17, no. 1, p. 218, 2017.
- [17] A. Yahyaoui, M. O. Arfaoui, G. Rigane et al., "Investigation on the chemical composition and antioxidant capacity of extracts from *Crataegus azarolus* L.: effect of growing location of an important Tunisian medicinal plant," *Chemistry Africa*, vol. 2, no. 3, pp. 361–365, 2019.
- [18] M. Dubois, K. A. Gilles, J. K. Hamilton, P. Rebers, and F. Smith, "Colorimetric method for determination of sugars and related substances," *Analytical Chemistry*, vol. 28, no. 3, pp. 350–356, 1956.

- [19] M. Monsigny, C. Petit, and A. C. Roche, "Colorimetric determination of neutral sugars by a resorcinol sulfuric acid micro-method," *Analytical Chemistry*, vol. 175, pp. 525–530, 1988.
- [20] V. L. Singleton, R. Orthofer, and R. M. Lamuela-Raventós, "Analysis of total phenols and other oxidation substrates and antioxidants by means of folin-ciocalteu reagent," *Method in Enzymology*, vol. 299, pp. 152–178, 1999.
- [21] N. Blumenkrantz and G. Asboe-Hansen, "New method for quantitative determination of uronic acids," *Analytical Chemistry*, vol. 54, pp. 484–489, 1973.
- [22] M. M. Bradford, "A rapid and sensitive method for the quantitation of microgram quantities of protein utilizing the principle of protein-dye binding," *Analytical Chemistry*, vol. 72, pp. 248–254, 1976.
- [23] Association of Official Analytical Chemists-AOAC, *Official Method of Analysis of AOAC Method 996.11*, AOAC International, Gaithersburg, MD, USA, 18th edition, 2005.
- [24] D. Rout, S. Mondal, I. Chakraborty, and S. S. Islam, "The structure and conformation of a water-insoluble (1→3)-, (1→6)- β -d-glucan from the fruiting bodies of *Pleurotus florida*," *Carbohydrate Research*, vol. 343, no. 5, pp. 982–987, 2008.
- [25] P. Bersuder, M. Hole, and G. Smith, "Antioxidants from a heated histidine-glucose model system. I: investigation of the antioxidant role of histidine and isolation of antioxidants by high-performance liquid chromatography," *Journal of American Oil Chemists' Society*, vol. 75, no. 2, pp. 181–187, 1998.
- [26] J. Liu, J. Luo, H. Ye, Y. Sun, Z. Lu, and X. Zeng, "In vitro and in vivo antioxidant activity of exopolysaccharides from endophytic bacterium *Paenibacillus polymyxa* EJS-3," *Carbohydrate Polymers*, vol. 82, no. 4, pp. 1278–1283, 2010.
- [27] N. R. Perron, H. C. Wang, S. N. DeGuire, M. Jenkins, M. Lawson, and J. L. Brumaghim, "Kinetics of iron oxidation upon polyphenol binding," *Dalton Transactions*, vol. 39, no. 41, pp. 9982–9987, 2010.
- [28] G. C. Yen and C. L. Hsieh, "Antioxidant activity of extracts from *Du-zhong* (*Eucommia ulmoides*) toward various lipid peroxidation models in vitro," *Journal of Agricultural and Food Chemistry*, vol. 46, no. 10, pp. 3952–3957, 1998.
- [29] G. L. Ellman, K. D. Courtney, V. Andres Jr., and R. M. Featherstone, "A new and rapid colorimetric determination of acetylcholinesterase activity," *Biochemical Pharmacology*, vol. 7, no. 2, pp. 88–95, 1961.
- [30] G. Oboh, A. O. Ademosun, P. O. Ayeni, O. S. Omojokun, and F. Bello, "Comparative effect of quercetin and rutin on α -amylase, α -glucosidase, and some pro-oxidant-induced lipid peroxidation in rat pancreas," *Comparative Clinical Pathology*, vol. 24, no. 5, pp. 1103–1110, 2015.
- [31] B. Gullon, M. E. Pintado, J. A. Pérez-Álvarez, and M. Viuda-Martos, "Assessment of polyphenolic profile and antibacterial activity of pomegranate peel (*Punica granatum*) flour obtained from co-product of juice extraction," *Food Control*, vol. 59, pp. 94–98, 2015.
- [32] Z. Y. Zhu, F. Dong, X. Liu et al., "Effects of extraction methods on the yield, chemical structure and anti-tumor activity of polysaccharides from *Cordyceps gunnii* mycelia," *Carbohydrate Polymers*, vol. 140, pp. 461–471, 2016.
- [33] J. Chen, X. Zhang, D. Huo et al., "Preliminary characterization, antioxidant and α -glucosidase inhibitory activities of polysaccharides from *Mallotus furetianus*," *Carbohydrate Polymers*, vol. 215, pp. 307–315, 2019.
- [34] N. Hammami, A. B. Gara, K. Bargougui, H. Ayedi, F. B. Abdal-leh, and K. Belghith, "Improved in vitro antioxidant and antimicrobial capacities of polysaccharides isolated from *Salicornia Arabica*," *International Journal of Biological Macromolecules*, vol. 120, no. Part B, pp. 2123–2130, 2018.
- [35] X. Xu, P. Chen, L. Zhang, and H. Ashida, "Chain structures of glucans from *Lentinus edodes* and their effects on NO production from RAW 264.7 macrophages," *Carbohydrate Polymers*, vol. 87, no. 2, pp. 1855–1862, 2012.
- [36] D. Stewart, H. M. Wilson, P. L. Hendra, and I. M. Morrison, "Fourier-transform infrared and Raman spectroscopic study of biochemical and chemical treatments of oak wood (*Quercus rubra*) and barley (*Hordeum vulgare*) straw," *Journal of Agricultural and Food Chemistry*, vol. 43, no. 8, pp. 2219–2225, 1995.
- [37] M. Kačuráková, N. Wellner, A. Ebringerová, Z. Hromádková, R. H. Wilson, and P. S. Belton, "Characterisation of xylan-type polysaccharides and associated cell wall components by FT-IR and FT-Raman spectroscopies," *Food Hydrocolloids*, vol. 13, no. 1, pp. 35–41, 1999.
- [38] Z. Chai, W. Huang, X. Zhao, H. Wu, X. Zeng, and C. Li, "Preparation, characterization, antioxidant activity and protective effect against cellular oxidative stress of polysaccharide from *Cynanchum auriculatum* Royle ex Wight," *International Journal of Biological Macromolecules*, vol. 119, pp. 1068–1076, 2018.
- [39] Q. Zhao, B. Dong, J. Chen et al., "Effect of drying methods on physicochemical properties and antioxidant activities of wolfberry (*Lycium barbarum*) polysaccharide," *Carbohydrate Polymers*, vol. 127, pp. 176–181, 2015.
- [40] R. Taylor and H. E. Conrad, "Stoichiometric depolymerization of polyuronides and glycosaminoglycuronans to monosaccharides following reduction of their carbodiimide-activated carboxyl group," *Biochemistry*, vol. 11, pp. 1383–1388, 2002.
- [41] B. H. Wang, J. J. Cao, B. Zhang, and H. Q. Chen, "Structural characterization, physicochemical properties and α -glucosidase inhibitory activity of polysaccharide from the fruits of wax apple," *Carbohydrate Polymers*, vol. 211, pp. 227–236, 2019.
- [42] E. I. Nep and B. R. Conway, "Characterization of grewia gum, a potential pharmaceutical excipient," *Journal of Excipients and Food Chemicals*, vol. 1, pp. 30–40, 2010.
- [43] K. P. Wang, J. Wang, Q. Li et al., "Structural differences and conformational characterization of five bioactive polysaccharides from *Lentinus edodes*," *Food Research International*, vol. 62, pp. 223–232, 2014.
- [44] X. Chen, H. Zhang, W. Du et al., "Comparison of different extraction methods for polysaccharides from *Crataegus pinnatifida* Bunge," *International Journal of Biological Macromolecules*, vol. 150, pp. 1011–1019, 2019.
- [45] W. Wang, X. Li, X. Bao, L. Gao, and Y. Tao, "Extraction of polysaccharides from black mulberry fruit and their effect on enhancing antioxidant activity," *International Journal of Biological Macromolecules*, vol. 120, no. Part B, pp. 1420–1429, 2018.
- [46] H. Chen, M. Zhang, and B. Xie, "Quantification of uronic acids in tea polysaccharide conjugates and their antioxidant properties," *Journal of Agricultural and Food Chemistry*, vol. 52, no. 11, pp. 3333–3336, 2004.
- [47] L. Tian, Y. Zhao, C. Guo, and X. Yang, "A comparative study on the antioxidant activities of an acidic polysaccharide and various solvent extracts derived from herbal *Houttuynia*

- cordata," *Carbohydrate Polymers*, vol. 83, no. 2, pp. 537–544, 2011.
- [48] M. S. Blois, "Antioxidant determinations by the use of a stable free radical," *Nature*, vol. 181, no. 4617, pp. 1199–1200, 1958.
- [49] I. Rjeibi, A. Feriani, A. B. Saad et al., "Lycium europaeum Linn as a source of polysaccharide with in vitro antioxidant activities and in vivo anti-inflammatory and hepatonephroprotective potentials," *Journal of Ethnopharmacology*, vol. 225, pp. 116–127, 2018.
- [50] C. Liu, J. Chang, L. Zhang, J. Zhang, and S. Li, "Purification and antioxidant activity of a polysaccharide from bulbs of *Fritillaria ussuriensis* Maxim," *International Journal of Biological Macromolecules*, vol. 50, no. 4, pp. 1075–1080, 2012.
- [51] N. Fakhfakh, O. Abdelhedi, H. Jdir, M. Nasri, and N. Zouari, "Isolation of polysaccharides from *Malva aegyptiaca* and evaluation of their antioxidant and antibacterial properties," *International Journal of Biological Macromolecules*, vol. 105, Part 2, pp. 1519–1525, 2017.
- [52] J. Wang, S. Hu, S. Nie, Q. Yu, and M. Xie, "Reviews on mechanisms of in vitro antioxidant activity of polysaccharides," *Oxidative Medicine and Cellular Longevity*, vol. 2016, 13 pages, 2016.
- [53] L. Chun-hui, W. Chang-hai, X. Zhi-liang, and W. Yi, "Isolation, chemical characterization and antioxidant activities of two polysaccharides from the gel and the skin of *Aloe barbadensis* Miller irrigated with sea water," *Process Biochemistry*, vol. 42, no. 6, pp. 961–970, 2007.
- [54] V. N. Talesa, "Acetylcholinesterase in Alzheimer's disease," *Mechanisms of Ageing and Development*, vol. 122, no. 16, pp. 1961–1969, 2001.
- [55] L. E. Collins, N. E. Paul, S. F. Abbas et al., "Oral tremor induced by galantamine in rats: a model of the parkinsonian side effects of cholinomimetics used to treat Alzheimer's disease," *Pharmacology Biochemistry and Behavior*, vol. 99, no. 3, pp. 414–422, 2011.
- [56] E. Esposito and S. Cuzzocrea, "New therapeutic strategy for Parkinson's and Alzheimer's disease," *Current Medicinal Chemistry*, vol. 17, no. 25, pp. 2764–2774, 2010.
- [57] Z. Y. Cheng, L. L. Lou, P. Y. Yang et al., "Seven new neuroprotective sesquiterpene lignans isolated from the seeds of *Crataegus pinnatifida*," *Fitoterapia*, vol. 133, pp. 225–230, 2019.
- [58] X. X. Huang, M. Bai, L. Zhou et al., "Food byproducts as a new and cheap source of bioactive compounds: lignans with antioxidant and anti-inflammatory properties from *Crataegus pinnatifida* seeds," *Journal of Agricultural and Food Chemistry*, vol. 63, no. 32, pp. 7252–7260, 2015.
- [59] M. Ali, S. Muhammad, M. R. Shah et al., "Neurologically potent molecules from *Crataegus oxyacantha*; isolation, anticholinesterase inhibition, and molecular docking," *Frontiers in Pharmacology*, vol. 8, p. 327, 2017.
- [60] X. Liu, J. Bian, D. Li et al., "Structural features, antioxidant and acetylcholinesterase inhibitory activities of polysaccharides from stem of *Physalis alkekengi* L.," *Industrial Crops and Products*, vol. 129, pp. 654–661, 2019.
- [61] W. Yang, Y. Fang, J. Liang, and Q. Hu, "Optimization of ultrasonic extraction of *Flammulina velutipes* polysaccharides and evaluation of its acetylcholinesterase inhibitory activity," *Food Research International*, vol. 44, no. 5, pp. 1269–1275, 2011.
- [62] C. Chen, L. J. You, A. M. Abbasi, X. Fu, R. H. Liu, and C. Li, "Characterization of polysaccharide fractions in mulberry fruit and assessment of their antioxidant and hypoglycemic activities in vitro," *Food & Function*, vol. 7, no. 1, pp. 530–539, 2016.
- [63] N. Y. Yoon, D. N. Ngo, and S. K. Kim, "Acetylcholinesterase inhibitory activity of novel chitoooligosaccharide derivatives," *Carbohydrate Polymers*, vol. 78, no. 4, pp. 869–872, 2009.
- [64] Q. Meng, F. Chen, T. Xiao, and L. Zhang, "Inhibitory effects of polysaccharide from *Diaphragma juglandis fructus* on α -amylase and α -d-glucosidase activity, streptozotocin-induced hyperglycemia model, advanced glycation end-products formation, and H_2O_2 -induced oxidative damage," *International Journal of Biological Macromolecules*, vol. 124, pp. 1080–1089, 2019.
- [65] J. K. Yan, Y. Y. Wang, W. Y. Qiu, L. X. Wu, Z. C. Ding, and W. D. Cai, "Purification, structural characterization and bioactivity evaluation of a novel proteoglycan produced by *Corbicula fluminea*," *Carbohydrate Polymers*, vol. 176, pp. 11–18, 2017.
- [66] Y. Xu, Y. Guo, Y. Gao et al., "Separation, characterization and inhibition on α -glucosidase, α -amylase and glycation of a polysaccharide from blackcurrant fruits," *LWT-Food Science and Technology*, vol. 93, pp. 16–23, 2018.
- [67] C. Nie, P. Zhu, M. Wang, S. Ma, and Z. Wei, "Optimization of water-soluble polysaccharides from stem lettuce by response surface methodology and study on its characterization and bioactivities," *International Journal of Biological Macromolecules*, vol. 105, Part 1, pp. 912–923, 2017.
- [68] I. Khemakhem, O. Abdelhedi, I. Trigui, M. A. Ayadi, and M. Bouaziz, "Structural, antioxidant and antibacterial activities of polysaccharides extracted from olive leaves," *International Journal of Biological Macromolecules*, vol. 106, pp. 425–432, 2018.
- [69] C. Cueva, M. V. Moreno-Arribas, P. J. Martín-Álvarez et al., "Antimicrobial activity of phenolic acids against commensal, probiotic and pathogenic bacteria," *Research in Microbiology*, vol. 161, no. 5, pp. 372–382, 2010.
- [70] F. He, Y. Yang, G. Yang, and L. Yu, "Studies on antibacterial activity and antibacterial mechanism of a novel polysaccharide from *Streptomyces virginia* H03," *Food Control*, vol. 21, no. 9, pp. 1257–1262, 2010.
- [71] I. Khlusov, E. Avdeeva, V. Shupletsova et al., "Comparative in vitro evaluation of antibacterial and osteogenic activity of polysaccharide and flavonoid fractions isolated from the leaves of *Saussurea controversa*," *Molecules*, vol. 24, no. 20, p. 3680, 2019.
- [72] M. Sardarodiyani, A. Arianfar, A. M. Sani, and S. Naji-Tabasi, "Antioxidant and antimicrobial activities of water-soluble polysaccharide isolated from Balangu seed (*Lallemantia royleana*) gum," *Journal of Analytical Science and Technology*, vol. 10, no. 1, p. 17, 2019.

Research Article

Neuroprotective Effect of Chlorogenic Acid on Mitochondrial Dysfunction-Mediated Apoptotic Death of DA Neurons in a Parkinsonian Mouse Model

Saumitra Sen Singh ¹, Sachchida Nand Rai ², Hareram Birla ¹, Walia Zahra ¹,
Aaina Singh Rathore¹, Hagera Dilnashin ¹, Richa Singh¹ and Surya Pratap Singh ¹

¹Department of Biochemistry, Institute of Science, Banaras Hindu University, Varanasi 221005, India

²Centre of Biotechnology, University of Allahabad, Prayagraj 211002, India

Correspondence should be addressed to Surya Pratap Singh; suryasinghbhu16@gmail.com

Received 7 March 2020; Revised 23 April 2020; Accepted 29 April 2020; Published 27 May 2020

Guest Editor: Francisco Jaime B. Mendonça Junior

Copyright © 2020 Saumitra Sen Singh et al. This is an open access article distributed under the Creative Commons Attribution License, which permits unrestricted use, distribution, and reproduction in any medium, provided the original work is properly cited.

Mitochondrial dysfunction and oxidative stress characterize major factors involved in the activation of complex processes corresponding to apoptosis-mediated neuronal senescence of dopaminergic neurons (DA) in Parkinson's disease (PD). Here, we evaluated the molecular mechanisms participating in the treatment of a 1-methyl-4-phenyl-1,2,3,6-tetrahydropyridine- (MPTP-) intoxicated PD mouse model in response to chlorogenic acid (CGA). The results indicate that CGA treatment significantly improved the motor coordination of the MPTP-intoxicated mice. CGA also alleviated the fall in activity of mitochondrial complexes I, IV, and V in accordance with ameliorating the level of superoxide dismutase and mitochondrial glutathione in the midbrain of MPTP-induced mice. CGA inhibited the activation of proapoptotic proteins including Bax and caspase-3, while elevating the expression of antiapoptotic protein like Bcl-2 consequently preventing the MPTP-mediated apoptotic cascade. The study also revealed the improved phosphorylation state of Akt, ERK1/2, and GSK3 β which was downregulated as an effect of MPTP toxicity. Our findings signify that CGA may possess pharmacological properties and contribute to neuroprotection against MPTP induced toxicity in a PD mouse model associated with phosphorylation of GSK3 β via activating Akt/ERK signalling in the mitochondrial intrinsic apoptotic pathway. Thus, CGA treatment may arise as a potential therapeutic candidate for mitochondrial-mediated apoptotic senescence of DA neurons in PD.

1. Introduction

Research has made it quite prominent that aging plays a prime factor in the onset and progression of the sporadic form of the neurodegenerative disorder Parkinson's disease (PD) characterized by the progressive depletion in the dopaminergic (DA) neurons along with the formation and accumulation of Lewy bodies primarily in the substantia nigra pars compacta (SNpc) region of the midbrain and striatum [1, 2]. While the exact mechanism of PD is yet to be elucidated, promising evidences indicate that oxidative stress and mitochondrial dysfunction play a crucial part in its pathogenesis [3–5]. Lewy body formation, com-

prising aggregates of abnormal or misfolded α -synuclein protein, is a hallmark feature of both familial and sporadic forms of PD. α -Synuclein undergoes aggregation predominantly in the cytoplasm of the neurons present in SN and leads to multifactorial etiopathogenesis of PD [6, 7]. Numerous pathogenic signals including increased oxidative stress, mitochondrial impairment, ubiquitin-proteasomal dysfunction, and activation of apoptotic cascade along with progressive loss of DA neurons cause the pathogenesis of PD [8, 9]. The clinical evidences from PD patients show the formation of free radicals consisting of reactive oxygen species (ROS), reactive nitrogen species (RNS), mitochondrial dysfunction, adenosine triphosphate (ATP)

depletion, and the initiation of caspase-mediated apoptotic cascade in the SN [10].

At the present time, the chief treatment options for PD are dopamine agonists or L-DOPA which simply provide symptomatic relief and show less efficiency with prolonged use resulting in disabling fluctuations and dyskinesias [11]. Therefore, finding treatments with neuroprotective potential against PD in correspondence with effectiveness in relieving symptoms is the main therapeutic target for slowing disease progression. Emerging evidences prove the vital role of apoptosis in PD pathogenesis. Hence, the apoptotic pathway can be prohibited by providing neuroprotection through the use of phytochemicals [12, 13].

Various cell culture models and animal models of PD have been developed using environmental neurotoxins including rotenone, 6-hydroxydopamine, and 1-methyl-4-phenyl-1,2,3,6-tetrahydropyridine (MPTP) [14]. The charged metabolite of MPTP is 1-methyl-4-phenylpyridinium (MPP⁺) acting as the main toxic agent against the DA neurons in the brain of MPTP-intoxicated *in vivo* models [15, 16]. MPP⁺ readily enters the nigrostriatal neurons via dopamine transporters and affects the SN neuronal loss contributing to striatal dopamine depletion further causing a parkinsonian syndrome. It also disturbs the mitochondrial membrane potential causing mitochondrial stress. It is reported to be an inhibitor of complex I of the electron transport chain (ETC) and contributes to considerable oxidative stress along with ATP depletion, consequently leading to neuronal loss [17]. MPP⁺ activates the proapoptotic proteins, making the mitochondrial membrane permeable for cytochrome c to be released into the cytosol. Associated signalling inactivates protein kinases (MAPKs) which might have a neuroprotective role.

Akt and ERK signalling pathways play crucial parts in neuroprotection via cell differentiation, proliferation, survival, and apoptosis [18, 19]. Numerous recent researches have highlighted the neuroprotective role of plant-based compounds and polyphenols in PD against neurotoxins and neuroinflammation, by promoting cell survival through their antioxidative, anti-inflammatory, and immunomodulatory effects [20–22]. Evidences prove the pivotal role of polyphenols in replenishing the neurons via increased activity of ETC, regulating the effects on redox potential, and restraining the apoptosis as a result of increased mitochondrial biogenesis [23–25]. CGA, a type of phenolic acid, is reported to demonstrate antiapoptotic, anti-inflammatory, antioxidative, neurotrophic, anticancerous, and neuroprotective properties. CGA is formed as an ester of the cinnamic acids including caffeic acid and quinic acid forming the second major component of coffee after caffeine [26–28]. In our previous study, we reported the antioxidative and anti-inflammatory property of CGA against the neurotoxic effect of MPTP in mice [26]. The present study was undertaken to assess the neuroprotective effect of CGA in an MPTP-induced PD mouse model via modulation of Akt, ERK1/2, and GSK3 β signalling pathways. Under this context, the effect of CGA was evaluated against MPP⁺-mediated DA neuronal injury in MPTP-intoxicated mice showing its neuroprotective role via the activation of Akt and ERK1/2 signal-

ling pathways by inhibiting the mitochondrial dysfunction. Our findings may be helpful in designing a CGA-based treatment strategy against PD.

2. Chemical and Reagents

2.1. Reagents and Antibodies. Mannitol, sodium dihydrogen phosphate, bovine serum albumin (BSA), oxidized cytochrome c, digitonin, disodium hydrogen phosphate, potassium chloride, ammonium chloride, and reduced nicotinamide adenine dinucleotide phosphate (NADPH) were purchased from Sisco Research Laboratories (SRL, Mumbai, India). MPTP, DABCO, 5,5-dithiobis 2-nitrobenzoic acid (DTNB), normal goat serum (NGS), and chlorogenic acid were obtained from Sigma-Aldrich (St. Louis, MO, United States). Sucrose and sodium carbonate were purchased from Merck (Darmstadt, Germany), and EGTA and sodium dodecyl sulphate (SDS) were obtained from HiMedia (Mumbai, India). Glycylglycine buffer, sodium fluoride, paraformaldehyde, Tris buffer, and trichloroacetic acid were bought from LobaChemie, India. Primary antibodies for Akt, p-Akt, caspase-3, ERK, p-ERK, and Bcl-2 were acquired from Abcam Life Science, Biogenuix Medsystems Pvt. Ltd. (New Delhi, India), and primary antibodies for GSK3 β , p-GSK3 β , TH, β -actin, and Bax were purchased from Santa Cruz Biotechnology (Santa Cruz, CA, United States).

2.2. Experimental Animals. The experiment was conducted using male Swiss albino mice (25 ± 5 g), obtained from the Institute of Medical Sciences' animal facility, Banaras Hindu University, Varanasi (India). The mice were kept in clean polypropylene cages with constant light-dark cycles of 12 h prior to the start of experiment. Mice were provided with *ad libitum* water and standard diet pellet until the dosing was completed. The experimental protocol was established according to the Animal Ethics Committee's guidelines of Banaras Hindu University, Varanasi, India.

2.2.1. Animal Dosing. Experimental animals were randomized into four groups: control, MPTP, MPTP+CGA, and CGA ($n = 10$ /group). The dosing was administered in accordance with our previous study with some modifications [26]. The mice in the control group received normal saline orally, once consequently for 24 days. In MPTP+CGA and CGA groups, the oral administration of 50 mg/kg of CGA was done, once daily for 24 days. Except for the control and drug-only groups, all the mice received MPTP (30 mg/kg) intraperitoneally, dissolved in normal saline for five consecutive days (from the 20th to 24th day of CGA dosing). After completion of dosing, a behavioral test was performed from the 25th to 28th day, and thereafter, mice were sacrificed to isolate the brains for the mitochondrial dysfunction assay, Western blotting, and immunohistochemical analysis.

2.2.2. Behavioral Test. To assess the effect of MPTP intoxication on motor function impairment in the parkinsonian mouse model, four behavioral tests were conducted, including the rotarod test, pole test, catalepsy test, and traction test.

2.2.3. Rotarod Test. The training for 3 consecutive days was given to the animals from all the groups at a speed of 5 rpm for the rotarod test. Thereafter, the time on the rotarod for each animal was noted down for maximum 5 min. The test was done four times, and finally, the average time for which the mice stayed on the rotarod was noted down [29]. After the completion of dosing, the rotarod test was again conducted and the time spent on the instrument was noted down for each mouse.

2.2.4. Pole Test. Bradykinesia in PD mouse models is usually evaluated by this test [30]. The test was done after the last MPTP injection was given. Mice were supported on the top of a pole (diameter 10 mm, height 52 cm, with a rough surface). The T-turn (time to turn) was recorded accordingly to the time taken by mice to step down the length of the pole.

2.2.5. Traction Test. Equilibrium and the muscle strength are measured by performing the traction test [30], and it was also conducted on the same day as the pole test. The forepaws of a mouse were located on a suspended horizontal bar, while its hind limb placements were scored from 1 to 3, with the lowest score indicating the severe motor and balance impairment. The following criteria were used to evaluate the score: the score was 3, if both hind limbs seized the bar, while it was 2 or 1, if one or no hind limb seized the bar, respectively.

2.2.6. Catalepsy Test. Catalepsy is a state of the behavioral test that characterizes the muscle stiffness in which the mice fail to change its posture which is imposed to them and is estimated by making the animals to stand on a wooden platform where their hind limbs were placed on a wood and forelimbs on the ground [31]. The intensity of catalepsy was measured when a mouse moved its hind limbs from a wooden platform (3 cm). The mice were adapted for 3 min, and if the latency exceeds more than 180 sec, the test was ended.

2.3. Mitochondrial Parameter Analysis

2.3.1. Isolation of Mitochondria. Differential centrifugation was done to isolate the mitochondrial pellet from the mouse brain [32]. The midbrain regions of the mice were homogenized in homogenizing buffer, prepared by mixing 5 mM HEPES, 225 mM mannitol, 1 mM ethylene glycol tetra acetic acid (EGTA), 75 mM sucrose, and 1 mg/ml BSA (pH 7.4). Centrifugation of the homogenates was done at 2,000 g for 30 min at 4°C. The pellet was disposed, and the supernatant obtained was again set to centrifugation for 10 min at 12,000 g. The resultant pellet constituting the mixture of mitochondria and synaptosomes was dissolved in the homogenizing buffer containing digitonin (0.02%). Crude mitochondrial fraction was finally obtained by the centrifugation of the suspended mixture for 10 min at 12,000 g. Homogenizing buffer without BSA and EGTA was used to wash the crude mitochondrial fraction twice, and finally, the resuspension was done in phosphate buffer (50 mM, pH 7.4). The Bradford assay was performed to estimate proteins in all the samples. The assays were done within 24 h of the mitochondrial isolation using 20 μ g proteins.

2.3.2. Complex I-III Assay. The assay of complexes I-III was done by incorporating the method of Sood et al. in our study [33]. In this assay, the catalytic oxidation of NADH to NAD⁺ is done by subsequently reducing cytochrome c. The reaction mixture was prepared by the addition of glycylglycine buffer (0.2 M, pH 8.5), NADH (6 mM in 2 mM glycylglycine buffer), and cytochrome c (10.5 mM). 20 μ g mitochondrial protein was added to the reaction mixture, and the absorbance change was recorded at 550 nm for 2 min. At 340 nm, the extinction coefficient for NADH is 6.22/mM/cm. The activity of the enzyme was expressed in terms of nmol NADH oxidized/min/mg protein.

2.3.3. Complex IV Assay. Complex IV activity was determined by measuring the oxidation of reduced cytochrome c by complex IV at 550 nm [33]. The reaction mixture consisted of mitochondrial protein (20 μ g) along with 10 mM phosphate buffer (pH 7.4), reduced cytochrome c, and potassium ferricyanide. Cytochrome c (oxidized) solution (10 mg/ml) was used to prepare cytochrome c (reduced), by adding few crystals of sodium borohydride in it. Absorbance change was monitored for about 3 min. The activity of complex IV was calculated in nmol cytochrome c oxidized/min/mg of protein.

2.3.4. Complex V Assay. Griffiths and Houghton's method was used to perform the mitochondrial ATPase test [34]. In this assay, the amount of inorganic phosphorus liberated is measured that is obtained by the hydrolysis of ATP to ADP. The incubation of the reaction mixture (1.0 ml) containing the mitochondrial sample and ATPase buffer (2 mM MgCl₂, 5 mM ATP, and 50 mM Tris HCl, pH 8.5) was done for 5 min at 30°C. After the addition of 10% TCA, the reaction mixture was spun at 3,000 g for 10 min. Phosphorus was assayed, and the results were expressed as nmol inorganic phosphate (Pi) liberated/min/mg protein.

2.3.5. Mitochondrial GSH. Mitochondrial GSH (reduced) content was estimated by using the mitochondrial protein sample (20 μ g) suspended in phosphate buffer. The addition of 25% trichloroacetic acid (TCA) was done to the samples, followed by a brief centrifugation at 1,500 g. The supernatant was collected, and 5,5-dithiobis 2-nitrobenzoic acid (DTNB) was added that reacts with thiol groups to form 2-nitro-5mercapto benzoic acid. Absorbance was recorded at 412 nm. Further, commercially available GSH was used to prepare the standard curve, and the amount was expressed as mmol of GSH/g mitochondrial protein [35].

2.3.6. Manganese SOD. The activity of manganese superoxide dismutase (Mn-SOD) was estimated by adding hydrogen peroxide that selectively inhibits Cu/Zn-SOD, in order to distinguish the enzyme's activity from that of Cu/Zn-SOD. The reaction mixture consists of sodium carbonate (50 mM), EDTA (0.1 mM), Triton-X (0.6%), and NBT (90 mM) and hydroxylamine hydrochloride [35]. Hydroxylamine hydrochloride undergoes photooxidation to produce superoxide that further reduces nitroblue tetrazolium (NBT) in the reaction medium, and this reaction was inhibited by SOD. The

reading was taken at 560 nm for 3 min, and the SOD activity was expressed as units. The one enzymatic unit of SOD was defined as the amount of enzyme required for 50% inhibition.

2.4. Western Blot (WB) Analysis. The SN of the mouse brain was homogenized using the lysis buffer (RIPA) and agitated for 2 h at 4°C. The homogenate was centrifuged (12,000 rpm, 30 min) to collect the supernatant, and the Bradford assay was performed to quantify the protein concentration. The total protein extract (50 µg) was loaded onto the polyacrylamide gels. After electrophoresis, proteins were transblotted to PVDF membranes and sequentially incubated overnight at 4°C with Bax (1:1000), Bcl-2 (1:800), caspase-3 (1:1000), p-Akt (1:1000), Akt (1:1000), p-ERK1/2 (1:1000), ERK1/2 (1:800), p-GSK3β (1:1000), GSK3β (1:1000), and β-actin (1:1000) and then with a horseradish peroxidase- (HRP-) conjugated secondary antibody for 2 h at room temperature. TBST washing (twice) separated each step. Blots were visualized using the DAB system (buffer +substrate+chromogen), and for each band, the relative density was calculated with respect to that of β-actin. Quantity One software (Windows, Bio-Rad) was used to indicate the expression of relative density.

2.5. Immunohistochemistry (IHC). Mice from each group were sacrificed using pentobarbital perfused intracardially with chilled 0.9% saline solution and further using 4% paraformaldehyde solution (prepared in 0.1 M phosphate-buffered saline, pH 7.4). Again, paraformaldehyde (10%) was used to postfix the brains overnight, and further, 30% sucrose solution was used to immerse the brains. Using the standard protocol, immunohistochemical staining was performed for TH, p-Akt, p-Erk1/2, and p-GSK3β [36]. Coronal brain sections were cut to 20 µm thickness using a cryotome (Leica, Wetzlar, Germany). Tissue sections were washed with 0.01 M PBS (pH 7.4) 2 × 10 min, followed by 1 h blocking with 10% NGS in PBST and then 1% BSA-PBST. The sections were rinsed with PBS and incubated with primary antibodies for TH (1:1000), p-Akt1 (1:500), p-ERK1/2 (1:500), and p-GSK3β (1:500) at 4°C (16 h). The brain sections were then treated with FITC-conjugated (for anti-mouse primary) and TRITC-conjugated (for anti-rabbit primary) secondary antibodies (diluted in 1% BSA-PBS) at room temperature (2 h). Tissue sections were washed thrice at each step with 1% BSA-PBS and PBS, respectively, and mounted with polyvinyl alcohol with DABCO. Images were captured with a fluorescent microscope (Nikon, Thermo Fisher Scientific). All images were then processed by ImageJ software (NIH, United States). Results expressed as a % area were reported.

2.6. Statistical Analysis. The analysis of data was done by one-way analysis of variance (ANOVA) using the Student–Newman–Keuls test and by Student’s two-tailed *t*-test using GraphPad Prism software. The results are expressed as the mean ± SEM. *p* values < 0.05 were considered statistically significant.

3. Results

3.1. Behavioral Parameter Analysis. The results from our study suggested that the MPTP-intoxicated animal falls early from the rotarod in comparison to the control ($p < 0.001$, Figure 1(a)). On the other hand, when CGA was administered to the MPTP-treated mice, the time on the rotarod was significantly increased ($p < 0.001$). The pole test clued that MPTP-treated mice showed prolonged locomotor activity time ($p < 0.01$ Figure 1(b)). The time duration was shortened significantly ($p < 0.01$) in pretreated mice with CGA, suggesting that bradykinesia induced by MPTP was alleviated by CGA treatment. Results of the traction test (Figure 1(c)) showed that PD mice have decreased strength and latency time as their hind limb grip score was lower ($p < 0.01$) than that of the control group. However, pretreatment with CGA increased the traction score ($p < 0.05$). This indicates that prophylactic treatment with CGA could mitigate the initial lesions induced by MPTP. Catalepsy was observed among the MPTP group of mice after MPTP injection. Latency in the catalepsy test among the MPTP group showed increased tendency with time ($p < 0.001$, Figure 1(d)), and the observed data was of considerable difference from that of the control group, while the mice treated with CGA showed little latency time ($p < 0.001$) than the MPTP-intoxicated group. Any significant changes did not appear in the neurobehavioral activity between the control and CGA-alone-treated animals. Thus, results have suggested that CGA improved the neurobehavioral lesion of MPTP-injected PD mice.

3.2. CGA Modulates MPTP-Induced Mitochondrial ETS Impairment in Mice. Oxidative phosphorylation in mitochondria produces ATP as energy, and this process requires the organized action of five enzyme complexes located in the inner membrane. Catastrophic consequences can be observed by any defect in these energy-generating complexes, not only because of the ATP loss but also due to the downstream functional loss. Therefore, the consequences of MPTP intoxication on the energy metabolism in the mouse brain were studied. MPTP being a known complex I inhibitor of the electron transport chain (ETC) was analysed to study its effect on the activities of various complexes in the respiratory chain. As Figure 2 depicted, the effect of CGA treatment on MPTP induced alterations in the complex I-III (Figure 2(a)), IV (Figure 2(b)), and V activities (Figure 2(c)). There was significant attenuation in the activities of complexes I-III ($p < 0.01$), complex IV ($p < 0.01$), and complex V ($p < 0.001$) in MPTP-intoxicated PD mice as compared to control mice. CGA administration before MPTP intoxication to the animals helped improve the activities of complexes I-III ($p < 0.01$), complex IV ($p < 0.01$), and complex V ($p < 0.001$) in comparison with MPTP-intoxicated mice. No potential change was observed when the control group was treated with CGA.

3.3. Mitochondrial Glutathione and Superoxide Dismutase Level Analysis. Further, the increase in oxidative stress resulting in the reduced function of ETC leads to the utilization of

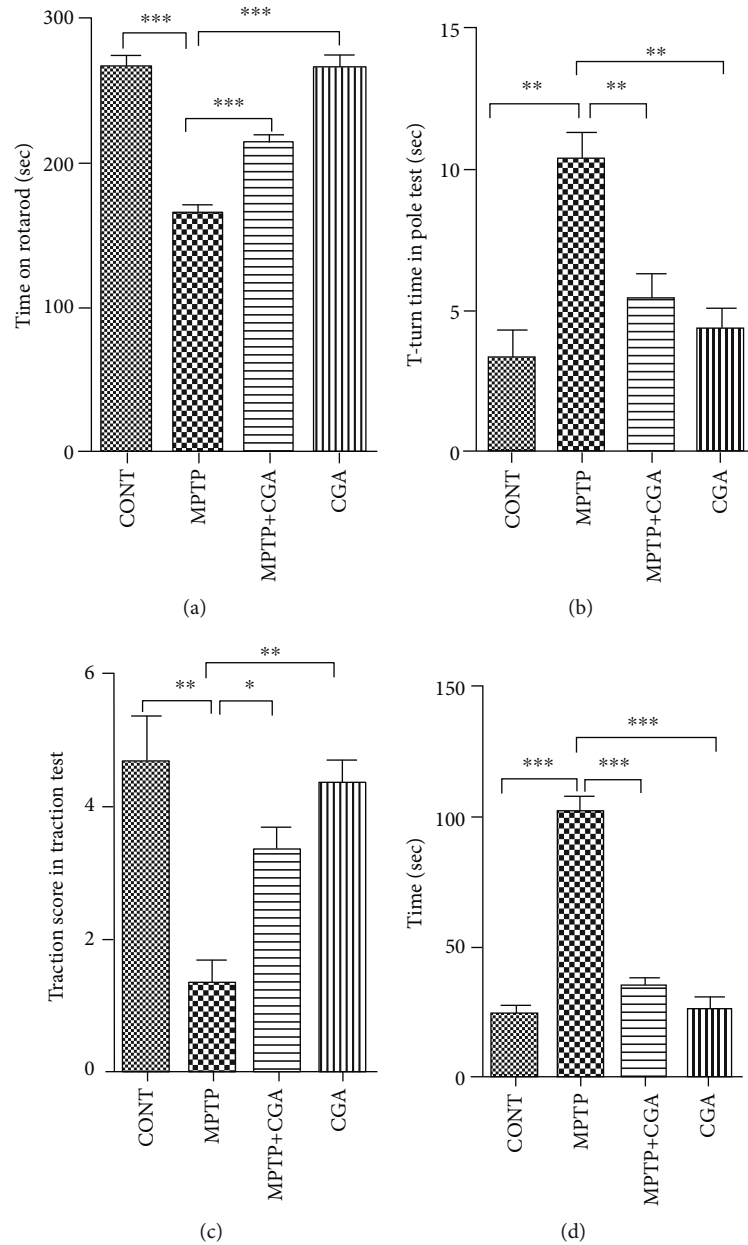


FIGURE 1: Mouse behavioral analysis. CGA mediated alteration in the neurobehavior of MPTP-injected mice. (a) Time on the rotarod test. (b) T-turn time in the pole test. (c) Traction score in the traction test. (d) Cataleptic test. Values are represented in the form of mean \pm SEM ($n = 10$). * $p < 0.05$, ** $p < 0.01$, and *** $p < 0.001$. Results were studied using the one-way ANOVA and further using the Newman-Keuls test.

mitochondrial GSH (mtGSH, reduced) and reduction in activity of Mn-SOD (Figures 3(a) and 3(b)). In the MPTP-treated group, a significant reduction ($p < 0.001$) in the levels of mtGSH was observed when compared to the control group. Consequently, a decline in the Mn-SOD activity ($p < 0.001$) was also analysed with MPTP intoxication (Figure 2(b)). On the other hand, CGA has reduced the ROS generation and ameliorated the function of ETS which has ultimately increased the level of mtGSH ($p < 0.001$) and Mn-SOD ($p < 0.001$) significantly.

3.4. CGA Inhibited the MPTP-Induced Activation of Mitochondrial Apoptosis Signalling in SN of Mice. Various

apoptosis-linked molecules were investigated to study the effect of CGA on MPTP-induced cell apoptosis rate (Figures 4(a)–4(c)). The MPTP-intoxicated group showed a considerable increment in the Bax/Bcl-2 ratio ($p < 0.001$) as compared to the control group whereas in CGA-treated PD mice, the Bax/Bcl-2 ratio ($p < 0.001$) was observed to be significantly reduced, which shows the antiapoptotic property of CGA in the parkinsonian mouse model (Figure 4(b)). The expression level of cleaved caspase-3 ($p < 0.01$) was observed to be elevated in the SN of PD mice whereas attenuated expression of cleaved caspase-3 ($p < 0.05$) was observed in the drug-treated group, which shows the antiapoptotic property of CGA in the parkinsonian mouse model (Figure 4(c)).

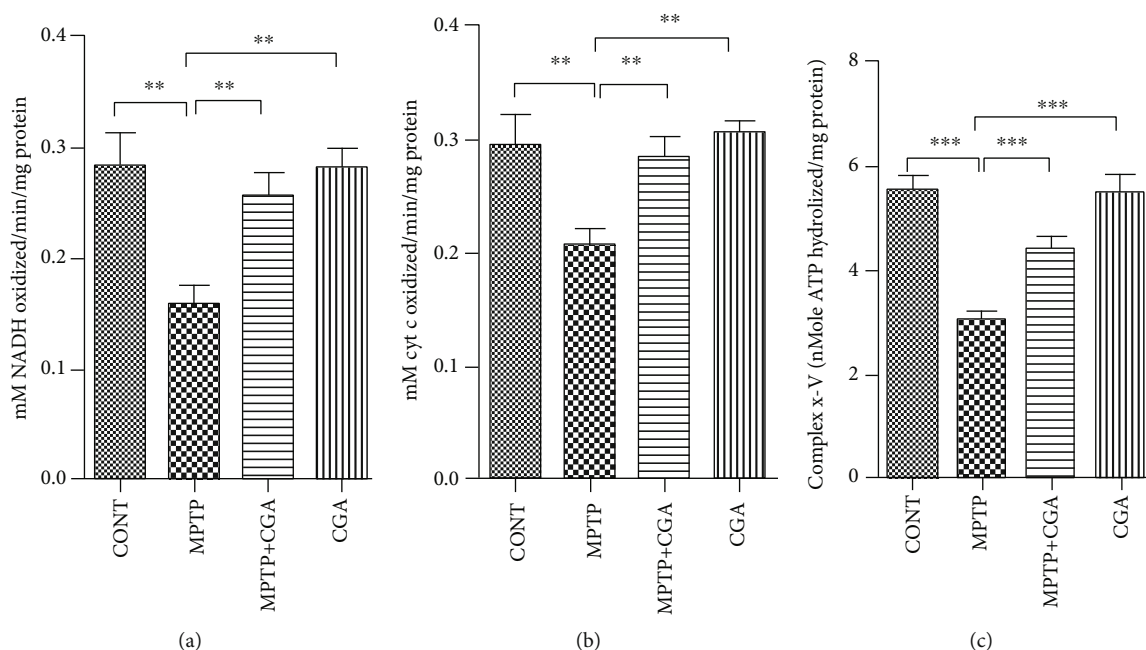


FIGURE 2: CGA mediated alterations on mitochondrial complexes I-III (a), IV (b), and V (c) of the electron transport chain in the midbrain of mice. Values are represented in the form of mean \pm SEM ($n = 5$). * $p < 0.05$, ** $p < 0.01$, and *** $p < 0.001$. Results were studied using the one-way ANOVA and further using the Newman-Keuls test.

3.5. CGA Ameliorates the Dysregulation of Akt and ERK Activation and GSK3 β Phosphorylation in the MPTP-Induced Parkinsonian Mouse Model. Expression of Akt, ERK1/2, and GSK3 β was examined by WB (Figures 4(a) and 4(d)–4(f)) and immunohistochemical analysis techniques (Figures 5–7). Akt and ERK1/2 are the major downstream key components of the MAPK signalling pathway. Our WB data emphasised that MPTP treatment significantly attenuated the p-Akt/Akt ratio ($p < 0.001$) compared with the control group, whereas in CGA treatment, the p-Akt/Akt ratio ($p < 0.01$) was observed to be elevated in PD mice (Figure 4(d)). Similar results were also observed through the IHC technique showing reduced Akt phosphorylation in MPTP-treated mice ($p < 0.001$) whereas increased p-Akt was observed in the case of CGA-treated PD mice (Figure 5). Furthermore, WB results depicted downregulation in the p-ERK1/2/ERK1/2 ratio in MPTP-treated mice ($p < 0.001$). On the contrary, the p-ERK1/2/ERK1/2 ratio ($p < 0.001$) was upregulated in CGA-treated PD mice (Figure 4). Likewise, in IHC, the ERK1/2 phosphorylation was seen to be decreased on MPTP intoxication ($p < 0.001$) whereas CGA treatment has significantly increased the phosphorylation of ERK1/2 ($p < 0.001$) (Figure 7).

GSK3 β has recently been linked to the mitochondrial intrinsic apoptosis. The WB result for GSK3 β revealed a reduced p-GSK3 β /GSK3 β ratio ($p < 0.001$) in MPTP-intoxicated mice whereas in CGA-treated PD mice, the ratio of p-GSK3 β /GSK3 β was seen to be increased ($p < 0.001$, Figure 4(f)). To further confirm the results, IHC was performed presenting a substantial decrease in GSK3 β phosphorylation after MPTP treatment in comparison with the control group ($p < 0.01$). On the other hand, CGA adminis-

tration leads to the enhanced phosphorylation of GSK3 β when compared to that of MPTP-intoxicated mice ($p < 0.001$, Figure 6).

3.6. CGA Ameliorates MPTP-Induced Degeneration of TH-Positive DA Neurons in SN of PD Mice. IHC of TH was performed to assess the loss of DA neurons in SN of MPTP-intoxicated mice (Figure 8). The data obtained in this study reveals the significant reduction of DA neurons in SN of an MPTP-intoxicated mouse as compared to control ($p < 0.001$). Alternatively, CGA pretreatment has done a significant increment in the expression of TH ($p < 0.01$) in SNpc of an MPTP-intoxicated mouse as compared with the MPTP-induced PD mouse model. Therefore, CGA administration was beneficial in protecting the DA neurons from MPTP-induced toxicity, as suggested by our findings.

4. Discussion

PD occurs due to multiple factors, and various pathways interact to induce the neurotoxic pathways that result in the loss of DA neurons in SN [6, 9]. The pathways that lead to neurodegeneration are influenced by each other, yet their contribution is independent of each other. All the involved processes work in an interdependent manner influencing one another and finally leading to the neuronal senescence [37, 38]. Hence, neuroprotection in the case of PD can only be achieved when combination of drugs or treatments targeting the collective pathways is used for PD therapy. In this context, it has been seen that CGA shows multiple biological effects such as antioxidant, anti-inflammatory, neuroprotective, and neurotrophic activities [27, 39–41]. In this study,

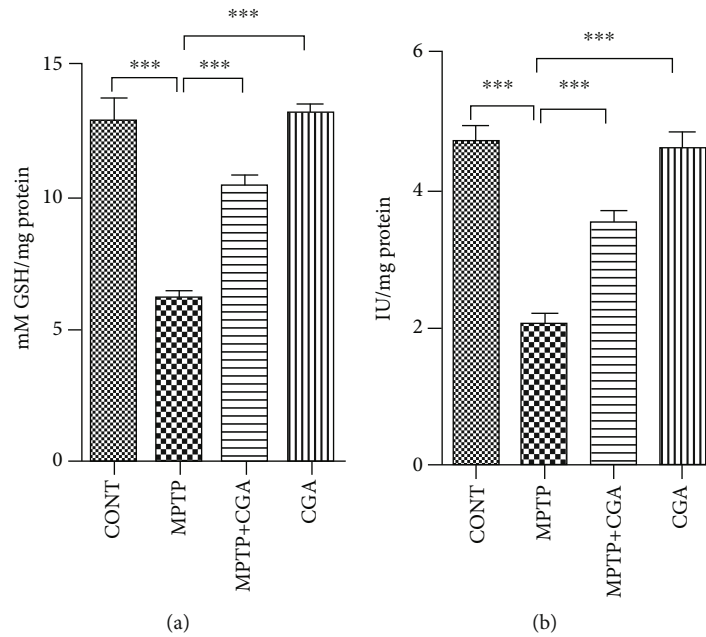


FIGURE 3: Alterations in mitochondrial antioxidant defence in respective treatment groups. (a) Mitochondrial reduced glutathione level. (b) Mitochondrial superoxide dismutase level. Values are represented in the form of mean \pm SEM ($n = 5$). * $p < 0.05$, ** $p < 0.01$, and *** $p < 0.001$. Results were studied using the one-way ANOVA and further using the Newman-Keuls test.

CGA act as a potent neuroprotective agent by preventing mitochondrial dysfunction and suppressing the apoptotic death of DA neurons. Also, these neuroprotective effects of CGA were found to be mediated by Akt, ERK1/2, and GSK3 β pathways. Different behavioral tests such as pole, catalepsy, rotarod, and traction tests have helped determine severe motor abnormalities in MPTP-intoxicated PD animal models [42–45] (Figure 1). Similar coordination deficits and motor impairment were also seen in our study too upon MPTP toxicity in mice, thereby validating our mouse model of PD in accordance with previous researches, whereas the neurobehavioral lesion was found to be alleviated by CGA as suggested by the behavioral tests which is in correspondence with earlier reports [30, 46–48].

The key pathogenic events of PD mainly constitute oxidative stress and mitochondrial dysfunction, and these two further lead to the onset of cell apoptosis [49, 50]. The neurotoxin MPTP serves as an excellent animal model for PD as it mimics the symptoms of PD extensively. The neurotoxin after crossing the blood-brain barrier (BBB) is acted upon by monoamine oxidase B to get converted into MPP $^+$ and enters into DA neurons specifically via the dopamine transporter. MPP $^+$ is the toxic metabolite of MPTP, and its accumulation inside the neurons leads to the inhibition of complex I of mitochondria and induces the ROS generation and depletion of ATP, prompting to the loss of the DA neurons [51, 52]. Both *in vivo* and *in vitro* models have been studied for the effects of antioxidants on the reduced mitochondrial dysfunction along with the enhanced growth of certain bioactive compounds in the mitochondria [53, 54]. In this study, MPTP intoxication reduced the activity of complexes I-III, complex IV, and complex V of ETS (Figure 2). Thus, the pattern of electron transfer was disturbed by MPTP

toxicity, which has led to the reduction in the effectiveness of the enzymes NADH dehydrogenase and cytochrome oxidase causing structural damage to the mitochondria leading to its dysfunction. Further, because of the reduced functioning of ETC, oxidative stress arises triggering the reduced activity of Mn-SOD and excessive consumption of mitochondrial GSH (mtGSH, reduced). A research done by Davey et al. in 1998 proposed that the reduced activity of complex I occurs because of the depletion in the level of GSH in PC12 cells, which also leads to the abolition of the threshold effect [55]. The mechanism involved in the threshold hindrance of complexes I-III by the GSH level is still unknown. The antioxidant GSH is known to protect the mitochondria from lipid peroxidation [56], and hence, its depletion might make complexes I-III prone to the attack of the free radicals. Also, in previous researches, it has been described that the depleted level of GSH causes the degeneration and enlargement of the brain mitochondria [57] and induces the reduced activity of complex IV in the purified brain mitochondrial preparations [58]. The decreased level of the reduced glutathione or the generation of reactive oxygen and nitrogen species by the activated glial cells might be the main factors for the decline in complex IV activity. Moreover, mitochondrial damage also takes place by the production of NO as a result of inflammation-mediated expression of iNOS induction, which causes the loss of the cytochrome oxidase pathway by producing RNS consequently inducing protein nitration in the ETC. Moreover, various *in vivo* studies have reported the pivotal role of GSH in protecting DA neurons against the adverse effects of MPTP on PD [59, 60]. Therefore, the findings suggest that the fall in the reduced GSH level increased the sensitization of mitochondria against the additional metabolic insult resulting in its dysfunction and cell

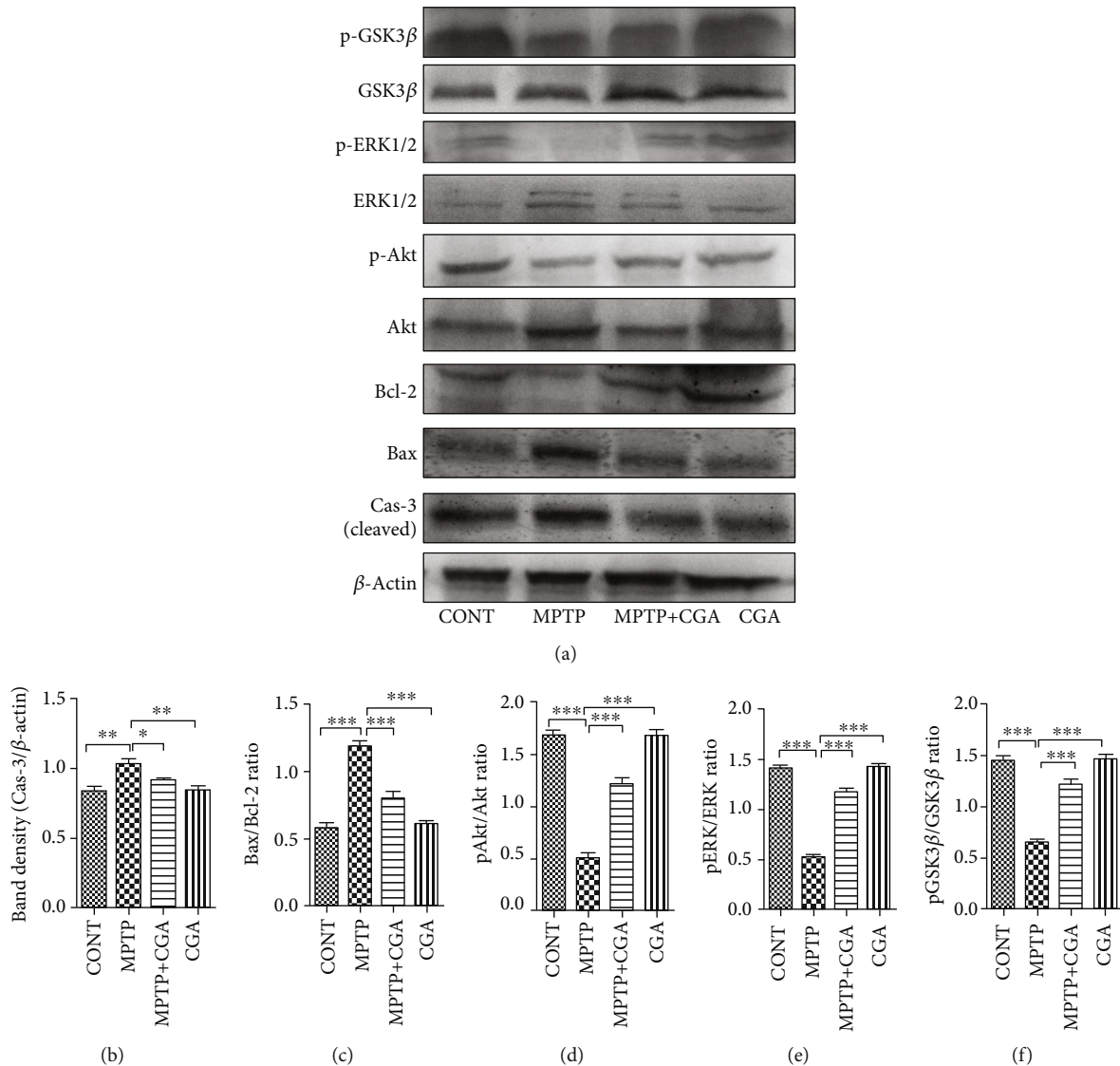


FIGURE 4: (a–f) Relative expression of Bax, Cas-3, Bcl-2, p-Akt, p-ERK1/2, and p-GSK3 β in SN of mice was studied using the Western blot technique and densitometry analysis of proteins. CGA suppressed MPTP-induced apoptosis via Akt, GSK3 β , and ERK1/2 signalling pathways in parkinsonian mice. It has normalized the deregulated expression of Bax, Bcl-2, and Cas-3 in MPTP-injected mice (a, b). β -Actin protein served as an internal control. Values are represented in the form of mean \pm SEM ($n = 5$). * $p < 0.05$, ** $p < 0.01$, and *** $p < 0.001$. Results were studied using the one-way ANOVA and further using the Newman-Keuls test. Abbreviations: CGA: chlorogenic acid; MPTP: 1-methyl-4-phenyl-1,2,3,6-tetrahydropyridine; SEM: standard error of the mean.

death. However, in our study, CGA was found to be potent in maintaining the appropriate activity of the ETC complexes (Figure 3). Furthermore, as reflected by the enhanced levels of reduced mtGSH and Mn-SOD, CGA was also effective in reducing the burden on the mitochondrial antioxidative defence by inhibiting the generation of the ROS. Thus, the ability of CGA to improve the activities of the complexes of ETC might be due to increased availability of reduced glutathione which is known to be the primary defence of mitochondrial functions.

The mitochondrion, an intracellular powerhouse, plays various crucial roles including energy production, free reactive oxygen and nitrogen species production along with critically modulating the apoptosis, and cell survival which are essential factors of aging. During the pathological alterations,

the leakage of cytochrome c and various proapoptotic molecules in the cytoplasm from the mitochondria, as a result of the mitochondrial membrane permeabilization, induces the cascade of events leading to cell death [61]. Mitochondrial dysfunction is generally estimated by measuring the membrane potential which is found impaired in the intrinsic apoptotic pathway [62]. The regulation of caspase activation is maintained as a result of the equilibrium between the expression levels of proapoptotic and prosurvival proteins in the Bcl-2 family [63], although Bcl-2 and Bax have contrasting functions while being from the same Bcl-2 family. While Bcl-2 is known for its antiapoptotic activity, Bax exhibits the proapoptotic function [64]. Numerous studies have suggested that the neurotoxin MPTP disturbs the balance of Bax/Bcl-2, which increases the activity of caspase-3 in the

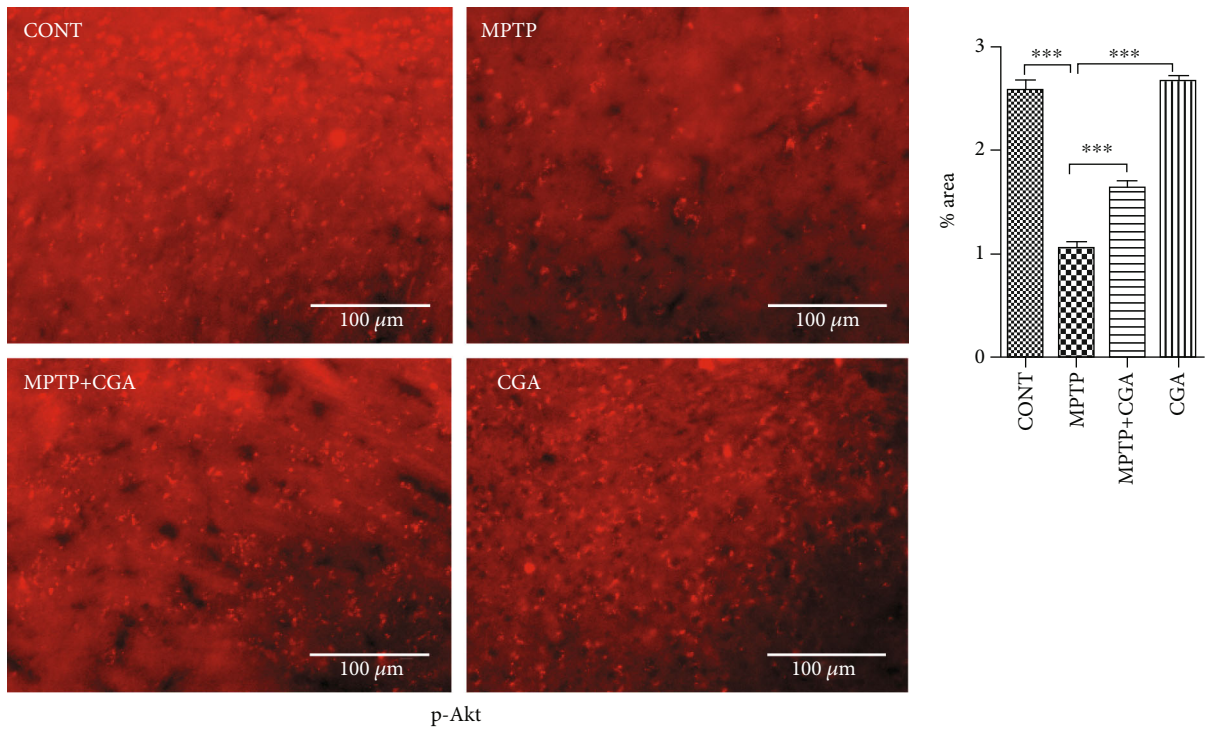


FIGURE 5: Immunohistochemical staining to analyse the expression of p-Akt in SN of different experimental groups. CGA administration enhanced the expression of p-Akt in SN of parkinsonian mice (20x magnification after staining). Values are expressed as mean \pm SEM ($n = 5$). * $p < 0.05$, ** $p < 0.01$, and *** $p < 0.001$. Results were studied using the one-way ANOVA and further using the Newman-Keuls test.

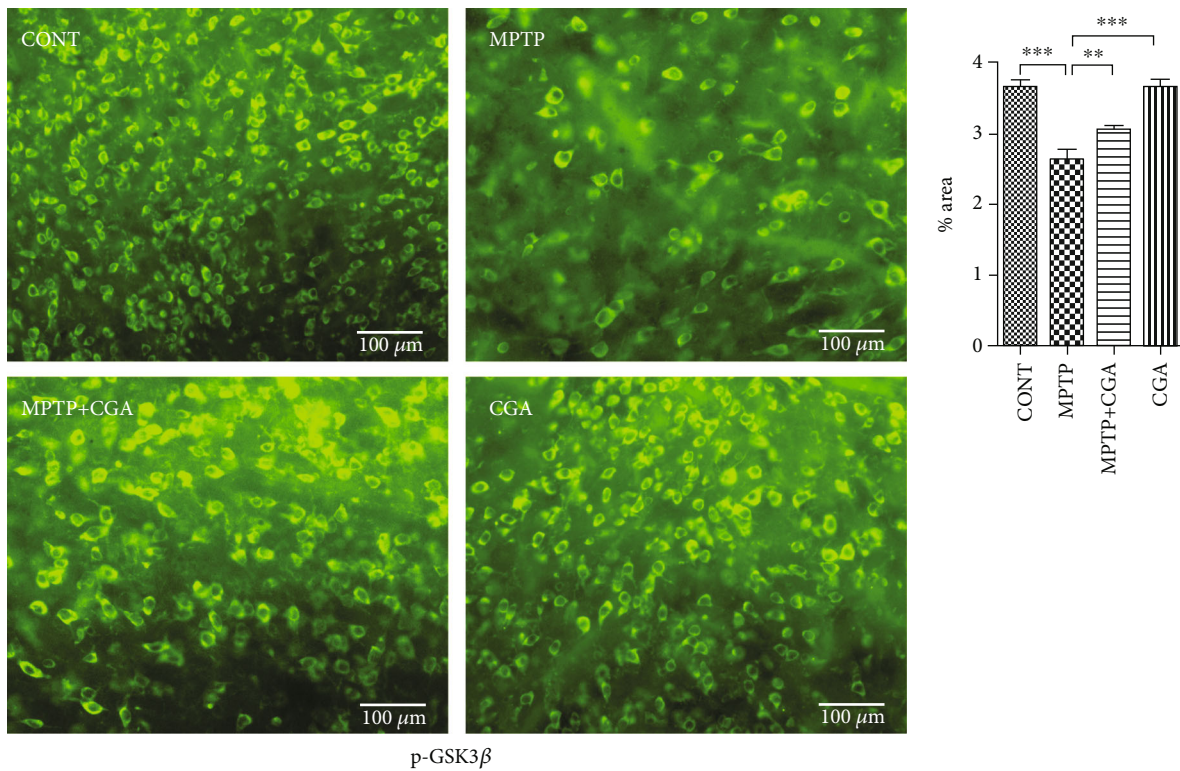


FIGURE 6: Immunohistochemical staining to analyse the expression of p-GSK3 β in SN of different experimental groups (a, b). Profound expression of p-GSK3 β in the CGA-administered group compared to the MPTP-intoxicated PD mice (20x). Values are represented as mean \pm SEM ($n = 5$). * $p < 0.05$, ** $p < 0.01$, and *** $p < 0.001$. Results were studied using the one-way ANOVA and further by the Newman-Keuls test.

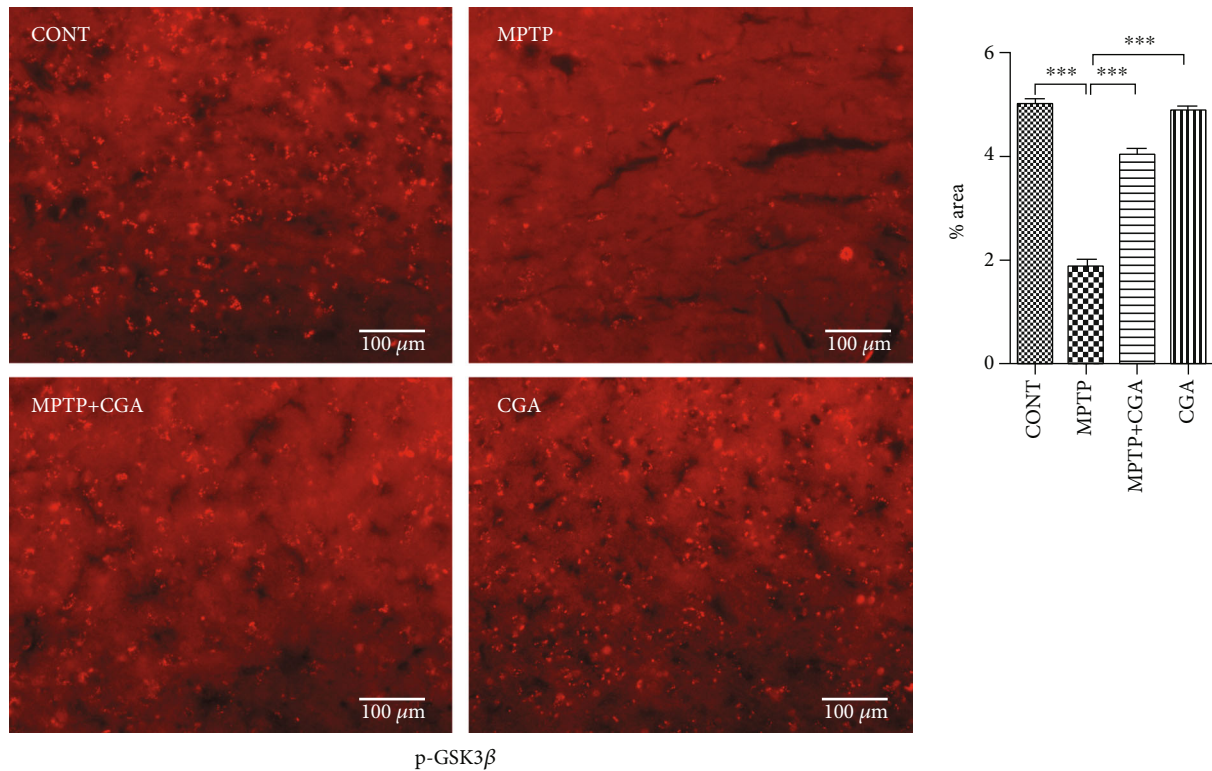


FIGURE 7: Immunohistochemical staining to analyse the expression of p-ERK1/2 in SN of different experimental groups. Upregulated expression of p-ERK1/2 due to CGA administration in parkinsonian mice (20x). Values are represented as mean \pm SEM ($n = 5$). * $p < 0.05$, ** $p < 0.01$, and *** $p < 0.001$. Results were studied using the one-way ANOVA and further by the Newman-Keuls test.

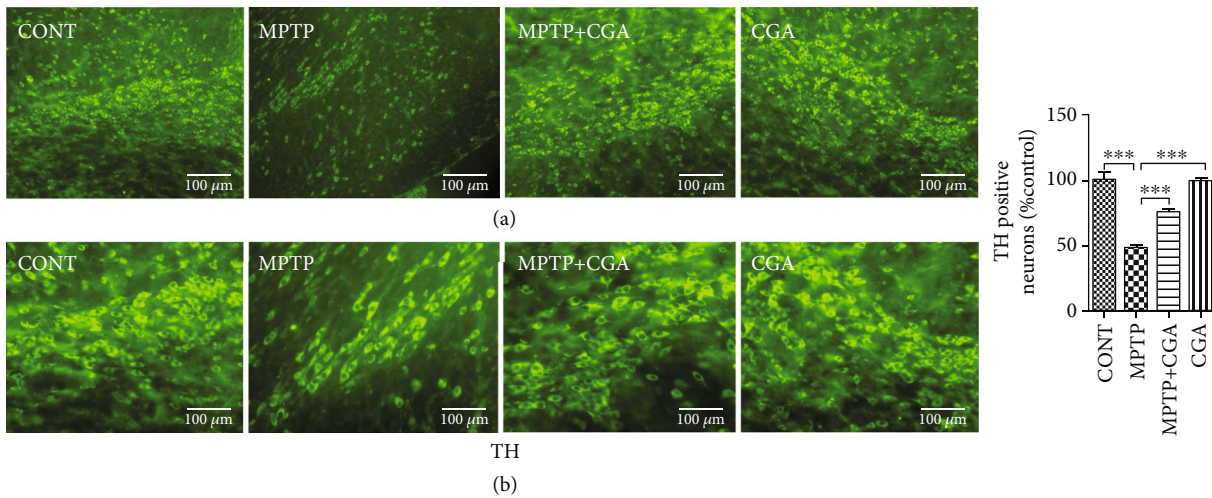


FIGURE 8: (a, b) Immunohistochemical staining to analyse the expression of TH-positive DA neurons in SN of different experimental groups. CGA protected the TH-positive DA neurons in MPTP-induced mice. (a) 10x and (b) 20x. TH immunoreactivity in SN of mice. Values are represented as mean \pm SEM ($n = 5$). * $p < 0.05$, ** $p < 0.01$, and *** $p < 0.001$. Results were studied using the one-way ANOVA and further by the Newman-Keuls test.

DA neurons [65, 66]. The release of apoptogenic proteins like cytochrome c into the cytosol from mitochondria mediates the activation of caspase-3 which occurs because of the loss of membrane integrity by the action of Bax, hence leading to cell death. Both *in vivo* and *in vitro* studies have suggested

the increased expression of caspase-3 upon MPTP toxicity [67]. The activation of caspase-9 provokes the initiation of the apoptotic cascade on the release of cytochrome c into the cytosol after mitochondrial dysfunction. As a result, caspase-3 gets activated by changing the morphology of

mitochondria leading to apoptosis [68]. However, CGA treatment has protected the DA neurons from MPTP-induced toxicity and inhibited the apoptosis (Figure 4).

Different cellular processes like growth, proliferation, survival, and apoptosis are regulated by the phosphorylation of some key proteins such as Akt, ERK1/2, and GSK3 β [69, 70]. The activation of Akt is found to be linked with the survival pathways of various cell types including neuronal cells as reported in several *in vitro* studies. Moreover, the survival of different neurons is linked with different neurotrophic factors, whose activation is mediated by Akt [71–73]. Also, transfection with a constitutively activated form of Akt is observed to promote the survival of the neurons without any other support whereas the cultured neurons were found to be dead when the activation of the kinase was interfered [74]. Studies from different sources have suggested the role of GSK3 β in the modulation of apoptosis, and the inhibition of GSK3 β has protected the DA neurons from MPTP toxicity as suggested by different cell and animal models of PD [45, 75, 76]. The localization of GSK3 β has been mainly observed in the cytosol, but its expression in lower amounts has also been seen in the nucleus and mitochondria [77, 78]. Furthermore, it is also linked with the regulation of the mitochondrial cell death pathway by eliciting numerous stressful conditions within the neurons [78]. Researchers have also suggested that inhibition of GSK3 β rescues the DA neurons from MPTP toxicity, indicating its association with the pathogenesis of PD [45, 76]. The neurotoxin MPTP has been found to decrease the phosphorylation of Akt and GSK3 β as suggested by previous studies, leading to the death of the DA neurons [70, 79]. MPTP-induced cell injury is mediated by GSK3 β , which is the downstream target of Akt [75, 80]. Mitochondrial dysfunction is seen to be facilitated by GSK3 β , and its inhibition prevents the loss of neurons mediated by the suppression of proapoptotic proteins [76, 81]. In accordance with previous studies, MPTP has decreased the phosphorylation of Akt (Figures 4 and 5) and GSK3 β (Figures 4 and 6), and CGA on the other hand has protected Akt and GSK3 β from dephosphorylation in the MPTP-intoxicated mouse model. It has been observed that Akt controls the phosphorylation of GSK3 β and thereby inhibits its activity [82]. MAPK signalling pathways also play a pivotal role in many cellular events, such as proliferation, differentiation, and apoptosis. The three major MAPK subfamilies have been chiefly characterized including ERK, JNK, and p38 [83]. Among them, ERK is known to enhance the DA neuronal survival rate, as in SH-SY5Y cells, the phosphorylation of ERK was seen to be suppressed after 4 h of MPP⁺ toxicity [84, 85]. Our study also shows the dephosphorylation of ERK upon MPTP intoxication, while the neuroprotective agent CGA was potent in abolishing the neurotoxic effect in the PD mouse model (Figures 4 and 7).

TH immunoreactivity in this study was performed to examine the CGA-mediated alterations on the functions of DA neurons in the SN of the MPTP-intoxicated parkinsonian mouse model [86] (Figure 8). Our immunohistochemical study has shown the reduction expression of TH-positive DA neurons in SN of an MPTP-intoxicated mouse, i.e., the characteristic feature of PD, as suggested by numerous

reports [44, 60, 86]. However, CGA has rescued this debilitating effect and hence conferred about protecting the DA neurons against MPTP-induced neurodegeneration in the mouse model of PD.

Hence, our results have therefore suggested that the neuroprotective effect of CGA is mediated by the GSK3 β phosphorylation-associated Akt/ERK pathway and is potent in inhibiting the mitochondrial intrinsic apoptosis due to MPTP toxicity in the mouse brain.

5. Conclusion

This study demonstrates the neuroprotective effect of CGA against MPTP-induced apoptotic cell death in mice. The Bax/Bcl-2 ratio, mitochondrial dysfunction, and expression of caspase-3 were seen to be significantly increased on MPTP intoxication. Furthermore, the phosphorylation of Akt, ERK1/2, and GSK3 β was also reduced by the neurotoxic action of MPTP. However, CGA was potent in protecting the neurons against MPTP-induced cytotoxicity through the phosphorylation of GSK3 β via activation of Akt and ERK1/2 signalling pathways in the mouse model of PD. Thus, this study helps to understand the neuroprotective mechanism of CGA in PD which can be further explored for clinical interventions.

Data Availability

The data used to support the findings of this study are available from the corresponding author upon request.

Ethical Approval

This work has been approved by the institutional animal ethical committee, BHU, Varanasi, India. All efforts were made to minimize animal suffering.

Conflicts of Interest

All authors have no conflict of interest to report.

Authors' Contributions

SSS conceived and designed the study, wrote the manuscript, and analysed and interpreted the data. SNR, HB, WZ, ASR, HD, and RS help in animal dosing, behavioral study, and manuscript preparation. SPS supervised the study. All authors read and approved the final manuscript.

Acknowledgments

SSS, SNR, HB, RS, WZ, ASR, and HD are sincerely thankful to ICMR, UGC, DBT, CSIR, and BHU, India, for their respective fellowship. The authors are also thankful to the head of the Department of Biochemistry, IOS, BHU, for providing the basic departmental facility and ISLS, BHU, for their central instrument facility.

References

- [1] H. Sawada, R. Hishida, Y. Hirata et al., "Activated microglia affect the nigro-striatal dopamine neurons differently in neonatal and aged mice treated with 1-methyl-4-phenyl-1, 2, 3, 6-tetrahydropyridine," *Journal of Neuroscience Research*, vol. 85, no. 8, pp. 1752–1761, 2007.
- [2] W. Poewe, K. Seppi, C. M. Tanner et al., "Parkinson disease," *Nature Reviews Disease Primers*, vol. 3, no. 1, article 17013, 2017.
- [3] M. P. Mattson, "Apoptosis in neurodegenerative disorders," *Nature Reviews Molecular Cell Biology*, vol. 1, no. 2, pp. 120–130, 2000.
- [4] J. K. Youn, D. W. Kim, S. T. Kim et al., "PEP-1-HO-1 prevents MPTP-induced degeneration of dopaminergic neurons in a Parkinson's disease mouse model," *BMB Reports*, vol. 47, no. 10, pp. 569–574, 2014.
- [5] S. R. Subramaniam and M.-F. Chesselet, "Mitochondrial dysfunction and oxidative stress in Parkinson's disease," *Progress in Neurobiology*, vol. 106-107, pp. 17–32, 2013.
- [6] I. Ferrer, "Early involvement of the cerebral cortex in Parkinson's disease: convergence of multiple metabolic defects," *Progress in Neurobiology*, vol. 88, no. 2, pp. 89–103, 2009.
- [7] Q.-L. Ma, P. Chan, M. Yoshii, and K. Ueda, "α-Synuclein aggregation and neurodegenerative diseases," *Journal of Alzheimer's Disease*, vol. 5, no. 2, pp. 139–148, 2003.
- [8] P. Gong, F. Deng, W. Zhang et al., "Tectorigenin attenuates the MPP⁺-induced SH-SY5Y cell damage, indicating a potential beneficial role in Parkinson's disease by oxidative stress inhibition," *Experimental and Therapeutic Medicine*, vol. 14, no. 5, pp. 4431–4437, 2017.
- [9] R. Kaur, S. Mehan, and S. Singh, "Understanding multifactorial architecture of Parkinson's disease: pathophysiology to management," *Neurological Sciences*, vol. 40, no. 1, pp. 13–23, 2019.
- [10] H. E. Moon and S. H. Paek, "Mitochondrial dysfunction in Parkinson's disease," *Experimental Neurobiology*, vol. 24, no. 2, pp. 103–116, 2015.
- [11] B. Thanvi, N. Lo, and T. Robinson, "Levodopa-induced dyskinesia in Parkinson's disease: clinical features, pathogenesis, prevention and treatment," *Postgraduate Medical Journal*, vol. 83, no. 980, pp. 384–388, 2007.
- [12] N. A. Tatton, A. Maclean-Fraser, W. G. Tatton, D. P. Perl, and C. O. Warren, "A fluorescent double-labeling method to detect and confirm apoptotic nuclei in Parkinson's disease," *Annals of Neurology*, vol. 44, Supplement 1, pp. S142–S148, 1998.
- [13] H. Mochizuki, K. Goto, H. Mori, and Y. Mizuno, "Histochemical detection of apoptosis in Parkinson's disease," *Journal of the Neurological Sciences*, vol. 137, no. 2, pp. 120–123, 1996.
- [14] J. Bové, D. Prou, C. Perier, and S. Przedborski, "Toxin-induced models of Parkinson's disease," *NeuroRx*, vol. 2, no. 3, pp. 484–494, 2005.
- [15] H. Birla, S. N. Rai, S. S. Singh et al., "Tinospora cordifolia suppresses neuroinflammation in parkinsonian mouse model," *Neuromolecular Medicine*, vol. 21, no. 1, pp. 42–53, 2019.
- [16] K. Chiba, A. J. Trevor, and N. Castagnoli Jr., "Active uptake of MPP⁺, a metabolite of MPTP, by brain synaptosomes," *Biochemical and Biophysical Research Communications*, vol. 128, no. 3, pp. 1228–1232, 1985.
- [17] D. Jantas, A. Greda, S. Golda et al., "Neuroprotective effects of metabotropic glutamate receptor group II and III activators against MPP (+)-induced cell death in human neuroblastoma SH-SY5Y cells: the impact of cell differentiation state," *Neuropharmacology*, vol. 83, pp. 36–53, 2014.
- [18] K. Nakaso, N. Tajima, Y. Horikoshi et al., "The estrogen receptor β-PI3K/Akt pathway mediates the cytoprotective effects of tocotrienol in a cellular Parkinson's disease model," *Biochimica et Biophysica Acta (BBA)-Molecular Basis of Disease*, vol. 1842, no. 9, pp. 1303–1312, 2014.
- [19] L. Teng, C. Kou, C. Lu et al., "Involvement of the ERK pathway in the protective effects of glycyrrhizic acid against the MPP⁺-induced apoptosis of dopaminergic neuronal cells," *International Journal of Molecular Medicine*, vol. 34, no. 3, pp. 742–748, 2014.
- [20] D. Vauzour, K. Vafeiadou, A. Rodriguez-Mateos, C. Rendeiro, and J. P. E. Spencer, "The neuroprotective potential of flavonoids: a multiplicity of effects," *Genes & Nutrition*, vol. 3, no. 3-4, pp. 115–126, 2008.
- [21] R. J. Williams and J. P. E. Spencer, "Flavonoids, cognition, and dementia: actions, mechanisms, and potential therapeutic utility for Alzheimer disease," *Free Radical Biology & Medicine*, vol. 52, no. 1, pp. 35–45, 2012.
- [22] S. S. Singh, S. N. Rai, H. Birla, W. Zahra, A. S. Rathore, and S. P. Singh, "NF-κB-mediated neuroinflammation in Parkinson's disease and potential therapeutic effect of polyphenols," *Neurotoxicity Research*, vol. 37, no. 3, pp. 491–507, 2020.
- [23] L. Gibellini, E. Bianchini, S. de Biasi, M. Nasi, A. Cossarizza, and M. Pinti, "Natural compounds modulating mitochondrial functions," *Evidence-based Complementary and Alternative Medicine*, vol. 2015, Article ID 527209, 13 pages, 2015.
- [24] I. Solanki, P. Parihar, M. L. Mansuri, and M. S. Parihar, "Flavonoid-based therapies in the early management of neurodegenerative diseases," *Advances in Nutrition*, vol. 6, no. 1, pp. 64–72, 2015.
- [25] M. R. de Oliveira, S. F. Nabavi, A. Manayi, M. Daglia, Z. Hajheydari, and S. M. Nabavi, "Resveratrol and the mitochondria: from triggering the intrinsic apoptotic pathway to inducing mitochondrial biogenesis, a mechanistic view," *Biochimica et Biophysica Acta (BBA)-General Subjects*, vol. 1860, no. 4, pp. 727–745, 2016.
- [26] S. S. Singh, S. N. Rai, H. Birla et al., "Effect of chlorogenic acid supplementation in MPTP-intoxicated mouse," *Frontiers in Pharmacology*, vol. 9, 2018.
- [27] H. Ito, X. L. Sun, M. Watanabe, M. Okamoto, and T. Hatano, "Chlorogenic acid and its Metabolite-Coumaric acid evoke neurite outgrowth in hippocampal neuronal cells," *Bioscience, Biotechnology, and Biochemistry*, vol. 72, no. 3, pp. 885–888, 2014.
- [28] S.-H. Kwon, H. K. Lee, J. A. Kim et al., "Neuroprotective effects of chlorogenic acid on scopolamine-induced amnesia via anti-acetylcholinesterase and anti-oxidative activities in mice," *European Journal of Pharmacology*, vol. 649, no. 1-3, pp. 210–217, 2010.
- [29] S. Manna, D. Bhattacharyya, T. K. Mandal, and S. Dey, "Neuropharmacological effects of deltamethrin in rats," *Journal of Veterinary Science*, vol. 7, no. 2, pp. 133–136, 2006.
- [30] M. Hu, F. Li, and W. Wang, "Vitamin E protects dopaminergic neurons in MPTP-induced Parkinson's disease through PI3K/Akt signaling pathway," *Drug Design, Development and Therapy*, vol. Volume 12, pp. 565–573, 2018.
- [31] F. B. Wehmuller, M. Hadjiconstantinou, and J. P. Bruno, "Acute stress or neuroleptics elicit sensorimotor deficits in

- MPTP-treated mice,” *Neuroscience Letters*, vol. 85, no. 1, pp. 137–142, 1988.
- [32] S. B. Berman and T. G. Hastings, “Dopamine oxidation alters mitochondrial respiration and induces permeability transition in brain mitochondria: implications for Parkinson’s disease,” *Journal of Neurochemistry*, vol. 73, no. 3, pp. 1127–1137, 1999.
- [33] P. K. Sood, U. Nahar, and B. Nehru, “Curcumin attenuates aluminum-induced oxidative stress and mitochondrial dysfunction in rat brain,” *Neurotoxicity Research*, vol. 20, no. 4, pp. 351–361, 2011.
- [34] D. E. GRIFFITHS and R. L. HOUGHTON, “Studies on energy-linked reactions: modified mitochondrial ATPase of oligomycin-resistant mutants of *Saccharomyces cerevisiae*,” *European Journal of Biochemistry*, vol. 46, no. 1, pp. 157–167, 1974.
- [35] P. Khanna and B. Nehru, “Antioxidant enzymatic system in neuronal and glial cells enriched fractions of rat brain after aluminum exposure,” *Cellular and Molecular Neurobiology*, vol. 27, no. 7, pp. 959–969, 2007.
- [36] O. S. Gorbatyuk, S. Li, L. F. Sullivan et al., “The phosphorylation state of Ser-129 in human α -synuclein determines neurodegeneration in a rat model of Parkinson disease,” *Proceedings of the National Academy of Sciences*, vol. 105, no. 2, pp. 763–768, 2008.
- [37] O. Riess and R. Krüger, “Parkinson’s disease—a multifactorial neurodegenerative disorder,” in *Diagnosis and Treatment of Parkinson’s Disease—State of the Art*, pp. 113–125, Springer, 1999.
- [38] P. P. Michel, E. C. Hirsch, and S. Hunot, “Understanding dopaminergic cell death pathways in Parkinson disease,” *Neuron*, vol. 90, no. 4, pp. 675–691, 2016.
- [39] S. M. Huang, H. C. Chuang, C. H. Wu, and G. C. Yen, “Cytoprotective effects of phenolic acids on methylglyoxal-induced apoptosis in neuro-2A cells,” *Molecular Nutrition & Food Research*, vol. 52, no. 8, pp. 940–949, 2008.
- [40] S. J. Hwang, S. H. Jun, Y. Park et al., “Green synthesis of gold nanoparticles using chlorogenic acid and their enhanced performance for inflammation,” *Nanomedicine: Nanotechnology, Biology and Medicine*, vol. 11, no. 7, pp. 1677–1688, 2015.
- [41] S. J. Hwang, Y. W. Kim, Y. Park, H. J. Lee, and K. W. Kim, “Anti-inflammatory effects of chlorogenic acid in lipopolysaccharide-stimulated RAW 264.7 cells,” *Inflammation Research*, vol. 63, no. 1, pp. 81–90, 2014.
- [42] M. Sedelis, R. K. W. Schwarting, and J. P. Huston, “Behavioral phenotyping of the MPTP mouse model of Parkinson’s disease,” *Behavioural Brain Research*, vol. 125, no. 1-2, pp. 109–125, 2001.
- [43] M.-F. Chesselet and F. Richter, “Modelling of Parkinson’s disease in mice,” *The Lancet Neurology*, vol. 10, no. 12, pp. 1108–1118, 2011.
- [44] S. N. Rai, H. Birla, S. S. Singh et al., “*Mucuna pruriens* protects against MPTP intoxicated neuroinflammation in Parkinson’s disease through NF- κ B/pAKT signaling pathways,” *Frontiers in Aging Neuroscience*, vol. 9, p. 421, 2017.
- [45] W. Wang, Y. Yang, C. Ying et al., “Inhibition of glycogen synthase kinase-3 β protects dopaminergic neurons from MPTP toxicity,” *Neuropharmacology*, vol. 52, no. 8, pp. 1678–1684, 2007.
- [46] X.-J. Xia, Y. G. Lian, H. Y. Zhao, and Q. L. Xu, “Curcumin protects from oxidative stress and inhibits α -synuclein aggregation in MPTP induced parkinsonian mice,” *International Journal of Clinical and Experimental Medicine*, vol. 9, no. 2, pp. 2654–2665, 2016.
- [47] J. Nataraj, T. Manivasagam, A. J. Thenmozhi, and M. M. Essa, “Lutein protects dopaminergic neurons against MPTP-induced apoptotic death and motor dysfunction by ameliorating mitochondrial disruption and oxidative stress,” *Nutritional Neuroscience*, vol. 19, no. 6, pp. 237–246, 2015.
- [48] S. N. Rai, W. Zahra, S. S. Singh et al., “Anti-inflammatory activity of ursolic acid in MPTP-induced parkinsonian mouse model,” *Neurotoxicity Research*, vol. 36, no. 3, pp. 452–462, 2019.
- [49] T. M. Dawson and V. L. Dawson, “Molecular pathways of neurodegeneration in Parkinson’s disease,” *Science*, vol. 302, no. 5646, pp. 819–822, 2003.
- [50] J. JIANG, J. JIANG, Y. ZUO, and Z. GU, “Rapamycin protects the mitochondria against oxidative stress and apoptosis in a rat model of Parkinson’s disease,” *International Journal of Molecular Medicine*, vol. 31, no. 4, pp. 825–832, 2013.
- [51] R. J. Smeyne and V. Jackson-Lewis, “The MPTP model of Parkinson’s disease,” *Molecular Brain Research*, vol. 134, no. 1, pp. 57–66, 2005.
- [52] B. B. Seo, E. Nakamaru-Ogiso, T. R. Flotte, A. Matsuno-Yagi, and T. Yagi, “In vivo complementation of complex I by the yeast Ndi1 enzyme possible application for treatment of Parkinson disease,” *Journal of Biological Chemistry*, vol. 281, no. 20, pp. 14250–14255, 2006.
- [53] M. Naoi, Y. Wu, M. Shamoto-Nagai, and W. Maruyama, “Mitochondria in neuroprotection by phytochemicals: bioactive polyphenols modulate mitochondrial apoptosis system, function and structure,” *International Journal of Molecular Sciences*, vol. 20, no. 10, p. 2451, 2019.
- [54] H. Jin, A. Kanthasamy, A. Ghosh, V. Anantharam, B. Kalyanaraman, and A. G. Kanthasamy, “Mitochondria-targeted antioxidants for treatment of Parkinson’s disease: pre-clinical and clinical outcomes,” *Biochimica et Biophysica Acta (BBA)-Molecular Basis of Disease*, vol. 1842, no. 8, pp. 1282–1294, 2014.
- [55] G. P. Davey, S. Peuchen, and J. B. Clark, “Energy thresholds in brain mitochondria potential involvement in neurodegeneration,” *Journal of Biological Chemistry*, vol. 273, no. 21, pp. 12753–12757, 1998.
- [56] A. Meister, “Glutathione deficiency produced by inhibition of its synthesis, and its reversal; applications in research and therapy,” *Pharmacology & Therapeutics*, vol. 51, no. 2, pp. 155–194, 1991.
- [57] A. Jain, J. Martensson, E. Stole, P. A. Auld, and A. Meister, “Glutathione deficiency leads to mitochondrial damage in brain,” *Proceedings of the National Academy of Sciences*, vol. 88, no. 5, pp. 1913–1917, 1991.
- [58] R. Heales, S. E. C. Davies, T. E. Bates, and J. B. Clark, “Deletion of brain glutathione is accompanied by impaired mitochondrial function and decreased N-acetyl aspartate concentration,” *Neurochemical Research*, vol. 20, no. 1, pp. 31–38, 1995.
- [59] X. H. Li, C. F. Dai, L. Chen, W. T. Zhou, H. L. Han, and Z. F. Dong, “7, 8-Dihydroxyflavone ameliorates motor deficits via suppressing α -synuclein expression and oxidative stress in the MPTP-induced mouse model of Parkinson’s disease,” *CNS Neuroscience & Therapeutics*, vol. 22, no. 7, pp. 617–624, 2016.
- [60] S. Mani, S. Sekar, R. Barathidasan et al., “Naringenin decreases α -synuclein expression and neuroinflammation in MPTP-

- induced Parkinson's disease model in mice," *Neurotoxicity Research*, vol. 33, no. 3, pp. 656–670, 2018.
- [61] X. Liu, C. N. Kim, J. Yang, R. Jemmerson, and X. Wang, "Induction of apoptotic program in cell-free extracts: requirement for dATP and cytochrome c," *Cell*, vol. 86, no. 1, pp. 147–157, 1996.
- [62] D. C. Joshi and J. C. Bakowska, "Determination of mitochondrial membrane potential and reactive oxygen species in live rat cortical neurons," *Journal of Visualized Experiments*, no. 51, article e2704, 2011.
- [63] S. Cory and J. M. Adams, "The Bcl2 family: regulators of the cellular life-or-death switch," *Nature Reviews Cancer*, vol. 2, no. 9, pp. 647–656, 2002.
- [64] L. Singh, N. Pushker, N. Saini et al., "Expression of proapoptotic Bax and anti-apoptotic Bcl-2 proteins in human retinoblastoma," *Clinical & Experimental Ophthalmology*, vol. 43, no. 3, pp. 259–267, 2015.
- [65] Y. Li, W. Z. Liu, L. Li, and C. Hölscher, "Neuroprotective effects of a GIP analogue in the MPTP Parkinson's disease mouse model," *Neuropharmacology*, vol. 101, pp. 255–263, 2016.
- [66] X. Wang, L. Zhao, T. Han, S. Chen, and J. Wang, "Protective effects of 2, 3, 5, 4'-tetrahydroxystilbene-2-O-beta-d-glucoside, an active component of *Polygonum multiflorum* Thunb, on experimental colitis in mice," *European Journal of Pharmacology*, vol. 578, no. 2-3, pp. 339–348, 2008.
- [67] A. Hartmann, S. Hunot, P. P. Michel et al., "Caspase-3: a vulnerability factor and final effector in apoptotic death of dopaminergic neurons in Parkinson's disease," *Proceedings of the National Academy of Sciences*, vol. 97, no. 6, pp. 2875–2880, 2000.
- [68] R. M. Friedlander, "Apoptosis and caspases in neurodegenerative diseases," *New England Journal of Medicine*, vol. 348, no. 14, pp. 1365–1375, 2003.
- [69] G. Chen, K. A. Bower, C. Ma, S. Fang, C. J. Thiele, and J. Luo, "Glycogen synthase kinase 3 β (GSK3 β) mediates 6-hydroxydopamine-induced neuronal death," *The FASEB Journal*, vol. 18, no. 10, pp. 1162–1164, 2004.
- [70] Q. Zhao, J. Ye, N. Wei, C. Fong, and X. Dong, "Protection against MPP+-induced neurotoxicity in SH-SY5Y cells by tormentic acid via the activation of PI3-K/Akt/GSK3 β pathway," *Neurochemistry International*, vol. 97, pp. 117–123, 2016.
- [71] H. Dudek, S. R. Datta, T. F. Franke et al., "Regulation of neuronal survival by the serine-threonine protein kinase Akt," *Science*, vol. 275, no. 5300, pp. 661–665, 1997.
- [72] V. Duronio, "The life of a cell: apoptosis regulation by the PI3K/PKB pathway," *Biochemical Journal*, vol. 415, no. 3, pp. 333–344, 2008.
- [73] N. Orike, G. Middleton, E. Borthwick, V. Buchman, T. Cowen, and A. M. Davies, "Role of PI 3-kinase, Akt and Bcl-2-related proteins in sustaining the survival of neurotrophic factor-independent adult sympathetic neurons," *The Journal of Cell Biology*, vol. 154, no. 5, pp. 995–1006, 2001.
- [74] V. Ries, H. C. Cheng, A. Baohan et al., "Regulation of the postnatal development of dopamine neurons of the substantia nigra in vivo by Akt/protein kinase B," *Journal of Neurochemistry*, vol. 110, no. 1, pp. 23–33, 2009.
- [75] A. Petit-Paitel, F. Brau, J. Cazareth, and J. Chabry, "Involvement of cytosolic and mitochondrial GSK-3 β in mitochondrial dysfunction and neuronal cell death of MPTP/MPP+-treated neurons," *PLoS One*, vol. 4, no. 5, article e5491, 2009.
- [76] T. D. King, G. N. Bijur, and R. S. Jope, "Caspase-3 activation induced by inhibition of mitochondrial complex I is facilitated by glycogen synthase kinase-3 β and attenuated by lithium," *Brain Research*, vol. 919, no. 1, pp. 106–114, 2001.
- [77] I. J. Xavier, P. A. Mercier, C. M. McLoughlin, A. Ali, J. R. Woodgett, and N. Ovsenek, "Glycogen synthase kinase 3 β negatively regulates both DNA-binding and transcriptional activities of heat shock factor 1," *Journal of Biological Chemistry*, vol. 275, no. 37, pp. 29147–29152, 2000.
- [78] D. W. Li, Z. Q. Liu, Wei-Chen, Min-Yao, and G. R. Li, "Association of glycogen synthase kinase-3 β with Parkinson's disease (review)," *Molecular Medicine Reports*, vol. 9, no. 6, pp. 2043–2050, 2014.
- [79] A.-R. Doo, S. N. Kim, J. Y. Park et al., "Neuroprotective effects of an herbal medicine, Yi-Gan San on MPP+/MPTP-induced cytotoxicity in vitro and in vivo," *Journal of Ethnopharmacology*, vol. 131, no. 2, pp. 433–442, 2010.
- [80] D. A. E. Cross, D. R. Alessi, P. Cohen, M. Andjelkovich, and B. A. Hemmings, "Inhibition of glycogen synthase kinase-3 by insulin mediated by protein kinase B," *Nature*, vol. 378, no. 6559, pp. 785–789, 1995.
- [81] S.-S. Park, H. Zhao, R. A. Mueller, and Z. Xu, "Bradykinin prevents reperfusion injury by targeting mitochondrial permeability transition pore through glycogen synthase kinase 3 β ," *Journal of Molecular and Cellular Cardiology*, vol. 40, no. 5, pp. 708–716, 2006.
- [82] M. Medina, J. J. Garrido, and F. G. Wandosell, "Modulation of GSK-3 as a therapeutic strategy on tau pathologies," *Frontiers in Molecular Neuroscience*, vol. 4, p. 24, 2011.
- [83] T. S. Lewis, P. S. Shapiro, and N. G. Ahn, "Signal transduction through MAP kinase cascades," in *Advances in Cancer Research*, pp. 49–139, Elsevier, 1998.
- [84] J. Zhu, C. Horbinski, F. Guo, S. Watkins, Y. Uchiyama, and C. T. Chu, "Regulation of autophagy by extracellular signal-regulated protein kinases during 1-methyl-4-phenylpyridinium-induced cell death," *The American Journal of Pathology*, vol. 170, no. 1, pp. 75–86, 2007.
- [85] Z. Weng, A. P. Signore, Y. Gao et al., "Leptin protects against 6-hydroxydopamine-induced dopaminergic cell death via mitogen-activated protein kinase signaling," *Journal of Biological Chemistry*, vol. 282, no. 47, pp. 34479–34491, 2007.
- [86] J.-M. Lee, D. S. Hwang, H. G. Kim, C. H. Lee, and M. S. Oh, "Dangguijakyak-san protects dopamine neurons against 1-methyl-4-phenyl-1, 2, 3, 6-tetrahydropyridine-induced neurotoxicity under postmenopausal conditions," *Journal of Ethnopharmacology*, vol. 139, no. 3, pp. 883–888, 2012.

Research Article

Baicalin Represses C/EBP β via Its Antioxidative Effect in Parkinson's Disease

Kecheng Lei ^{1,2}, **Yijue Shen**,¹ **Yijing He**,¹ **Liwen Zhang**,^{3,4} **Jingxing Zhang**,¹ **Weifang Tong**,¹ **Yichun Xu**,^{3,4} and **Lingjing Jin** ¹

¹Neurotoxin Research Center of Key Laboratory of Spine and Spinal Cord Injury Repair and Regeneration of Ministry of Education, Neurological Department of Tongji Hospital, Tongji University School of Medicine, 200065 Shanghai, China

²Department of Pathology and Laboratory Medicine, Emory University School of Medicine, 30322 Atlanta, Georgia, USA

³National Engineering Research Center for Biochip, Shanghai Biochip Limited Corporation, Shanghai, China

⁴Institute of Digestive Diseases, School of Medicine, Tongji University, China

Correspondence should be addressed to Lingjing Jin; lingjingjin@163.com

Received 18 February 2020; Revised 19 April 2020; Accepted 2 May 2020; Published 22 May 2020

Guest Editor: Francisco Jaime B. Mendonça Junior

Copyright © 2020 Kecheng Lei et al. This is an open access article distributed under the Creative Commons Attribution License, which permits unrestricted use, distribution, and reproduction in any medium, provided the original work is properly cited.

Parkinson's disease (PD) is a neurodegenerative disease characterized by the gradual loss of dopaminergic (DA) neurons in the substantia nigra (SN) and the formation of intracellular Lewy bodies (LB) in the brain, which aggregates α -synuclein (α -Syn) as the main component. The interest of flavonoids as potential neuroprotective agents is increasing due to its high efficiency and low side effects. Baicalin is one of the flavonoid compounds, which is a predominant flavonoid isolated from *Scutellaria baicalensis* Georgi. However, the key molecular mechanism by which Baicalin can prevent the PD pathogenesis remains unclear. In this study, we used bioinformatic assessment including Gene Ontology (GO) to elucidate the correlation between oxidative stress and PD pathogenesis. RNA-Seq methods were used to examine the global expression profiles of noncoding RNAs and found that C/EBP β expression was upregulated in PD patients compared with healthy controls. Interestingly, Baicalin could protect DA neurons against reactive oxygen species (ROS) and decreased C/EBP β and α -synuclein expression in pLVX-Tet3G- α -synuclein SH-SY5Y cells. In a 1-methyl-4-phenyl-1,2,3,6-tetrahydropyridine (MPTP) induced PD mouse model, the results revealed that treatment with Baicalin improved the PD model's behavioral performance and reduced dopaminergic neuron loss in the substantia nigra, associated with the inactivation of proinflammatory cytokines and oxidative stress. Hence, our study supported that Baicalin repressed C/EBP β via redox homeostasis, which may be an effective potential treatment for PD.

1. Background

Oxidative stress has been implicated as a key contributor to the progression of Parkinson's disease (PD) [1]. Because of the presence of enzymes such as tyrosine hydroxylase (TH) and monoamine oxidase (MAO), the neurotransmitter dopamine can be a major source of oxidative stress [2]. Although the human brain comprises less than 5% of total body weight, over 20% of the whole body's total oxygen is supplied to it, with part of oxygen subsequently converted into reactive oxygen species (ROS) [3]. Oxidative stress is considered as the common underlying source that leads to cellular dysfunction and demise, the idiopathic and genetic causes of PD [3, 4]. Overexpression of oxidative stress may lead to excitotoxicity,

mitochondrial dysfunction, protein misfolding and aggregation, and cellular apoptosis, which are all *in vitro* indicators of PD [5]. It is also believed that the increased levels of oxidized lipids are the common underlying mechanism that leads to dopaminergic neuronal loss in the substantia nigra (SN) and motor dysfunctions in PD patients [6].

α -Synuclein accumulates in Lewy bodies, which is the hallmark in PD pathology and leads to neurodegeneration and the progression of the clinical symptoms [7]. Although its exact role in neuropathology is unclear, evidence suggests that overexpression of α -synuclein might lead to oxidative stress [8] and neuroinflammation [9]. Then, oxidative stress can modulate the α -synuclein structure, leading to other formations of the protein, including fibrils and oligomers [10],

the latter of which can develop into positive regulation of ROS. The phosphorylation of α -synuclein at Ser-129, the major phosphorylation site, has been demonstrated from an animal model study to produce neurotoxic effects [11]. Moreover, oxidative stress leading to ROS production and α -synuclein aggregation is one of the proposed mechanisms for the death of dopaminergic neurons in PD patients [12].

It is also notable that the mitochondrial complex I damage is demonstrated to be one of the primary PD pathological animal models due to the administration of mitochondrial toxins, such as MPTP and rotenone, leading to the formation of α -synuclein aggregates and oxidative stress [13]. Methyl-4-phenyl-1,2,3,6-tetrahydropyridine (MPTP), a mitochondrial complex I inhibitor, is metabolized into the toxin 1-methyl-4-phenylpyridine (MPP⁺) by monoamine oxidase B (MAO-B) and later taken up by dopaminergic neurons, which finally lead to neuronal death and ROS production [14]. In rats, chronic administration of rotenone caused selective nigral dopaminergic neuron loss and a significant reduction in complex I activity while at the same time, the ROS level increased [15]. Altogether, these findings suggest that mitochondrial respiratory chain impairment, in particular, complex I deficiency, and the subsequent increase in ROS production may directly contribute to the pathology of PD.

Usually, it is mitochondria's ability to produce ATP appropriately in response to energy demands [16]. Meanwhile, the transcription factor CCAAT/enhancer-binding protein beta (C/EBP β), which is expressed in the brain, is also involved in the regulation of ATP synthesis [17]. Remarkably, C/EBP β -/- mice exhibit resistance to excitotoxicity-induced neuronal cell death, which indicates that C/EBP β might regulate gene expression implicated in brain damage [18].

There have been many reports discussing effective antioxidant treatment for PD, as well as conventional compounds that possessed antioxidant activity [19, 20]. Therefore, it is reasonable to suggest that targeting oxidative stress may be an effective strategy for PD medicine. Natural compounds have always been attractive targets for discovering new drug candidates, and many flavonoid derivatives are effective in preventing oxidative stress [21]. For instance, Hesperidin, the main flavanone derivative of citrus fruits, can alleviate cognitive impairment and oxidative stress in a mouse model of Alzheimer's disease [22]. Similarly, myricitrin, a flavonoid isolated from Chinese bayberry bark and fruit, demonstrated a protective effect on MPP⁺ induced mitochondrial dysfunction in a DJ-1-dependent manner in SN4741 cells [23]. Taking into account information about flavonoids, the focus of our paper is to discuss Baicalin, which is also the flavonoid derivatives, the principal component in the roots of *Scutellaria radix*, known as Huang Qin in Chinese traditional medicine [21, 24]. In recent years, several studies have shown that Baicalin displays a potent neuroprotective effect in various *in vitro* and *in vivo* models of neuronal injuries [25]. In particular, Baicalin effectively prevents neurodegenerative diseases through various pharmacological mechanisms, including antiexcitotoxicity, antiapoptosis, and anti-inflammation, promoting the expression of neuronal protective factors [26]. However, the mechanism of which

Baicalin can inhibit neurodegeneration and regulate redox homeostasis is unclear. In this study, we used RNA-Seq to examine the global expression profiles of noncoding RNAs in PD patients and healthy controls, and then, we demonstrated that Baicalin could protect cells from neurotoxicity *in vitro* and *in vivo*. Subsequently, Gene Ontology analysis displayed that, compared with the healthy controls, many processes overrepresented in PD patients were related to glucocorticoid receptor binding and cellular response to oxidative stress. Our study may help extend understanding of the roles of oxidative stress and provide new research directions for PD.

2. Materials and Methods

2.1. Cell Lines and Cell Culture. Human cell line pLVX-Tet3G- α -synuclein SH-SY5Y was provided by Dr. Jingxing Zhang and supplemented with G418 (100 μ g/ml). The cells were cultured in 1640 medium (Life Technologies, USA), supplemented with 10% fetal bovine serum (Hyclone, USA), penicillin (100 U/ml), and streptomycin (100 U/ml) (ABAM Life Technologies, California, USA). Cell cultures were maintained in 5% CO₂ and air humidified in a 37°C incubator [27].

2.2. Chemicals and Reagents. Baicalin was purchased from the company (Sigma, USA), and the stock solutions were prepared in dimethyl sulfoxide (DMSO) (Sigma, USA). For *in vivo* experiments, Baicalin was dissolved in sterile PBS.

2.3. Bioinformatic Analysis. Differentially expressed genes (DEGs) were determined from a treated versus control comparison of log₂-transformed expression measurements using the R package (<http://www.bioconductor.org/packages/release/bioc/html/edgeR.html>), and the resulting *p* values were adjusted using Benjamini and Hochberg's approach for controlling the false discovery rate (FDR) [28]. Differentially expressed genes (DEGs) with statistical significance were identified through volcano plot filtering. The thresholds for DEG were absolute log₂ fold change > 1 and *p* value < 0.01. Hierarchical clustering was performed using pheatmap package in R. To understand the potential biological functions of DEGs, we used clusterProfiler on R platform (<https://bioconductor.org/packages/release/bioc/html/clusterProfiler.html>). GO terms with corrected *p* value less than 0.05 were considered significantly enriched by DEGs.

2.4. Quantitative Real-Time PCR. Total RNA was extracted using a TRIzol reagent (Invitrogen, California, USA) according to the manufacturer's instructions. Reverse transcription was performed with SuperScript III reverse transcriptase (Life Technologies, #18080085), and primers were designed and purchased from TaqMan: CEBPB (Hs00270923_s1), Cebp (Mm00843434_s1), SNCA (Hs00240906_m1), Snca (Mm01188700_m1), Il1b (Mm00434228_m1), Il6 (Mm00446190_m1), TNF- α (Mm00443258_m1), and TGF β (Mm01178820_m1). Real-time PCR was performed with a TaqMan Universal Master Mix Kit (Life Technologies, #4304473) by ABI 7500 Fast Real-Time PCR System. The relative quantification of the target genes was calculated by the

comparative cycle threshold (CT) ($2^{-\Delta\Delta CT}$) method. The expression of GAPDH was used as an endogenous control. The relative quantification of gene expression was calculated by the $2^{-\Delta\Delta CT}$ method. All tests were performed in triplicate [29].

2.5. Protein Extraction and Western Blot Analysis. After the cell treatment under different conditions, the cells were harvested and the total proteins were extracted. Equal amounts of the proteins were loaded on SDS-PAGE gels, and the western blot assays were performed as previously described. α -Synuclein (#610787, BD Biosciences, USA), α -synuclein pS-129 (ab51253, Abcam, USA), p-C/EBP β (#3084, CST, USA), C/EBP β (#7962, Santa Cruz, USA), TH (#2792 CST, USA), and cleaved caspase-3 (#9664, CST, USA) were used at a final concentration of 1 mg/ml and were incubated overnight at 4°C in the presence of 5% nonfat milk powder. β -Actin (#3700, CST, USA) was used as the loading control [30].

2.6. Cell Viability Assay. Cell cytotoxicity was assessed in vitro using the 3-(4,5-dimethylthiazol-2-yl)-2,5-diphenyltetrazolium bromide (MTT) assay. After different treatments, 20 μ l of MTT (5 mg/ml in PBS, Sigma, USA) was added to each well and the plates were incubated for 2 h. The resulting formazan product was dissolved with DMSO, and the absorbance at a wavelength of 490 nm was read using a microplate reader (BioTek Instruments Inc., USA) [31]. All tests were performed in triplicate.

2.7. Intracellular ROS Measurement. The level of intracellular reactive oxygen species (ROS) was detected by the DCFH-DA method. After different treatments, cells were collected and then incubated with 10 μ M DCFH-DA (ROS dye, #C6827, Invitrogen, USA) for 1 hour at 37°C. The fluorescence intensity was measured by a microplate reader (BioTek Instruments Inc., USA) with settings at excitation and emission equal to 485/535 nm, and all tests were performed in triplicate [32].

2.8. Lactate Dehydrogenase (LDH) Cytotoxicity Assay. The level of LDH was detected by LDH assay kits (Promega Corporation, USA). After different treatments, the 100 μ l cell medium of each sample was collected and incubated with 50 μ l of the CytoTox 96[®] Reagent for 30 minutes at room temperature. Then, 50 μ l of Stop Solution was added to each well, and the absorbance at 490 nm was recorded. All tests were performed in triplicate.

2.9. Protein Carbonyl Assay Measurements and GSH/GSSG Ratio. After different treatments, the protein carbonyl level and GSH/GSSG ratio were measured from cell homogenates using a Protein Carbonyl Assay Kit (#ab126287, Abcam, Cambridge, MA, USA) and GSH/GSSG-Glo[™] (Promega Corporation, USA), respectively, according to the manufacturer's guidelines [33]. All tests were performed in triplicate.

2.10. JC-1 Mitochondrial Membrane Potential Assay. After different treatments, the cells were washed by PBS and stained with 10 μ M JC-1 (Cayman, USA) for 1 hour at

37°C. Finally, the cells were photographed with a fluorescence microscope (Nikon, Japan) at Ex488 nm/Em535 nm and Ex 540 nm/Em570 nm [34].

2.11. In Vivo Mouse Model Experiments. Male C57BL/6 mice (weighing 20–30 g) were purchased from Shanghai SLAC Laboratory Animal, housed, and maintained at constant temperature and humidity with a 12 h light/dark cycle in Tongji University. Three-month-old mice (8 per group) were injected a daily i.p. injection of MPTP (30 mg/kg) or saline treatment for 5 days [35] and then i.p. injection with 20 mg/kg and 40 mg/kg Baicalin for 2 weeks. Motor impairments were tested with rotarod tests and grid tests after Baicalin treatment (8 mice per group). In the rotarod tests, mice were trained for 2 min at a speed of 4 r.p.m. and then performed eight trials for a maximum of 5 min with increasing speed starting from 4 r.p.m. to 40 r.p.m. The fall-off time was recorded. For inverted grid tests, mice were placed in the center of a 30 \times 30 cm screen with 1 cm wide mesh. The screen was inverted head-over-tail and placed on supports 40 cm above an open cage with deep bedding. Mice were timed until they released their grip or remained for 60 s.

2.12. Tissue Preparation. After 2 weeks of treatment and behavior test, mice (3 per group) intended for immunofluorescence (IF) staining and immunohistochemistry (IHC) analysis were euthanasia and transcardially perfused with PBS followed by 4% paraformaldehyde (PFA) in PBS. Brains were postfixed for 24 h in 4% PFA at 4°C and transferred to a solution of 30% sucrose in PBS for 24 h at 4°C. The coronal section of SN and STR was sectioned as 30 μ m free-floating sections on a cryostat (Leica CM3050) and kept in PBS at 4°C [36]. The mouse brains intended for cell lysis (2 per group) and mRNA (3 per group) were transcardially perfused with ice-cold PBS and later performed western blotting and quantitative real-time PCR individually.

2.13. Immunofluorescence Staining. The number of TH- and GFAP-positive cells in the substantia nigra was estimated using a random sampling stereological counting method. Images were sampled from at least four different points within each substantia nigra section [37]. TH (ab6211), GFAP (ab7260), and DAPI (ab104139) were from Abcam, USA. All immunoreactive cells were counted regardless of the intensity of labeling. The slides were photographed with a fluorescence microscope (Nikon, Japan).

2.14. Immunohistochemistry Staining. Sections were prepared, and the expression of 4-HNE in the striatum and substantia nigra was assessed using a technique that has been reported previously [38]. In brief, the endogenous peroxidase activity was inactivated with 10% methanol and 3% hydrogen peroxide (H₂O₂) solution in PBS, pH 7.4, for 10 min, and nonspecific binding was blocked with 10% normal serum in TBS containing 0.5% Triton X-100. The sections were incubated overnight at 4°C with anti-4-HNE antibody (1:200 dilution in 1% normal serum in PBS containing 0.5% Triton X-100; ab46545, Abcam). The sections were then incubated with HRP-conjugated secondary antibody for 1 h. The slides were identified following DAB incubation for 10 min at room

temperature. Finally, photographs were taken using a microscope (Nikon, Japan).

2.15. Statistical Analysis. Data visualization and analysis were performed with GraphPad Prism 6 (GraphPad Software Inc., La Jolla, CA, USA). Statistical analysis was performed using either Student's *t*-test or one-way ANOVA. Significant difference among groups was assessed as * $p < 0.05$, ** $p < 0.01$, and *** $p < 0.001$.

3. Results

3.1. The Functional Annotation of Bioinformatic Analysis in PD Patients. To profile differentially expressed mRNAs of PD patients and healthy controls, we obtained blood samples from both groups. Then, the whole-genome sequencing and alteration were analyzed. The mRNA was upregulated or downregulated, respectively, by more than twofold in PD patients vs. healthy controls ($p < 0.05$) (Figure 1(a)). Among them, the results showed that *C/EBP β* was upregulated in PD patient blood samples compared with healthy controls (Figure 1(b)). Gene Ontology (GO) is a commonly used bioinformatic tool that provides comprehensive information on gene function of individual genomic products based on defined features [39]. This analysis was performed to establish the role of enrichment in molecular functions (MF), biological processes (BP), and cellular components (CC) in the interaction networks of *C/EBP β* . The enrichment analysis showed that for biological processes in the *C/EBP β* system, most of the genes were enriched at "cellular response to oxidative stress." The cellular component analysis showed that most of the genes were "nuclear chromatin." The typical molecular functions were "glucocorticoid receptor binding" and "protein heterodimerization activity" (Figure 1(c)). Hence, these results indicated that oxidative stress can be an effective target for PD research and presented more possible research directions for in-depth investigation.

3.2. Baicalin Inhibits the Toxicity and Oxidative Stress in pLVX-Tet3G- α -Synuclein SH-SY5Y Cell Lines. To examine the neurotoxicity of α -synuclein *in vitro*, the Doxycycline inducible pLVX-Tet3G- α -synuclein stable cell line was constructed, and the transfected efficiency was validated by mRNA and western blotting, as presented in Figures 2(a) and 2(b). To identify natural compounds capable of inhibiting the toxicity, we initiated a cell-based assay to screen chemicals extracted from Chinese herbal medicine [25]. The toxicity was evaluated by the release of lactate dehydrogenase (LDH). We found that 25 μ M or 50 μ M groups of Baicalin (Figure 2(c)) showed the significant ability ($p = 0.036$ and $p = 0.02$ individually) to protect cells from Dox-induced cell death (Figure 2(d)). Further study indicated that Baicalin exerted the protection effect on Dox-induced cells in a dose-dependent manner (Figure 2(e)). The quantitative oxidative stress level analysis showed that the 50 μ M Baicalin group decreased the ROS level (Figure 2(f)) ($p = 0.007$) and carbonyl expression (Figure 2(g)) ($p = 0.039$) while increasing the GSH/GSSH level ($p = 0.048$) (Figure 2(h)) compared to the Dox-induced group. Hence, Baicalin inhibited toxicity

and balanced the redox homeostasis in pLVX-Tet3G- α -synuclein SH-SY5Y cell lines.

3.3. Baicalin Protects against Dox-Induced Mitochondrial Dysfunctions. To determine whether Baicalin possesses the preventive effects against mitochondrial dysfunctions, parameters of mitochondrial function were studied in pLVX-Tet3G- α -synuclein SH-SY5Y cell lines. Mitochondrial membrane potential ($\Delta\psi$ M) is an important parameter of the mitochondrial function used as an indicator of cell health [40]. JC-1 is a dye that can selectively enter into mitochondria and reversibly change color from green to red as the membrane potential increases [41]. In Figure 3(a), Dox-induced JC-1 monomers were detected, which means that damaged or unhealthy cells were upregulated. On the other hand, increasing the concentration of Baicalin could induce JC-1 aggregates (healthy cells), especially at 50 μ M ($p = 0.024$). These results indicated that Baicalin could protect membrane potential from Dox-induced toxicity. To assess whether Baicalin regulates *CEBPB* and *SNCA* mRNA expression, we conducted quantitative RT-PCR (qRT-PCR) assays with pLVX-Tet3G- α -synuclein SH-SY5Y cells and found that *CEBPB* and *SNCA* were upregulated after DOX treatment and it can be reversed by Baicalin in a dose-dependent way (Figure 3(b)). Immunoblotting showed that TH proteins revealed a dose-dependent elevation while *p-C/EBP β* , *C/EBP β* , α -synuclein, and α -synuclein pS129 decreased in pLVX-Tet3G- α -synuclein SH-SY5Y cells upon Baicalin treatment. The results demonstrated that Baicalin could reverse Dox-induced α -synuclein aggregation. Interestingly, Dox-induced caspase-3 activation indicates that active oxidative stress triggers apoptosis. On the other hand, Baicalin reduced caspase-3 activation in a dose-dependent manner (Figure 3(c)).

3.4. Baicalin Protects Dopaminergic Neurons and Rescues Motor Dysfunction against MPTP-Induced Neurotoxicity In Vivo. To investigate the *in vivo* roles of Baicalin, three-month-old C57BL mice (8 per group) were treated with MPTP (i.p., 30 mg/kg) or saline for 5 days. Motor behavioral tests showed that MPTP incurred significant motor disorder, which was ameliorated upon two weeks of 20 mg/kg and 40 mg/kg Baicalin treatment. Remarkably, in the 40 mg/kg Baicalin group, MPTP elicited in the rotarod test ($p = 0.042$) and grid test ($p = 0.047$) were significantly less severe than the control group (Figures 4(a) and 4(b)), supporting the fact that Baicalin was highly neuroprotective and prevented MPTP-elicited motor dysfunctions in mice. We also monitored dopaminergic neuron loss after Baicalin treatment. Immunofluorescence staining showed that dopaminergic neurons in SN were substantially diminished by MPTP as compared to the vehicle group. Again, Baicalin attenuated the loss of dopaminergic neurons (Figure 4(c)). The maximal neuroprotective effects occurred with the 40 mg/kg Baicalin group ($p = 0.012$).

3.5. Baicalin Regulates the Redox Balance in the MPTP Treatment Group. For manifesting the oxidative stress in Parkinson's disease, we employed 4-HNE staining, one of the

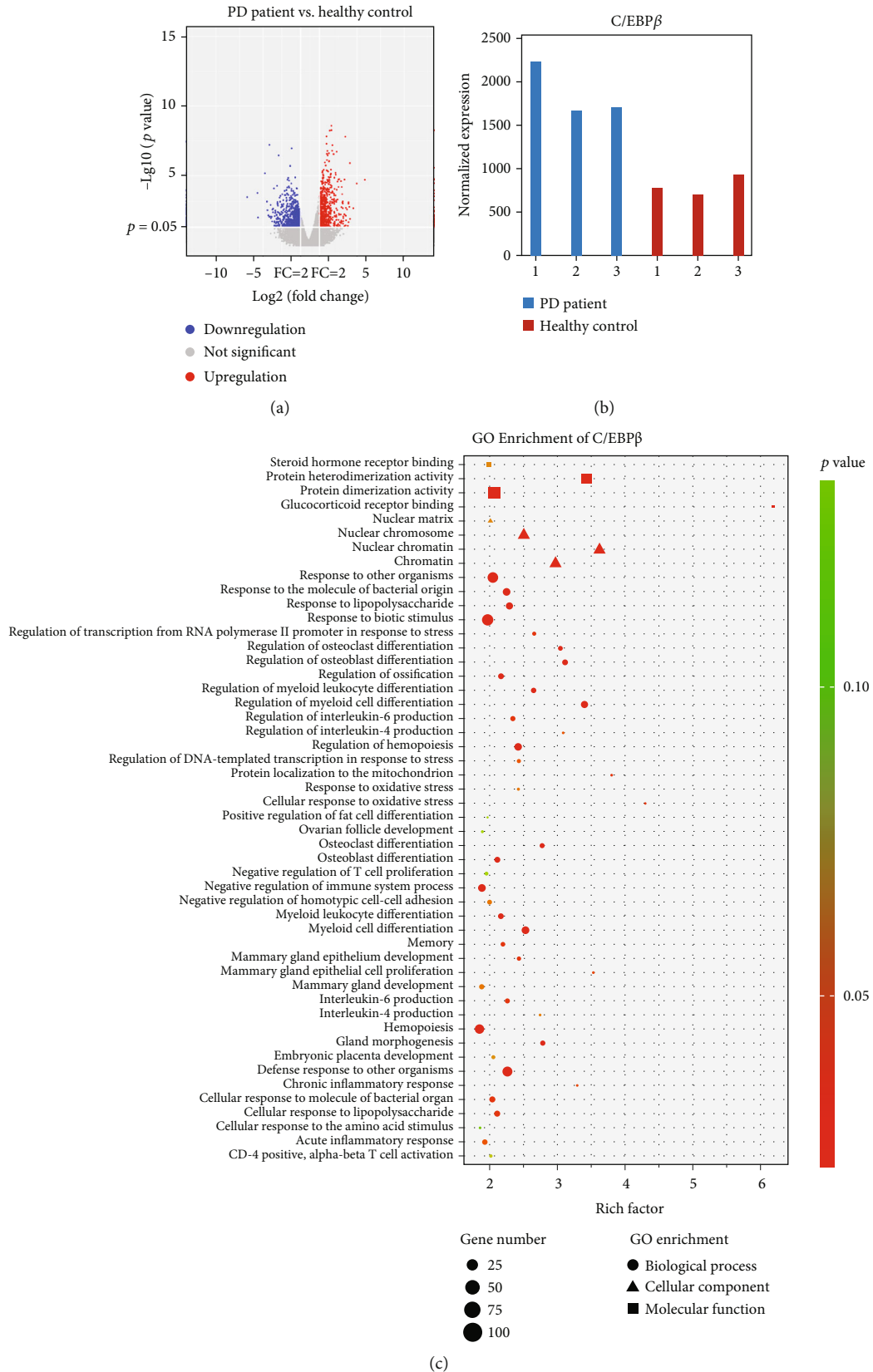


FIGURE 1: Expression profiles and Gene Ontology (GO) terms for differentially expressed mRNAs between PD patients and healthy control blood samples. (a) Volcano analysis exhibited differentially expressed mRNAs. Blue dots illustrated downregulated genes, and red dots illustrated upregulated genes. (b) C/EBP β was upregulated in PD patient samples compared to healthy control samples. (c) GO enrichment analysis for biological processes, cellular component, and molecular function in the interaction networks of C/EBP β .

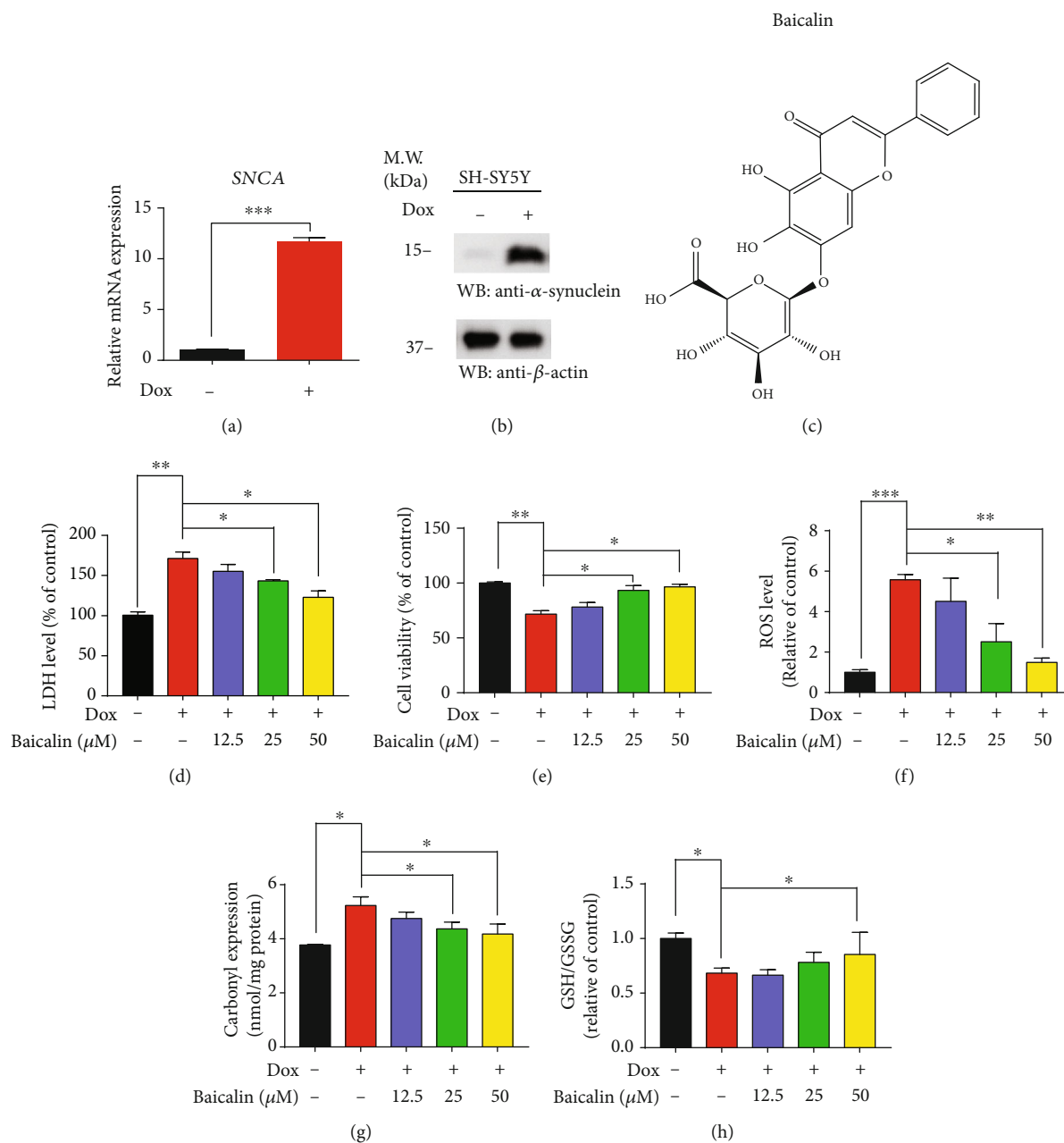
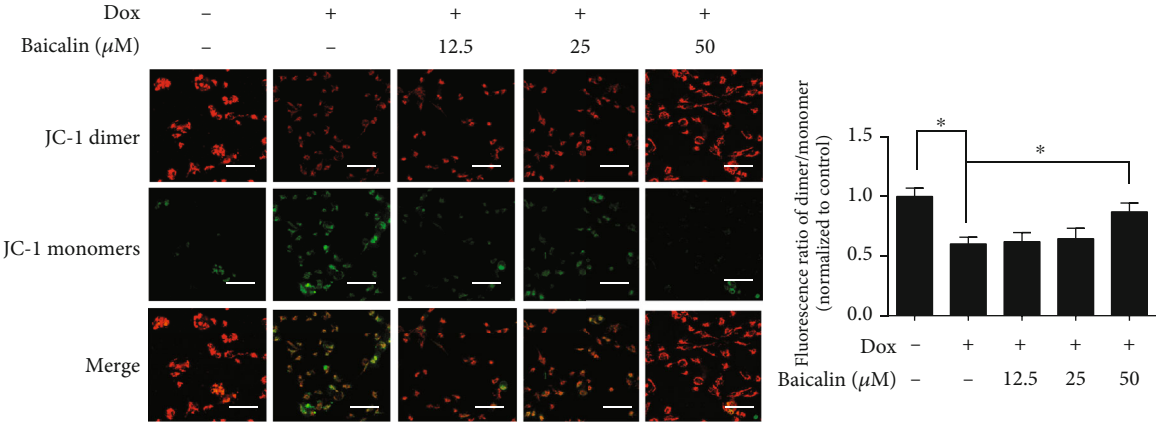


FIGURE 2: Baicalin inhibited toxicity and oxidative stress in pLVX-Tet3G- α -synuclein SH-SY5Y cell lines. (a) The mRNA level of α -synuclein in pLVX-Tet3G- α -synuclein SH-SY5Y stable cell line. (b) The protein level of α -synuclein in pLVX-Tet3G- α -synuclein SH-SY5Y stable cell line. (c) The chemical structure of Baicalin. (d) The LDH level of Baicalin. (e) Cell viability by MTT assay. (f) The ROS level, (g) carbonyl expression, and (h) GSH/GSSG level of Baicalin. The pLVX-Tet3G- α -synuclein SH-SY5Y cells were incubated with various concentrations (0–50 μ M) of Baicalin for 24 h. All data represented the mean and standard error of three independent experiments. * $p < 0.05$; ** $p < 0.01$; *** $p < 0.001$.

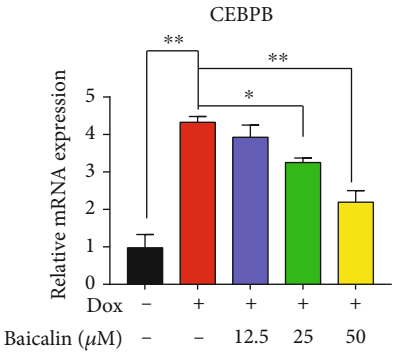
most bioactive and studied lipid peroxidation biomarkers [42]. IHC analysis demonstrated that Baicalin group mice possessed the least oxidative stress among the experimental groups, provoked by MPTP treatment, in alignment with its prominent neuroprotective activity in the striatum and substantia nigra (Figure 5(a)). We observed that *Cebpb* ($p = 0.021$) and *Snca* ($p = 0.0042$) mRNA expression decreased after 40 mg/kg Baicalin treatment in SN compared to the MPTP group (Figure 5(b)). Immunoblotting analysis revealed the comparable protein levels expressed in the

mouse brains. MPTP treatment elicited prominent dopaminergic neuronal TH loss, which was partially alleviated by Baicalin. As expected, α -synuclein pS129, α -synuclein, p-C/EBP β , and C/EBP β were strongly upregulated in the MPTP group after Baicalin treatment (Figure 5(c)). Hence, Baicalin possesses strong antioxidative activity, rescuing dopaminergic neurons from MPTP-induced cell death.

3.6. Baicalin Protects against Neuroinflammation and Oxidative Stress Triggered by MPTP Treatment. Activated



(a)



(b)

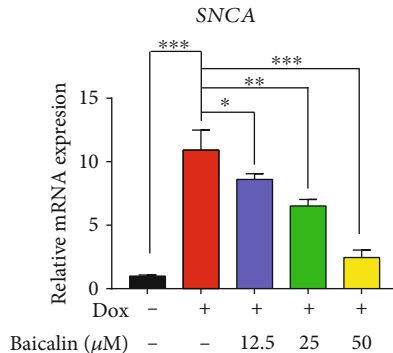


FIGURE 3: Continued.

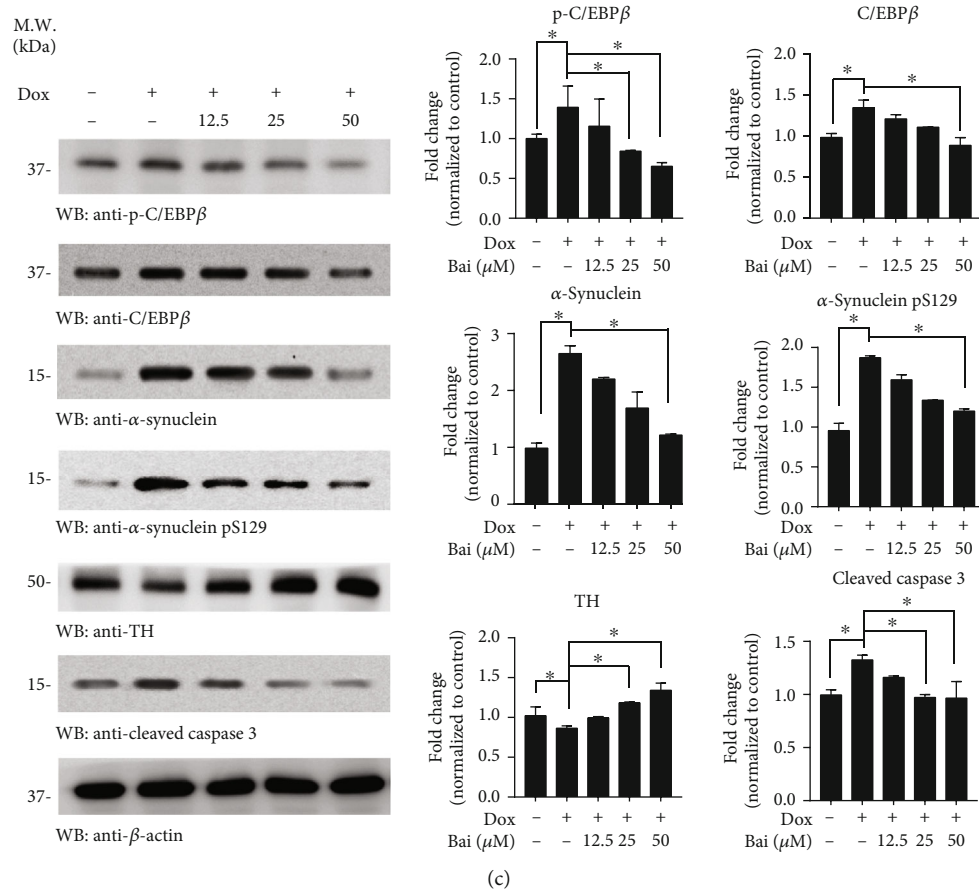


FIGURE 3: Baicalin protected Dox-induced mitochondrial dysfunction. (a) The representative image of pLVX-Tet3G- α -synuclein SH-SY5Y cell with an accumulation of JC-1 staining after incubation with various concentrations (0–50 μ M) of Baicalin for 24 h. Scale bars: 50 μ m. (b) The mRNA level of pLVX-Tet3G- α -synuclein SH-SY5Y cells treated with various concentrations (0–50 μ M) of Baicalin for 24 h. (c) Western blot analysis of pLVX-Tet3G- α -synuclein SH-SY5Y cell treated with various concentrations (0–50 μ M) of Baicalin for 24 h. All data represented the mean and standard error of three independent experiments. * $p < 0.05$; ** $p < 0.01$; *** $p < 0.001$.

microglia and increased levels of inflammatory mediators are detected in the striatum of deceased PD patients [43, 44]; meanwhile, a large body of animal studies supports the contributory role of inflammation in dopaminergic cell loss [45]. Quantification of neuroinflammation revealed that IL-1 β , IL-6, and TNF- α mRNA levels were decreased after Baicalin treatment, while the TGF- β mRNA level was increased (Figure 6(a)). Increased expression of GFAP is considered as markers of ROS production and the inflammatory process. In Figure 6(b), immunofluorescence staining of GFAP in the striatum showed a remarkably higher expression of GFAP-positive astrocytes in MPTP treatment when compared to the saline group ($p = 0.0025$). However, Baicalin decreased the GFAP-positive cells as well ($p = 0.032$). Again, our results indicated that Baicalin reduced oxidative stress in the MPTP treatment group.

4. Discussion

Over thousands of years, Chinese herbs have been used by the Chinese pharmacologists as treatment of diseases, including cancer [46], climacteric syndrome [47], schizophrenia [48], Alzheimer's disease [49], and Parkinson's disease [50].

Baicalin is one of the most important flavonoid compounds, which is mainly isolated from the root of *Scutellaria baicalensis* Georgi, which is an indispensable Chinese medicinal herb [51]. Besides, Baicalin does not display any significant toxicity to the mice at a dose even of 15 g/kg [52], which indicates its low toxicity, making it highly acceptable and safe for application in humans. However, one major limitation in the clinical application of Baicalin is their poor oral bioavailability and low aqueous solubility. There is increasing evidence that Baicalin plays an important role in various diseases, such as cardiovascular disease, depression, Alzheimer's disease, and Parkinson's disease. Baicalin alleviates cardiac dysfunction and myocardial remodeling in a chronic pressure overload mouse model [53]. In AD, Baicalin can reduce Alzheimer-like pathological changes and memory impairment caused by amyloid β 1-42. Jin et al. reported that Baicalin can reduce cognitive impairment and protect neurons from microglia-mediated neuroinflammation TLR4/NF- κ B signaling [54]. In a recent study, Baicalin inhibited TLR4 expression through the PI3K/AKT/FoxO1 pathway and improved depression-like behavior [55]. Noticeably, Baicalin, which is the aglycone of Baicalin, inhibits α -synuclein fibrillation and disaggregates the

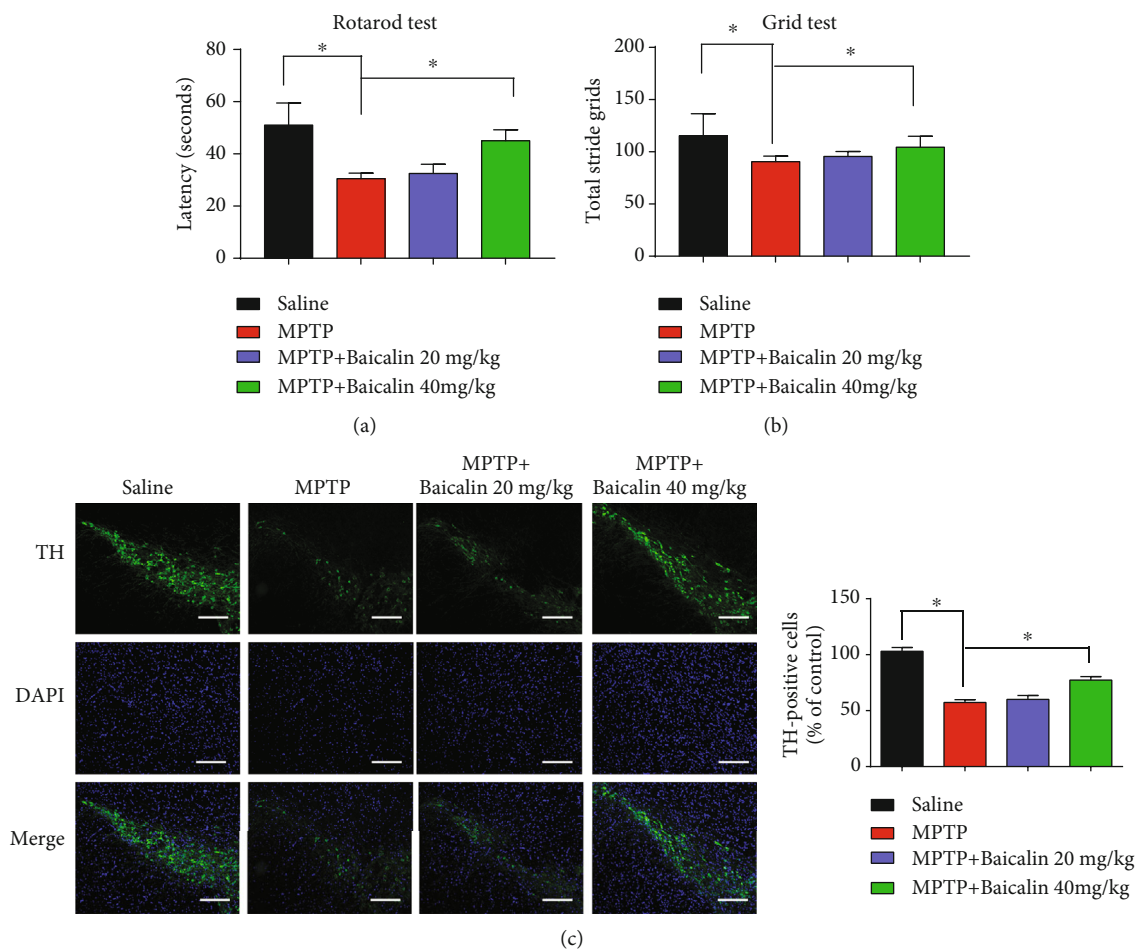


FIGURE 4: Baicalin protected dopaminergic neurons and rescues motor dysfunction against MPTP-induced neurotoxicity *in vivo*. (a) Rotarod tests and (b) grid tests were conducted by a blinded observer after two weeks of 20 mg/kg and 40 mg/kg Baicalin treatment. Data were the mean \pm SEM ($n = 8$ per group). (c) TH staining of the substantia nigra (SN) of the above mice. Scale bars: 200 μ m. All data represented the mean and standard error of three independent experiments. * $p < 0.05$; ** $p < 0.01$; *** $p < 0.001$.

performed fibrils [56]. The medical mechanism of Baicalin inhibiting α -synuclein aggregates is still unclear. In our experiment, an *in vitro* experimental model, Baicalin (50 μ M) protected pLVX-Tet3G- α -synuclein SH-SY5Y cells against Dox-induced toxicity and also prevented the loss of cell viability (Figure 2(e)). Other researchers also found that lack of α -synuclein in mice is associated with reduced vulnerability to MPTP and reduced dopaminergic neuronal cell death [57]. The previous study also showed that abnormal posture, gait, and stiffness of the limbs are directly related to the loss of dopaminergic neurons, which is the root cause of PD [58]. Baicalin and deferoxamine can reduce iron accumulation in SN of Parkinson's disease rats [59]. In our results, we showed that Baicalin blocked α -synuclein expression and aggregation and protected dopaminergic neurons and rescues motor dysfunction against MPTP-induced neurotoxicity *in vivo* (Figure 4); presumably, Baicalin's therapeutic efficacy might partially result from its inhibition against α -synuclein.

Additionally, Baicalin may sustain redox homeostasis by protecting mitochondrial systems after treating with MPP+ [60]. Maintaining homeostasis is essential for preventing

and curing disease [61]. Unbalanced homeostasis with the more oxidized environment, for example, higher oxidative stress, facilitated more cell death. In our research, Baicalin inactivated ROS (25 μ M and 50 μ M) production, carbonyl expression, and lactate dehydrogenase (LDH) level, meanwhile, alternated in GSH/GSSG ratio (Figures 2(d) and 2(f)–2(h)), facilitating a dramatically less oxidized environment for cell survival. Interestingly, Baicalin was effective in blocking the Dox-induced toxicity on the mitochondrial membrane potential (Figure 3(a)), resulting in increased ATP synthesis.

Currently, with the advent of next-generation sequencing technologies, RNA-Seq is gradually replacing microarrays for the detection of transcript expression profiling [62]. Although a lot of papers reported the RNA networks in PD, microarray methods were primarily employed [63, 64]. In this study, we used RNA-Seq to examine the global expression profiles of noncoding RNAs. Using RNA-Seq technology, we found that C/EBP β was upregulated in PD patient's blood samples (Figure 1(b)). Moreover, the target mRNAs of differentially expressed mRNAs were mostly involved in "glucocorticoid receptor binding," "cellular response to

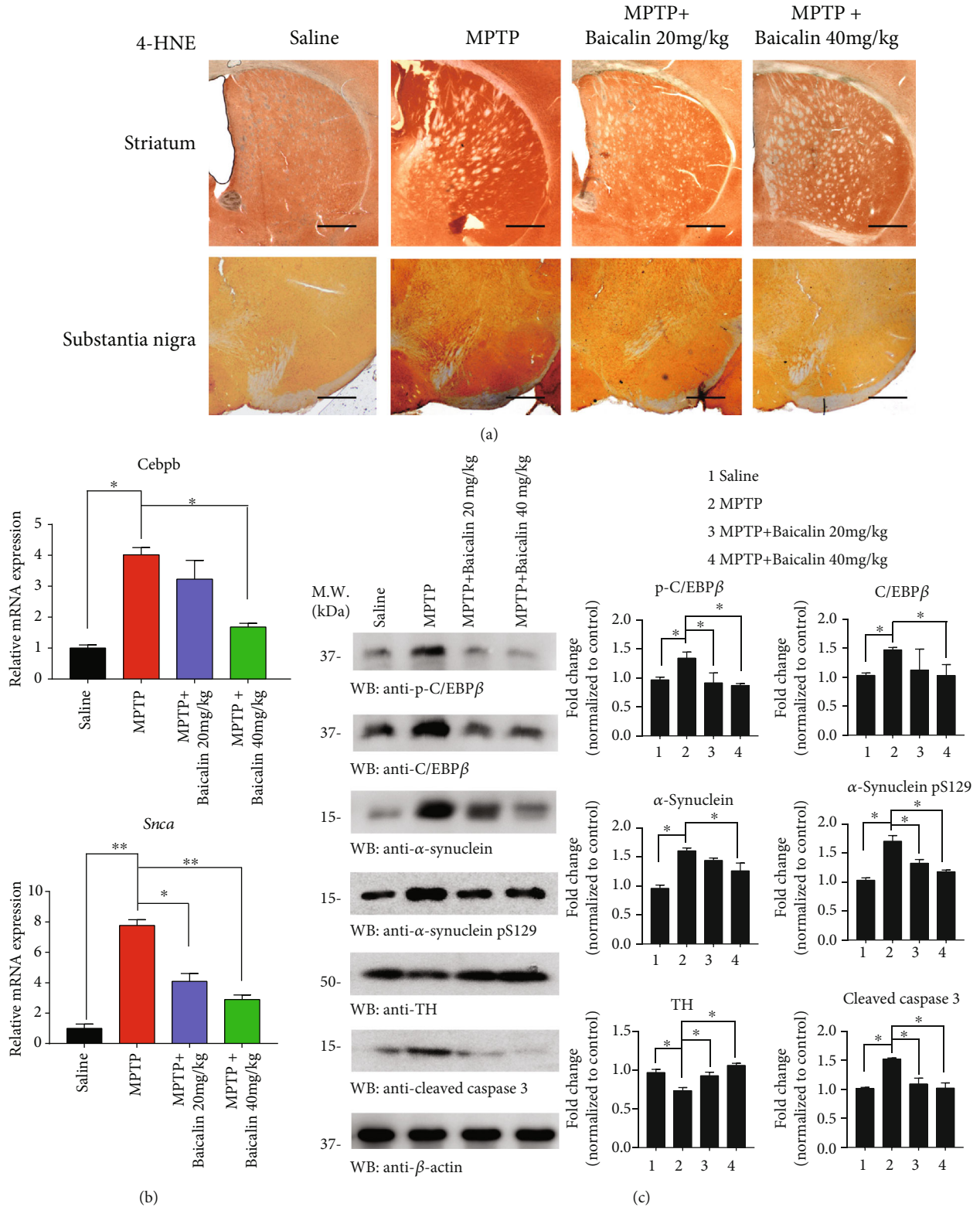


FIGURE 5: Baicalin protected dopaminergic neuron oxidative stress against MPTP treatment. (a) Immunohistochemical analysis for assessment of 4-HNE in the substantia nigra (SN) and striatum of saline, MPTP, MPTP+20 mg/kg Baicalin, and MPTP+40 mg/kg Baicalin groups. Scale bars: 500 μ m. (b) The *Cebpb* and *Snca* mRNA levels of represented groups. (c) SN lysates were probed with various indicated antibodies. The band densitometric data of WB. All data represented the mean and standard error of three independent experiments. * $p < 0.05$; ** $p < 0.01$; *** $p < 0.001$.

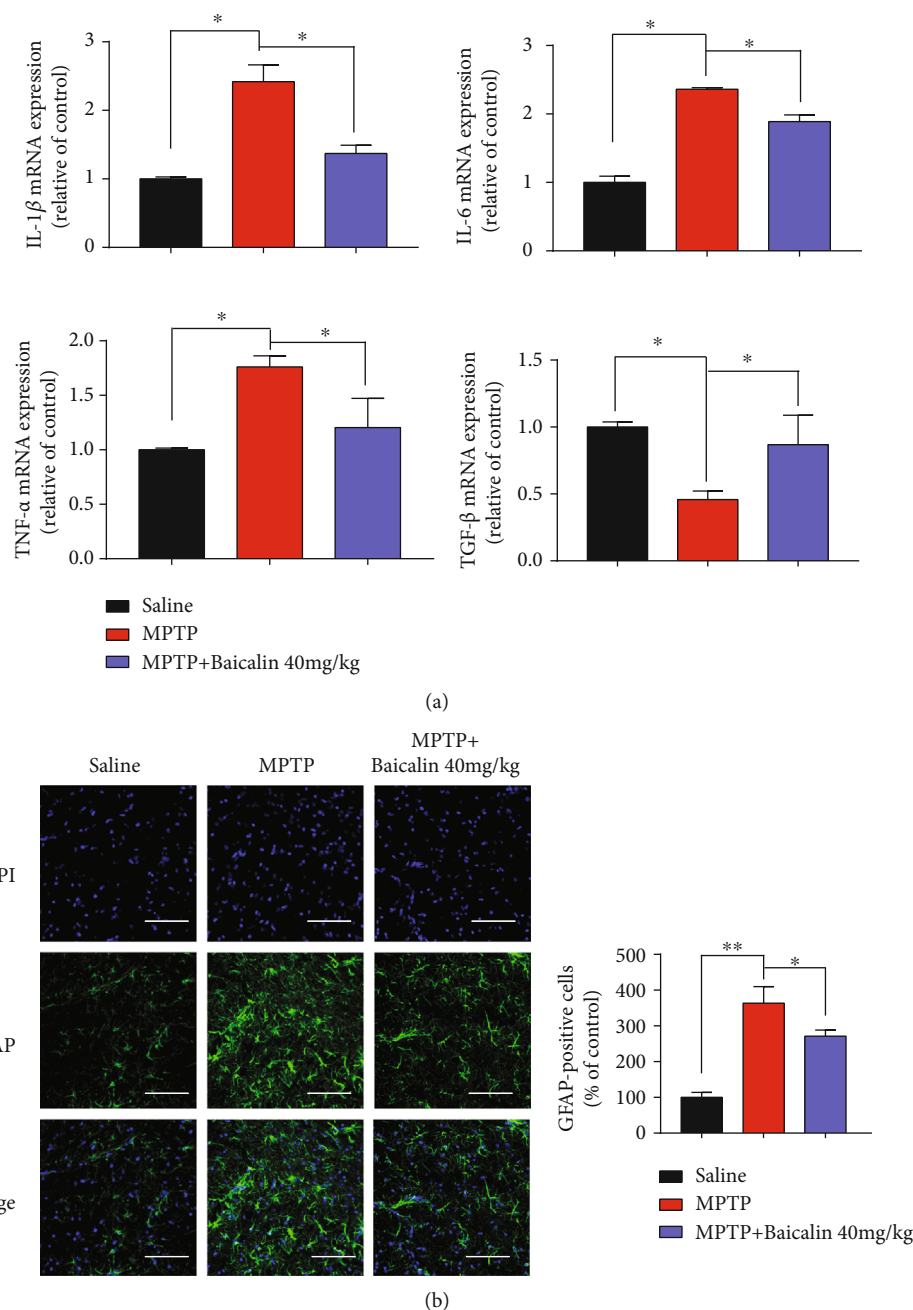


FIGURE 6: Baicalin protected against neuroinflammation and oxidative stress triggered by MPTP treatment. (a) IL-1 β , IL-6, TNF- α , and TGF- β mRNA levels of SN measured by q-RT-PCR in saline, MPTP, and MPTP+40 mg/kg Baicalin groups. (b) Immunofluorescence staining to detect the expression of the glial fibrillary acidic protein- (GFAP-) positive astrocyte (green) in saline, MPTP, and MPTP+40 mg/kg Baicalin groups. Scale bars: 100 μ m. All data represented the mean and standard error of three independent experiments. * $p < 0.05$; ** $p < 0.01$; *** $p < 0.001$.

oxidative stress,” and “protein localization to the mitochondria” (Figure 1(c)). These results were partly consistent with those of our data. Also, RNA-Seq data showed new findings in that regulation of “protein heterodimerization” and “nuclear chromatin” were involved in the pathogenesis of PD, which are interesting targets for further investigation.

Our previous work demonstrated that C/EBP β , which is the transcription factor of α -synuclein and MAO-B, mediates the pathogenesis of Parkinson’s disease [65]. C/EBP β is one

of the family members of transcription factors in the basic-leucine zipper (bZIP) class. In glial cells, C/EBP β regulates the proinflammatory program. Because of its role in neuroinflammation, C/EBP β is a potential target for the treatment of neurodegenerative disorders [66]. In our study, Baicalin repressed DOX-induced C/EBP β level and α -synuclein as indicated in mRNA and protein level (Figures 3(b) and 3(c)). In addition, it was demonstrated that Baicalin inhibited MPTP-triggered inflammatory mediators, including the

classical proinflammatory triad of IL-1 β , IL-6, and TNF- α (Figure 6(a)). Notably, Baicalin was involved in the regulation of proinflammatory gene expression in glial activation, especially GFAP expression, and played a key role in the reduction of neurotoxic effects by inactivating microglia (Figure 6(b)).

There may be some other limitations to our study that should be shortly mentioned: (1) Further studies are necessary to reveal how Baicalin regulates the inactivation of glial cells in PD models. (2) Although flavonoids are nonspecific inhibitors [67], our future research will focus on this basis and look for structural elements with high specificity and beneficial effects in PD treatment.

5. Conclusions

Our data strongly supported that the analysis of the gene expression profile may enable the identification of targets for PD diagnosis and treatment. The results confirmed that C/EBP β and oxidative stress played important roles in the progression of PD. Meanwhile, Baicalin functioned as an antioxidant for dictating the expression of C/EBP β and regulated oxidative stress in the pLVX-Tet3G- α -synuclein SH-SY5Y cell model and MPTP treatment mouse model, further indicating Baicalin's neuroprotective effect in neurotoxin-triggered Parkinson's disease.

Data Availability

The data used to support the findings of this study have not been made available because the data also form part of an ongoing study.

Ethical Approval

All applicable international, national, and/or institutional guidelines for the care and use of animals were followed.

Consent

All subjects agreed to be in the study, and biological specimens were obtained after informed consent with approval from Shanghai Tongji Hospital.

Conflicts of Interest

The authors declare that they have no competing interests.

Authors' Contributions

Kecheng Lei and Yijue Shen contributed equally to this work. They carried out the experiment and wrote the manuscript. Yijing He and Weifang Tong helped with animal work. Jingxing Zhang offered the cell lines. Liwen Zhang and Yichun Xu performed the analytic calculations. Lingjing Jin supervised the project. Kecheng Lei and Yijue Shen are co-first authors.

Acknowledgments

The authors would like to thank Dr. Keqiang Ye from Emory University for revising the manuscript. This article is supported by the "National Key R&D Program of China" (2018YFC1314700 and 2018YFA0108000), National Natural Science Foundation of China (81974196 and 81873779), Shanghai municipal medical and health excellent academic leaders training program (2017BR029), and China Postdoctoral Science Foundation (2018M632168).

References

- [1] M. Al Shahrani, S. Heales, I. Hargreaves, and M. Orford, "Oxidative stress: mechanistic insights into inherited mitochondrial disorders and Parkinson's disease," *Journal of Clinical Medicine*, vol. 6, no. 11, p. 100, 2017.
- [2] N. Mahy, N. Andrés, C. Andrade, and J. Saura, "Age-related changes of MAO-A and -B distribution in human and mouse brain," *Neurobiology*, vol. 8, no. 1, pp. 47–54, 2000.
- [3] G. F. Crotty, A. Ascherio, and M. A. Schwarzschild, "Targeting urate to reduce oxidative stress in Parkinson disease," *Experimental Neurology*, vol. 298, Part B, pp. 210–224, 2017.
- [4] D. N. Hauser and T. G. Hastings, "Mitochondrial dysfunction and oxidative stress in Parkinson's disease and monogenic parkinsonism," *Neurobiology of Disease*, vol. 51, pp. 35–42, 2013.
- [5] C. W. Olanow, "The pathogenesis of cell death in Parkinson's disease—2007," *Movement Disorders*, vol. 22, no. S17, pp. S335–S342, 2007.
- [6] A. Barzilai and E. Melamed, "Molecular mechanisms of selective dopaminergic neuronal death in Parkinson's disease," *Trends in Molecular Medicine*, vol. 9, no. 3, pp. 126–132, 2003.
- [7] W. J. Schulz-Schaeffer, "The synaptic pathology of α -synuclein aggregation in dementia with Lewy bodies, Parkinson's disease and Parkinson's disease dementia," *Acta Neuropathologica*, vol. 120, no. 2, pp. 131–143, 2010.
- [8] M. Hashimoto, L. J. Hsu, E. Rockenstein, T. Takenouchi, M. Mallory, and E. Masliah, " α -Synuclein protects against oxidative stress via inactivation of the c-Jun N-terminal kinase stress-signaling pathway in neuronal cells," *Journal of Biological Chemistry*, vol. 277, no. 13, pp. 11465–11472, 2002.
- [9] E. C. Hirsch, S. Vyas, and S. Hunot, "Neuroinflammation in Parkinson's disease," *Parkinsonism & Related Disorders*, vol. 18, pp. S210–S212, 2012.
- [10] V. N. Uversky, "A protein-chameleon: conformational plasticity of α -synuclein, a disordered protein involved in neurodegenerative disorders," *Journal of Biomolecular Structure and Dynamics*, vol. 21, no. 2, pp. 211–234, 2003.
- [11] O. S. Gorbatyuk, S. Li, L. F. Sullivan et al., "The phosphorylation state of Ser-129 in human α -synuclein determines neurodegeneration in a rat model of Parkinson disease," *Proceedings of the National Academy of Sciences of the United States of America*, vol. 105, no. 2, pp. 763–768, 2008.
- [12] K. J. Barnham, C. L. Masters, and A. I. Bush, "Neurodegenerative diseases and oxidative stress," *Nature Reviews Drug Discovery*, vol. 3, no. 3, pp. 205–214, 2004.
- [13] R. Betarbet, T. B. Sherer, and J. T. Greenamyre, "Animal models of Parkinson's disease," *BioEssays*, vol. 24, no. 4, pp. 308–318, 2002.

- [14] N. Schmidt and B. Ferger, "Neurochemical findings in the MPTP model of Parkinson's disease," *Journal of Neural Transmission*, vol. 108, no. 11, pp. 1263–1282, 2001.
- [15] C. M. Testa, T. B. Sherer, and J. T. Greenamyre, "Rotenone induces oxidative stress and dopaminergic neuron damage in organotypic substantia nigra cultures," *Molecular Brain Research*, vol. 134, no. 1, pp. 109–118, 2005.
- [16] M. D. Brand and D. G. Nicholls, "Assessing mitochondrial dysfunction in cells," *Biochemical Journal*, vol. 435, no. 2, pp. 297–312, 2011.
- [17] Q. Du, Z. Tan, F. Shi et al., "PGC1 α /CEBPB/CPT1A axis promotes radiation resistance of nasopharyngeal carcinoma through activating fatty acid oxidation," *Cancer Science*, vol. 110, no. 6, pp. 2050–2062, 2019.
- [18] Z.-H. Wang, K. Gong, X. Liu et al., "C/EBP β regulates delta-secretase expression and mediates pathogenesis in mouse models of Alzheimer's disease," *Nature Communications*, vol. 9, no. 1, article 1784, 2018.
- [19] K. Aquilano, S. Baldelli, G. Rotilio, and M. R. Ciriolo, "Role of nitric oxide synthases in Parkinson's disease: a review on the antioxidant and anti-inflammatory activity of polyphenols," *Neurochemical Research*, vol. 33, no. 12, pp. 2416–2426, 2008.
- [20] The Parkinson Study Group, "Effects of tocopherol and deprenyl on the progression of disability in early Parkinson's disease," *New England Journal of Medicine*, vol. 328, no. 3, pp. 176–183, 1993.
- [21] M. R. de Oliveira, S. F. Nabavi, S. Habtemariam, I. E. Orhan, M. Daglia, and S. M. Nabavi, "The effects of baicalin and baicalin on mitochondrial function and dynamics: a review," *Pharmacological Research*, vol. 100, pp. 296–308, 2015.
- [22] D. Wang, L. Liu, X. Zhu, W. Wu, and Y. Wang, "Hesperidin alleviates cognitive impairment, mitochondrial dysfunction and oxidative stress in a mouse model of Alzheimer's disease," *Cellular and Molecular Neurobiology*, vol. 34, no. 8, pp. 1209–1221, 2014.
- [23] Z. Cai, W. Zeng, K. Tao, F. Lu, G. Gao, and Q. Yang, "Myricitrin alleviates MPP $^{+}$ -induced mitochondrial dysfunction in a DJ-1-dependent manner in SN4741 cells," *Biochemical and Biophysical Research Communications*, vol. 458, no. 2, pp. 227–233, 2015.
- [24] K. Sowndhararajan, P. Deepa, M. Kim, S. J. Park, and S. Kim, "Neuroprotective and cognitive enhancement potentials of baicalin: a review," *Brain Sciences*, vol. 8, no. 6, p. 104, 2018.
- [25] J. Dong, Y. Zhang, Y. Chen et al., "Baicalin inhibits the lethality of ricin in mice by inducing protein oligomerization," *Journal of Biological Chemistry*, vol. 290, no. 20, pp. 12899–12907, 2015.
- [26] W. Liang, X. Huang, and W. Chen, "The effects of baicalin and baicalin on cerebral ischemia: a review," *Aging and Disease*, vol. 8, no. 6, pp. 850–867, 2017.
- [27] E. H. Ahn, D. W. Kim, M. J. Shin et al., "PEP-1-ribosomal protein S3 protects dopaminergic neurons in an MPTP-induced Parkinson's disease mouse model," *Free Radical Biology and Medicine*, vol. 55, pp. 36–45, 2013.
- [28] Y. Xing, Z. Zhao, Y. Zhu, L. Zhao, A. Zhu, and D. Piao, "Comprehensive analysis of differential expression profiles of mRNAs and lncRNAs and identification of a 14-lncRNA prognostic signature for patients with colon adenocarcinoma," *Oncology Reports*, vol. 39, no. 5, pp. 2365–2375, 2018.
- [29] K. Lei, X. Liang, Y. Gao et al., "Lnc-ATB contributes to gastric cancer growth through a miR-141-3p/TGF β 2 feedback loop," *Biochemical and Biophysical Research Communications*, vol. 484, no. 3, pp. 514–521, 2017.
- [30] K. Lei, W. du, S. Lin et al., "3B, a novel photosensitizer, inhibits glycolysis and inflammation via miR-155-5p and breaks the JAK/STAT3/SOCS1 feedback loop in human breast cancer cells," *Biomedicine & Pharmacotherapy*, vol. 82, pp. 141–150, 2016.
- [31] K. Lei, S. Tan, W. Du et al., "3B, a novel of photosensitizer, exhibited anti-tumor effects via mitochondrial apoptosis pathway in MCF-7 human breast carcinoma cells," *Tumor Biology*, vol. 36, no. 7, pp. 5597–5606, 2015.
- [32] E. H. Ahn, D. W. Kim, M. J. Shin et al., "PEP-1-PEA-15 protects against toxin-induced neuronal damage in a mouse model of Parkinson's disease," *Biochimica et Biophysica Acta (BBA)-General Subjects*, vol. 1840, no. 6, pp. 1686–1700, 2014.
- [33] S. Luo, K. Lei, D. Xiang, and K. Ye, "NQO1 is regulated by PTEN in glioblastoma, mediating cell proliferation and oxidative stress," *Oxidative Medicine and Cellular Longevity*, vol. 2018, Article ID 9146528, 16 pages, 2018.
- [34] H. Ding, Y. Xiong, J. Sun, C. Chen, J. Gao, and H. Xu, "Asiatic acid prevents oxidative stress and apoptosis by inhibiting the translocation of α -synuclein into mitochondria," *Frontiers in Neuroscience*, vol. 12, p. 431, 2018.
- [35] Z. Li, X. Bao, X. Bai et al., "Design, synthesis, and biological evaluation of phenol bioisosteric analogues of 3-hydroxymorphinan," *Scientific Reports*, vol. 9, no. 1, article 2247, 2019.
- [36] R. Svarcbahts, U. H. Julku, and T. T. Myöhänen, "Inhibition of prolyl oligopeptidase restores spontaneous motor behavior in the α -synuclein virus vector-based Parkinson's disease mouse model by decreasing α -synuclein oligomeric species in mouse brain," *Journal of Neuroscience*, vol. 36, no. 49, pp. 12485–12497, 2016.
- [37] H. Jiang, S. U. Kang, S. Zhang et al., "Adult conditional knockout of PGC-1 α leads to loss of dopamine neurons," *eNeuro*, vol. 3, no. 4, pp. ENEURO.0183–ENEURO16.2016, 2016.
- [38] R. Jia, T. Kurita-Ochiai, S. Oguchi, and M. Yamamoto, "Periodontal pathogen accelerates lipid peroxidation and atherosclerosis," *Journal of Dental Research*, vol. 92, no. 3, pp. 247–252, 2013.
- [39] Gene Ontology Consortium, "The Gene Ontology (GO) database and informatics resource," *Nucleic Acids Research*, vol. 32, no. 9, pp. 2580–2592, 2004.
- [40] B. Acton, A. Jurisicova, I. Jurisica, and R. Casper, "Alterations in mitochondrial membrane potential during preimplantation stages of mouse and human embryo development," *Molecular Human Reproduction*, vol. 10, no. 1, pp. 23–32, 2004.
- [41] M. V. Martin, D. Fiol, E. Zabaleta, and G. Pagnussat, "Arabidopsis thaliana embryo sac mitochondrial membrane potential stain," *Bio-Protocol*, vol. 4, no. 10, 2014.
- [42] M. Guichardant and M. Lagarde, "Analysis of biomarkers from lipid peroxidation: a comparative study," *European Journal of Lipid Science and Technology*, vol. 111, no. 1, pp. 75–82, 2009.
- [43] A. Hald and J. Lotharius, "Oxidative stress and inflammation in Parkinson's disease: is there a causal link?," *Experimental Neurology*, vol. 193, no. 2, pp. 279–290, 2005.
- [44] K. Kaur, J. S. Gill, P. K. Bansal, and R. Deshmukh, "Neuroinflammation - A major cause for striatal dopaminergic degeneration in Parkinson's disease," *Journal of the Neurological Sciences*, vol. 381, pp. 308–314, 2017.

- [45] P. Whitton, "Inflammation as a causative factor in the aetiology of Parkinson's disease," *British Journal of Pharmacology*, vol. 150, no. 8, pp. 963–976, 2007.
- [46] M. McCulloch, C. See, X. J. Shu et al., "Astragalus-based Chinese herbs and platinum-based chemotherapy for advanced non-small-cell lung cancer: meta-analysis of randomized trials," *Journal of Clinical Oncology*, vol. 24, no. 3, pp. 419–430, 2006.
- [47] S. Eisenhardt and J. Fleckenstein, "Traditional Chinese medicine valuably augments therapeutic options in the treatment of climacteric syndrome," *Archives of Gynecology and Obstetrics*, vol. 294, no. 1, pp. 193–200, 2016.
- [48] J. Rathbone, L. Zhang, M. Zhang et al., "Chinese herbal medicine for schizophrenia: cochrane systematic review of randomised trials," *The British Journal of Psychiatry*, vol. 190, no. 5, pp. 379–384, 2007.
- [49] T.-Y. Wu, C.-P. Chen, and T.-R. Jinn, "Traditional Chinese medicines and Alzheimer's disease," *Taiwanese Journal of Obstetrics and Gynecology*, vol. 50, no. 2, pp. 131–135, 2011.
- [50] L.-W. Chen, Y.-Q. Wang, L.-C. Wei, M. Shi, and Y.-S. Chan, "Chinese herbs and herbal extracts for neuroprotection of dopaminergic neurons and potential therapeutic treatment of Parkinson's disease," *CNS & Neurological Disorders - Drug Targets*, vol. 6, no. 4, pp. 273–281, 2007.
- [51] Q. Zhao, X.-Y. Chen, and C. Martin, "*Scutellaria baicalensis*, the golden herb from the garden of Chinese medicinal plants," *Science Bulletin*, vol. 61, no. 18, pp. 1391–1398, 2016.
- [52] X. Zhang, Q. Cheng, and Y. Zhang, "Acute toxicity test of baicalin capsule in mice," *Journal of Medical Research*, 2006.
- [53] Y. Zhang, P. Liao, M. Zhu et al., "Baicalin attenuates cardiac dysfunction and myocardial remodeling in a chronic pressure-overload mice model," *Cellular Physiology and Biochemistry*, vol. 41, no. 3, pp. 849–864, 2017.
- [54] X. Jin, M. Y. Liu, D. F. Zhang et al., "Baicalin mitigates cognitive impairment and protects neurons from microglia-mediated neuroinflammation via suppressing NLRP3 inflammasomes and TLR4/NF- κ B signaling pathway," *CNS Neuroscience & Therapeutics*, vol. 25, no. 5, pp. 575–590, 2019.
- [55] L.-T. Guo, S.-Q. Wang, J. Su et al., "Baicalin ameliorates neuroinflammation-induced depressive-like behavior through inhibition of toll-like receptor 4 expression via the PI3K/AKT/FoxO1 pathway," *Journal of Neuroinflammation*, vol. 16, no. 1, p. 95, 2019.
- [56] M. Caruana, T. Högen, J. Levin, A. Hillmer, A. Giese, and N. Vassallo, "Inhibition and disaggregation of α -synuclein oligomers by natural polyphenolic compounds," *FEBS Letters*, vol. 585, no. 8, pp. 1113–1120, 2011.
- [57] P. Klivenyi, D. Siwek, G. Gardian et al., "Mice lacking alpha-synuclein are resistant to mitochondrial toxins," *Neurobiology of Disease*, vol. 21, no. 3, pp. 541–548, 2006.
- [58] P. Eichhammer, M. Johann, A. Kharraz et al., "High-frequency repetitive transcranial magnetic stimulation decreases cigarette smoking," *Journal of Clinical Psychiatry*, vol. 64, no. 8, pp. 951–953, 2003.
- [59] P. Xiong, X. Chen, C. Guo, N. Zhang, and B. Ma, "Baicalin and deferoxamine alleviate iron accumulation in different brain regions of Parkinson's disease rats," *Neural Regeneration Research*, vol. 7, article 2092, 2012.
- [60] A. J. Y. Guo, R. C. Y. Choi, A. W. H. Cheung et al., "Baicalin, a flavone, induces the differentiation of cultured osteoblasts," *Journal of Biological Chemistry*, vol. 286, no. 32, pp. 27882–27893, 2011.
- [61] F. Ursini, M. Maiorino, and H. J. Forman, "Redox homeostasis: the Golden Mean of healthy living," *Redox Biology*, vol. 8, pp. 205–215, 2016.
- [62] S. Tarazona, F. García-Alcalde, J. Dopazo, A. Ferrer, and A. Conesa, "Differential expression in RNA-seq: a matter of depth," *Genome Research*, vol. 21, no. 12, pp. 2213–2223, 2011.
- [63] S. Mandel, O. Weinreb, and M. B. H. Youdim, "Using cDNA microarray to assess Parkinson's disease models and the effects of neuroprotective drugs," *Trends in Pharmacological Sciences*, vol. 24, no. 4, pp. 184–191, 2003.
- [64] K. Häbig, M. Walter, S. Poths, O. Riess, and M. Bonin, "RNA interference of LRRK2—microarray expression analysis of a Parkinson's disease key player," *Neurogenetics*, vol. 9, no. 2, pp. 83–94, 2008.
- [65] Z. Wu, Y. Xia, Z. Wang et al., "C/EBP β / δ -secretase signaling mediates Parkinson's disease pathogenesis via regulating transcription and proteolytic cleavage of α -synuclein and MAOB," *Molecular Psychiatry*, 2020.
- [66] M. Pulido-Salgado, J. M. Vidal-Taboada, and J. Saura, "C/EBP β and C/EBP δ transcription factors: Basic biology and roles in the CNS," *Progress in Neurobiology*, vol. 132, pp. 1–33, 2015.
- [67] B. Wright, J. P. E. Spencer, J. A. Lovegrove, and J. M. Gibbins, "Insights into dietary flavonoids as molecular templates for the design of anti-platelet drugs," *Cardiovascular Research*, vol. 97, no. 1, pp. 13–22, 2013.

Research Article

Apigenin Protects Mouse Retina against Oxidative Damage by Regulating the Nrf2 Pathway and Autophagy

Yuanzhong Zhang,¹ Yan Yang,² Haitao Yu,³ Min Li,⁴ Li Hang,¹ and Xinrong Xu ¹

¹Department of Ophthalmology, Jiangsu Province Hospital of Chinese Medicine (Affiliated Hospital of Nanjing University of Chinese Medicine), Nanjing 210029, China

²Department of Ophthalmology, The Second Affiliated Hospital of Nanjing University of Chinese Medicine, Nanjing 210017, China

³School of Pharmacy, Nanjing University of Chinese Medicine, Nanjing 210023, China

⁴Department of Ophthalmology, Liyang Branch of Jiangsu Province Hospital of Chinese Medicine, Liyang 213300, China

Correspondence should be addressed to Xinrong Xu; 13851641312@qq.com

Received 27 March 2020; Accepted 29 April 2020; Published 14 May 2020

Guest Editor: Francisco Jaime B. Mendonça Junior

Copyright © 2020 Yuanzhong Zhang et al. This is an open access article distributed under the Creative Commons Attribution License, which permits unrestricted use, distribution, and reproduction in any medium, provided the original work is properly cited.

Oxidative stress is a critical factor in the pathology of age-related macular degeneration (AMD). Apigenin (AP) is a flavonoid with an outstanding antioxidant activity. We had previously observed that AP protected APRE-19 cells against oxidative injury *in vitro*. However, AP has poor water and fat solubility, which determines its low oral bioavailability. In this study, we prepared the solid dispersion of apigenin (AP-SD). The solubility and dissolution of AP-SD was significantly better than that of the original drug, so the oral bioavailability in rats was better than that of the original drug. Then, the effects of AP-SD on the retina of a model mouse with dry AMD were assessed by fundus autofluorescence (FAF), optical coherence tomography (OCT), and electron microscopy; the results revealed that AP-SD alleviated retinopathy. Further research found that AP-SD promoted the nuclear translocation of Nrf2 and increased expression levels of the Nrf2 and target genes HO-1 and NQO-1. AP-SD enhanced the activities of SOD and GSH-Px and decreased the levels of ROS and MDA. Furthermore, AP-SD upregulated the expressions of p62 and LC3II in an Nrf2-dependent manner. However, these effects of AP-SD were observed only in the retina of Nrf2 WT mice, not in Nrf2 KO mice. In addition, the therapeutic effect of AP-SD was dose dependent, and AP did not work. In conclusion, AP-SD significantly enhanced the bioavailability of the original drug and reduced retinal oxidative injury in the model mouse of dry AMD *in vivo*. The results of the underlying mechanism showed that AP-SD upregulated the expression of antioxidant enzymes through the Nrf2 pathway and upregulated autophagy, thus inhibiting retinal oxidative damage. AP-SD may be a potential compound for the treatment of dry AMD.

1. Introduction

Age-related macular degeneration (AMD) is a leading cause of vision loss in the elderly. Clinically, AMD falls into two categories: dry AMD and wet AMD. The dry AMD presents as retinal pigment proliferation or depigmentation, drusen, and advanced geographic atrophy. The wet AMD is characterized by choroidal neovascularization (CNV), leading to retinal exudation and hemorrhage, and eventually severe visual impairment. In recent years, the treatment of wet AMD has made significant progress due to the widespread use of antivascular endothelial growth factor (VEGF) drugs

[1]. Currently, there are no effective treatment options for dry AMD.

A large number of evidences indicate that oxidative damage of retinal pigment epithelium (RPE) is a main etiology of AMD. The RPE cell has abundant mitochondria and produces a large amount of reactive oxygen species (ROS) in a high-oxygen environment [2]. In addition, one of the major functions of RPE is the phagocytosis and degradation of photoreceptor outer segments (POS). POS is rich in unsaturated fatty acids, and the part being not degraded by RPE forms lipofuscin, which increases ROS generation while exposed to light [3]. The nuclear factor E2-related factor 2 (Nrf2)

pathway is a primary system employed by the RPE to neutralize oxidative stress and maintain cellular homeostasis [4]. In a physiological condition, Nrf2 is constitutively targeted for degradation by the multisubunit, E3 ubiquitin ligase KEAP1. Oxidative stress dissociates KEAP1 and stabilizes Nrf2. The transcription factor rapidly translocates to the nucleus, heterodimerizes with Maf proteins, and binds to the antioxidant response elements (AREs) in the promoters of its cognate target genes, inducing the expression of genes encoding heme oxygenase-1 (HO-1), quinone oxidoreductase-1 (NQO-1), glutathione peroxidase (GSH-Px), superoxide dismutase (SOD), and catalase (CAT). These enzymes can quickly scavenge ROS and protect the body from injuries caused by active substances or toxic substances [5]. Thus, the activation of the Nrf2 pathway could reduce the oxidative damage of RPE, suggesting that the Nrf2 pathway is a potential target for AMD treatment [6].

As Nrf2 pathway does, autophagy keeps cellular homeostasis in situations of oxidative stress; therefore, its failure is associated with aging and many diseases, such as cancer, cardiovascular diseases, and neurodegenerative diseases [7]. The impairment of autophagy has been shown to be one cause of the development and progression of AMD [8]. Impaired autophagy significantly reduced the degradation of POS, leading to a deposit of undegraded POS under RPE, and finally an increase of ROS generation [9, 10]. The autophagy is increased and the Nrf2 pathway is activated at the same time while the cell is in oxidative stress. Polyunsaturated fatty acids rapidly increase the generation of ROS in RPE and upregulate the expression of Nrf2 and SQSTM1/p62 proteins [11]. Studies have shown that many inducers of the Nrf2 pathway can also induce autophagy [12–14]. Correspondingly, a deficiency of Nrf2 reduces SQSTM1/p62 expression [15]. Clearly, there is a strong correlation between autophagy and Nrf2 pathways, which makes sense for AMD.

Apigenin (AP) is a bioactive flavonoid which is obtained from several fruits and vegetables. AP has been reported to exhibit antioxidant, anti-inflammatory, and anticancer activities [16, 17]. Our previous study has shown that AP exhibited protective effects on ARPE-19 cells against tert-butyl hydroperoxide- (t-BHP-) induced oxidative injury, which were associated with its antioxidant properties dependent upon the activation of Nrf2 signaling [18]. However, AP has the disadvantages of poor water and fat solubility and low bioavailability. Studies have indicated that the preparation of solid dispersion could significantly increase the solubility and dissolution rate of drugs, which can further enhance the bioavailability of drugs [19, 20]. In the current study, we prepared the solid dispersion of apigenin (AP-SD), determined its bioavailability in rats, and evaluated its protective effects on retinal injury induced by oxidative stress in Nrf2 WT and Nrf2 KO mice.

2. Materials and Methods

2.1. Chemicals, Reagents, and Antibodies. Apigenin was from Sigma Chemical (St. Louis, MO, USA). Polyvinylpyrrolidone (PVP K30) was from J&K Chemical Ltd. (Shanghai, China). Hydroquinone (HQ) was from Alfa Aesar (Heysham, Lanca-

shire, UK). The primary antibodies used in western blot were obtained from the following source: Nrf2, HO-1, NQO-1, p62, GAPDH, and Lamin B (Abcam, UK) and LC3 (Cell Signaling Technology, USA); the secondary antibody Goat Anti-Rabbit IgG/HRP was from (Abcam, UK).

2.2. Preparation of AP-SD. With the orthogonal experiment, we assigned PVP K30 as the carrier to prepare the solid dispersion of AP, the mass ratio of AP and PVK V30 is 1: 9, and anhydrous ethanol is used as the reaction solvent to prepare AP-SD. Briefly, AP and PVK V30 at a mass ratio of 1:9 were dissolved in absolute ethanol of adequate volume with full mixing. After the mixture was evaporated in vacuo and vacuum drying at 50°C, the AP-SD was obtained for experiments.

We then determined the standard curve of AP-SD. The chromatographic conditions were Waters 600 C₁₈ column, methanol-0.1% CH₃COONa solution (*v/v* 60:40) as the mobile phase, 337 nm wavelength, 1.0 mL/min flow velocity, 40°C column temperature, and 10 μ L sample size. The control solution was prepared according to following the procedures. AP of 10 mg was dissolved in ethanol and volumed in 50 mL volumetric flask, and thereby the AP control solution at a concentration of 1 mg/mL was obtained. Anhydrous ethanol was used to dilute the control solution to yield a series of solutions at 1, 2, 4, 8, 16, and 32 μ g/mL. Each solution of 10 μ L was injected into a high-performance liquid chromatograph (HPLC, Waters 600, USA) for measurement of the peak area. Concentrations of AP ($[C]$) were marked at the horizontal ordinate and peak areas (A) at the longitudinal coordinate giving the standard curve equation: $A = 32786.6 \times [C] - 160.4$ ($R = 0.9991$), linear range 0.56–32.7 μ g/mL.

2.3. Determination of Solubility. AP and AP-SD (equivalent to 10 mg of AP) were precisely weighted and added into 100 mL conical flask, and then, distilled water/chloroform of 20 mL was added. The solutions were incubated in a 25°C thermostatic oscillator for 24 hr. Each sample of 5 mL was filtered through a 0.45 μ m microporous membrane. The successive filtrate of 10 μ L was subjected to HPLC analyses. Control solution of 10 μ L at 8 μ g/mL was spontaneously analyzed by HPLC. The equilibrium solubility of both samples in water and chloroform was measured, respectively, based on the peak area.

2.4. Determination of Dissolution Rate. AP and AP-SD (both containing 10 mg pure AP) were evenly dispersed in the dissolution medium (phosphate buffer saline, pH 7.4, 37°C, $V = 900$ mL) and centrifuged at 100 r/min. Each sample of 5 mL was collected at the time points of 5, 10, 15, 20, 30, 45, 60, and 90 min, respectively, and subjected to filtration. The successive filtrate of 1 mL was volumed in 10 mL volumetric flask with distilled water. HPLC analyses were used, and mass concentrations were calculated through introducing a peak area into the standard curve equation followed by calculation of the cumulative dissolution percentage.

2.5. Determination of Plasma Concentrations of AP. Twelve Sprague Dawley rats (Model Animal Research Centre of Nanjing University (Nanjing, China) were randomly divided

into two groups: the AP and AP-SD groups ($n = 6$). Rats of both groups were intragastrically administrated with corresponding drugs containing pure AP at 50 mg/kg. Blood samples were collected from orbit at time points of 0.25, 0.5, 1, 2, 4, 8, 12, and 24 hr of each rat. After adding heparin, blood samples were centrifuged at 3000 r/min for 15 min, and the supernatants were collected for examination. 200 μ L plasma was mixed with 600 μ L of silybin solution (internal standard, 13.3 μ g/mL in methanol) and vortex mixed for 5 min. After centrifugation for 5 min at 10000 r/min, the supernatant was collected. The rest of the residue was extracted with another 300 μ L of methanol by vortex mixing for 5 min and centrifuged for 5 min at 10000 r/min again, and the obtained supernatant was pooled together with the previous supernatant. Then, the total supernatant was dried under a nitrogen flow at 35°C and the obtained residues were reconstituted with 200 μ L of methanol. After centrifugation for another 5 min at 10000 r/min, an aliquot of 20 μ L supernatant was analyzed by HPLC for determining drug concentrations. Maximum plasma concentration (C_{max}) and time to reach maximum concentration (T_{max}) were obtained directly from the concentration-time curve; area under the plasma concentration-time curve from zero to the time of the final sample measurement (AUC_{0-24}) was calculated using the statistical software GraphPad Prism 5 (GraphPad Software Inc., CA, USA).

2.6. Animal Experimental Procedures. C57BL/6 mice (6 months old, bodyweight 25-33 g, Nrf2 WT and KO) were obtained from the Model Animal Research Centre of Nanjing University (Nanjing, China). All mice were domesticated under a 12 h light/dark cycle at a controlled temperature (25°C) with free access to food and tap water. Nrf2 WT mice were divided into 6 groups: the aging control, model control, AP 60 (60 mg/kg), and AP-SD groups (20, 40, and 60 mg/kg). Nrf2 KO mice were divided into 3 groups: the aging control, model control, and AP-SD 60 groups (60 mg/kg). The doses were defined by the content of pure AP in the solid dispersion and were determined by preliminary experiments. Animals were treated according to the following procedures: aging control mice were fed normal diet for 9 months; model control mice were fed normal diet during months 1-3, high-fat diet and intake of HQ dissolved in the drinking water (0.8%) during months 4-6, normal diet and intragastric administration with 0.5% CMC-Na suspension daily during months 7-9. For the treated group mice, model control mice were intragastrically administrated with corresponding drugs (suspended in 0.5% CMC-Na) at the last 3 months. All experimental procedures were approved by the institutional and local committee for the care and use of animals, and all animals received humane care according to the National Institutes of Health (USA) guidelines.

2.7. Fundus Autofluorescence. The mice were anesthetized using a ketamine (120 mg/kg body weight) and xylazine (8 mg/kg body weight) intraperitoneal injection, and the pupil was fully dilated with tropicamide phenylephrine eye drops (Kanda Pharmaceutical, Japan). The mouse was placed on the table with its head in the chinrest. To maintain corneal

hydration and improve image quality, the viscoelastic material (Viscoat, Alcon-Couvreur, Belgium) was smeared on the cornea covering with a coverslip. A 90D noncontact slit lamp lens was fixated directly in front of the confocal scanning laser ophthalmoscope (Heidelberg Engineering, Heidelberg, Germany). Fluorescence was excited using a 488 nm argon laser or a 790 nm diode laser. As Charbel Issa did [21], images were recorded using the ART mode for the quantitative analysis of fundus autofluorescence (FAF); the mean grey level on mouse FAF images was measured using ImageJ software (version 1.52, NIH, Bethesda, USA).

2.8. Optical Coherence Tomography. Like the FAF assessment, the animal was anesthetized, the pupil fully dilated, and the viscoelastic material was smeared on the cornea covering with a coverslip; then, a 90D noncontact slit lamp lens was placed in front of an optical coherence tomography (OCT) device (Cirrus HD-OCT 4000, Carl Zeiss Meditec, Dublin, CA); cross-sectional images of the retina were undertaken. The average thickness of the mouse retina was obtained using the macular cube scan mode according to the methods reported by Song [22].

2.9. Transmission Electron Microscopy. Eyeballs were fixed in 4% paraformaldehyde for 20 min. The cornea, lens, and vitreous were removed. The yye wall tissue (2 × 4 mm) was excised from the bilateral area of the optic disc and fixed with glutaral/osmic acid, coated with epoxy resins, and sectioned. After double staining with uranyl acetate and lead citrate, the sections were examined with transmission electron microscope (Tecnai G2 Spirit BioTWIN; FEI, Hillsboro, OR, USA) and images were taken. The area of the sediment beneath RPE was determined according to the methods reported by Edward [23]. Briefly, images were opened in ImageJ software and calibrated using the embedded scale bar. The region of the sediment was drawn using free selection tool, and the area was measured. The thickness of the Bruch membrane (BrM) was directly measured by electron microscopy.

2.10. Measurements of ROS, MDA, and Antioxidant Enzymes. The retina was isolated, and tissue homogenates were prepared via centrifugation at 4°C, 3000 r/min for 10 min. Levels of ROS were determined using the DCFH-DA method. Levels of MDA were measured using the thio-barbituric acid method. In addition, activities of SOD and GSH-PX were measured using the corresponding enzyme-linked immunosorbent assay kits at the wavelength of 450 and 412 nm, respectively. Kits above were from Nanjing Jiancheng Bioengineering Institute (Nanjing, China), and experiments were performed according to the instructions provided by the manufactures.

2.11. Western Blot Analysis. The mouse retina/choroid tissue was lysed in the RIPA buffer containing a protease inhibitor.

For examining the Nrf2 expression, nuclear and cytoplasmic proteins were separated using a Bioepitope Nuclear and Cytoplasmic Extraction Kit (Bioworld Technology, St. Louis Park, MN, USA) following the manufacturer's guidelines. Proteins (50 μ g/well) were separated by SDS-polyacrylamide gel and transferred to a PVDF membrane (Millipore, Burlington,

MA, USA). After blocking with 5% skim milk in Tris-buffered saline containing 0.1% Tween 20, the membranes were incubated with primary corresponding primary antibodies. The blots were then incubated with a secondary antibody (anti-rabbit horseradish peroxidase-conjugate/anti-mouse HRP-conjugate), and the protein bands were visualized using a chemiluminescence reagent (Millipore, Burlington, MA, USA). Equivalent loading was confirmed using an antibody against GAPDH for total proteins and against Lamin B for nuclear proteins. The levels of target protein bands were densitometrically determined using Quantity One 4.4.1.

2.12. Statistical Analysis. Data were presented as mean \pm SD, and results were analyzed using GraphPad Prism 5 software. The significance of difference was determined by Student's *t*-test for comparison between two groups and one-way ANOVA with post hoc Tukey's test for comparison between multiple groups. A value of $p < 0.05$ was considered to be statistically significant.

3. Results

3.1. AP-SD Increases the Solubility and Dissolution of AP In Vitro. We determined the equilibrium solubility of AP and AP-SD in water and chloroform. The results showed that the equilibrium solubility of AP-SD in both water and chloroform was significantly higher than that of AP (Table 1). Determination of the dissolution rate showed that AP-SD had significantly higher cumulative dissolution rates than AP at each time points (Figure 1).

3.2. AP-SD Enhances the Absorption of AP In Vivo. We obtained the plasma concentration-time curve of AP and AP-SD in rats (Figure 2). C_{\max} , T_{\max} , and AUC_{0-24} for AP and AP-SD were calculated with ImageJ software (Table 2). The results showed that AP-SD had better bioavailability than AP.

3.3. AP-SD Alleviated Pathological Changes of the Retina. In clinical, fundus AF and OCT are the most used noninvasive means for monitoring of dry AMD [24, 25]. Fundus AF generated with wavelength between 500 and 750 nm is dominated by RPE lipofuscin, a complex mixture of fluorophores being accumulated in the RPE after phagocytosis of POS [26]. Therefore, AF intensity indicates the level of lipofuscin in vivo in the RPE. Spectral-domain- (SD-) OCT provides high-quality, cross-sectional images of the retina including RPE with resolution approaching histology performed with light microscopy [27]. To evaluate the therapeutic effects of AP-SD, we established a dry AMD mouse model that mimics three risk factors for AMD in humans: aging, hyperlipidemia, and smoking (HQ is abundant in cigarette smoke) [28]. HQ, an electrophilic, could inhibit the binding of BACH1 with Nrf2, thus activating the Nrf2 pathway [29]. Our results showed that AF intensity in model mice was significantly enhanced compared with that in aging mice, and in Nrf2KO mouse higher than in Nrf2WT mice. AF intensity was attenuated after treatment with AP-SD in Nrf2WT mice (Figures 3(a) and 3(b)). Correspondingly, the images of OCT scanning showed that the outer layer struc-

TABLE 1: Equilibrium solubility of AP of both dosage forms (37°C, $n = 3$).

Solvents	Concentration ($\mu\text{g/mL}$)	
	AP	AP-SD
Water	1.33 ± 0.15	$352.09 \pm 22.56^{**}$
Chloroform	2.18 ± 0.21	$1.43 \times 10^3 \pm 187.11^{**}$

Significance: $**p < 0.01$ versus AP.

ture of the retina including photoreceptors, RPE, and Bruch membrane (BrM) became unclear, and the retina was thinner in model mice compared with aging mice, more significant in Nrf2 KO mice than in Nrf2 WT mice (Figure 4). Treatment with AP-SD could restore the retinal structure in Nrf2WT mice.

We further observed the retinal ultrastructure; the results demonstrated that there were undigested phagosomes (Figure 5(a)) and autophagosome (Figure 5(b)) present in the RPE of the model mouse. There were obvious sediments under RPE and thickened BrM in the model mice compared to the aging mice, and it is more severe in Nrf2 KO mice. AP-SD reduced the area of the sediment and thinned BrM in Nrf2WT mice (Figure 6). In particular, AP-SD only alleviated retinopathy in Nrf2 WT mice and had no effects in Nrf2 KO mice. In addition, the therapeutic effect of AP-SD was dose dependent, and AP did not work. Collectively, these data indicated that AP-SD more potently improved pathological changes of the retina in Nrf2 WT model mice with dry AMD.

3.4. AP-SD Induced Nrf2 Nuclear Translocation and Increased Antioxidant Gene Expression. To explore the underlying mechanism for AP-SD reducing retinopathy in model mice with dry AMD, we first assessed the effects of AP-SD on Nrf2 pathway. As shown in Figure 7(a), the level of nuclear Nrf2 was increased and the level of cytoplasmic Nrf2 was reduced in model mice compared with those in aging mice. AP-SD decreased the level of cytoplasmic Nrf2 and increased the level of nuclear Nrf2 in a dose-effect manner, indicating that AP-SD promoted Nrf2 nuclear translocation (Figure 7(b)). Furthermore, we examined the ability of AP-SD to upregulate the expressions of the targeted genes of Nrf2, upon its increased nuclear translocation. The expressions of HO-1 and NQO-1 were upregulated in the Nrf2 WT model mice and downregulated in the Nrf2 KO model mice, compared with those in aging mice (Figure 8(a)). AP-SD dose dependently increased the expressions of HO-1 and NQO-1 in Nrf2 WT mice but had no effects in Nrf2 KO mice as expected (Figure 8(b)).

3.5. AP-SD Restored Activities of SOD and GSH-Px Enzyme and Decreased Levels of SOD and MDA. We measured the activity of SOD and GSH-Px enzyme in mouse, two important antioxidant enzymes of the retina. The results showed that the activities of SOD and GSH-Px were significantly decreased in Nrf2 WT model mice and are more remarkable in Nrf2 KO model mice. AP-SD dose dependently restored

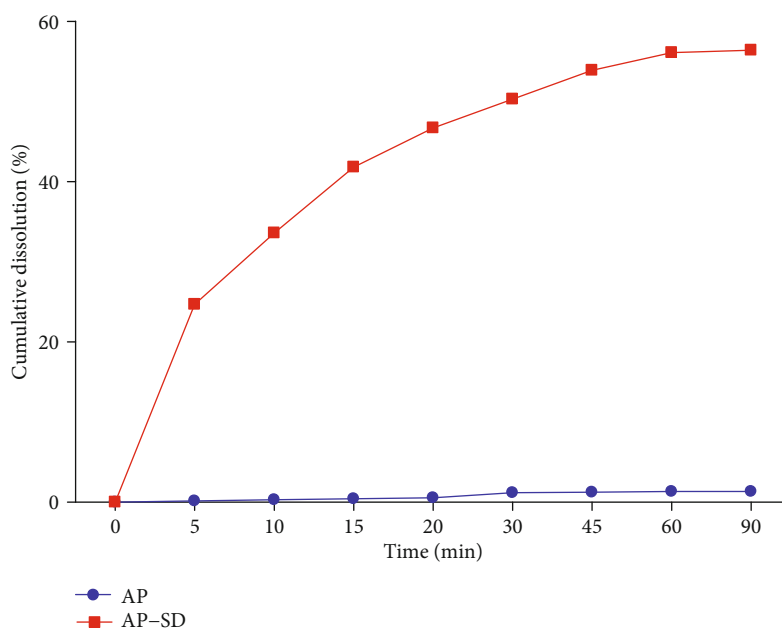


FIGURE 1: AP-SD had significantly higher cumulative dissolution rates than AP. Determination of cumulative dissolution rates of AP and AP-SD at indicated time points. Data are means \pm standard deviation ($n = 6$).

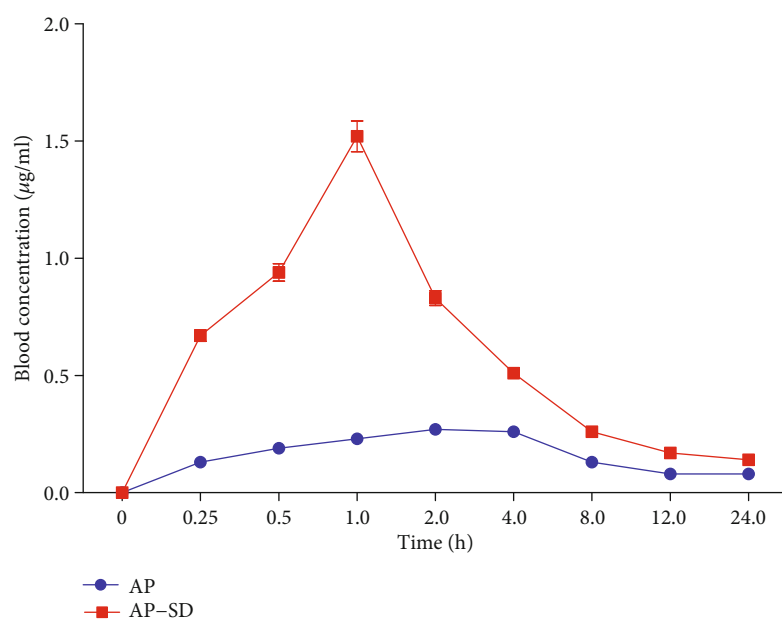


FIGURE 2: AP-SD had better oral bioavailability than AP. Determination of blood concentrations of AP and AP-SD at indicated time points in rats. Data are means \pm standard deviation ($n = 6$).

TABLE 2: Pharmacokinetic parameters of AP after oral administration of pure AP and AP-SD in rats (dose 50 mg/kg, $n = 6$, mean \pm SD).

Parameters	AP	AP-SD
C_{\max} ($\mu\text{g/mL}$)	0.27	1.52**
T_{\max} (hr)	2.0	1*
AUC_{0-24} ($\mu\text{gh/mL}$)	3.10	7.68**

Significance: * $p < 0.05$, ** $p < 0.01$ versus AP.

the activities of SOD and GSH-Px in Nrf2 WT mice, not in Nrf2 KO mice (Figures 9(a) and, 9(b)). ROS is a by-product of cellular oxidative phosphorylation and its level is consistent with oxidative stress. ROS causes lipid peroxidation of the biomembrane, which leads to the production of a large amount of MDA [2]. Therefore, we examined the levels of ROS and MDA in the mouse retina. The results showed that the levels of ROS and MDA were significantly elevated in Nrf2 WT and Nrf2 KO model mice, but higher in Nrf2 KO mice. AP-SD decreased the ROS and MDA levels in dose-

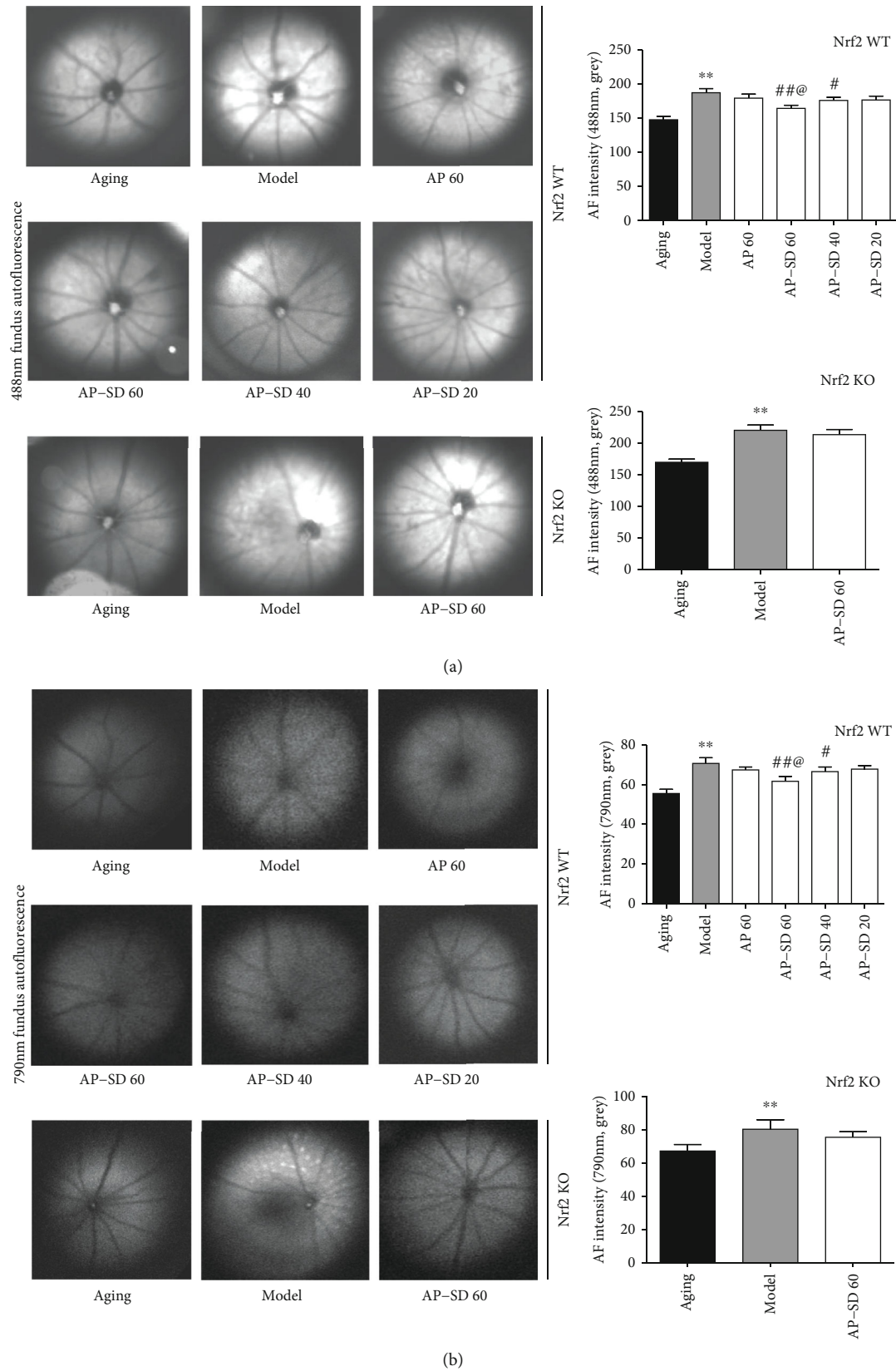


FIGURE 3: Representative images of fundus AF excited at 488 (a) and 790 nm (b) in Nrf2 WT and KO mice. AF intensity in model mice was significantly enhanced compared with that in aging mice, and in Nrf2 KO mice higher than in Nrf2 WT mice. AF intensity was decreased after treatment with AP-SD in Nrf2 WT mice, but not in Nrf2 KO mice. ** $p < 0.01$, model control versus aging control; # $p < 0.05$, ## $p < 0.01$, AP-SD versus model control; @ $p < 0.05$, AP-SD 60 versus AP-SD 40. Data are means \pm standard deviation ($n = 5$).

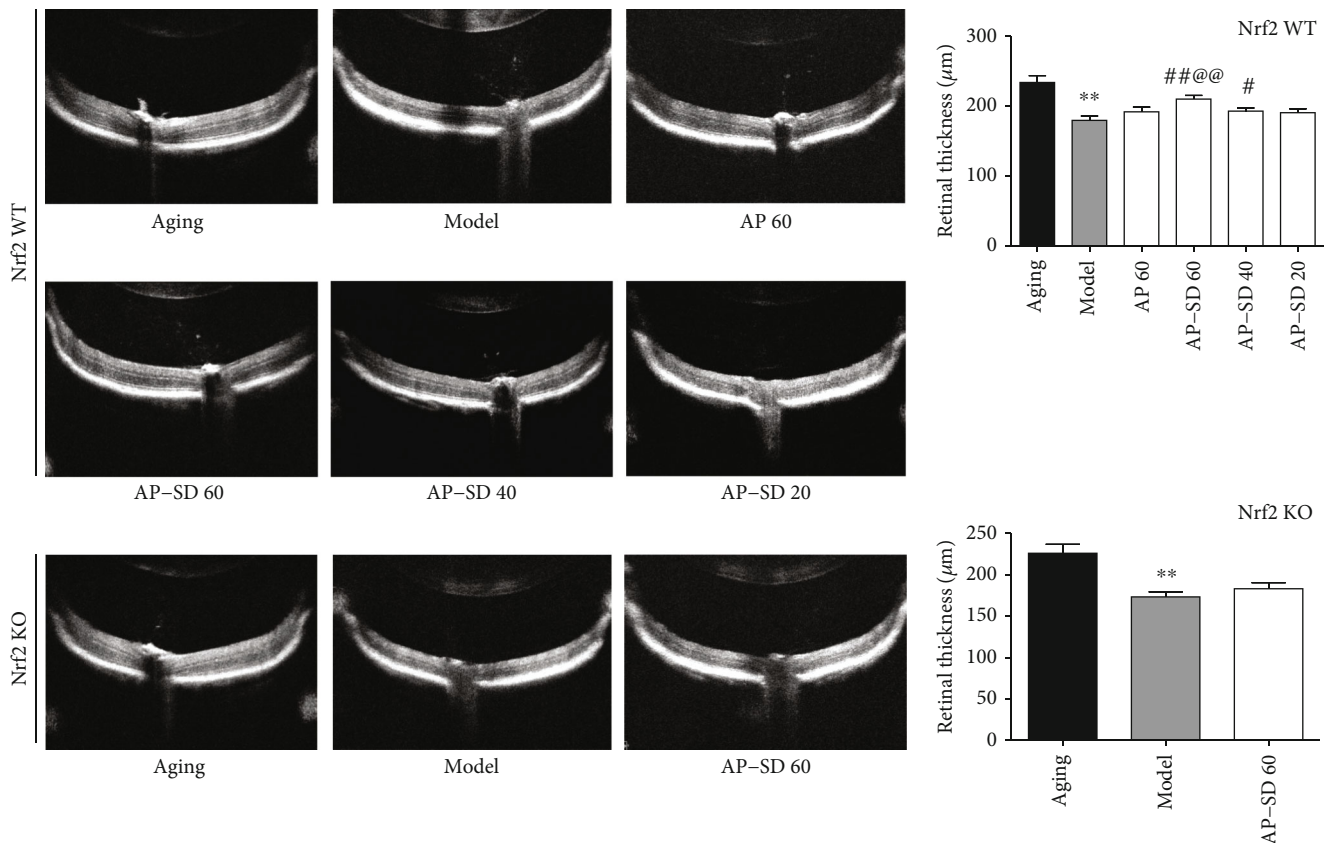


FIGURE 4: Representative images of OCT in Nrf2 WT and KO mice. Outer layer structure of the retina was unclear and the retina was thinner in model mice compared with aging mice, more significant in Nrf2 KO mice. Treatment with AP-SD dose dependently restored the retinal structure in Nrf2 WT mice and did not in Nrf2 KO mice. ** $p < 0.01$, model control versus aging control; # $p < 0.05$, ## $p < 0.01$, AP-SD versus model control; @ $p < 0.01$, AP-SD 60 versus AP-SD 40. Data are means \pm standard deviation ($n = 5$).

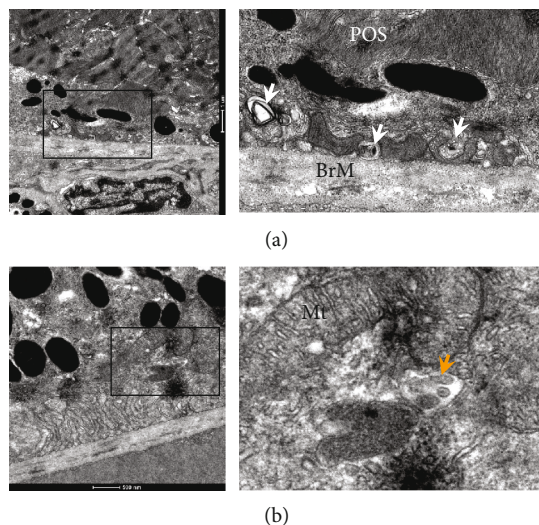


FIGURE 5: Transmission electron microscopy showed that there were undigested phagosomes (a, white arrow) and autophagosome (b, orange arrow) present in the RPE of the model mouse. POS: photoreceptor outer segment; Mt: mitochondria; BrM: Bruch membrane.

effect manner in Nrf2 WT mice, not in Nrf2 KO mice (Figures 10(a) and 10(b)).

3.6. AP-SD Increased p62 Protein Expression and Regulated Autophagy in an Nrf2-Dependent Manner. The p62 protein and LC3 have been widely regarded as markers for autophagic activity. p62 is used as a marker of autophagic degradation [30] and LC3-II serves as a marker for autophagosome formation [31]. Autophagy increases often coincides with the induction of the Nrf2 pathway in stressed conditions [32]. Based on these findings, we assessed whether Nrf2 directly upregulated the expression of p62. As shown in Figure 10(a), the upregulation of p62 expression was only found in Nrf2 WT model mice, but not in Nrf2 KO model mice, compared with the aging mice. Under the same conditions, Nrf2 levels in the nucleus significantly increased in Nrf2 WT model mice, as shown in the previous results. Our findings are consistent with those of several reports [33, 34]. In addition, AP-SD dose dependently increased p62 expression in Nrf2 WT mice, not in Nrf2KO mice (Figure 11(b)). Meanwhile, the upregulation of LC3 II expression was also only shown in Nrf2 WT mice, but not in Nrf2 KO mice, compared with the aging mice. In Nrf2 WT mice (Figure 11(a)), the expression of LC3 II increased in dose-dependent manner after treatment with AP-SD,

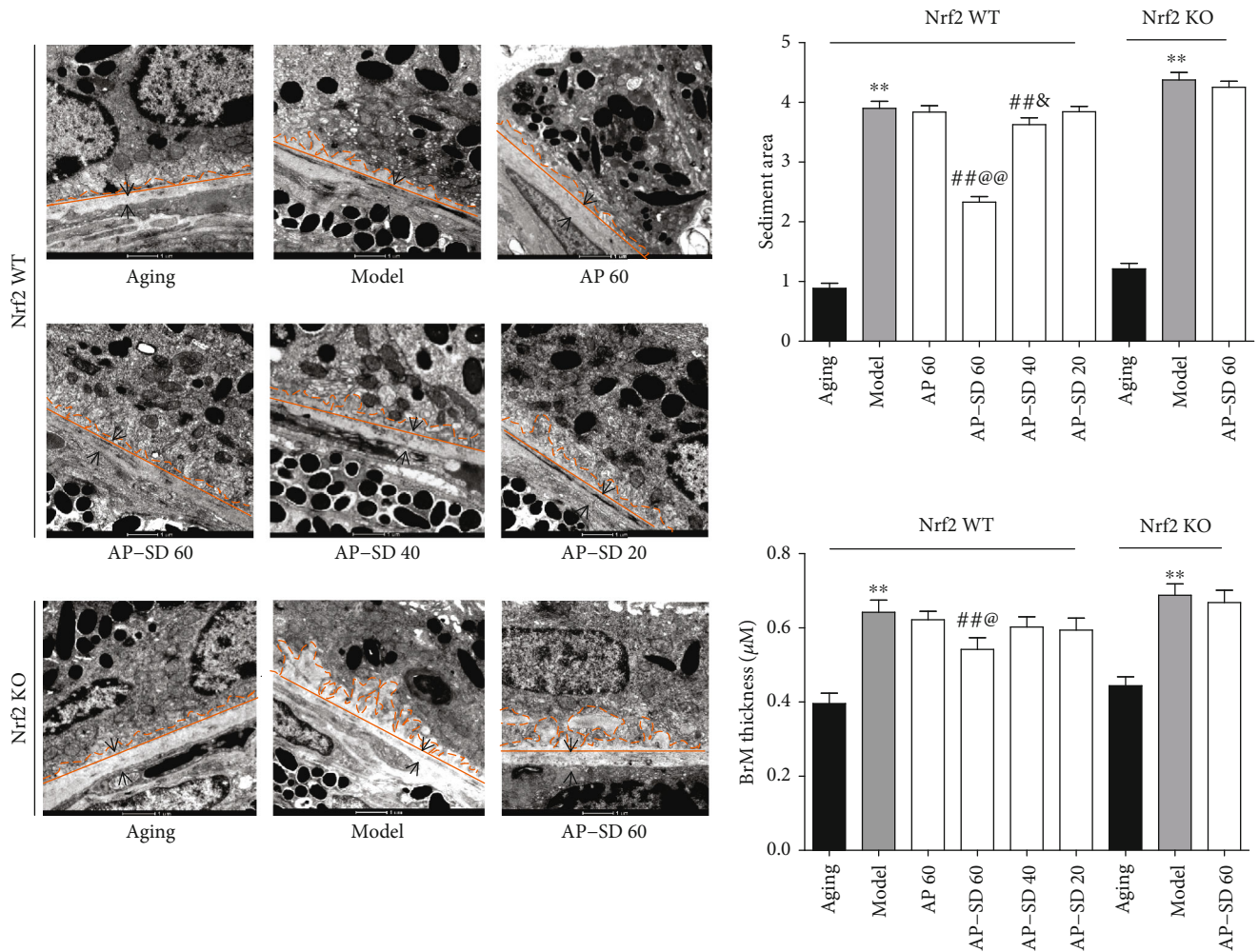


FIGURE 6: Representative images of TEM in Nrf2 WT and KO mice. There were obvious sediments under RPE (orange area) and thickened BrM (black arrow) in model mice compared to the aging mice, and it is more severe in Nrf2 KO mice. AP-SD reduced the area of the sediment and thinned BrM in Nrf2 WT mice and not in Nrf2 KO mice. ** $p < 0.01$, model control versus aging control; ## $p < 0.01$, AP-SD versus model control; @ $p < 0.05$, @@ $p < 0.01$, AP-SD 60 versus AP-SD 40; & $p < 0.05$, AP-SD 40 versus AP-SD 20. Data are means \pm standard deviation ($n = 5$).

but there was no significant change in Nrf2 KO mice (Figure 11(b)). Together, these results imply that Nrf2 is a mediator of the activation of autophagy in the model mice with dry AMD.

4. Discussion

Up to now, no therapy options are approved for the treatment of dry AMD. Several pathways, including oxidative stress, deposits of lipofuscin, and chronic inflammation, seem to play important roles in the pathogenesis of dry AMD and represent possible targets [35]. Oxidative stress has been suggested to be a critical component of AMD pathogenesis. Many reports demonstrated that natural products are able to decrease the occurrence of several diseases induced by oxidative injury, including AMD [36, 37]. Dietary supplements containing high dose of antioxidants and minerals (vitamins C and E, β -carotene, and zinc) delayed the progression of AMD intermediate to advanced stages [38]. Quercetin, lutein, zeaxanthin, and hesperetin have also been shown to have the potential to prevent AMD progress [39–

41]. It has been reported that AP plays a protective role in treating diseases associated with the oxidative process, such as cardiovascular and neurological disorders [42, 43]. However, like other flavonoids, AP has poor solubility in water and fat, therefore having low bioavailability. PVP, a hydrophilic excipient, could convert drugs to an amorphous form, and immensity enhances the solubility and dissolution of drugs [44, 45]. In this study, we prepared AP-SD with PVP K30; the results showed that the formation of solid dispersion increased the solubility and dispersion of AP, so the oral bioavailability of AP-SD was better than that of AP in rats. We then used dry AMD model mouse to verify the benefits of AP-SD in improving bioavailability. The results showed that AP-SD could reduce retinopathy, while AP could not, indicating that the formation of solid dispersion reasonably enhanced the protective effects of AP on the mouse retina on account of the increased bioavailability.

Recently, the Nrf2 pathway was considered a key contributor to the response to increased oxidative stress in RPE. Nrf2 knockout mouse has been shown to induce AMD-like pathological changes, manifested by the accumulation of

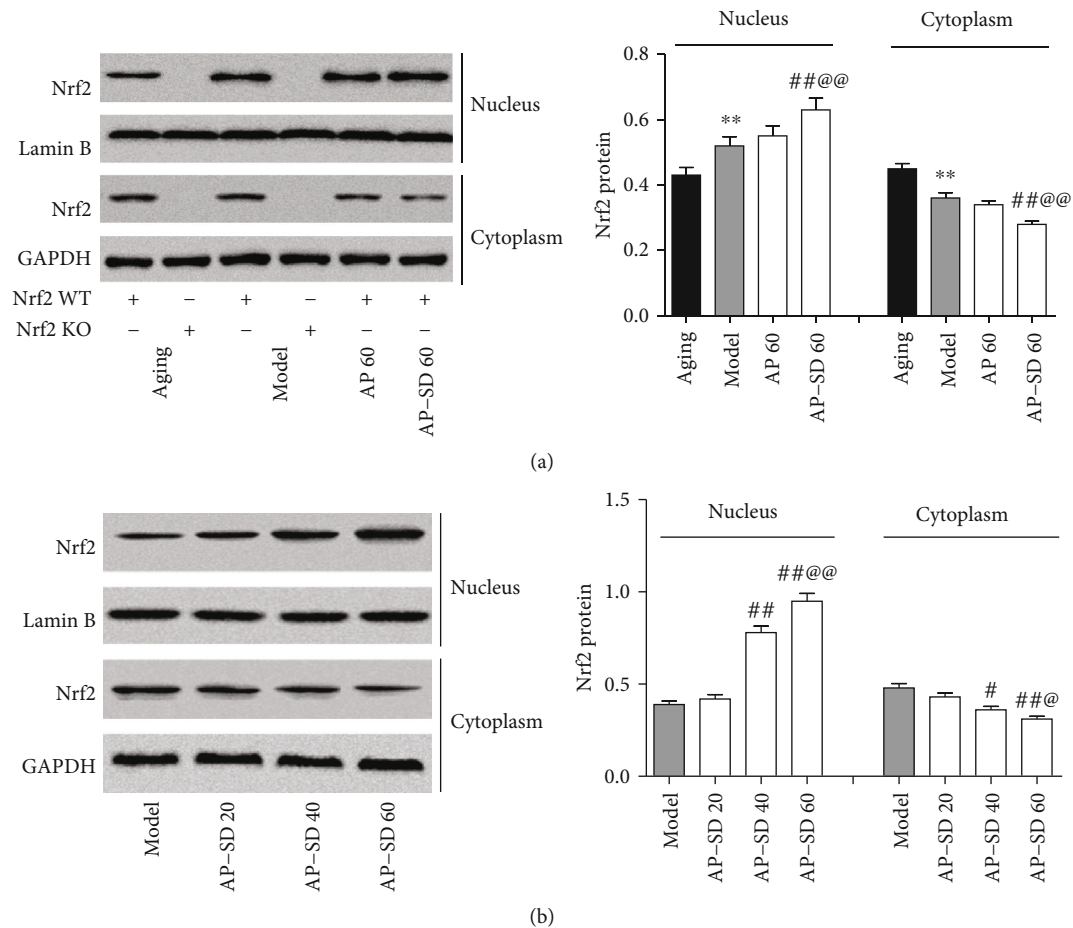


FIGURE 7: AP-SD promoted Nrf2 nuclear translocation. (a) The level of nuclear Nrf2 was increased and the level of cytoplasmic Nrf2 was reduced in model mice compared with those in aging mice. (b) AP-SD decreased the level of cytoplasmic Nrf2 and increased the level of nuclear Nrf2. $^{**}p < 0.01$, model control versus aging control; $^{##}p < 0.01$, AP-SD versus model control; $^{\textcircled{p}}p < 0.05$, $^{\textcircled{p}p}p < 0.01$, AP-SD 60 versus AP-SD 40. Data are means \pm standard deviation ($n = 5$).

lipofuscin, drusen, choroidal neovascularization and accumulation of the autophagosome [46]. In this study, similar lesions were showed in the retina of the model mouse. Activation of the Nrf2 pathway could have a therapeutic potential in protecting RPE cells against oxidative stress, so it may be beneficial for dry AMD [47]. Based on this point, we have previously reported that AP protected ARPE-19 cells against oxidative injury by the activation of Nrf2 signaling *in vitro*. In the present study, the effects of AP were validated in model mouse of dry AMD *in vivo*. The upregulation of Nrf2 expression and nuclear translocation were observed in Nrf2 WT mice. AP-SD promoted Nrf2 nuclear translocation, upregulated the expression of Nrf2 and targeted protein HO-1 and GCL, restored activities of SOD and GSH-PX, and decreased the levels of ROS and MDA in Nrf2 WT mice. As expected, similar results were not observed in Nrf2 KO mice. In conclusion, our findings suggested that AP-SD protected the retina against oxidative injury via activation of the Nrf2 signaling pathway.

It was reported that AP regulate autophagy. For example, AP promoted autophagy through the mTOR/AMPK/ULK1 pathway and could play an antidepressant effect [48], inhibited the growth of cisplatin-resistant colon cancer cells by

inducing autophagy and apoptosis [49], and restored impairment of autophagy and downregulation of unfolded protein response regulatory proteins in keratinocytes exposed to ultraviolet B radiation [50]. Studies have suggested that p62 protein is regulated by oxidative stress and is a transcriptional target of Nrf2 [51, 52]. This study focused on the effect of AP on autophagy pathway in the retina of model mice and the relationship between the p62 expression, autophagy, and Nrf2 pathway. The results showed that the expression of p62 and LC3 in Nrf2 KO mice were significantly lower than that in Nrf2 WT mice. In Nrf2 WT mice, AP-SD dose dependently upregulated the expression of p62 and LC3 but had no effect in Nrf2KO mice. Our finding suggested that AP-SD upregulated the autophagy in an Nrf2-dependent manner. It has been well known that the nuclear translocation of Nrf2 is increased and the expression of Nrf2 is upregulated in oxidative stress. Nrf2 could regulate the transcription of autophagy genes, such as p62, ULK1, Atg7 and GABARAPL1, Atg2B, Atg5, and Atg4D, because there is an ARE sequence in their promoter regions. The expressions of several autophagy markers (including LC3) were decreased in Nrf2-deficient mice [33, 53]. However, it has been reported that trehalose upregulate Nrf2 and autophagy in a p62-

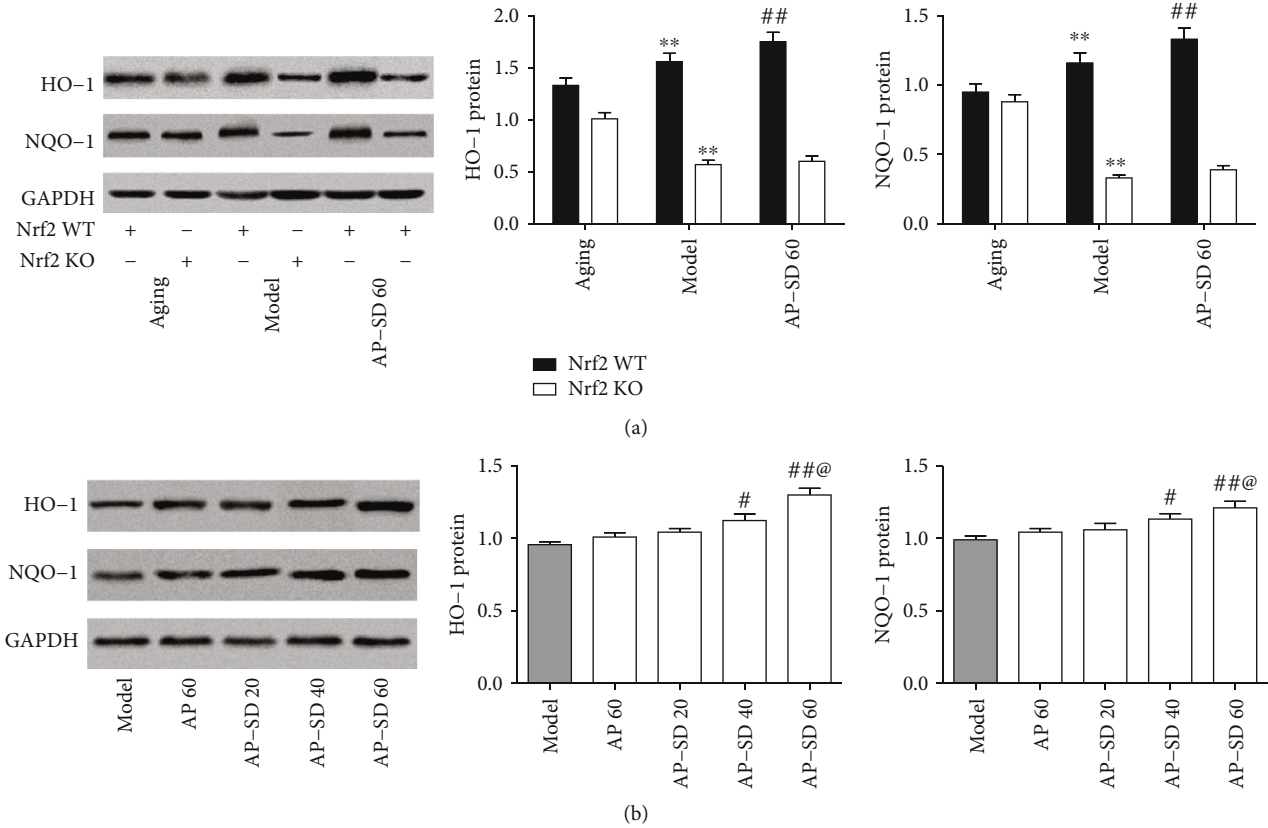


FIGURE 8: AP-SD upregulated the expressions of the targeted genes of Nrf2. (a) The expressions of HO-1 and NQO-1 were upregulated in the Nrf2 WT model mice and downregulated in Nrf2 KO model mice, compared with those in aging mice. (b) AP-SD increased the expressions of HO-1 and NQO-1 in Nrf2 WT mice but not in Nrf2 KO mice. $^{**}p < 0.01$, model control versus aging control; $^{\#}p < 0.05$, $^{##}p < 0.01$, AP-SD versus model control; $^{\textcircled{a}}p < 0.05$, AP-SD 60 versus AP-SD 40. Data are means \pm standard deviation ($n = 5$).

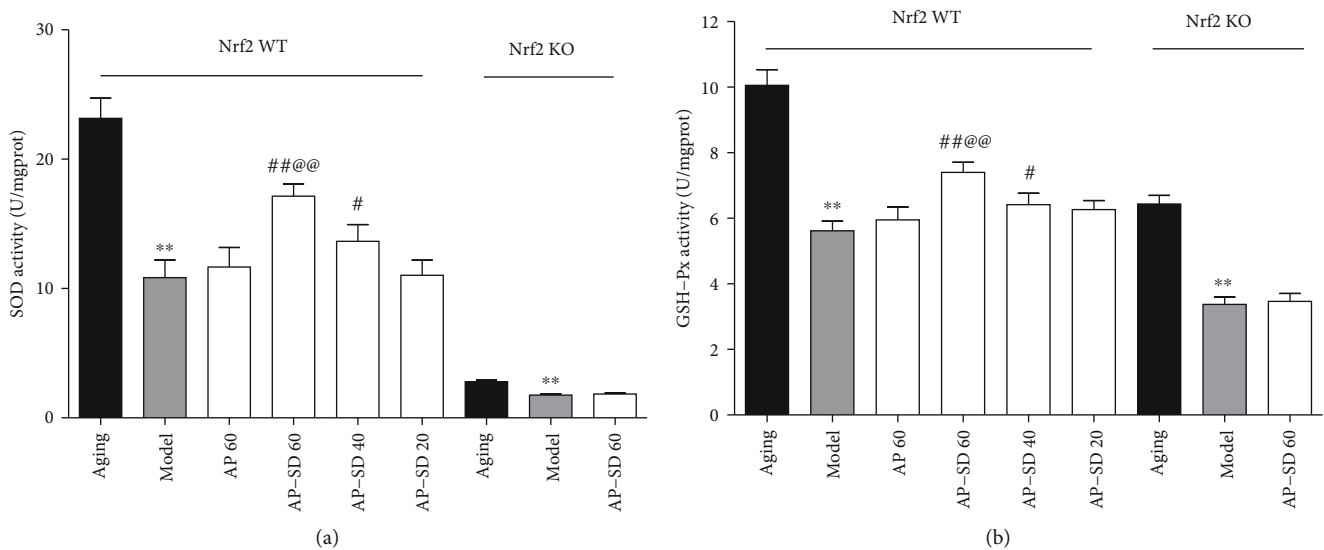


FIGURE 9: AP-SD restored the activities of SOD and GSH-Px. The activities of SOD (a) and GSH-Px (b) were decreased in Nrf2 WT model mice and more remarkable in Nrf2 KO model mice. AP-SD restored the activities of SOD and GSH-Px in Nrf2 WT mice, not in Nrf2 KO mice. $^{**}p < 0.01$, model control versus aging control; $^{\#}p < 0.05$, $^{##}p < 0.01$, AP-SD versus model control; $^{\textcircled{a}}p < 0.01$, AP-SD 60 versus AP-SD 40. Data are means \pm standard deviation ($n = 5$).

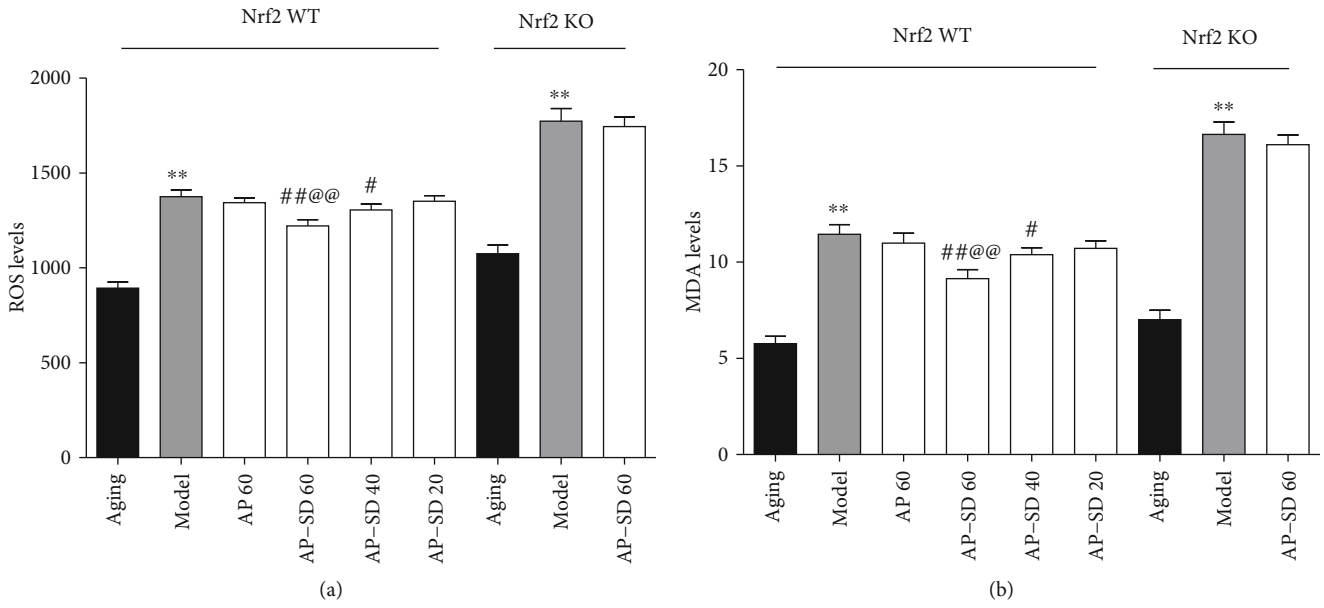


FIGURE 10: AP-SD decreased the ROS and MDA levels. The levels of ROS (a) and MDA (b) were significantly elevated in Nrf2 WT and Nrf2 KO model mice, but higher in Nrf2 KO mice. AP-SD decreased the ROS and MDA levels in Nrf2 WT mice, not in Nrf2 KO mice. $**p < 0.01$, model control versus aging control; $\#p < 0.05$, $\#\#p < 0.01$, AP-SD versus model control; $@@p < 0.01$, AP-SD 60 versus AP-SD 40. Data are means \pm standard deviation ($n = 5$).

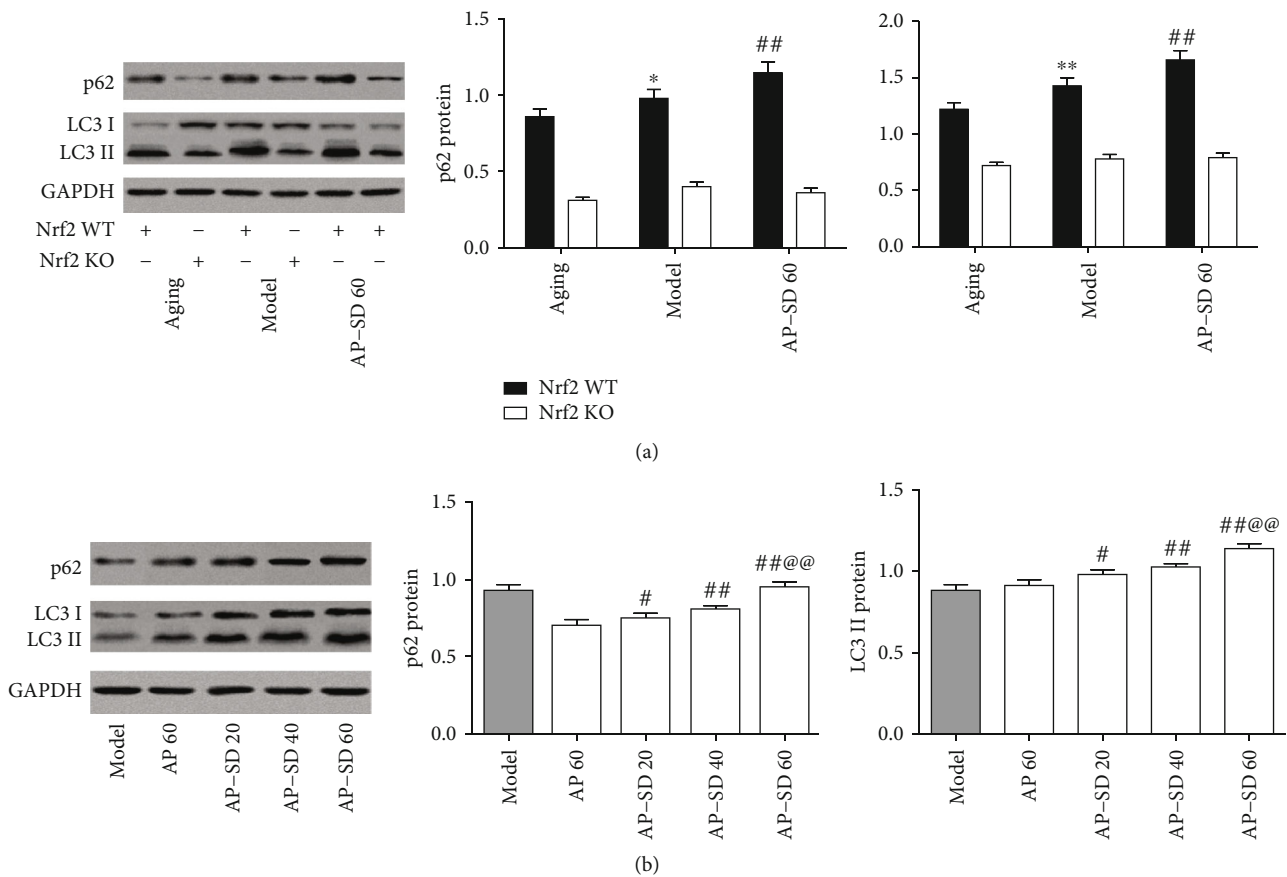


FIGURE 11: AP-SD regulated autophagy. (a) The expressions of p62 and LC3 II were upregulated in Nrf2 WT model mice, but not in Nrf2 KO model mice, compared with those in aging mice. (b) AP-SD increased the expressions of p62 and LC3 II in Nrf2 WT mice, but not in Nrf2 KO mice. $*p < 0.05$, $**p < 0.01$, model control versus aging control; $\#p < 0.05$, $\#\#p < 0.01$, AP-SD versus model control; $@@p < 0.01$, AP-SD 60 versus AP-SD 40. Data are means \pm standard deviation ($n = 5$).

dependent manner in oxidative stress [12]. Therefore, the underlying mechanism of AP regulating the Nrf2 pathway and autophagy remains to be further studied.

In summary, AP-SD significantly enhanced the bioavailability of the original drug and reduced retinal oxidative injury in model mouse of dry AMD *in vivo*. Meanwhile, we provided evidence that AP not only activates Nrf2 pathway but also upregulates p62 and autophagy. AP-SD upregulated the expressions of antioxidant enzymes through the Nrf2 pathway and upregulated the autophagy in an Nrf2-dependent manner to suppress retinal oxidative damage. The results suggest that AP-SD is a potential compound for the treatment of dry AMD.

Data Availability

The data used to support the findings of this study are included within the article.

Disclosure

The authors declare that the research was conducted in the absence of any commercial or financial relationships that could be construed as a potential conflict of interest.

Conflicts of Interest

The authors declare that they have no conflicts of interest.

Acknowledgments

The work was supported by the Jiangsu Provincial Key Research and Development Program (Grant No. BE2018757).

References

- [1] S. J. Bakri, J. E. Thorne, A. C. Ho et al., "Safety and efficacy of anti-vascular endothelial growth factor therapies for neovascular age-related macular degeneration: a report by the American Academy of ophthalmology," *Ophthalmology*, vol. 126, no. 1, pp. 55–63, 2019.
- [2] J. T. Handa, "How does the macula protect itself from oxidative stress?," *Molecular Aspects of Medicine*, vol. 33, no. 4, pp. 418–435, 2012.
- [3] C. Roehlecke, U. Schumann, M. Ader et al., "Stress reaction in outer segments of photoreceptors after blue light irradiation," *PLoS One*, vol. 8, no. 9, article e71570, 2013.
- [4] S. Datta, M. Cano, K. Ebrahimi, L. Wang, and J. T. Handa, "The impact of oxidative stress and inflammation on RPE degeneration in non-neovascular AMD," *Progress in Retinal and Eye Research*, vol. 60, pp. 201–218, 2017.
- [5] T. Suzuki and M. Yamamoto, "Molecular basis of the Keap1–Nrf2 system," *Free Radical Biology and Medicine*, vol. 88, Part B, pp. 93–100, 2015.
- [6] S. H. Kim and J. W. Park, "Morin hydrate attenuates CSE-induced lipid accumulation, ER stress, and oxidative stress in RPE cells: implications for age-related macular degeneration," *Free Radical Research*, vol. 53, no. 8, pp. 865–874, 2019.
- [7] B. Levine and G. Kroemer, "Autophagy in the pathogenesis of disease," *Cell*, vol. 132, no. 1, pp. 27–42, 2008.
- [8] P. Boya, L. Esteban-Martínez, A. Serrano-Puebla, R. Gómez-Sintes, and B. Villarejo-Zori, "Autophagy in the eye: development, degeneration, and aging," *Progress in Retinal and Eye Research*, vol. 55, pp. 206–245, 2016.
- [9] K. Kaarniranta, P. Tokarz, A. Koskela, J. Paterno, and J. Blasiak, "Autophagy regulates death of retinal pigment epithelium cells in age-related macular degeneration," *Cell Biology and Toxicology*, vol. 33, no. 2, pp. 113–128, 2017.
- [10] E. Keeling, A. Lotery, D. Tumbarello, and J. Ratnayaka, "Impaired cargo clearance in the retinal pigment epithelium (RPE) underlies irreversible blinding diseases," *Cells*, vol. 7, no. 2, p. 16, 2018.
- [11] I. Johansson, V. T. Monsen, K. Pettersen et al., "The marine n-3 PUFA DHA evokes cytoprotection against oxidative stress and protein misfolding by inducing autophagy and NFE2L2 in human retinal pigment epithelial cells," *Autophagy*, vol. 11, no. 9, pp. 1636–1651, 2015.
- [12] Y. Mizunoe, M. Kobayashi, Y. Sudo et al., "Trehalose protects against oxidative stress by regulating the Keap1–Nrf2 and autophagy pathways," *Redox Biology*, vol. 15, pp. 115–124, 2018.
- [13] L. Zhang, H. Wang, Y. Fan et al., "Fucoxanthin provides neuroprotection in models of traumatic brain injury via the Nrf2–ARE and Nrf2–autophagy pathways," *Scientific Reports*, vol. 7, no. 1, article 46763, 2017.
- [14] Y. Saito, Y. Kuse, Y. Inoue, S. Nakamura, H. Hara, and M. Shimazawa, "Transient acceleration of autophagic degradation by pharmacological Nrf2 activation is important for retinal pigment epithelium cell survival," *Redox Biology*, vol. 19, pp. 354–363, 2018.
- [15] S. Dayalan Naidu, D. Dikovskaya, E. Gaurilcikaite et al., "Transcription factors NRF2 and HSF1 have opposing functions in autophagy," *Scientific Reports*, vol. 7, no. 1, article 11023, 2017.
- [16] F. Li, F. Lang, H. Zhang et al., "Apigenin Alleviates Endotoxin-Induced Myocardial Toxicity by Modulating Inflammation, Oxidative Stress, and Autophagy," *Oxidative Medicine and Cellular Longevity*, vol. 2017, Article ID 2302896, 10 pages, 2017.
- [17] W. J. Hu, J. Liu, L. K. Zhong, and J. Wang, "Apigenin enhances the antitumor effects of cetuximab in nasopharyngeal carcinoma by inhibiting EGFR signaling," *Biomedicine & Pharmacotherapy*, vol. 102, pp. 681–688, 2018.
- [18] X. Xu, M. Li, W. Chen, H. Yu, Y. Yang, and L. Hang, "Apigenin attenuates oxidative injury in ARPE-19 cells thorough activation of Nrf2 pathway," *Oxidative Medicine and Cellular Longevity*, vol. 2016, Article ID 4378461, 9 pages, 2016.
- [19] Y. Huang and W. G. Dai, "Fundamental aspects of solid dispersion technology for poorly soluble drugs," *Acta Pharmaceutica Sinica B*, vol. 4, no. 1, pp. 18–25, 2014.
- [20] A. W. Khan, S. Kotta, S. H. Ansari, R. K. Sharma, and J. Ali, "Enhanced dissolution and bioavailability of grapefruit flavonoid naringenin by solid dispersion utilizing fourth generation carrier," *Drug Development and Industrial Pharmacy*, vol. 41, no. 5, pp. 772–779, 2014.
- [21] P. Charbel Issa, A. R. Barnard, M. S. Singh et al., "Fundus autofluorescence in the Abca4(-/-) mouse model of Stargardt disease –correlation with accumulation of A2E, retinal function, and histology," *Investigative Ophthalmology & Visual Science*, vol. 54, no. 8, pp. 5602–5612, 2013.
- [22] Q. Song, X. Sun, Q. Nie et al., "A novel method of multi-parameter measurements for the mouse retina *in vivo* using optical coherence tomography," *Experimental Eye Research*, vol. 121, pp. 66–73, 2014.

- [23] M. M. Edwards, D. S. McLeod, I. A. Bhutto, R. Grebe, M. Duffy, and G. A. Luttj, "Subretinal glial membranes in eyes with geographic atrophy," *Investigative Ophthalmology & Visual Science*, vol. 58, no. 3, pp. 1352–1367, 2017.
- [24] G. Landa, R. B. Rosen, J. Pilavas, and P. M. T. Garcia, "Drusen characteristics revealed by spectral-domain optical coherence tomography and their corresponding fundus autofluorescence appearance in dry age-related macular degeneration," *Ophthalmic Research*, vol. 47, no. 2, pp. 81–86, 2012.
- [25] M. G. Nittala, H. Ruiz-Garcia, and S. R. Sadda, "Accuracy and reproducibility of automated drusen segmentation in eyes with non-neovascular age-related macular degeneration," *Investigative Ophthalmology & Visual Science*, vol. 53, no. 13, pp. 8319–8324, 2012.
- [26] F. C. Delori, C. K. Dorey, G. Staurengi, O. Arend, D. G. Goger, and J. J. Weiter, "In vivo fluorescence of the ocular fundus exhibits retinal pigment epithelium lipofuscin characteristics," *Investigative Ophthalmology & Visual Science*, vol. 36, no. 3, pp. 718–729, 1995.
- [27] J. Lei, S. Balasubramanian, N. S. Abdelfattah, M. G. Nittala, and S. V. R. Sadda, "Proposal of a simple optical coherence tomography-based scoring system for progression of age-related macular degeneration," *Graefes Archive for Clinical and Experimental Ophthalmology*, vol. 255, no. 8, pp. 1551–1558, 2017.
- [28] J. M. Seddon, B. Rosner, R. D. Sperduto et al., "Dietary fat and risk for advanced age-related macular degeneration," *Archives of Ophthalmology*, vol. 119, no. 8, pp. 1191–1199, 2001.
- [29] C. Su, Z. Liu, Y. Wang, Y. Wang, E. Song, and Y. Song, "The electrophilic character of quinones is essential for the suppression of Bach1," *Toxicology*, vol. 387, pp. 17–26, 2017.
- [30] G. Bjørkøy, T. Lamark, A. Brech et al., "p 62/SQSTM1 forms protein aggregates degraded by autophagy and has a protective effect on huntingtin-induced cell death," *Journal of Cell Biology*, vol. 171, no. 4, pp. 603–614, 2005.
- [31] Y. Kabeya, N. Mizushima, T. Ueno et al., "LC3, a mammalian homologue of yeast Apg8p, is localized in autophagosomal membranes after processing," *The EMBO Journal*, vol. 19, no. 21, pp. 5720–5728, 2000.
- [32] Q. M. Chen and A. J. Maltagliati, "Nrf2 at the heart of oxidative stress and cardiac protection," *Physiological Genomics*, vol. 50, no. 2, pp. 77–97, 2018.
- [33] M. Pajares, N. Jiménez-Moreno, Á. J. García-Yagüe et al., "Transcription factor NFE2L2/NRF2 is a regulator of macroautophagy genes," *Autophagy*, vol. 12, no. 10, pp. 1902–1916, 2016.
- [34] D. P. Frias, R. L. N. Gomes, K. Yoshizaki et al., "Nrf2 positively regulates autophagy antioxidant response in human bronchial epithelial cells exposed to diesel exhaust particles," *Scientific Reports*, vol. 10, no. 1, article 3704, 2020.
- [35] L. F. Hernández-Zimbrón, R. Zamora-Alvarado, L. Ochoa-de la Paz et al., "Age-related macular degeneration: new paradigms for treatment and management of AMD," *Oxidative Medicine and Cellular Longevity*, vol. 2018, Article ID 8374647, 14 pages, 2018.
- [36] R. K. Saini, K. R. R. Rengasamy, F. M. Mahomoodally, and Y. S. Keum, "Protective effects of lycopene in cancer, cardiovascular, and neurodegenerative diseases: an update on epidemiological and mechanistic perspectives," *Pharmacological Research*, vol. 155, article 104730, 2020.
- [37] H. H. Dieguez, H. E. Romeo, A. Alaimo et al., "Oxidative stress damage circumscribed to the central temporal retinal pigment epithelium in early experimental non-exudative age-related macular degeneration," *Free Radical Biology and Medicine*, vol. 131, pp. 72–80, 2019.
- [38] Age-Related Eye Disease Study Research Group, "A randomized, placebo-controlled, clinical trial of high-dose supplementation with vitamins C and E and beta carotene for age-related cataract and vision loss: AREDS report no. 9," *Archives of Ophthalmology*, vol. 119, no. 10, pp. 1439–1452, 2001.
- [39] X. R. Xu, H. T. Yu, Y. Yang, L. Hang, X. W. Yang, and S. H. Ding, "Quercetin phospholipid complex significantly protects against oxidative injury in ARPE-19 cells associated with activation of Nrf2 pathway," *European Journal of Pharmacology*, vol. 770, pp. 1–8, 2016.
- [40] B. Eisenhauer, S. Natoli, G. Liew, and V. Flood, "Lutein and zeaxanthin-food sources, bioavailability and dietary variety in age-related macular degeneration protection," *Nutrients*, vol. 9, no. 2, p. 120, 2017.
- [41] C. Zhu, Y. Dong, H. Liu, H. Ren, and Z. Cui, "Hesperetin protects against H₂O₂-triggered oxidative damage via upregulation of the Keap1-Nrf2/HO-1 signal pathway in ARPE-19 cells," *Biomedicine & Pharmacotherapy*, vol. 88, pp. 124–133, 2017.
- [42] P. Zeng, B. Liu, Q. Wang et al., "Apigenin Attenuates Atherogenesis through Inducing Macrophage Apoptosis via Inhibition of AKT Ser473 Phosphorylation and Downregulation of Plasminogen Activator Inhibitor-2," *Oxidative Medicine and Cellular Longevity*, vol. 2015, Article ID 379538, 12 pages, 2015.
- [43] M. Kim, J. Jung, N. Y. Jeong, and H. J. Chung, "The natural plant flavonoid apigenin is a strong antioxidant that effectively delays peripheral neurodegenerative processes," *Anatomical Science International*, vol. 94, no. 4, pp. 285–294, 2019.
- [44] J. Zhao, J. Yang, and Y. Xie, "Improvement strategies for the oral bioavailability of poorly water-soluble flavonoids: an overview," *International Journal of Pharmaceutics*, vol. 570, article 118642, 2019.
- [45] Y. Shao, H. Yu, Y. Yang, M. Li, L. Hang, and X. Xu, "A solid dispersion of quercetin shows enhanced Nrf2 activation and protective effects against oxidative injury in a mouse model of dry age-related macular degeneration," *Oxidative Medicine and Cellular Longevity*, vol. 2019, Article ID 1479571, 12 pages, 2019.
- [46] Z. Zhao, Y. Chen, J. Wang et al., "Age-related retinopathy in NRF2-deficient mice," *PLoS One*, vol. 6, no. 4, article e19456, 2011.
- [47] K. T. Vu and J. D. Hulleman, "An inducible form of Nrf2 confers enhanced protection against acute oxidative stresses in RPE cells," *Experimental Eye Research*, vol. 164, pp. 31–36, 2017.
- [48] X. Zhang, H. Bu, Y. Jiang et al., "The antidepressant effects of apigenin are associated with the promotion of autophagy via the mTOR/AMPK/ULK1 pathway," *Molecular Medicine Reports*, vol. 20, no. 3, pp. 2867–2874, 2019.
- [49] X. Chen, H. Xu, X. Yu, X. Wang, X. Zhu, and X. Xu, "Apigenin inhibits in vitro and in vivo tumorigenesis in cisplatin-resistant colon cancer cells by inducing autophagy, programmed cell death and targeting m-TOR/PI3K/Akt signaling pathway," *Journal of BUON*, vol. 24, no. 2, pp. 488–493, 2019.

- [50] L. Li, M. Li, S. Xu, H. Chen, X. Chen, and H. Gu, "Apigenin restores impairment of autophagy and downregulation of unfolded protein response regulatory proteins in keratinocytes exposed to ultraviolet B radiation," *Journal of Photochemistry and Photobiology B*, vol. 194, pp. 84–95, 2019.
- [51] Z. Tang, B. Hu, F. Zang, J. Wang, X. Zhang, and H. Chen, "Nrf2 drives oxidative stress-induced autophagy in nucleus pulposus cells via a Keap1/Nrf2/p62 feedback loop to protect intervertebral disc from degeneration," *Cell Death & Disease*, vol. 10, no. 7, p. 510, 2019.
- [52] W. Liao, Z. Wang, Z. Fu et al., "p 62/SQSTM1 protects against cisplatin-induced oxidative stress in kidneys by mediating the cross talk between autophagy and the Keap 1-Nrf2 signalling pathway," *Free Radical Research*, vol. 53, no. 7, pp. 800–814, 2019.
- [53] T. Jiang, B. Harder, M. Rojo de la Vega, P. K. Wong, E. Chapman, and D. D. Zhang, "p62 links autophagy and Nrf2 signaling," *Free Radical Biology and Medicine*, vol. 88, Part B, pp. 199–204, 2015.

Research Article

***Tetrastigma hemsleyanum* Vine Flavone Ameliorates Glutamic Acid-Induced Neurotoxicity via MAPK Pathways**

Qiang Chu,^{1,2} Yonglu Li,² Zheng Hua,² Yaxuan Wang,² Xin Yu,² Ruoyi Jia,² Wen Chen,² and Xiaodong Zheng^{ID}²

¹State Key Laboratory of Silicon Materials, School of Materials Science and Engineering, Zhejiang University, Hangzhou 310027, China

²Department of Food Science and Nutrition, National Engineering Laboratory of Intelligent Food Technology and Equipment, National-Local Joint Engineering Laboratory of Intelligent Food Technology and Equipment, Key Laboratory for Agro-Products Postharvest Handling of Ministry of Agriculture, Zhejiang Key Laboratory for Agro-food Processing, Fuli Institute of Food Science, Zhejiang University, Hangzhou 310058, China

Correspondence should be addressed to Xiaodong Zheng; xdzhengzju@163.com

Received 4 February 2020; Accepted 21 February 2020; Published 22 March 2020

Guest Editor: Francisco Jaime B. Mendonça Junior

Copyright © 2020 Qiang Chu et al. This is an open access article distributed under the Creative Commons Attribution License, which permits unrestricted use, distribution, and reproduction in any medium, provided the original work is properly cited.

Glutamic acid (Glu) is a worldwide flavor enhancer with various positive effects. However, Glu-induced neurotoxicity has been reported less. *Tetrastigma hemsleyanum* (TH), a rare herbal plant in China, possesses high medicinal value. More studies paid attention to tuber of TH whereas vine part (THV) attracts fewer focus. In this study, we extracted and purified flavones from THV (THVF), and UPLC-TOF/MS showed THVF was consisted of 3-caffeoylquinic acid, 5-caffeoylquinic acid, quercetin-3-O-rutinoside, and kaempferol-3-O-rutinoside. *In vitro*, Glu caused severe cytotoxicity, genotoxicity, mitochondrial dysfunction, and oxidative damage to rat pheochromocytoma (PC12) cells. Conversely, THVF attenuated Glu-induced toxicity via MAPK pathways. *In vivo*, the neurotoxicity triggered by Glu restrained the athletic ability in *Caenorhabditis elegans* (*C. elegans*). The treatment of THVF reversed the situation induced by Glu. In a word, Glu could cause neurotoxicity and THVF owns potential neuroprotective effects both *in vitro* and *in vivo* via MAPK pathways.

1. Introduction

Glutamic acid (Glu), as one of the basic amino acids, is widely applied in industry. Glu is involved in many crucial chemical reactions in the body and plays an important role in protein metabolism in organisms [1]. Meanwhile, it is ubiquitous in the human diet; as a flavor enhancer and food additive in food field, Glu is widely used to improve the taste of beverages and foods and preserves the freshness of animal food [2, 3]. For example, sodium glutamate, commonly known as monosodium glutamate, is a typical flavor agent that can be used alone or with other amino acids [4]. In addition, studies have proven that Glu is an excellent hair-generating agent. Ottersen et al. reported that Glu effectively promoted the proliferation of hair papilla cells; besides, it can also expand blood vessels and accelerated blood circulation,

resulting in hair regeneration [5, 6]. It has also been estimated that Glu poses the ability to reduce wrinkles [7]. As an auxiliary drug for liver diseases, Glu is taken and combined with blood ammonia to form glutamine, which can relieve the toxic effect of ammonia in the metabolic process, thus preventing and treating hepatic coma [8, 9]. Besides, brain tissue cannot oxidize amino acids except glutamate, and therefore, glutamine can be used as an energy substance to improve the function of the brain [10, 11]. As a supplement to the nerve center and cerebral cortex, Glu exhibits a certain effect on the treatment of concussion, nerve damage, epilepsy, and mental retardation [12, 13]. Data show that Glu peaks the largest productive amino acid variety worldwide.

Although Glu shows an irreplaceable role in various fields, it may also turn from a protective agent to a neurotoxin in many cases. A growing number of studies have

found that the Glu is closely associated with the etiology and pathology of many neurological and psychiatric disorders, such as cerebral ischemia, epilepsy, Alzheimer's disease, Huntington's disease, schizophrenia, and Pico disease [14]. Oxidative stress caused by Glu is an important cause of neurodegenerative diseases [15, 16], high concentration of Glu inhibits cysteine/glutamate antiporter or system x-CT in neuronal cells, causes calcium overload that interferes with mitochondrial respiratory chain function, thereby inhibiting cysteine uptake and causing intracellular glutathione (GSH) deprivation and ROS accumulation, and ultimately leading to cell necrosis or apoptosis [17, 18]. Moreover, studies have shown that the caspase-dependent apoptotic pathway is related with Glu-neurotoxicity [19].

Natural plant extracts are attracting researchers' attention because of their safety, nontoxicity, and various biological activities [20]. Many natural plants have been already proved to exhibit various bioactive capacities such as antioxidative activity, anti-inflammatory activity, hypolipidemic effects, and even antitumor capacity [20]. *Tetragium hemsleyanum* Diels et. Gilg (TH), initially used for folk treatment of cancer (Li et al., 2019), is now not only a traditional Chinese medicine but also a type of functional food. Previous studies have shown that TH has antioxidant, anti-inflammatory, anticancer, and immunomodulatory properties that can effectively treat high fever, infantile febrile seizures, pneumonia, asthma, hepatitis, rheumatism, menstrual disorders, sore throats, and sores [21, 22]. It has reported that TH contains many phytochemicals, such as flavonoids, phenolic acids, polysaccharides, and phytosterols, resulting in its various biological activities such as anti-inflammatory, antioxidant, antiproliferative, antitumor, and antiviral effects [22–24]. However, there are fewer studies that paid attention to vine of TH, which is usually regarded useless and often discarded as a by-product, resulting in a waste of source.

In this study, we have extracted and purified the THVF, then identified and characterized the main compounds of THVF by UPLC-TOF/MS. In addition, we adopted the PC12 cell line and evaluated the protective effects of the THVF against damage induced by Glu *in vitro*. Meanwhile, western blot assay was conducted to unearth the underlying mechanism and the possible signal pathways involved in the protective effects. Furthermore, we assessed THVF's possible protective effects for *Caenorhabditis elegans* (*C. elegans*) against Glu-induced injury and its potential function in nematode physiological activity.

2. Materials and Methods

2.1. Extraction and Purification of THVF. *T. hemsleyanum* vines were first washed, dried, smashed into powder, and extracted with 80% ethanol at 45°C for 90 min by ultrasonication (with the ratio of material and solution in 1:5). The above extraction produce was repeated three times. Then, the filtered fluid was collected and settled at 4°C overnight. On the second day, the filtrate was centrifuged at 4000 r/min for 10 min to gain the supernatants. Then, the supernatants were evaporated to concentrate under reduced pressure at 45°C, the concentrations were later

centrifuged at 10000 r/min, and then the supernatants were loaded onto an equilibrated AB-8macroporous resin column ($\varnothing 3.2 \times 60$ cm) for further purification. Finally, the eluted fluid was evaporated and lyophilized and later stored at -80°C for further research.

2.2. Identification of THVF. An Ultra Performance Liquid Chromatography (UPLC) system (Waters, Milford, MA, USA) equipped with a triple-Time-of-Flight mass spectrometry (TOF/MS) system (AB SCIEX, Triple TOF 5600+, Framingham, MA, USA) on a Promosil C18 column (4.6 mm \times 250 mm, 5 μ m) was used to identify flavonoid compounds. The ingredients of the mobile phase are acetonitrile (A) and 0.1% aqueous formic acid (B). The linear gradient of phase B was 0–1 min (95%), 1–21 min (95–85%), 21–46 min (85–75%), 46–56 min (75–95%), and 56–60 min (95%). The flow rate was 0.8 mL/min, and the injection amount was 5 μ L. The mass spectrometry was operated in a negative ion mode at a temperature of 550°C, and the source voltage was 4.5 kV. Ions were recorded from *m/z* 100–1500, and the wavelength for the ultraviolet (UV) detector was set as 280 nm.

2.3. Cell Culture and Treatments. PC12 cell line was obtained from Shanghai Institute of Cell Biology (Shanghai, China) and cultured in Dulbecco's modified Eagle's medium (DMEM) supplemented with 10% fetal bovine serum (FBS) and 1% penicillin-streptomycin solution in an incubator with 5% CO₂ at 37°C. THVF powder was always freshly dissolved in DMEM with 10% FBS before use. After being cultured for 24 h, the cells were washed with phosphate-buffered saline (PBS) twice and then pretreated with different concentrations of THVF for another 24 hours. Later, Glu (20 mM) was added for 24 h in the absence/presence of different concentrations of THVF.

2.4. Cell Viability Assays. The assays of cell viability were carried out according to our previous protocol [21]. PC12 cells were seeded onto a 96-well plate, and 3-(4,5-dimethyl-2-thiazolyl)-2,5-diphenyl-2-H-tetrazolium bromide (MTT) diluted with serum-free DMEM at a final concentration of 0.5 mg/mL was added to each well after different treatments. After 4 h of incubation at 37°C, the formazan precipitate was dissolved in 150 μ L of dimethyl sulfoxide (DMSO) and shook for 15 minutes and the absorbance was measured at 570 nm with a spectrophotometer. The viability of the untreated group was regarded as 100%, and each experiment was repeated at least three times.

2.5. Fluorescent Probes Staining for PC12 Cells. After cell treatment, serum-free DMEM, respectively, containing 6 kinds of fluorescent probes were applied, including 2,7-dichlorofluorescein diacetate (DCFH-DA), DHE, apha-thalene-2,3-dicarboxaldehyde (NDA), Rhodamine 123, 10-N nonyl acridine orange (NAO), and Hoechst 33258. Cells were washed twice in PBS buffer after treatments and incubated in free-serum DMEM containing the probe at 37°C for 30 min. Then, cells were washed three times with PBS buffer and detected on a fluorescence microscope (Nikon) with different

filters at identical acquisition settings. Image-Pro Plus 6.0 software was adopted to analyze the densitometry.

2.6. Determination of the Level of SOD, MDA, and GSH. Cells were treated with different treatments, after washing with PBS buffer twice, 500 μ L WB/IP cell lysis buffer was added, and cells were scratched and collected. An ultrasonic shredder and centrifuge (Sigma, USA) were used, and the supernatants were collected for further assay. SOD, MDA, and GSH contents were determined with assay kits purchased from Beyotime Biotechnology (Jiangsu, China).

2.7. Western Blot. Total protein of cells was prepared using the WB/IP lysis buffer (Beyotime Biotechnology, Jiangsu, China). Equal amounts of protein were subjected to sodium dodecyl sulfate-polyacrylamide gel electrophoresis (SDS-PAGE) and transferred to polyvinylidene fluoride (PVDF) membranes. Membranes were probed with primary antibodies, and primary antibodies against p-p38 mitogen-activated protein kinase (MAPK), p38 MAPK, p-JNK, c-Jun N-terminal kinase JNK, and β -actin were purchased from Abcam (Shanghai, China). They were detected with horseradish-peroxidase-conjugated secondary antibodies using the enhanced chemiluminescence (ECL) detection system. β -Actin was used as a loading control, and ImageJ software was used to analyze densitometry.

2.8. C. Elegans Strains and Treatment. *C. elegans* bristol N2 (wild-type) was provided by Dr. Du (Zhejiang University, China). The mutants were maintained at 20°C on a standard nematode growth medium (NGM) with *E. coli* OP50 as food resources. To collect eggs, adult animals on NGM were dissolved in bleaching solution. Then, the eggs were transferred into a new plate for hatching and synchronized at the same period.

Synchronized L3 stage *C. elegans* were collected and transferred to NGM containing THVF of different concentrations (2.5, 5, and 10 μ g/mL). After 24-hour treatments, 20 mM of glutamate was added while the concentration of TVE kept the same as before.

2.9. Determination of Survival Rate, Body Length, and Body Width. The survival rate assays were performed in the 24-well plates. A total of 40 young nematodes were raised in each well with culture medium (NaCl 3.1 g/L, KCl 2.4 g/L, cholesterol 1 mg/L), and *E. coli* OP50 was added for food supply. 0, 2.5, 5, and 10 μ g/mL THVF were added into medium, respectively. After treating for 24 h, 20 mM Glu was later added for another 24 h. Survival rate was defined as survival rate (%) = the living worm numbers after treatment/total worm numbers before treatment * 100%.

The survival rate in the control group was regarded as 100% when calculated. Meanwhile, the photos of *C. elegans* were captured by a microscope and animals' body length and body width were measured by Auto CAD.

2.10. Locomotion Behavior Assay. Head thrash and body bend assays were used to evaluate locomotion behavior ability of nematodes. Once, head thrash was defined as a change in the direction of bending in the mid body which was

counted for 1 min. A body bend was defined as a change in the direction of the part of nematodes corresponding to the posterior bulb of the pharynx along the y -axis, assuming that the long axis of the body was the x -axis ($n = 30$ per replicate; three replicates per group).

2.11. Visualization of ROS, Superoxide, and GSH. To measure the level of ROS, superoxide, and GSH, three fluorescence probes (DCFH-DA, DHE, and NDA) were added, respectively. Images of animals were obtained through a fluorescence microscope.

2.12. Statistical Analysis. Data were expressed as mean \pm standard deviations (SDs) from at least three independent experiments. Significant differences were determined by one-way analysis of variance (ANOVA) followed by the multiple comparison at $p < 0.05$. Significant differences were all analyzed using SPSS. Densitometry analyses were performed using Image-Pro Plus 6.0 software.

3. Results

3.1. The Main Compounds of THVF. UPLC-TOF/MS results showed that THVF was composed of four main compounds; we numbered these four compounds as peak 1, 2, 3, and 4 (Figure 1(a)). As Figure 1(b) illustrated, peak 1 with a molecular ion at m/z 191.0506 [quinic acid-H]⁻ was identified as C₁₆H₁₈O₉, while a series of fragments of m/z 191.0561, 179.0345, 161.0242, 127.0403, and 85.0315 appeared in peak 2 secondary mass spectrum (Figure 1(c)). According to TOF/MS results and previous studies, peaks 1 and 2 were deduced as 3-caffeoylquinic acid and 5-caffeoylquinic acid [21, 25]. Peak 3 with a retention time at 33.923 min and fragment at m/z 301 [M-H-146-162]⁻ was identified as quercetin-3-O-rutinoside. Furthermore, the relative molecular mass of peak 4 was 594, and a fragment of m/z 309 was lost at m/z 285 [M-H-308]⁻ that could correspond to the loss of one rutinoside and peak 7 could be kaempferol-3-O-rutinoside. Therefore, it could be deduced that THVF is consisted of 3-caffeoylquinic acid, 5-caffeoylquinic acid, quercetin-3-O-rutinoside, and kaempferol-3-O-rutinoside.

3.2. THVF Alleviated Oxidative Stress Caused by Glu. According to the results of MTT assay (Figure 1(f)), we found that the concentration range of 0.78–25 μ g/mL showed no toxicity to PC12 cells. Thus, we choose 2.5, 5, 10, and 20 μ g/mL of THVF for further study. DNA damage is a key feature of cytotoxicity [26]. Therefore, Hoechst 33258, a specific DNA fluorescence probe, was adopted to assess nuclear fragmentation. As shown in Figure 2(a), the number of high light blue dots was markedly elevated after Glu stimulation while THVF treatments decreased such light dots at a dose-related manner.

Besides genotoxicity, Glu further caused intracellular redox disturbance, resulting in overproduction of ROS [27]. Since plant flavones were regarded as a potent free radical scavenger both *in vitro* and *in vivo* [28], we tested the intracellular ROS level in the presence or absence of THVF by DCFH-DA, a specific ROS fluorescence probe. An enhanced DCF fluorescence intensity was observed in Glu-treated cells

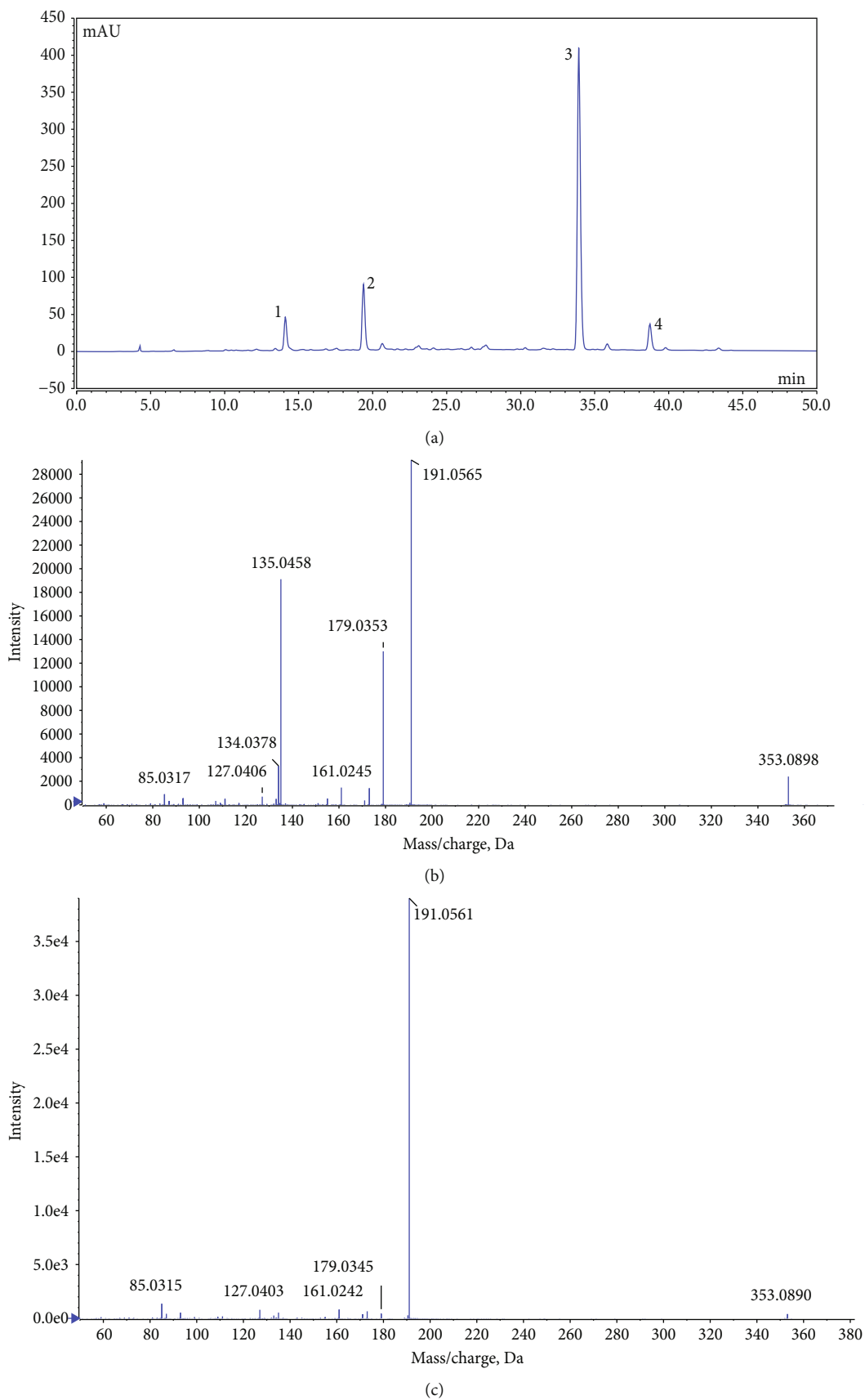


FIGURE 1: Continued.

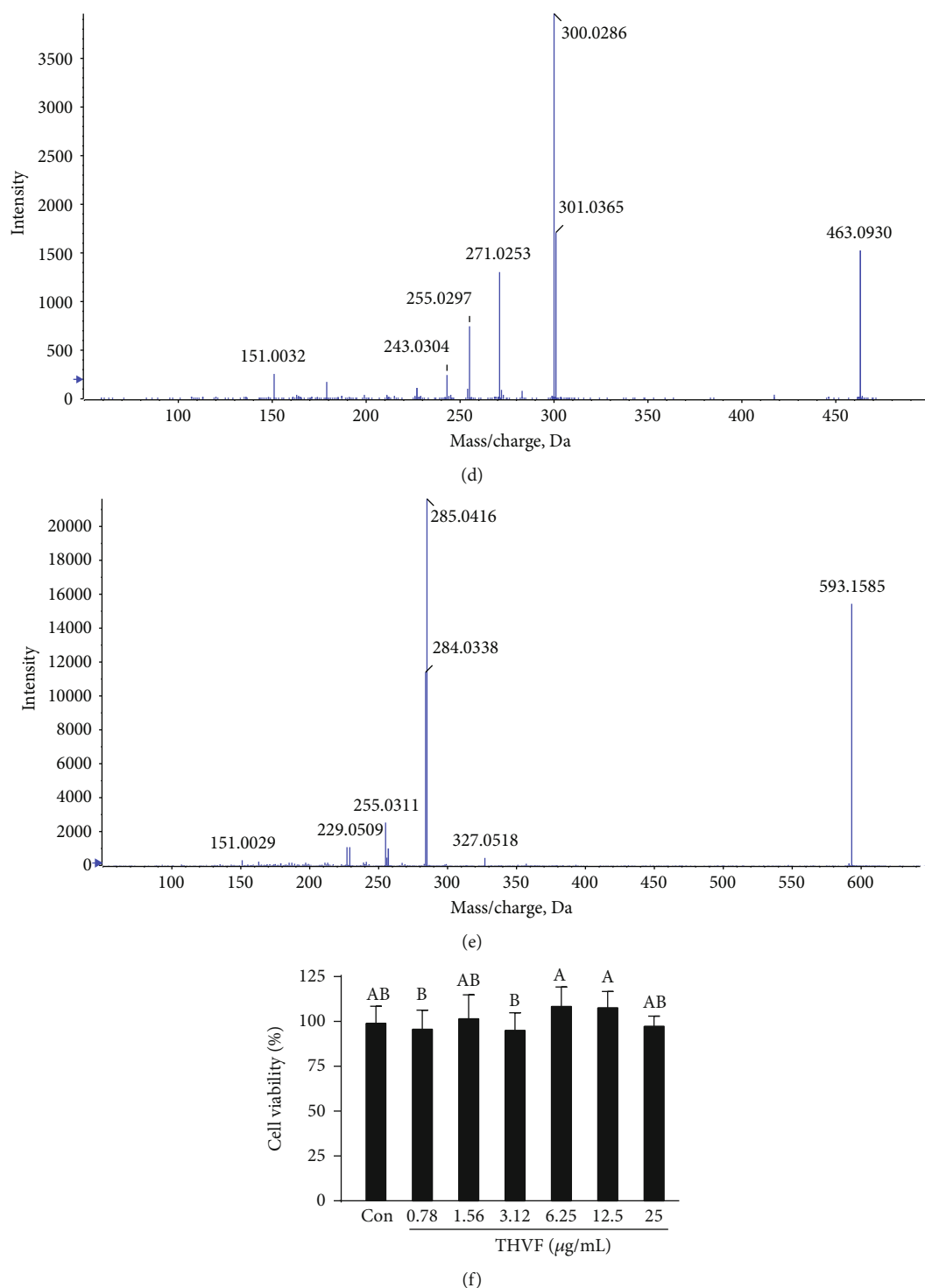


FIGURE 1: HPLC elution profile of compounds in THVF and effects of THVF on cytotoxicity in PC12 cells. (a) The liquid chromatography profile of THVF. The peak numbers were labeled according to the retention times. (b) MS/MS information for peak 1. (c) MS/MS information for peak 2. (d) MS/MS information for peak 3. (e) MS/MS information for peak 4. (f) PC12 cell viability was measured by the MTT method after treated with THVF at different concentrations for 24 h ($n = 6$).

compared with the control group (Figures 2(a) and 2(b)). Intriguingly, 10 and 20 $\mu\text{g/mL}$ THVF significantly declined the ROS level, with the DCF fluorescence intensity decreased to 0.18 and 0.15, respectively. Meanwhile, DHE, a unique probe of intracellular superoxide anion radicals,

was further used to analyze O_2^- contents. Similar findings were got, Glu significantly raised the mean DHE fluorescence intensity of PC12 cells (Figures 2(a) and 2(b)). In contrast, the intervention of THVF helped scavenging the overproduced O_2^- with the DHE fluorescence intensity

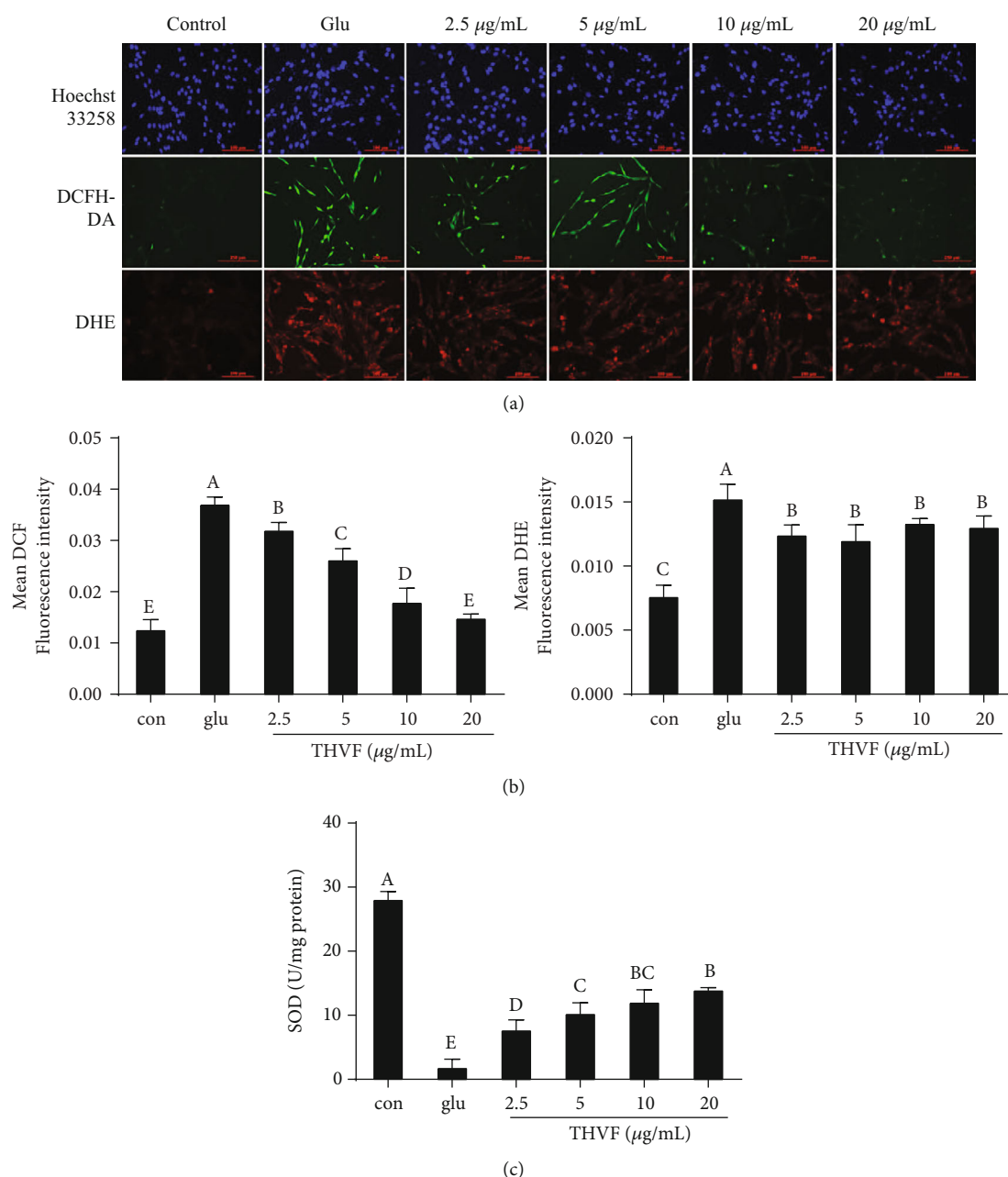


FIGURE 2: Effects of THVF on Glu-induced oxidative damage in PC12 cells ($n = 3$). (a) Hoechst 33258, DCFH-DA, DHE staining for genotoxicity, ROS, and O_2^- . (b) The quantitative data of panel DCFH-DA and DHE. (c) SOD activity of PC12 cells with or without Glu and THVF treatments. THVF-treated cells were inoculated in different concentrations of THVF for 24 hours, and then, 20 mM Glu was added for a total of 24 hours. Cells without Glu and THVF were used as negative control group. Cells treated with Glu alone were used as a glu group. Images were captured with a fluorescence microscope in the same settings. All the fluorescence images were quantified in the whole field with the background removed and represented by normalized fluorescence (y-axes) via Image-Pro Plus 6.0 ($n = 3$). Significance analysis was carried out according to the one-way ANOVA test, and different letters in figures mean statistically significant differences among the groups (a, b, c, etc., were labeled from large to small and once columns containing a same word means statistically insignificant, otherwise means statistically significant, $p < 0.05$).

declined. Superoxide dismutase (SOD) is an antioxidant metalloenzyme that specifically acts as a disproportionation catalyst to suppress superoxide anion radical generation [29]. As Figure 2(c) demonstrated, Glu severely inhibited activity of SOD in PC12 cells. Fortunately, THVF reversed this situation and 20 $\mu\text{g/mL}$ THVF could even recover the

SOD activity similar to control. These dates jointly revealed the protective effect of THVF under Glu-induced toxicity.

3.3. THVF Relieved Mitochondrial Dysfunction Induced by Glu. ROS is often regarded as a by-product of mitochondrial dysfunction [30], and mitochondrial dysfunction could

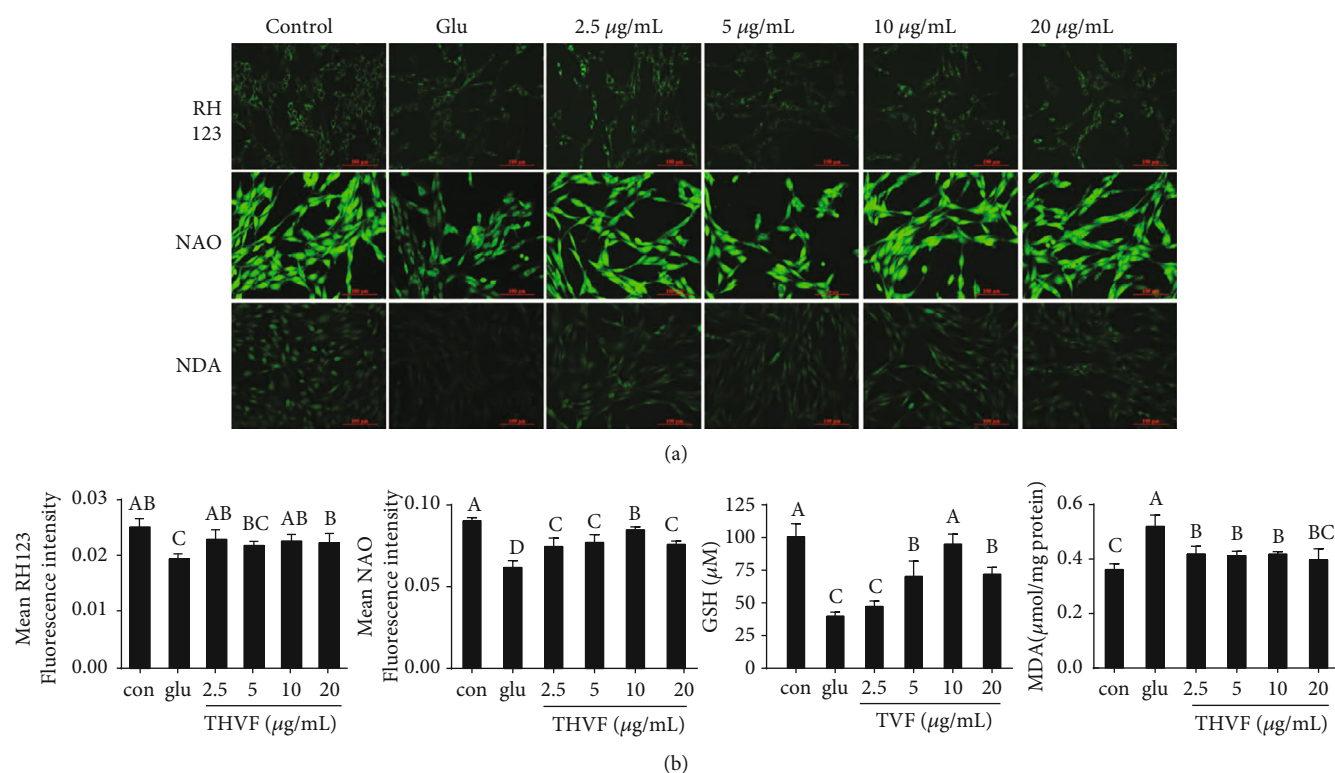


FIGURE 3: Effect of THVF on Glu-induced mitochondrial dysfunction in PC12 cells ($n = 3$). (a) Mitochondrial membrane potential, mitochondrial membrane lipid peroxidation, and GSH alterations of PC12 cells in the presence of Glu and THVF under different treatments and were incubated with RH123, NAO, and NDA probes. (b) The quantitative data of panel (a). Images were captured with a fluorescence microscope in the same settings. All the fluorescence images were quantified in the whole field with the background removed and represented by normalized fluorescence (y -axes) via Image-Pro Plus 6.0 ($n = 3$). Significance analysis was carried out according to one-way ANOVA test and different letters in figures mean statistically significant differences among the groups (a, b, c, etc., were labeled from large to small and once columns containing a same word means statistically insignificant, otherwise means statistically significant, $p < 0.05$).

further accelerate the progression of various diseases, such as atherosclerosis, diabetes, Alzheimer's disease, and Parkinson's disease [31]. Based on these findings, we suspected that THVF might provide a defense effect to the toxicity via recovering mitochondrial function. RH123 fluorescence probe is specific for mitochondrial membrane potential (MMP) detection and NAO is for mitochondrial membrane lipid peroxidation (MMLP), respectively. As Figure 3(a) illustrated, a Rh123 fluorescence intensity decline could be observed with the stimulation of Glu, suggesting the decreased MMP, which is usually regarded as prerequisite and a landmark event in early apoptosis. Similarly, the NAO fluorescence intensity was markedly suppressed by Glu, indicating the disturbed MMLP. However, after THVF treatments, NAO intensity increased compared with Glu-treated cells. Malondialdehyde (MDA) is a crucial product of MMLP, and its production can aggravate damage and leading to aging and resistance physiology [32]. Consistent with previous results, Glu stimulation triggered MDA production and accumulation in PC12 cells while $2.5 \mu\text{g}/\text{mL}$ was sufficient to decrease intracellular MDA content. Mitochondrial dysfunction could further facilitate consumption of glutathione (GSH), and NDA fluorescence intensity reduction was found after Glu stimulation. Conversely, THVF treatments increased intensity significantly, suggest-

ing the alleviation of mitochondrial damage and enhancement of antioxidative ability. Based on these results, we believe THVF exerted a beneficial effect against Glu-induced mitochondrial dysfunction.

3.4. THVF Promoted Cell Proliferation Inhibited by Glu. Besides genotoxicity, ROS generation, and mitochondrial dysfunction, Glu also directly induce PC12 cells apoptosis. B-cell lymphoma-2 (Bcl-2) protein family is closely related to apoptosis [33]. As Figure 4(a) showed, Glu upregulated the Bax expression and suppressed the protein level of Bcl-2, which manifested the apoptotic state of PC12 cells. Besides, the production level of caspase-9 was also increased to 3-fold of control. However, we found THVF obviously down-regulated expressions of Bax, caspase-9, and up-regulated Bcl-2 levels at a dose-dependent manner. PCNA plays a crucial role in cell proliferation and regulating cell cycle [34]. Consists with previous results, Glu significantly inhibited the expression of PCNA, indicating the damage of PC12 cell proliferation caused by Glu. On the contrary, THVF reversed such inhibition and up-regulated PCNA level to 2 times of control. These results suggested that THVF reversed apoptosis induced by Glu and facilitated cell proliferation.

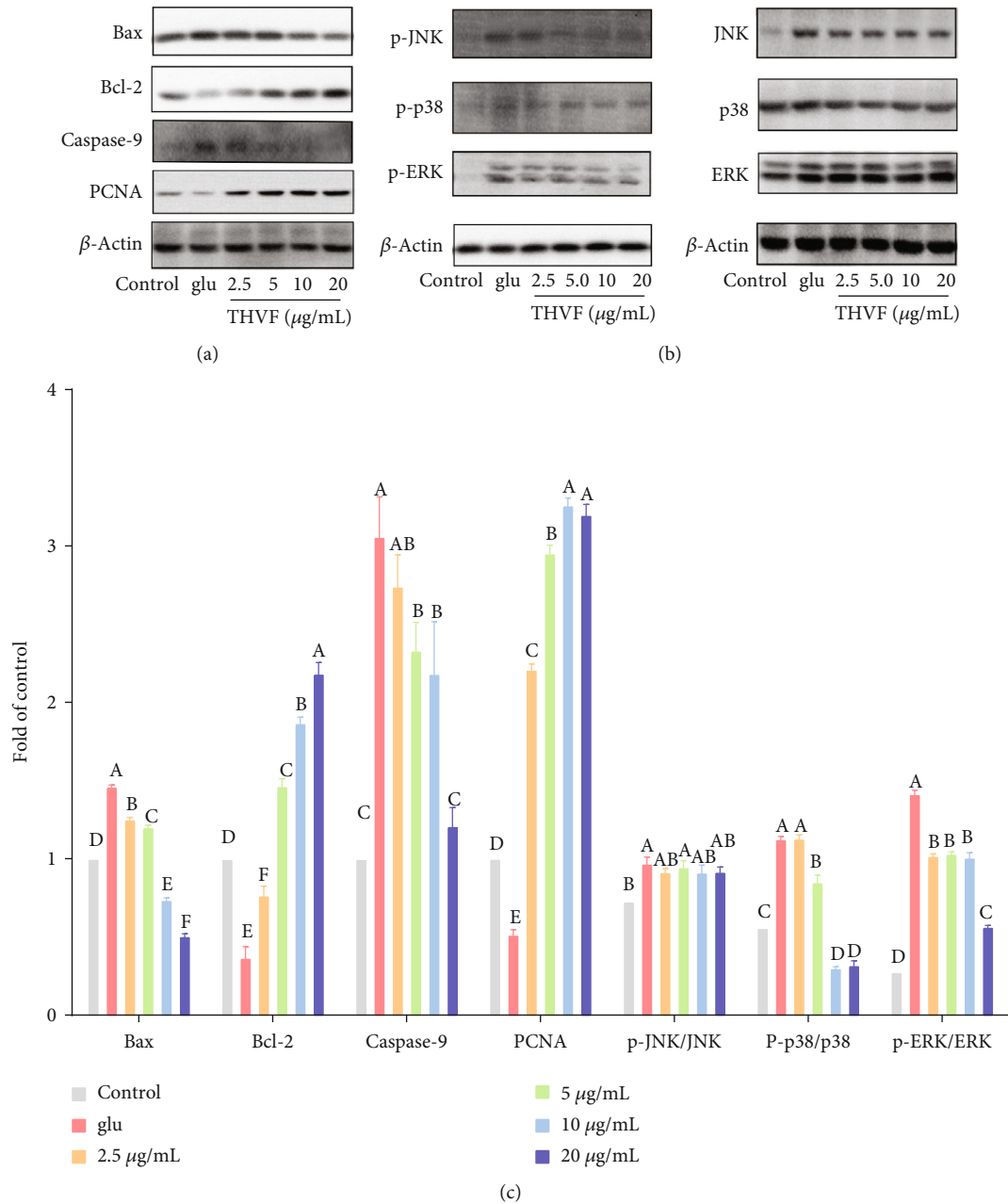


FIGURE 4: THVF treatment altered expressions of proteins in PC12 cells. (a) Western blot bands of Bax, Bcl-2, caspase-9, PCNA, and β -actin ($n = 3$). (b) Western blot bands of MAPKs. p-JNK, p-p38, and p-ERK represent phosphorylation of JNK, p38, and ERK. (c) Relative expressions of Bax, Bcl-2, caspase-9, PCNA, p-JNK, p-p38, p-ERK, JNK, p38, and ERK. The images were quantified by ImageJ software, the intensity of bands was corrected by β -actin ($n = 3$), and vertical lines in the histogram represent SDs of three replicates. Significance analysis was carried out according to the one-way ANOVA test, and different letters mean statistically significant differences among the groups (a, b, c, etc., were labeled from large to small and once columns containing a same word means statistically insignificant, otherwise means statistically significant, $p < 0.05$).

3.5. *The Protective Effect of THVF Involved in MAPK Pathways.* As an important transmitter of signals from the cell surface to the interior of the nucleus, MAPKs can be activated by different extracellular stimuli such as cytokines, hormones, and cellular stress [35]. Figure 4(b) showed that with the stimulation of Glu, the phosphorylation of JNK, ERK, and p38 was upregulated. However, after THVF treatments, downregulation of phospho-p38 and phosphor-ERK was observed. Meanwhile, though

THVF had both inhibited the expression level of total JNK and p-JNK, the ratio of p-JNK/JNK had not changed compared to Glu-induced cells. Based on these results, we deduced that THVF protect PC12 cells from toxicity via ERK/p38 pathways.

3.6. *THVF Recovered the Locomotory Ability of C. elegans.* With short lifespan and low cost, *C. elegans* is regarded as an ideal *in vivo* model to study toxicity [36]. As shown

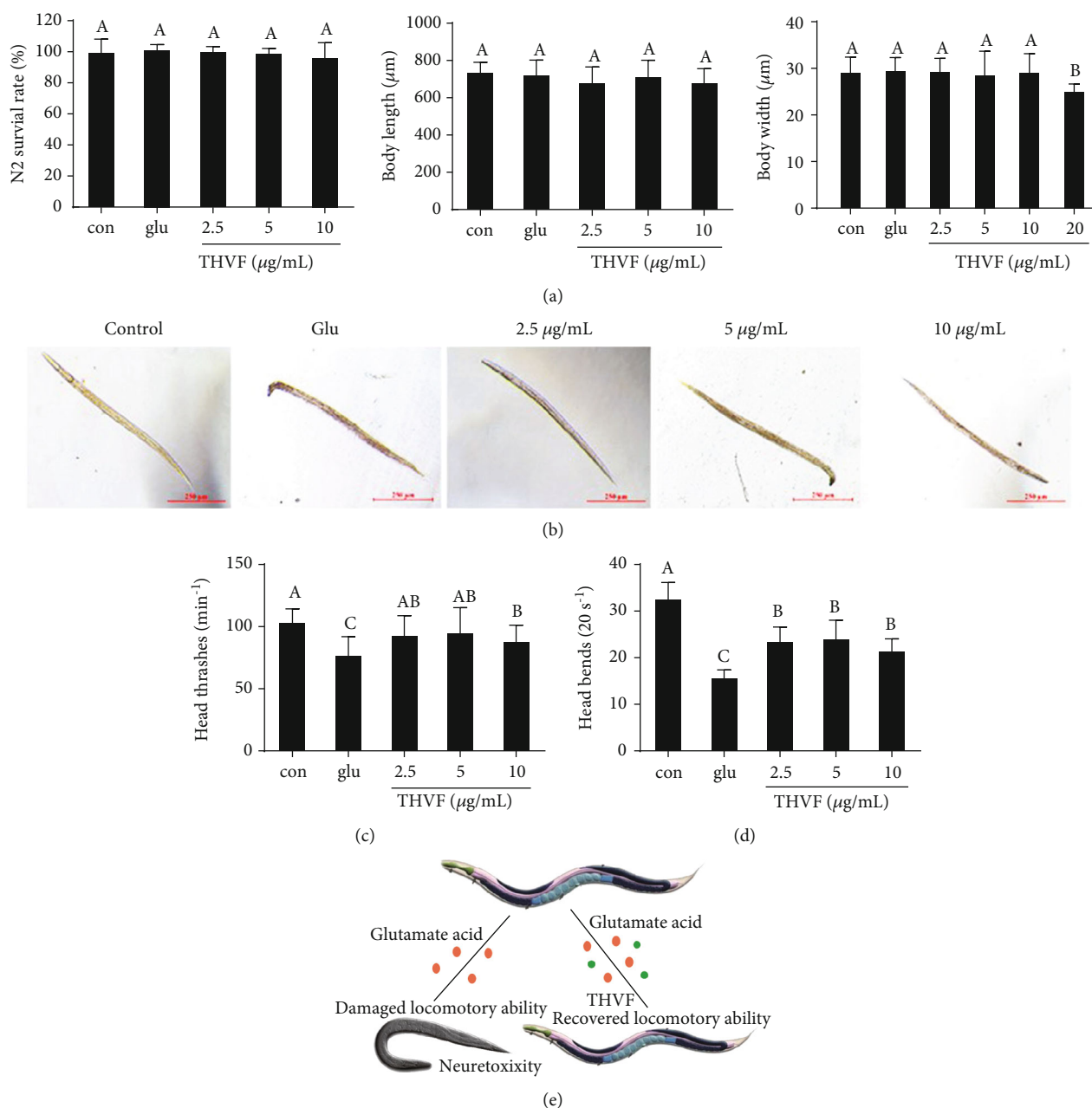


FIGURE 5: Effect of THVF on Glu-induced toxicity in *C. elegans* ($n = 30$). (a) Survival rate, body length, and body width of different groups in N2. (b) Representative photographs of *C. elegans* with different treatments. (c) Head thrashes of different groups in N2. (d) Body-bending frequency of different groups in N2. (e) Scheme illustration of Glu and THVF on nematode locomotory activity. Significance analysis was carried out according to the one-way ANOVA test, and different letters show statistically significant differences among the groups ($p < 0.05$).

in Figures 5(a) and 5(b), both Glu and THVF had not affected the survival rate, body length, and body width of nematode. However, Glu stimulation caused severe damage to nematodes' locomotory ability. Our results showed significant decreases in body bends and head thrashes of *C. elegans* after exposure to Glu (Figures 5(c) and 5(d)), implying the neurotoxicity of Glu, while THVF partly recovered the locomotory abilities of nematodes. Based on these results, our results demonstrated that Glu could induce considerably severe locomotor defects and THVF

was capable to protect nematodes from Glu-induced neurotoxicity (Figure 5(e)).

3.7. THVF Protected *C. elegans* from Glu-Induced Oxidative Stress. In *in vitro* study, Glu induced oxidative toxicity to PC12 cells and THVF effectively alleviated oxidative stress. To confirm whether THVF could help prevent from oxidative damage *in vivo*, we used DCF, DHE, and NDA probes to measure intracellular ROS, O_2^- , and GSH depletion in *C. elegans*, respectively. Figure 6 demonstrated that the

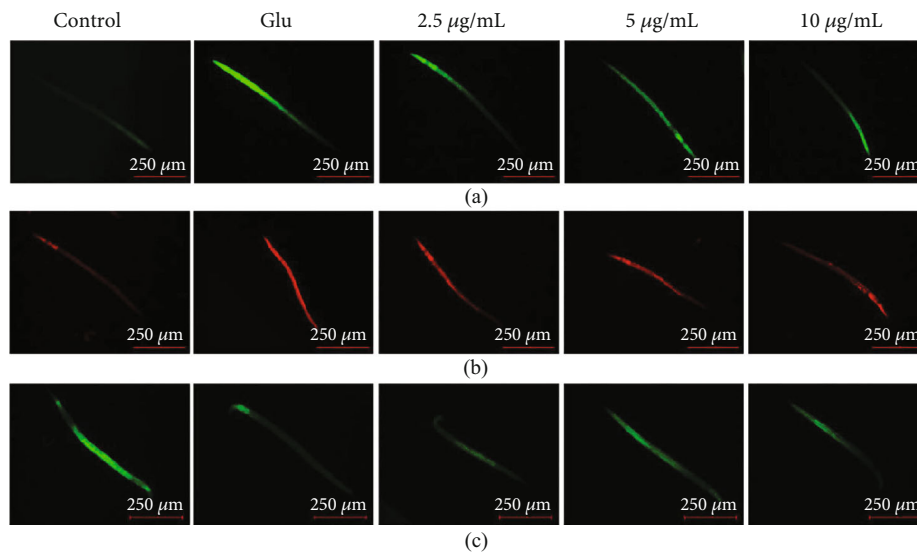


FIGURE 6: Fluorescence staining for *C. elegans* ($n = 30$). (a) DCFH-DA staining for ROS alteration. (b) DHE staining for O_2^- alteration. (c) NDA staining for GSH contents. Images were captured with a fluorescence microscope in the same settings ($n = 6$).

treatment of Glu remarkably increased the mean DCF fluorescence intensity whereas the addition of THVF restored the mean DCF fluorescence intensity as expected at a dose-related manner. Moreover, Glu enhanced the level of O_2^- and facilitated the GSH depletion in nematodes. On the contrary, THVF intervention suppressed the generation of O_2^- and restrained GSH depletion. These results above suggested that THVF could attenuate Glu-induced oxidative damage in *C. elegans*.

4. Discussion

The Chinese have used certain seaweeds to enhance the flavor of food for some 2,000 years. In 1908, the flavor-enhancing agent was identified as glutamic acid [37]. Nowadays, Glu has been applied to a large amount of industrial production with its various applications such as flavor enhancer, wrinkles reducer, energy supplier, and neurotherapeutic agent. However, the toxicity especially neurotoxicity of Glu has been continuously uncovered recently. Many studies have revealed that natural products are able to help alleviate toxicity and protect from outer stimulation. TH is a traditional Chinese herb and food with various confirmed bioactive functions, while TH vine is usually regarded useless and often discarded as a by-product, resulting in a waste of source. We extracted and purified the flavones of TH and use UPLC-TOF/MS to characterized the main compounds of THVF. Results showed that THVF was composed of 3-caffeoylquinic acid, 5-caffeoylquinic acid, quercetin-3-O-rutinoside, and kaempferol-3-O-rutinoside.

With extreme versatility for pharmacological manipulation, ease of culture, and the large amount of background knowledge on their proliferation and neuro characterization, rat pheochromocytoma (PC12) cells have been widely used as a model for neural research [38]. Glu caused severe genotoxicity to PC12, hereby triggered enhanced ROS generation and overproduction of O_2^- , which were by-products of mito-

chondrial dysfunction induced by Glu. Additionally, Glu inhibited the SOD enzyme activity and then increased the MDA accumulation as results. Conversely, THVF attenuated the Glu-induced toxicity by alleviating the genotoxicity, relieving oxidative stress, and recovering mitochondrial functions. It is implying that cell death in central nervous system irregularly may play a part in an etiology of cancer, AIDS, autoimmune diseases, and degenerative diseases such as Alzheimer's disease (AD), amyotrophic lateral sclerosis (ALS), and Huntington's disease. Similarly, PC12 cell proliferation was inhibited by Glu with down-regulation of PCNA and Bcl-2, as well as up-regulation of Bax and caspase-9, suggesting the apoptosis of cells. As expected, THVF recovered the cell proliferate ability and enhanced the expression levels of PCNA, Bcl-2.

Mitogen-activated protein kinase (MAPK), as an important transmitter of signal transmission from the cell surface to the interior of the nucleus, plays a key role in stress response [35]. Glu markedly activated the phosphorylation of p38, JNK, and ERK. Nevertheless, down-regulation of p38 phosphorylation was found in THVF treated cells. Considering p38 MAPK is vital in immune response to stress and cell survival [39], THVF can inactivate, at least partly, the p38 MAPK pathway. Besides, THVF suppressed the expression of Glu-induced ERK over-phosphorylation. Previous studies have reported that ERKs, as a downstream protein of various growth factors (EGF, NGF, PDGF), regulate cell proliferation, differentiation, and survival. It acts like a receptor of signals from growth factors, mitogens, and environmental stimuli and then regulates nuclear transcription factors through the ERK signal cascade [40]. Thus, THVF might help protect PC12 cells from Glu-induced toxicity by suppressing over-phosphorylation of ERK and p38.

It has been proved that neurotransmitters and their metabolism, vesicle circulation, and synaptic transmission are highly conserved, and all 302 neurons of the nematode have been well studied, which makes *C. elegans* an ideal

model to learn neurotoxicity and behavior *in vivo* [41]. Locomotor behaviors require the control of neural circuits [42]. Our results implied that Glu toxicity might be involved in the disruption of motor control function or appropriate synaptic contacts between neurons and muscle cells. As *C. elegans* lacks a functional blood-brain barrier, Glu could quickly diffuse into the nervous system and directly produce neurotoxic actions, resulting in damaged head thrashes and body bends. Fortunately, here THVF turned to be a neuroprotective agent and recovered the locomotory ability of nematodes. Consistent with *in vitro* results, Glu elevated the intracellular ROS, O₂⁻ generation, and GSH depletion in nematodes and THVF prevented larvae from Glu-toxicity. However, it is unclear whether MAPK pathways are also involved in the THVF-treated nematodes, and further research is needed to confirm the inner mechanism in *C. elegans* level.

5. Conclusion

In this study, we focus on Glu neurotoxicity rather than its wide applications and well-known protective effects. As results illustrated, Glu caused damage to PC12 cells and *C. elegans* while THVF, flavones extracted, and purified from TH vine was able to protect Glu-induced toxicity via MAPK pathways. These data provide a novel insight and raise worthwhile questions about the Glu-accompanied side-toxicity and THVF potential neuroprotective effects both *in vitro* and *in vivo*, as well as MAPK pathways' role in neurotoxicity.

Data Availability

The data used to support the findings of this study are available from the corresponding author upon request.

Conflicts of Interest

The authors have declared no conflict of interest.

Authors' Contributions

Qiang Chu and Yonglu Li contributed equally to this work.

Acknowledgments

This work was supported by the Science and Technology Department of Zhejiang Province (No. 2018C02045) and Shanghai Zhengyue Enterprise Management Co., Ltd.

References

- [1] P. J. Reeds, "Dispensable and indispensable amino acids for humans," *The Journal of Nutrition*, vol. 130, no. 7, pp. 1835S–1840S, 2000.
- [2] S. Jinap and P. Hajeb, "Glutamate. Its applications in food and contribution to health," *Appetite*, vol. 55, no. 1, pp. 1–10, 2010.
- [3] T. Populin, S. Moret, S. Truant, and L. S. Conte, "A survey on the presence of free glutamic acid in foodstuffs, with and without added monosodium glutamate," *Food Chemistry*, vol. 104, no. 4, pp. 1712–1717, 2007.
- [4] A. N. Williams and K. M. Woessner, "Monosodium glutamate 'allergy': menace or myth?," *Clinical and Experimental Allergy*, vol. 39, no. 5, pp. 640–646, 2009.
- [5] O. P. Ottersen, Y. Takumi, A. Matsubara, A. S. Landsend, J. H. Laake, and S. Usami, "Molecular organization of a type of peripheral glutamate synapse: the afferent synapses of hair cells in the inner ear," *Progress in Neurobiology*, vol. 54, no. 2, pp. 127–148, 1998.
- [6] P. Pichler and L. Lagnado, "The transfer characteristics of hair cells encoding mechanical stimuli in the lateral line of zebrafish," *The Journal of Neuroscience*, vol. 39, no. 1, pp. 112–124, 2019.
- [7] A. Ogunleye, A. Bhat, V. U. Irorere, D. Hill, C. Williams, and I. Radecka, "Poly- γ -glutamic acid: production, properties and applications," *Microbiology*, vol. 161, no. 1, pp. 1–17, 2015.
- [8] H. A. Krebs, "Metabolism of amino-acids: the synthesis of glutamine from glutamic acid and ammonia, and the enzymic hydrolysis of glutamine in animal tissues," *The Biochemical Journal*, vol. 29, no. 8, pp. 1951–1969, 1935.
- [9] J. S. Najarian and H. A. Harper, "Comparative effect of arginine and monosodium glutamate on blood ammonia," *Proceedings of the Society for Experimental Biology and Medicine*, vol. 92, no. 3, pp. 560–563, 1956.
- [10] K. Krnjevic, "Glutamate and gamma-aminobutyric acid in brain," *Nature*, vol. 228, no. 5267, pp. 119–124, 1970.
- [11] M. Kobayashi, C. Benakis, C. Anderson et al., "AGO CLIP reveals an activated network for acute regulation of brain glutamate homeostasis in ischemic stroke," *Cell Reports*, vol. 28, no. 4, pp. 979–991.e6, 2019.
- [12] A. da Silva-Candal, A. Pérez-Díaz, M. Santamaría et al., "Clinical validation of blood/brain glutamate grabbing in acute ischemic stroke," *Annals of Neurology*, vol. 84, no. 2, pp. 260–273, 2018.
- [13] Z. Zhou, G. L. Austin, L. Young, L. A. Johnson, and R. Sun, "Mitochondrial metabolism in major neurological diseases," *Cells*, vol. 7, no. 12, p. 229, 2018.
- [14] S. Bleich, K. Romer, J. Wiltfang, and J. Kornhuber, "Glutamate and the glutamate receptor system: a target for drug action," *International Journal of Geriatric Psychiatry*, vol. 18, Supplement 1, pp. S33–S40, 2003.
- [15] M. T. Islam, "Oxidative stress and mitochondrial dysfunction-linked neurodegenerative disorders," *Neurological Research*, vol. 39, no. 1, pp. 73–82, 2017.
- [16] J. T. Coyle and P. Puttfarcken, "Oxidative stress, glutamate, and neurodegenerative disorders," *Science*, vol. 262, no. 5134, pp. 689–695, 1993.
- [17] R. D. Randall and S. A. Thayer, "Glutamate-induced calcium transient triggers delayed calcium overload and neurotoxicity in rat hippocampal neurons," *The Journal of Neuroscience*, vol. 12, no. 5, pp. 1882–1895, 1992.
- [18] N. Plotegher, D. Perocheau, R. Ferrazza et al., "Impaired cellular bioenergetics caused by GBA1 depletion sensitizes neurons to calcium overload," *Cell Death & Differentiation*, 2019.
- [19] S. A. Novgorodov, J. R. Voltin, M. A. Gooz, L. Li, J. J. Lemasters, and T. I. Guduz, "Acid sphingomyelinase promotes mitochondrial dysfunction due to glutamate-induced regulated necrosis," *Journal of Lipid Research*, vol. 59, no. 2, pp. 312–329, 2018.

- [20] Y. Yu, M. Shen, Q. Song, and J. Xie, "Biological activities and pharmaceutical applications of polysaccharide from natural resources: a review," *Carbohydrate Polymers*, vol. 183, pp. 91–101, 2018.
- [21] Y. Li, Q. Chu, Y. Liu, X. Ye, Y. Jiang, and X. Zheng, "Radix *Tetragium* flavonoid ameliorates inflammation and prolongs the lifespan of *Caenorhabditis elegans* through JNK, p38 and Nrf2 pathways," *Free Radical Research*, vol. 53, no. 5, pp. 562–573, 2019.
- [22] Q. Chu, R. Jia, W. Chen et al., "Purified *Tetragium hemsleyanum* vines polysaccharide attenuates EC-induced toxicity in Caco-2 cells and *Caenorhabditis elegans* via DAF-16/FOXO pathway," *International Journal of Biological Macromolecules*, 2019.
- [23] Q. Chu, R. Jia, M. Chen et al., "*Tetragium hemsleyanum* tubers polysaccharide ameliorates LPS-induced inflammation in macrophages and *Caenorhabditis elegans*," *International Journal of Biological Macromolecules*, vol. 141, pp. 611–621, 2019.
- [24] X. Chen, L. Tao, Y. Ru et al., "Antibacterial mechanism of *Tetragium hemsleyanum* Diels et Gilg's polysaccharides by metabolomics based on HPLC/MS," *International Journal of Biological Macromolecules*, vol. 140, pp. 206–215, 2019.
- [25] J. Kolniak-Ostek, "Identification and quantification of polyphenolic compounds in ten pear cultivars by UPLC-PDA-Q/TOF-MS," *Journal of Food Composition and Analysis*, vol. 49, pp. 65–77, 2016.
- [26] M. Pagano and C. Faggio, "The use of erythrocyte fragility to assess xenobiotic cytotoxicity," *Cell Biochemistry and Function*, vol. 33, no. 6, pp. 351–355, 2015.
- [27] A. Sharma, "Monosodium glutamate-induced oxidative kidney damage and possible mechanisms: a mini-review," *Journal of Biomedical Science*, vol. 22, no. 1, p. 93, 2015.
- [28] S. H. Nile, Y. S. Keum, A. S. Nile, S. S. Jalde, and R. V. Patel, "Antioxidant, anti-inflammatory, and enzyme inhibitory activity of natural plant flavonoids and their synthesized derivatives," *Journal of Biochemical and Molecular Toxicology*, vol. 32, no. 1, article e22002, 2018.
- [29] S. Signorella, C. Palopoli, and G. Ledesma, "Rationally designed mimics of antioxidant manganoenzymes: role of structural features in the quest for catalysts with catalase and superoxide dismutase activity," *Coordination Chemistry Reviews*, vol. 365, pp. 75–102, 2018.
- [30] J. M. Flynn and S. Melov, "SOD2 in mitochondrial dysfunction and neurodegeneration," *Free Radical Biology & Medicine*, vol. 62, pp. 4–12, 2013.
- [31] T. Jiang, Q. Sun, and S. Chen, "Oxidative stress: a major pathogenesis and potential therapeutic target of antioxidative agents in Parkinson's disease and Alzheimer's disease," *Progress in Neurobiology*, vol. 147, pp. 1–19, 2016.
- [32] S. Feng, H. Cheng, Z. Xu et al., "Thermal stress resistance and aging effects of *Panax notoginseng* polysaccharides on *Caenorhabditis elegans*," *International Journal of Biological Macromolecules*, vol. 81, pp. 188–194, 2015.
- [33] R. J. Youle and A. Strasser, "The BCL-2 protein family: opposing activities that mediate cell death," *Nature Reviews Molecular Cell Biology*, vol. 9, no. 1, pp. 47–59, 2008.
- [34] W. Strzalka and A. Ziemienowicz, "Proliferating cell nuclear antigen (PCNA): a key factor in DNA replication and cell cycle regulation," *Annals of Botany*, vol. 107, no. 7, pp. 1127–1140, 2011.
- [35] B. Su and M. Karin, "Mitogen-activated protein kinase cascades and regulation of gene expression," *Current Opinion in Immunology*, vol. 8, no. 3, pp. 402–411, 1996.
- [36] M. C. Leung, P. L. Williams, A. Benedetto et al., "*Caenorhabditis elegans*: an emerging model in biomedical and environmental toxicology," *Toxicological Sciences*, vol. 106, no. 1, pp. 5–28, 2008.
- [37] A. Samuels, "The toxicity/safety of processed free glutamic acid (MSG): a study in suppression of information," *Accountability in Research*, vol. 6, no. 4, pp. 259–310, 1999.
- [38] R. H. S. Westerink and A. G. Ewing, "The PC12 cell as model for neurosecretion," *Acta Physiologica*, vol. 192, no. 2, pp. 273–285, 2008.
- [39] T. M. Thornton and M. Rincon, "Non-classical p38 map kinase functions: cell cycle checkpoints and survival," *International Journal of Biological Sciences*, vol. 5, no. 1, pp. 44–51, 2009.
- [40] B. Sparta, M. Pargett, M. Minguet, K. Distor, G. Bell, and J. G. Albeck, "Receptor level mechanisms are required for epidermal growth factor (EGF)-stimulated extracellular signal-regulated kinase (ERK) activity pulses," *The Journal of Biological Chemistry*, vol. 290, no. 41, pp. 24784–24792, 2015.
- [41] K. Kamireddy, S. Chinnu, P. S. Priyanka, P. S. Rajini, and P. Giridhar, "Neuroprotective effect of *Decalepis hamiltonii* aqueous root extract and purified 2-hydroxy-4-methoxy benzaldehyde on 6-OHDA induced neurotoxicity in *Caenorhabditis elegans*," *Biomedicine & Pharmacotherapy*, vol. 105, pp. 997–1005, 2018.
- [42] H. Kohsaka, P. A. Guertin, and A. Nose, "Neural circuits underlying fly larval locomotion," *Current Pharmaceutical Design*, vol. 23, no. 12, pp. 1722–1733, 2017.